

Some pages of this thesis may have been removed for copyright restrictions.

If you have discovered material in AURA which is unlawful e.g. breaches copyright, (either yours or that of a third party) or any other law, including but not limited to those relating to patent, trademark, confidentiality, data protection, obscenity, defamation, libel, then please read our [Takedown Policy](#) and [contact the service](#) immediately

**COMPUTER SIMULATION FOR TUBE-MAKING
BY THE COLD ROLL-FORMING PROCESS**

TAKAAKI TOYOOKA

Doctor of Philosophy

THE UNIVERSITY OF ASTON IN BIRMINGHAM

October 1999

This copy of the thesis has been supplied on condition that anyone who consults it is understood to recognise that its copyright rests with its author and that no quotation from the thesis and no information derived from it may be published without proper acknowledgement.

COMPUTER SIMULATION FOR TUBE-MAKING BY THE COLD ROLL-FORMING PROCESS

Takaaki Toyooka

Doctor of Philosophy 1999

SUMMARY

The conventional design of forming rolls depends heavily on the individual skills of roll designers which is based on intuition and knowledge gained from previous work. Roll design is normally a trial and error procedure, however with the progress of computer technology, CAD/CAM systems for the cold roll-forming industry have been developed. Generally, however, these CAD systems can only provide a flower pattern based on the knowledge obtained from previously successful flower patterns.

In the production of ERW(Electric Resistance Welded) tube and pipe, the need for a theoretical simulation of the roll-forming process, which can not only predict the occurrence of the edge buckling but also obtain the optimum forming condition, has been recognised. A new simulation system named "CADFORM" has been devised that can carry out the consistent forming simulation for this tube-making process. The CADFORM system applies an elastic-plastic stress-strain analysis and evaluates edge buckling by using a simplified model of the forming process. The results can also be visualised graphically.

The calculated longitudinal strain is obtained by considering the deformation of lateral elements and takes into account the reduction in strains due to the fin-pass roll. These calculated strains correspond quite well with the experimental results. Using the calculated strains, the stresses in the strip can be estimated. The addition of the fin-pass roll reduction significantly reduces the longitudinal compressive stress and therefore effectively suppresses edge buckling.

If the calculated longitudinal stress is controlled, by altering the forming flower pattern so it does not exceed the buckling stress within the material, then the occurrence of edge buckling can be avoided.

CADFORM predicts the occurrence of edge buckling of the strip in tube-making and uses this information to suggest an appropriate flower pattern and forming conditions which will suppress the occurrence of the edge buckling.

KEYWORDS: Cold Roll Forming
Tube-Making
Computer Simulation
Elastic-Plastic Stress-Strain Analysis
Edge Buckling

Dedicated to my parents
and family

ACKNOWLEDGEMENTS

I would like to take the opportunity to express my gratitude to everyone who has helped me complete this research.

In particular, I would like to thank the Kawasaki Steel Corporation, for giving me the opportunity to undertake this PhD research at Aston University, and my supervisor Dr Ian Cole, who sadly past away just before the completion of my thesis.

I would also like to acknowledge the help of ;

Dr J. E. T. Penny,	Main supervisor Head of Department Mechanical and Electrical Engineering Aston University
Dr K. Baines,	Advisor Department of Mechanical Engineering Adelaide University
Dr D.A. Milner,	Advisor Aston University
Dr R. J. Downes,	Computer advisor Southampton University
Miss Katy Barry	Administrative assistant School of Engineering and Applied Science Aston University
Mr. Y Hashimoto	Senior Researcher Technical Research Laboratories Kawasaki Steel Corporation
Dr T. Fujii	Director and Superintendent Technical Research Laboratories Kawasaki Steel Corporation
Mr E. Yamanaka	Director and Superintendent Chita Works Kawasaki Steel Corporation

Contents

	Page
Summary	2
Dedication	3
Acknowledgements	4
Lists of Contents	5
Lists of Figures	8
Lists of Tables	14
Lists of Photographs	15
Chapter 1. Tube-making by the Cold Roll Forming Process	
1.1 Introduction	16
1.2 Production of ERW tube and pipe	18
1.3 Background of this research	21
1.4 Research objectives	25
Chapter 2. Roll-Forming Technology for ERW Tube- and Pipe-making	
2.1 Design of forming rolls and mill for ERW tube- and pipe-making	27
2.2 Newly developed ERW tube- and pipe-making	28
2.3 Pass-line conditions for ERW tube- and pipe-making	32
Chapter 3. Computer Aids in Cold Roll-Forming	
3.1 CAD/CAM system	33
3.2 Theoretical analysis of cold roll-forming	34
3.2.1 Minimum energy method	34
3.2.2 Finite element analysis	43
Chapter 4. Application of the "ROLFOM" Package to Tube-making	45
Chapter 5. New Computer Simulation for Tube-making	
5.1 Outline of new computer simulation, "CADFORM"	54
5.2 Two-dimensional flower pattern design	57
5.2.1 Flower pattern design programme	57

5.2.2	Two-dimensional flower pattern drawing	58
5.3	Procedures and modelling for elastic-plastic stress-strain analysis in tube making	71
5.3.1	Modelling for elastic-plastic stress-strain analysis	71
5.3.2	Model-1 of stress-strain analysis	75
5.3.3	Model-2 of stress-strain analysis	79
5.3.4	Consideration of fin-pass roll reduction	81
5.3.5	Elastic-plastic stress-strain analysis	84
5.4	Algorithm of elastic-plastic stress-strain analysis	89
5.5	Evaluation of edge buckling	92
5.6	Three-dimensional graphics display and drawing	96
Chapter 6.	Results of Calculation by the CADFORM System	
6.1	Three-dimensional deformed surface of the strip in the forming passes	98
6.2	Stress and strain of the strip in the forming passes	105
Chapter 7.	Verification of the CADFORM System by Measured Forming Strains	
7.1	Strain measurement experiment	117
7.2	Comparison of calculated to measured strains	121
Chapter 8.	Discussion	
8.1	Simulation of stress and strain of the tube with large D/t ratio formed in the 4inch model mill	125
8.1.1	Forming conditions of thin walled tube	125
8.1.2	Comparison of stress and strain between Model-1 and Model-2	149
8.1.3	Evaluation of edge buckling	153
8.2	Effects of pass-line conditions on the tube stress and strain	157
8.3	Effect of the number of divided elements in the lateral direction on the tube stress and strain	160
8.4	Effect of forming flower patterns on the stress and strain in tube-making by the cold roll forming process	165
8.5	Application of the CADFORM system to production mills	181
Chapter 9	Conclusions	
9.1	Introduction	187
9.2	Development of the CADFORM system	188

9.2.1	Flower pattern design	189
9.2.2	Elastic-plastic stress-strain analyses	190
9.2.3	Verification of the CADFORM system	190
9.2.4	Comparison of stress and strain by two theoretical models	191
9.2.5	Evaluation of edge buckling	191
9.2.6	Effects of pass-line conditions	192
9.2.7	Effects of the number of laterally divided elements	193
9.2.8	Effects of forming flower patterns	193
9.4	Application of the CADFORM system	194
Chapter 10 Future Work		195
REFERENCES		198
Appendix -1	Programme of the CADFORM	205
Appendix -2	Input data of tube $D = 60.5\text{mm} \times t = 1.75\text{mm}$	291
Appendix -3	Input data of tube $D = 42.7\text{mm} \times t = 1.5\text{mm}$	293
Appendix -4	Input and output data of tube $D = 100\text{mm} \times t = 1.0\text{mm}$	295
Appendix -5	Input and data of centre bend flower pattern	314
Appendix -6	Input and data of edge bend flower pattern	3106
Appendix -7	Input and data of circular bend flower pattern	318
Appendix -8	Input and data of tube $D = 146.0\text{mm} \times t = 2.0\text{mm}$	320

List of Figures

Fig.1	Schematic view of the cold roll-forming process for ERW tube-making	17
Fig.2	Typical shapes of sections produced by the cold roll-forming process	17
Fig.3	Typical layout of tube-making process using cold roll-forming and high frequency electric resistance welding	19
Fig.4	Variation of annual production of tube and pipes in Japan	20
Fig.5	Illustration of occurrence of edge buckling in tube-making by the cold roll-forming process	24
Fig.6	Typical flower pattern used in ERW tube- and pipe-making	29
Fig.7	New flower patterns developed in the CBR forming process	29
Fig.8	Typical layout of forming mill for production of ERW tube and pipe	30
Fig.9	Schematic view of forming of sheet metal in major forming passes	31
Fig.10	Pass-line conditions for ERW tube- and pipe-making	32
Fig.11	Main factors defining the cold roll-forming process and their relationships	35
Fig.12	Illustration of concept of shape function $S(x)$ by Kiuchi	39
Fig.13	Flow-chart of total simulation process by Kiuchi	39
Fig.14	Variation of longitudinal membrane strain ϵ_{x0} occurring at transversally different positions	40
Fig.15	Configuration of CAD/CAM system for cold roll forming developed by Aston University	46
Fig.16	Example of hat shape finished section by using the ROLFOM section programme	47
Fig.17	Example of flower pattern A and flower pattern B by the ROLFOM flower pattern programme	49
Fig.18	Application of the ROLFOM to flower pattern design of tube at the break-down roll forming stage	50
Fig.19	Application of the ROLFOM to flower pattern design of tube at the fin-pass roll forming stage	51
Fig.20	Application of the ROLFOM to flower pattern design and flower sequence	52
Fig.21	Construction of CADFORM system for tube and pipe	56
Fig.22	Drawing of planned forming flower at entry pass by flower pattern A using the CADFORM system	60

Fig.23	Drawing of planned forming flower at 1st pass by flower pattern A using the CADFORM system	61
Fig.24	Drawing of planned forming flower at 2nd pass by flower pattern A using the CADFORM system	62
Fig.25	Drawing of forming flower at 3rd pass by flower pattern A using the CADFORM system	63
Fig.26	Drawing of forming flower at 4th pass by flower pattern A using the CADFORM system	64
Fig.27	Drawing of forming flower at 5th pass by flower pattern A using the CADFORM system	65
Fig.28	Drawing of forming flower at 6th pass by flower pattern A using the CADFORM system	66
Fig.29	Drawing of forming flower at 7th pass by flower pattern A using the CADFORM system	67
Fig.30	Drawing of forming flower at 8th pass by flower pattern A using the CADFORM system	68
Fig.31	Drawing of flower sequence in bottom constant pass-line forming by flower pattern B using the CADFORM system	69
Fig.32	Drawing of flower sequence in downhill pass-line forming by flower pattern B using the CADFORM system	70
Fig.33	Flow-chart of elastic-plastic stress strain analysis	74
Fig.34	Schematic diagram of division of strip into elements and definition of dimensions of divided elements in Model-1	75
Fig.35	Definition of dimensions of divided elements and their deformation without adjustment of coordinate points in the lateral direction in Model-1	78
Fig.36	Illustration of division of sheet metal into elements and definition of dimensions of divided elements in Model-2	80
Fig.37	Procedure for consideration of fin-pass roll reduction	83
Fig.38	Definition of strain components in fin-pass roll forming	83
Fig.39	Schematic diagram of the von Mises yield criterion for material yielding in the plane stress condition	86
Fig.40	Definition of elastic and plastic strain increments in yielding of material	86
Fig.41	Pattern of material yielding conditions to obtain the elastic increment strain	88
Fig.42	Flow-chart of stepwise analysis of strains of divided elements in Model-2	90
Fig.43	Flow-chart of stepwise analysis of stresses of divided elements in Model-2	91
Fig.44	Model of edge buckling at strip edge	93
Fig.45	Definition of sector of hollow circle	95

Fig.46	Definition of coordinates and rotation for 3-D drawing	97
Fig.47	Example of 3-D deformed surface of strip drawn using planned flowers in forming passes of tube with $D = 60.5\text{mm}$, $t = 1.75\text{mm}$ and $\sigma_Y = 295\text{MPa}$	101
Fig.48	Example of 3-D deformed surface of strip drawn using planned flowers in forming passes of tube with $D = 60.5\text{mm}$, $t = 1.75\text{mm}$ and $\sigma_Y = 295\text{MPa}$ (View from the direction of Z-axis/bank(θ_B) = 0° , Y-axis/heading(θ_H) = 0° and X-axis/pitch(θ_P) = 40°)	102
Fig.49	Example of deformed surface of strip drawn using planned flowers in different deformation emphasis scale ratios of R_{zx} and R_{zy} in forming passes of tube with $D = 60.5\text{mm}$, $t = 1.75\text{mm}$ and $\sigma_Y = 295\text{MPa}$ (View from the direction of Z-axis/bank(θ_B) = 0° , Y-axis/heading(θ_H) = 50° and X-axis/pitch(θ_P) = 30°)	103
Fig.50	Example of deformed surface of strip drawn using planned flowers in the bottom constant pass-line and downhill pass-line forming of tube with $D = 60.5\text{mm}$, $t = 1.75\text{mm}$ and $\sigma_Y = 295\text{MPa}$ (View from the direction of Z-axis/bank(θ_B) = 0° , Y-axis/heading(θ_H) = 50° and X-axis/pitch(θ_P) = 30°)	104
Fig.51	Computer graphic drawing of the 3-D deformed surface of strip drawn using planned flowers in the forming passes (View from the direction of Z-axis/bank(θ_B) = 0° , Y-axis/heading(θ_H) = 50° and X-axis/pitch(θ_P) = 40°)	107
Fig.52	3-D graphics drawing of longitudinal membrane strain increment $d\epsilon_z$, calculated by CADFORM system (View from the direction of Z-axis/bank(θ_B) = 0° , Y-axis/heading(θ_H) = 50° and X-axis/pitch(θ_P) = 40°)	108
Fig.53	3-D graphics drawing of lateral membrane strain increment $d\epsilon_x$, calculated by CADFORM system (View from the direction of Z-axis/bank(θ_B) = 0° , Y-axis/heading(θ_H) = 50° and X-axis/pitch(θ_P) = 40°)	109
Fig.54	3-D graphics drawing of longitudinal strain ϵ_z , calculated by CADFORM system (View from the direction of Z-axis/bank(θ_B) = 0° , Y-axis/heading(θ_H) = 50° and X-axis/pitch(θ_P) = 40°)	110
Fig.55	3-D graphics drawing of lateral strain ϵ_x , calculated by CADFORM system (View from the direction of Z-axis/bank(θ_B) = 0° , Y-axis/heading(θ_H) = 50° and X-axis/pitch(θ_P) = 40°)	111

Fig.56	3-D graphics drawing of longitudinal stress increment $d\sigma_z$, calculated by CADFORM system (View from the direction of Z-axis/bank(θ_B) = 0° , Y-axis/heading(θ_H) = 50° and X-axis/pitch(θ_P) = 40°)	112
Fig.57	3-D graphics drawing of lateral stress increment $d\sigma_x$, calculated by CADFORM system (View from the direction of Z-axis/bank(θ_B) = 0° , Y-axis/heading(θ_H) = 50° and X-axis/pitch(θ_P) = 40°)	113
Fig.58	3-D graphics drawing of longitudinal stress σ_z , calculated by CADFORM system (View from the direction of Z-axis/bank(θ_B) = 0° , Y-axis/heading(θ_H) = 50° and X-axis/pitch(θ_P) = 40°)	114
Fig.59	3-D graphics drawing of lateral stress σ_x , calculated by CADFORM system (View from the direction of Z-axis/bank(θ_B) = 0° , Y-axis/heading(θ_H) = 50° and X-axis/pitch(θ_P) = 40°)	115
Fig.60	3-D graphics drawing of equivalent stress $\bar{\sigma}$, calculated by CADFORM system (View from the direction of Z-axis/bank(θ_B) = 0° , Y-axis/heading(θ_H) = 50° and X-axis/pitch(θ_P) = 40°)	116
Fig.61	Schematic layout of the CBR forming pilot mill used in strain measurements	118
Fig.62	Position of strain gages pasted on strip surface	120
Fig.63	Variation of longitudinal measured surface strain	122
Fig.64	Occurrence of longitudinal strain peak due to deformation of strip in fin-pass roll forming	123
Fig.65	Comparison of calculated strains to measured strain in the longitudinal direction	124
Fig.66	Schematic layout of 4inch full cage roll forming type model mill installed at Yamanashi University	127
Fig.67	Drawing of planned flower with large D/t ratio at No.6 pass (No.1 fin-pass roll) by flower pattern A	128
Fig.68	Drawing of planned flowers with large D/t ratio in bottom constant pass-line forming by flower pattern B	129
Fig.69	Computer graphic drawing of 3-D deformed surface of strip drawn using planned flowers with D = 100.0mm and t = 1.0mm in bottom constant pass-line forming	133
Fig.70	3-D graphics drawing of longitudinal membrane strain increment $d\epsilon_z$ calculated by CADFORM system	134
Fig.71	3-D graphics drawing of lateral membrane strain increment $d\epsilon_x$ calculated by CADFORM system	135

Fig.72	3-D graphics drawing of longitudinal strain ϵ_z , calculated by CADFORM system	136
Fig.73	3-D graphics drawing of lateral strain ϵ_x , calculated by CADFORM system	137
Fig.74	3-D graphics drawing of longitudinal stress increment $d\sigma_z$, calculated by CADFORM system	138
Fig.75	3-D graphics drawing of lateral stress increment $d\sigma_x$, calculated by CADFORM system	139
Fig.76	3-D graphics drawing of longitudinal stress σ_z , calculated by CADFORM system	140
Fig.77	3-D graphics drawing of lateral stress σ_x , calculated by CADFORM system	141
Fig.78	3-D graphics drawing of equivalent stress $\bar{\sigma}$, calculated by CADFORM system	142
Fig.79	Variation of calculated longitudinal membrane strain increment and strain at strip edge in forming of tube with D/t ratio 100	146
Fig.80	Variation of calculated longitudinal membrane stress increment, stress and equivalent stress at strip edge in forming of tube with D/t ratio 100	146
Fig.81	Variation of maximum longitudinal membrane strain at edge of strip between each pass obtained by Kiuchi	147
Fig.82	Lateral distribution of calculated longitudinal strain increment and strain at strip edge at pass No.5	148
Fig.83	Lateral distribution of calculated longitudinal stress increment and stress at strip edge at pass No.5	148
Fig.84	Comparison of theoretical longitudinal strain increments using stress and strain analyses from Model-1 and -2	151
Fig.85	Comparison of theoretical longitudinal strains using stress and strain analyses from Model-1 and -2	151
Fig.86	Comparison of calculated longitudinal stress increments using stress and strain analyses from Model-1 and -2	152
Fig.87	Comparison of calculated longitudinal stresses using stress and strain analyses from Model-1 and -2	152
Fig.88	Comparison of theoretical longitudinal stresses with calculated buckling stresses for the case of N = 1	156
Fig.89	Comparison of theoretical longitudinal stresses with calculated buckling stresses for the case of N = 4	156

Fig.90	Pass-line conditions for bottom constant and downhill forming	157
Fig 91	Effect of downhill forming on longitudinal strain increment calculated by Model-2	158
Fig 92	Effect of downhill forming on longitudinal strain calculated by the Model-2	158
Fig 93	Effect of downhill forming on longitudinal stress increment calculated by the Model-2	159
Fig 94	Effect of downhill forming on longitudinal stress calculated by the Model-2	159
Fig.95	Computer graphic drawing of the 3-D deformed surface of strip in the case of twenty divided elements calculated by Model-2	162
Fig 96	3-D graphic drawing of longitudinal membrane strain ϵ_z , in the case of twenty divided elements calculated by Model-2	163
Fig 97	3-D graphic drawing of longitudinal membrane stress σ_z , in the case of twenty divided elements calculated by Model-2	164
Fig.98	Centre bending flower pattern by computer graphic drawing	168
Fig.99	Computer graphic drawing of 3-D deformed surface of the strip in centre bending flower pattern	169
Fig.100	3-D graphic drawings of calculated longitudinal membrane strain ϵ_z , for centre bending flower pattern	170
Fig.101	3-D graphic drawings of calculated longitudinal membrane stress σ_z , for centre bending flower pattern	171
Fig.102	Edge bending flower pattern by computer graphic drawing	172
Fig.103	Computer graphic drawing of 3-D deformed surface of the strip, for edge bending flower pattern	173
Fig.104	3-D graphic drawings of calculated longitudinal membrane strain ϵ_z , for edge bending flower pattern	174
Fig.105	3-D graphic drawings of calculated longitudinal membrane stress σ_z , for edge bending flower pattern	175
Fig.106	Circular bending flower pattern by computer graphic drawing	176
Fig.107	Computer graphic drawing of 3-D deformed surface of the strip, for circular bending flower pattern	177
Fig.108	3-D graphic drawings of calculated longitudinal membrane strain ϵ_z , for circular bending flower pattern	178

Fig.109	3-D graphic drawings of calculated longitudinal membrane stress σ_z , for circular bending flower pattern	179
Fig.110	Comparison of longitudinal membrane strain ϵ_z , employing three different forming flower patterns	180
Fig.111	Comparison of longitudinal membrane stress σ_z , employing three different forming flower patterns	180
Fig.112	Comparison of microstructure between HISTORY and conventional ERW steel tubes	183
Fig.113	Comparison of mechanical properties between HISTORY and conventional ERW steel tubes	184
Fig.114	Examples of calculated results in the 6inch CBR forming mill of The HISTORY mill	185
Fig.115	Variation of longitudinal membrane stress σ_z	186

List of Tables

Table 1	Stresses and strains at pass No.4 calculated by Models-1 and -2	150
Table 2	Calculation of theoretical elastic and plastic buckling stresses for the case of $N = 1$	155
Table 3	Calculation of theoretical elastic and plastic buckling stresses for the case of $N = 4$	155
Table 4	Comparison of stress and strain between the divided elements ten and twenty in a half width of strip	161

List of Photographs

Photo.1	Appearance of the 26in ERW full cage roll forming mill at the Chita works of Kawasaki Steel Corporation	23
Photo.2	Appearance of the CBR forming mill for manufacturing ERW stainless steel tube at the Chita works	23
Photo.3	Appearance of edge buckling in actual production of thin walled pipe, with $D = 609.6\text{mm}$ by $t = 6.0\text{mm}$, $D/t = 100$	24
Photo.4	Computer graphic display example of the planned flower pattern A	59
Photo.5	Computer graphic display example of the planned flower pattern B	59
Photo.6	Appearance of edge buckling in actual production of thin walled pipe with $D = 146.0\text{mm}$, $t = 2.0\text{mm}$ and $\sigma_Y = 730\text{MPa}$	93
Photo.7	Examples of 3-D graphics displaying calculated longitudinal stress and strain by the CADFORM system in forming passes of the tube with $D = 100\text{mm}$, $t = 1.0\text{mm}$ and $\sigma_Y = 340\text{MPa}$	100
Photo.8	Appearance of the CBR forming pilot mill used in the strain measurements	118
Photo.9	Appearance of the strip deformation in cage roll forming stage of the CBR forming pilot mill	119
Photo.10	Appearance of strain gages pasted on strip surface at the entry side of the edge bend rolls	120
Photo.11	Appearance of thin walled tube formed in cage roll forming zone	127
Photo.12	Appearance of the HISTORY mill	182

Chapter 1. Tube-making by the Cold Roll Forming Process

1.1 Introduction

Cold roll-forming is a continuous process of progressively bending metal strip without changing the material thickness, into shapes of essentially constant cross-section, using successive sets of rotating tools called "Forming Rolls". As such, it provides a very useful sheet metal (strip) forming process, capable of consistently and accurately producing a comprehensive range of profiles in a wide range of ferrous and non-ferrous metals, with little restriction on length. Recently, demand for cold roll-formed sections has increased.

Fig.1 shows a schematic view of the cold roll-forming process for producing tube. The strip is passed through a series of rolls which progressively bend it to the required section geometry. Rolls are set on horizontal axes and vertical axes as shown in the figure.

Cold roll-formed sections have been used in wide areas of the construction industry, the automobile industry, the oil industry and the housing industry due to their particular features, i.e. high strength-to-weight ratio, high productivity, high economic production, large overall length, high dimensional accuracy and high quality of surface texture. These sections have also found application in the manufacture of a wide variety of consumer goods.

Fig.2 shows typical shapes of sections produced by the cold roll-forming process. The cold roll-forming process produces a wide range of products with complicated cross-sectional shapes. In recent years, the importance of cold roll-forming has continued to grow with the increasing needs for its products.

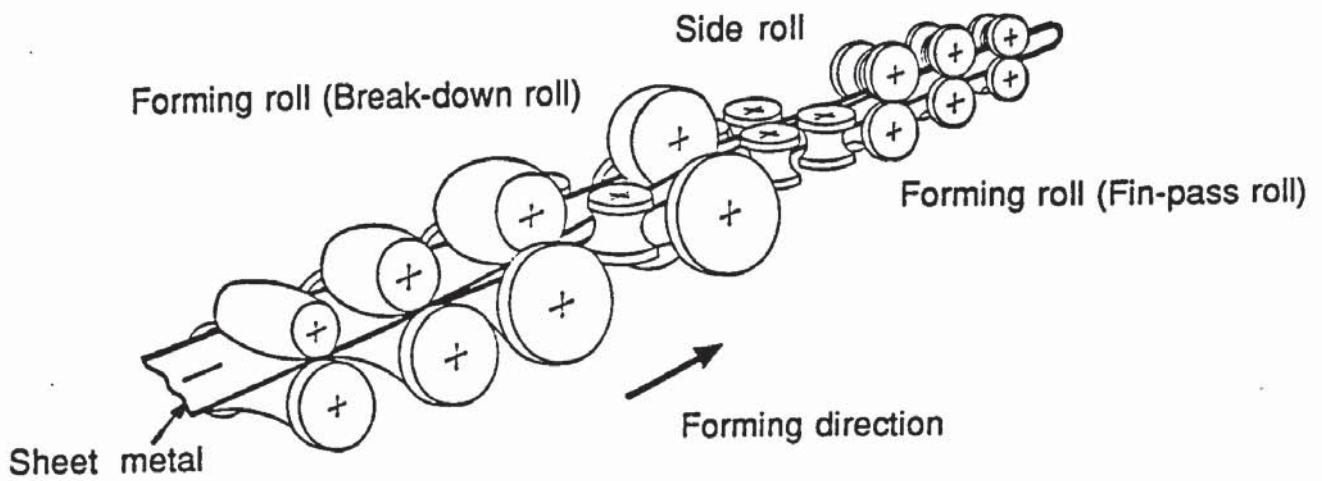


Fig.1 Schematic view of the cold roll-forming process for ERW(Electric Resistance Welded) tube-making

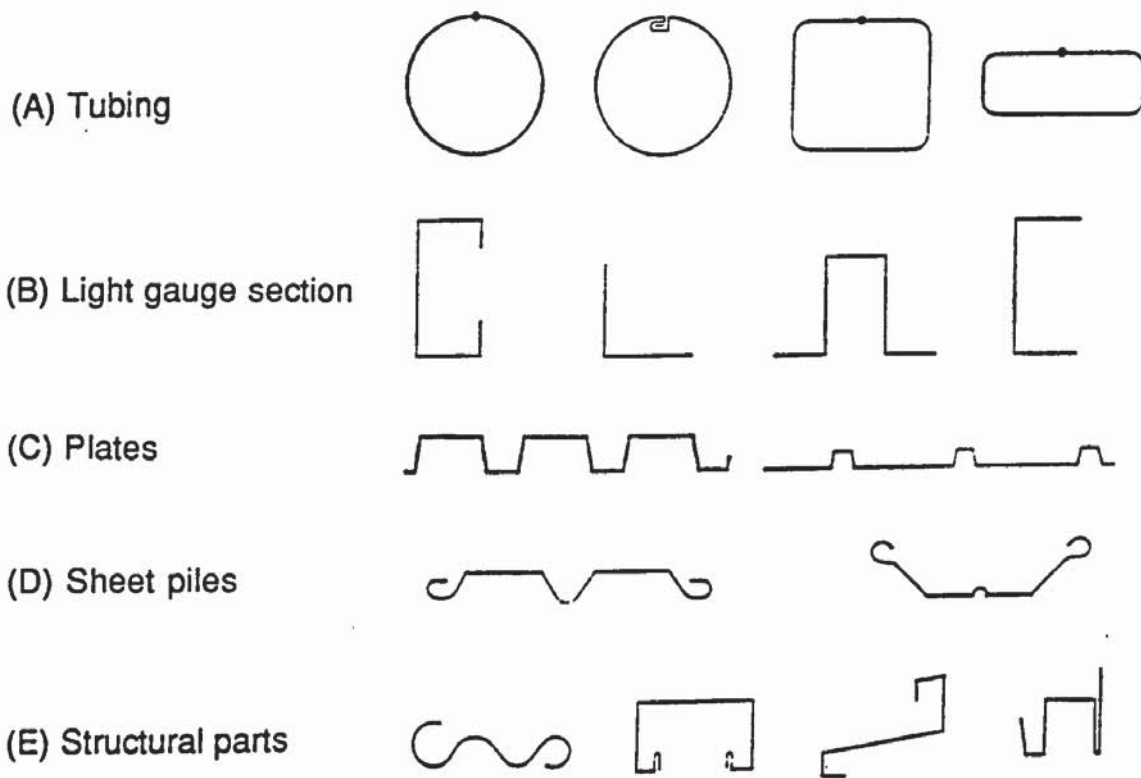


Fig.2 Typical shapes of sections produced by the cold roll-forming process

1.2 Production of ERW tube and pipe

Since the production of ERW (Electric Resistance Welded) tube and pipe began in the beginning of the 1900's, its technology has been developed by using the cold roll-forming process and great progress has been made together with the development and improvement of welding techniques and the technique of rolling strip material. In particular, remarkable progress has been made during the last twenty years. Fig.3 shows the layout of a typical tube-making process using cold roll-forming and high frequency electric resistance welding.

Because of their high reliability and low cost, ERW tube and pipe have also been used in fields such as the oil industry, the automobile industry and heat exchanger and chemical plant, instead of seamless tube and pipe.

Fig.4 shows the variation of the Japanese annual production¹ of tubes and pipes for ERW, seamless, press brake (press brake formed and expanded) and CBW (Continuous Butt Welded) in the decade from 1986. Total production tends to reduce gradually each year. This tendency is especially remarkable in seamless products. However production of ERW products increased to more than five million tons a year in 1990 and after 1990 production of ERW also tended to slightly reduce, however, it still contributes half of the total production of tubes and pipes. This means that greater importance has been attached to ERW products, and their uses have expanded.

ERW tube and pipe mills can produce tubes and pipes with the outside diameter D , up to 660.4 mm (26in), the wall-thickness t , up to 22 mm (0.866in), the D/t ratio from 4 to 125 and the yield strength σ_Y , as-rolled up to X-80 grade (minimum $\sigma_Y = 550\text{MPa}$) specified by API (American Petroleum Institute). Forming speed can approach 200m/min in the smaller diameter ERW tube mills.

Main tubular products consist of line pipes, OCTG (Oil Country Tubular Goods), mechanical and structural tubing, structural pipes, boiler and heat

exchanger tubes, and gas and water transportation pipes.

In recent years, automobile companies have actively studied an application of the hydroformed tube to sub-frame parts and body frame parts of automobiles. ERW mechanical*, tubes with thin wall gauge, have been used for tube hydroforming and it is predicted that the amount of ERW mechanical tubes used to hydroformed tube will be greatly increased in several years.

According to the demand of tubes and pipes mentioned above, it has become apparent that ERW tubes and pipes have tended towards small batch, multi-kind production, higher valued added/higher quality products, shorter delivery terms, higher productivity and flexible forming systems. Such systems can reduce the size changing time, the number of operators and can also expand the available size range.

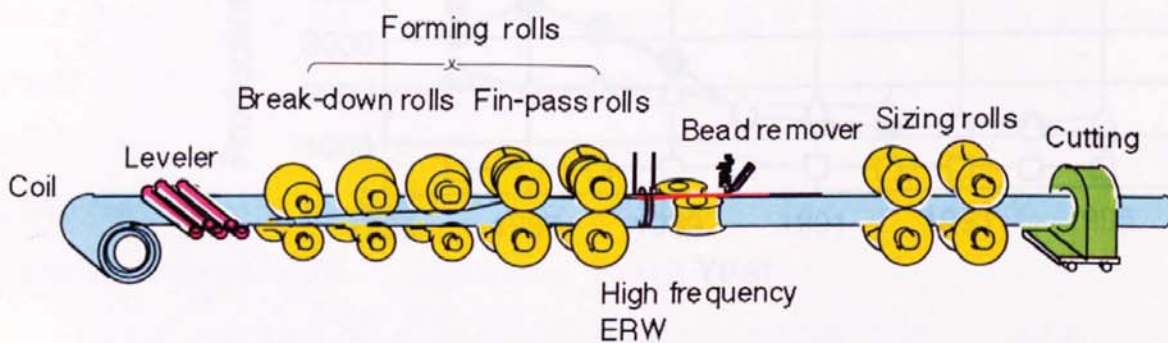


Fig.3 Typical layout of tube-making process using cold roll-forming and high frequency electric resistance welding

*mechanical tube: Tube for machine structural purposes

1.3 Background of this research

Research and development programs were conducted using production experience and experimental data. The requirement for an understanding of the forming process by theoretical analysis has been increased through the need of research and development in order to reduce the number of experiments employing trial and error and to get an estimate of the appropriate forming schedules prior to experimental work.

Although some theoretical studies on the roll-forming process have already been done in response to these needs, they have not yet reached a

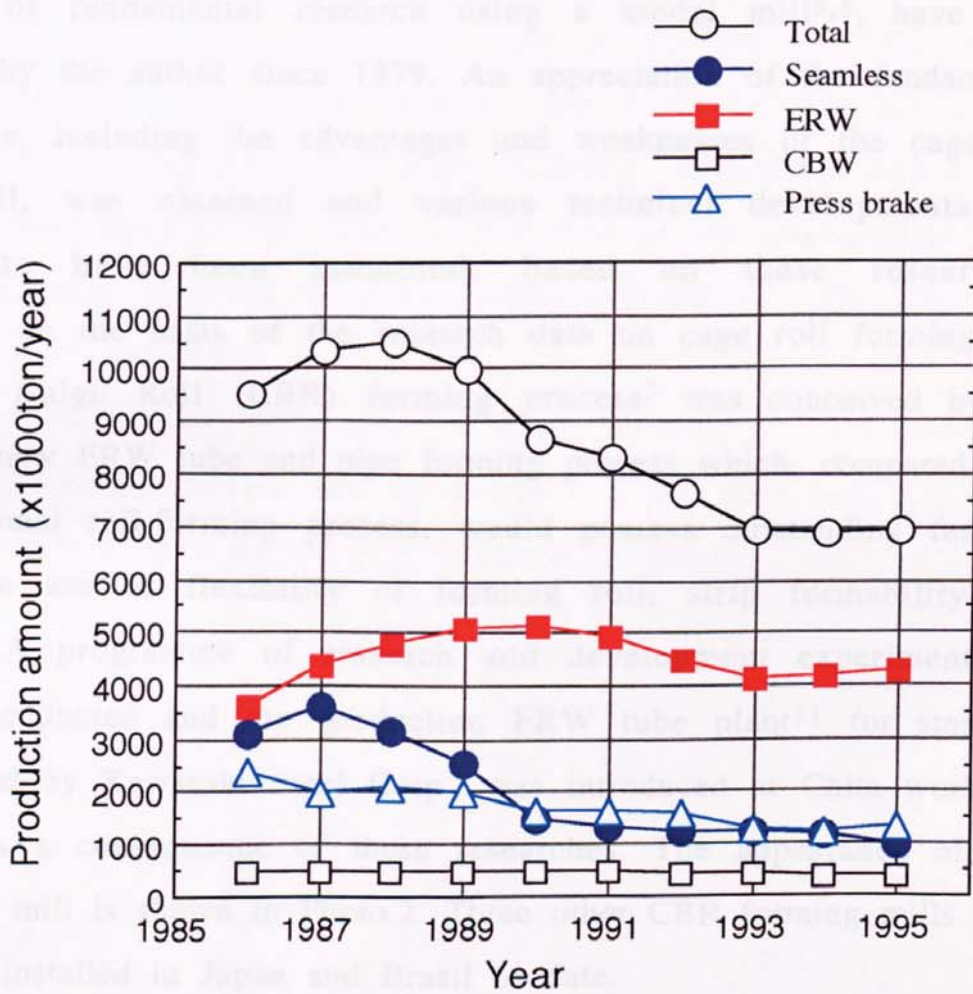


Fig.4 Variation of annual production of tubes and pipes in Japan

1.3 Background of this research

Kawasaki Steel Corporation introduced the 26in ERW full cage roll forming mill² (IHI-Yoder) in Japan in 1978. Its appearance is shown in Photo.1. In order to establish this cage roll forming technology, experimental investigations using the actual production mill^{3,4} and a programme of fundamental research using a model mill^{5,6}, have been carried out by the author since 1979. An appreciation of the fundamental characteristics, including the advantages and weaknesses of the cage roll forming mill, was obtained and various technical developments and improvements have been promoted, based on these researches. Furthermore, on the basis of the research data on cage roll forming, the Chance-free Bulge Roll (CBR) forming process⁷ was conceived by the author as a new ERW tube and pipe forming process which, compared with the conventional roll-forming process, would possess outstanding features including the use of flexibility of forming roll, strip formability and weldability. A programme of research and development experiments⁸⁻¹⁰ have been conducted and the production ERW tube plant¹¹ for stainless steel, designed by Kawasaki Steel Corp., was introduced at Chita works in June 1990 as a consequence of these researches. The appearance of this CBR forming mill is shown in Photo.2. Three other CBR forming mills have already been installed in Japan and Brazil to date.

These research and development programmes were conducted using production experience and experimental data. The requirement for an understanding of the forming process by theoretical analysis has been increased through this kind of research and development. This is in order to reduce the number of experiments employing trial and error and to get an estimate of the appropriate forming schedules prior to experimental work.

Although some theoretical studies on the roll-forming process have already been done in response to these needs, they have not yet reached a

stage at which the occurrence of shape defects in the products can be evaluated. In the field of CAD/CAM, the evaluation system of the flower pattern designed by CAD has also not been completed.

Most CAD systems, which have taken account of the basic elastic-plastic theory, can only draw the flower pattern or the roll profiles based on the data and knowledge which has been stored through past experience. This research, therefore, aims at creating a CAD system, including theoretical analyses, which can evaluate the stress-strain conditions for the occurrence of edge buckling, commonly called "edge wave" that take place at the edges of the strip in the roll-forming stages. In particular, edge buckling is a most serious problem in the forming of thin walled tube and pipe.

Fig.5 illustrates the occurrence of edge buckling in tube-making by the cold roll-forming process and an example of the edge buckling in the actual production of thin walled pipe is shown in Photo.3.

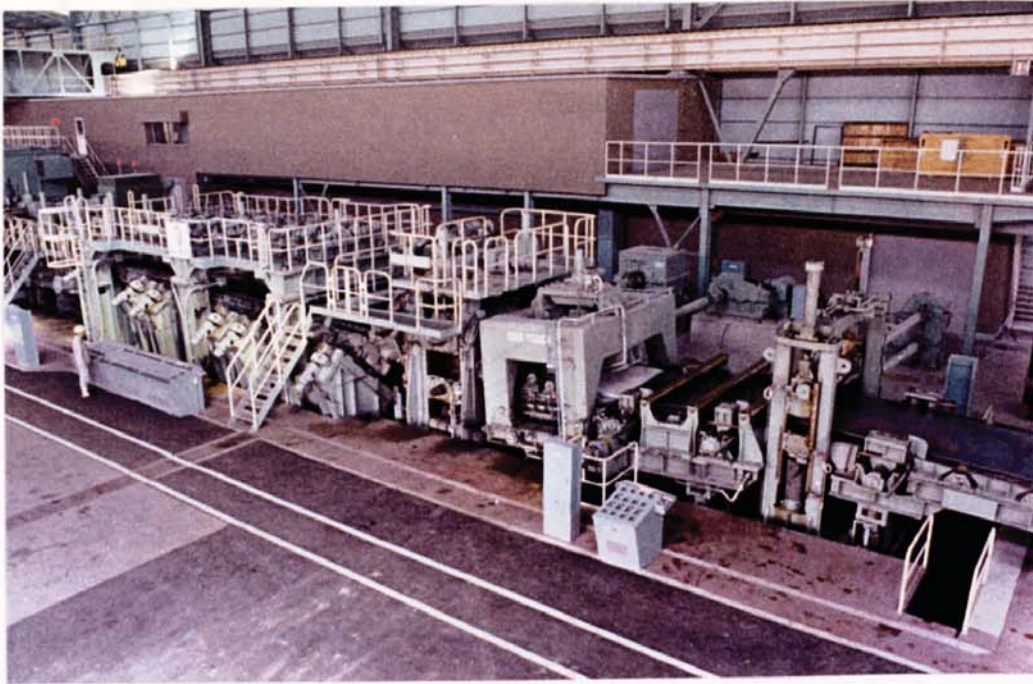


Photo.1 Appearance of the 26in ERW full cage roll forming mill at the Chita works of Kawasaki Steel Corporation

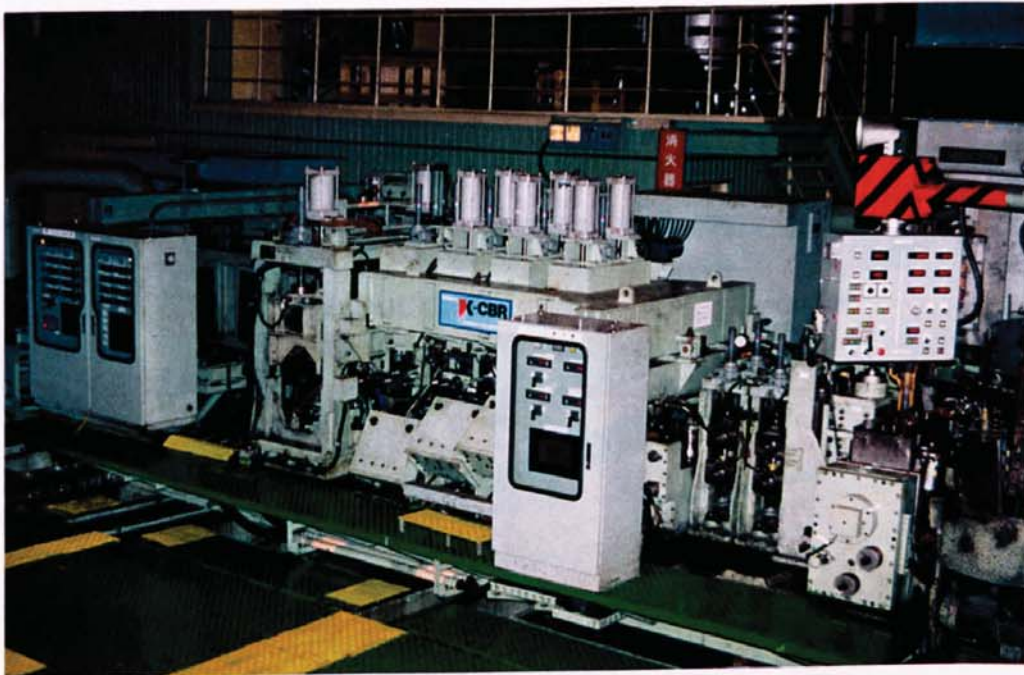


Photo.2 Appearance of the CBR forming mill for manufacturing ERW stainless steel tube at the Chita works

Photo.3 Appearance of edge burking in actual production of thin-walled pipe with $D = 819 \text{ mm}$ by $t = 6.0 \text{ mm}$, $L/D = 100$

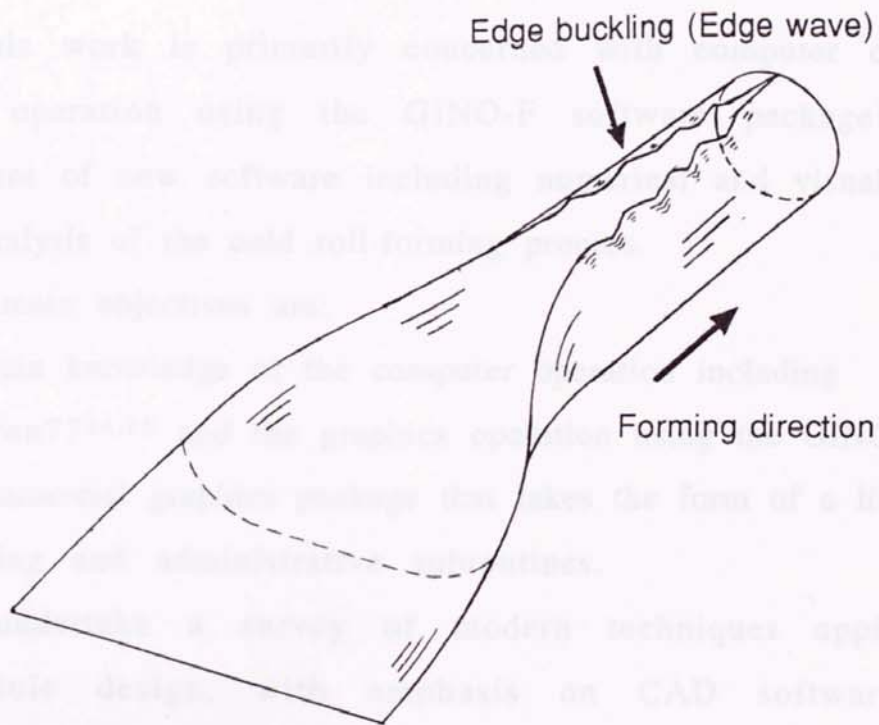


Fig.5 Illustration of occurrence of edge buckling in tube-making by cold roll-forming process

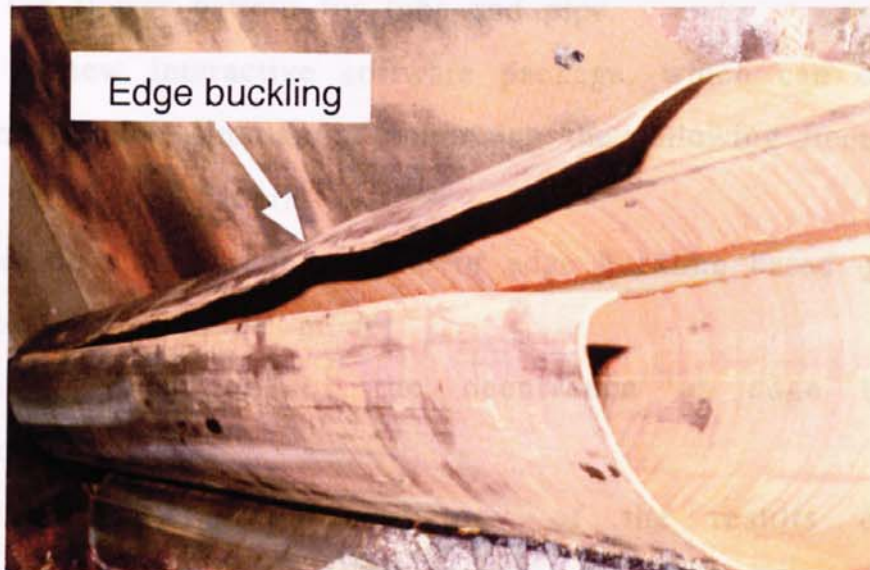


Photo.3 Appearance of edge buckling in actual production of thin walled pipe with $D = 609.6\text{mm}$ by $t = 6.0\text{mm}$, $D/t = 100$

1.4 Research objectives

This work is primarily concerned with computer operation and graphics operation using the GINO-F software package^{12,13} and the development of new software including numerical and visual programmes for the analysis of the cold roll-forming process.

The main objectives are:

- (1) To gain knowledge of the computer operation including Fortran77^{14,15} and the graphics operation using the GINO-F, which is a commercial graphics package that takes the form of a library of drawing and administrative subroutines.
- (2) To undertake a survey of modern techniques applied to roll schedule design, with emphasis on CAD softwares for the flower pattern and numerical analyses of the roll-forming process.
- (3) To attempt to apply the existing CAD/CAM system, "ROLFOM" developed by previous research students at Aston University, to the design of the flower pattern for tube and pipe.
- (4) To create a new interactive software package, which can carry out a consistent forming simulation comprising the following items:
 - (a) CAD of the flower pattern
 - (b) Elastic-plastic stress-strain analysis of edge buckling based on a geometrical deformation model
 - (c) Theoretical evaluation of the occurrence of edge buckling in the forming stages
 - (d) Three-dimensional graphics display of the results obtained by this new interactive package.
- (5) To verify the results of the theoretical analysis by the experimental data
- (6) To investigate effects of the forming factors such as the flower pattern, the pass height condition, the material properties, the tube

stress-strain in the forming stages and the occurrence of edge buckling.

Chapter 2. Roll-Forming Process of ERW Tube- and Pipe-making

2.1 Design of forming rolls and mill for ERW tube- and pipe-making

The roll-forming technology for tube and pipe consists of two components, (1) the forming sequence called the "flower pattern", which determines how the strip is bent ("soft" technology), and (2) the equipment for forming the strip to the shape of the planned flower pattern ("hard" technology).

Fig.6 shows four typical flower patterns for : (A) Edge bending, (B) Centre bending, (C) Circular bending and (D) W-bending. Usually, a combined flower pattern will be used in production. The design of the flower pattern and expert knowledge are very important key factors. The W-bending flower pattern, in which the edge portion of the strip is bent, whilst the centre portion of the strip is reverse-bent, has often been used in the production of heavy walled tubes in recent years.

The new flower pattern shown in Fig.7, which is characterised by bulge-bending and bend-unbending in the fin-pass (the term fin-pass is used throughout to denote the finishing passes) roll stands, has been developed in the previously mentioned CBR forming process⁷.

On the other hand, the design of the forming mill including the design of roll construction, is also a very significant matter. This is not only to obtain the appropriate forming of the strip but also to provide a flexibility of forming roll profiles that enables the products to be manufactured in a wide range of sizes.

Fig.8 shows the typical layout of a forming mill for the production of ERW tube and pipe. The "break-down roll forming mill", also called "the step forming mill", is a common process and has been introduced mainly in small or medium diameter tube production.

The "Cage roll forming mill", also called the "natural forming mill", was originally developed by Yoder¹⁶ and the Torrance Machinery and

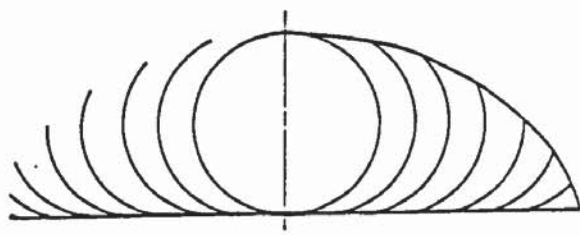
Engineering Inc.¹⁷ in the USA in the 1960's and it has been introduced mainly in large diameter pipe production. This mill enables the pipes to be manufactured in a wide range of size by the common use of some rolls without roll-changing. Fig.9 shows a schematic view of the forming of the strip in the main forming stages (passes) such as break-down roll-forming, cage roll forming, and fin-pass roll forming which is the finishing stage where the formed strip is reduced in the circumferential direction.

2.2 Newly developed ERW tube- and pipe-making mills

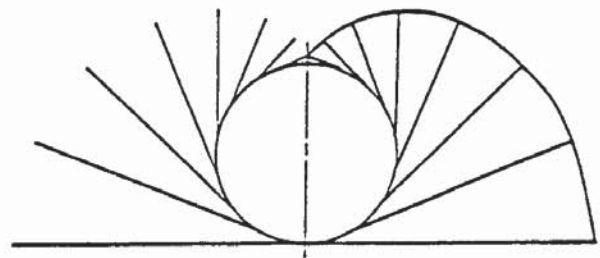
Recently, flexible forming mills have been developed for the principal purpose of realising forming roll flexibility in order to achieve small-batch multi-kind production. Typical new ERW tube and pipe forming mills developed currently may be listed as follows:

(1) Lineal Forming mill	Mannesmann Demag Germany	1982 ¹⁸
(2) CTA Forming mill	Voest-Alpine Austria	1987 ¹⁹
(3) FF mill	Nakata Japan	1987 ²⁰
(4) Roll-less Forming mill	Nisshin Seiko Japan	1990 ²¹
(5) CBR Forming mill	Kawasaki Steel Japan	1990 ¹¹

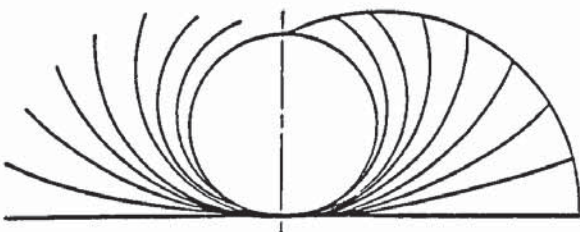
An automated and computerised 16in ERW pipe mill²² was introduced at Nagoya works of Nippon Steel Corp. in 1987. Furthermore, Kawasaki Steel Corporation has recently developed a new manufacturing process for the welded tube, termed "HISTORY", that can recreate material property of tube with high strength and excellent formability.



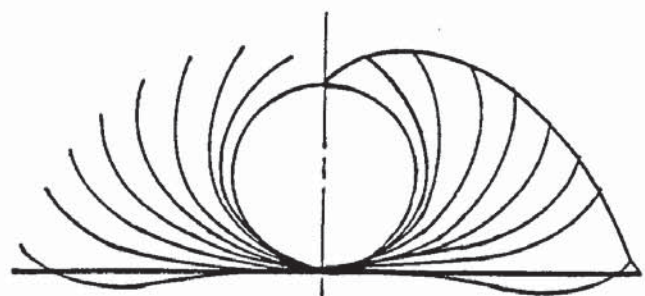
(A) Edge bend forming



(B) Centre bend forming

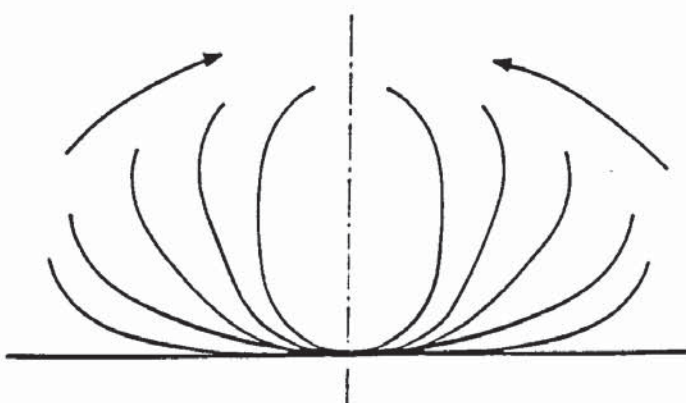


(C) Circular bend forming

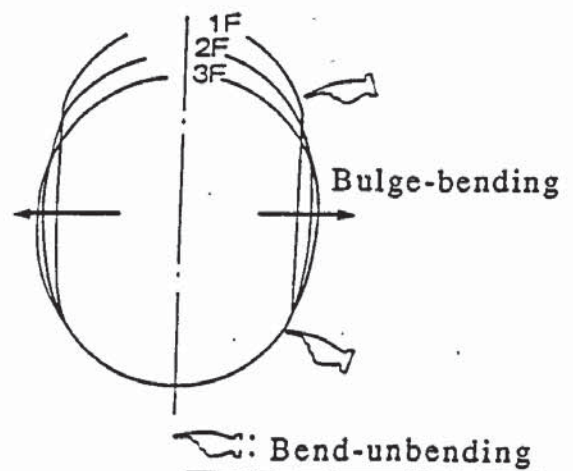


(D) W-bend forming

Fig.6 Typical flower pattern used in ERW tube- and pipe-making

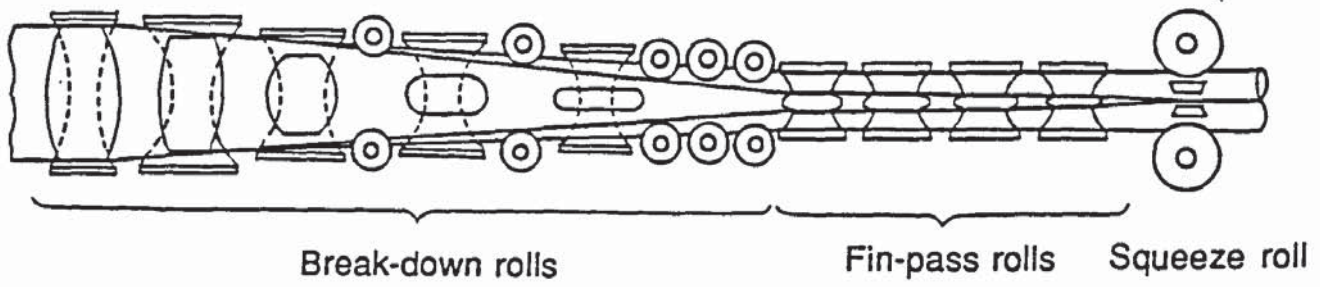


(A) Cage roll forming

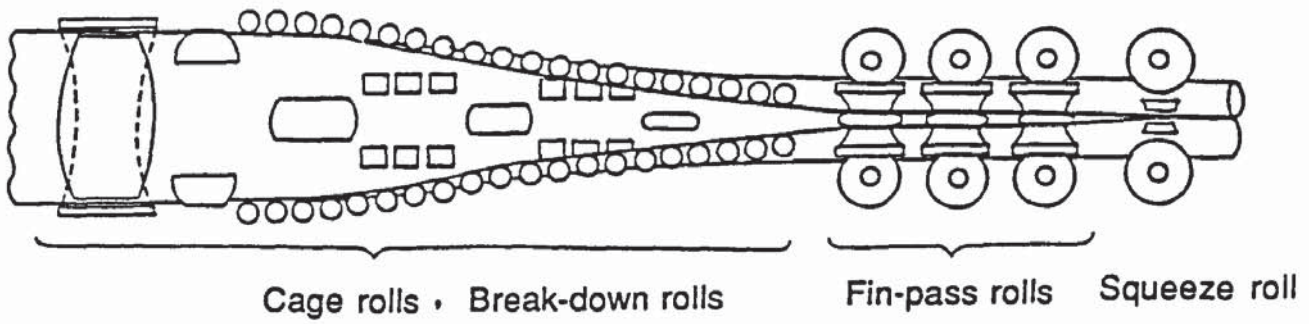


(B) Fin-pass roll forming

Fig.7 New flower patterns developed in the CBR forming process⁷

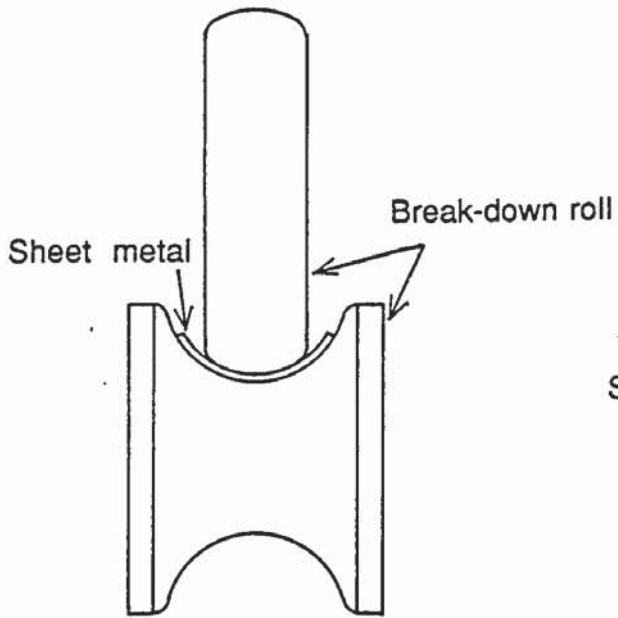


(a) Break-down roll forming mill(process)

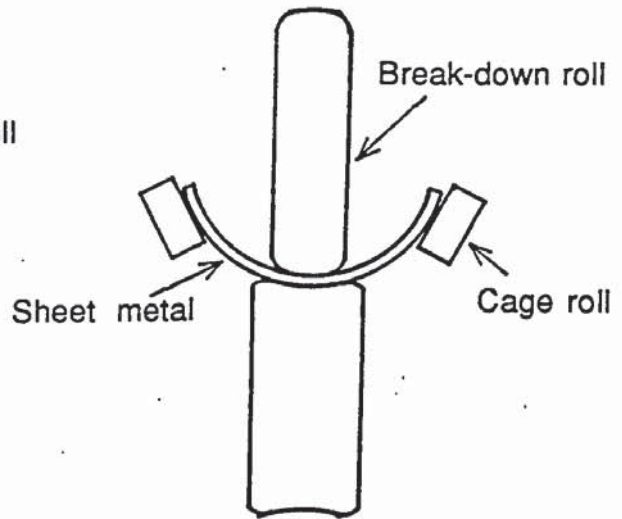


(b) Cage roll forming mill(process)

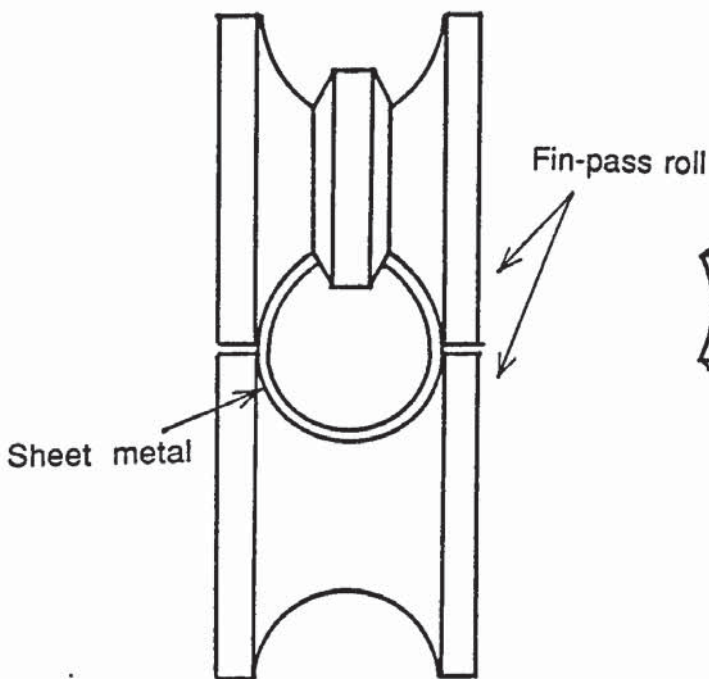
Fig.8 Typical layout of forming mill for production of ERW tube and pipe



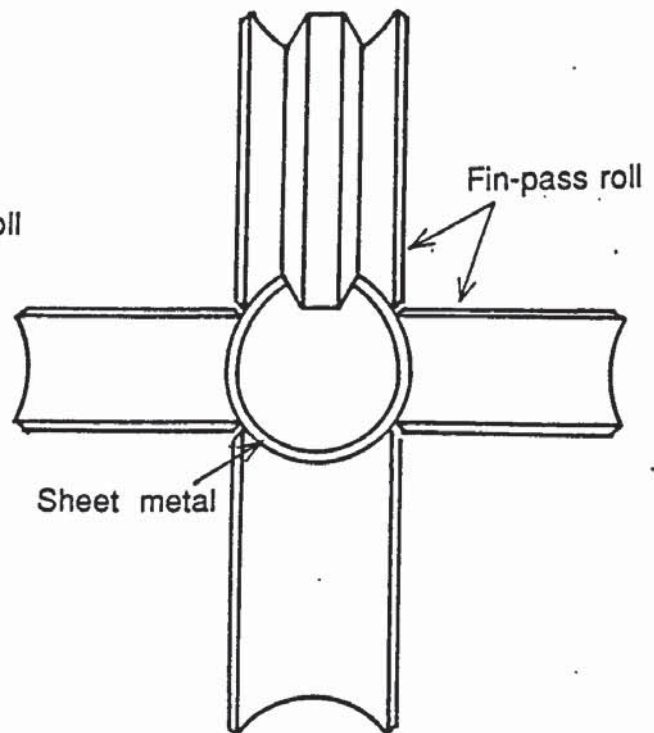
(a) Break-down roll forming



(b) Cage roll forming



(c) Two rolls type fin-pass roll forming



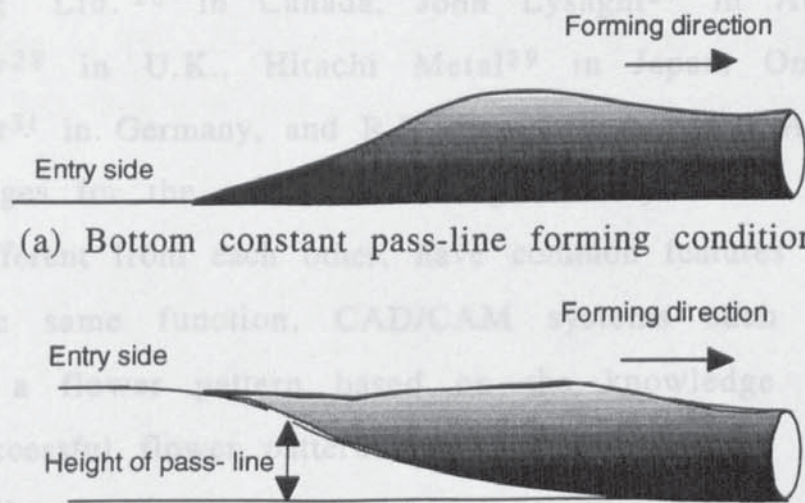
(d) Four rolls type fin-pass roll forming

Fig.9 Schematic view of forming of sheet metal in major forming passes

2.3 Pass-line conditions for ERW tube- and pipe-making

3.1 CAD/CAM system

In ERW tube and pipe manufacturing, the bottom constant pass-line condition is generally applied, as shown in Fig.10(a). However, edge buckling easily occurs in the case of large diameter thin-walled tube and pipe. The trace length of the strip is the three dimensional forming pass length which indicates the space trace of each strip part in the forming. In the cold roll-forming of strip for tube- and pipe-making, the trace length of the strip edge becomes larger than that of the strip centre in the middle forming stage, thus the trace length of the strip edge is decreased gradually, closing to the trace length of the strip centre after the middle forming stage. In the downstream forming stages, the edge portion of the strip is subjected to a compressive stress condition due to the shrinkage of stretched edge. Due to this compression, edge buckling easily occurs in the forming of thin walled tube and pipe. Thus, the downhill pass-line forming condition is applied in the case of manufacturing thin walled tube and pipe, to decrease the compression at the strip edge, due to the difference of trace length between the strip edge and centre. The height of the strip centre position is gradually decreased in advance of the forming in the downhill pass-line forming condition as shown in Fig.10(b).



(a) Bottom constant pass-line forming condition

(b) Downhill pass-line forming condition

Fig.10 Pass-line conditions for ERW tube- and pipe-making

Chapter 3. Computer Aids in Cold Roll-Forming

3.1 CAD/CAM system

The conventional design and manufacture of forming rolls depended on the individual skill of the cold forming roll designer, which was normally based on the experience and knowledge gained from previous work. There was no universally recognized scientific design theory which could provide guiding principles. The roll schedule design was normally a trial and error procedure and it was not efficient.

With the advent and progress of computer technology, computer aided design (CAD) and computer aided manufacturing (CAM) have improved design techniques. CAD/CAM systems or packages for cold roll-forming, based on some geometrical considerations, including the basic bending theory and primitive design rules, have now been devised.

There are a number of examples of CAD/CAM software packages which have been developed for the cold roll-forming industry, such as the package developed by Rhodes²³ for the Machine Tool Industry Research Association. There are also publications describing the systems in use in other countries, for example the programme developed by Industrie Secco²⁴ in Italy and packages devised by ROLL DATA²⁵ in the USA, Delta Engineering Ltd.²⁶ in Canada, John Lysaght²⁷ in Australia, Aston University²⁸ in U.K., Hitachi Metal²⁹ in Japan, Ona³⁰ in Japan, A.Sedlmaier³¹ in Germany, and R.Baranowski³² in the USA. All are tailor-made packages for the cold roll-forming industry. These CAD systems, although different from each other, have common features and essentially perform the same function. CAD/CAM systems such as these can recommend a flower pattern based on the knowledge obtained from previous successful flower patterns.

Generally, however, all the decisions involved in flower pattern design will be made by the designer without substantial assistance from the computer; the flower pattern designed by the previously mentioned

CAD/CAM systems is not based on a theoretical evaluation of the forming stages. However, there is no doubt that the application of these systems has resulted in the reduction of the designers' workload, shortened lead times, reduced error and increased efficiency.

3.2 Theoretical analysis of cold roll-forming

3.2.1 Minimum energy method

Experimental investigations and fundamental studies of cold roll-forming have been rigorously carried forward by a number of researchers such as Masuda et al.³³, Sarantidis et al.³⁴, Suzuki and Kiuchi³⁵, Kiuchi and Shintani³⁶, Jimma and Ona³⁷, Nakajima and Mizutani³⁸, Kato and Saito³⁹, Onoda and Toyooka⁶, Kuriyama and Adaka⁴⁰, Kasuga and Jimma⁴¹, Jimma and Morimoto⁴², and Kokado and Onoda⁴³. These investigations and studies were carried out under the four main subject areas as follows:

- (1) Fundamental studies of cold roll-forming.
- (2) Investigations of optimum roll pass schedules.
- (3) Investigations of specific sectional problems, including the cause of their occurrence and the method of their suppression.
- (4) Studies of the development of new forming processes.

As shown in Fig.11, a large number of factors are involved in cold roll-forming and they can make the deformation process very complex.

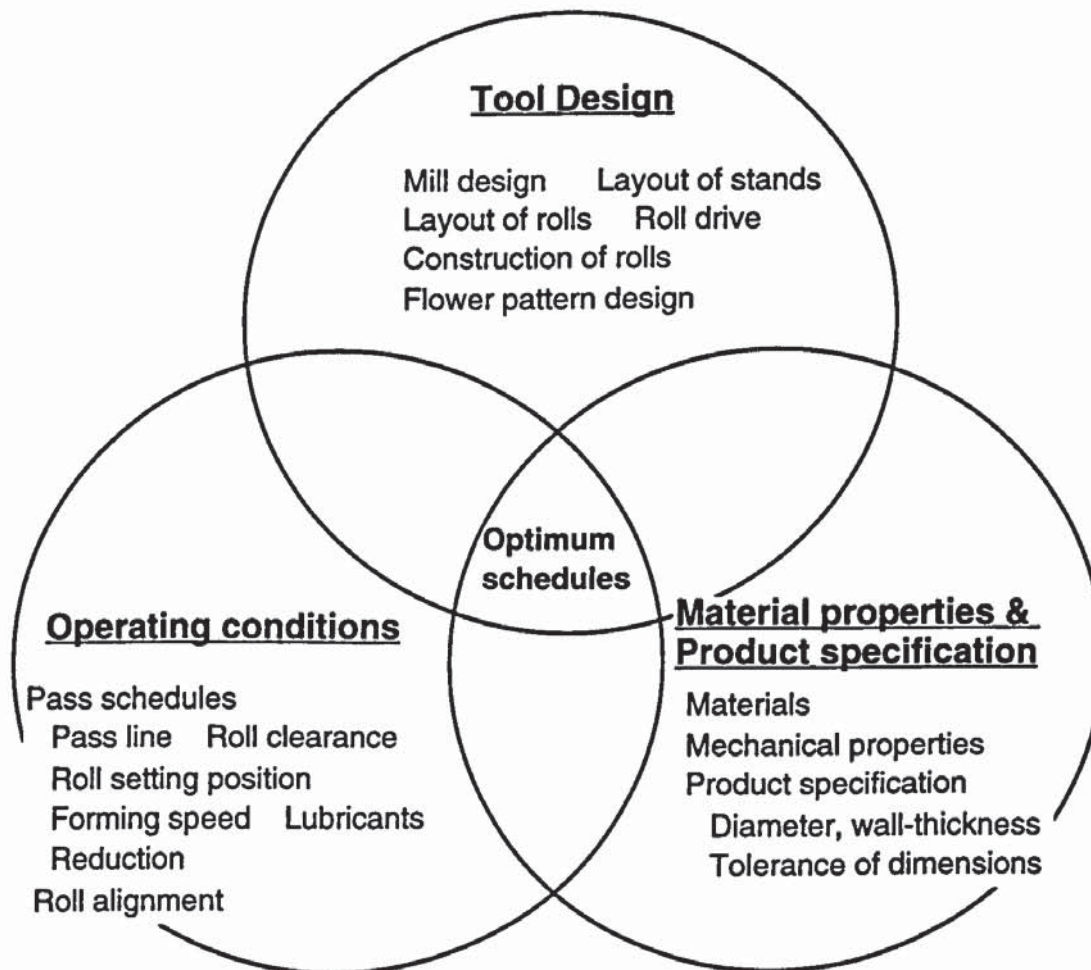


Fig.11 Main factors defining cold roll-forming process and their relationships

Cold roll-forming, therefore, becomes an extremely complex three-dimensional deformation process with elastic-plastic deformation. Thus, the mathematical model of cold roll-forming is a problematic exercise. The creation of a model, which can consistently represent the total deformation of the strip, is also very difficult.

There are several major factors that cause difficulty in the theoretical analysis of cold roll-forming. These reasons are:

- (1) The deformed strip is a complex three-dimensional body.
- (2) It is essential to deal with the analysis as elastic-plastic deformation without ignoring the elastic deformation.
- (3) Boundary conditions are not defined and the shape of material between passes is not known.
- (4) The forces acting on the strip cannot be quantified.
- (5) It is necessary to consider work-hardening, because the direction of strain is reversed many times.
- (6) The deformation strain is small, but high accuracy of the analysis is required.

The necessity of a comprehensive design theory for roll pass schedules, including the flower pattern, is clearly required. Thus the introduction of scientific principles will help to reduce the requirement for trial and error procedures which have traditionally been applied.

The most comprehensive theoretical analysis of cold roll-forming for the forming of tubes and other sections has been performed by Kiuchi and his collaborators^{44,45}. He realised that the first step in modelling the roll-forming process was in predicting the shape of the strip between successive stages. The shape function, $S(x)$, as shown in Fig.12, represents the flow pattern of each part of the strip between passes, where the flow pattern was given by the following equation:

$$S(x) = \sin\left[\frac{\pi}{2} \left(\frac{x}{L_s}\right)^n\right] \quad (1)$$

where,

x = the distance of some position between the (i)th and the (i+1)th stage

L_s = the distance between the neighbouring stages

n = an unknown value decided by the minimum energy method

In this analysis the sheet strip was divided into small elements. Kiuchi then devised an expression for the membrane strain in each element based on simple trigonometry, and the calculated bending strain by using the sheet curvature along the X (longitudinal) and Y (lateral) axes. The magnitude of the strain in each element was evaluated by summation of these strains. The constitutive equations for the plastic stress-strain relationship were adopted from a technique derived by Yamada⁴⁶, by inverting the Prandtl-Reuss equations.

Some assumptions were applied in order to simplify the modelling, as listed below:

- (1) The front and rear cross-sectional profiles are always included in planes which are perpendicular to the X-axis and which can traverse along the X-axis.
- (2) The summation of stress in the X direction in each element is constant or equal to zero at each stage.
- (3) The directions of principal strain are coincident with the X- and Y-axes, and the plane strain condition can be applied.
- (4) The shear strain and shear stress are ignored.
- (5) The stress σ_z , in the wall-thickness direction, is negligible and equal to zero

The variable n in the equation (1) is then adjusted until the power of deformation is minimised as shown in Fig.13. By this simulation method a series of forming processes for welded tubes was investigated and the effects of forming conditions on the deformation characteristics of the strip analysed. Kiuchi then went on to develop the optimum flower pattern for tubes by either equalizing the longitudinal membrane strain of the edge of the strip, or the total power at each pass, using results from simulation.⁴⁷

Fig.14 shows simulated results of the variation of the longitudinal membrane strain occurring at different lateral positions. Here the strain behaviour, with increasing and decreasing strain, that caused the strain peak just before each stand, was calculated consecutively.

Kiuchi's work can be said to be important and innovative because it is, to date, probably the most comprehensive attempt to model the cold roll-forming process. However, there is a lack of experimental verification of this theoretical model by correlation of simulated and actual values of stress and strain. Results for longitudinal stress by this simulation were not reported. Furthermore, although he focussed his attention on the longitudinal membrane strain, he did not evaluate it from the point of view of the occurrence of forming defects, such as edge buckling. It was considered that it was not easy to devise the model of edge buckling in this theoretical model because the longitudinal shape of the strip, which would have to be considered as a factor of the dimension for calculation of edge buckling, is very complex. Only the results of the longitudinal membrane strain and the total power at each pass are shown.

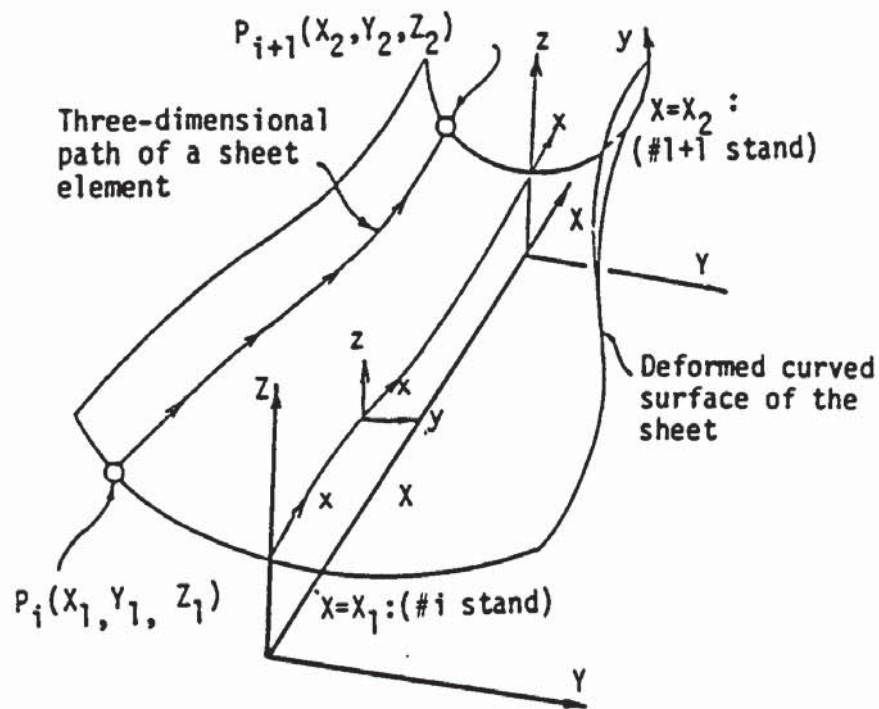


Fig.12 Illustration of the concept of shape function $S(x)$ by Kiuchi 44,45

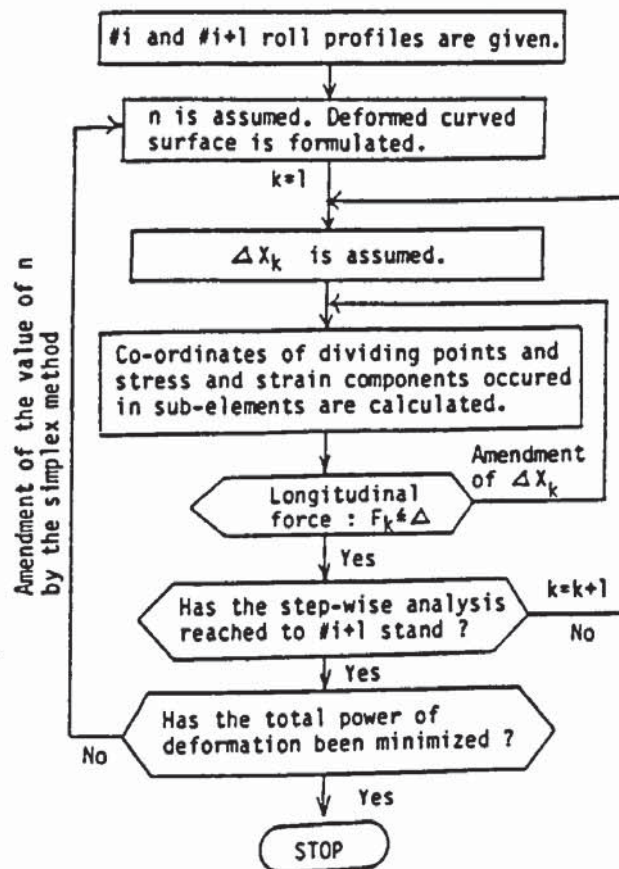
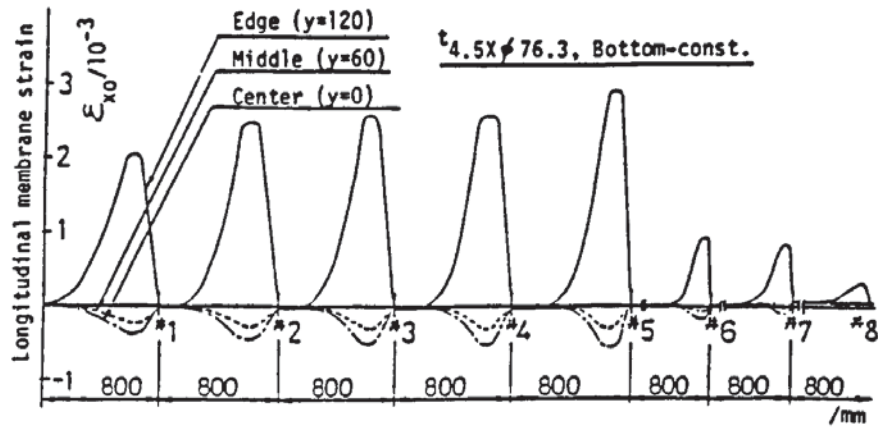
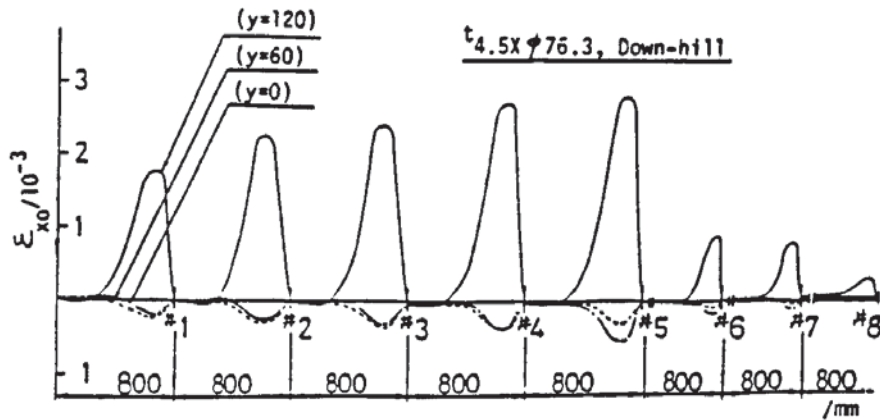


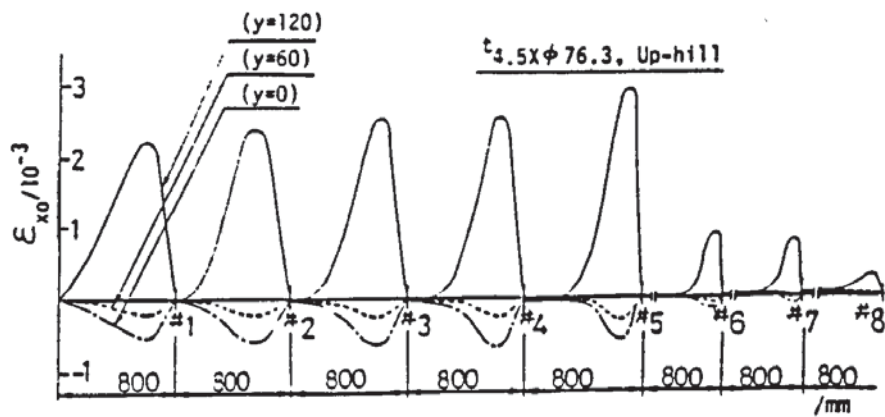
Fig.13 Flow-chart of the total simulation process by Kiuchi 44,45



(a) Bottom-constant pass-line type



(b) Down-hill pass-line type



(c) Up-hill pass-line type

Fig.14 Variation of the longitudinal membrane strain ϵ_{x_0} occurring at transversally different positions

The theoretical model presented by Panton⁴⁸ was very similar to that of Kiuchi. A new shape function, $S(x)$, which can define the geometrical shape of the strip between successive passes in the cold roll-forming process, was devised following a series of experimental investigations. The shape function of the strip, which describes the bending distribution of the strip between passes, is defined by the following equations:

$$S(x) = e^{-a[(L-x)/x]^b} \quad (2)$$

$$\theta(x) = S_\theta + (F_\theta - S_\theta) S(x) \quad (3)$$

where,

x = the distance from the preceding pass

L = the distance between successive passes (the pass length)

$\theta(x)$ = the angle of bending at a distance X from the preceding pass

S_θ = the angle of bending at the preceding pass

F_θ = the angle of bending at the end of the pass

a and b are variables.

The elastic-perfectly plastic model of the stress-strain relationship was applied and the work-hardening of the material was ignored. He verified the theoretical model by experimental data obtained from the forming of a simple U-section channel, but a high accuracy could not be achieved.

Bhattacharyya⁴⁹ constructed a theoretical model for a simple U-section channel. This theoretical work is concerned with predicting the shape of the strip between stands, which is a similar method to that of the previously mentioned two workers; a minimum energy method has also been adopted. It is assumed that no forming will take place in the pass until a certain point in the longitudinal position is reached. The idea of "deformation length", adopted by Bhattacharyya, was introduced to define the shape of the strip. He also assumed that, (i) the material can be treated

as rigid-perfectly plastic, (ii) bending takes place only along the fold line, and (iii) the flange adopts the shape which minimises the plastic work. This work was extended into estimating the roll load⁵⁰. Bhattacharyya recognized the limitations of the analysis, but claimed that the equations to determine the forming length were a good approximation which was verified by the experimental investigations.

Thus, these described studies take a similar analytical approach, i.e. they estimate the shape of the strip between passes by using a special function or definition, optimising its shape by the minimum energy solution. However, by using the results obtained from their theoretical models, they have not extended their analyses to the evaluation of the occurrence of forming defects. It seems that there are some difficulties in considering an evaluation model for the occurrence of forming defects. These are, for example, how to decide the shapes and regions of the strip which are affected by the stress or forces that cause the forming defects, and how to assume the point where these forces act.

3.2.2 Finite element analysis

Recently, following advances in computer technology, numerical methods have increasingly been applied to the modelling of a wide area of industrial forming processes.

Finite element analysis (FEA) is typical of these numerical methods and it has become the most popular method of stress-strain analysis. At present, there are very many commercial finite element packages available.

Onoda^{51,52,53} has studied the deformation features of the strip in the break-down rolls, and the fin-pass rolls, in an ERW pipe mill by a three-dimensional rigid-plastic finite element method. He estimated the effects of forming conditions on circumferential distributions of the wall-thickness strain and outer curvature of the formed steel sheets. However, his analysis was limited to the simulation of a few forming features. Furthermore, Onoda⁵⁴ has tried to calculate the deformation features of a Hat-section, roll formed from steel sheet using a three-dimensional elastic-plastic finite element method. He estimated the membrane strains and membrane stresses in the roll formed steel sheet, however, he was still unable to evaluate shape defects such as pocket waves. Furthermore, long calculation times are needed to analyse the deformation of the steel sheet by FEM.

Downes⁵⁵ studied the analysis of the strain, which is created in the strip between passes in the cold roll-forming process, by using his software package called "ROLFEA", which is an elastic-plastic finite element method. He considered the deformation model which consisted of a combination of press brake forming and strip torsion between stands. The strains obtained by ROLFEA are approximately 25% larger than the actual strain measured by a strain gauge, however, he could achieve a close estimate of the strain behaviour.

Itami^{56,57} analysed the residual stress and the deformation of ERW

pipe in the sizing rolls, i.e. the final stages, by a three-dimensional elastic-plastic finite element method from a commercial package, called "MARC". A reasonably accurate simulation was achieved.

Kiuchi and Wang^{58,59} have carried out a numerical analysis of the deformation of steel sheet at the break-down forming stage in tube-making by a two-dimensional elastic-plastic finite element method. They estimated only the outer curvature of the formed sheet. However, they have not analysed the deformation of steel sheet in the longitudinal direction.

As mentioned already, many investigations of cold roll-forming have been carried out, especially in Japan. Research activities have also been performed progressively under the Japan Roll Forming Committee of the Japan Society for Technology of Plasticity (JSTP). However, there are few studies which deal with the consistent forming simulation, including the evaluation of the occurrence of forming defects. One of the reasons may be that the cold roll-forming process has many unknown factors, as well as a number of other characteristics. This is because it has an extremely complicated three-dimensional deformation, with small strains and a large free deformed surface, compared with that of other forming processes such as rolling, forging, extrusion and sheet forming. However, consistent roll forming simulation for tube-making has been the objective of many engineers and operators to predict the occurrence of the forming defects, prior to actual tube production, and to suppress forming defects.

Thus this work seeks to develop a more consistent forming simulation for tube-making in this field, based on professional experience and knowledge gained in the cold roll-tube forming process for more than twenty years.

Chapter 4. Application of the "ROLFOM" Package to Tube Making

Research students at Aston University have developed the CAD/CAM system for cold roll-forming called "ROLFOM" in association with Hadley Industries. ROLFOM is written in FORTRAN 77¹⁵ using the GINO-F graphics package¹². This software runs on the Vax 8650 and Textronix 4107 equipment at Aston University.

The ROLFOM system consists of computer aided design (CAD) and computer aided manufacturing (CAM) programmes. The configuration of the ROLFOM system is shown diagrammatically in Fig.15.

The CAD software comprises five parts:

- (1) Finished section programme
- (2) Flower pattern programme
- (3) Template programme
- (4) Roll design programme
- (5) Roll editor programme

The CAM software comprises three parts:

- (1) Roll machining programme
- (2) Post-processor programme
- (3) Tape check programme

As an example, Fig.16 shows a hat-shape finished section produced by the finished section programme. This programme has the purpose of defining and drawing the finished section, however it can calculate only the required sheet width, based on a consideration of the bending allowance of the strip. Although this consideration is not necessary in the case of $R/t > 5$ (R being the radius of bending and t the wall-thickness of the strip, i.e. $D/t > 10$) as reported by Kaltprofil⁶⁰.

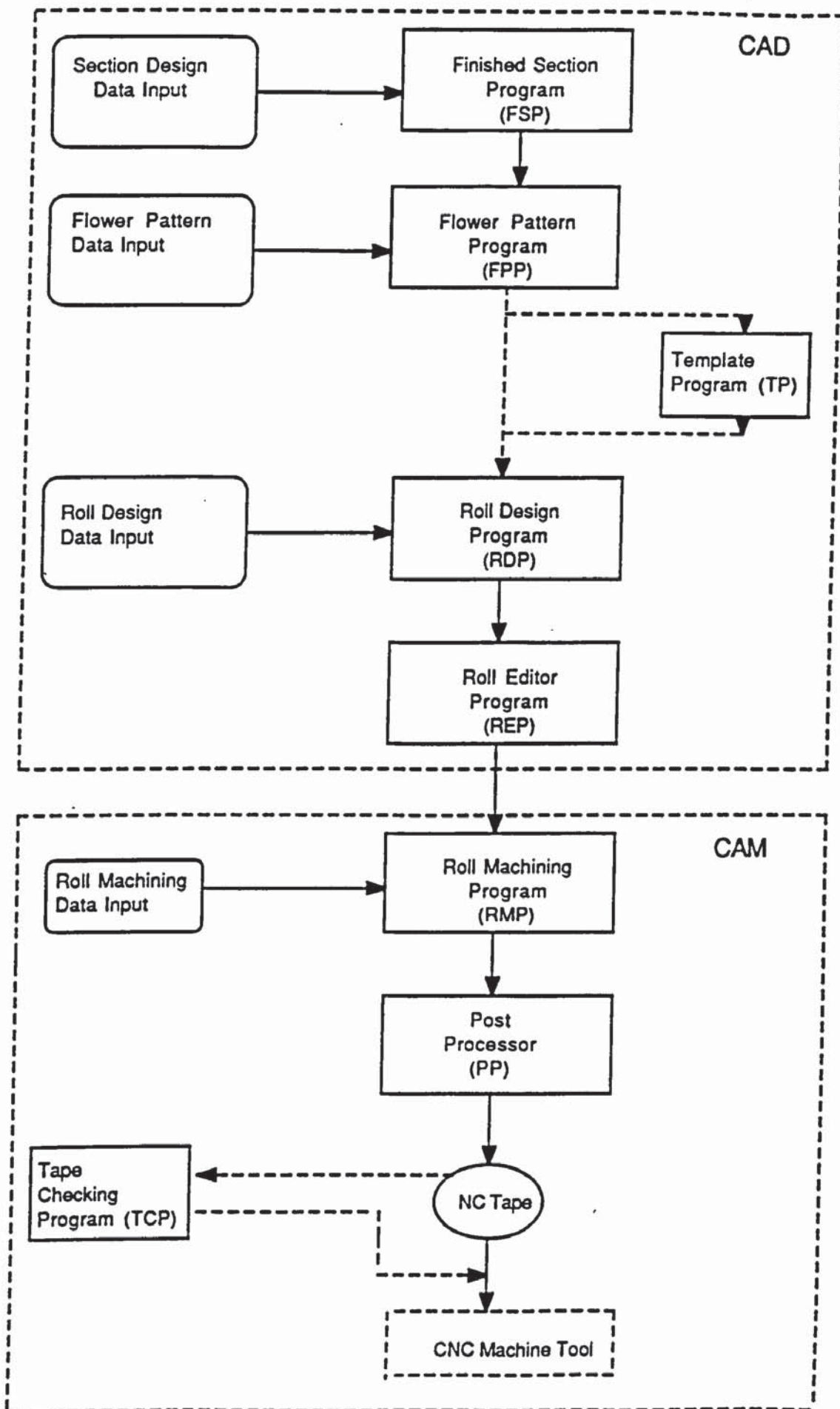


Fig.15 Configuration of CAD/CAM system for cold roll forming developed by Aston University

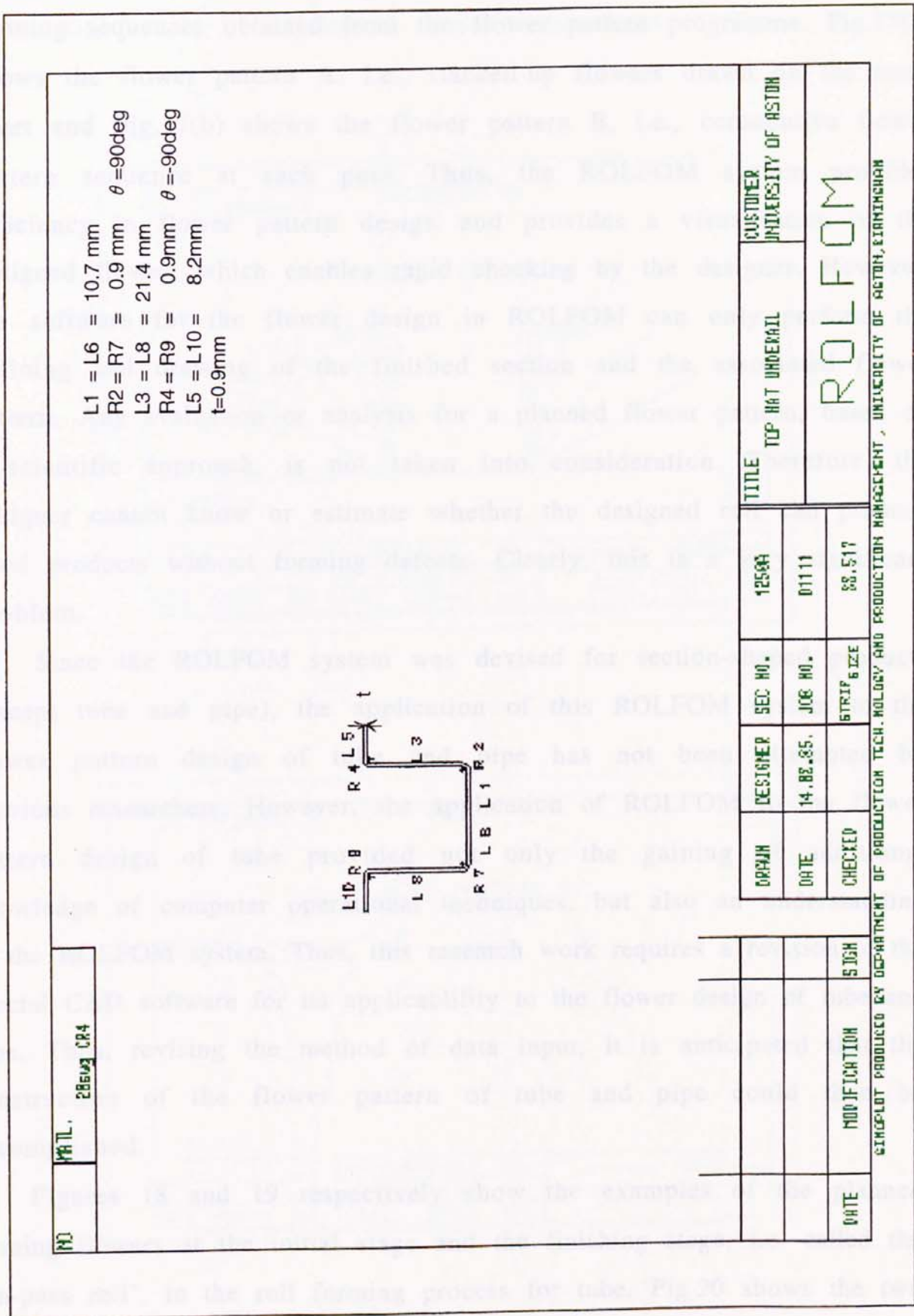


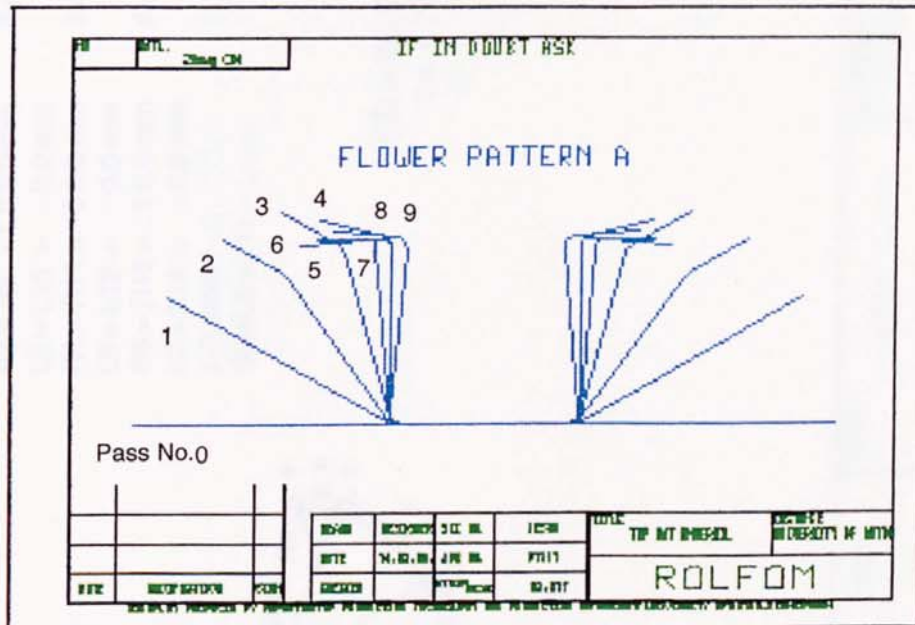
Fig.16 Example of hat shape finished section using the ROLFOM section programme

Fig.17 shows examples of planned flower patterns which visualises forming sequences obtained from the flower pattern programme. Fig.17(a) shows the flower pattern A, i.e., stacked-up flowers drawn on the same chart and Fig.17(b) shows the flower pattern B, i.e., consecutive flower pattern sequence at each pass. Thus, the ROLFOM system provides efficiency in flower pattern design and provides a visualisation of the designed flower, which enables rapid checking by the designer. However, the software for the flower design in ROLFOM can only perform the defining and drawing of the finished section and the associated flower pattern. Any evaluation or analysis for a planned flower pattern, based on a scientific approach, is not taken into consideration. Therefore, the designer cannot know or estimate whether the designed roll can produce good products without forming defects. Clearly, this is a very significant problem.

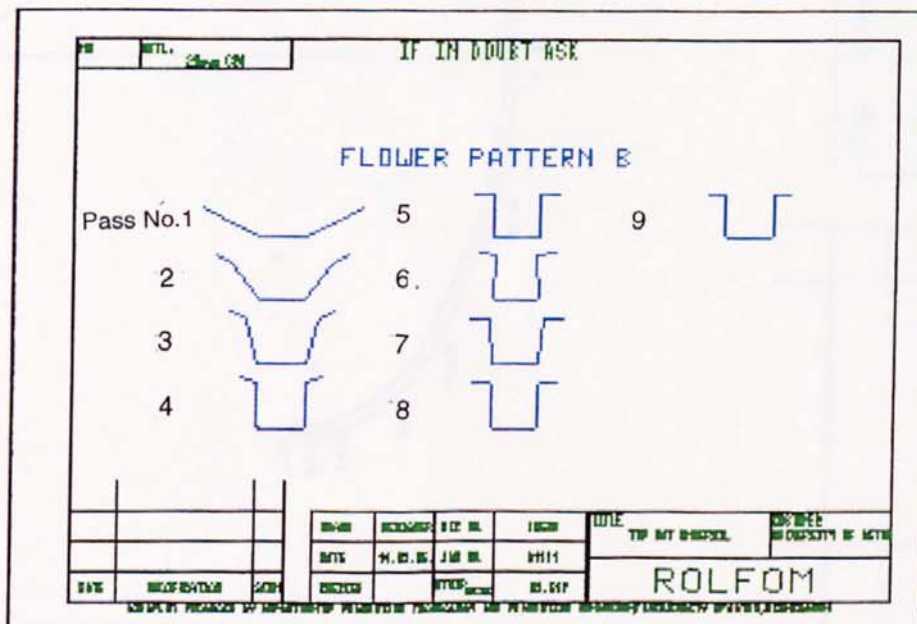
Since the ROLFOM system was devised for section-shaped products (except tube and pipe), the application of this ROLFOM system to the flower pattern design of tube and pipe has not been attempted by previous researchers. However, the application of ROLFOM to the flower pattern design of tube provided not only the gaining of additional knowledge of computer operational techniques, but also an understanding of the ROLFOM system. Thus, this research work requires a revision of the special CAD software for its applicability to the flower design of tube and pipe. Thus, revising the method of data input, it is anticipated that the construction of the flower pattern of tube and pipe could then be accomplished.

Figures 18 and 19 respectively show the examples of the planned forming flowers at the initial stage and the finishing stage, i.e. called the "fin-pass roll", in the roll forming process for tube. Fig.20 shows the two kinds of planned flower patterns from start to the first fin-pass roll stage. Each flower was drawn with respect to the outside surface and the wall-

thickness was neglected. Fig.20(a) shows the stacked-up flower pattern A and Fig.20(b) shows the consecutive flower pattern B, as detailed in Fig.16.



(a) Flower pattern A



(b) Flower pattern B

Fig.17 Example of flower pattern A and flower pattern B by the ROLFOM flower pattern programme

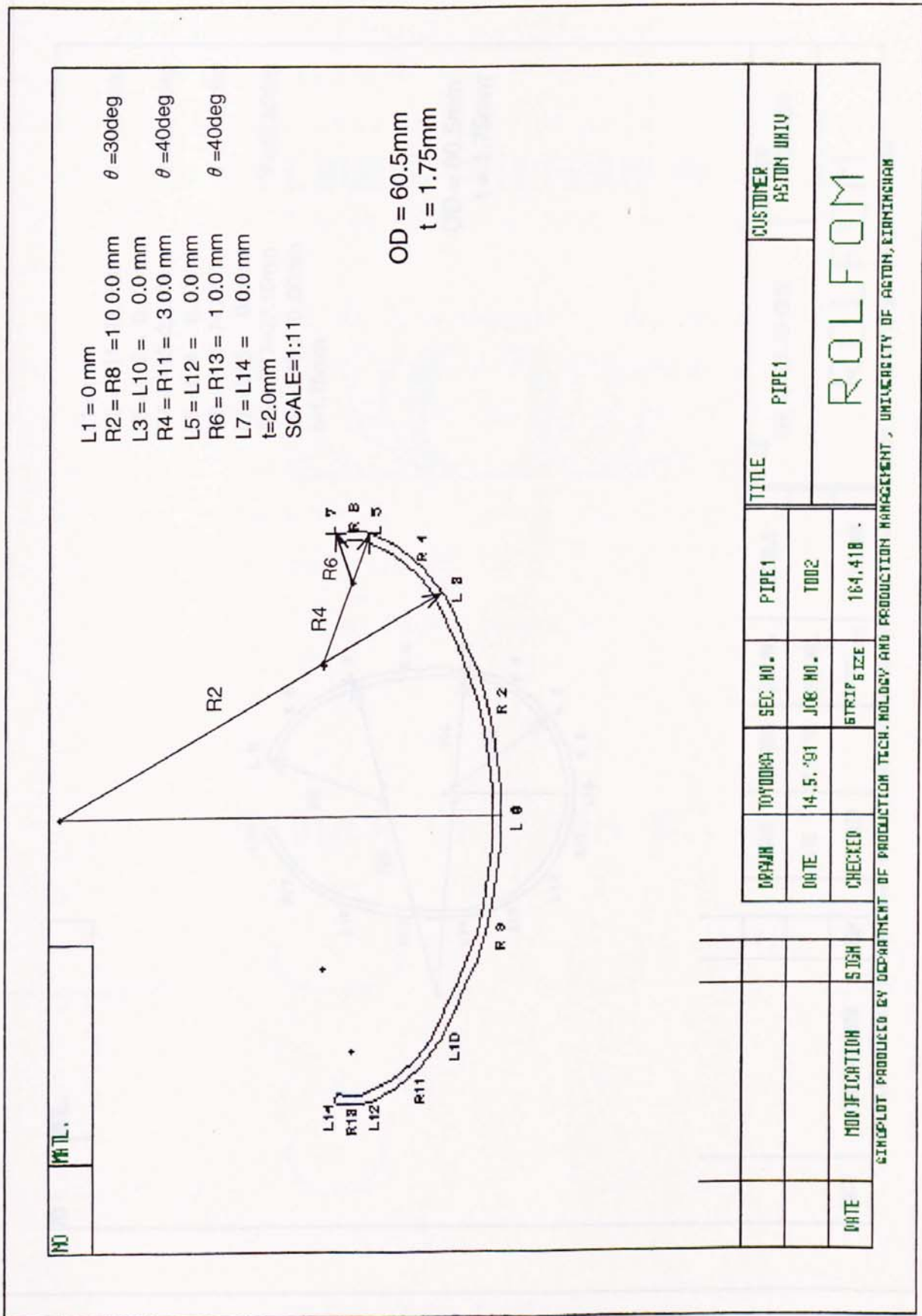


Fig.18 Application of the ROLFOM to flower pattern design of tube at break-down roll forming stage

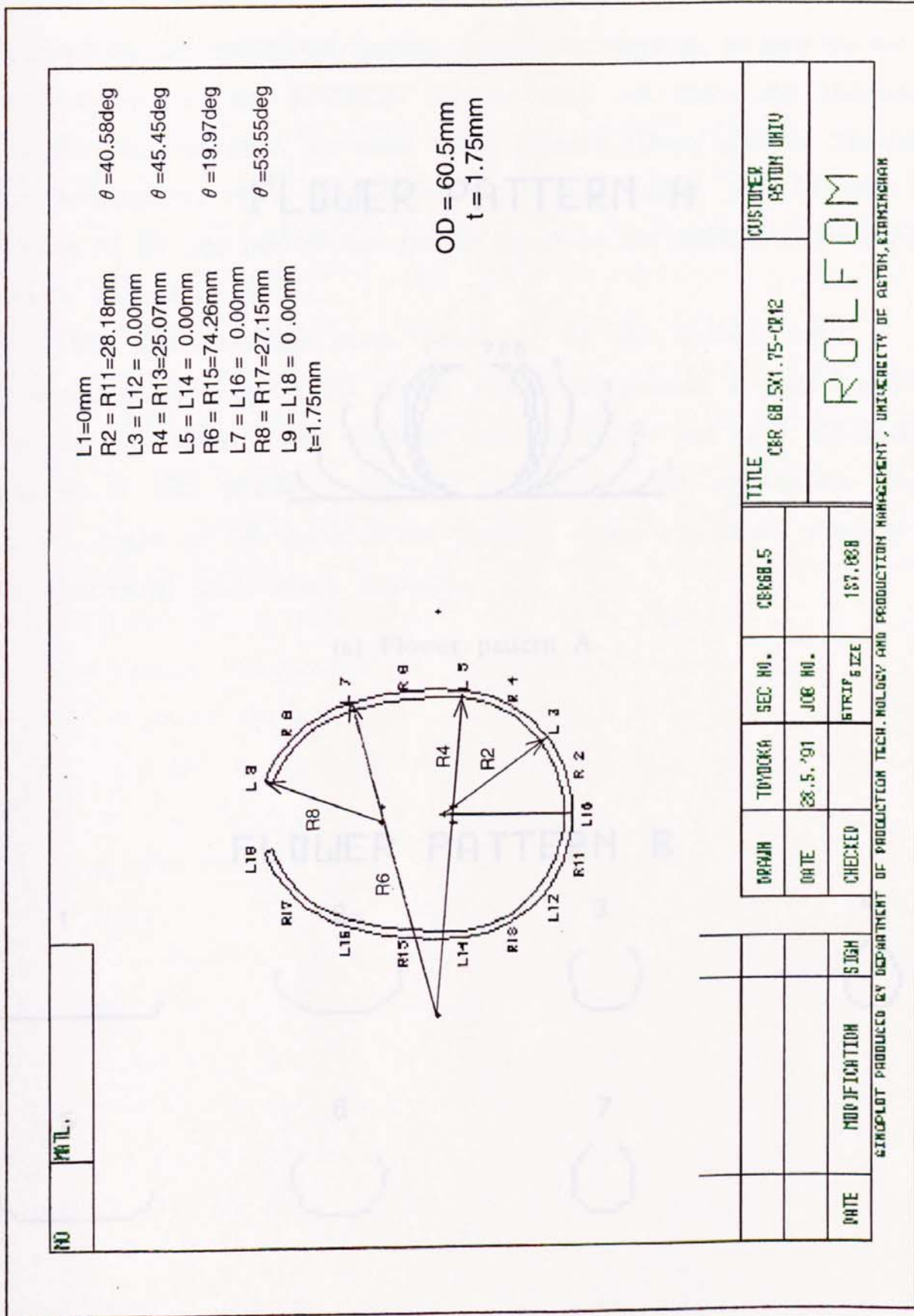
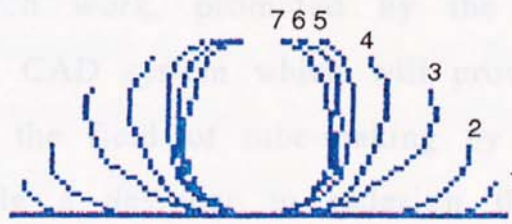


Fig.19 Application of the ROLFOM to flower pattern design of tube at the fin-pass roll forming stage

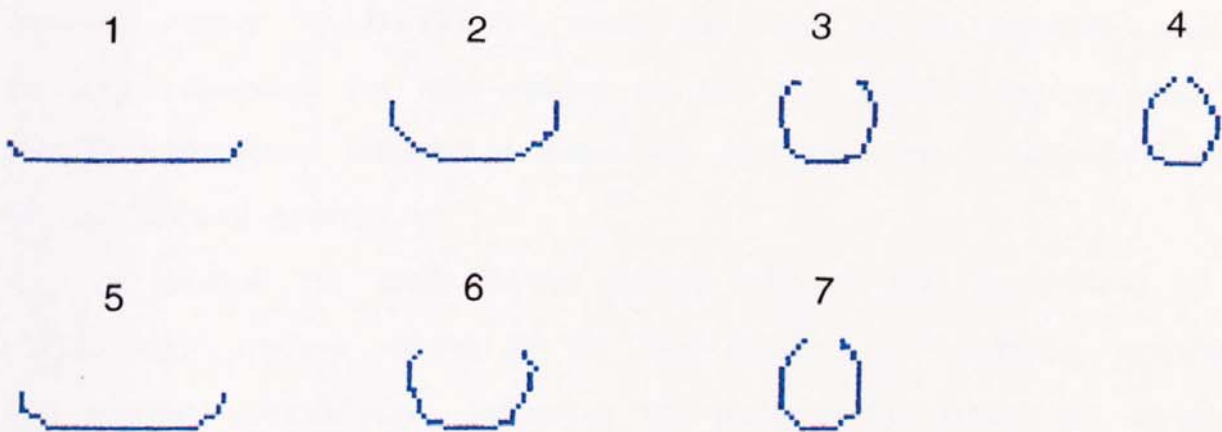
However, as mentioned previously, the validity of the flower pattern, obtained by the ROLFOM system, cannot be verified if it cannot be checked whether the ROLFOM system does not have any conceptual errors and evaluation procedure for a planned flower pattern. Therefore, the investigation of the validity of the designed flower pattern based on the theoretical analysis is clearly required.

FLOWER PATTERN A



(a) Flower pattern A

FLOWER PATTERN B



(b) Flower pattern B

Fig.20 Application of the ROLFOM to flower pattern design and flower sequence

However, as mentioned previously, the validity of this flower pattern, obtained by the ROLFOM system, cannot be verified. It also cannot be checked because the ROLFOM system does not have any theoretical analysis and evaluation provision for a planned flower pattern. Therefore, the development of a new software package, which can evaluate the validity of the designed flower pattern based on the theoretical analysis, is clearly required.

Thus this research work, promoted by the author, aims at the development of a new CAD system which will provide a more consistent forming simulation in the field of tube-making by the cold roll-forming process. It will enable a designer to redesign the appropriate flower pattern, based on the result of the forming defect evaluation proposed by the theoretical stress-strain analysis.

Chapter 5. New Computer Simulation for Tube-making

5.1 Outline of new computer simulation, "CADFORM"

As previously mentioned, very little research has been conducted that deals with a consistent forming simulation and evaluation of forming defects in the cold roll-forming processes. This is because of the extremely complicated three-dimensional small strain deformations, and because of the many uncertain boundary conditions, which are difficult to estimate or define. However, it is considered that it would be possible to carry out the required consistent forming simulation by a modelling simplification based on original but acceptable assumptions. In some cases, greater value is attached to a consistent complete forming simulation which can provide an approximate estimation, rather than a localised forming simulation with high accuracy. This is especially the case in the production of ERW tube and pipe, where development of consistent software has been required, not only to predict the occurrence of forming defects in the forming of new products, but also to obtain an optimum forming condition and procedures in order to minimise such forming defects.

Thus, this research deals with the development of a new software package named "CADFORM", which can carry out the required consistent forming simulation for tube-making by the cold roll-forming process. The CADFORM system includes a theoretical analysis using a simplified model of the forming process.

In general, the main factors which have to be considered in the roll-forming process consist of the tool design, the operating conditions and product specification, including the material properties, as shown in Fig.11 (page 35). Every factor influences every other and all have a close relationship. In normal production, operating conditions are mainly controlled by the product specification because the tool design has already been fixed. However, three major factors have to be determined to obtain the optimum forming of the strip and to achieve high quality products.

The optimum design of the forming tools exists in the area which satisfies the three major factors, as shown in Fig.11.

The outline of this research work is shown in Fig.21. The construction of the CADFORM system, which will be developed for tube and pipe, comprises four main parts:

- (1) Flower pattern design programme with the data input and the two dimensional (2-D) drawing
- (2) Elastic-plastic, stress-strain analysis programme
- (3) Evaluation of edge buckling programme
- (4) Three dimensional (3-D) graphics display and drawing programme

This interactive data input system has to be created in order to provide easy use and access. Amendment of data, creating data files and calling the data from the file by the interactive method, are also taken into consideration in order to give satisfactory operations for the designer. Furthermore, all main results are to be displayed on the Tektronix colour screen by newly devised 2-D and 3-D graphics programmes associated with the GINO-F graphics package. They are visualised in order to enable the designer to gain rapid understanding and checking of the results.

The originality of this research is the realisation of predicting a forming defect and enabling designer to redesign the appropriate flower pattern, based on the result of the edge buckling evaluation. The consistent forming simulation, which consists of the construction of forming flower patterns, the analysis of stress-strain using the designed flower pattern and the evaluation of the edge buckling occurrence is a new approach by this research work to realise a more effective tube-making analysis.

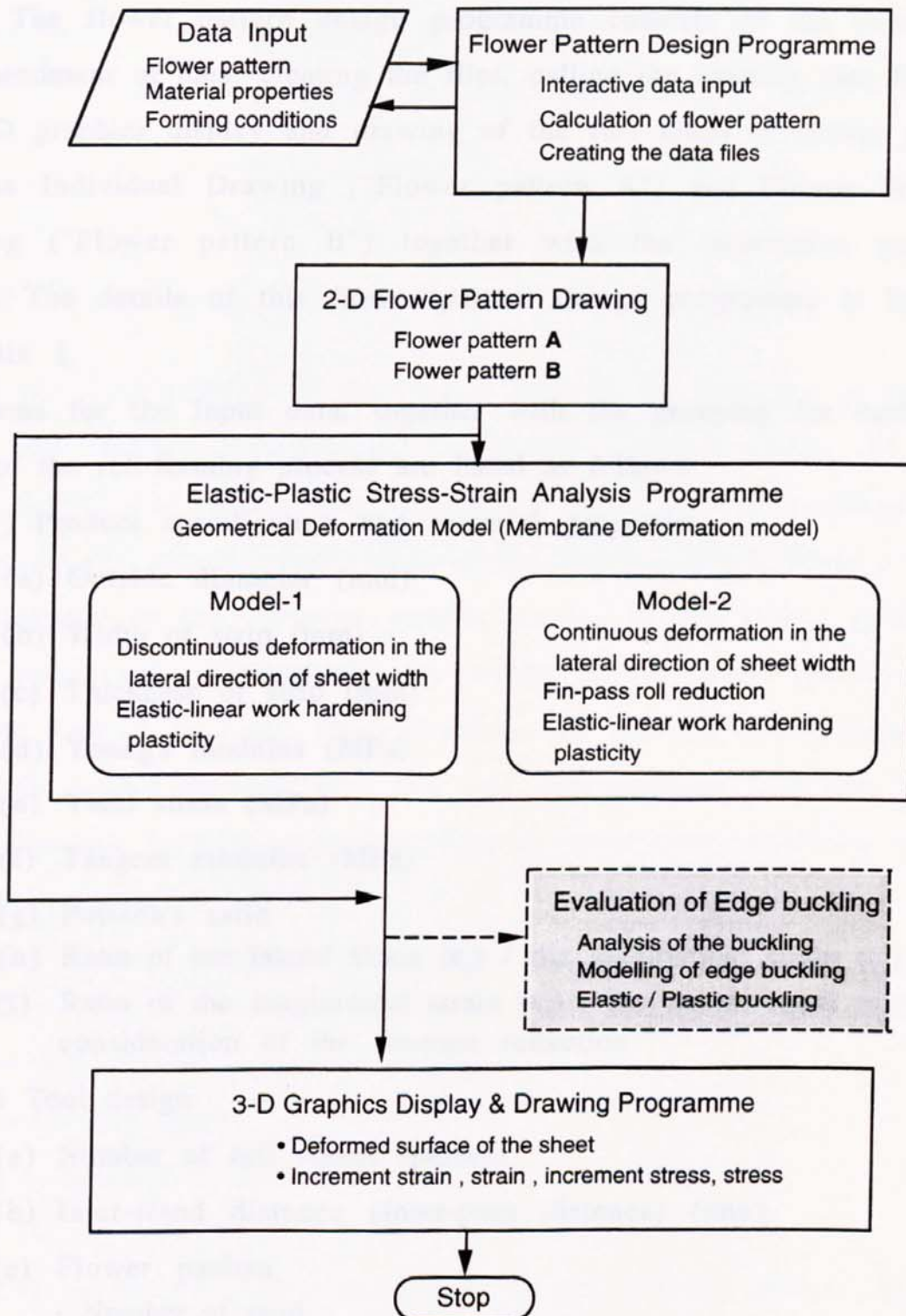


Fig.21 Construction of CADFORM system for tube and pipe

5.2 Two dimensional flower pattern design

5.2.1 Flower pattern design programme

The flower pattern design programme consists of the data input, the amendment of data, creating the files, calling the existing data file, and the 2-D graphics display and drawing of the two kinds of flower patterns such as Individual Drawing ("Flower pattern A") and Flower Sequence Drawing ("Flower pattern B") together with the interactive operation system. The details of this flower pattern design programme is listed in Appendix 1.

Items for the input data, together with the grouping for each main factor of the roll-forming process are listed as follows:

- (1) Product specification and material properties
 - (a) Outside diameter (mm)
 - (b) Width of strip (mm)
 - (c) Thickness of strip (mm)
 - (d) Young's modulus (MPa)
 - (e) Yield stress (MPa)
 - (f) Tangent modulus (MPa)
 - (g) Poisson's ratio
 - (h) Ratio of the lateral strain (ϵ_y) / the longitudinal strain (ϵ_x)
 - (i) Ratio of the longitudinal strain (ϵ_x) / the lateral strain (ϵ_y) for consideration of the fin-pass reduction
- (2) Tool design
 - (a) Number of roll stands (passes)
 - (b) Inter-stand distance (Inter-pass distance) (mm)
 - (c) Flower pattern
 - Number of radii
 - Radius (mm) and angle (deg)
- (3) Operating conditions
 - (a) Pass line height (mm)
 - Bottom constant (constant pass line) forming

- Downhill (pass line) forming
- Uphill (pass line) forming

(b) Forming speed (m/min)

(4) Stress strain analysis

(a) Number of the divided elements in the lateral direction.

5.2.2 Two-dimensional flower pattern drawing

In the 2-D drawing of the flower pattern, the designer is provided with a menu screen at each stage. The flower pattern A and/or the flower pattern B, for the optional pass sequence, are obtained by calculation of some of the geometrical dimensions of the flower pattern. Photo.4 and 5 show examples of the computer graphic display of the flower patterns A and B, respectively. Furthermore, the results of the flower pattern A are shown in Figures 22 - 30. These drawings are planned flower patterns of tubes with outside diameter 60.5 mm and wall-thickness 1.75 mm for the bottom constant forming condition. The notation used in flower pattern drawings is defined as follows:

TL0 = outside surface length of formed sheet

TLN = neutral axis length of formed sheet

R = outer radius

A = bending angle

DH = downhill forming height

Fig.31 shows the flower pattern B for the planned flower sequence described in the previous paragraph. Fig.32 shows the flower pattern B for the application of downhill forming to the forming of the same size of tube. Any size of tube and pipe can be drawn with this CADFORM system using the automatic scaling provision.

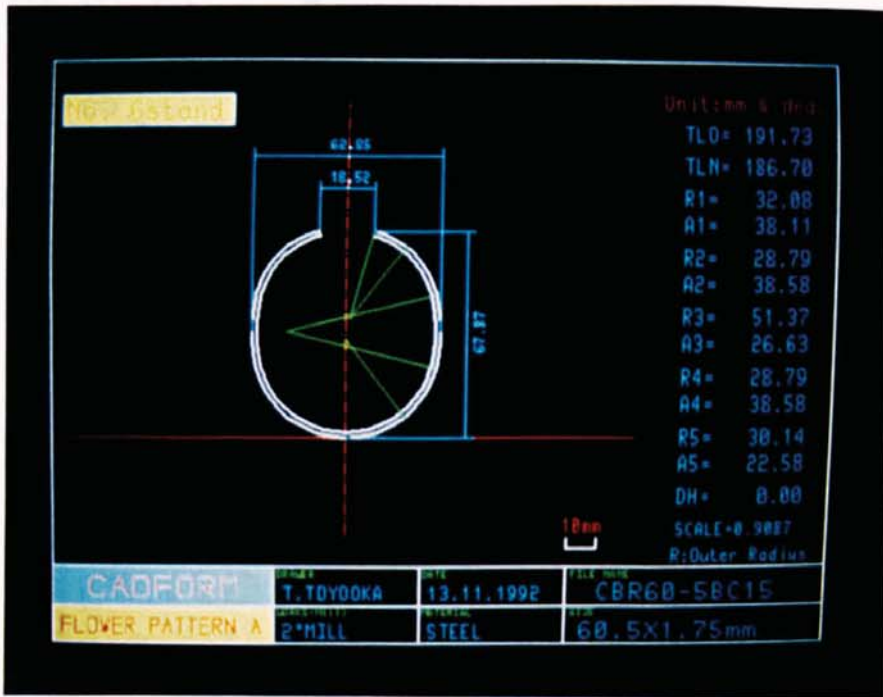


Photo.4 Computer graphic display example of the planned flower pattern A

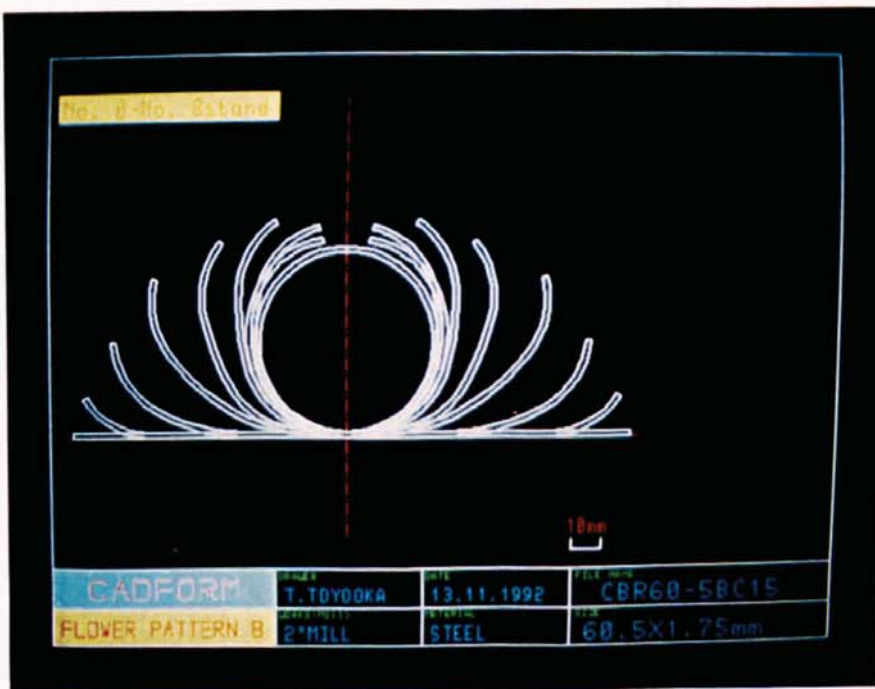


Photo.5 Computer graphic display example of the planned flower pattern B

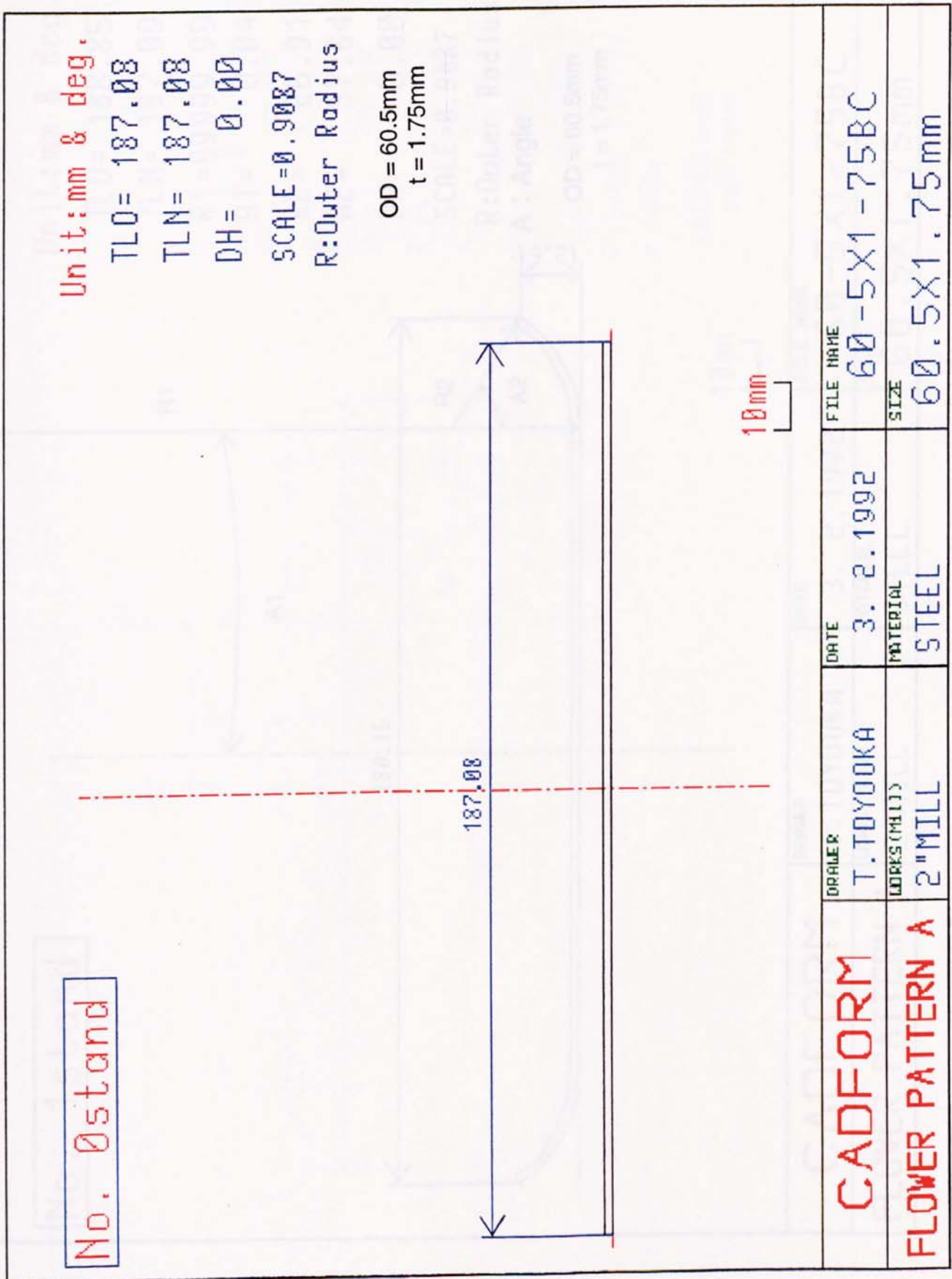


Fig.22 Drawing of planned forming flower at entry pass by flower pattern A using the CADFORM system

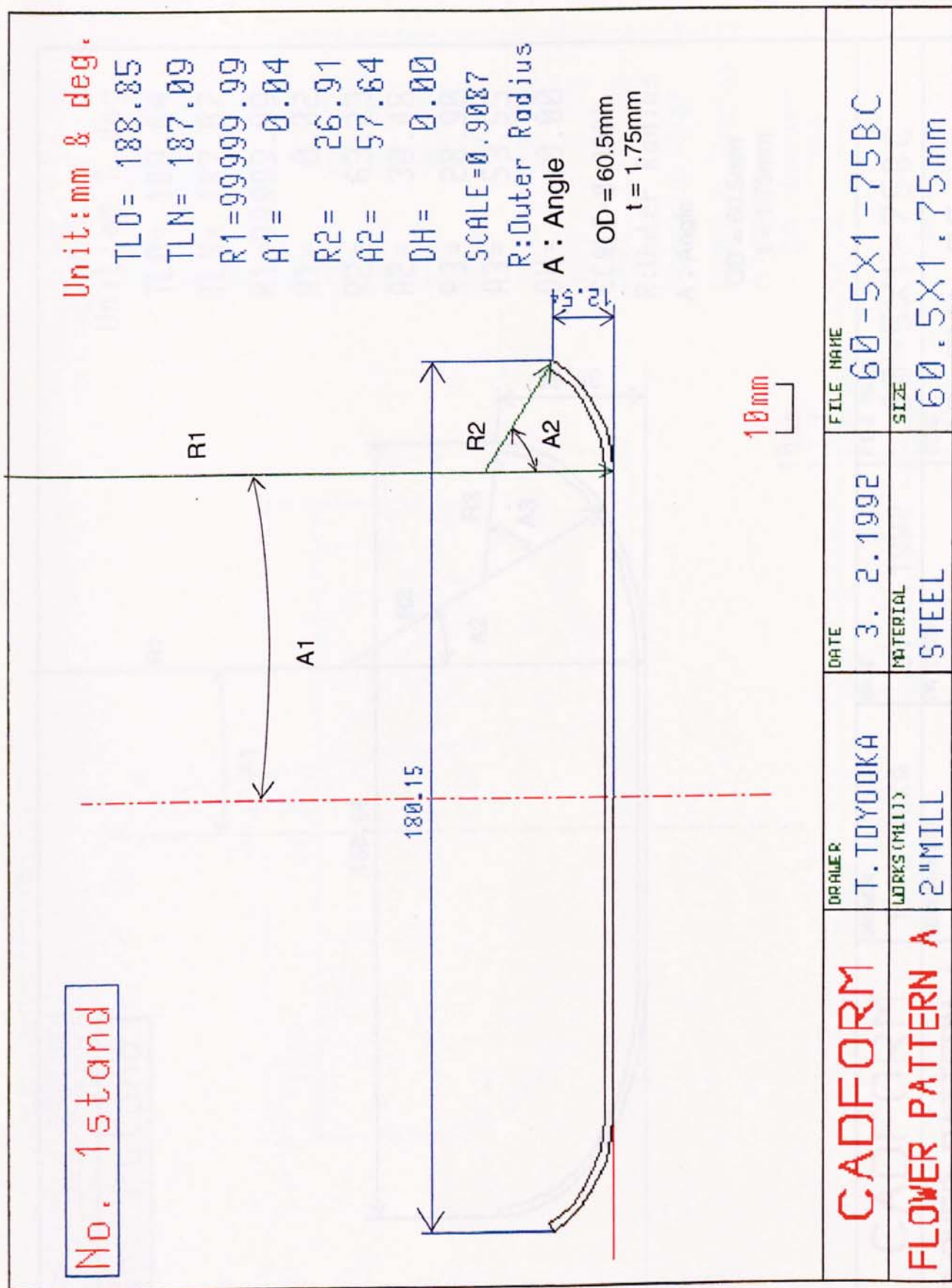


Fig.23 Drawing of planned forming flower at 1st pass by flower pattern A using the CADFORM system

No. 2stand

Unit: mm & deg.

TLO= 189.64

TLN= 187.07

R1=99999.99

A1= 0.02

R2= 63.23

A2= 30.48

R3= 28.90

A3= 53.55

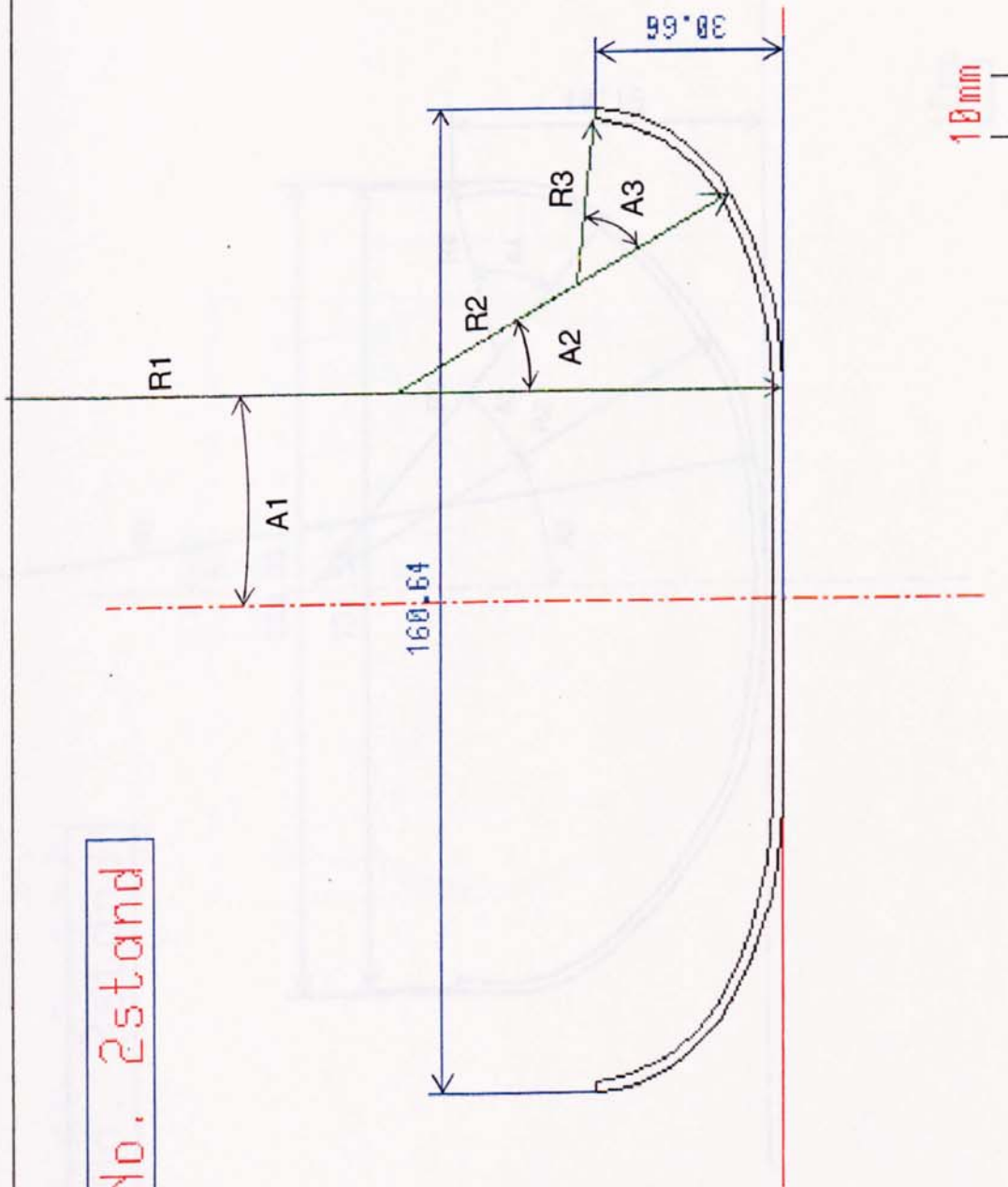
DH= 0.00

SCALE=0.9087

R:Outer Radius

A : Angle

OD = 60.5mm
t = 1.75mm



CADFORM	DRAWER T.TOYOOKA	DATE 3. 2.1992	FILE NAME 60-5X1-75BC
FLOWER PATTERN A	WORKS (PH11) 2" MILL	MATERIAL STEEL	SIZE 60.5X1.75mm

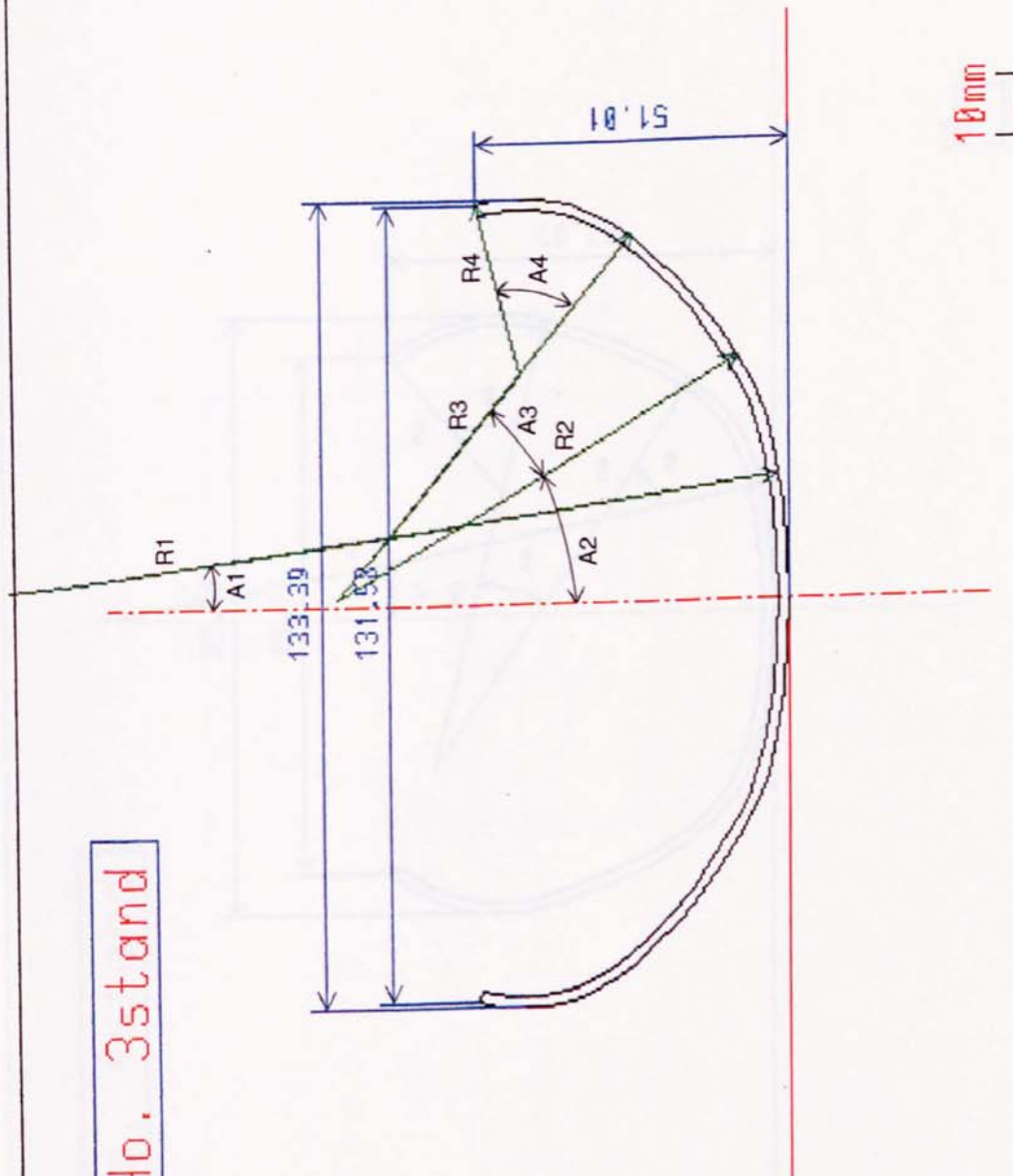
Fig.24 Drawing of planned forming flower at 2nd pass by flower pattern A using the CADFORM system

No. 3stand

Unit: mm & deg.

- TLO= 190.26
- TLN= 187.08
- R1= 148.26
- A1= 8.00
- R2= 52.52
- A2= 22.83
- R3= 76.01
- A3= 19.97
- R4= 28.90
- A4= 53.55
- DH= 0.00

SCALE=0.9087
 R:Outer Radius
 A: Angle
 OD = 60.5mm
 t = 1.75mm



CADFORM	DRAWER T. TOYOOKA	DATE 3. 2. 1992	FILE NAME 60-5X1-75BC
FLOWER PATTERN A	WORKS (MILL) 2" MILL	MATERIAL STEEL	SIZE 60.5X1.75mm

Fig.25 Drawing of planned forming flower at 3rd pass by flower pattern A using the CADFORM system

No. 4 stand

Unit: mm & deg.

TL0 = 191.05

TLN = 187.08

R1 = 109.25

A1 = 10.88

R2 = 26.82

A2 = 45.45

R3 = 76.01

A3 = 19.97

R4 = 28.90

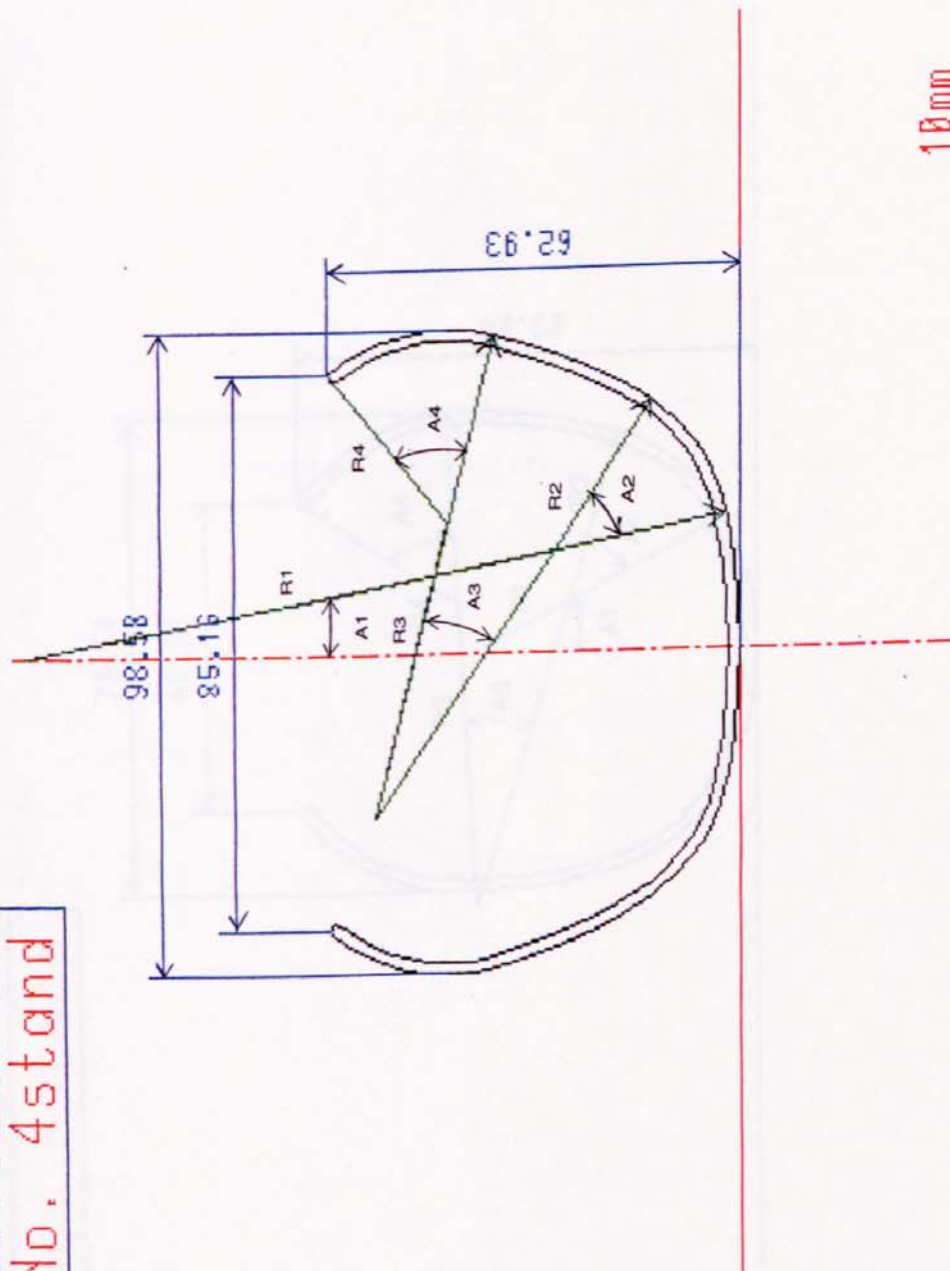
A4 = 53.55

DH = 0.00

SCALE = 0.9087

R: Outer Radius

OD = 60.5mm
t = 1.75mm



CADFORM	DRAWER T. TOYOOKA	DATE 3. 2. 1992	FILE NAME 60-5X1-75BC
FLOWER PATTERN A	WORKS (MILL) 2" MILL	MATERIAL STEEL	SIZE 60.5X1.75mm

Fig.26 Drawing of planned forming flower at 4th pass by flower pattern A using the CADFORM system

No. 5stand

OD = 60.5mm
t = 1.75mm

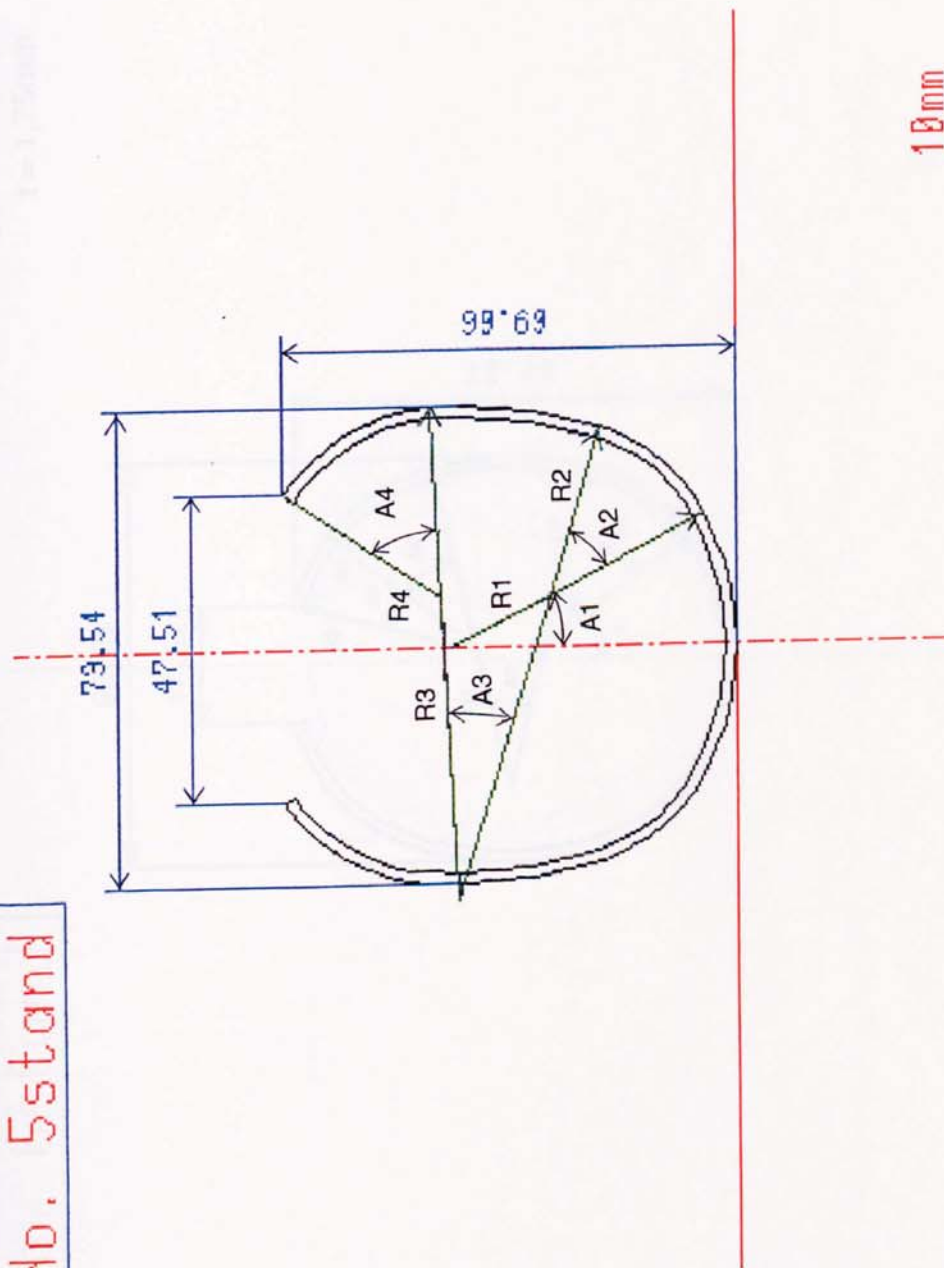
Unit: mm & deg.

TL0 = 191.56
 TLN = 187.08
 R1 = 43.69
 A1 = 27.54
 R2 = 26.82
 A2 = 45.45
 R3 = 76.01
 A3 = 19.97
 R4 = 28.90
 A4 = 53.55
 DH = 0.00

SCALE = 0.9087

R: Outer Radius

OD = 60.5mm
t = 1.75mm



CADFORM	DRAYER T. TOYOOKA	DATE 3. 2. 1992	FILE NAME 60-5X1-75BC
FLOWER PATTERN A	WORKS (MILL) 2" MILL	MATERIAL STEEL	SIZE 60.5X1.75mm

Fig.27 Drawing of planned forming flower at 5th pass by flower pattern A using the CADFORM system

No. 6stand

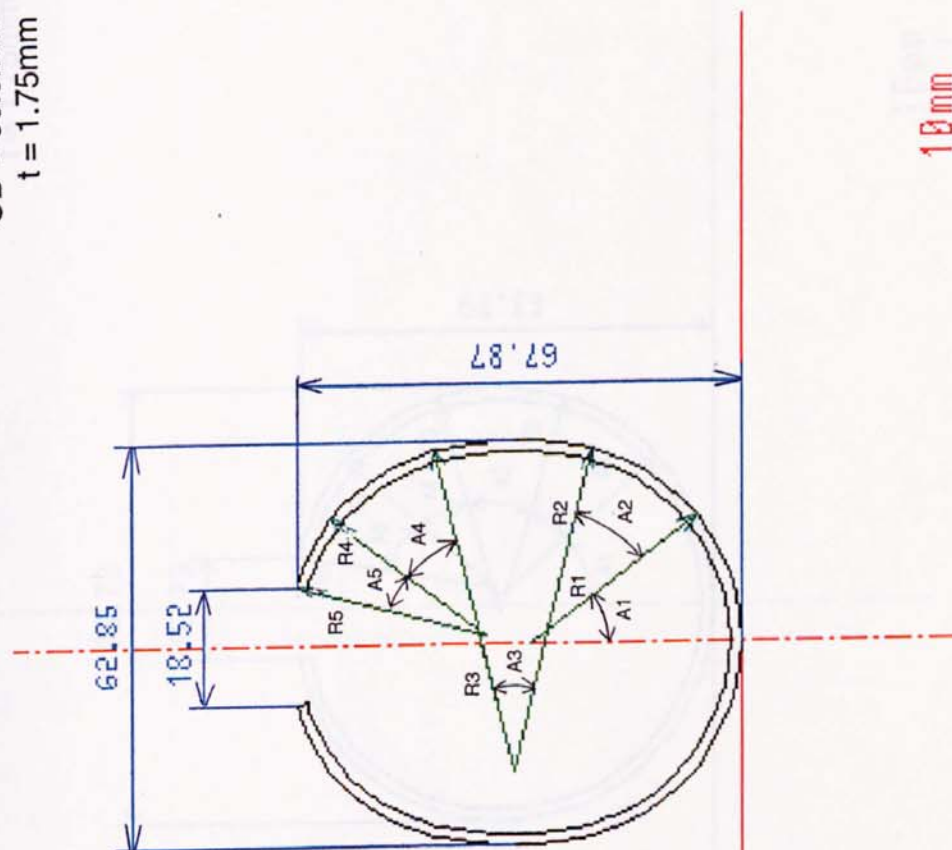
OD = 60.5mm
t = 1.75mm

Unit: mm & deg.

- TLD = 191.73
- TLN = 186.70
- R1 = 32.08
- A1 = 38.11
- R2 = 28.79
- A2 = 38.58
- R3 = 51.37
- A3 = 26.63
- R4 = 28.79
- A4 = 38.58
- R5 = 30.14
- A5 = 22.58
- DH = 0.00

SCALE = 0.9087

R: Outer Radius



10mm

CADFORM	DRAWER T. TOYOOKA	DATE 3. 2. 1992	FILE NAME 60-5X1-75BC
FLOWER PATTERN A	WORKS (MILL) 2" MILL	MATERIAL STEEL	SIZE 60.5X1.75mm

Fig.28 Drawing of planned forming flower at 6th pass by flower pattern A using the CADFORM system

No. 7 stand

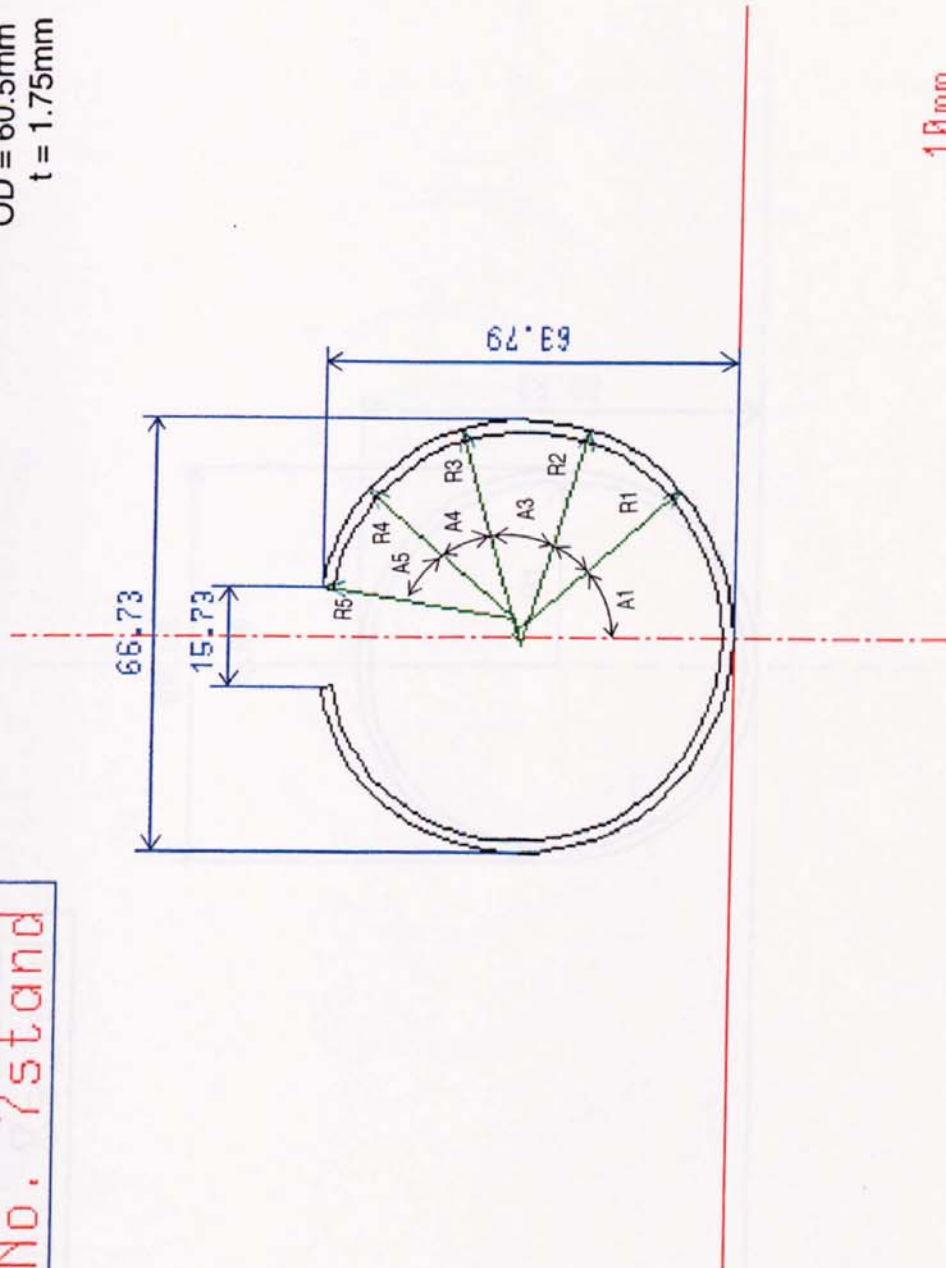
OD = 60.5mm
t = 1.75mm

Unit: mm & deg.

TL0 = 191.74
TLN = 186.52
R1 = 34.62
A1 = 41.35
R2 = 30.42
A2 = 32.28
R3 = 34.62
A3 = 32.74
R4 = 30.42
A4 = 32.28
R5 = 30.16
A5 = 31.96
DH = 0.00

SCALE = 0.9087

R: Outer Radius



10mm

CADFORM	DRAWER	T. TOYOOKA	DATE	3. 2. 1992	FILE NAME	60-5X1-75BC
	WORKS (MILL)	2" MILL	MATERIAL	STEEL	SIZE	60.5X1.75mm

Fig.29 Drawing of planned forming flower at 7th pass by flower pattern A using the CADFORM system

No. 8stand

Unit: mm & deg.

TLO= 191.01

TLN= 185.51

R1= 30.40

A1= 180.00

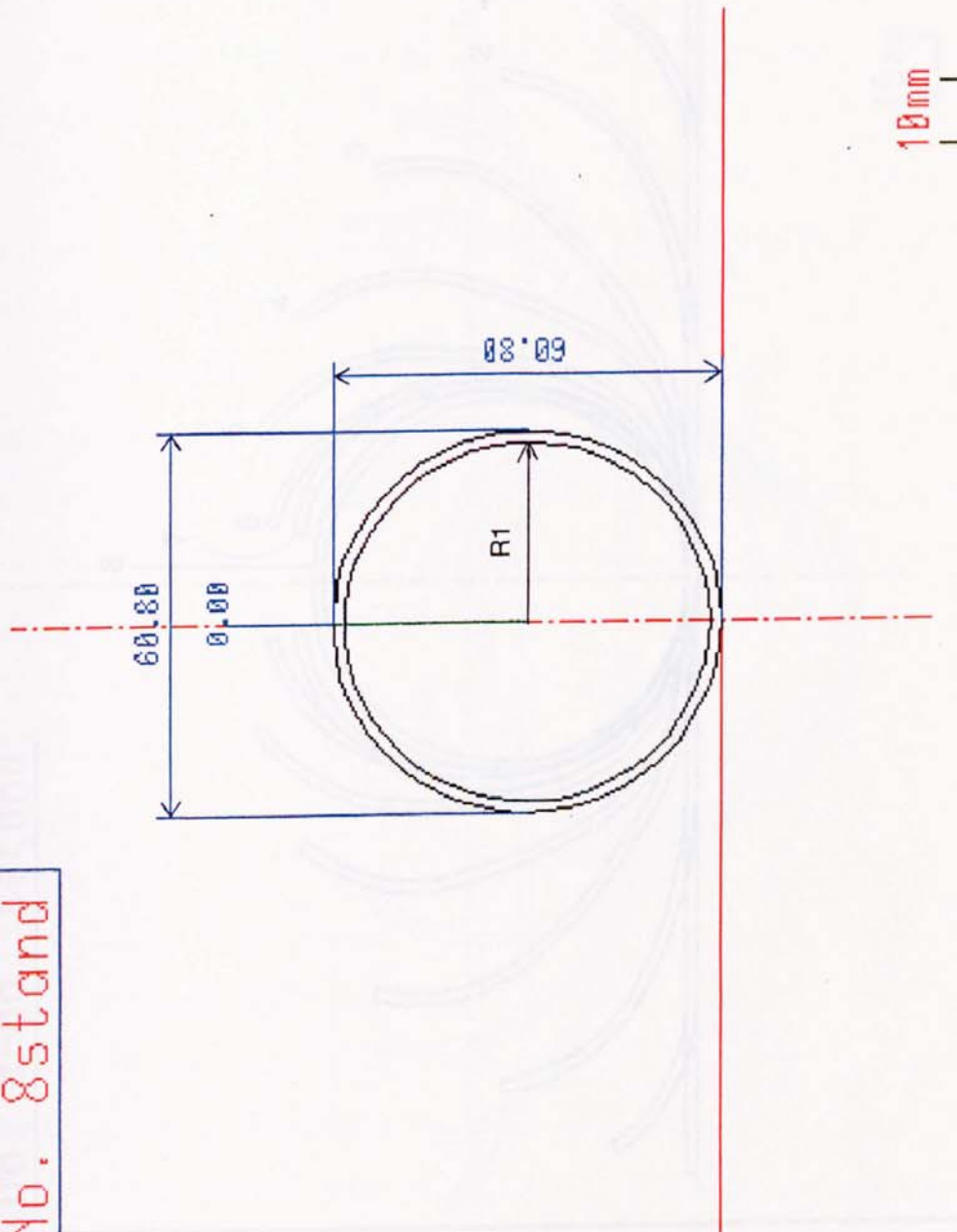
DH= 0.00

SCALE=0.9087

R:Outer Radius

OD = 60.5mm

t = 1.75mm

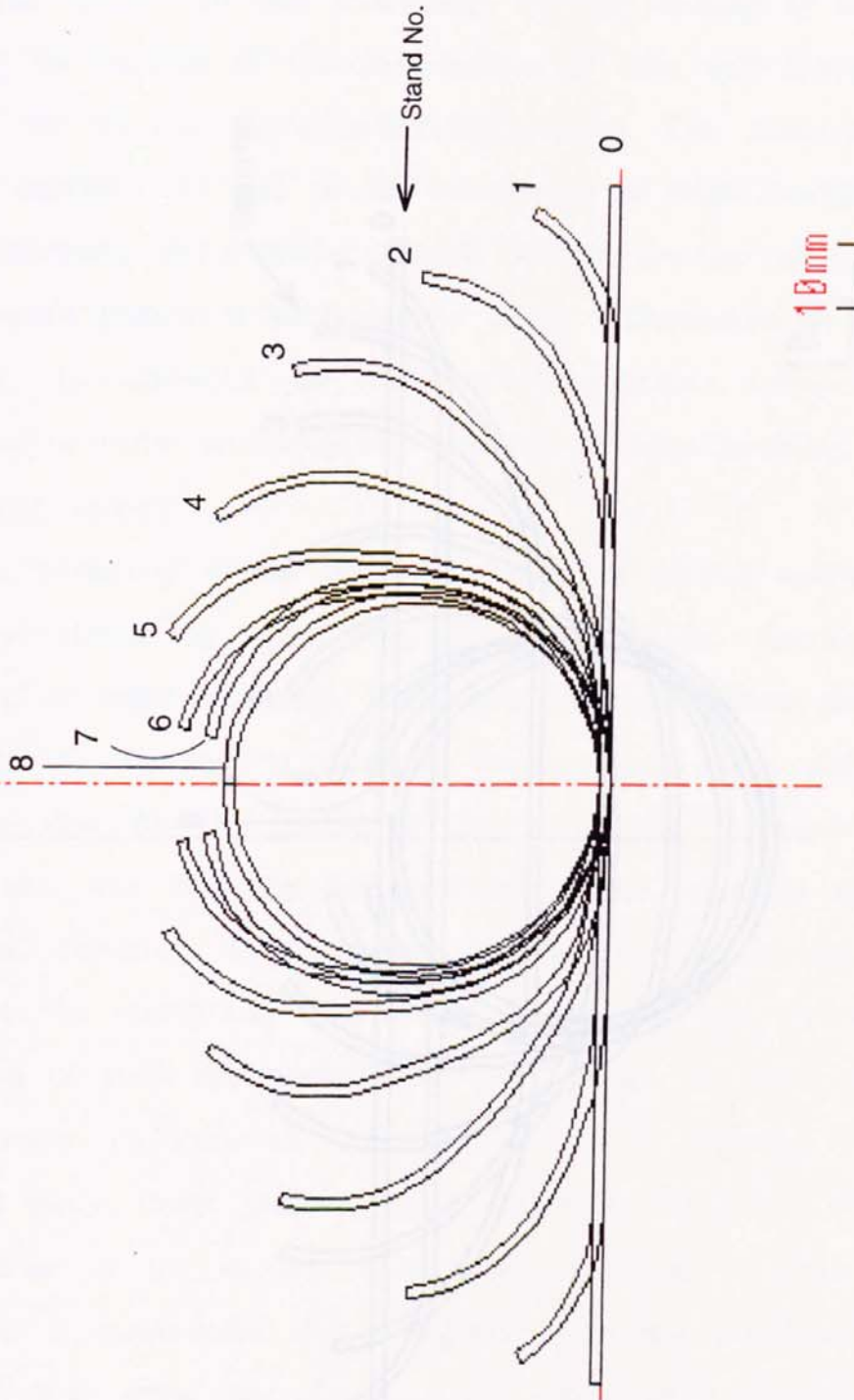


CADFORM	DRAWER T.TDYOOKA	DATE 3. 2.1992	FILE NAME 60-5X1-75BC
FLOWER PATTERN A	WORKS (MILL) 2" MILL	MATERIAL STEEL	SIZE 60.5X1.75mm

Fig.30 Drawing of planned forming flower at 8th pass by flower pattern A using the CADFORM system

No. 0-No. 8stand

OD = 60.5mm
t = 1.75mm

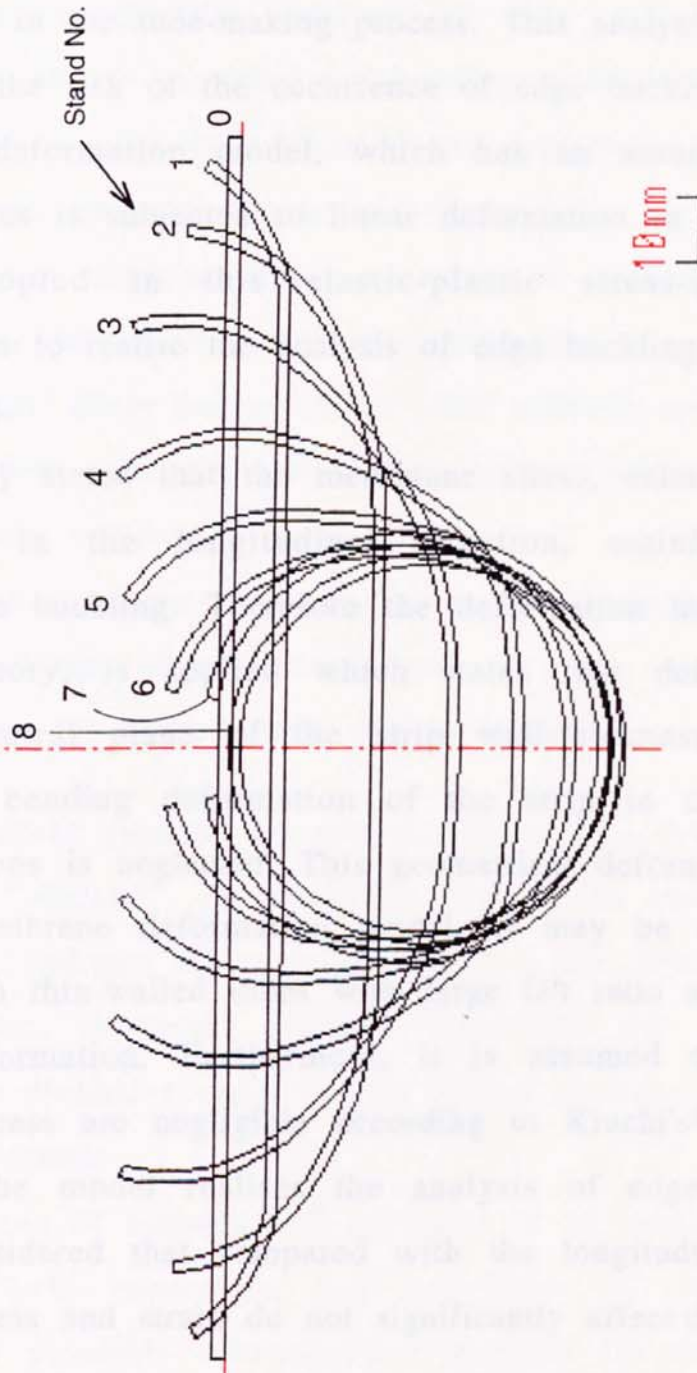


CADFORM	DRAYER T.TOYOOKA	DATE 3. 2.1992	FILE NAME 60-5x1-75BC
FLOWER PATTERN B	LORES (PH I) 2" MILL	MATERIAL STEEL	SIZE 60.5X1.75mm

Fig.31 Drawing of planned flower sequence in bottom constant pass-line forming by flower pattern B using the CADFORM system

OD = 60.5mm
t = 1.75mm

No. 0-No. 8stand



CADFORM	DRAWER T. TOYOOKA	DATE 4. 3. 1992	FILE NAME 60-5X1-75DH
FLOWER PATTERN B	WORKS (MILL) 2" MILL	MATERIAL STEEL	SIZE 60.5X1.75mm

Fig.32 Drawing of planned flower sequence in downhill pass-line forming by flower pattern B using the CADFORM system

5.3 Procedures and modelling for elastic-plastic stress-strain analysis in tube-making

5.3.1 Modelling for elastic-plastic stress-strain analysis

The concept of this modelling, for the forming of tube, is based on obtaining the outline of the deformation of tube and analysing the stress-strain of the strip in the tube-making process. This analysis is required in order to consider the risk of the occurrence of edge buckling of the strip. The geometrical deformation model, which has an assumption that the strip between passes is subjected to linear deformation in the longitudinal direction, is adopted in this elastic-plastic stress-strain analysis programme in order to realise the analysis of edge buckling of the strip in the forming passes.

It is generally stated that the membrane stress, calculated from the membrane strain in the longitudinal direction, mainly affects the occurrence of edge buckling. Therefore the deformation model, based on the membrane theory, is applied which states that deformation only occurs on the neutral plane of the strip wall-thickness. This model assumes that the bending deformation of the strip in the lateral and longitudinal directions is neglected. This geometrical deformation can also be termed the membrane deformation model. It may be noted that the deformation of such thin-walled tubes with large D/t ratio approximates to the membrane deformation. Furthermore, it is assumed that the shear strain and shear stress are negligible according to Kiuchi's⁴⁴ report. This simplification of the model realises the analysis of edge buckling. In addition, it is considered that compared with the longitudinal membrane stress, the shear stress and strain do not significantly affect the occurrence of edge buckling.

In order to simplify the modelling and to enable a consistent forming simulation to be achieved several assumptions are introduced in this

stress-strain analysis. These are as follows:

- (1) The material deforms whereby its cross-sectional profile is perpendicular to the material neutral plane.
- (2) The direction of the principal strain coincide with the X (longitudinal) and Y (lateral) axes.
- (3) Plane stress condition and the stress $\sigma_z = 0$ in the wall-thickness direction apply.
- (4) Membrane theory is applied and bending strains in the lateral and longitudinal direction are neglected.
- (5) Shear strain and shear stress are ignored.
- (6) Elastic-linear work-hardening plasticity is assumed where relevant as the mechanical property.
- (7) The material obeys the von Mises yield criterion and the Prandtl-Reuss stress-strain relationship in the plastic deformation regions.
- (8) Stress and strain are homogeneous in the element.
- (9) The Bauschinger effect is neglected.
- (10) The material is homogeneous and isotropic.

In the CADFORM system, the two deformation models were devised as "Model-1" and "Model-2". As shown in Fig.33, the Model-1 calculates the strain for the condition of no deformation of the divided elements in the lateral direction. However, Model-2 calculates the strain of both deformations of the divided elements in the lateral direction, and that due to fin-pass roll reduction.

The consideration of fin-pass roll reduction is an original idea of the author, based on long experience and knowledge of tube- and pipe-making. Thus it is generally acknowledged that the fin-pass reduction is very important to suppress the edge buckling occurrence of the strip in ERW pipe production. However, no research work has taken into consideration of the fin-pass roll reduction in the theoretical analysis to

date. This is because the mechanism of the suppression of the strip edge buckling by the fin-pass roll reduction has not been appreciated.

Both proposed deformation models have elements which are divided in the longitudinal and lateral directions and these models analyse the stress and strain of each element. The strip mesh is defined at each stand in the longitudinal direction. Although there are a few studies which present the strain variations of the strip to date, there is little work which details the stress variations of the strip in tube-making by the cold roll-forming process. Therefore, this research is important and useful for suppression of the forming defects by considering the stress condition of the strip in the forming stages.

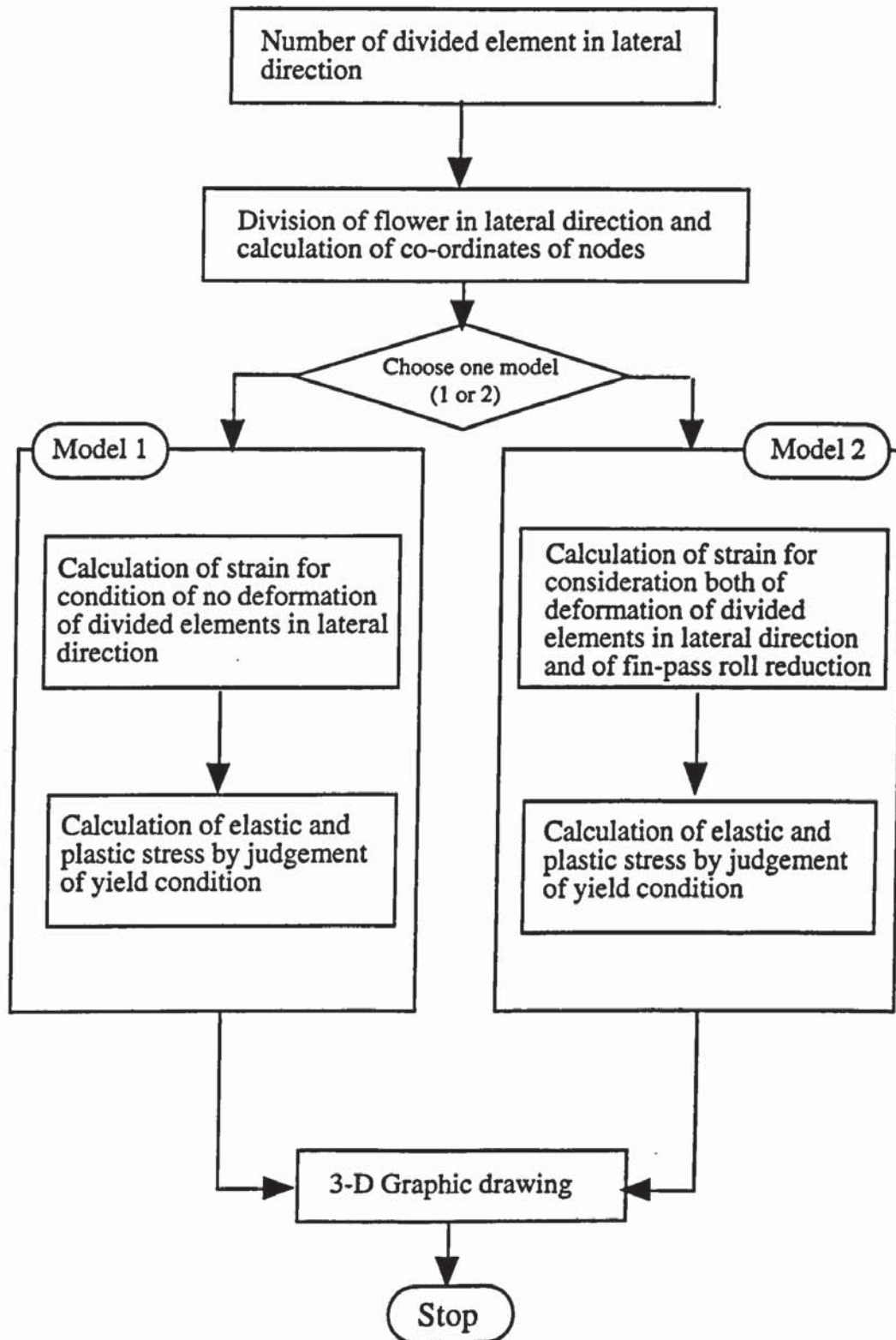


Fig.33 Flow-chart of elastic-plastic stress strain analysis

5.3.2 Model-1 of stress-strain analysis

Fig.34 illustrates the division of the strip into elements in the longitudinal and lateral directions, and the definition of the dimensions of the divided elements in Model-1. The coordinate point $P(i, j)$ of the element (i, j) is defined as the cross point of the line i and the line j as shown in Fig. 34. The length of line element $\Delta l_{(i,j)}$ between the coordinate point $P(i, j)$ and the coordinate point $P(i-1, j)$ is calculated on the basis of simple trigonometry. The coordinate point $P(i, j)$ is defined as $P(i, j)(X(i, j), Y(i, j), Z(i, j))$ and the coordinate point $P(i-1, j)$ is also defined as $P(i-1, j)(X(i-1, j), Y(i-1, j), Z(i-1, j))$. The length of line element $\Delta l_{(i,j)}$ can be calculated by the following equation (4).

$$\Delta l_{(i,j)} = \left\{ \Delta X_{(i,j)}^2 + \Delta Y_{(i,j)}^2 + \Delta Z_{(i,j)}^2 \right\}^{1/2} \quad (4)$$

where,

$\Delta X_{(i,j)} = X_{(i,j)} - X_{(i-1,j)}$ is equal to the inter-stand distance ΔX_i .

$\Delta Y_{(i,j)} = Y_{(i,j)} - Y_{(i-1,j)}$

$\Delta Z_{(i,j)} = Z_{(i,j)} - Z_{(i-1,j)}$

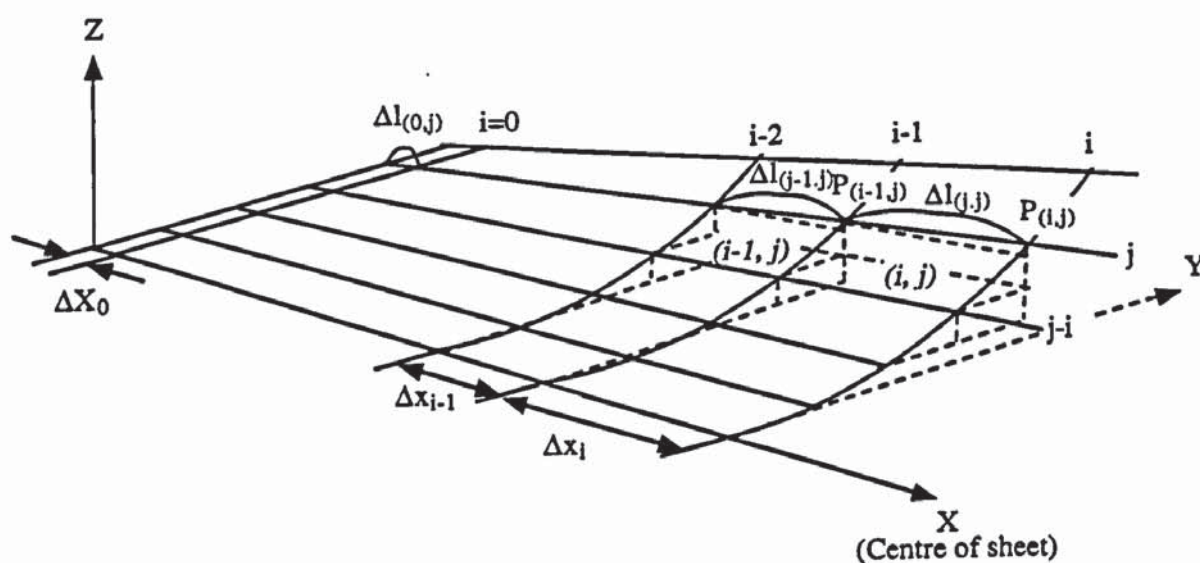


Fig.34 Schematic diagram of division of strip into elements and definition of dimensions of divided elements in Model-1.

The longitudinal membrane strain increment $d\varepsilon_x(i,j)$ and membrane strain $\varepsilon_x(i,j)$ in each element can be calculated by the following equations (5) and (6). In the equation (5), the difference of the inter-stand distance between the element $(i-1, j)$ and the element (i, j) is taken into consideration since the longitudinal divided length according to the inter-stand distance is not always equal.

$$d\varepsilon_x(i,j) = \ln \left\{ \frac{\Delta l(i,j) \Delta X_{i-1}}{\Delta l(i-1,j) \Delta X_i} \right\} \quad (5)$$

where, ΔX_{i-1} is the inter-stand distance between the $i-2$ stand and the $i-1$ stand and ΔX_i is the inter-stand distance between the $i-1$ stand and the i stand.

The longitudinal membrane strain $\varepsilon_x(i,j)$ can be calculated as the summation of the longitudinal membrane strain increment $d\varepsilon_x(i,j)$ by the following equation (6):

$$\begin{aligned} \varepsilon_x(i,j) &= \sum_{i=1}^i d\varepsilon_x(i,j) \\ &= \ln \{ (\Delta l_{(1,j)} \Delta X_0) / (\Delta l_{(0,j)} \Delta X_1) \} + \ln \{ (\Delta l_{(2,j)} \Delta X_1) / (\Delta l_{(1,j)} \Delta X_2) \} + \dots \\ &\dots + \ln \{ (\Delta l_{(i-1,j)} \Delta X_{i-2}) / (\Delta l_{(i-2,j)} \Delta X_{i-1}) \} + \ln \{ (\Delta l_{(i,j)} \Delta X_{i-1}) / (\Delta l_{(i-1,j)} \Delta X_i) \} \\ &= \ln \{ (\Delta l_{(i,j)} \Delta X_0 / \Delta l_{(0,j)} \Delta X_i) \} = \ln \{ \Delta l_{(i,j)} / \Delta X_i \} \end{aligned} \quad (6)$$

where, $\Delta l_{(0,j)}$ is equal to ΔX_0 .

The lateral membrane strain increment $d\varepsilon_y(i,j)$ is defined by introducing the ratio λ of the longitudinal membrane strain to the lateral membrane strain since it is very difficult to calculate both strains simultaneously and the longitudinal strain is more effective and larger than the lateral strain in the cold roll forming. The lateral membrane strain increment $d\varepsilon_y(i,j)$ and the lateral membrane strain $\varepsilon_y(i,j)$ can be calculated by the following equations (7) and (8):

$$d\varepsilon_y(i, j) = -\lambda d\varepsilon_x(i, j) \quad (7)$$

$$\varepsilon_y(i, j) = \sum_{i=1}^i d\varepsilon_y(i, j) = -\lambda \varepsilon_x(i, j) \quad (8)$$

λ is the ratio of $\varepsilon_y/\varepsilon_x$ and takes the appropriate value between 0 and 1.0

Fig.35(a) shows the more detailed illustration and definition of the dimensions of the divided elements in Model-1. Model-1 has discontinuous deformation of the elements in the lateral direction. Since the coordinate point P(i, j) of the element (i, j) has already been defined, the width $\Delta b(i, j)$ of the element (i, j) can be calculated by the following equations(9) and (10):

$$d\varepsilon_y(i, j) = \ln \{ \Delta b(i, j) / \Delta b(i-1, j) \} \quad (9)$$

$$\Delta b(i, j) = \Delta b(i-1, j) e^{d\varepsilon_y(i, j)} \quad (10)$$

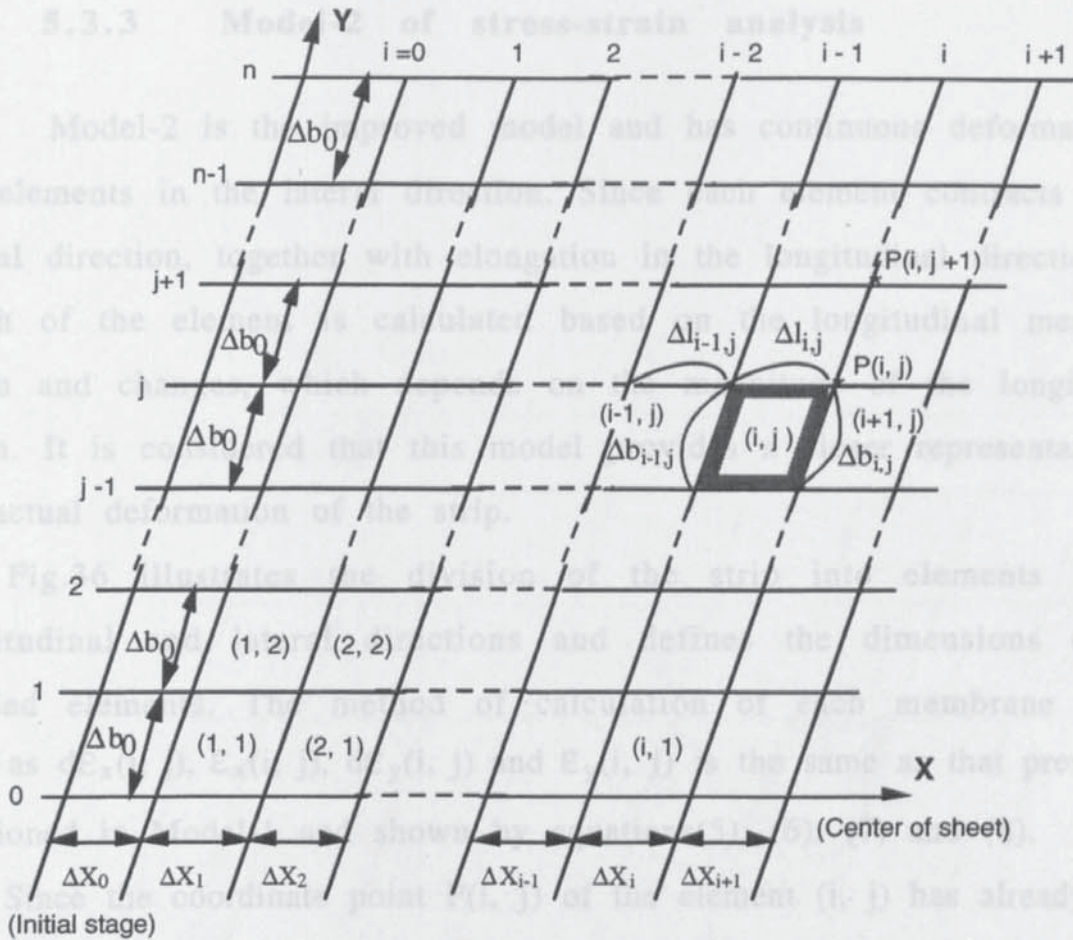
Model-1 does not accommodate the adjustment of the coordinate points in the lateral direction, owing to the deformation of elements. Thus, if the strip expands in the longitudinal direction and contracts in the lateral direction then, each element has a small clearance between elements close to each other in the lateral direction. The above mentioned deformation is shown schematically in Fig.35(b).

5.3.3

Model-2 of stress-strain analysis

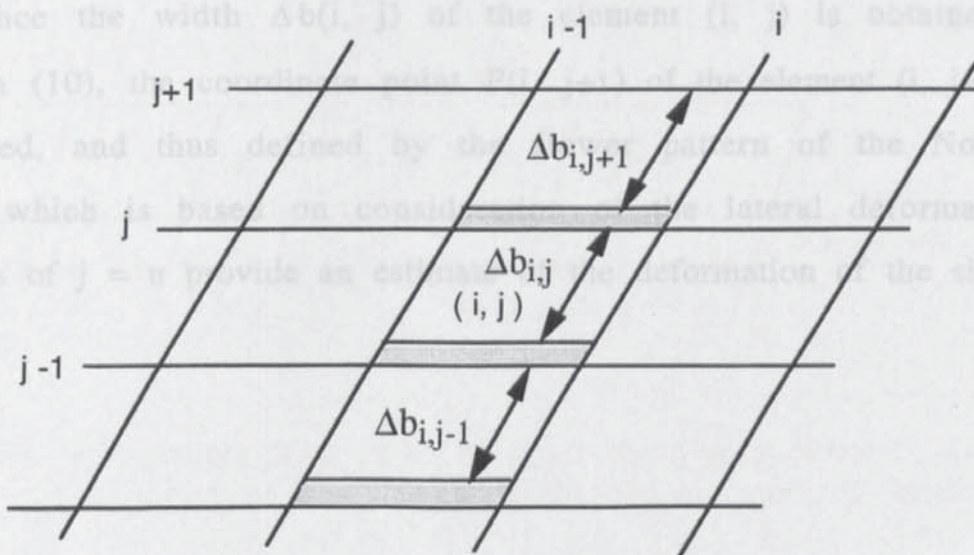
Model-2 is the improved model and has continuous deformation of the elements in the lateral direction. The calculation of the longitudinal strain and the lateral strain is calculated based on the longitudinal membrane strain and the lateral strain. It is considered that this model is a good representation to the actual deformation of the strip.

Fig. 25 illustrates the division of the strip into elements in the longitudinal direction. The method of calculation of each membrane strain, such as $\epsilon_{(i,j)}$ and $\epsilon_{(i,j)}$, is the same as that previously mentioned. The coordinate point (i,j) of the element (i,j) has already been defined, the width $\Delta b_{(i,j)}$ of the element (i,j) can be calculated by the equation



(a) Definition of dimensions of divided elements in Model-1

Since the width $\Delta b_{(i,j)}$ of the element (i,j) is obtained by the equation (10), $\Delta b_{(i,j)}$ can be calculated, and thus defined by the width of the element (i,j) stand (pass), which is based on considering lateral deformation. The elements of $j = n$ provide an estimate of deformation at the sheet edge.



(b) Occurrence of small clearance for elements in Model-1

Fig.35 Definition of dimensions of divided elements and their deformation without adjustment of coordinate points in the lateral direction in Model-1

5.3.3 Model-2 of stress-strain analysis

Model-2 is the improved model and has continuous deformation of the elements in the lateral direction. Since each element contracts in the lateral direction, together with elongation in the longitudinal direction, the width of the element is calculated based on the longitudinal membrane strain and changes, which depends on the magnitude of the longitudinal strain. It is considered that this model provides a closer representation to the actual deformation of the strip.

Fig.36 illustrates the division of the strip into elements in the longitudinal and lateral directions and defines the dimensions of the divided elements. The method of calculation of each membrane strain, such as $d\epsilon_x(i, j)$, $\epsilon_x(i, j)$, $d\epsilon_y(i, j)$ and $\epsilon_y(i, j)$ is the same as that previously mentioned in Model-1 and shown by equations(5), (6), (7) and (8).

Since the coordinate point $P(i, j)$ of the element (i, j) has already been defined, the width $\Delta b(i, j)$ of the element (i, j) can be calculated by the equation (10) that previously mentioned.

Since the width $\Delta b(i, j)$ of the element (i, j) is obtained by the equation (10), the coordinate point $P(i, j+1)$ of the element $(i, j+1)$ can be calculated, and thus defined by the flower pattern of the No.(i) stand (pass), which is based on consideration of the lateral deformation. The elements of $j = n$ provide an estimate of the deformation of the sheet edge.

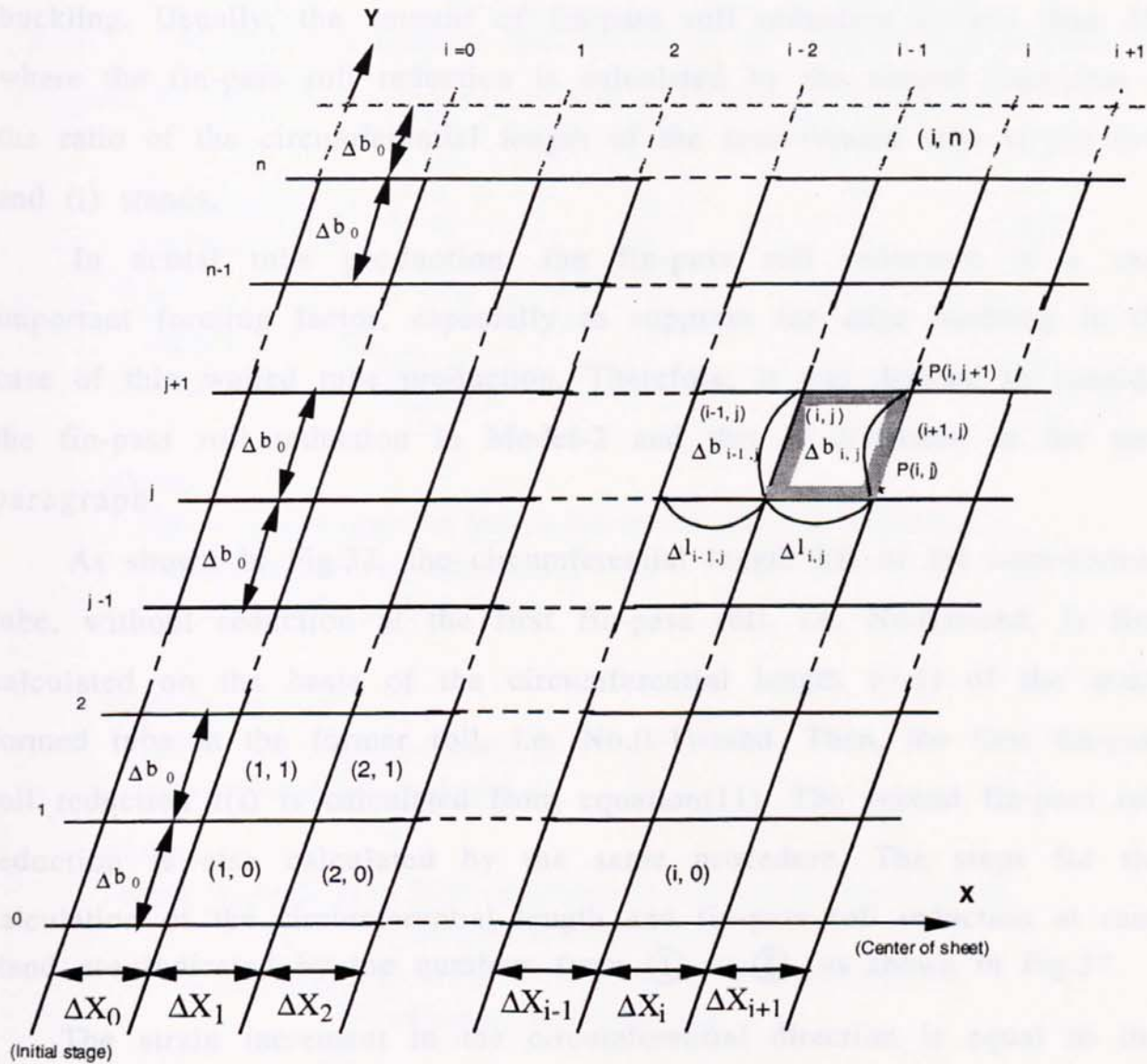


Fig.36 Illustration of division of sheet metal into elements and definition of dimensions of divided elements in Model-2

5.3.4 Consideration of fin-pass roll reduction

In fin-pass roll forming, the circumferential length of the semi-formed tube is reduced at each fin-pass roll, in order to get an appropriate edge shape for the electric resistance welding and to suppress the edge buckling. Usually, the amount of fin-pass roll reduction is less than 2%, where the fin-pass roll reduction is calculated by the natural logarithm of the ratio of the circumferential length of the semi-formed tube at the (i-1) and (i) stands.

In actual tube production, the fin-pass roll reduction is a very important forming factor, especially to suppress the edge buckling in the case of thin walled tube production. Therefore, it was decided to consider the fin-pass roll reduction in Model-2 and this is discussed in the next paragraph.

As shown in Fig.37, the circumferential length $l(i)$ of the semi-formed tube, without reduction at the first fin-pass roll, i.e. No.(i)stand, is first calculated on the basis of the circumferential length $l(i-1)$ of the semi-formed tube at the former roll, i.e. No.(i-1)stand. Then, the first fin-pass roll reduction $r(i)$ is calculated from equation(11). The second fin-pass roll reduction is also calculated by the same procedure. The steps for the calculation of the circumferential length and fin-pass roll reduction at each stand are indicated by the numbers from ① to ⑤, as shown in Fig.37.

The strain increment in the circumferential direction is equal to the fin-pass roll reduction. The definition of the strain components in the fin-pass roll forming is shown in Fig.38. In the CADFORM system the strain component in the thickness direction is ignored as stated by the membrane theory. The relationship between the strain $d\epsilon_y(i, j)$ in the circumferential direction and the strain $d\epsilon_x(i, j)$ in the longitudinal direction is defined by equation(12) in order to simplify the modelling.

The actual deformation of the semi-formed tube in the fin-pass roll is not uniform in the circumferential direction, however, uniform

deformation is assumed in the circumferential direction. According to the results of some investigations^{4,6,36} regarding the deformation behaviour of the semi-formed tube in the fin-pass and sizing stage, the ratio of $d\epsilon_x(i, j)/d\epsilon_y(i, j)$ takes an appropriate value between 0.35 and 0.5. Thus, a mean value of 0.45 was applied in the calculations using the CADFORM system. The strain increments and strains in the fin-pass roll forming are calculated by the following analysis and equations (13) and (14):

$$\left. \begin{aligned} r(i) &= \ln(l(i)/l_r(i)) \\ l_r(i) &= l(i) e^{-r(i)} \end{aligned} \right\} \quad (11)$$

$$\left. \begin{aligned} d\epsilon_{fy}(i, j) &= -r(i) \\ d\epsilon_{fx}(i, j) &= -\lambda_F d\epsilon_{fy}(i, j) \end{aligned} \right\} \quad (12)$$

where,

$l_r(i)$ = Circumferential length due to fin-pass roll reduction

$r(i)$ = Fin-pass roll reduction at i stand

λ_F = the ratio of $d\epsilon_{fx} / d\epsilon_{fy}$

Strain increment

$$\left. \begin{aligned} d\epsilon_x(i, j) &= d\epsilon_x(i, j) + d\epsilon_{fx}(i, j) \\ d\epsilon_y(i, j) &= d\epsilon_y(i, j) + d\epsilon_{fy}(i, j) \end{aligned} \right\} \quad (13)$$

where,

$d\epsilon_x(i, j), d\epsilon_y(i, j)$ = Strain increments without consideration of
fin-pass roll reduction

$d\epsilon_x(i, j), d\epsilon_y(i, j)$ = Strain increments with consideration of
fin-pass roll reduction

Strain

$$\left. \begin{aligned} \epsilon_x(i, j) &= \epsilon_x(i, j) + d\epsilon_{fx}(i, j) \\ \epsilon_y(i, j) &= \epsilon_y(i, j) + d\epsilon_{fy}(i, j) \end{aligned} \right\} \quad (14)$$

where,

$\epsilon_x(i, j), \epsilon_y(i, j)$ = Strains without consideration of
fin-pass roll reduction

$\epsilon_x(i, j), \epsilon_y(i, j)$ = Strains with consideration of
fin-pass roll reduction

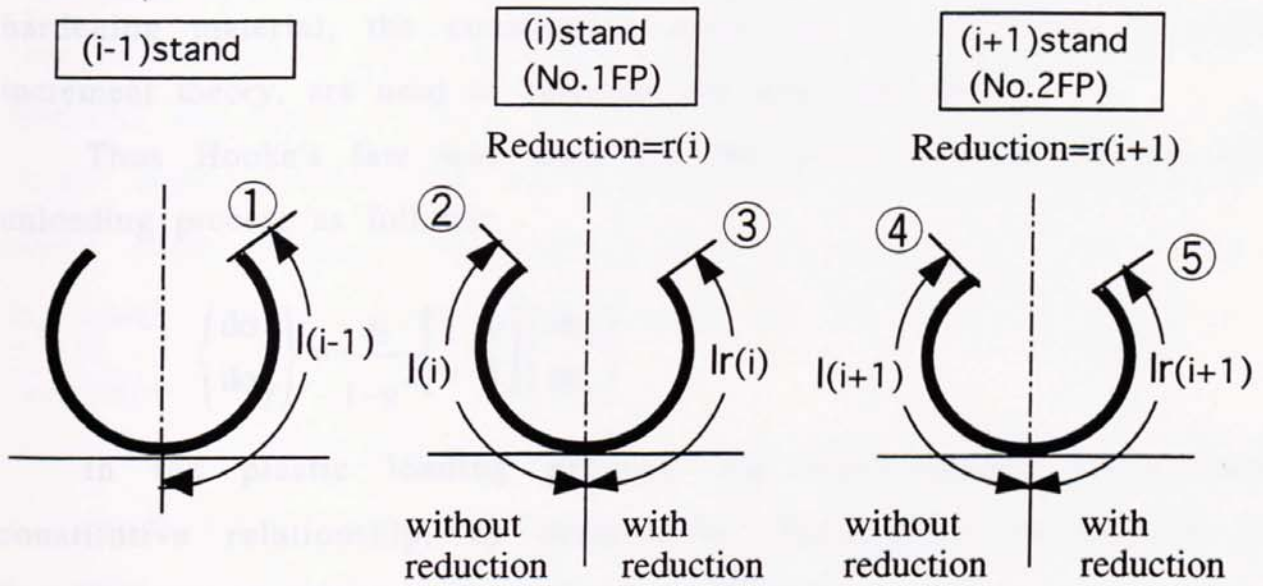


Fig.37 Procedure for consideration of fin-pass roll reduction

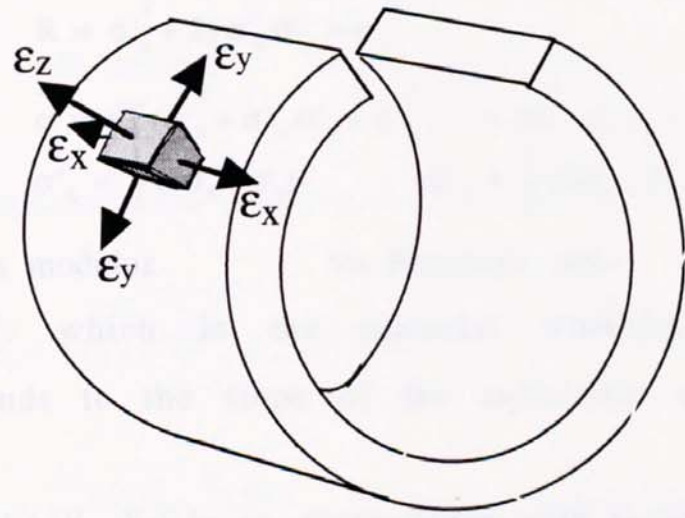


Fig.38 Definition of strain components in fin-pass roll forming

5.3.5 Elastic-plastic stress-strain analysis

In the deformation of the strip, assuming an elastic-linear work-hardening material, the constitutive equations, on the basis of strain increment theory, are used to calculate the stress and strain.

Thus Hooke's law was used for the elastic loading process and unloading process as follows:

$$\begin{pmatrix} d\sigma_x \\ d\sigma_y \end{pmatrix} = \frac{E}{1-\nu^2} \begin{bmatrix} 1 & \nu \\ \nu & 1 \end{bmatrix} \begin{pmatrix} d\varepsilon_x \\ d\varepsilon_y \end{pmatrix} \quad (15)$$

In the plastic loading process, the elastic-plastic stress-strain constitutive relationship, as derived by Yamada⁴⁶, (an inversion of Prandtl-Reuss equations) was utilised as follows:

$$\begin{pmatrix} d\sigma_x \\ d\sigma_y \end{pmatrix} = \frac{E}{Q} \begin{bmatrix} \sigma_y'^2 + 2P & -\sigma_x' \sigma_y' + 2\nu P \\ -\sigma_x' \sigma_y' + 2\nu P & \sigma_x'^2 + 2P \end{bmatrix} \begin{pmatrix} d\varepsilon_x \\ d\varepsilon_y \end{pmatrix} \quad (16)$$

where,

$$\begin{aligned} P &= \frac{2H}{9E} \sigma^2 & Q &= R + 2(1-\nu^2)P \\ R &= \sigma_x'^2 + 2\nu\sigma_x'\sigma_y' + \sigma_y'^2 \\ \sigma &= \sqrt{3} (\sigma_x'^2 + \sigma_x'\sigma_y' + \sigma_y'^2)^{1/2} = (\sigma_x^2 - \sigma_x\sigma_y + \sigma_y^2)^{1/2} \\ \sigma_x' &= \frac{1}{3}(2\sigma_x - \sigma_y) & \sigma_y' &= \frac{1}{3}(2\sigma_y - \sigma_x) \end{aligned}$$

E = Young's modulus

ν = Poisson's ratio

$H = \overline{d\sigma} / \overline{d\varepsilon^p}$, which is the material work-hardening rate and corresponds to the slope of the equivalent stress-plastic strain curve,

$H = (E \times E_t) / (E - E_t)$ in an elastic-linear work hardening material.

E_t = Tangent modulus, and

σ_x' and σ_y' are deviatoric stresses

The method of determining the yielding of the material is now described. As shown in Fig.39, it is assumed that the material is deformed from point A to point B, and then to point C, where B is the yield point. This deformation of the material is shown in Fig.40 using the stress-strain diagram. The material has a strain increment $d\bar{\epsilon}$, which consists of the elastic strain increment $d\bar{\epsilon}_e$, due to passing from A to B, and the elastic-plastic strain increment $d\bar{\epsilon}_{(p+\epsilon)}$, due to passing from B to C. Thus, $d\epsilon_x^e$ and $d\epsilon_y^e$, which define $d\bar{\epsilon}_e$, can be obtained by the solution given in the next paragraph.

It is considered that the stress increments, $d\sigma_x^e$ and $d\sigma_y^e$ from point A to point B, causes yielding of the material. The yielding of the material, in the plane stress condition of the von Mises yield criterion, is represented by the following equations (17) and (18).

$$\bar{\sigma} = \left\{ \left(\sigma_{x(k-1)} + d\sigma_x^e \right)^2 - \left(\sigma_{x(k-1)} + d\sigma_x^e \right) \left(\sigma_{y(k-1)} + d\sigma_y^e \right) + \left(\sigma_{y(k-1)} + d\sigma_y^e \right)^2 \right\}^{1/2} \quad (17)$$

$$\sigma_Y = \bar{\sigma} \quad (18)$$

where,

$\sigma_Y =$ Yield strength

$\bar{\sigma} =$ Equivalent stress

The following equation (19) is obtained from the equations (17) and (18).

$$\left(d\sigma_x^e{}^2 - d\sigma_x^e d\sigma_y^e + d\sigma_y^e{}^2 \right) + 3 \left(\sigma'_{x(k-1)} d\sigma_x^e + \sigma'_{y(k-1)} d\sigma_y^e \right) + \sigma_{(k-1)}^2 - \sigma_Y^2 = 0 \quad (19)$$

where,

$$\sigma'_{x(k-1)} = \frac{2\sigma_{x(k-1)} - \sigma_{y(k-1)}}{3} \quad \sigma'_{y(k-1)} = \frac{2\sigma_{y(k-1)} - \sigma_{x(k-1)}}{3}$$

$$\bar{\sigma}_{(k-1)} = \left(\sigma_{x(k-1)}^2 - \sigma_{x(k-1)} \sigma_{y(k-1)} + \sigma_{y(k-1)}^2 \right)^{1/2}$$

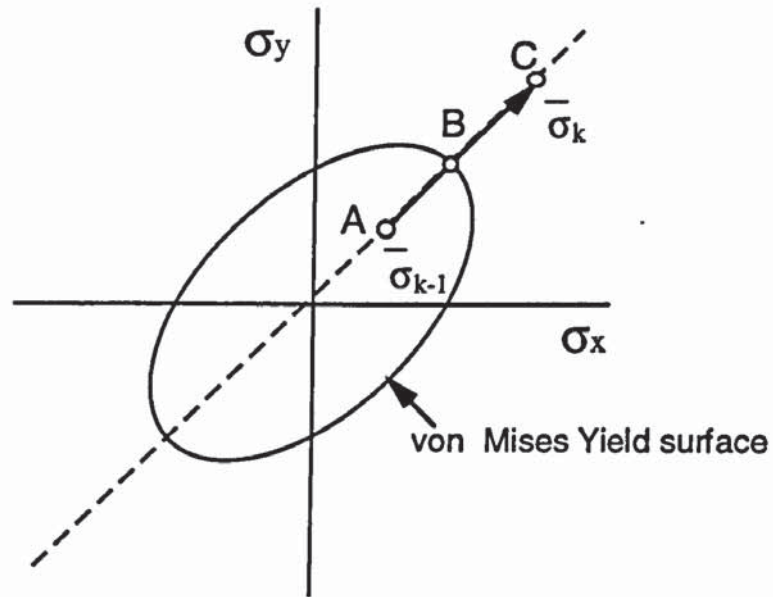


Fig.39 Schematic diagram of the von Mises yield criterion for material yielding in the plane stress condition

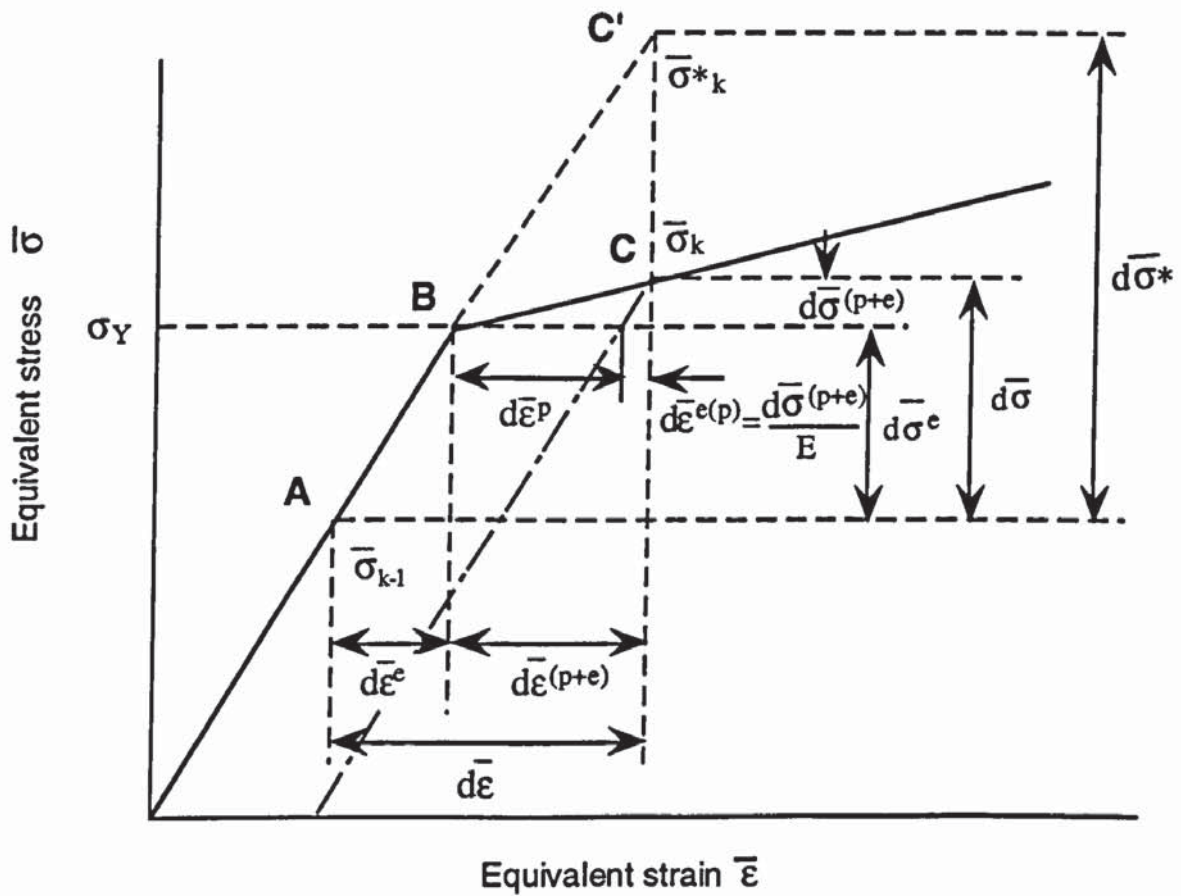


Fig.40 Definition of elastic and plastic strain increments in yielding of material

By assuming the elastic deformation from point A to point C', the stress increments $d\sigma_x$ and $d\sigma_y$ are obtained. Thus, the following relationships between stress and strain are defined:

$$d\sigma_x^e = d\sigma_x \left(\frac{d\varepsilon_x^e}{d\varepsilon_x} \right) \quad (20)$$

$$d\sigma_y^e = d\sigma_y \left(\frac{d\varepsilon_y^e}{d\varepsilon_y} \right) = d\sigma_y \left(\frac{d\varepsilon_x^e}{d\varepsilon_x} \right) \quad (21)$$

where,

$$\frac{d\varepsilon_x^e}{d\varepsilon_x} = \frac{d\varepsilon_y^e}{d\varepsilon_y}$$

The following equation (22), from which the elastic strain increment $d\varepsilon_x^e$ may be obtained, is derived from equations (19), (20) and (21).

$$\left(d\sigma_x^2 - d\sigma_x d\sigma_y + d\sigma_y^2 \right) \left(\frac{d\varepsilon_x^e}{d\varepsilon_x} \right)^2 + 3 \left(\sigma'_x d\sigma_x + \sigma'_y d\sigma_y \right) \left(\frac{d\varepsilon_x^e}{d\varepsilon_x} \right) + \sigma_{(k-1)}^{-2} - \sigma_Y^2 = 0 \quad (22)$$

where the subscript (k-1) is omitted from $d\sigma_x$, $d\sigma_y$, σ'_x and σ'_y .

The elastic strain increment $d\varepsilon_x^e$, which causes the yielding of the material, can be obtained by the solution of equation (22). The eight different patterns of the yielding condition are defined in order to obtain the elastic strain increment $d\varepsilon_x^e$, and are shown in Fig.41. The stress-strain analysis for the plastic deformation is carried out by using the elastic-plastic strain increments, $d\varepsilon_x^{(p+e)}$ and $d\varepsilon_y^{(p+e)}$, which are calculated by the following equations (23).

$$\left. \begin{aligned} d\varepsilon_x^{(p+e)} &= d\varepsilon_x - d\varepsilon_x^e \\ d\varepsilon_y^{(p+e)} &= d\varepsilon_y - d\varepsilon_y^e \end{aligned} \right\} (23)$$

Furthermore, Hooke's law shown in the equation (15) is applied in the unloading process in the plastic deformation region as shown in Fig.40.

The plastic strain increments $d\epsilon_x^p$ and $d\epsilon_y^p$ can be calculated by the following equation (23):

$$\left. \begin{aligned} d\epsilon_x^p &= d\epsilon_x^{(p+e)} - d\epsilon_x^{e(p)} = d\epsilon_x^{(p+e)} - \frac{d\sigma_x^{(p+e)}}{E} \\ d\epsilon_y^p &= d\epsilon_y^{(p+e)} - d\epsilon_y^{e(p)} = d\epsilon_y^{(p+e)} - \frac{d\sigma_y^{(p+e)}}{E} \end{aligned} \right\} (24)$$

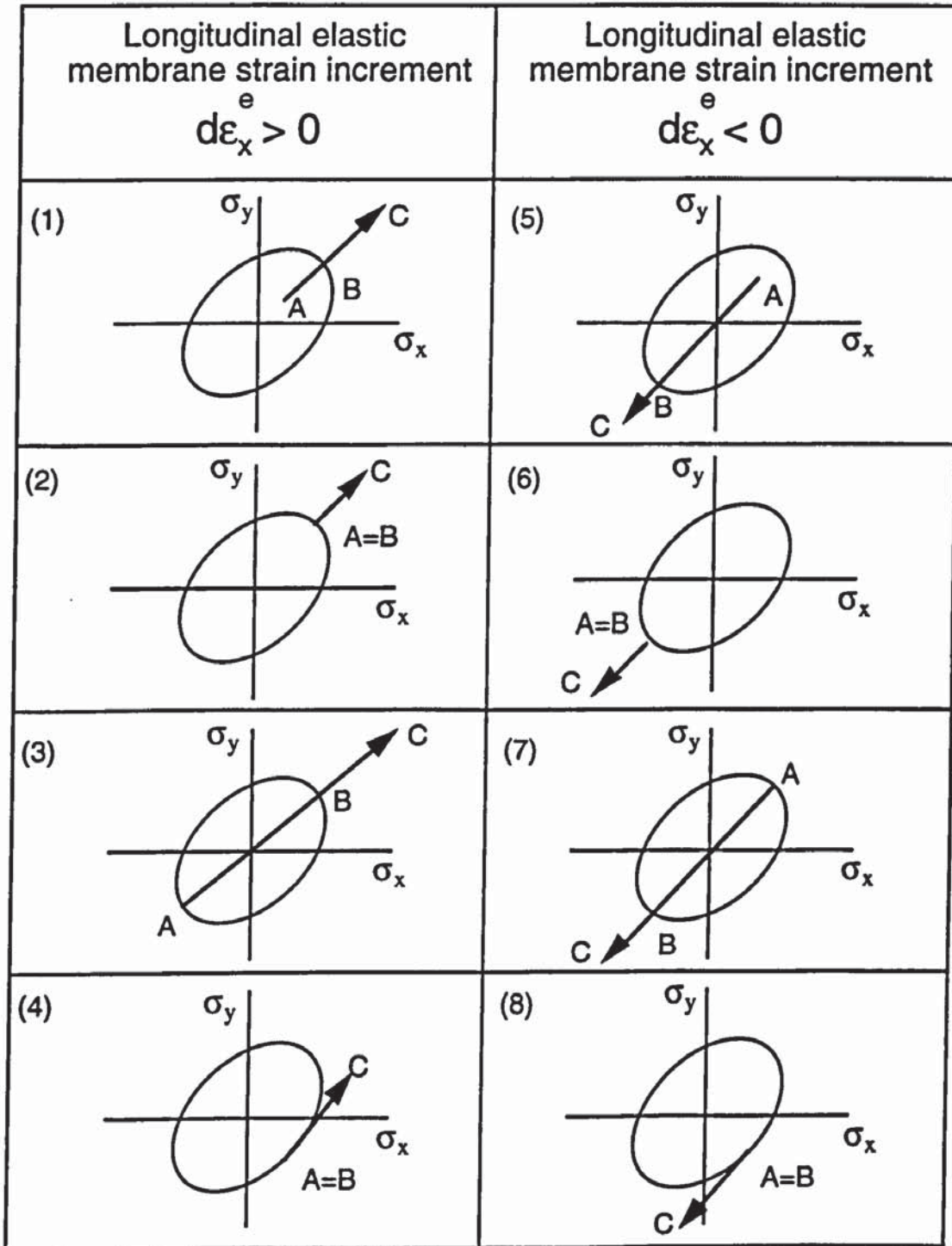


Fig.41 Pattern of material yielding conditions to obtain the elastic increment strain

5.4 Algorithm of elastic-plastic, stress-strain analysis

On the basis of the previously mentioned procedures of the elastic-plastic, stress-strain analysis, the flow-chart of the stepwise analysis of strains of the divided elements in Model-2 has been devised as shown in Fig.42. Furthermore, the calculation of the node coordinates in each forming stand has already been carried out prior to the commencement of this analysis. Thus membrane strain increments and membrane strains are first calculated and the coordinates of nodes in the lateral direction are then recalculated. Finally, the fin-pass roll reduction is considered at the forming stage for that particular roll stand.

The flow-chart of the stepwise analysis of stresses of the divided elements in Model-2 is then devised and shown in Fig.43. Stress increments are first calculated by using strain increments calculated in the previously explained strain analysis. Stresses are calculated by stress increments and the equivalent stress is then obtained. Secondly, the yielding condition is evaluated and the yielding pattern determined. Then, elastic-plastic strain increments and stress increments are calculated. In particular, plastic stress increments are calculated by equation (16). Finally, stresses are obtained from the stresses generated at the former stand and the stress increments.

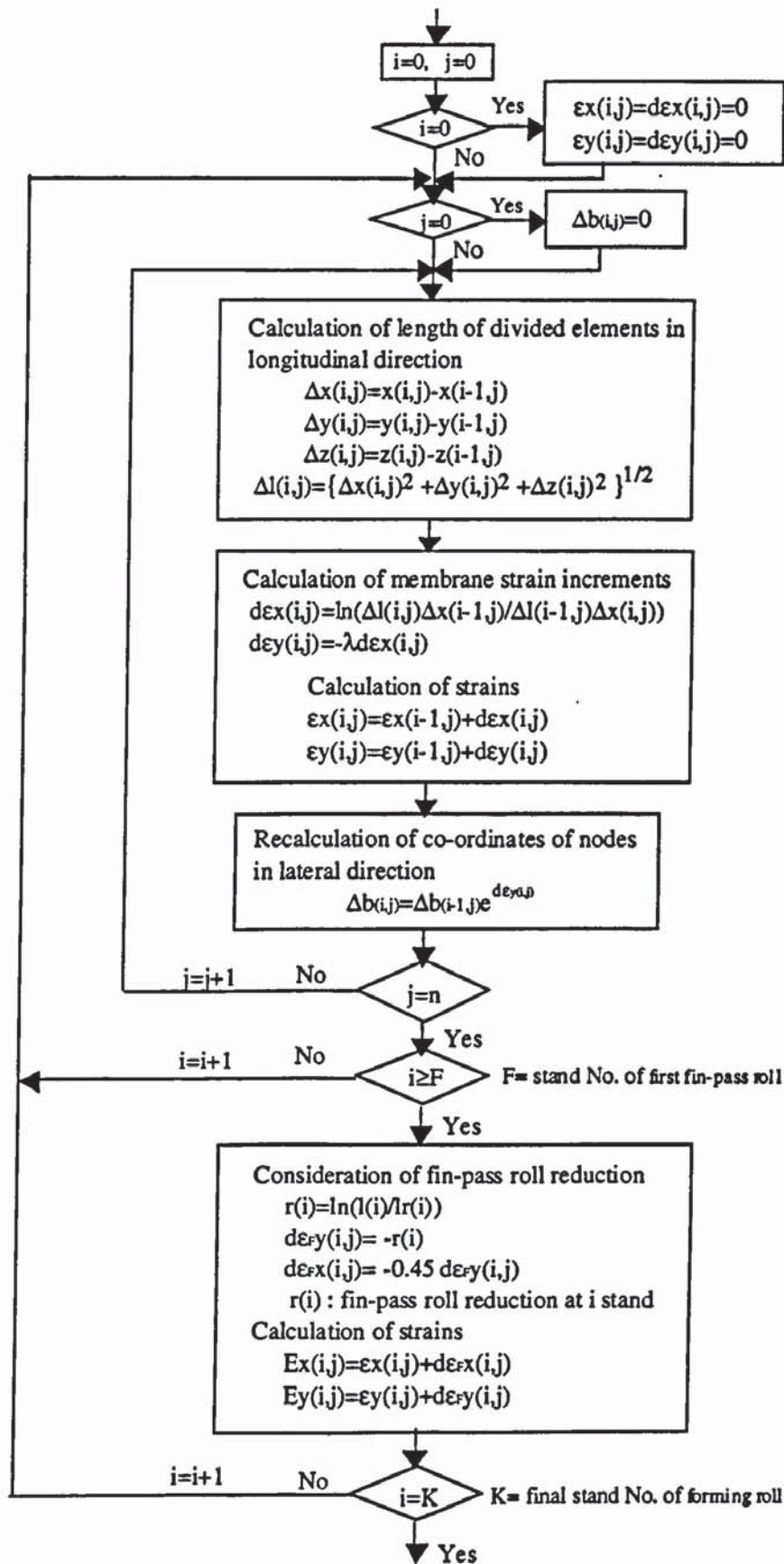


Fig.42 Flow-chart of stepwise analysis of strains of divided elements in Model-2

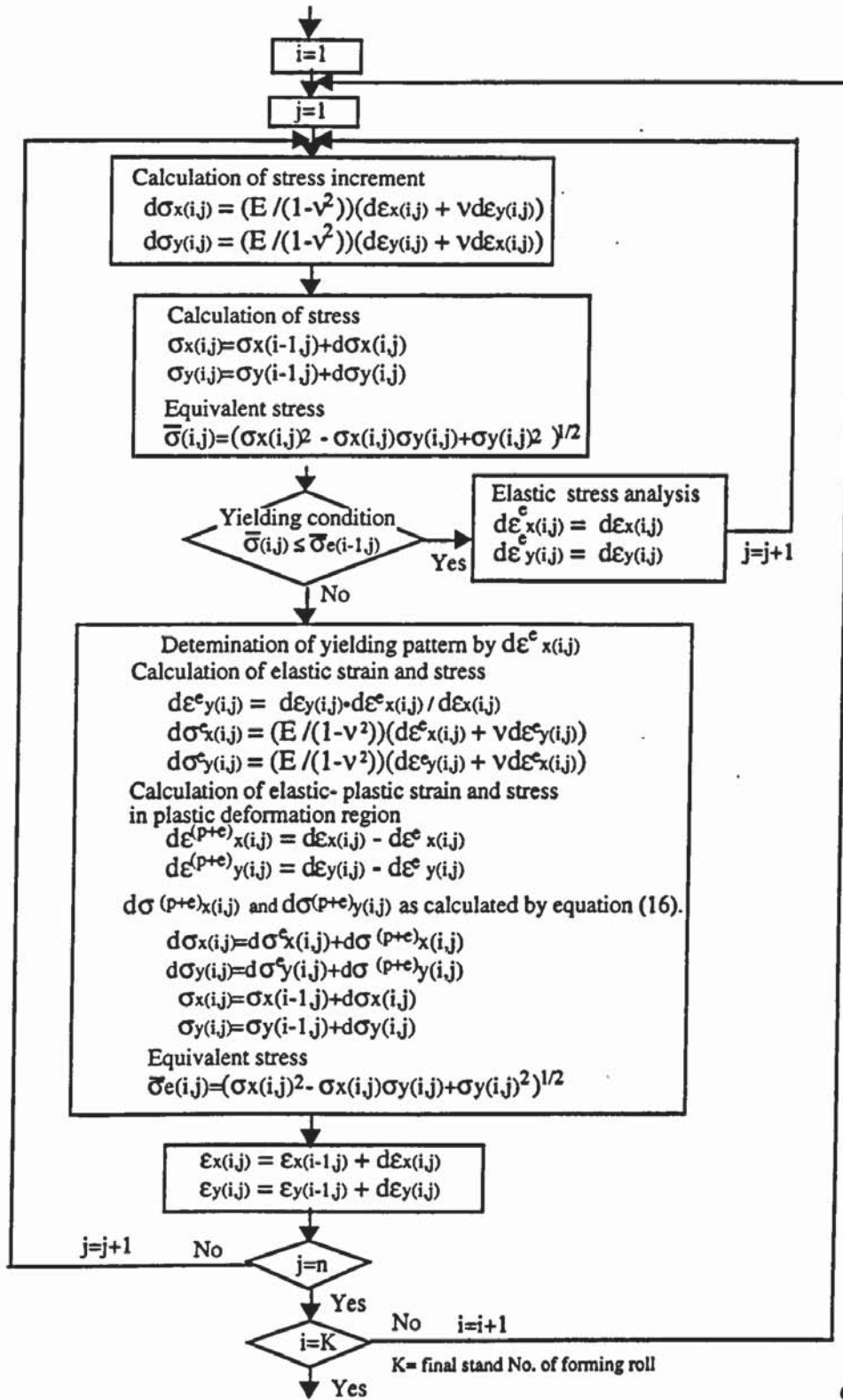


Fig.43 Flow-chart of stepwise analysis of stresses of divided elements in Model-2

5.5 Evaluation of edge buckling

In order to make a model of edge buckling of the tube, the buckling model of a long column was applied. Divided elements in the lateral direction between roll stands were considered as thin walled columns respectively to realise a evaluation of edge buckling of the tube as shown in Fig.44. Fig.44 shows the model of edge buckling at the strip edge where the tensile strains in the longitudinal direction are generally occurred. However, compressive stresses are acted at both sides of these divided elements at the strip edge due to decrease in tensile strains shown in Fig.44. Thus, when the compressive stress in the longitudinal direction is acted at both sides of the divided element at the strip edge, it is estimated whether this divided element at the strip edge is buckled.

In this model, the Euler⁶¹ theory was applied to the elastic buckling in the elastic deformation and both of the tangent modulus theory and the reduced modulus theory were also applied to the plastic buckling in the plastic deformation. Furthermore, the edge buckling generally occurs at the edge portion within ten percent of the total lateral width of the strip sheet and a single edge buckling usually occurs at the strip edge between roll stands as shown in Photo.6. Photo.6 shows an appearance of a single edge buckling at the strip edge in actual production of thin walled pipe with $D = 146.0\text{mm}$, $t = 2.0\text{mm}$ and $\sigma_Y = 730 \text{ MPa}$. Thus, this simplified buckling model was considered. The following assumptions are introduced in order to simplify the edge buckling analysis.

- (1) The stress $\sigma_{(i,n)}$, obtained by the stress analysis, acts homogeneously on the element (i,n) , with the wall-thickness(t) forming the edge portion of the tube.
- (2) The force obtained by $\sigma_{(i,n)} \times A$ acts at both sides of the element (i,n) , that is at the No.($i-1$) stand and No.(i) stand, where A is the cross sectional area of the element.

- (3) The lateral region of the strip which is subjected to the occurrence of edge buckling, is limited by the number of elements in the lateral direction of this model. However, it is necessary that the dimensions of the actual affected areas and the effects of tube sizes on the edge buckling, are investigated in the tube-making experiments.
- (4) The divided element has the cross section with sector of hollow circle in the longitudinal direction as shown in Fig.45.

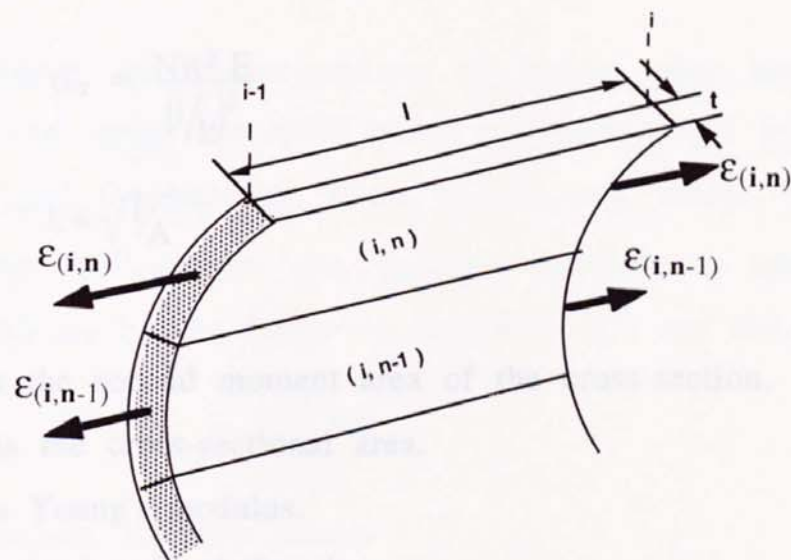


Fig.44 Model of edge buckling at strip edge



Photo.6 Appearance of edge buckling in actual production of thin walled pipe with $D = 146.0\text{mm}$, $t = 2.0\text{mm}$ and $\sigma_Y = 730\text{MPa}$.

The judgement of the occurrence of elastic edge buckling can be carried out by comparing the acted stress $\bar{\sigma}_{(i)}$ represented by the following equations (22) and (23), and the buckling stress σ_{cr} , obtained by equations based on the Euler⁶¹ equation (24), as follows:

$$\bar{\sigma}_{(i)} = f(\sigma_{(i, n-k)}, \dots, \sigma_{(i, n)}) \quad (22)$$

For example,

$$\bar{\sigma}_{(i)} = \frac{\sum_{j=n-k}^n \sigma_{(i, j)}}{k+1} \quad (23)$$

$$\sigma_{cr} = \frac{N\pi^2 E}{(l/k)^2} \quad (24)$$

$$k = \sqrt{I/A}$$

where,

I is the second moment area of the cross-section.

A is the cross-sectional area.

E is Young's modulus.

l is the length of the element.

N is a constant depending on the condition of the action of the load.

N = 1/4 : one end fixed and one end free

N = 1 : both hinged ends

N = 2 : one end hinged and one end fixed

N = 4 : both fixed ends

I is obtained by the following equation (25) taken into consideration of the sector of the hollow circle⁶² as shown in Fig.45.

$$I = R^3 t \left[\left(1 - \frac{3t}{2R} + \frac{t^2}{R^2} - \frac{t^3}{4R^3} \right) \left(\alpha + \sin \alpha \cos \alpha - \frac{2 \sin^2 \alpha}{\alpha} \right) + \frac{t^2 \sin^2 \alpha}{3R^2 \alpha (2 - t/R)} \left(1 - \frac{t}{R} + \frac{t^2}{6R^2} \right) \right] \quad (25)$$

where, $A = \alpha t (2R - t)$

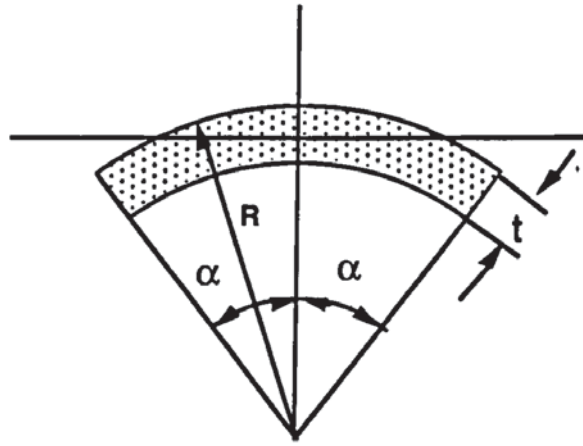


Fig.45 Definition of sector of hollow circle

The judgement of the occurrence of plastic edge buckling can be carried out by comparing the acted stress $\bar{\sigma}_{(i)}$ represented by the equation (22) and (23), and the buckling stress $\sigma_{cr}^* = (\sigma_{cr} + \sigma_Y)$, where σ_{cr} is obtained by the equation (26) where the Young's modulus is replaced to the modulus EE defined by the following equations (27) and (28):

$$\sigma_{cr} = \frac{N\pi^2 EE}{(l/k)^2} \quad (26)$$

(i) Tangent modulus theory

$$EE = E_t \quad (27)$$

(ii) Reduced-modulus theory (Equivalent elastic coefficient)

$$EE = \bar{E} = \frac{4E E_t}{(\sqrt{E} + \sqrt{E_t})^2} \quad (28)$$

where,

E_t is the tangent modulus and \bar{E} is the reduced-modulus.

Generally, E_t provides the smaller buckling stress σ_{cr} as a safer evaluation than \bar{E} provides, because E_t is smaller than \bar{E} .

N is a constant depending on the condition of the action of the load. In this model, the condition of both sides of the divided element are estimated to be both hinged ends $N=1$ or both fixed ends $N=4$ because the strip sheet is pinched by forming rolls.

5.6 Three-dimensional graphic displaying and drawing

The main results, such as the three-dimensional (3-D) deformed surface of the strip, strain increments, strains, stresses and equivalent stress are displayed on the Tektronix colour screen by a newly developed 3-D graphics programme which is associated with the GINO-F graphics package. The definition of the coordinate axes, shown in graphic drawing by the stress-strain analysis, is different from the previous definition, in that the Z-axis is the longitudinal direction and X-axis is the lateral direction.

By converting the coordinates, the 3-D graphics are obtained on the 2-D plane. The displayed objects, i.e. the results, can be viewed from any direction of view by changing the values of the bank θ_B , the heading θ_H , and the pitch θ_P , as shown in Fig.46. The coordinates are converted as follows:

(1) Rotation of Z-axis / bank(θ_B)

$$X = x \cos(\theta_B) - y \sin(\theta_B)$$

$$Y = x \sin(\theta_B) + y \cos(\theta_B)$$

(2) Rotation of Y-axis / heading(θ_H)

$$Z = z \cos(\theta_H) - x \sin(\theta_H)$$

$$X = z \sin(\theta_H) + x \cos(\theta_H)$$

(3) Rotation of X-axis / pitch(θ_P)

$$Y = y \cos(\theta_P) - z \sin(\theta_P)$$

$$Z = y \sin(\theta_P) + z \cos(\theta_P)$$

Furthermore, the scale ratios to emphasise the deformation R_{zx} and R_{zy} , are defined by the following equations (24) and (25):

$$X = P_x(i,j) \cdot \frac{L}{R_{zx} \cdot D} \quad (24)$$

$$Y = P_y(i,j) \cdot \frac{L}{R_{zy} \cdot D} \quad (25)$$

where, L = total length of forming passes

D= outside diameter

These values are optional. In order to emphasise the deformation of the strip, smaller values of R_{zx} and R_{zy} are required. Furthermore, R_{xy} and R_{xz} are usually set at the same value between five and twenty.

The whole programme included in the CADFORM system is shown in Appendix-1.

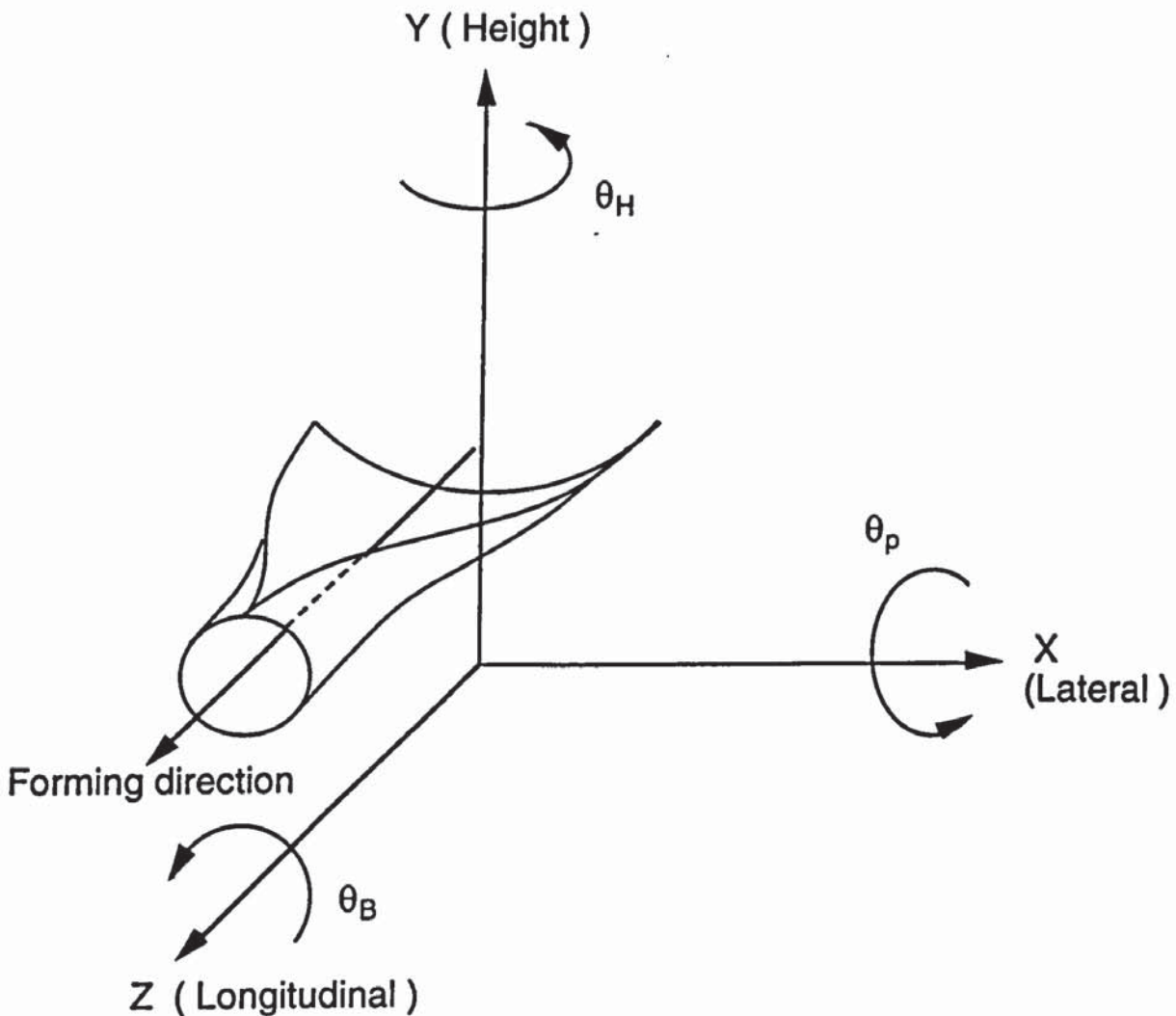


Fig.46 Definition of coordinates and rotation for 3-D drawing

Chapter 6. Results of Calculation by the CADFORM System

6.1 Three-dimensional deformed surface of the strip in the forming passes

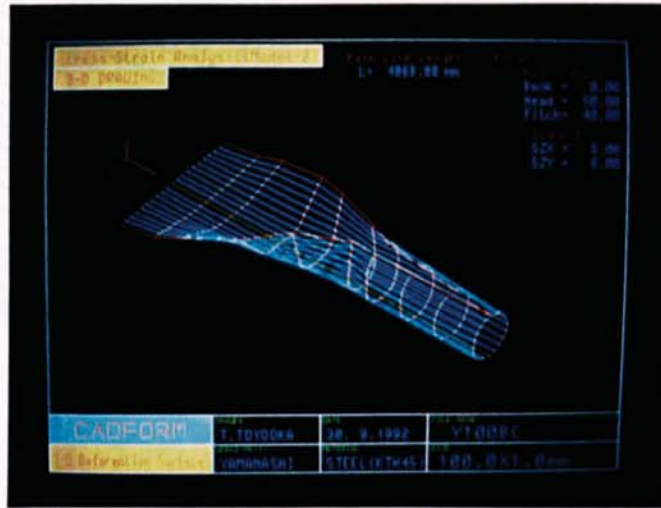
Examples of the three dimensional graphics displayed by the CADFORM system are shown in Photo.7. These photographs express results of the 3-D deformed surface of the strip shown in: (a), the 3-D variation of longitudinal strain ϵ_z ; (b) and the 3-D variation of longitudinal stress σ_z ; (c) in the forming passes of the tube with $D = 100$ mm, $t = 1.0$ mm and $\sigma_Y = 340$ MPa.

Figures 47 and 48 show examples of the 3-D deformed surface of the strip in the forming passes of the tube with $D = 60.5$ mm, $t = 1.75$ mm and $\sigma_Y = 295$ MPa using the 3-D graphics programme. Each drawing shows a view from different directions by changing the values of the bank θ_B , the heading θ_H , and the pitch θ_P , as explained in the previous chapter. Fig.47(a) shows the 3-D deformed surface of the strip viewed from the direction of bank(θ_B) = 0° , heading(θ_H) = 50° and pitch(θ_P) = 40° . Fig.47(b) shows the 3-D deformed surface of the strip viewed from the direction of bank(θ_B) = 0° , heading(θ_H) = 150° and pitch(θ_P) = 30° . Fig.48 shows the 3-D deformed surface of the strip viewed from the direction of bank(θ_B) = 0° , heading(θ_H) = 0° and pitch(θ_P) = 40° . Since the situation for complete deformation can be visualized clearly, the designer can identify the outline of the deformation behaviour of the strip in the forming process.

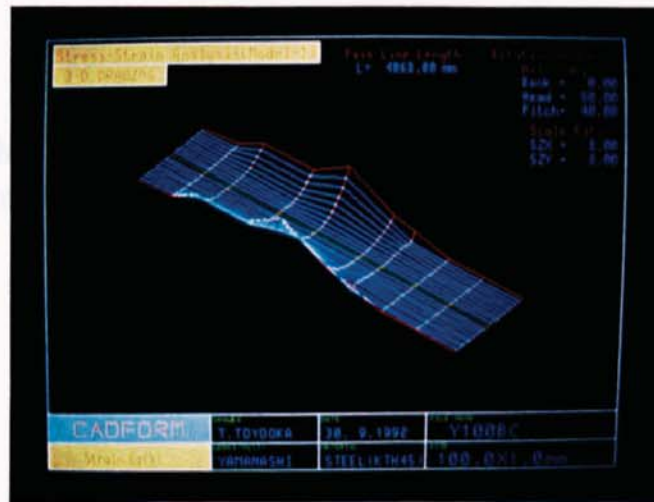
Fig.49 shows an example of the 3-D deformed surface of the strip using different scale ratios of R_{zx} and $R_{zy} = 15, 12$ and 8 . The smaller values of R_{zx} and $R_{zy} = 8$ can emphasise the deformation of the strip as shown in Fig.49(c). Usually, R_{xy} and R_{xz} are preferably used with the same value from five to twenty. The designer can have a different image of the outline of the deformation behaviour of the strip in the forming process by the programme setting of the scale ratios.

Fig.50 shows the drawing of the 3-D deformed surface for the

different pass-line forming conditions of bottom constant pass-line, and downhill pass-line. The downhill pass-line, shown in Fig.50(b), expresses a forming condition in which the vertical position of the forming rolls in the longitudinal direction is gradually reduced compared with the entry position of the strip. This is done in order to suppress the edge buckling. The strip is viewed from the same position, thus the difference in the deformed sheet is due to the difference in the pass-line, which can clearly be visualized.



(a) 3-D deformed surface of strip

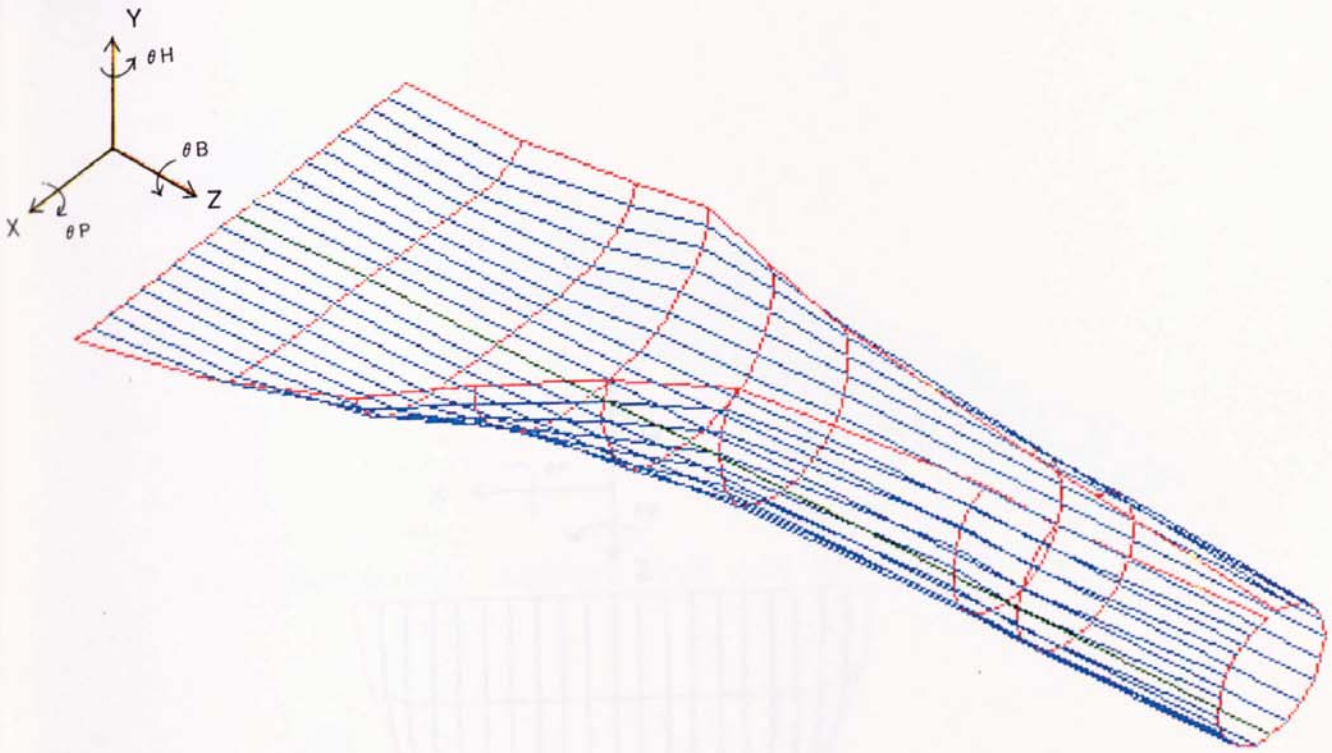


(b) 3-D variation of longitudinal strain ϵ_z

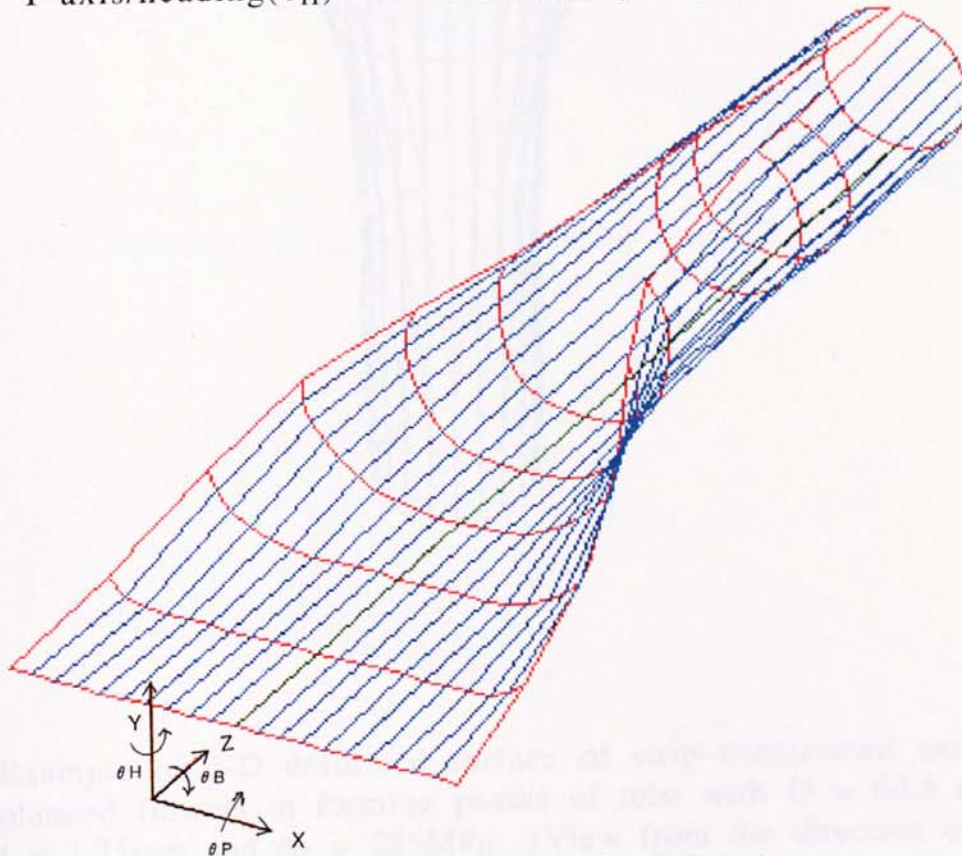


(c) 3-D variation of longitudinal stress σ_z

Photo.7 Examples of 3-D graphics displaying calculated longitudinal stress and strain by the CADFORM system in forming passes of the tube with $D = 100\text{mm}$, $t = 1.0\text{mm}$ and $\sigma_Y = 340\text{MPa}$



(a) View from the direction of Z-axis/bank(θ_B)= 0° ,
Y-axis/heading(θ_H)= 50° and X-axis/pitch(θ_P)= 40°



(b) View from the direction of Z-axis/bank(θ_b)= 0° ,
Y-axis/heading(θ_h)= 150° and X-axis/pitch(θ_p)= 30°

Fig.47 Example of 3-D deformed surface of strip constructed using planned flowers in forming passes of tube with $D = 60.5\text{mm}$, $t = 1.75\text{mm}$ and $\sigma_Y = 295\text{MPa}$.

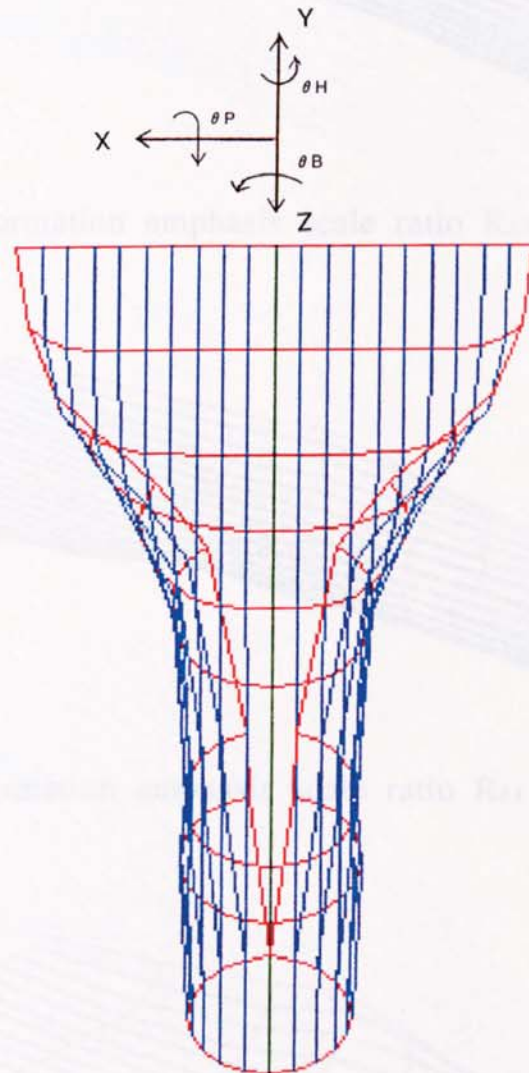


Fig.48 Example of 3-D deformed surface of strip constructed using planned flowers in forming passes of tube with $D = 60.5$ mm, $t = 1.75$ mm and $\sigma_Y = 295$ MPa (View from the direction of Z-axis/bank(θ_B) = 0° , Y-axis/heading(θ_H) = 0° and X-axis/pitch(θ_P) = 40°)

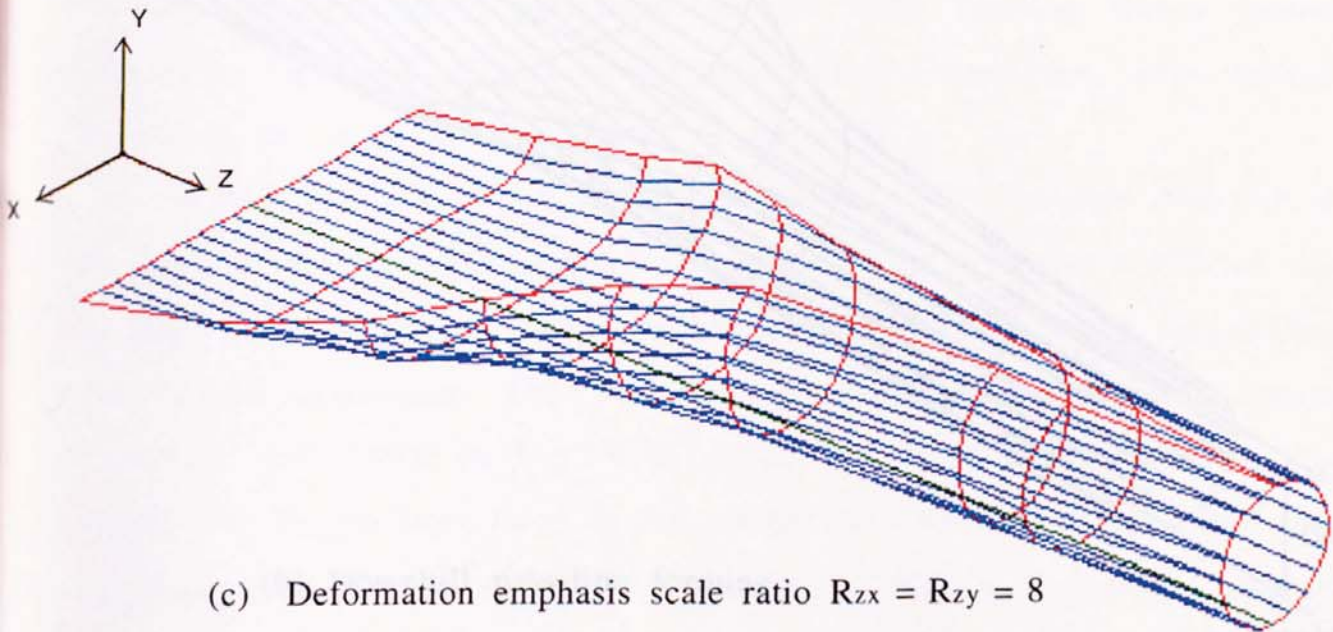
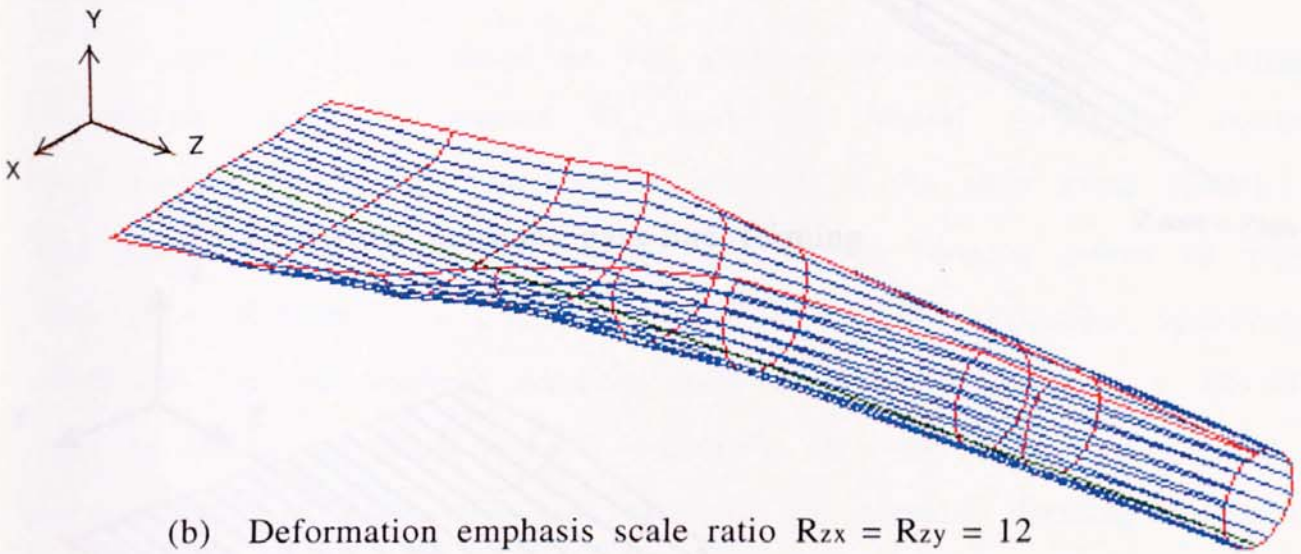
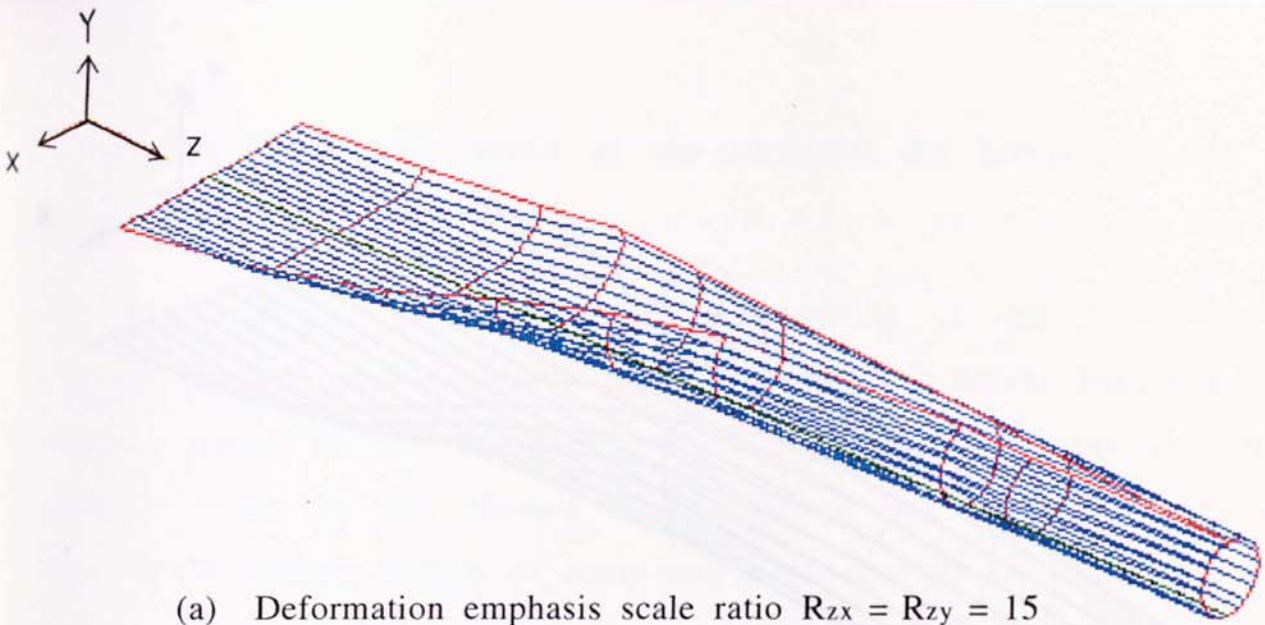
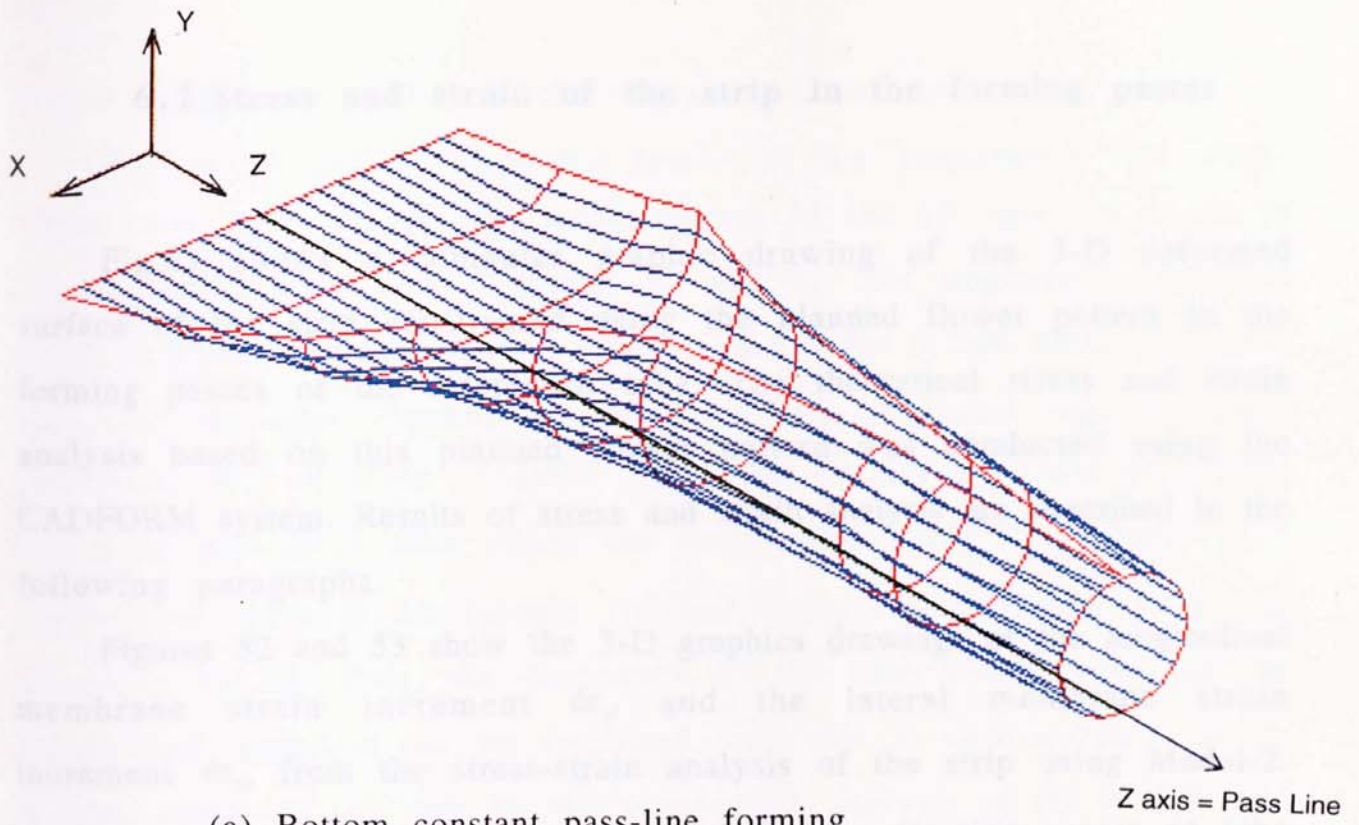
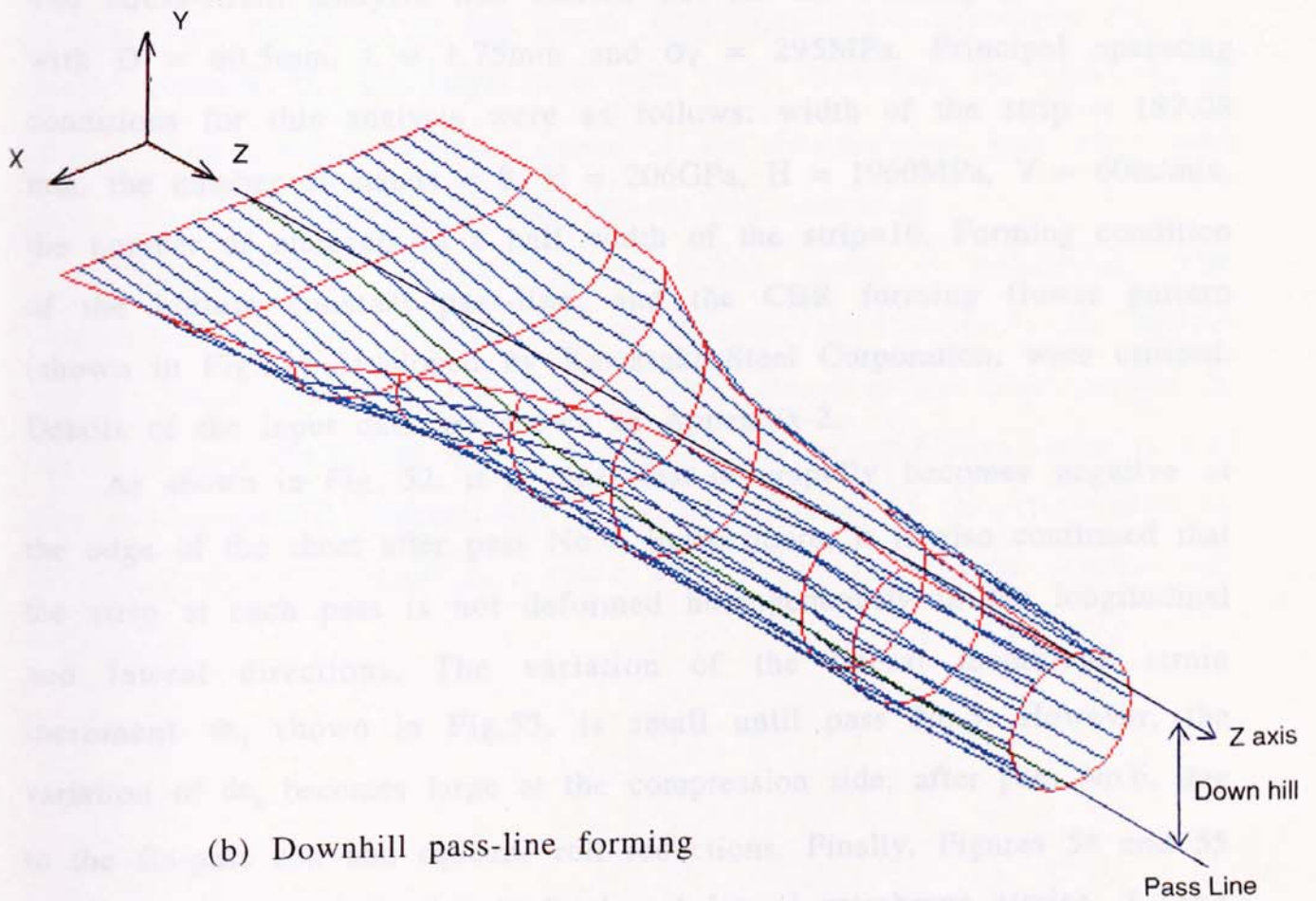


Fig.49 Example of deformed surface of strip constructed using planned flowers in different deformation emphasis scale ratios of R_{zx} and R_{zy} in forming passes of tube with $D = 60.5\text{mm}$, $t = 1.75\text{mm}$ and $\sigma_Y = 295\text{MPa}$ (View from the direction of Z-axis/bank(θ_B) = 0° , Y-axis/heading(θ_H) = 50° and X-axis/pitch(θ_P) = 30°)



(a) Bottom constant pass-line forming



(b) Downhill pass-line forming

Fig.50 Example of deformed surface of strip constructed using planned flowers in the bottom constant pass-line and downhill pass-line forming of tube with $D = 60.5\text{mm}$, $t = 1.75\text{mm}$ and $\sigma_Y = 295\text{MPa}$ (View from the direction of Z-axis/bank(θ_B) = 0° , Y-axis/heading(θ_H) = 50° and X-axis/pitch(θ_P) = 30°)

6.2 Stress and strain of the strip in the forming passes

Fig.51 shows a computer graphic drawing of the 3-D deformed surface of the strip constructed using the planned flower pattern in the forming passes of the referenced tube. The theoretical stress and strain analysis based on this planned flower pattern was conducted using the CADFORM system. Results of stress and strain analysis are described in the following paragraphs.

Figures 52 and 53 show the 3-D graphics drawings of the longitudinal membrane strain increment $d\epsilon_z$, and the lateral membrane strain increment $d\epsilon_x$, from the stress-strain analysis of the strip using Model-2. The stress-strain analysis was carried out for the forming passes of tube with $D = 60.5\text{mm}$, $t = 1.75\text{mm}$ and $\sigma_Y = 295\text{MPa}$. Principal operating conditions for this analysis were as follows: width of the strip = 187.08 mm, the number of stands = 8, $E = 206\text{GPa}$, $H = 1960\text{MPa}$, $V = 60\text{m/min}$, the number of elements in a half width of the strip=10. Forming condition of the bottom constant pass-line, and the CBR forming flower pattern (shown in Fig.31) developed by Kawasaki Steel Corporation, were utilised. Details of the input data are shown in Appendix-2.

As shown in Fig. 52, it is clear that $d\epsilon_z$ rapidly becomes negative at the edge of the sheet after pass No.4. Furthermore, it is also confirmed that the strip at each pass is not deformed homogeneously in the longitudinal and lateral directions. The variation of the lateral membrane strain increment $d\epsilon_x$ shown in Fig.53, is small until pass No.5. However, the variation of $d\epsilon_x$ becomes large at the compression side, after pass No.6, due to the fin-pass roll and squeeze roll reductions. Finally, Figures 54 and 55 show the results of the longitudinal and lateral membrane strains, ϵ_z and ϵ_x . The variations of the longitudinal and lateral membrane strains are small prior to the squeeze roll pass. However, large variations of the longitudinal and lateral membrane strains are present due to high

frequency pressure welding at the squeeze roll reduction stage.

Figures 56 and 57 show the results of the longitudinal and lateral stress increments $d\sigma_z$ and $d\sigma_x$, whilst Figures 58 and 59 show the results of the longitudinal and lateral stresses σ_z and σ_x . The negative longitudinal stress increment $d\sigma_z$, of about -130MPa (this value is not clear in Fig.56) occurs at the edge element in pass No.5. An additional negative stress increment $d\sigma_z$, of about -130MPa (this value is also not clear in Fig.56) occurs in pass No.6 after which the longitudinal stress σ_z , changes to a compressive stress in the fin-pass roll and squeeze roll forming stages, as shown in Fig.58. Thus, the occurrence of the compressive stress in the longitudinal direction can be estimated, and this is demonstrated in the forming stages of the tube by the stress-strain analysis of the CADFORM system. The variations of the lateral membrane stress increment $d\sigma_x$, and lateral stresses σ_x , are small until pass No.5. However, the variations of these lateral stresses becomes large at the compression side after pass No.6, due to the fin-pass roll and squeeze roll reductions.

Finally, Fig.60 shows the equivalent stress $\bar{\sigma}$ behaviour. The longitudinal and lateral distribution of the equivalent stress in the middle forming stage is varied, and the equivalent stress at the edge portion is largest at pass No.3. The lateral distribution of the equivalent stress in fin-pass roll forming is uniform due to material yielding of the whole sheet in the lateral direction, again as a result of the fin-pass roll and squeeze roll reductions.

Stress-Strain Analysis(Model-2)

3-D DRAWING

Pass Line Length
L = 4820.00 mm

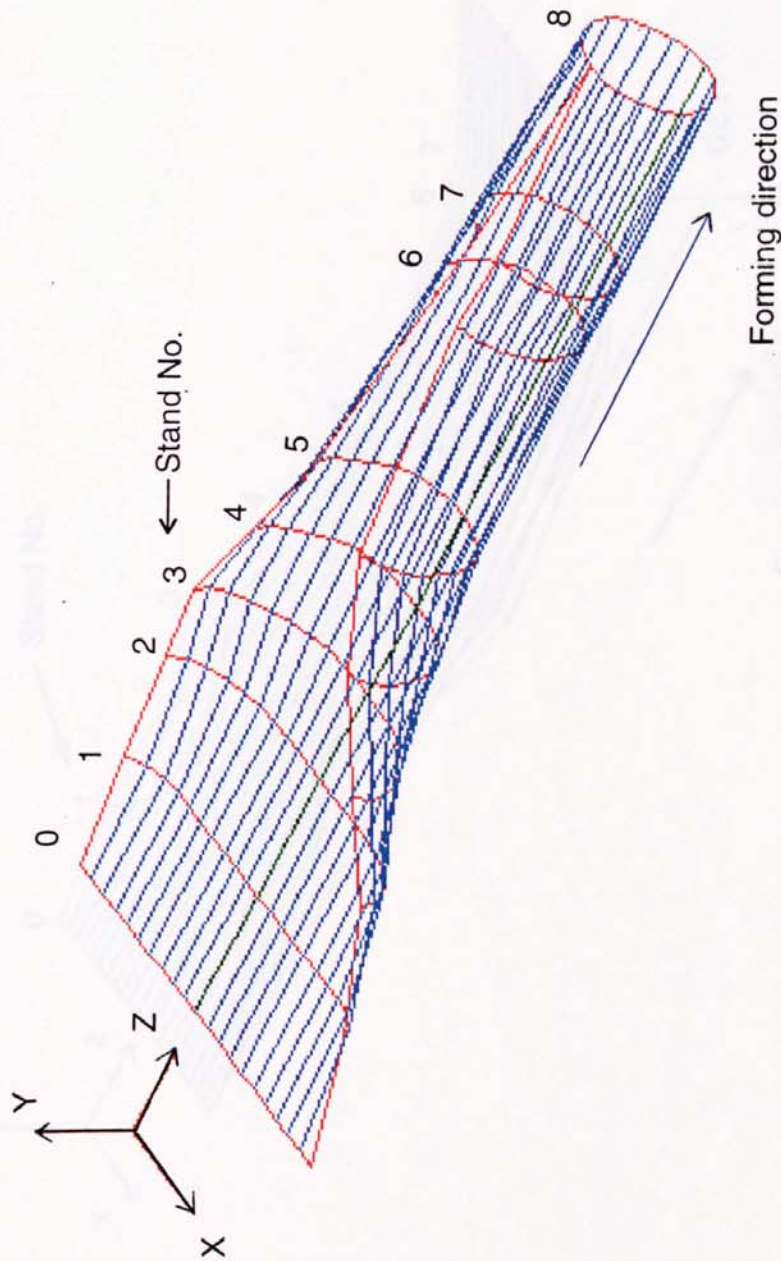
Rotation Angle of
Axis (deg.)

Bank = 0.00
Head = 50.00
Pitch = 40.00

Scale Ratio

SZX = 8.00
SZY = 8.00

OD = 60.5mm
t = 1.75mm



CADFORM

3-D Deformation Surface

DRAWER
T. TOYOOKA
WORKS (MILL)
2" MILL

DATE
30. 9. 1992
MATERIAL
STEEL

FILE NAME
CBR60-5BC
SIZE
60.5X1.75mm

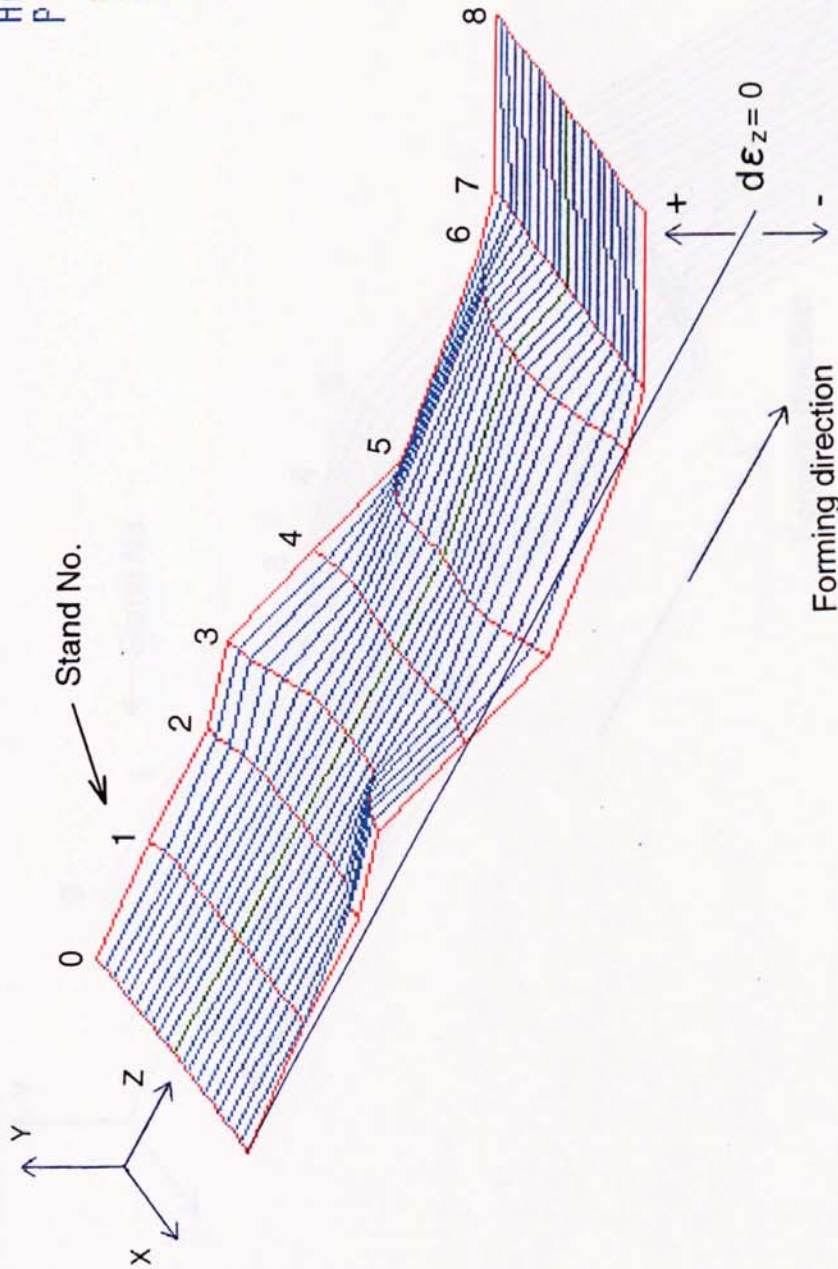
Fig.51 Computer graphic drawing of the 3-D deformed surface of strip constructed using planned flowers in the forming passes (View from the direction of Z-axis/bank(θ_B) = 0°, Y-axis/heading(θ_H) = 50° and X-axis/pitch(θ_P) = 40°)

Stress-Strain Analysis (Model-2)

3-D DRAWING

Pass Line Length
L = 4820.00 mm

Rotation Angle of Axis (deg.)
Bank = 0.00
Head = 50.00
Pitch = 40.00
Scale Ratio
SZX = 8.00
SZY = 8.00
OD = 60.5mm
t = 1.75mm



CADFORM
Strain Increment $d\epsilon_z(\%)$

DRAYER T.TOYOOKA	DATE 30. 9.1992	FILE NAME CBR60-5BC
WORKS (MILL) 2" MILL	MATERIAL STEEL	SIZE 60.5X1.75mm

Fig.52 3-D graphics drawing of longitudinal membrane strain increment $d\epsilon_z$, calculated by CADFORM system (View from the direction of Z-axis/bank(θ_B) = 0° , Y-axis/heading(θ_H) = 50° and X-axis/pitch(θ_P) = 40°)

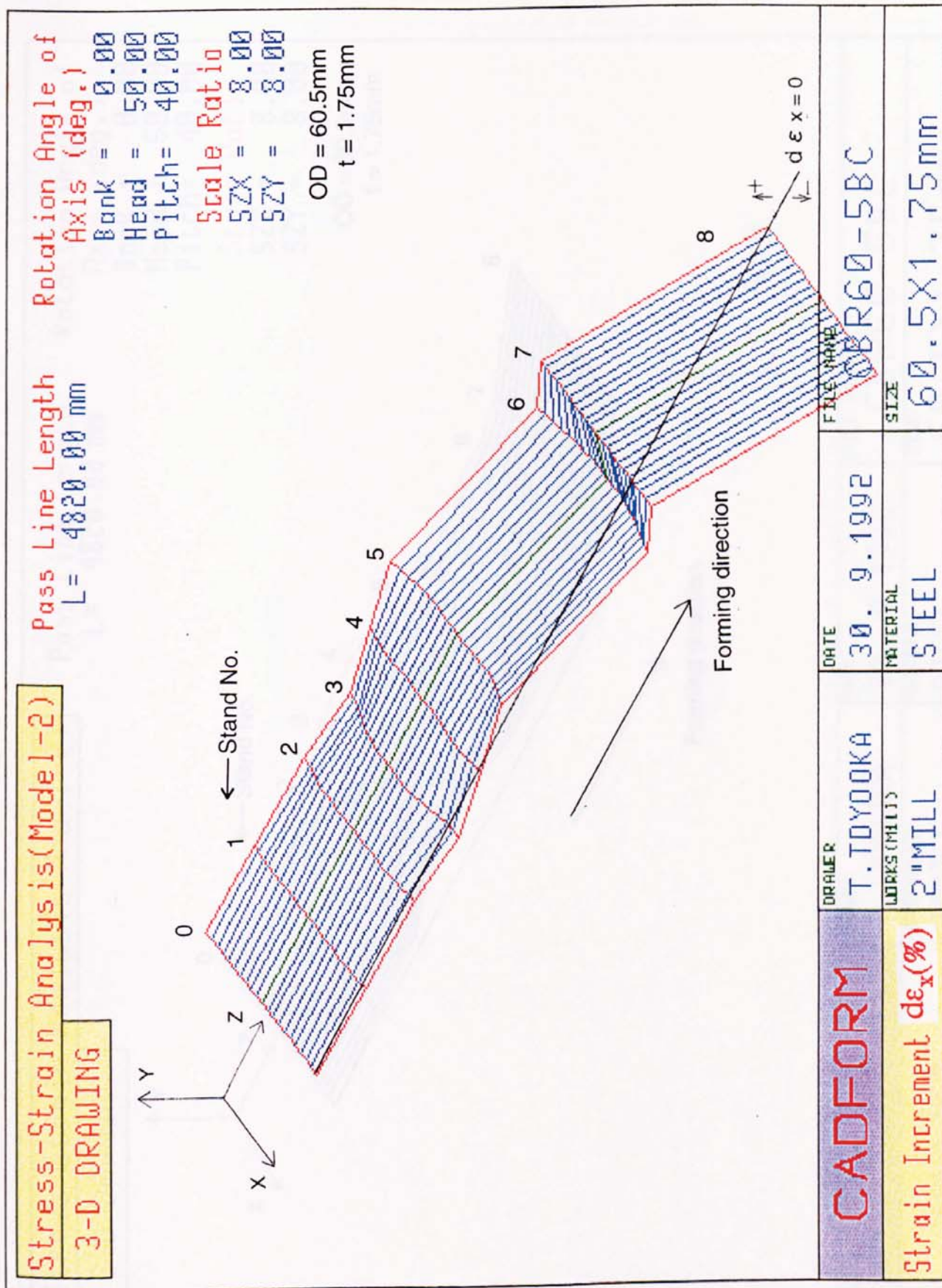


Fig.53 3-D graphics drawing of lateral membrane strain increment $d\epsilon_x$, calculated by CADFORM system (View from the direction of Z-axis/bank(θ_B) = 0°, Y-axis/heading(θ_H) = 50° and X-axis/pitch(θ_P) = 40°)

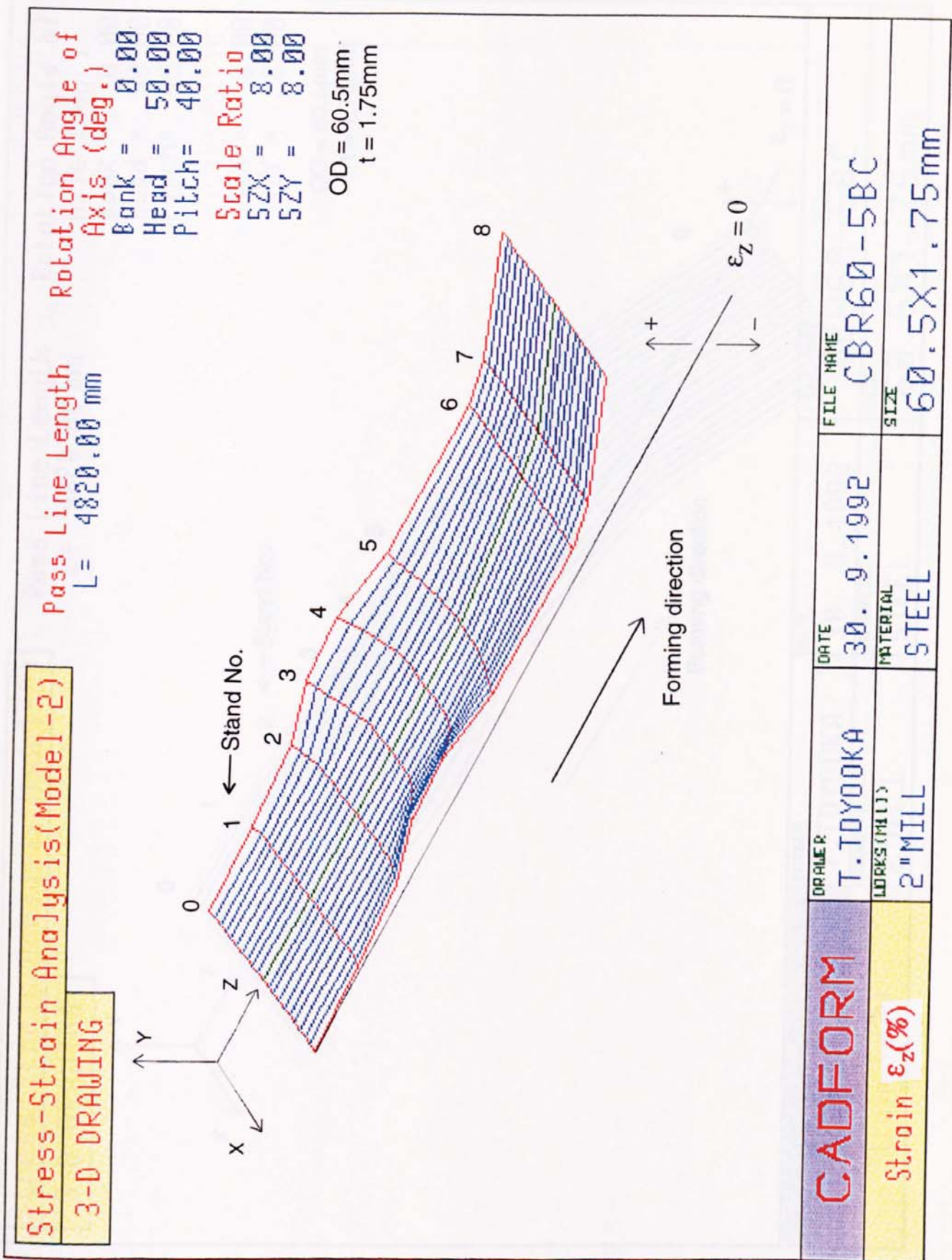


Fig.54 3-D graphics drawing of longitudinal strain ϵ_z , calculated by CADFORM system
 (View from the direction of Z-axis/bank(θ_B) = 0° ,
 Y-axis/heading(θ_H) = 50° and X-axis/pitch(θ_P) = 40°)

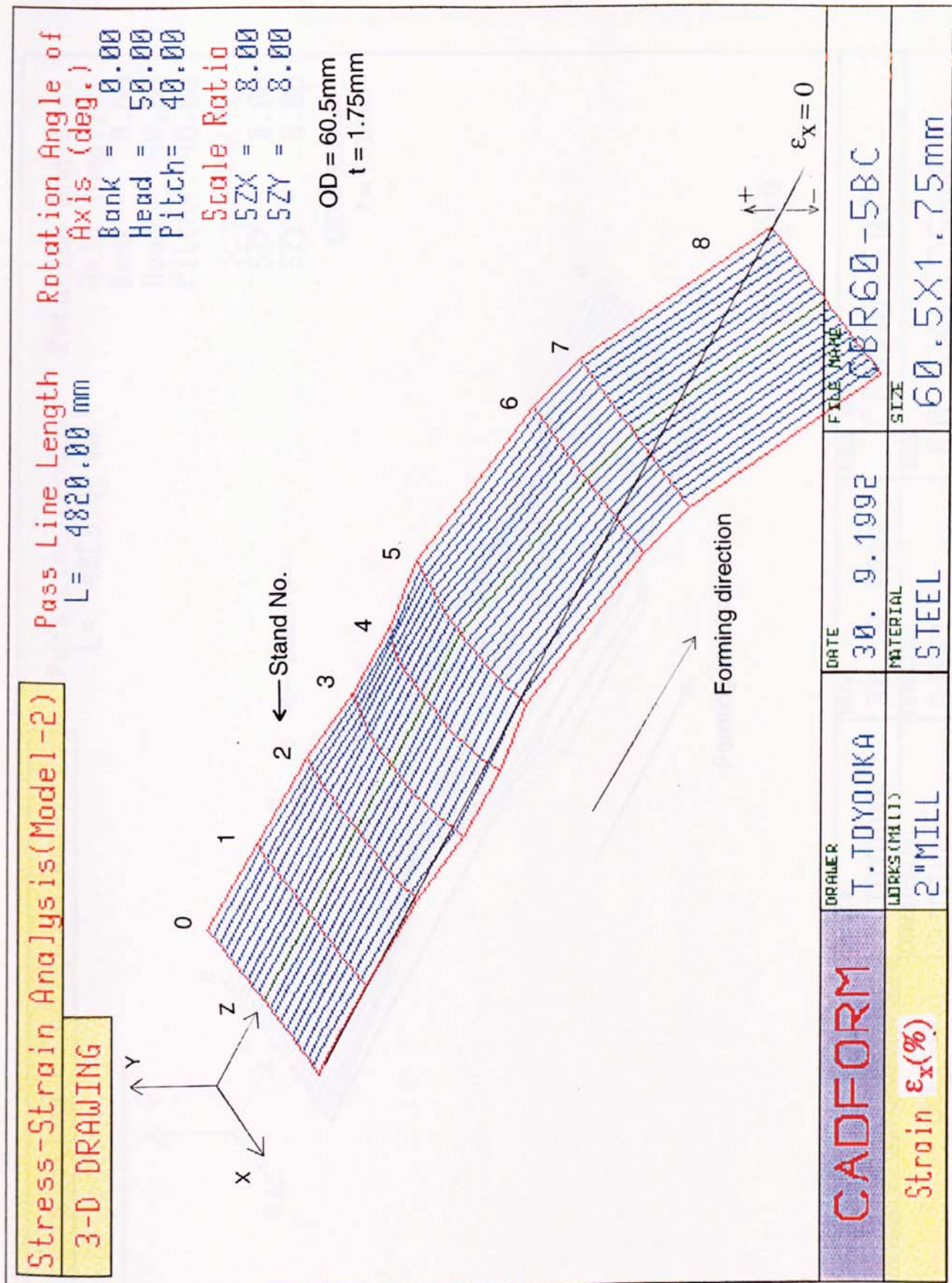


Fig.55 3-D graphics drawing of lateral strain ϵ_x , calculated by CADFORM system
 (View from the direction of Z-axis/bank(θ_B) = 0°,
 Y-axis/heading(θ_H) = 50° and X-axis/pitch(θ_P) = 40°)

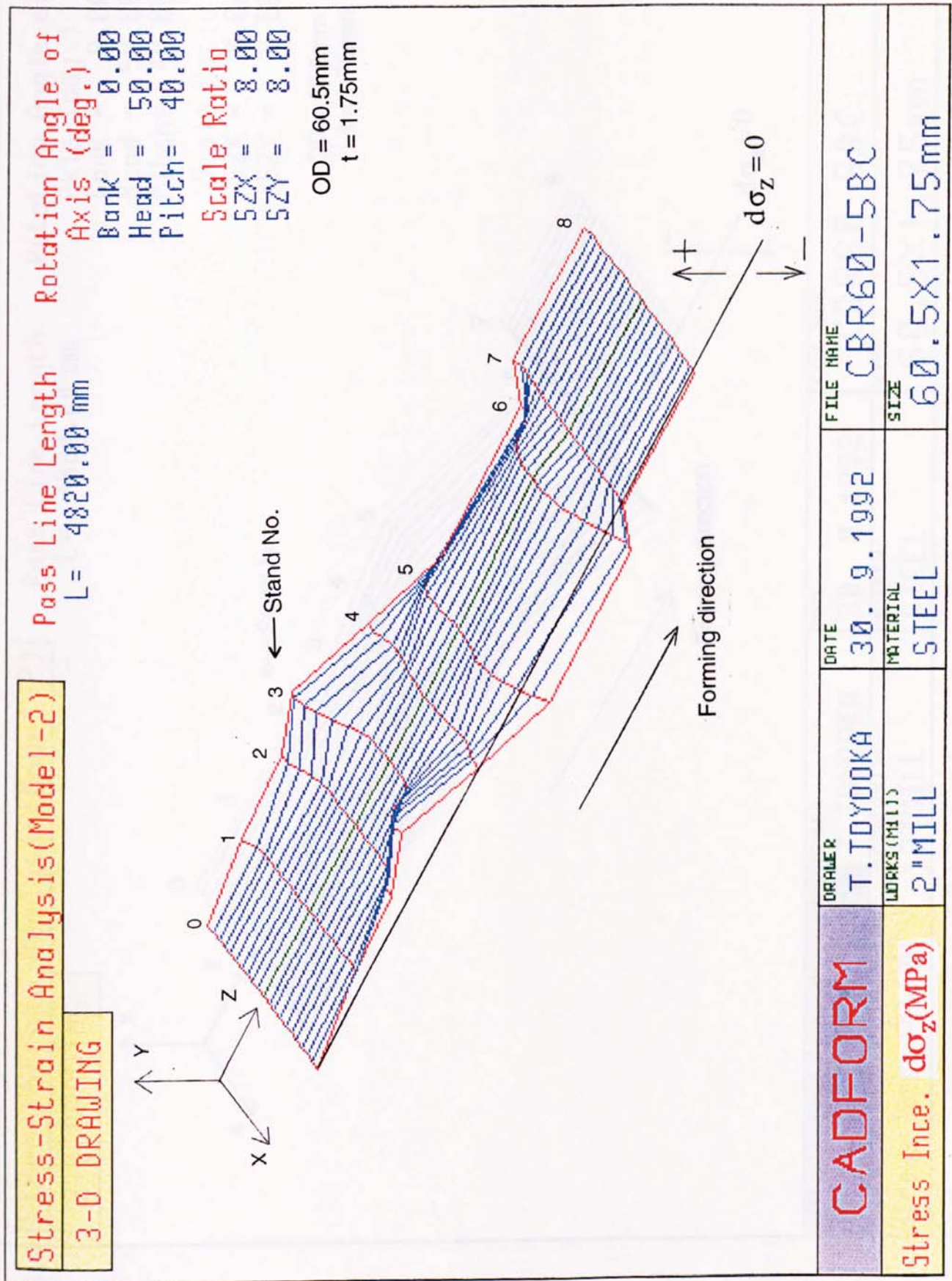


Fig.56 3-D graphics drawing of longitudinal stress increment $d\sigma_z$, calculated by CADFORM system
(View from the direction of Z-axis/bank(θ_B) = 0°, Y-axis/heading(θ_H) = 50° and X-axis/pitch(θ_P) = 40°)

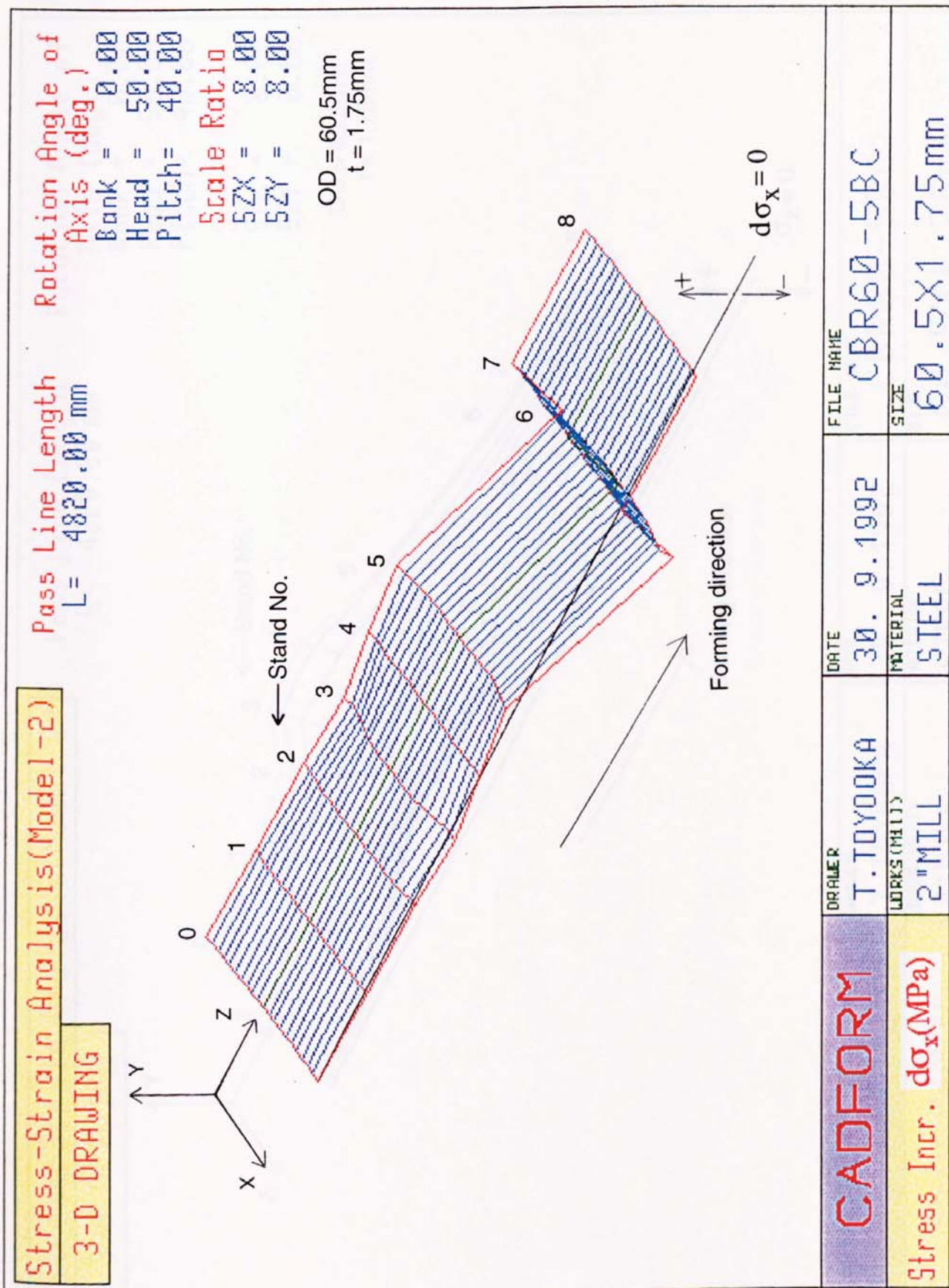


Fig.57 3-D graphics drawing of lateral stress increment $d\sigma_x$, calculated by CADFORM system
(View from the direction of Z-axis/bank(θ_B) = 0° ,
Y-axis/heading(θ_H) = 50° and X-axis/pitch(θ_P) = 40°)

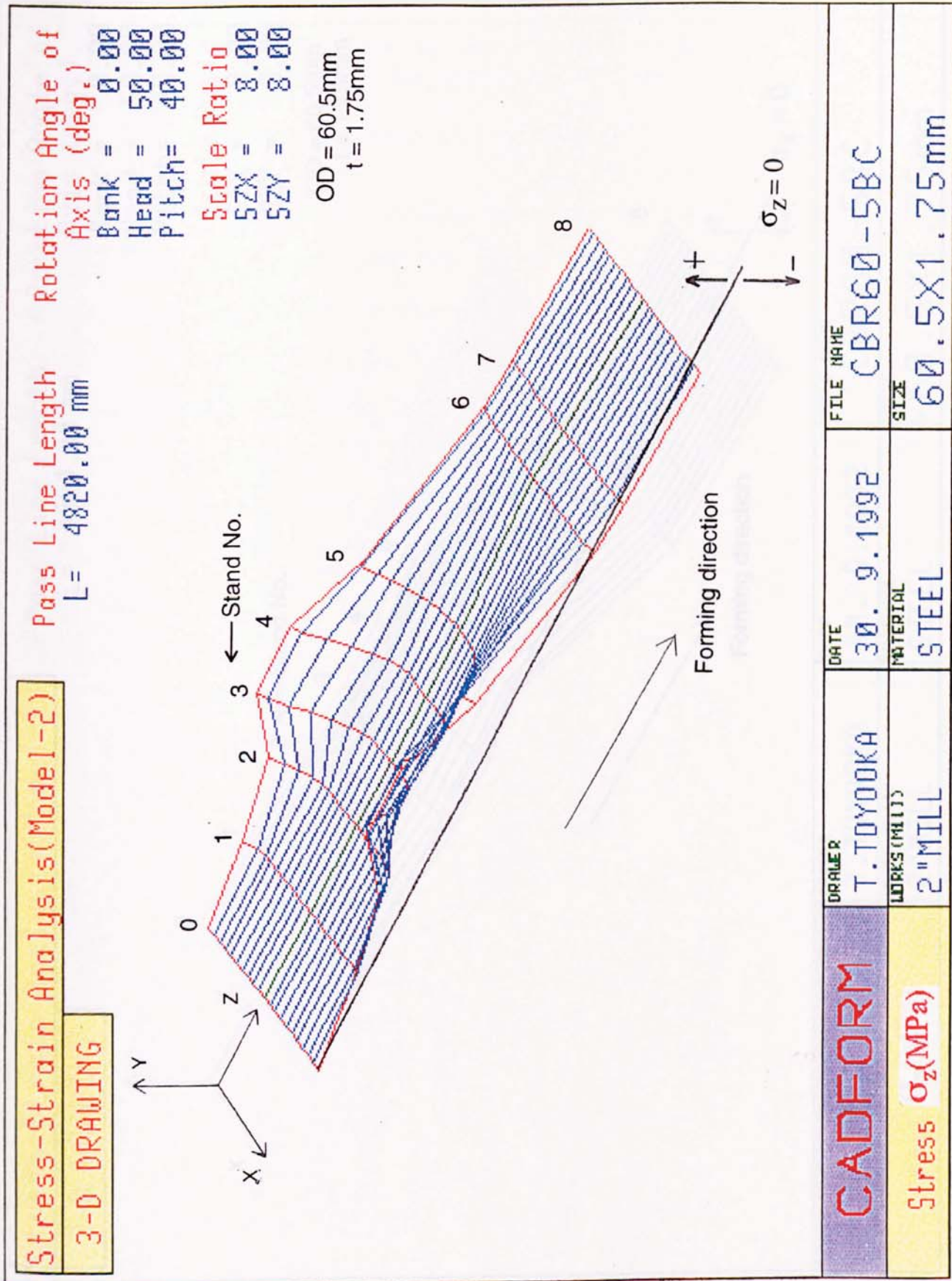


Fig.58 3-D graphics drawing of longitudinal stress σ_z , calculated by CADFORM system
 (View from the direction of Z-axis/bank(θ_B) = 0° ,
 Y-axis/heading(θ_H) = 50° and X-axis/pitch(θ_P) = 40°)

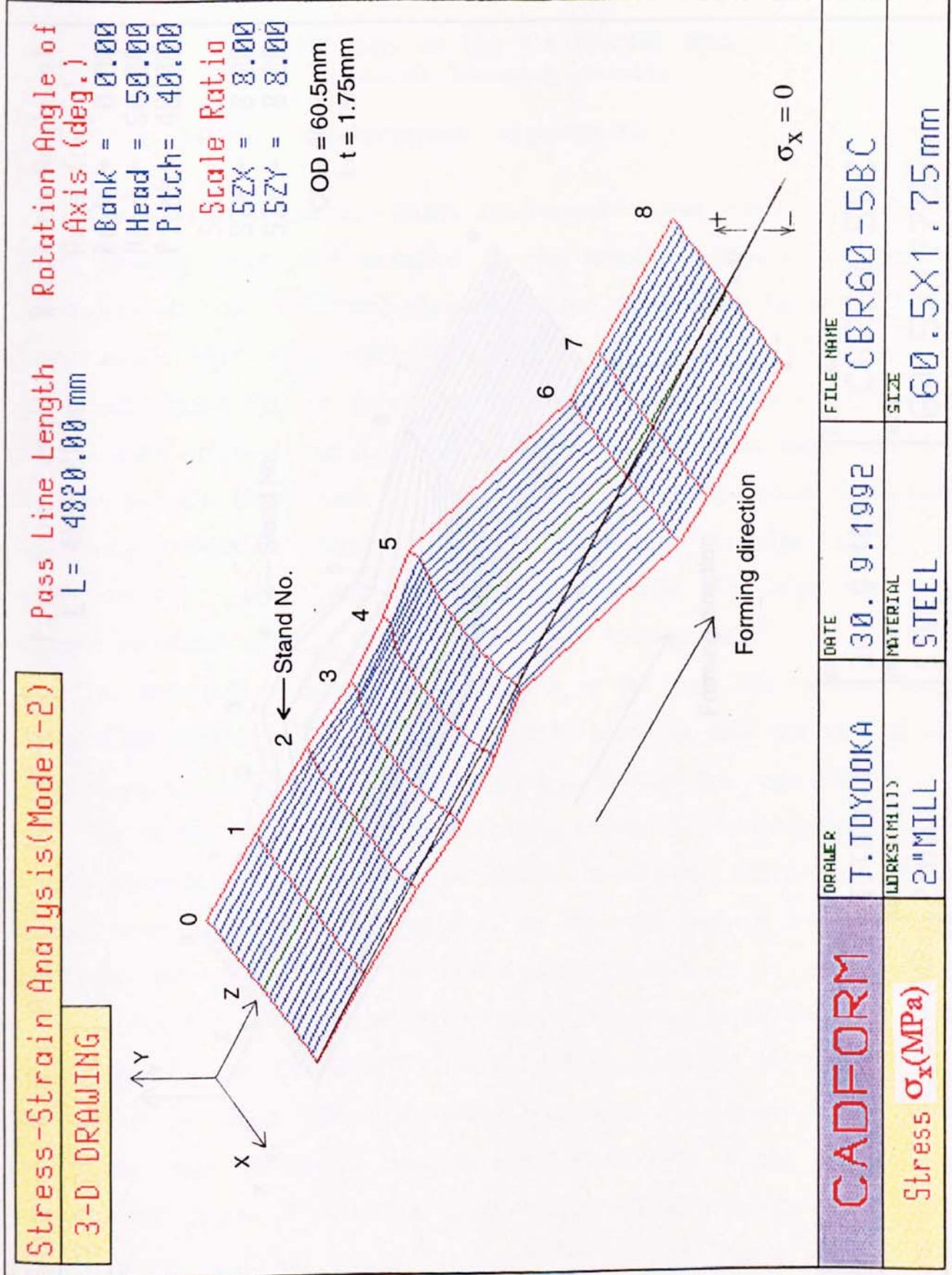


Fig.59 3-D graphics drawing of lateral stress σ_x , calculated by CADFORM system
 (View from the direction of Z-axis/bank(θ_B) = 0° ,
 Y-axis/heading(θ_H) = 50° and X-axis/pitch(θ_P) = 40°)

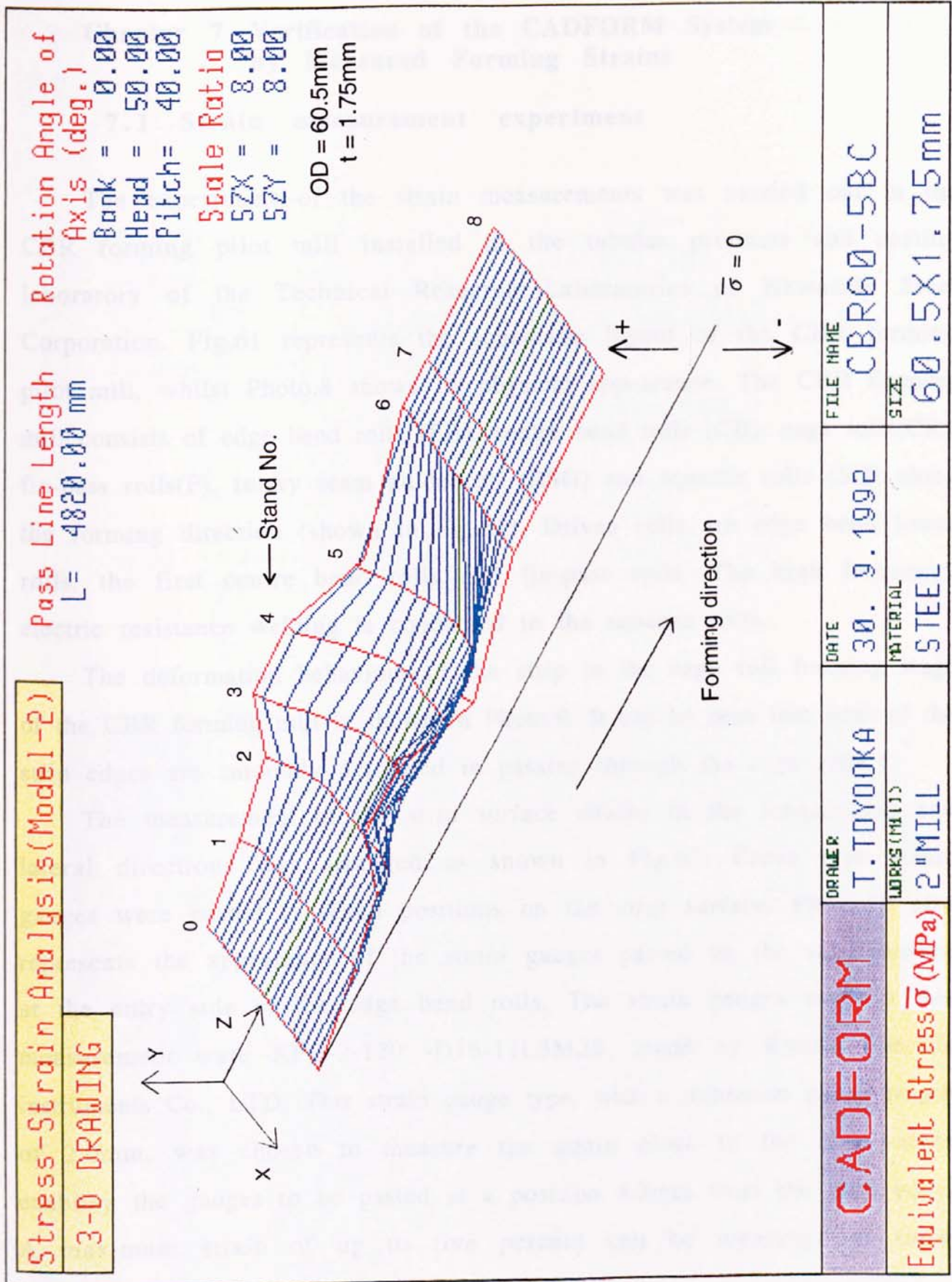


Fig.60 3-D graphics drawing of equivalent stress $\bar{\sigma}$, calculated by CADFORM system
 (View from the direction of Z-axis/bank(θ_B) = 0°,
 Y-axis/heading(θ_H) = 50° and X-axis/pitch(θ_P) = 40°)

Chapter 7 Verification of the CADFORM System by Measured Forming Strains

7.1 Strain measurement experiment

The experiment of the strain measurements was carried out in the CBR forming pilot mill installed in the tubular products and casting laboratory of the Technical Research Laboratories of Kawasaki Steel Corporation. Fig.61 represents the schematic layout of the CBR forming pilot mill, whilst Photo.8 shows its physical appearance. The CBR forming mill consists of edge bend rolls (EB), centre bend rolls (CB), cage rolls (CR), fin-pass rolls (F), rotary seam guide roll (RSG) and squeeze rolls (SQ) along the forming direction (shown in Fig.61). Driven rolls are edge bend lower rolls, the first centre bend rolls and fin-pass rolls. The high frequency electric resistance welding is conducted in the squeeze rolls.

The deformation behaviour of the strip in the cage roll forming stage of the CBR forming mill is shown in Photo.9. It can be seen that both of the strip edges are smoothly deformed in passing through the cage rolls.

The measurement of the strip surface strains in the longitudinal and lateral directions was arranged as shown in Fig.62. Cross type strain gauges were pasted at seven positions on the strip surface. Photo.10 also represents the appearance of the strain gauges pasted on the strip surface at the entry side of the edge bend rolls. The strain gauges used in this measurement were KFG-2-120 -D16-11L3M2S, made by Kyowa Electric instruments Co., LTD. This strain gauge type, with a minimum gauge length of 2.0mm, was chosen to measure the strain close to the strip edges enabling the gauges to be pasted at a position 4.2mm from the strip edge. A maximum strain of up to five percent can be measured at room temperature by this strain gauge.

The tube size used in this experiment was $D = 42.7\text{mm}$ and $t = 1.5\text{mm}$. In the experiments the upper edge bend roll was lifted during the passing through of the strip containing the pasted portion of strain gauges,

to prevent any damage to the strain gauges. The forming speed was about 5m/min.

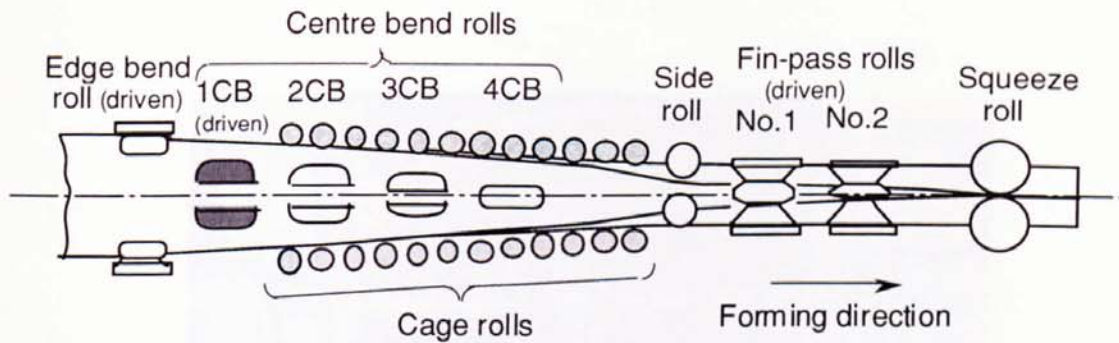


Fig.61 Schematic layout of the CBR forming pilot mill used in strain measurements

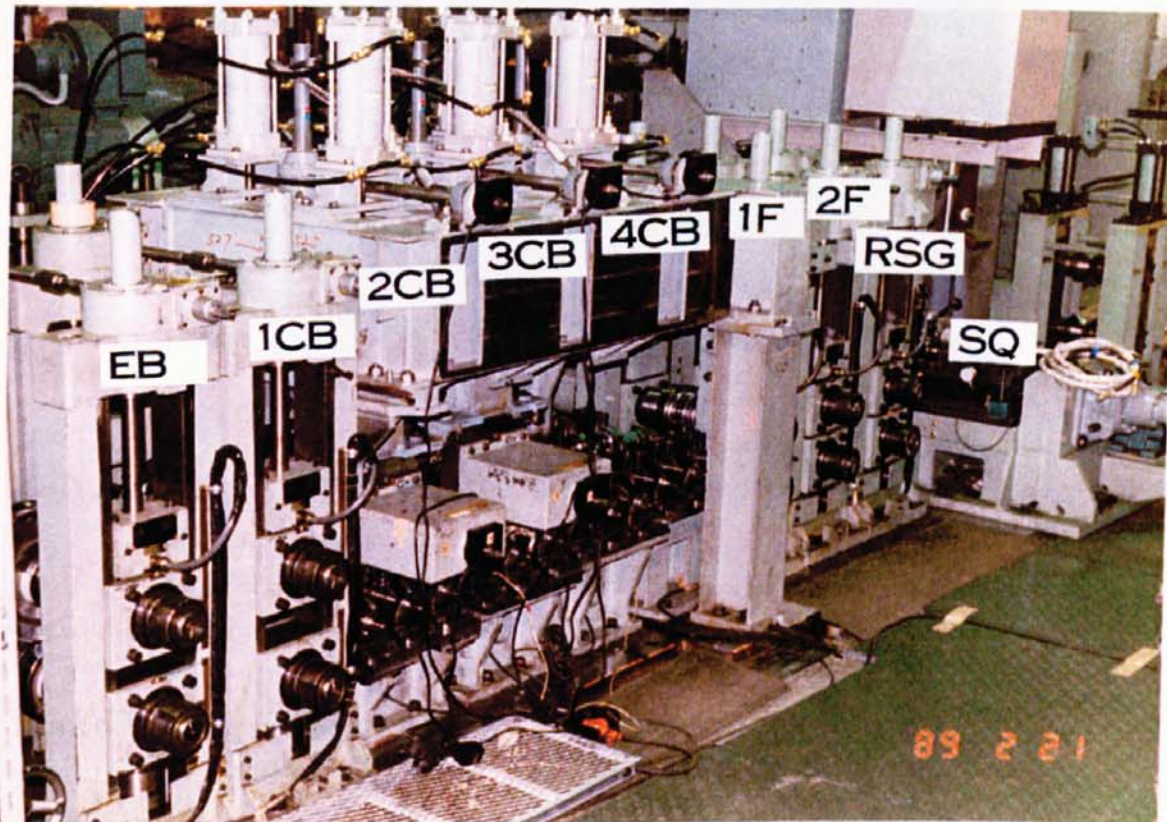


Photo.8 Appearance of the CBR forming pilot mill used in strain measurements

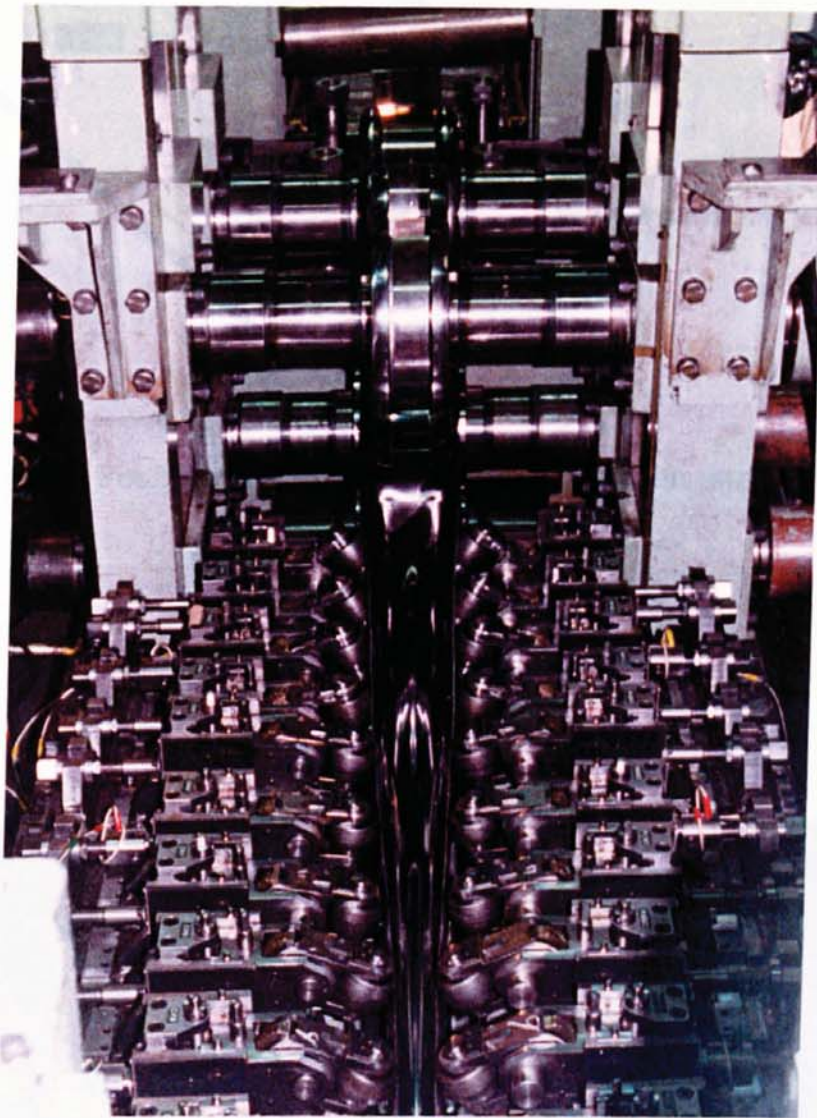


Photo.9 Appearance of the strip deformation in cage roll forming stage of the CBR forming pilot mill

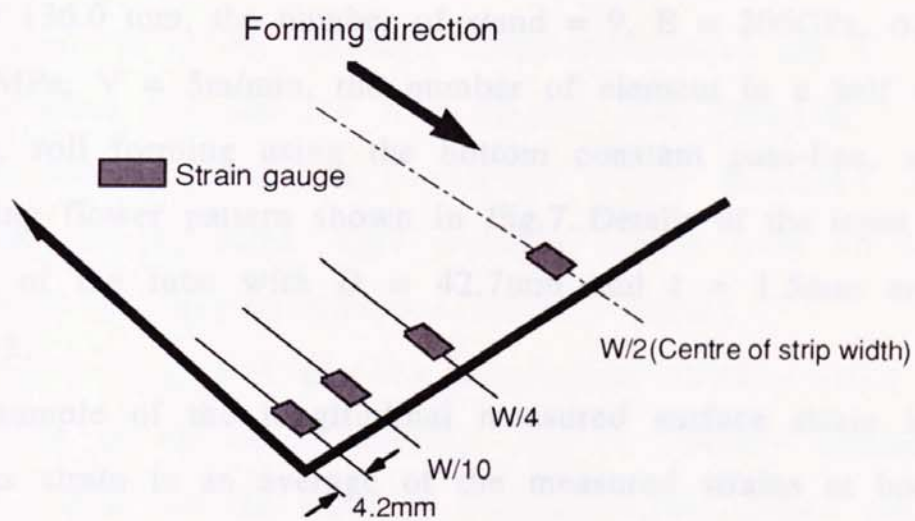


Fig.62 Position of strain gauges pasted on strip surface

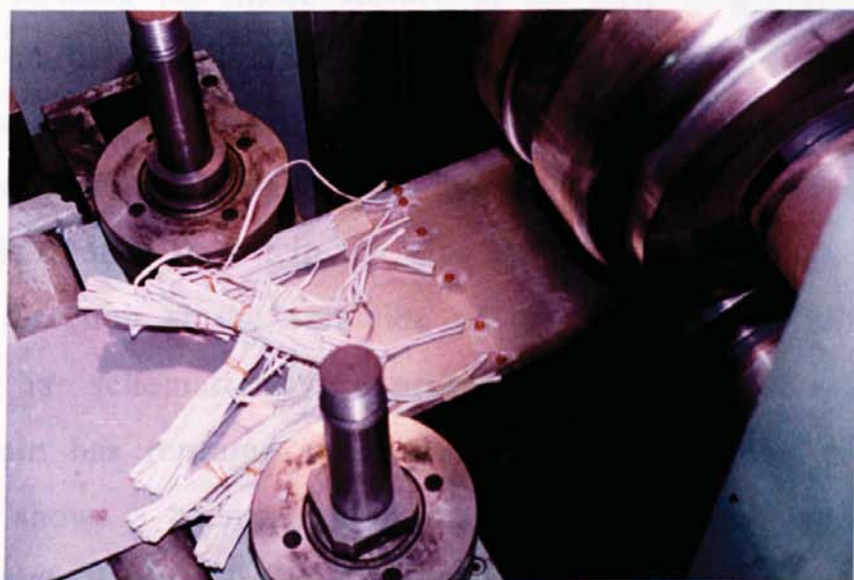


Photo.10 Appearance of strain gauges pasted on strip surface at the entry side of the edge bend rolls

7.2 Comparison of calculated to measured strains

Principal input conditions for this analysis were as follows; width of the strip = 136.0 mm, the number of stand = 9, $E = 206\text{GPa}$, $\sigma_Y = 295\text{MPa}$, $H = 1960\text{MPa}$, $V = 5\text{m/min}$, the number of element in a half width of the strip = 10, roll forming using the bottom constant pass-line, and with the CBR forming flower pattern shown in Fig.7. Details of the input data for the calculation of the tube with $D = 42.7\text{mm}$ and $t = 1.5\text{mm}$ are shown in Appendix-3.

An example of the longitudinal measured surface strain is shown in Fig.63. This strain is an average of the measured strains at both edges of the strip. Strains at other positions could not be satisfactorily measured due to the damage by the forming rolls. It is apparent that a strain peak occurs when the strip passes through each forming roll. The strain peak at the first fin-pass 1F, is the largest strain at 0.9%. Small and uniform variations of strain is apparent at the cage roll forming stage, and these strain variations suggests the superiority of cage roll forming.

In roll forming the inside surface of the strip is generally subjected to compression in the longitudinal direction at the entry side of the rolls due to pre-deformation and then, subsequently to tension in the longitudinal direction after contacting with rolls due to stretch bending along the roll radius. Furthermore, the strip is also subjected to compression in the longitudinal direction at the exit side of the rolls due to un-bending. This deformation is schematically expressed in Fig.64 showing that the measured strain has repeated strain peaks at each forming pass.

Fig. 65 shows a comparison of the calculated membrane strains to the measured surface strain in the longitudinal direction. Calculated strains were analysed by Model-1 and -2. The calculated strain is expressed as a point at each forming pass, and is not the same as the measured strain, since it is assumed that the strip is deformed only at the centre of each forming pass in this stress and strain analysis. Thus it is assumed that the

surface strain is roughly equal to the membrane strain for thin walled strip. Clearly, for thicker wall strip this is not the case, since a bending strain is also present. The calculated strain by Model-2 corresponds well with the measured strain, although strain differences are observed at the first center bend roll and the first fin-pass roll. However the calculated strain from Model-1 does not correspond to the measured strain at the fin-pass roll forming stage. This probably results from no consideration being given to the fin-pass reduction stage by Model-1.

Thus, it is confirmed that the longitudinal forming strain, controlling the occurrence of the edge buckling, can be roughly estimated by the CADFORM system. On the basis of these calculated strains, the stresses of the strip in tube-making can also be roughly estimated by the CADFORM system. Furthermore, the occurrence of edge buckling can be predicted by using the longitudinal calculated stress.

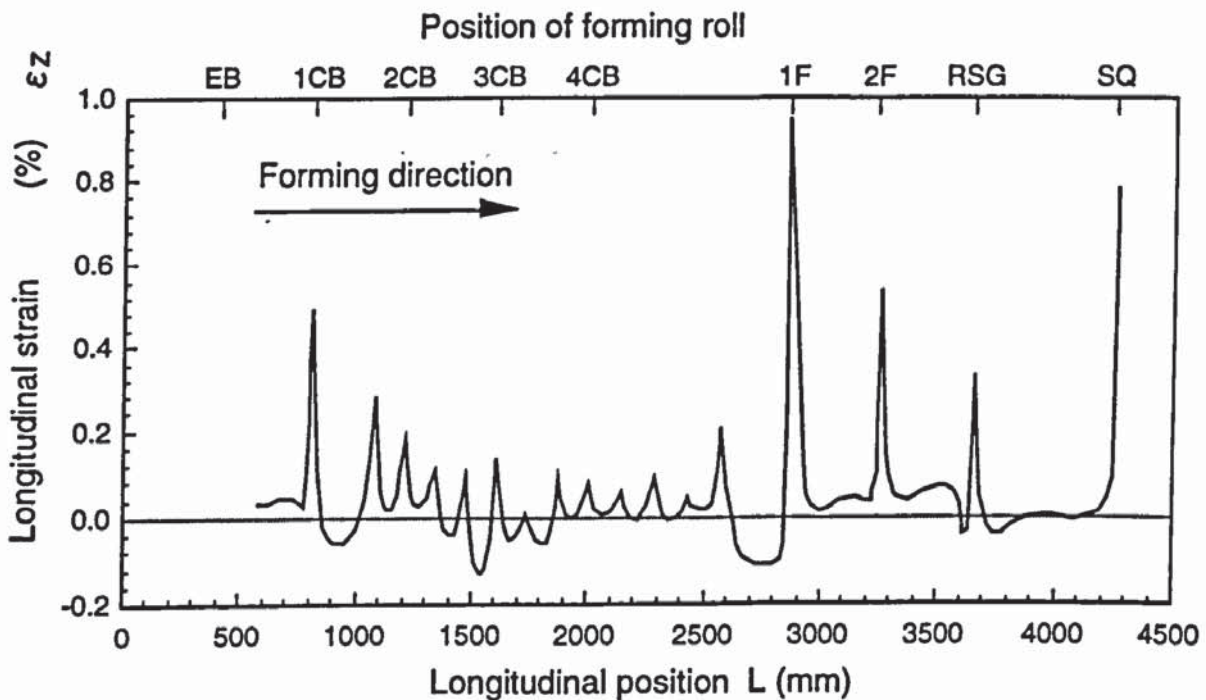


Fig.63 Variation of longitudinal measured surface strain

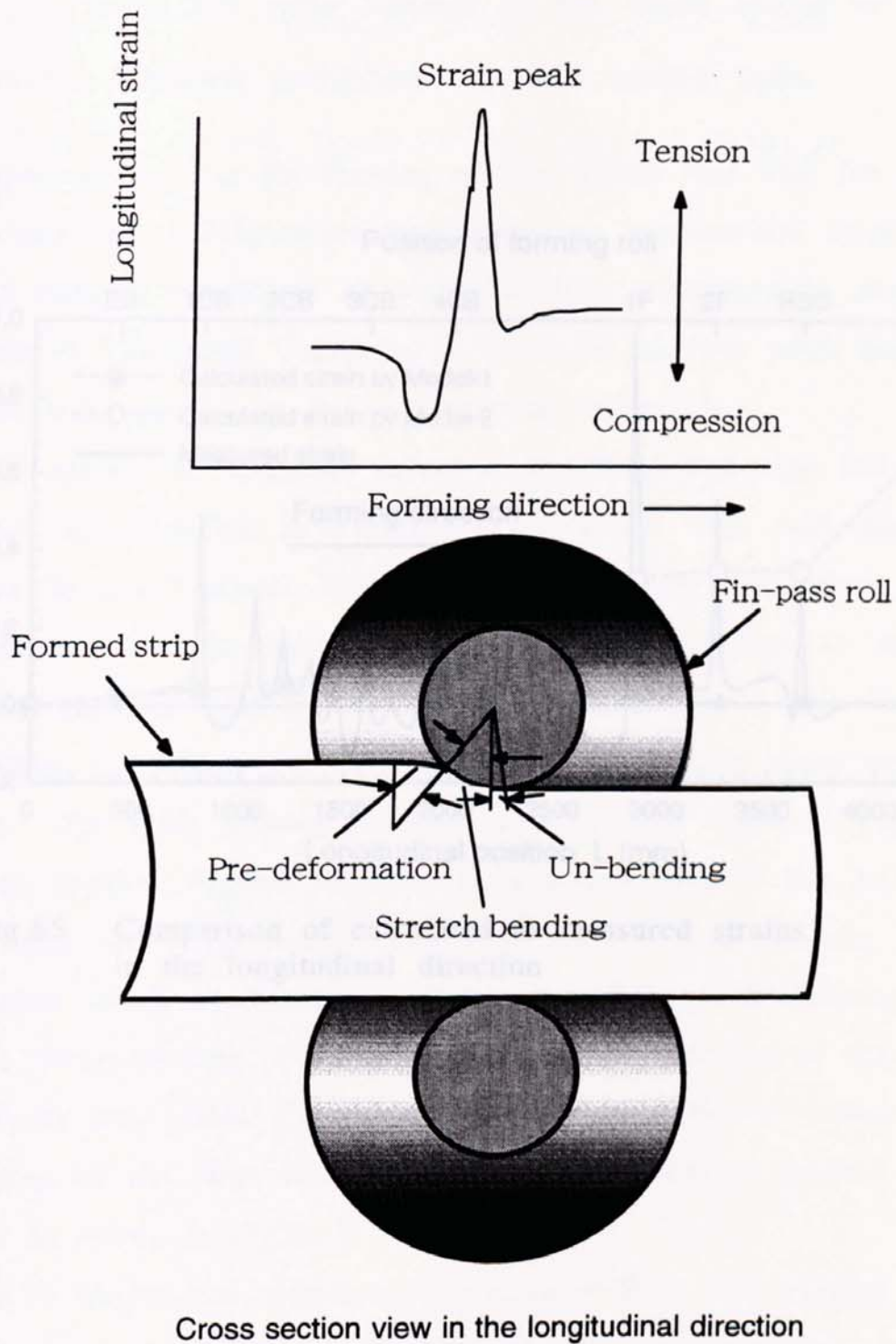


Fig.64 Occurrence of longitudinal strain peak due to deformation of strip in fin-pass roll forming

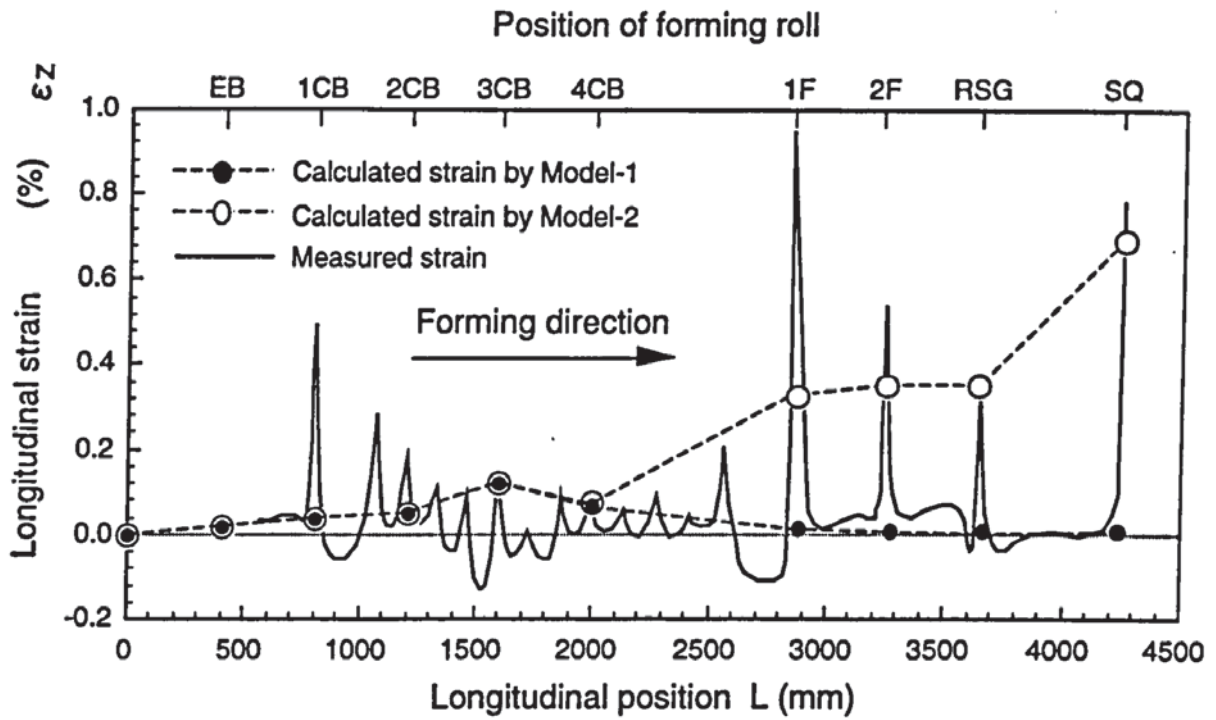


Fig.65 Comparison of calculated to measured strains in the longitudinal direction

Chapter 8 Discussion

8.1 Simulation of stress and strain of the tube with large D/t ratio formed in the 4inch model mill

8.1.1 Forming conditions of thin walled tube

In order to stabilize the forming of thin walled tube with D/t ratios of 100, Kawasaki Steel Corporation carried out an experimental study⁶ on the effects of forming conditions on edge buckling occurrence in cooperation with Onoda at Yamanashi University in Japan in the four years from 1980. The author was engaged in this experimental study.

Fig.66 shows the schematic layout of the 4inch full cage roll forming type model mill installed at Yamanashi University. This mill consists of four centre bend roll stands, thirty-eight pairs of cage rolls, three fin-pass roll stands and squeeze rolls along the forming direction as shown in Fig.66. The tube size used by Onoda and the author in this experiment was $D = 100.0\text{mm}$, $t = 1.0\text{mm}$ and $\sigma_Y = 340\text{MPa}$. The forming speed was about 7.5 m/min. The CBR forming planned flower pattern shown in Fig.67 and Fig.68 was applied. Figures 67 and 68 show examples of the 2-D flower pattern-A and -B. Fig.67 shows the first fin-pass roll forming planned flower pattern which expresses typical features of the CBR forming flower pattern, i.e. bulge-bending of R3 portion and bend-unbending of R2 and R4 portion of the strip sheet. Fig.68 shows the planned flower sequence. The edge bending of the strip and downhill forming were not applied in this experiment as shown in Fig.68.

Photo.11 shows the appearance of thin walled tube formed in the cage roll forming zone. In this experiment edge buckling often occurred around the stages of No.3 and No.4 center bend rolls in the cage forming roll zone. Therefore, stress-strain analysis of the strip in the cage forming roll zone, by the CADFORM system, was attempted to evaluate the occurrence of edge buckling.

Principal input conditions for this analysis were as follows: width of the strip = 315.0mm, the number of stand = 9, $E = 206\text{GPa}$, $H = 1960\text{MPa}$, $V = 7.5\text{m/min}$, and the number of divided element in a half width of the strip = 10. The forming configuration was by the bottom constant pass-line and the downhill pass-line. Details of the input and output data are shown in Appendix-4

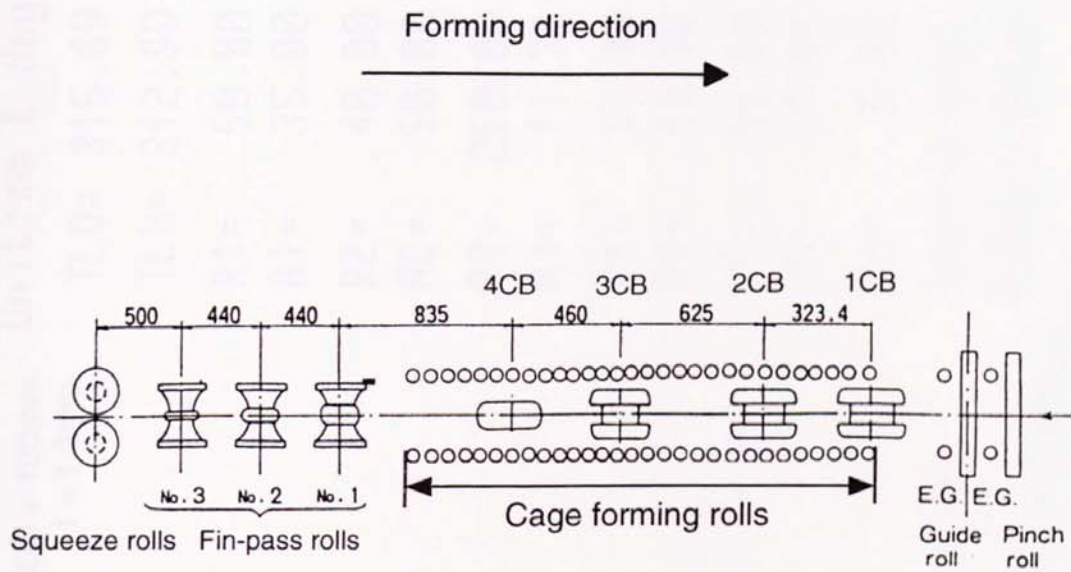


Fig.66 Schematic layout of 4inch full cage roll forming type model mill installed at Yamanashi University

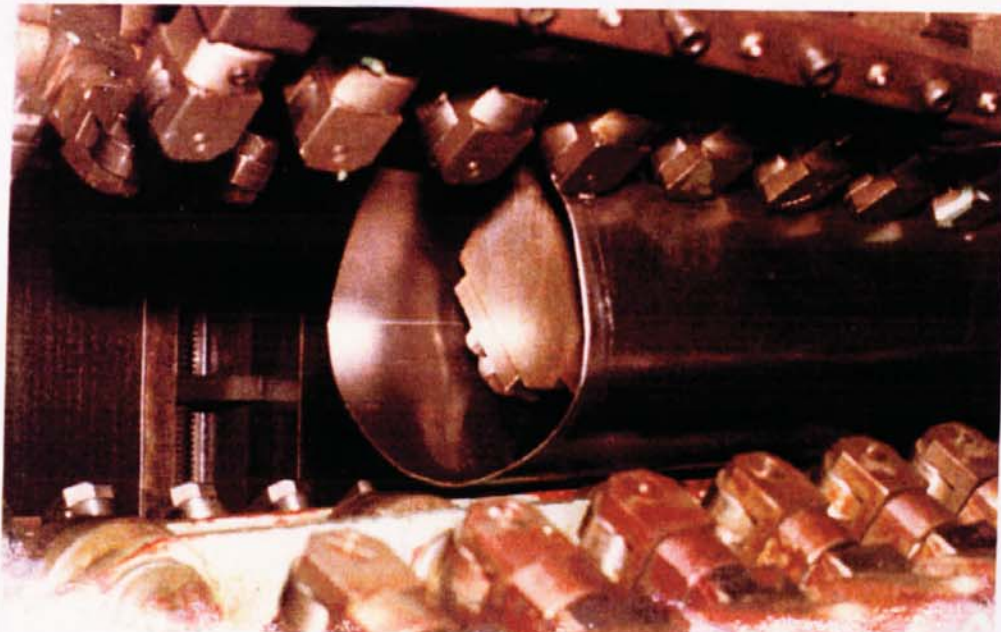


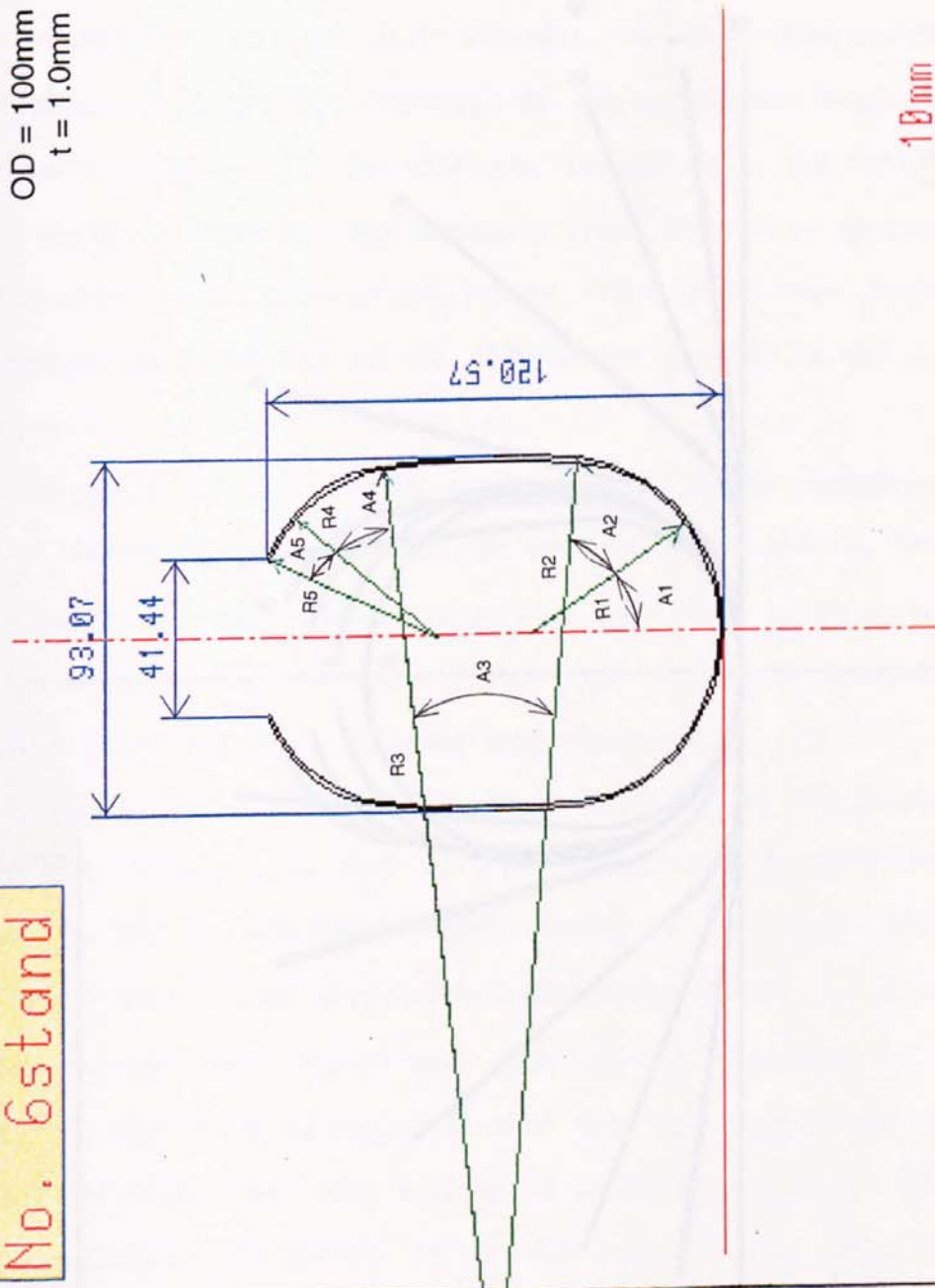
Photo.11 Appearance of forming of thin walled tube in the cage roll forming zone

No. 6stand

OD = 100mm
t = 1.0mm

Unit: mm & deg.

TL0 = 315.69
TLN = 312.99
R1 = 50.00
A1 = 35.00
R2 = 40.00
A2 = 50.00
R3 = 250.00
A3 = 11.70
R4 = 37.39
A4 = 43.30
R5 = 50.00
A5 = 15.00
DH = 0.00
SCALE = 0.5396
R: Outer Radius



10mm

CADFORM	DRAWER	T. TOYOOKA	DATE	30. 9. 1992	FILE NAME	Y100BC
	WORKS (M.I.)	YAMANASHI	MATERIAL	STEEL (KTH45)	SIZE	100 * 0X1 * 0mm

Fig.67 Drawing of planned flower with large D/t ratio at No.6 pass (No.1 fin-pass roll) by flower pattern A

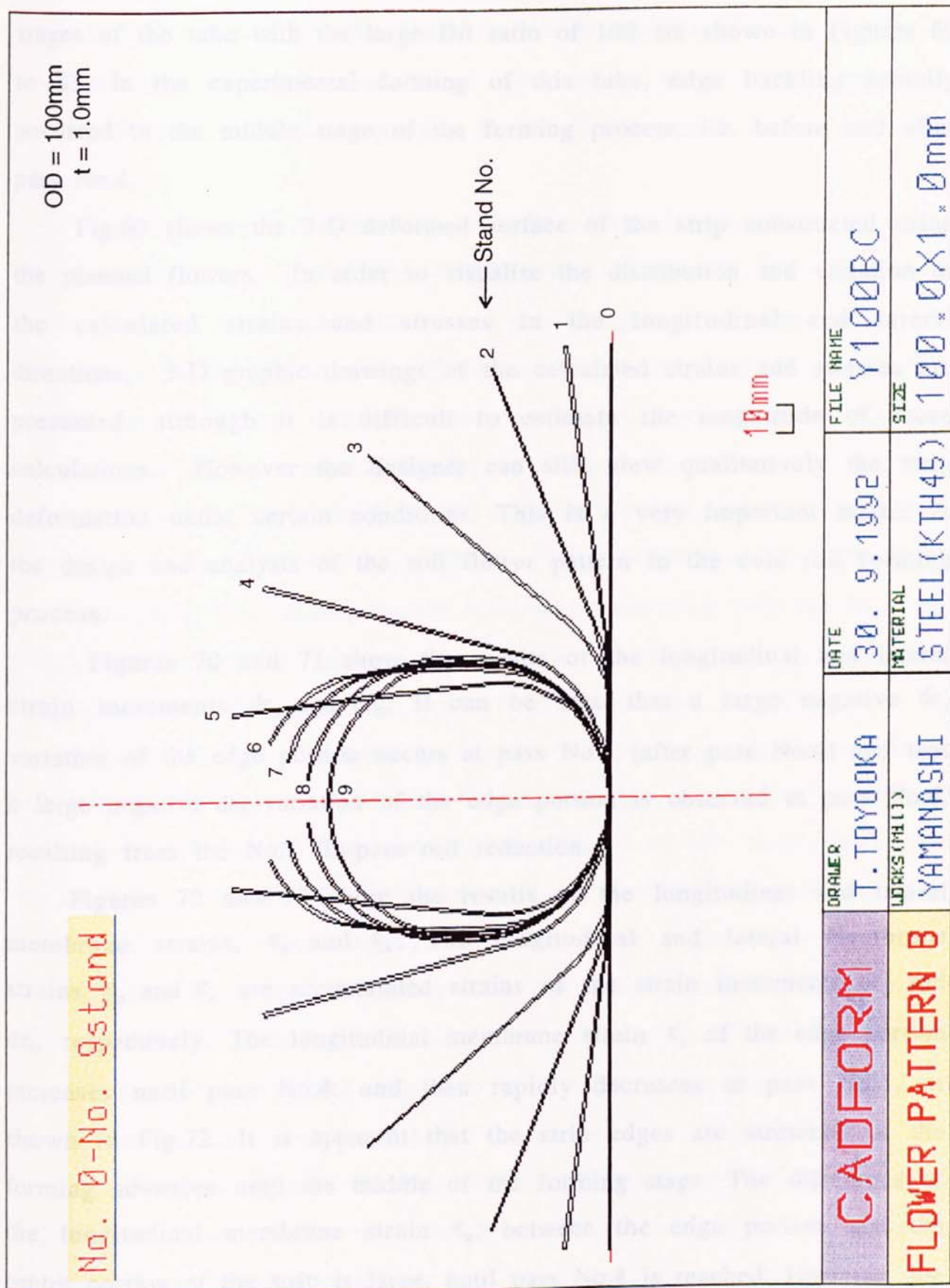


Fig.68 Drawing of planned flowers with large D/t ratio in bottom constant pass-line forming by flower pattern B

Results of the stress-strain analysis by Model-2 for the forming stages of the tube with the large D/t ratio of 100 are shown in Figures 69 to 83. In the experimental forming of this tube, edge buckling actually occurred in the middle stage of the forming process, i.e. before and after pass No.4.

Fig.69 shows the 3-D deformed surface of the strip constructed using the planned flowers. In order to visualise the distribution and variation of the calculated strains and stresses in the longitudinal and lateral directions, 3-D graphic drawings of the calculated strains and stresses are presented, although it is difficult to estimate the magnitude of these calculations. However the designer can still view qualitatively the strip deformation under certain conditions. This is a very important matter in the design and analysis of the roll flower pattern in the cold roll forming process.

Figures 70 and 71 show the results of the longitudinal and lateral strain increments $d\epsilon_z$ and $d\epsilon_x$. It can be seen that a large negative $d\epsilon_z$ variation of the edge portion occurs at pass No.5 (after pass No.4) and that a large negative $d\epsilon_x$ variation of the edge portion is observed at pass No.6, resulting from the No.1 fin-pass roll reduction.

Figures 72 and 73 show the results of the longitudinal and lateral membrane strains, ϵ_z and ϵ_x . The longitudinal and lateral membrane strains ϵ_z and ϵ_x are accumulated strains of the strain increments $d\epsilon_z$ and $d\epsilon_x$, respectively. The longitudinal membrane strain ϵ_z of the edge portion increases until pass No.4, and then rapidly decreases at pass No.5, as shown in Fig.72. It is apparent that the strip edges are stretched as the forming advances until the middle of the forming stage. The difference of the longitudinal membrane strain ϵ_z , between the edge portion and the centre portion of the strip is large, until pass No.4 is reached. However, the lateral distribution of the longitudinal membrane strain ϵ_z becomes uniform, and a tensile strain is apparent after pass No.5, i.e. in the fin-pass

roll forming and squeeze roll forming stages, due to the fin-pass roll and squeeze roll reductions. The lateral membrane strains ϵ_x , shown in Fig.73, homogeneously changes to a large compressive strain condition in the lateral direction of the strip, due to the fin-pass roll and squeeze roll reductions.

Figures 74 and 75 show the results of the longitudinal and lateral stress increments, $d\sigma_z$ and $d\sigma_x$, respectively. There are few reports that have presented up to date results of the theoretical forming strains and stresses in cold roll forming. Thus, this research work is an original presentation that expresses the stress increment distribution of the strip by the stress-strain analysis detailed in Chapter 5. Considering Fig.74 a large negative variation of $d\sigma_z$ at the edge portion also occurs at pass No.5, after pass No.4. However, as shown in Fig.74, substantial variation of $d\sigma_z$ to tensile stress is observed at pass No.6, again resulting from the No.1 fin-pass roll reduction. In Fig.75, a large negative variation of $d\sigma_x$ is observed at pass No.6, which is also due to the No.1 fin-pass roll reduction.

Figures 76 and 77 show the results of the longitudinal and lateral stresses, σ_z and σ_x , respectively. The longitudinal and lateral membrane stresses σ_z and σ_x are the accumulated stresses of the stress increments $d\sigma_z$ and $d\sigma_x$, respectively. The envisaged stress distribution of the strip could not be predicted, although there are some cases where the stress condition can be more informative than the strain condition. These results of the longitudinal and lateral membrane stresses σ_z and σ_x is also an original presentation which expresses the stress distribution of the strip by the stress-strain analysis detailed previously.

As shown in Fig.76, the longitudinal membrane stress σ_z of the strip edge increases to a tensile stress until pass No.4, then rapidly decreases to a compressive stress at pass No.5. The strip edges are subjected to a tensile stress condition and the difference of σ_z between the edge portion and the centre portion of the strip increases as the forming advances until

it reaches the middle of the forming stage. Here the strip at these stages is subjected to a fairly large compressive stress condition after pass No.4 due to the change of the trace length of the strip edge. It is also theoretically established that compression acts on the strip edge in the downstream forming stages.

Furthermore, the longitudinal membrane stress σ_z of the edge portion changes to a tensile stress at pass No.6, i.e. in the first fin-pass roll forming stage, due to the fin-pass roll reduction. However, the lateral distribution of σ_z becomes uniform in the squeeze roll forming stage. Furthermore, it is apparent that the strip sheet is subjected to a complex stress condition in the longitudinal and lateral directions as the forming advances.

The lateral membrane stress σ_x , shown in Fig.77, uniformly changes to a large compressive stress condition in the lateral direction of the strip from pass No.6, due to the fin-pass roll and squeeze roll reductions.

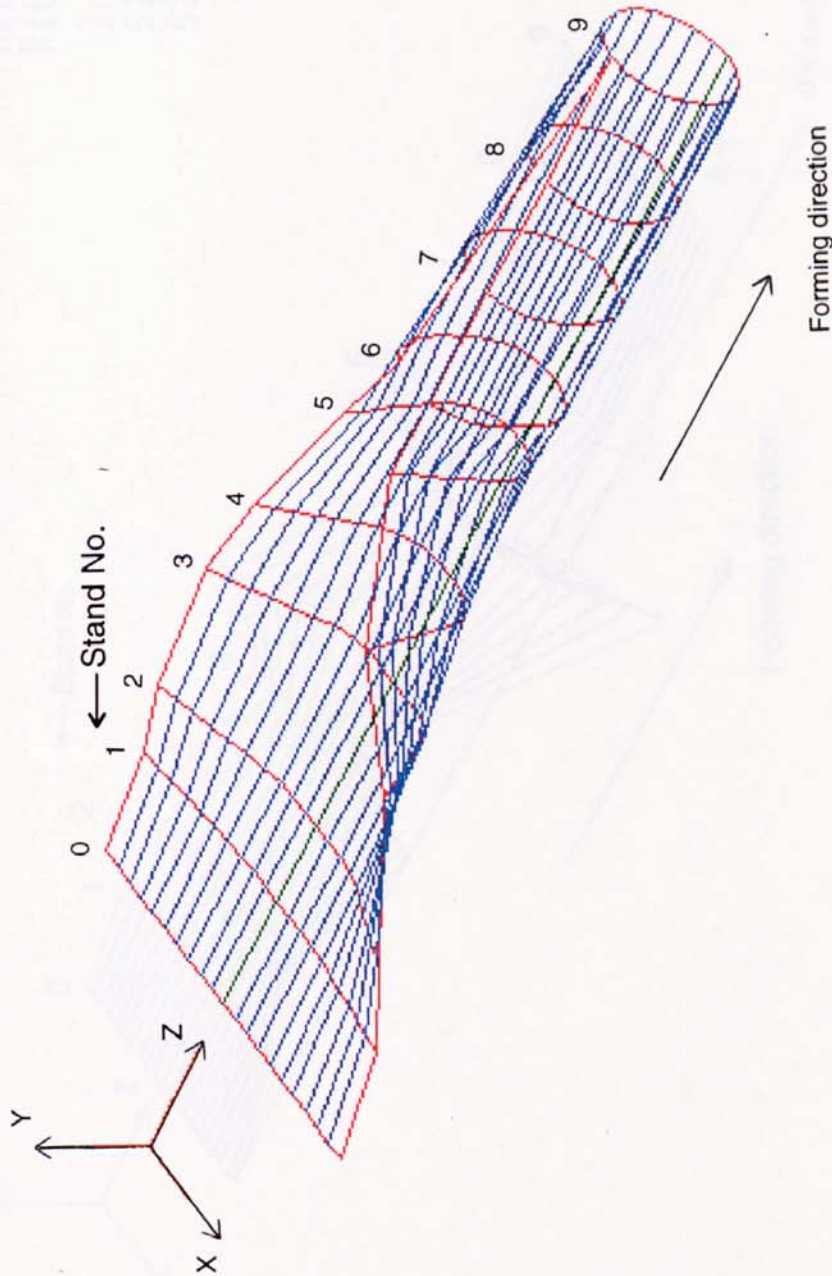
Fig.78 shows the equivalent stress, $\bar{\sigma}$. The equivalent stress $\bar{\sigma}$, of the edge portion, is large after pass No.2 since the material at the edges of the strip will be subjected to significant work-hardening in the early forming stages. The difference of the equivalent stress $\bar{\sigma}$, between the edge portion and the centre portion of the strip is noticeably large until pass No.5. This suggests that the strip edges are substantially more deformed, compared to the strip center portion. Thus, the complete material in the lateral direction is subjected to the significant work-hardening at pass No.6, again resulting from the No.1 fin-pass roll reduction. Thus, the lateral distribution of the equivalent stress, $\bar{\sigma}$ becomes uniform after pass No.5, i.e. in the fin-pass roll forming and squeeze roll forming stages, due to the fin-pass roll and squeeze roll reductions. The magnitude of the equivalent stress $\bar{\sigma}$, from pass No.6, appears to be of a constant value. However, this value gradually increases as a result of the material work-hardening as the forming advances. This work-hardening of the tube can also be estimated from the calculated equivalent stress.

Stress-Strain Analysis(Model-2)

3-D DRAWING

Pass Line Length
L = 4068.00 mm

Rotation Angle of Axis (deg.)
Bank = 0.00
Head = 50.00
Pitch = 40.00
Scale Ratio
SZX = 8.00
SZY = 8.00
OD = 100mm
t = 1.0mm



CADFORM	DRAWER T. TOYOOKA	DATE 30. 9. 1992	FILE NAME Y100BC
3-D Deformation Surface	WORKS (MILL) YAMANASHI	MATERIAL STEEL (KTH45)	SIZE 100 * 0X1 * 0mm

Fig.69 Computer graphic drawing of 3-D deformed surface of the strip constructed using planned flowers with $D = 100.0\text{mm}$ and $t = 1.0\text{mm}$ for bottom constant pass-line forming

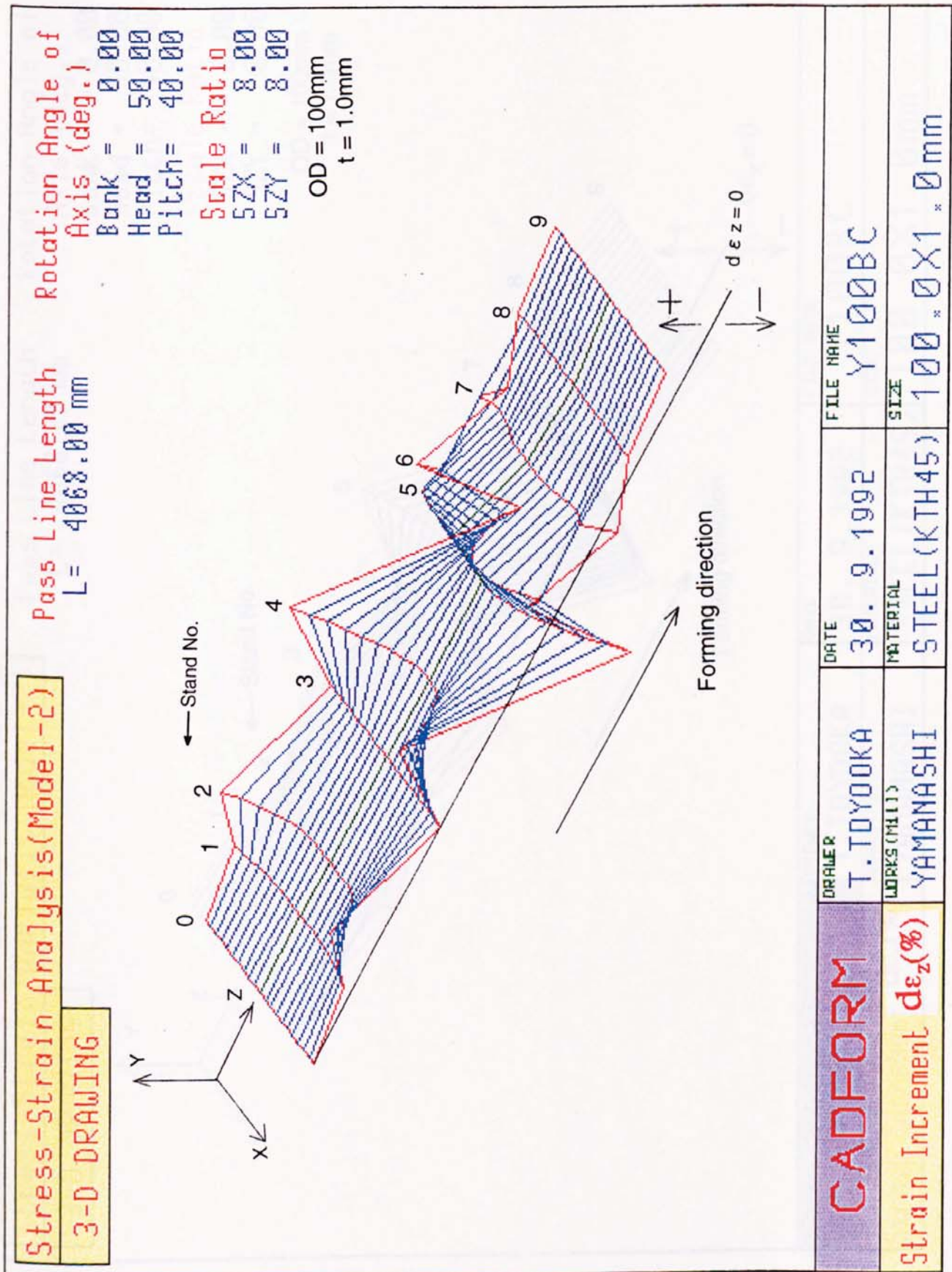


Fig.70 3-D graphics drawing of longitudinal membrane strain increment $d\epsilon_z$ calculated by CADFORM system

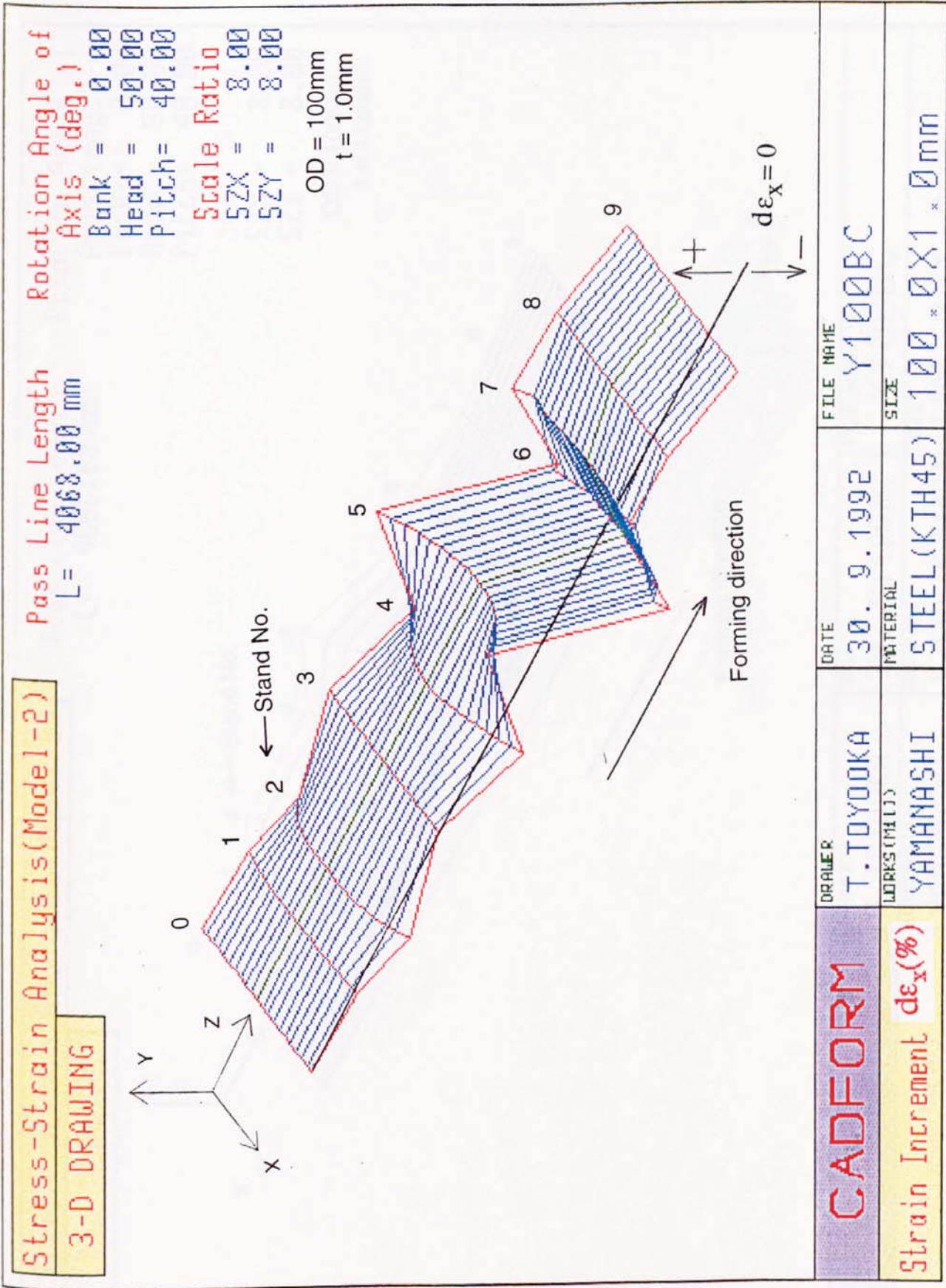


Fig.71 3-D graphics drawing of lateral membrane strain increment $d\epsilon_x$ calculated by CADFORM system

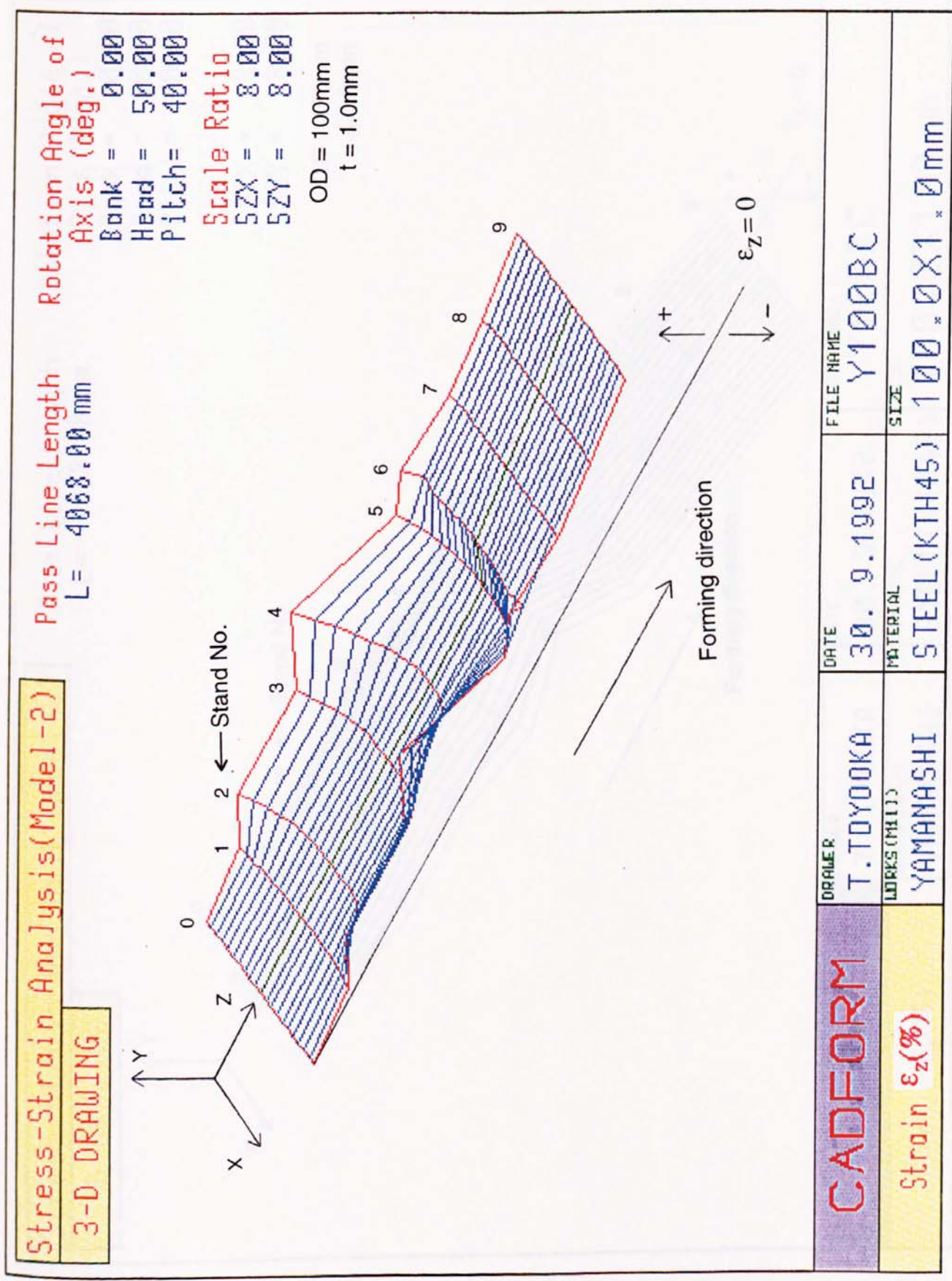


Fig.72 3-D graphics drawing of longitudinal strain ϵ_z calculated by CADFORM system

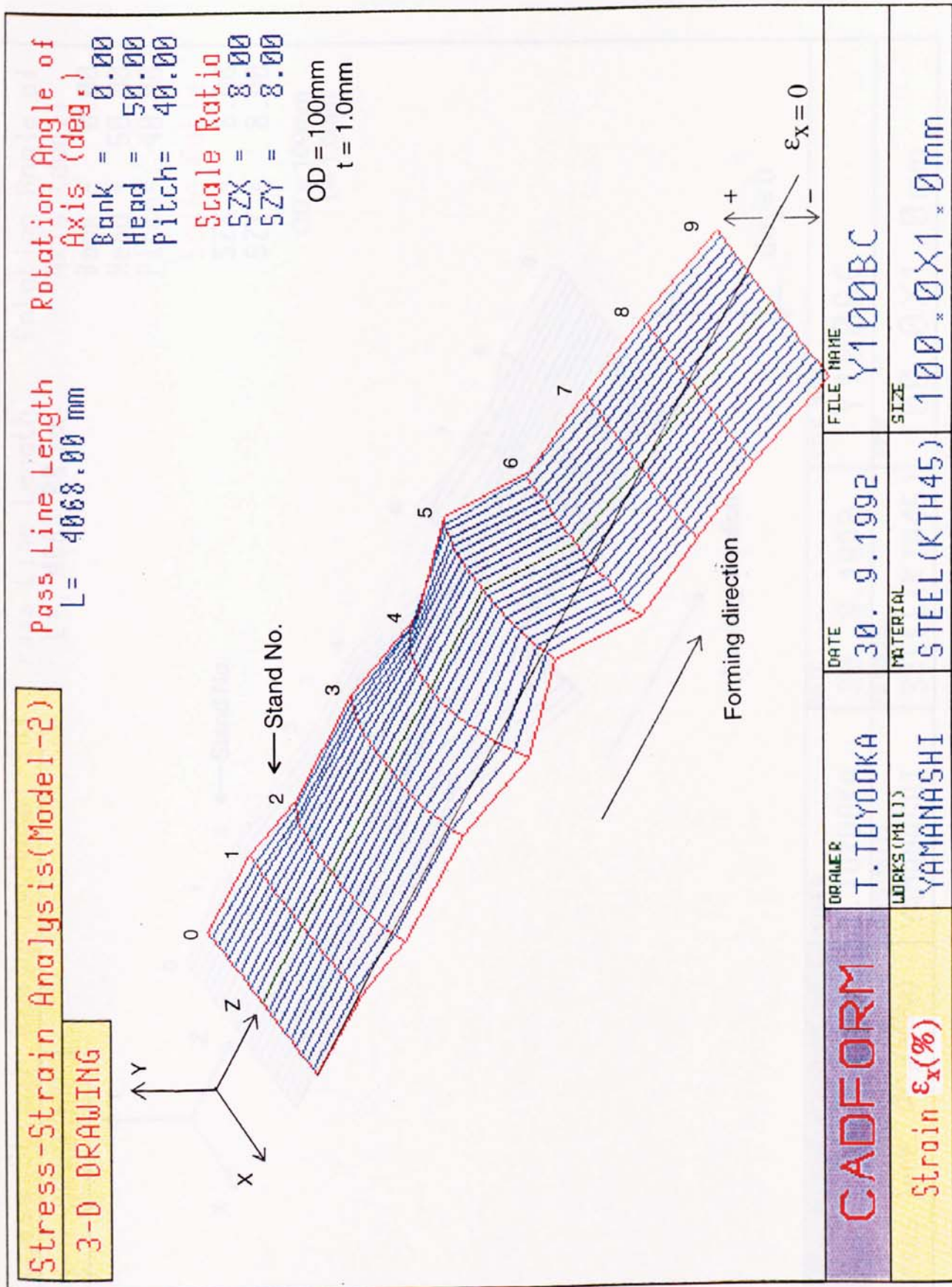


Fig.73 3-D graphics drawing of lateral strain ϵ_x calculated by CADFORM system

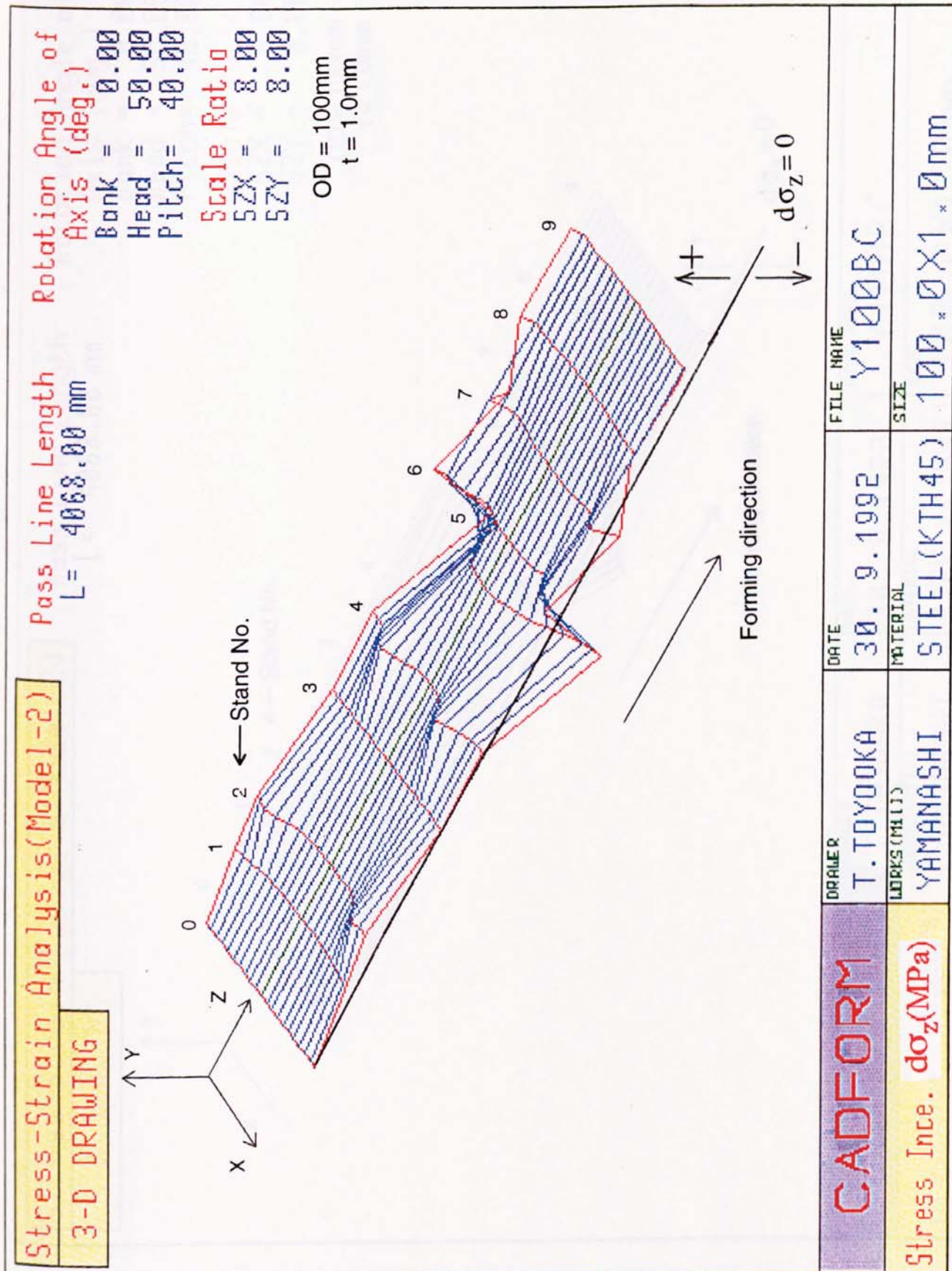


Fig.74 3-D graphics drawing of longitudinal stress increment $d\sigma_z$ calculated by CADFORM system

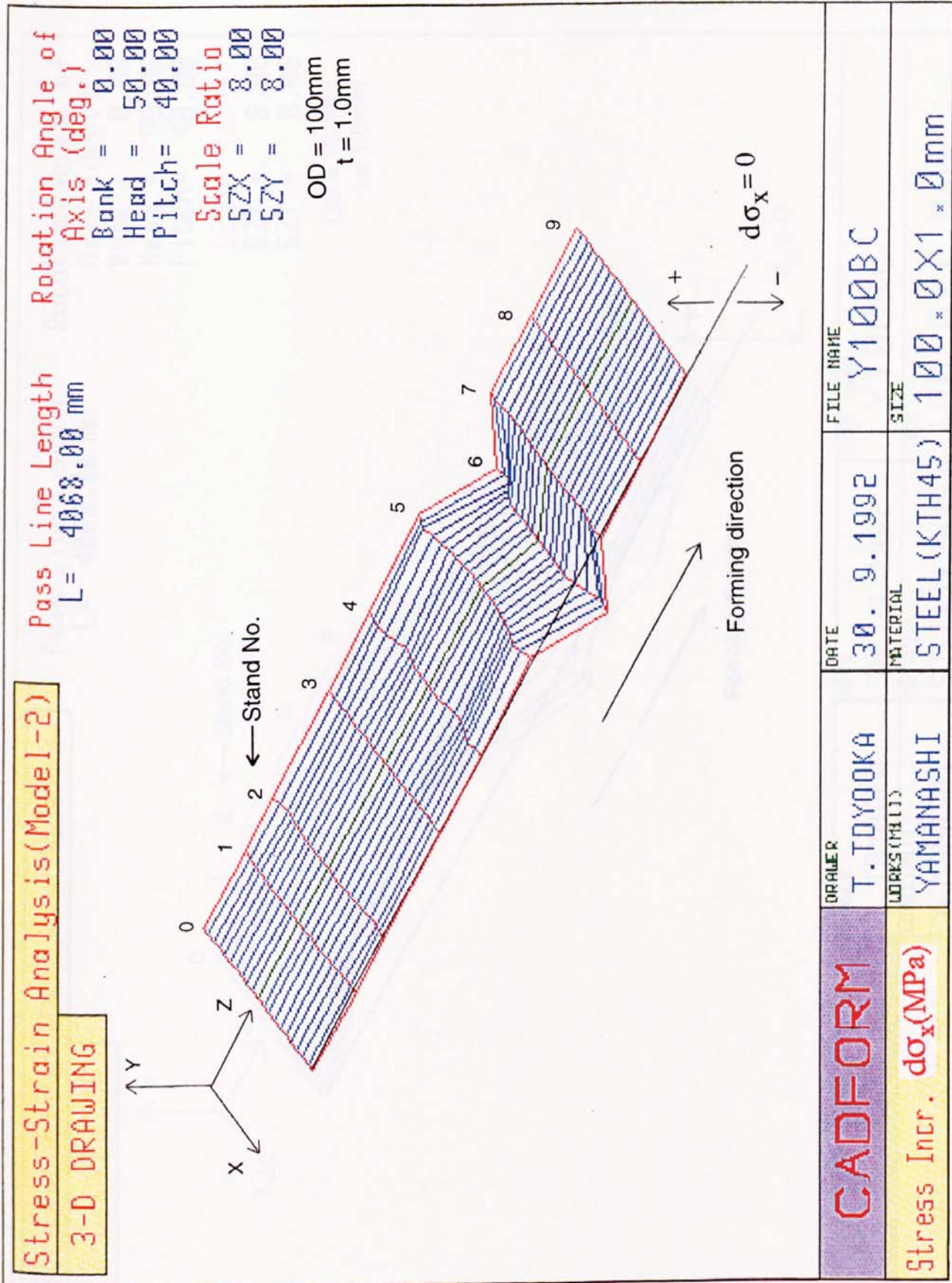


Fig.75 3-D graphics drawing of lateral stress increment $d\sigma_x$ calculated by CADFORM system

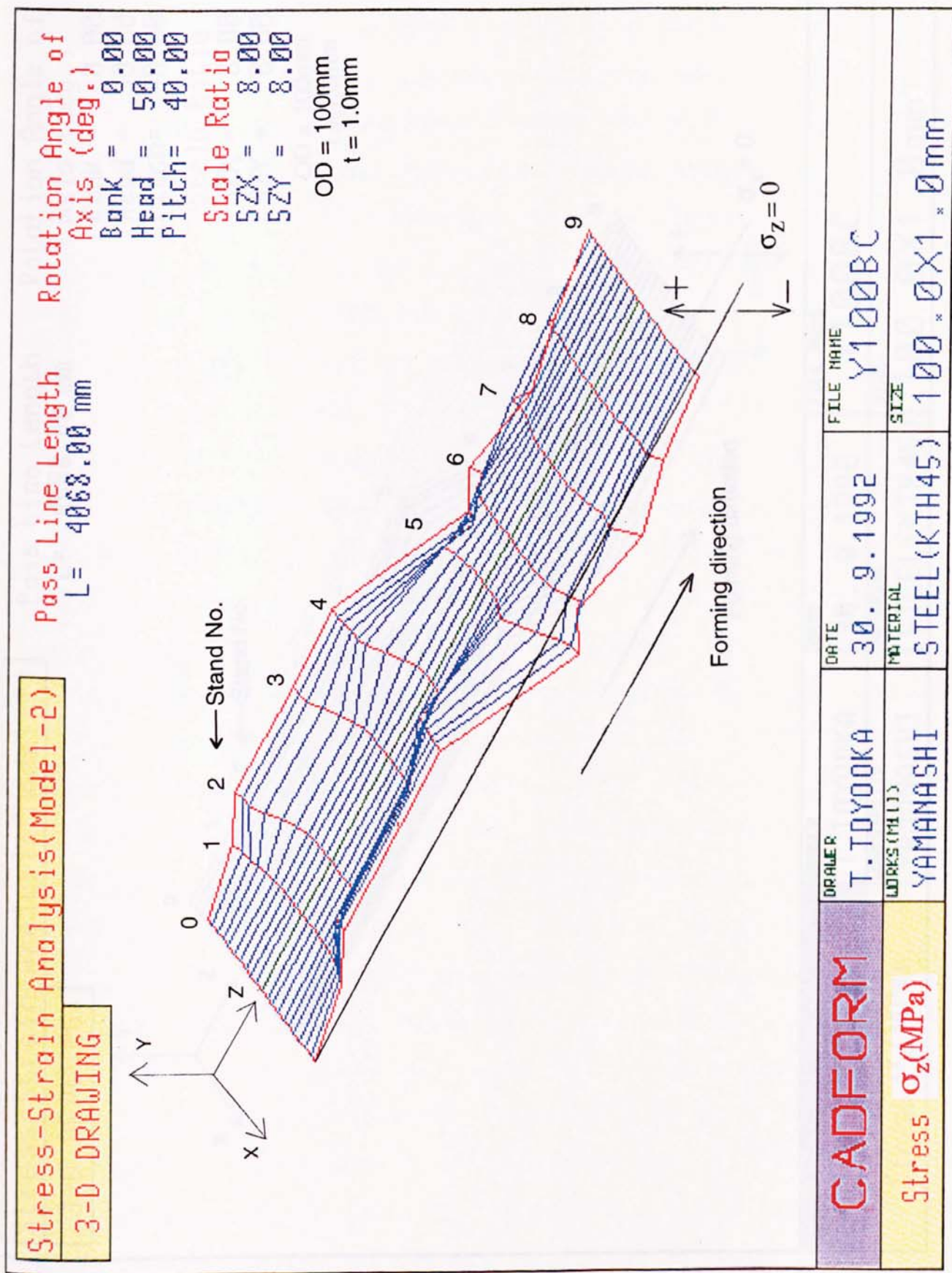


Fig.76 3-D graphics drawing of longitudinal stress σ_z calculated by CADFORM system

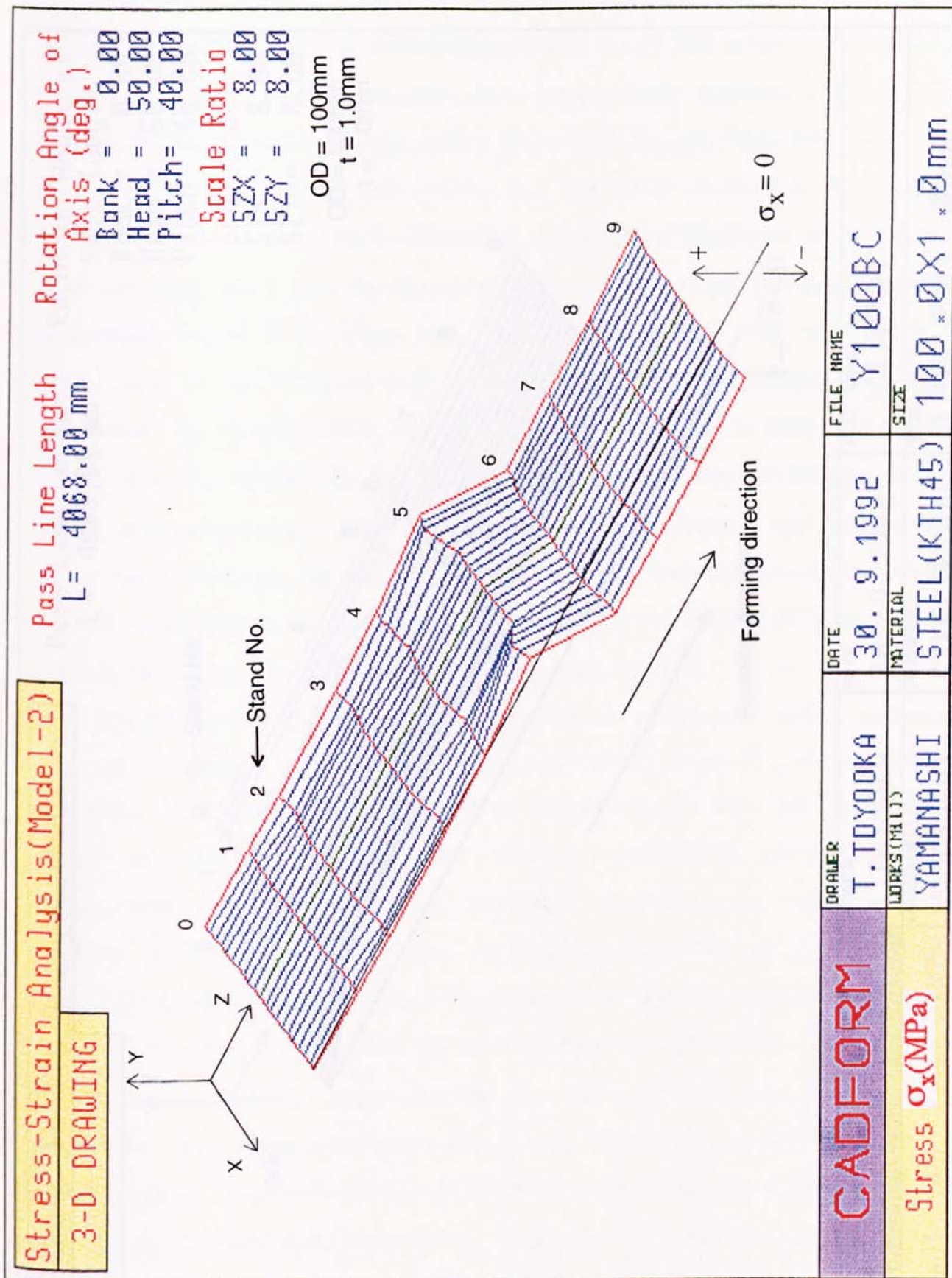


Fig.77 3-D graphics drawing of lateral stress σ_x calculated by CADFORM system

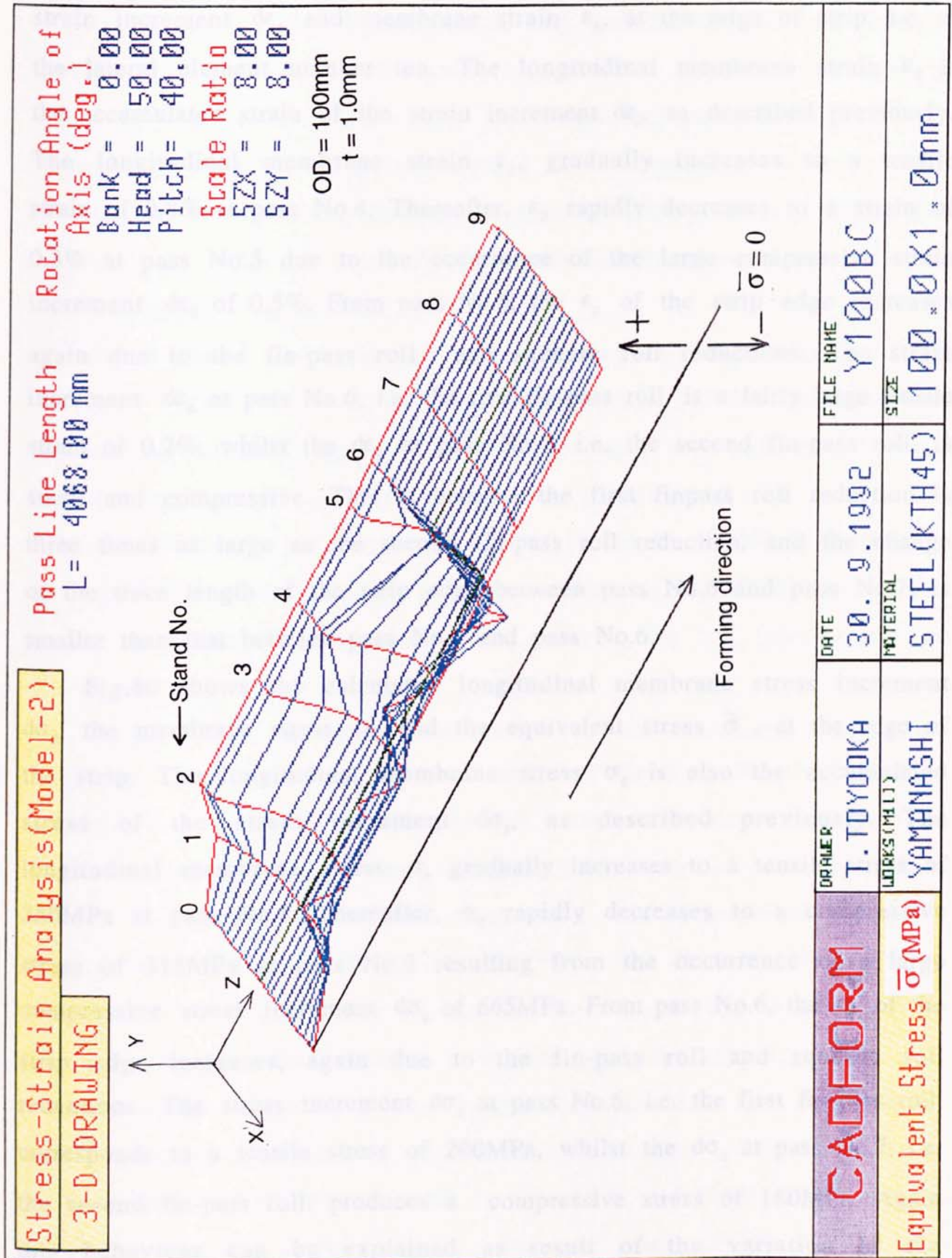


Fig.78 3-D graphics drawing of equivalent stress $\bar{\sigma}$ calculated by CADFORM system

Fig.79 shows the variation of the calculated longitudinal membrane strain increment $d\epsilon_z$ and membrane strain ϵ_z , at the edge of strip, i.e. at the lateral element number ten. The longitudinal membrane strain ϵ_z is the accumulated strain of the strain increment $d\epsilon_z$, as described previously. The longitudinal membrane strain ϵ_z , gradually increases to a tensile strain of 0.8% at pass No.4. Thereafter, ϵ_z rapidly decreases to a strain of 0.3% at pass No.5 due to the occurrence of the large compressive strain increment $d\epsilon_z$ of 0.5%. From pass No.6, the ϵ_z of the strip edge increases again due to the fin-pass roll and squeeze roll reductions. The strain increment $d\epsilon_z$ at pass No.6, i.e. the first fin-pass roll, is a fairly large tensile strain of 0.2%, whilst the $d\epsilon_z$ at pass No.7, i.e. the second fin-pass roll, is small and compressive. This is because the first finpass roll reduction is three times as large as the second fin-pass roll reduction, and the change of the trace length of the strip edge between pass No.6 and pass No.7, is smaller than that between pass No.5 and pass No.6.

Fig.80 shows the calculated longitudinal membrane stress increment $d\sigma_z$, the membrane stress σ_z and the equivalent stress $\bar{\sigma}$, at the edge of the strip. The longitudinal membrane stress σ_z is also the accumulated stress of the stress increment $d\sigma_z$, as described previously. The longitudinal membrane stress σ_z gradually increases to a tensile stress of 350MPa at pass No.4. Thereafter, σ_z rapidly decreases to a compressive stress of 315MPa at pass No.5 resulting from the occurrence of a large compressive stress increment $d\sigma_z$ of 665MPa. From pass No.6, the σ_z of the strip edge increases, again due to the fin-pass roll and squeeze roll reductions. The stress increment $d\sigma_z$ at pass No.6, i.e. the first fin-pass roll, corresponds to a tensile stress of 200MPa, whilst the $d\sigma_z$ at pass No.7, i.e. the second fin-pass roll, produces a compressive stress of 180MPa. Again this behaviour can be explained as result of the variation of the longitudinal membrane strain shown in Fig.79.

The large variation of each strain and stress is clearly confirmed at pass

No.5. It can be said that the strip edge is subjected to a critical occurrence of edge buckling in this forming stage, and thus the fin-pass roll reduction is effective in decreasing the compressive stress of the strip edge. As shown in Fig.80, the variation of the equivalent stress $\bar{\sigma}$, at the edge portion was predicted to yield according to the results of the stress-strain analysis, which considered the biaxial stress condition. It is apparent that the equivalent stress $\bar{\sigma}$ gradually increases as the material work-hardens with the advance of forming.

Fig.81 shows the result of the variation of the longitudinal maximum membrane strain $\epsilon_{z,max}$ at the edge of the strip between each pass, as obtained by Kiuchi⁵⁷. In this case the tube sizes were different, however Kiuchi's approximate magnitude and the variation of the longitudinal membrane strain ϵ_z , are reasonably similar to results of this analysis using the CADFORM system. Thus, it is suggested that the CADFORM system can provide a reasonable simulation of the strain in the roll forming of tube and pipe.

Fig.82 shows the lateral distribution of the calculated longitudinal membrane strain increment $d\epsilon_z$, and membrane strain ϵ_z , in a half width of the strip at pass No.5. The longitudinal compressive strain increment $d\epsilon_z$ occurs in the whole strip width at pass No.5, with its value increasing towards the strip edge. On the other hand, the longitudinal membrane strain ϵ_z is tensile across the whole strip width and its value also increases towards the strip edge. This is because the whole strip is substantially stretched until pass No.4. Thus it is apparent that the strip is subjected to a tensile strain condition in the longitudinal direction and consequently there is minimal occurrence of edge buckling according to the single result of the longitudinal membrane strain ϵ_z . Clearly it is difficult to estimate the occurrence of edge buckling from only one result of the longitudinal membrane strain.

Fig.83 shows the lateral distribution of the calculated longitudinal

membrane stress increment $d\sigma_z$ and membrane stress σ_z , for the same situation as in Fig.82. The longitudinal compressive stress increment $d\sigma_z$, occurs across the whole strip width at pass No.5. The value of $d\sigma_z$ increases approaching the strip edge, becoming large and compressive stress (665MPa) at the strip edge. The sections of approximately one quarter of the strip width from the edge, are subjected to a compressive stress due to the addition of this large compressive stress increment. In particular, elements towards the edge portion are subjected to a large compressive stress of 315MPa. It is therefore considered that there is a critical condition of edge buckling occurrence according to the result of longitudinal stress analysis, although the evaluation by the edge buckling analysis has not yet been shown here - see Figures 88 and 89. Thus the longitudinal stress analysis is more significant than the strain analysis in estimating a critical condition of the occurrence of edge buckling. There are few reports that actually present and discuss the stresses of the strip in the forming stages in respect of estimating the edge buckling occurrence.

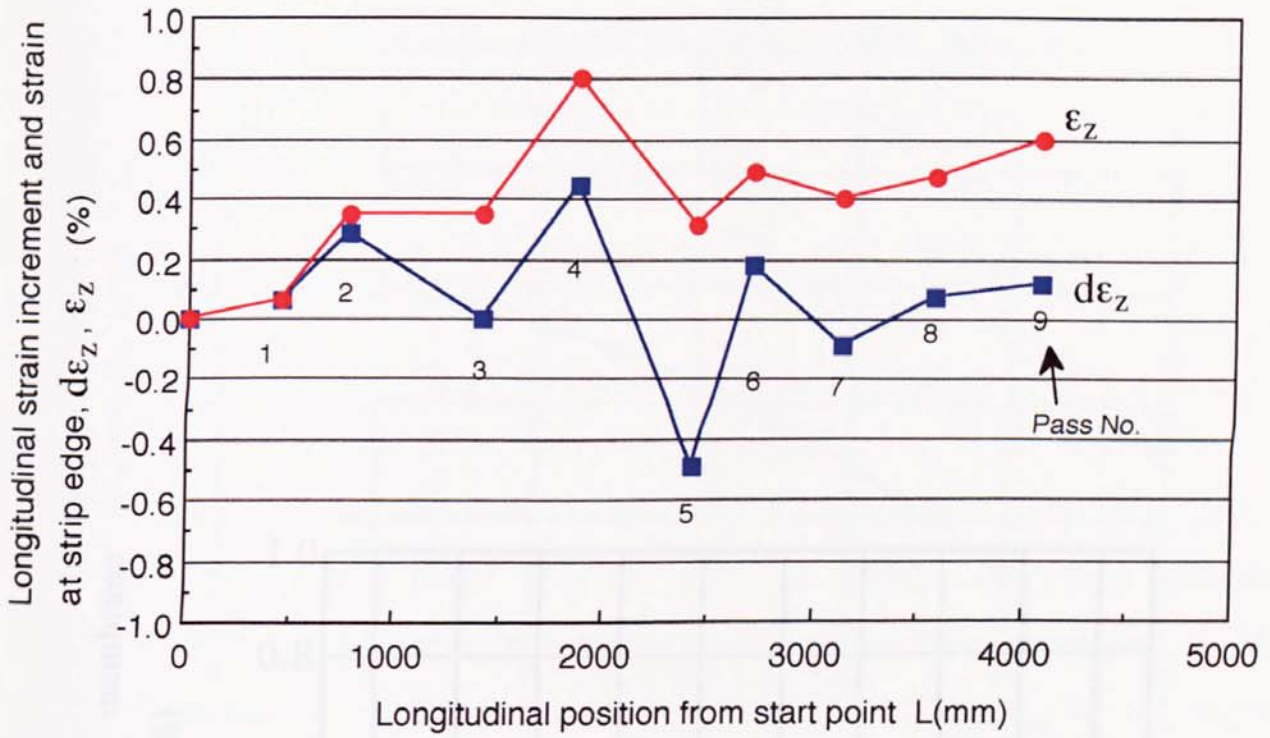


Fig.79 Variation of calculated longitudinal membrane strain increment and strain at strip edge in forming of tube with D/t ratio 100

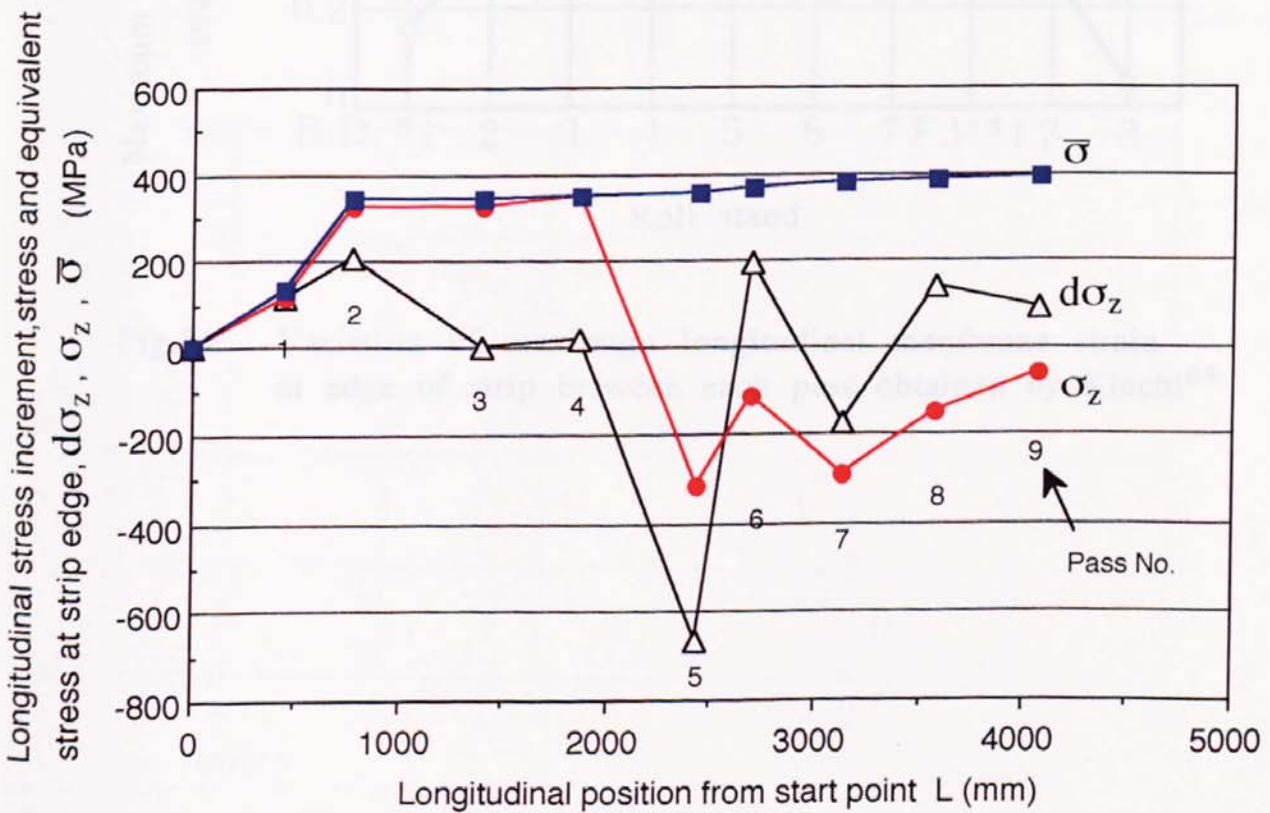


Fig.80 Variation of calculated longitudinal membrane stress increment, stress and equivalent stress at strip edge in forming of tube with D/t ratio 100

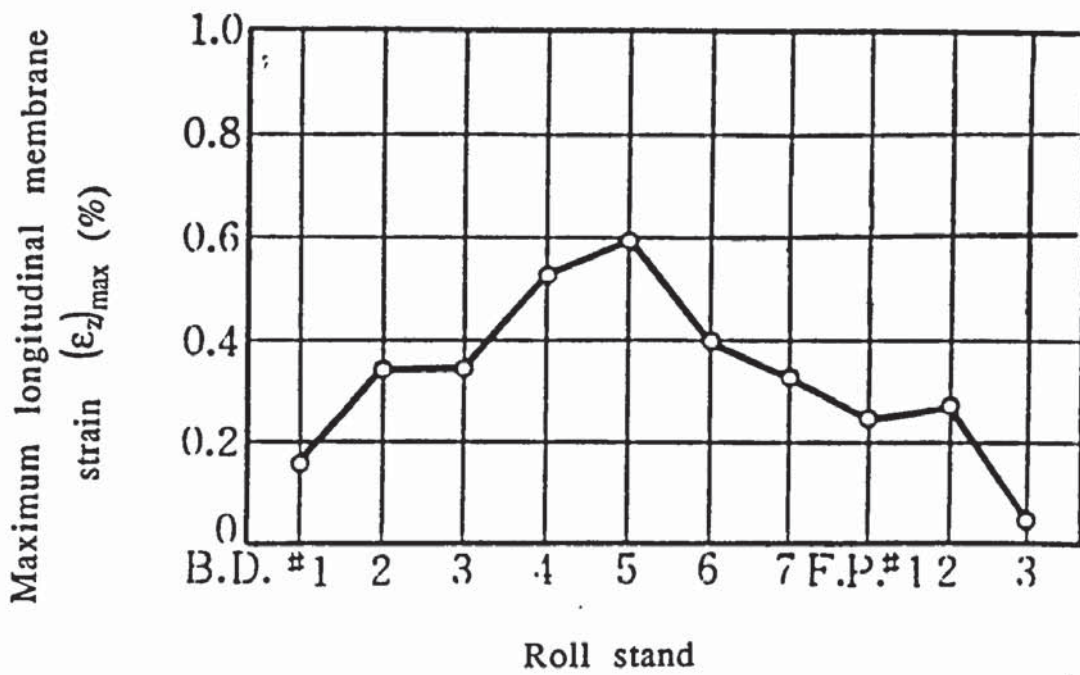


Fig.81 Variation of maximum longitudinal membrane strain at edge of strip between each pass obtained by Kiuchi⁶³

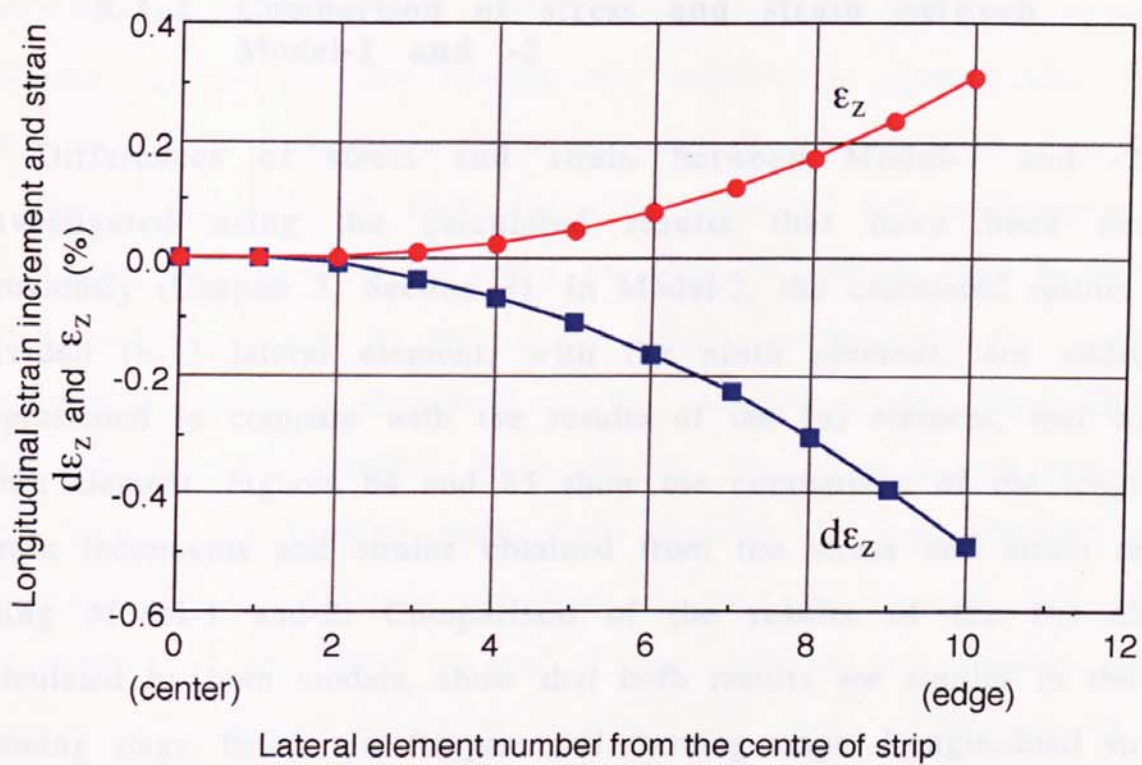


Fig.82 Lateral distribution of calculated longitudinal membrane strain increment and strain at strip edge at pass No.5

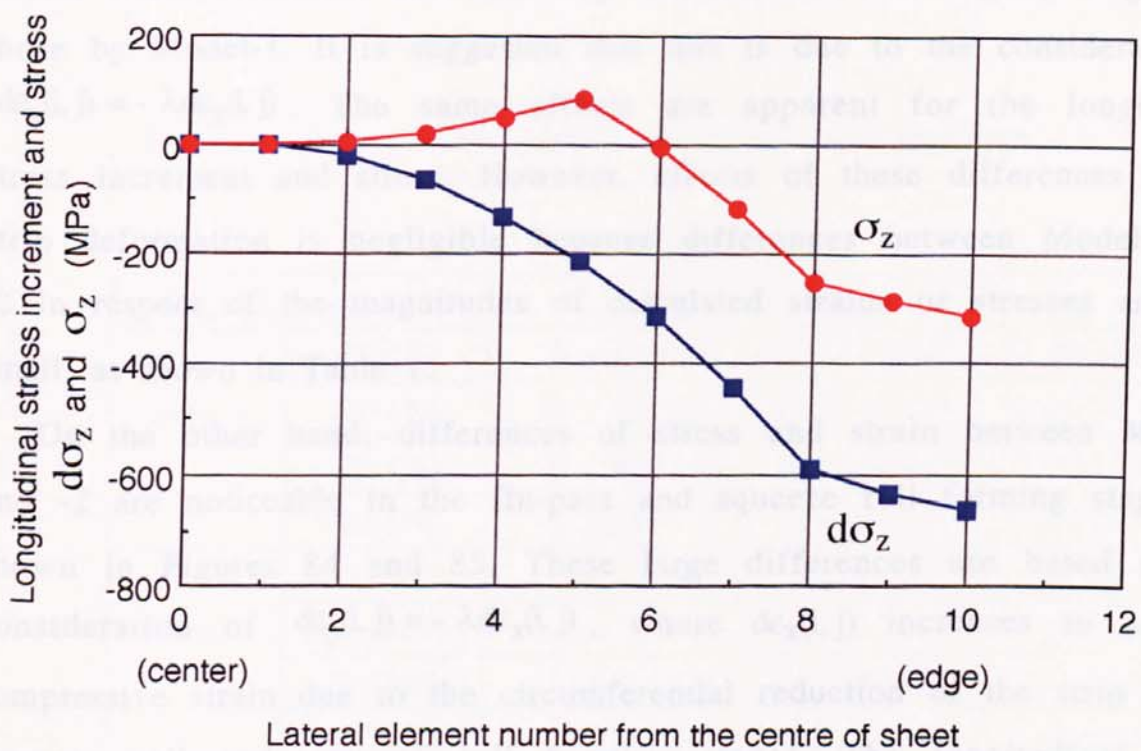


Fig.83 Lateral distribution of calculated longitudinal membrane stress increment and stress at strip edge at pass No.5

8.1.2 Comparison of stress and strain between Model-1 and -2

Differences of stress and strain between Model-1 and -2 were investigated using the calculated results that have been described previously (Chapter 5, Section 3). In Model-2, the calculated results of the divided (n-1) lateral element, with the ninth element, are additionally represented to compare with the results of the (n) element, and with the tenth element. Figures 84 and 85 show the comparison of the longitudinal strain increments and strains obtained from the stress and strain analyses using Model-1 and-2. Comparison of the results of the (n) element, calculated by both models, show that both results are similar in the upper forming stage, before the fin-pass roll forming stage. Longitudinal strain of the (n-1) element is generally smaller than that of the (n) element. As shown in Table 1, the longitudinal strain increment and strain predicted by Model-2, are slightly smaller than those given by Model-1, whilst the lateral strain increment and strain by the Model-2, are slightly larger than those by Model-1. It is suggested that this is due to the consideration of $d\epsilon_y(i, j) = -\lambda d\epsilon_x(i, j)$. The same effects are apparent for the longitudinal stress increment and stress. However, effects of these differences on the strip deformation is negligible because differences between Model-1 and -2 in respect of the magnitudes of calculated strains or stresses are very small, as shown in Table 1.

On the other hand, differences of stress and strain between Model-1 and -2 are noticeable in the fin-pass and squeeze roll forming stages, as shown in Figures 84 and 85. These large differences are based on the consideration of $d\epsilon_y(i, j) = -\lambda d\epsilon_x(i, j)$, where $d\epsilon_x(i, j)$ increases to a large compressive strain due to the circumferential reduction of the strip in the fin-pass roll and squeeze roll forming stages. The longitudinal strain increment and strain also increases in the fin-pass roll and squeeze roll forming stages due to the fin-pass reduction. Effects of the circumferential

reduction of the strip are apparent, especially in the first fin-pass roll forming, because the first fin-pass roll reduction is about 0.58%, and this value is two or three times larger than that at other forming stages.

Figures 86 and 87 show the comparison of the longitudinal stress increments and stresses calculated by Model-1 and -2. The behaviour of the stresses is similar to that of the strains. Furthermore, the longitudinal compressive stress is decreased by the addition of the compressive fin-pass reductions in Model-2. In particular, this effect is apparent for the first fin-pass roll forming stage. This suggests that edge buckling can be suppressed by the fin-pass reduction. It can also be seen that complex deformation at the edge portion of the strip in the fin-pass roll and squeeze roll forming stages is expressed by large differences of stress between the (n) and (n-1) elements in Model-2, as shown in Fig. 87.

Table 1 Stresses and strains at pass No.4 calculated by Models-1 and -2

At pass No.4		A:Model-2	B:Model-1	A-B
Strain	d ϵ_z (%)	0.447569	0.449034	-0.001465
	d ϵ_x (%)	-0.223784	-0.224517	0.000733
	ϵ_z (%)	0.799622	0.801365	-0.001743
	ϵ_x (%)	-0.399811	-0.400680	0.000869
Stress	d σ_z (MPa)	21.7505	21.7720	-0.0215
	d σ_x (MPa)	24.3363	24.3261	0.0102
	σ_z (MPa)	348.2573	348.3047	-0.0474
	σ_x (MPa)	-3.5575	-3.5314	-0.0261

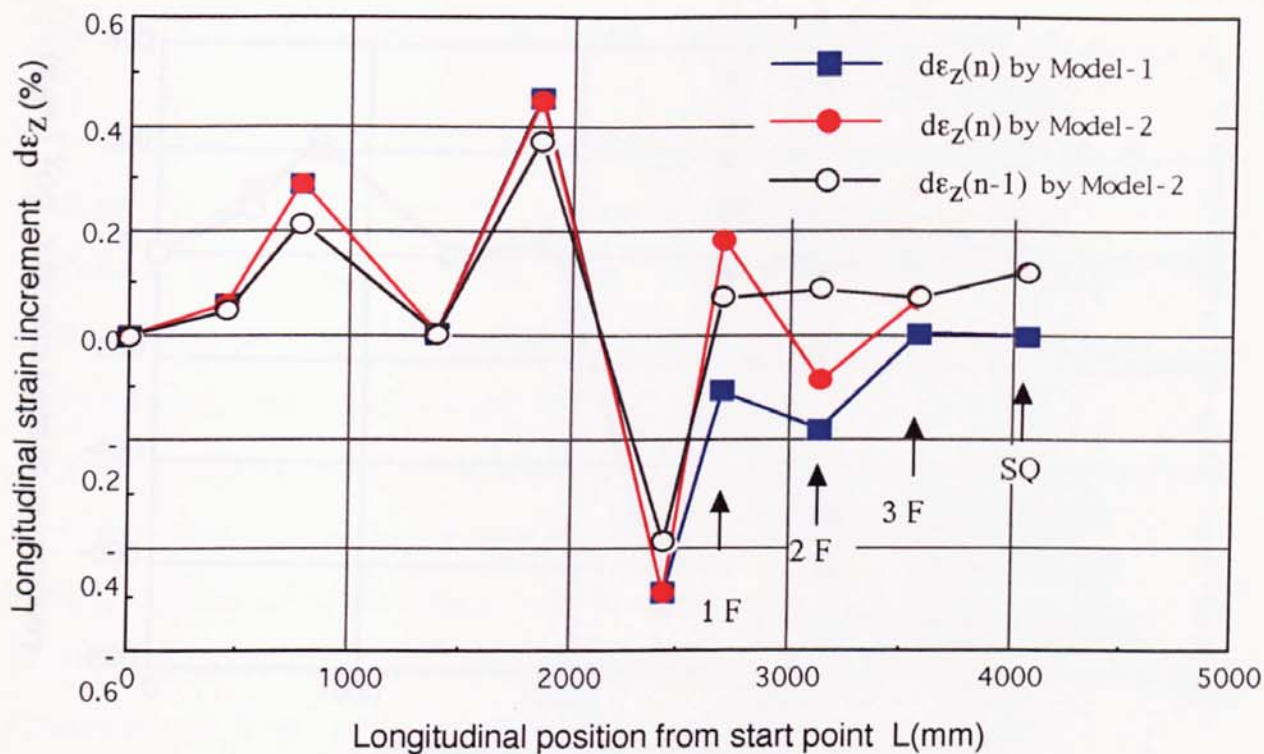


Fig.84 Comparison of calculated longitudinal strain increments using stress and strain analyses from Model-1 and -2

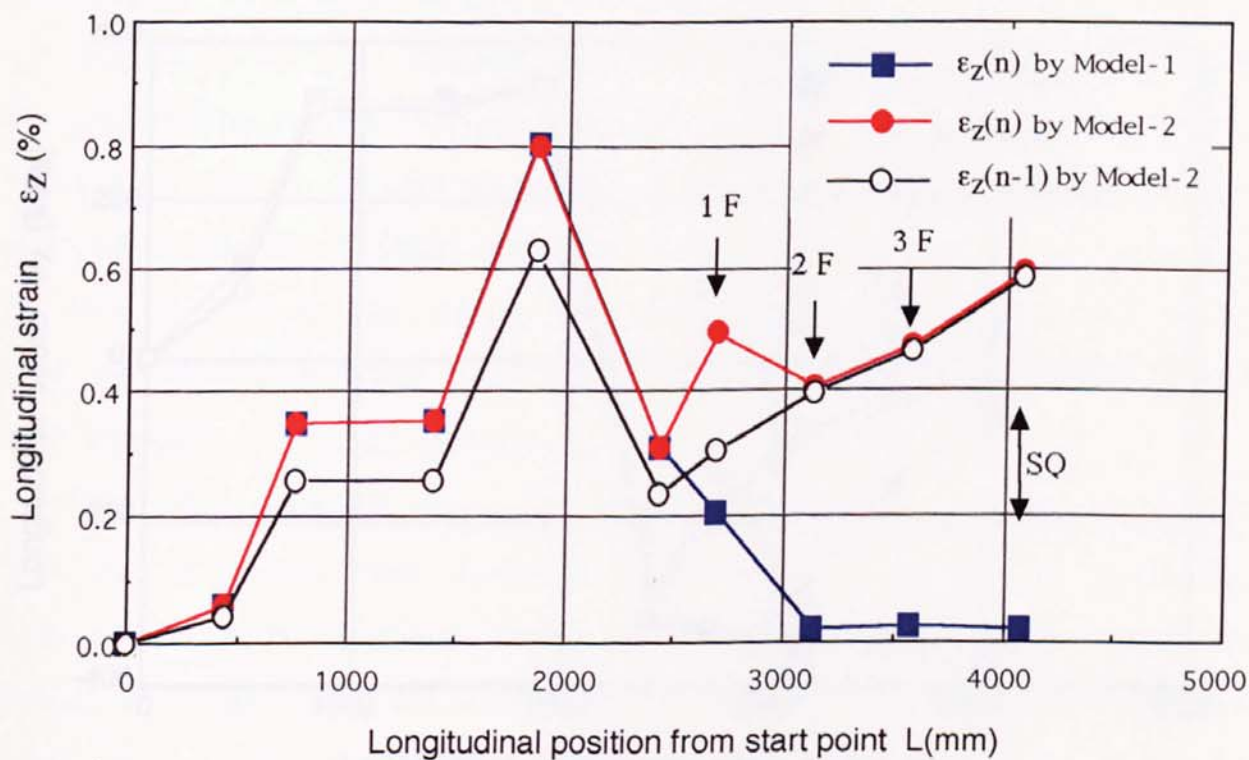


Fig.85 Comparison of calculated longitudinal strains using stress and strain analyses from Model-1 and -2

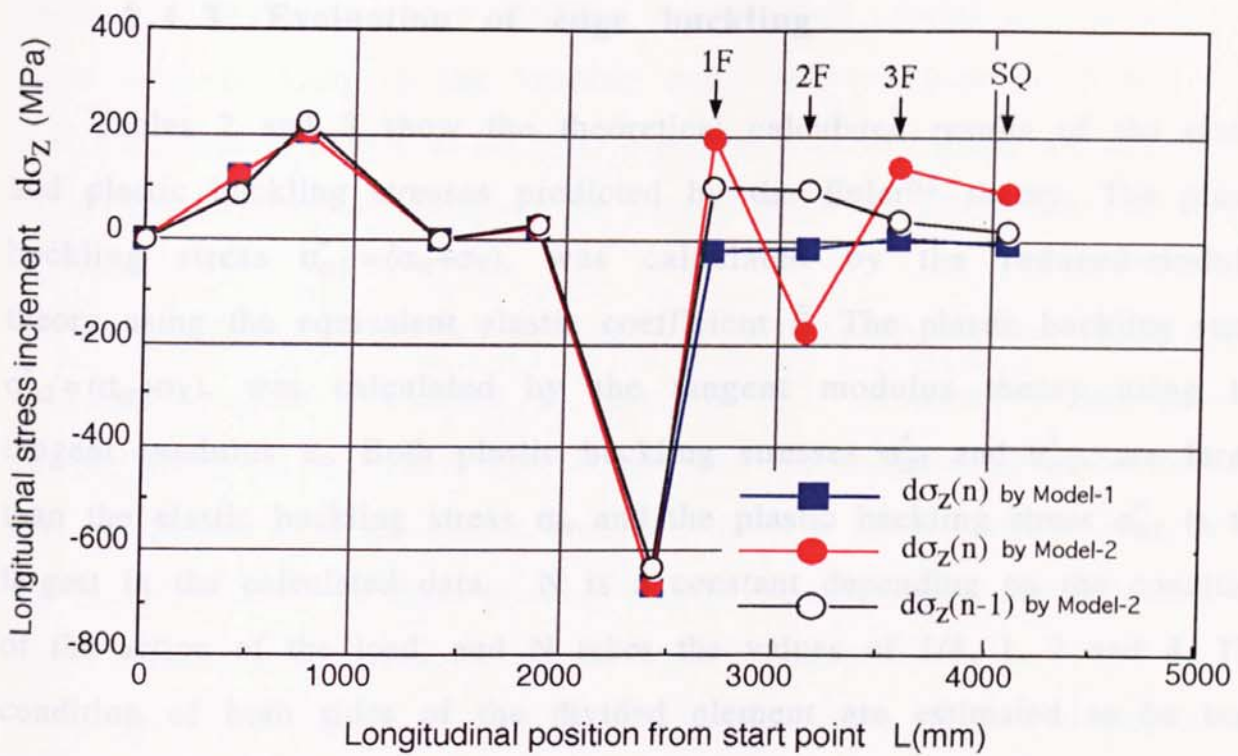


Fig.86 Comparison of calculated longitudinal stress increments using stress and strain analyses from Model-1 and -2

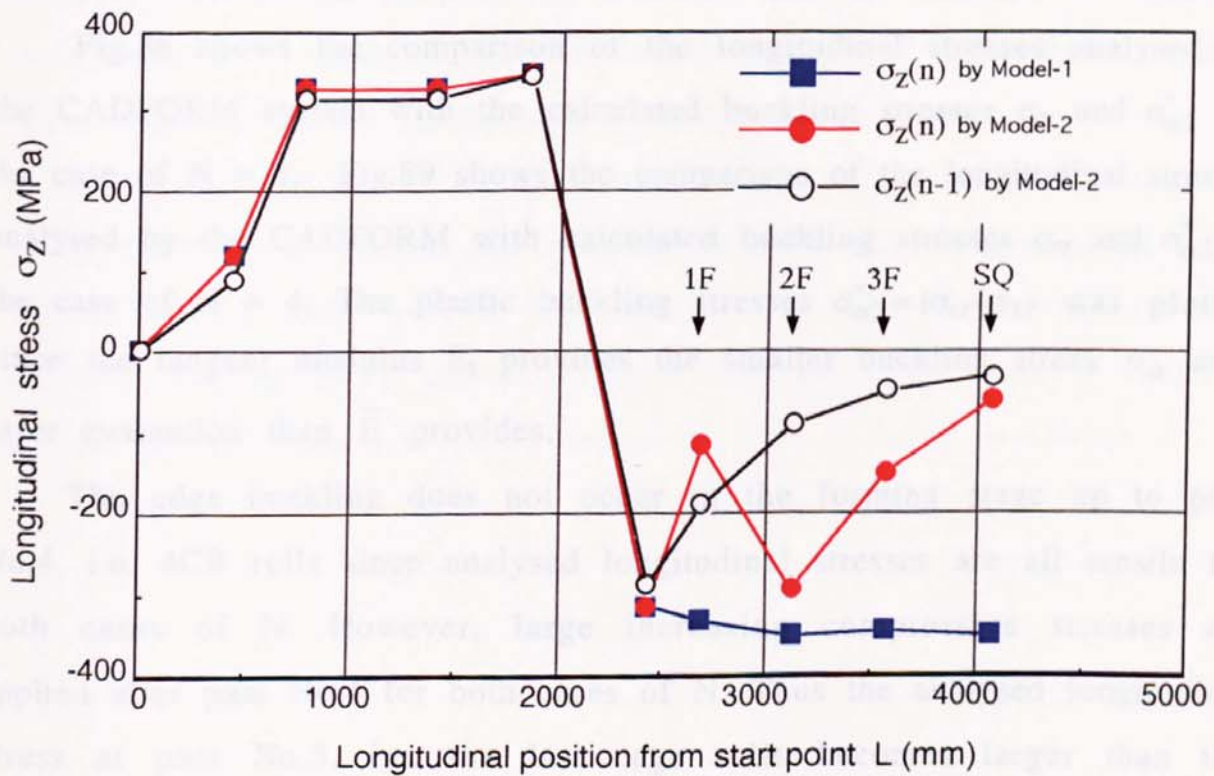


Fig.87 Comparison of calculated longitudinal stresses using stress and strain analyses from Model-1 and -2

8.1.3 Evaluation of edge buckling

Tables 2 and 3 show the theoretical calculated results of the elastic and plastic buckling stresses predicted by the Euler⁶¹ theory. The plastic buckling stress $\sigma_{cr1}^* = (\sigma_{cr} + \sigma_Y)$, was calculated by the reduced-modulus theory using the equivalent elastic coefficient \bar{E} . The plastic buckling stress $\sigma_{cr2}^* = (\sigma_{cr} + \sigma_Y)$, was calculated by the tangent modulus theory using the tangent modulus E_t . Both plastic buckling stresses σ_{cr1}^* and σ_{cr2}^* , are larger than the elastic buckling stress σ_{cr} and the plastic buckling stress σ_{cr1}^* is the largest in the calculated data. N is a constant depending on the condition of the action of the load, and N takes the values of 1/4, 1, 2 and 4. The condition of both sides of the divided element are estimated to be both hinged ends $N=1$ or both fixed ends $N=4$ because the strip sheet is pinched by forming rolls. Thus, the buckling stress calculation was carried out using N values of 1 and 4 although it is difficult to decide the actual fixing condition of both edges between each roll stand.

Fig.88 shows the comparison of the longitudinal stresses analysed by the CADFORM system with the calculated buckling stresses σ_{cr} and σ_{cr2}^* for the case of $N = 1$. Fig.89 shows the comparison of the longitudinal stresses analysed by the CADFORM with calculated buckling stresses σ_{cr} and σ_{cr2}^* in the case of $N = 4$. The plastic buckling stresses $\sigma_{cr2}^* = (\sigma_{cr} + \sigma_Y)$ was plotted since the tangent modulus E_t provides the smaller buckling stress σ_{cr} as a safer evaluation than \bar{E} provides.

The edge buckling does not occur in the forming stage up to pass No.4, i.e. 4CB rolls since analysed longitudinal stresses are all tensile for both cases of N . However, large increasing compressive stresses are applied after pass No.4 for both cases of N . Thus the analysed longitudinal stress at pass No.5, i.e. the last cage rolls becomes larger than the calculated elastic buckling stress in both case of N and is close to the plastic buckling stress σ_{cr2}^* .

It is therefore considered that the strip edges are subjected to the

condition of the elastic edge buckling or to a high critical condition of the elastic edge buckling in the forming stage between pass No.4 and pass No.6. This area is shown as the grey coloured zone in Figures 88 and 89. In the actual forming experiment, the elastic edge buckling occurred after pass No.4.

In the fin-pass roll and squeeze roll forming stages, the longitudinal compressive stress calculated by the Model-1 is close to the plastic buckling stress at pass No.6, i.e. 1F and then the analysed stress becomes a little bit larger than the plastic buckling stress at each forming pass after pass No. 7, i.e. 2F. In these forming stages, the strip edges are subjected to a high critical condition of the plastic edge buckling.

On the other hand, the longitudinal compressive stress calculated by the Model-2 with the consideration of the fin-pass roll reduction is decreased less than the plastic buckling stress by the circumferential reduction of the strip in the fin-pass roll and squeeze roll forming stages. This suggests that the fin-pass roll reduction is more effective to suppress the occurrence of edge buckling. However, both edges are still in a high critical condition of the elastic edge buckling.

As already mentioned, it can be stated that the stress-strain analysis by the CADFORM system can roughly simulate the occurrence of edge buckling of the strip in tube-making by the cold roll-forming process. Thus, this original study utilises a viable computer programme to simulate the total process from roll flower design to edge buckling evaluation.

Table 2 Calculation of theoretical elastic and plastic buckling stresses for the case of $N = 1$

$D=100 \phi \times t=1.0t$ Bottom constant pass-line $N = 1$

Stand No.	Thick-ness (mm)	Bending radius R (mm)	Bending length b (mm)	Bending angle α (RAD)	Span δ (mm)	Cross sectional area A (mm ²)	Youngs modulus E (Gpa)	Tangent modulus Et (Mpa)	Equivalent elastic coefficient E (Mpa)	Coefficient N	Second moment area I	k $\sqrt{I/A}$	Plastic σ_{cr1} (E=E (Mpa))	Plastic σ_{cr2} (E=E (Mpa))	Basic σ_{cr} (by E) E (Mpa)
1	1	----	15.75	----	230	15.7500	206	1961	6512	1	1.3125	0.2887	340.10	340.03	3.1997
2	1	---	15.75	----	50	15.7500	206	1961	6512	1	1.3125	0.2887	342.14	340.64	67.705
3	1	---	15.75	----	50	15.7500	206	1961	6512	1	1.3125	0.2887	342.14	340.64	67.705
4	1	----	15.75	---	50	15.7500	206	1961	6512	1	1.3125	0.2887	342.14	340.64	67.705
5	1	---	15.75	----	50	15.7500	206	1961	6512	1	1.3125	0.2887	342.14	340.64	67.705
6	1	----	15.75	----	260.99	15.7500	206	1961	6512	1	1.3125	0.2887	340.08	340.02	2.4849
7	1	50	15.82	0.1568	220	15.5274	206	1961	6512	1	1.7932	0.3398	340.15	340.05	4.8465
8	1	50	15.82	0.1568	220	15.5274	206	1961	6512	1	1.7932	0.3398	340.15	340.05	4.8465
9	1	50	15.82	0.1568	500	15.5274	206	1961	6512	1	1.7932	0.3398	340.03	340.01	0.8383

Table 3 Calculation of theoretical elastic and plastic buckling stresses for the case of $N = 4$

$D=100 \phi \times t=1.0t$ Bottom constant pass-line $N = 4$

Stand No.	Thick-ness (mm)	Bending radius R (mm)	Bending length b (mm)	Bending angle α (RAD)	Span δ (mm)	Cross sectional area A (mm ²)	Youngs modulus E (Gpa)	Tangent modulus Et (Mpa)	Equivalent elastic coefficient E (Mpa)	Coefficient N	Second moment area I	k $\sqrt{I/A}$	Plastic σ_{cr1} (E=E (Mpa))	Plastic σ_{cr2} (E=E (Mpa))	Basic σ_{cr} (by E) E (Mpa)
1	1	----	15.75	----	230	15.7500	206	1961	6512	4	1.3125	0.2887	340.40	340.12	12.798
2	1	----	15.75	---	50	15.7500	206	1961	6512	4	1.3125	0.2887	348.56	342.58	270.8219
3	1	----	15.75	---	50	15.7500	206	1961	6512	4	1.3125	0.2887	348.56	342.58	270.8219
4	1	----	15.75	---	50	15.7500	206	1961	6512	4	1.3125	0.2887	348.56	342.58	270.8219
5	1	----	15.75	---	50	15.7500	206	1961	6512	4	1.3125	0.2887	348.56	342.58	270.8219
6	1	----	15.75	----	260.99	15.7500	206	1961	6512	4	1.3125	0.2887	340.31	340.09	9.9398
7	1	50	15.82	0.1568	220	15.5274	206	1961	6512	4	1.7932	0.3398	340.61	340.18	19.3882
8	1	50	15.82	0.1568	220	15.5274	206	1961	6512	4	1.7932	0.3398	340.61	340.18	19.3882
9	1	50	15.82	0.1568	500	15.5274	206	1961	6512	4	1.7932	0.3398	340.12	340.04	3.7532

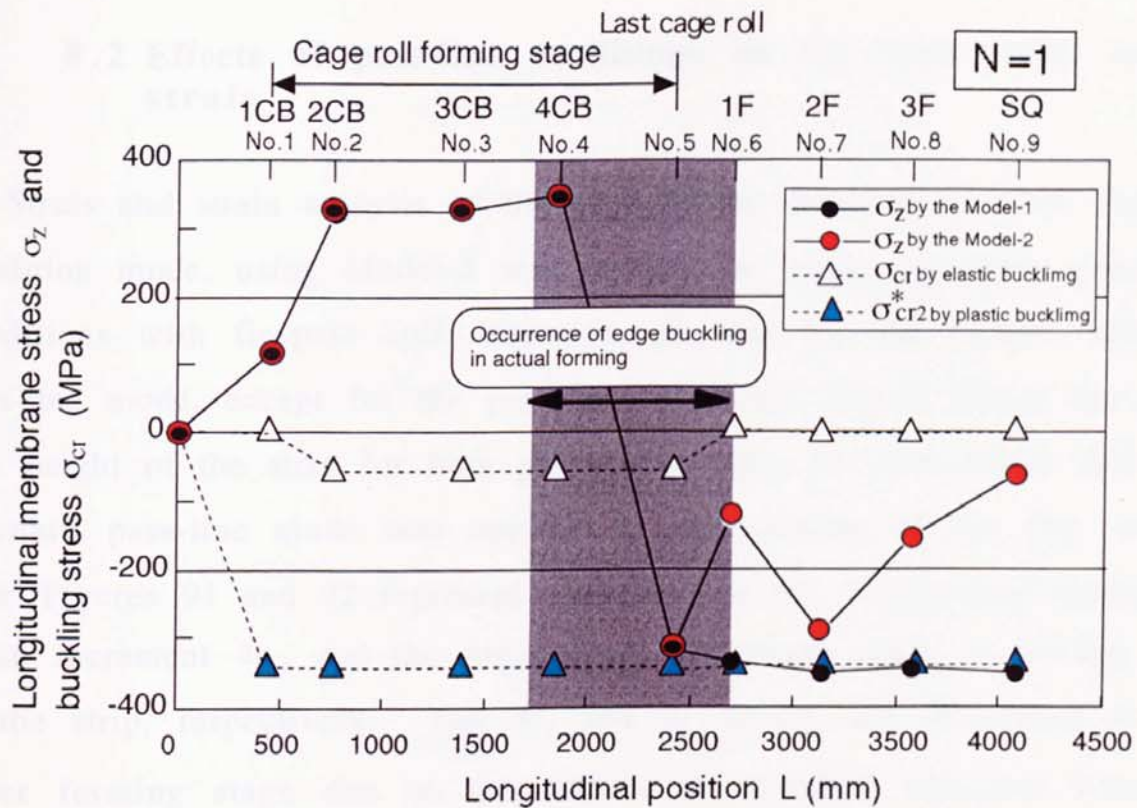


Fig.88 Comparison of theoretical longitudinal stresses with calculated buckling stresses for the case of $N = 1$

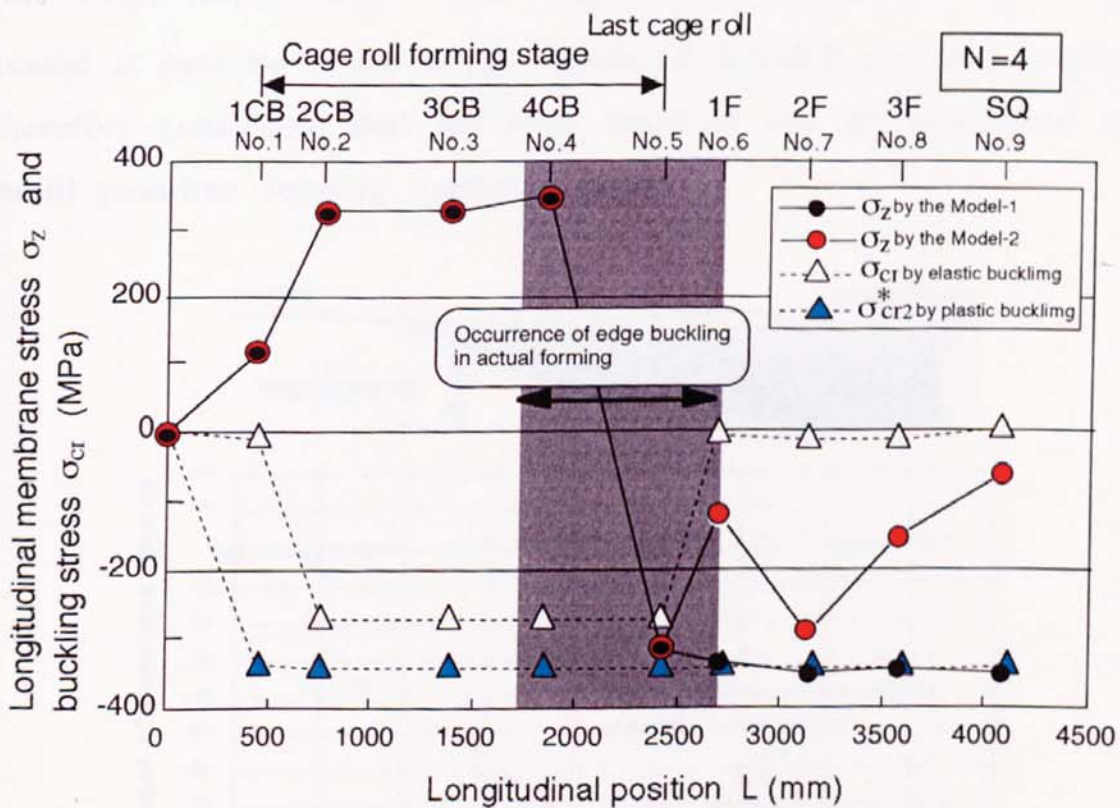


Fig.89 Comparison of theoretical longitudinal stresses with calculated buckling stresses for the case of $N = 4$

8.2 Effects of pass-line conditions on the tube stress and strain

Stress and strain analysis of the strip in the downhill pass-line forming condition mode, using Model-2 was carried out under the same operating conditions with fin-pass roll reduction, as that for the bottom constant pass-line mode, except for the pass-line condition. Fig.90 shows the pass-line height of the strip for both pass-lines. Thus, for this model mill, the downhill pass-line mode was applied to the forming of the thin walled tube. Figures 91 and 92 represent variations of the longitudinal membrane strain increment $d\epsilon_z$, and the longitudinal membrane strain ϵ_z , at the edge of the strip, respectively. The $d\epsilon_z$ and ϵ_z values are decreased at the upper forming stage due to the effects of downhill pass-line forming. Figures 93 and 94 represent variations of the longitudinal membrane stress increment $d\sigma_z$, and the longitudinal membrane stress σ_z , at the edge of the strip, respectively. The longitudinal compressive stress σ_z also decreased at pass No.5, due to the effects of downhill pass-line forming. It is therefore considered that the edge buckling can be suppressed by the downhill pass-line forming condition mode.

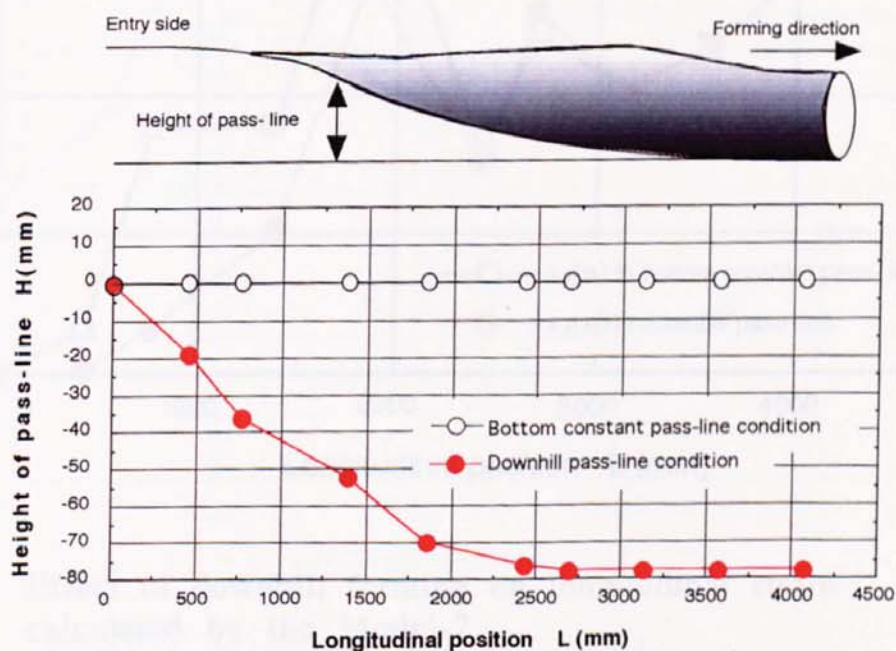


Fig.90 Pass-line conditions for bottom constant and downhill forming

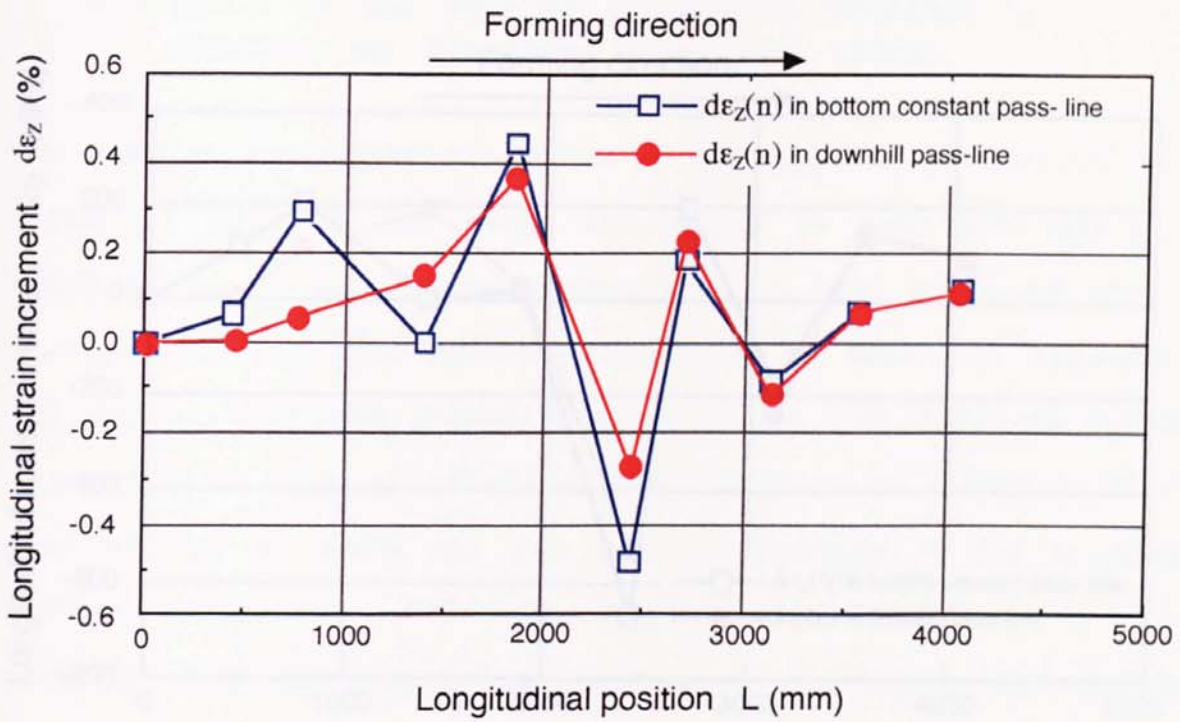


Fig 91 Effect of downhill forming on longitudinal strain increment calculated by Model-2

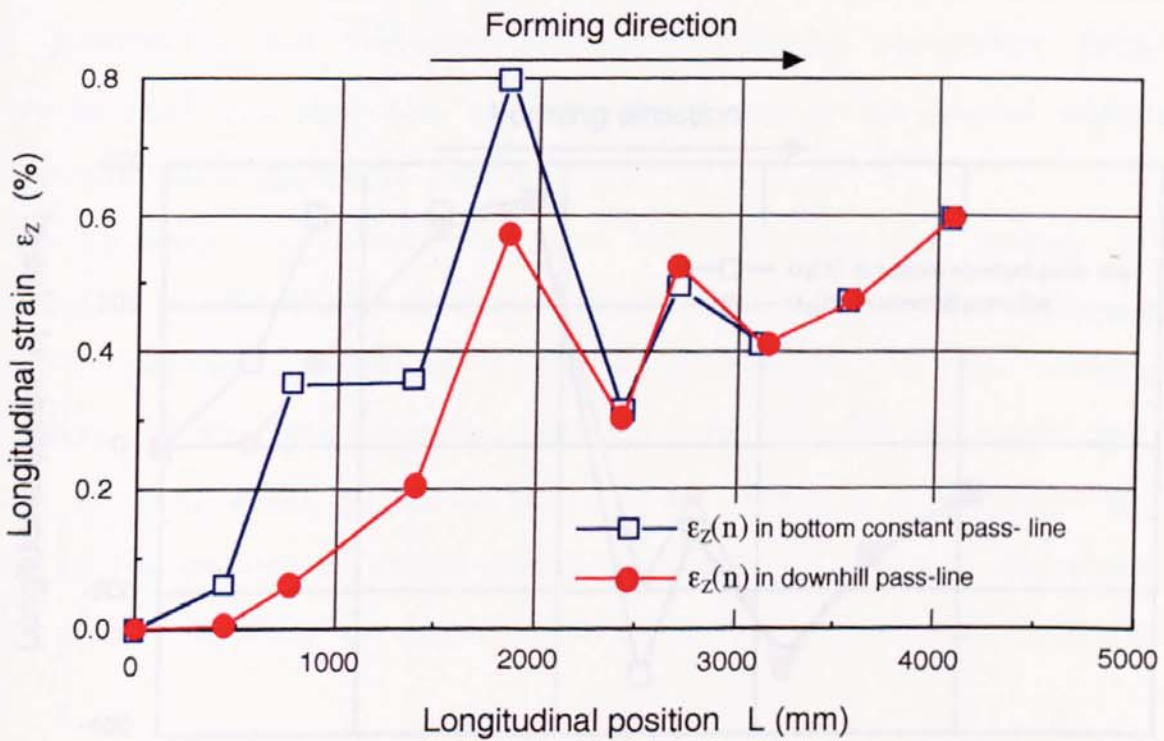


Fig 92 Effect of downhill forming on longitudinal strain calculated by the Model-2

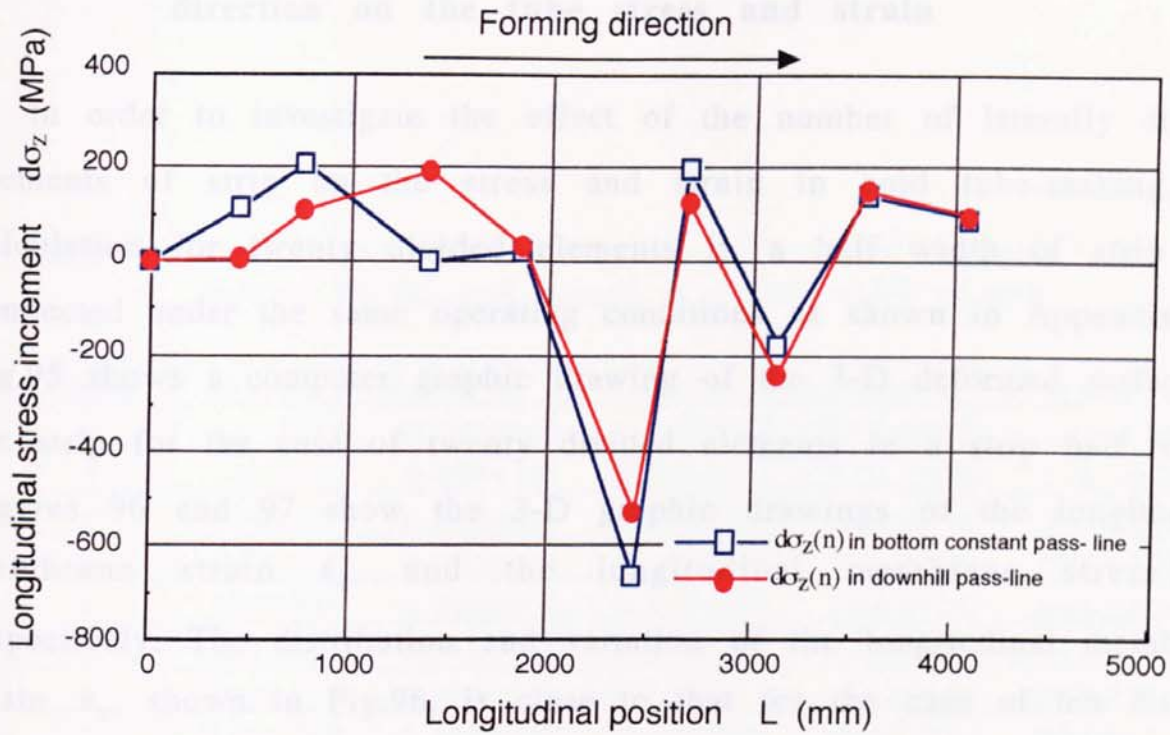


Fig 93 Effect of downhill forming on longitudinal stress increment calculated by the Model-2

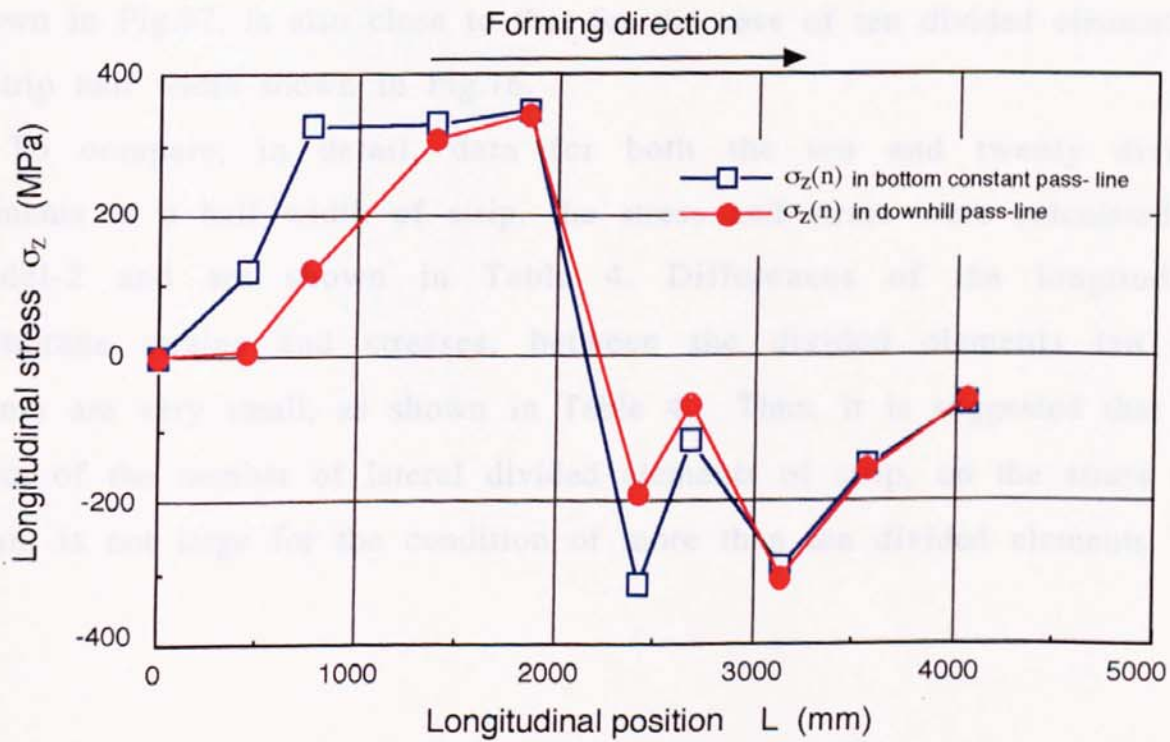


Fig 94 Effect of downhill forming on longitudinal stress calculated by the Model-2

8.3 Effect of the number of divided elements in the lateral direction on the tube stress and strain

In order to investigate the effect of the number of laterally divided elements of strip on the stress and strain in cold tube-making, the calculation for twenty divided elements in a half width of strip was conducted under the same operating conditions as shown in Appendix-4. . Fig.95 shows a computer graphic drawing of the 3-D deformed surface of the strip for the case of twenty divided elements in a strip half width. Figures 96 and 97 show the 3-D graphic drawings of the longitudinal membrane strain ϵ_z , and the longitudinal membrane stress σ_z , respectively. The distribution and variation of the longitudinal membrane strain ϵ_z , shown in Fig.96, is close to that for the case of ten divided elements in a strip half width, shown in Fig.72. The lateral distribution of the longitudinal membrane strain ϵ_z , become uniform after the first fin-pass roll forming stage, due to the circumferential fin-pass roll reduction. The distribution and variation of the longitudinal membrane stress σ_z , shown in Fig.97, is also close to that for the case of ten divided elements in a strip half width shown in Fig.76.

To compare, in detail, data for both the ten and twenty divided elements in a half width of strip, the stress and strain were calculated by Model-2 and are shown in Table 4. Differences of the longitudinal membrane strains and stresses, between the divided elements ten and twenty are very small, as shown in Table 4. Thus, it is suggested that the effect of the number of lateral divided elements of strip, on the stress and strain, is not large for the condition of more than ten divided elements.

Table 4 Comparison of stress and strain between elements divided by ten and twenty in a half width of strip

Stand	L (mm)	ϵ_z -10(%)	ϵ_z -20(%)	σ_z -10(MPa)	σ_z -20(MPa)
0	0.00	0.000000	0.000000	0.0000	0.0000
1	444.65	0.061415	0.061414	118.1388	118.1375
2	768.00	0.350487	0.350461	326.3670	326.3645
3	1393.00	0.352053	0.352012	326.5068	326.5029
4	1853.00	0.799622	0.799456	348.2573	348.2528
5	2427.01	0.310500	0.310470	-315.6649	-315.6340
6	2688.00	0.492781	0.491987	-117.4235	-117.8743
7	3128.00	0.405970	0.405866	-294.3778	-293.6175
8	3568.00	0.475579	0.475452	-152.2883	-151.8918
9	4068.00	0.594299	0.594183	-62.7636	-62.6334

Stress-Strain Analysis (Model-2)

3-D DRAWING

Pass Line Length
L = 4068.00 mm

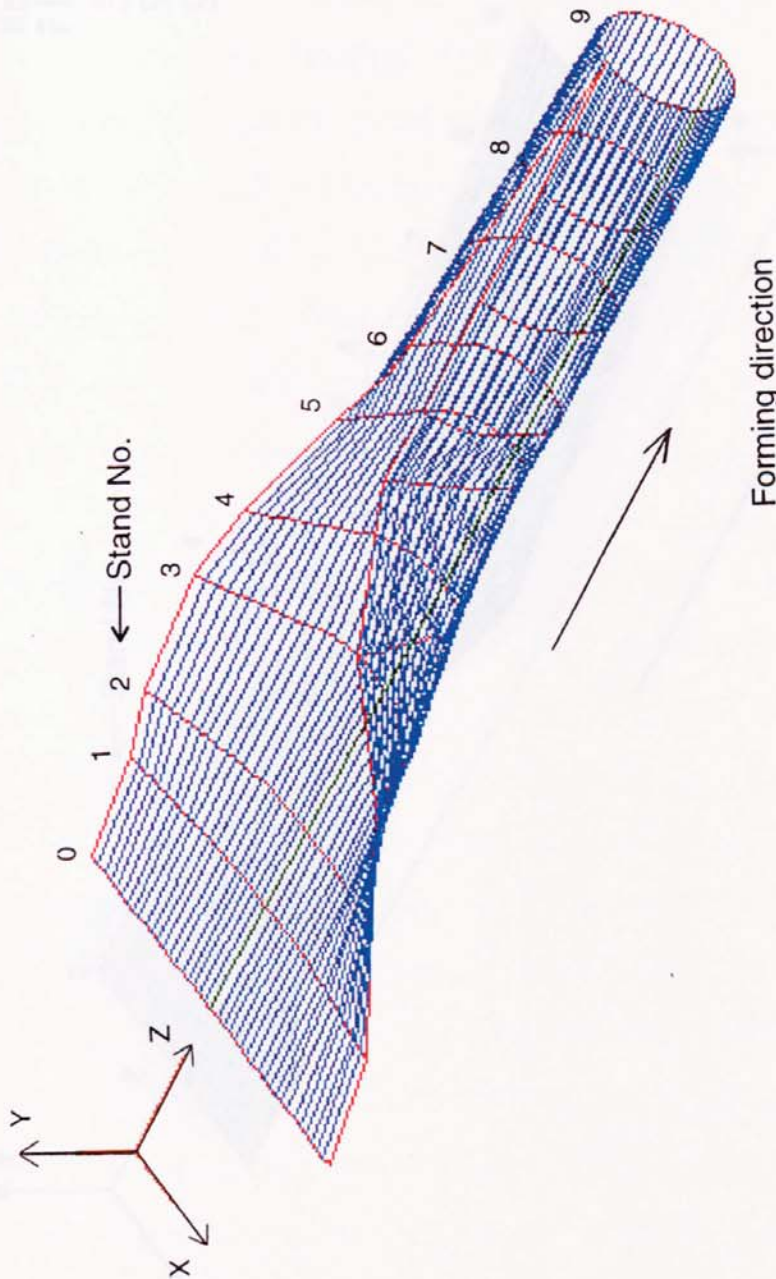
Rotation Angle of
Axis (deg.)

Bank = 0.00
Head = 50.00
Pitch = 40.00

Scale Ratio

SZX = 8.00
SZY = 8.00

OD = 100mm
t = 1.0mm



CADFORM

DRAWER
T. TOYOOKA

DATE
12.11.1992

FILE NAME
Y100BC20

3-D Deformation Surface

WORKS (PH.D.)
YAMANASHI

MATERIAL
STEEL(KTH45)

SIZE
100 * 0X1 * 0mm

Fig.95 Computer graphic drawing of the 3-D deformed surface of strip for the case of twenty divided elements calculated by Model-2

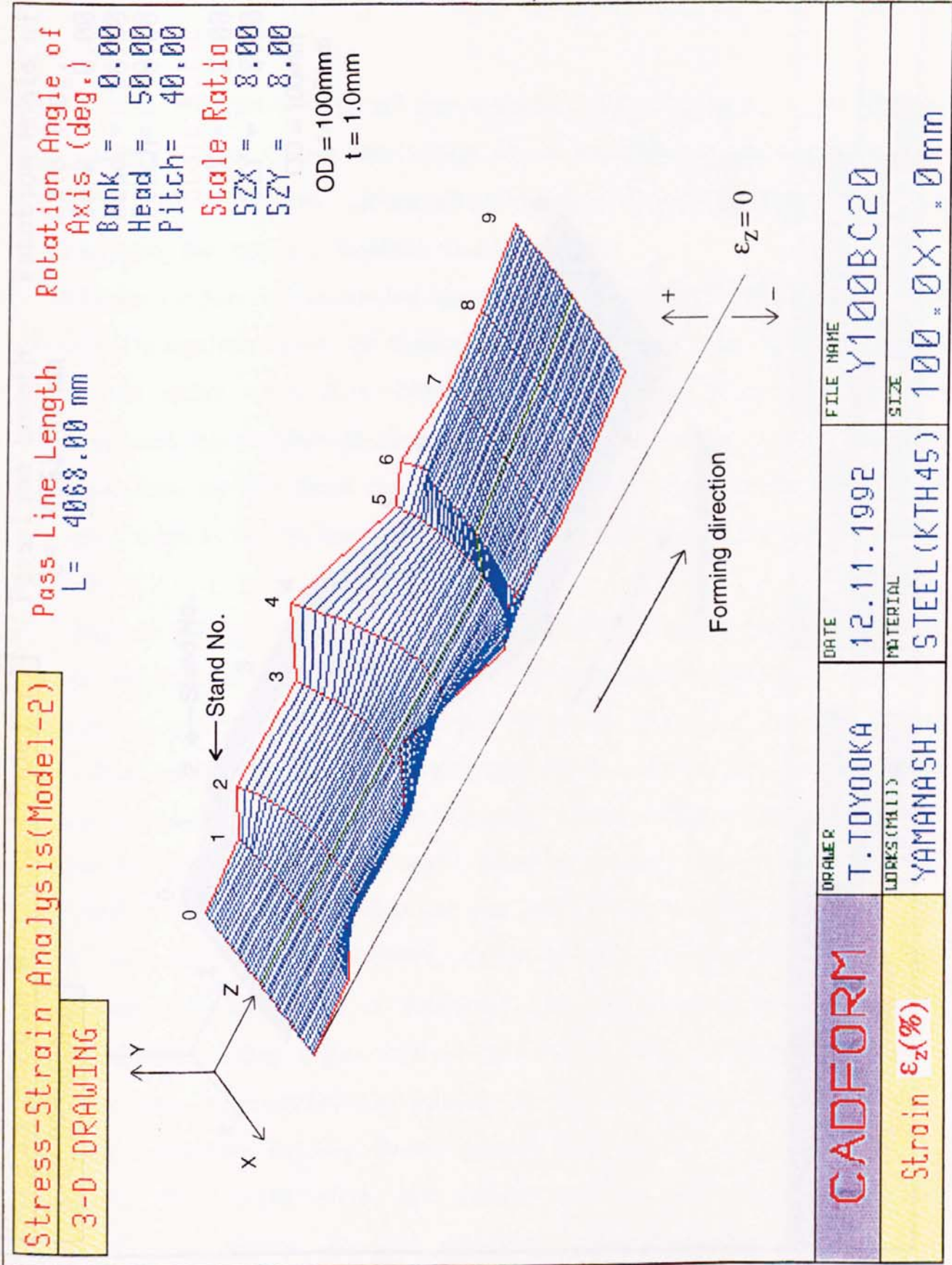


Fig 96 3-D graphic drawing of the longitudinal membrane strain ϵ_z for the case of twenty divided elements calculated by Model-2

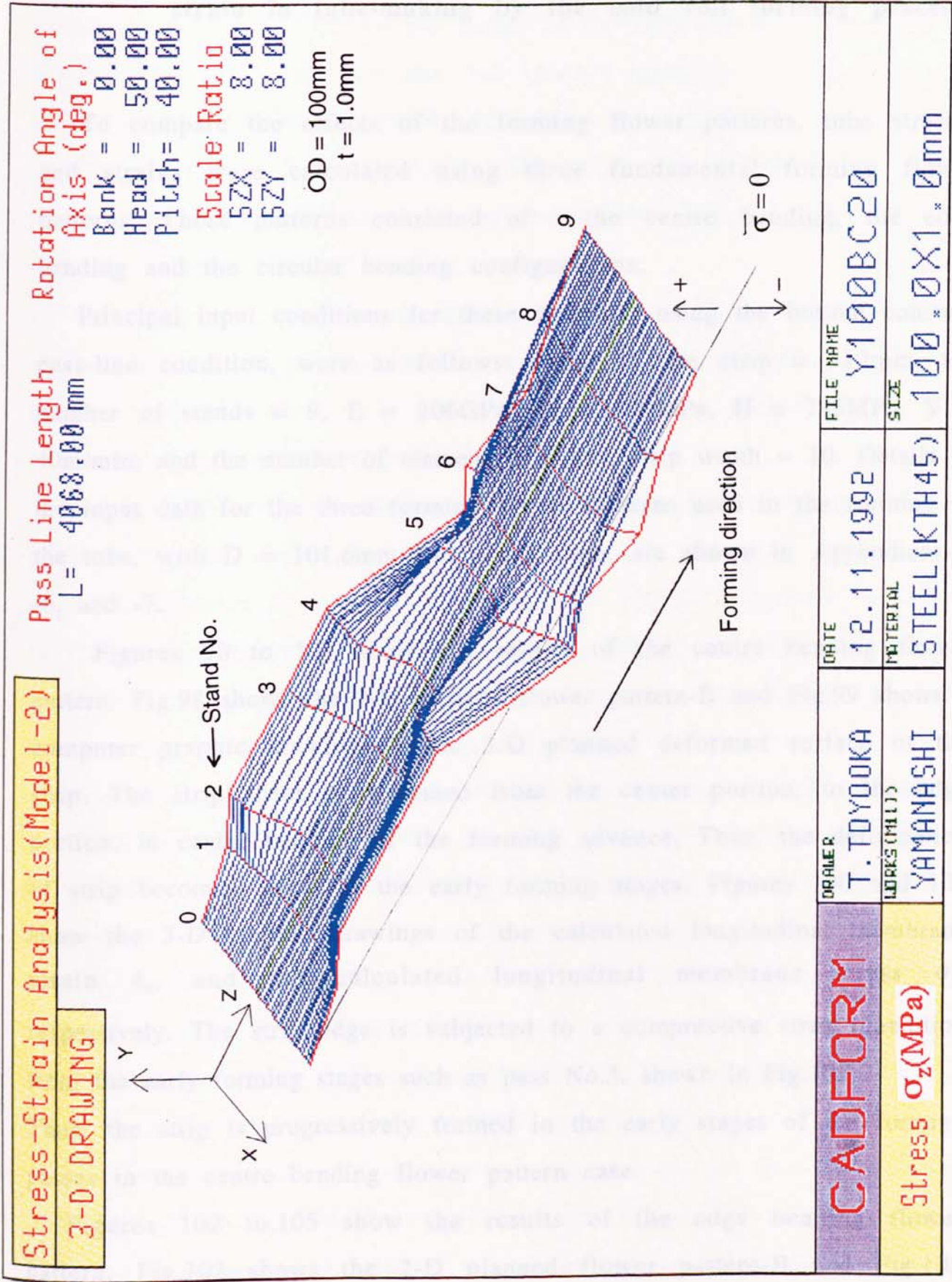


Fig 97 3-D graphic drawing of the longitudinal membrane stress σ_z for the case of twenty divided elements calculated by Model-2

8.4 Effect of forming flower patterns on the stress and strain in tube-making by the cold roll forming process

To compare the effects of the forming flower patterns, tube stresses and strains were calculated using three fundamental forming flower patterns. These patterns consisted of : the centre bending, the edge bending and the circular bending configurations.

Principal input conditions for these analyses, using the bottom constant pass-line condition, were as follows: width of the strip = 312mm, the number of stands = 9, $E = 206\text{GPa}$, $\sigma_Y = 309\text{MPa}$, $H = 785\text{MPa}$, $V = 40\text{m/min}$, and the number of element in a half strip width = 10. Details of the input data for the three forming flower patterns used in the forming of the tube, with $D = 101.6\text{mm}$ and $t = 2.3\text{mm}$, are shown in Appendices-5, -6, and -7.

Figures 98 to 101 show the results of the centre bending flower pattern. Fig.98 shows the 2-D planned flower pattern-B and Fig.99 shows a computer graphic drawing of the 3-D planned deformed surface of the strip. The strip sheet is deformed from the center portion, to the edge portion, in center bending as the forming advance. Thus, the deformation of strip becomes larger in the early forming stages. Figures 100 and 101 show the 3-D graphic drawings of the calculated longitudinal membrane strain ϵ_z , and the calculated longitudinal membrane stress σ_z , respectively. The strip edge is subjected to a compressive stress condition from the early forming stages such as pass No.3, shown in Fig.101. Thus, the strip is progressively formed in the early stages of the forming passes in the centre bending flower pattern case.

Figures 102 to.105 show the results of the edge bending flower pattern. Fig.102 shows the 2-D planned flower pattern-B and Fig.103 shows a computer graphic drawing of the 3-D planned deformed surface of the strip. The strip sheet is deformed from the edge portion, to the center

portion, in edge bending with the advance of forming. Thus, the deformation of the strip becomes larger in the downstream forming stages. Figures 104 and 105 show the 3-D graphic drawings of the calculated longitudinal membrane strain ϵ_z , and the calculated longitudinal membrane stress σ_z , respectively. The strip edge is subjected to the compressive stress condition from the downstream forming stages, such as pass No.7, shown in Fig.105.

In this case it is noted that the strip is progressively formed in the downstream stages of the forming passes in the edge bending flower pattern case. However, it is practically difficult to design forming rolls which can bend only the edge portion of the strip.

Figures 106 to 109 show the results of the circular bending flower pattern. Fig.106 shows the 2-D planned flower pattern-B, and Fig.107 shows a computer graphic drawing of the 3-D planned deformed surface of the strip. The strip sheet is deformed towards the whole portion of strip in circular bending as forming advances. Thus, the deformation of strip become homogeneous in all forming stages.

Figures 108 and 109 show the 3-D graphic drawings of the calculated longitudinal membrane strain ϵ_z , and the calculated longitudinal membrane stress σ_z , respectively. The strip edge is subjected to a compressive stress condition from the downstream forming stages, such as pass No.7, shown in Fig.109. Here it is noted that the strip is uniformly formed in all stages of the forming passes for the case of the circular bending flower pattern. Therefore, this circular bending flower pattern is generally used in the production of ERW tube and pipe.

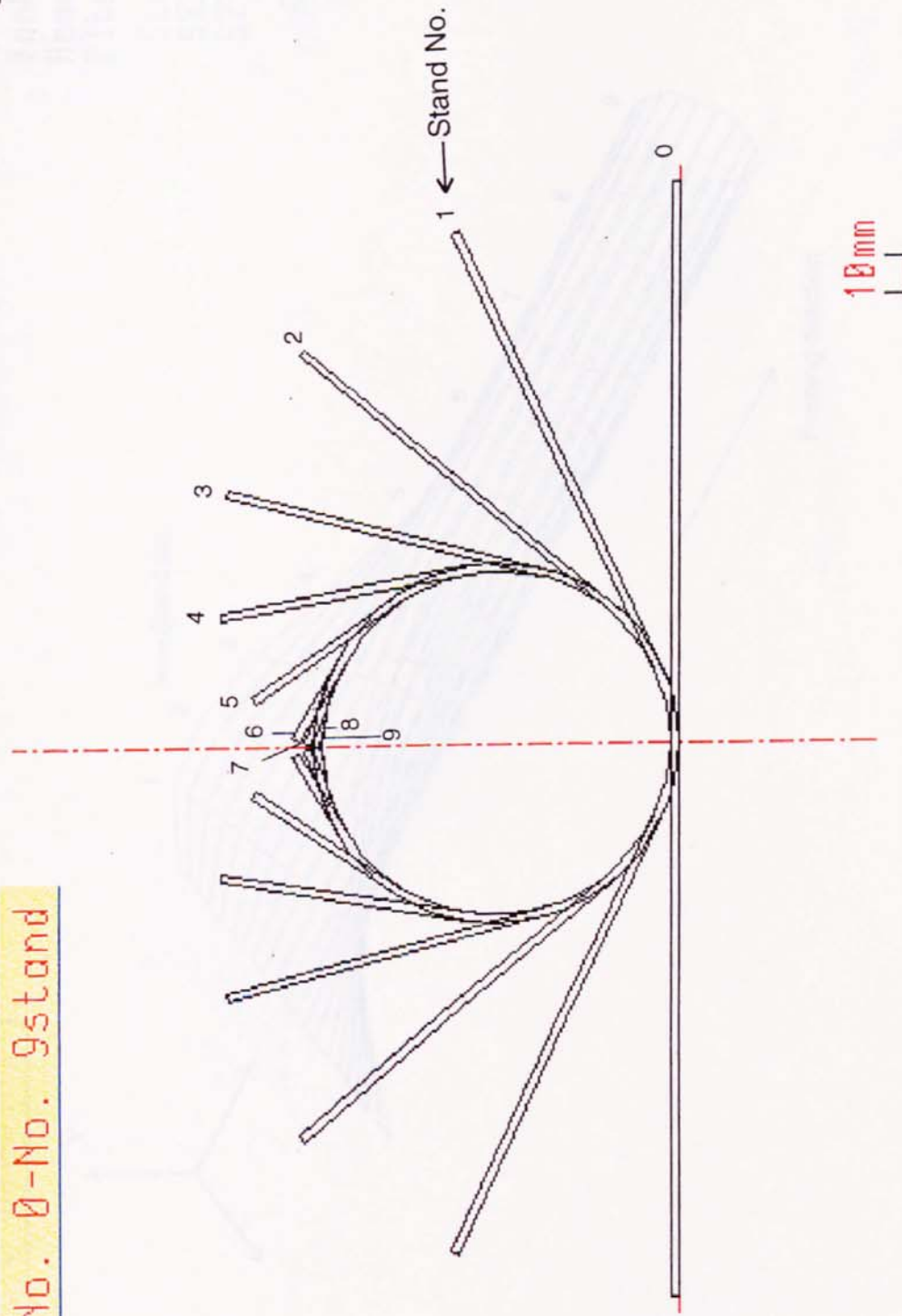
Figures 110 and 111 shows the comparison of the longitudinal membrane strain ϵ_z , and the longitudinal membrane stress σ_z , for each of the three forming flower patterns, respectively. It is seen that the strip in the centre bend forming is subjected to the most critical condition of edge buckling occurrence, as shown in Fig.111. However, the strip in the circular

bend forming is subjected to the most favorable condition of edge buckling suppression.

Thus, the features of the stress and strain characteristic for the three fundamental flower patterns are clarified by the analysis employing the CADFORM system. This confirms that the flower pattern design is very important in suppressing the occurrence of edge buckling.

OD = 101.6mm
t = 2.3 mm

No. 0-No. 9stand



CADFORM	DRAWER	T. TDYOOKA	DATE	14.10.1992	FILE NAME	CENTRE
	WORKS (PH. L.J.)	TOKYO UNIV.	MATERIAL	STEEL	SIZE	101.6X2.3mm
FLOWER PATTERN B						

Fig.98 Centre bending flower pattern by computer graphic drawing

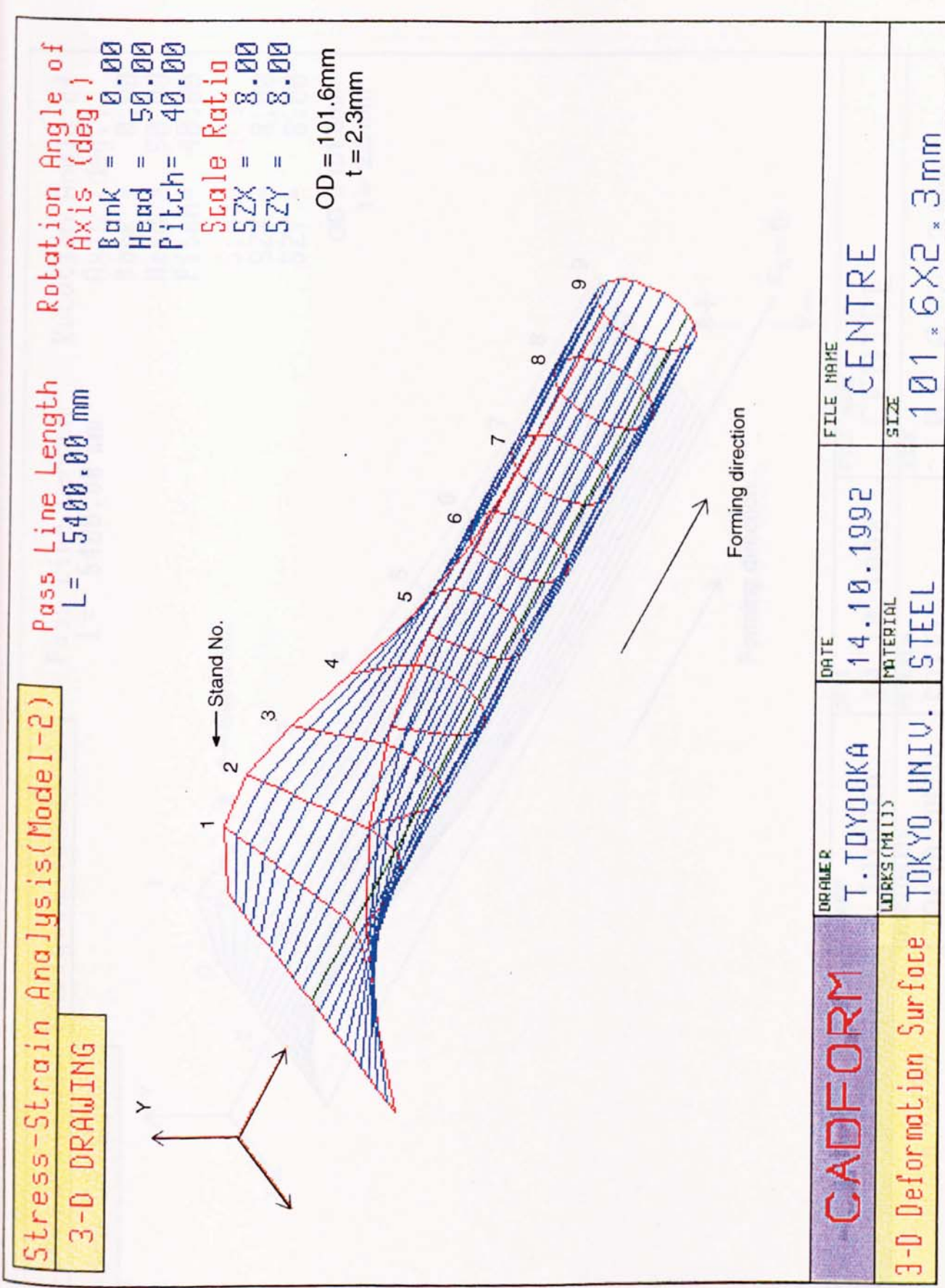


Fig.99 Computer graphic drawing of 3-D deformed surface of the strip for centre bending flower pattern

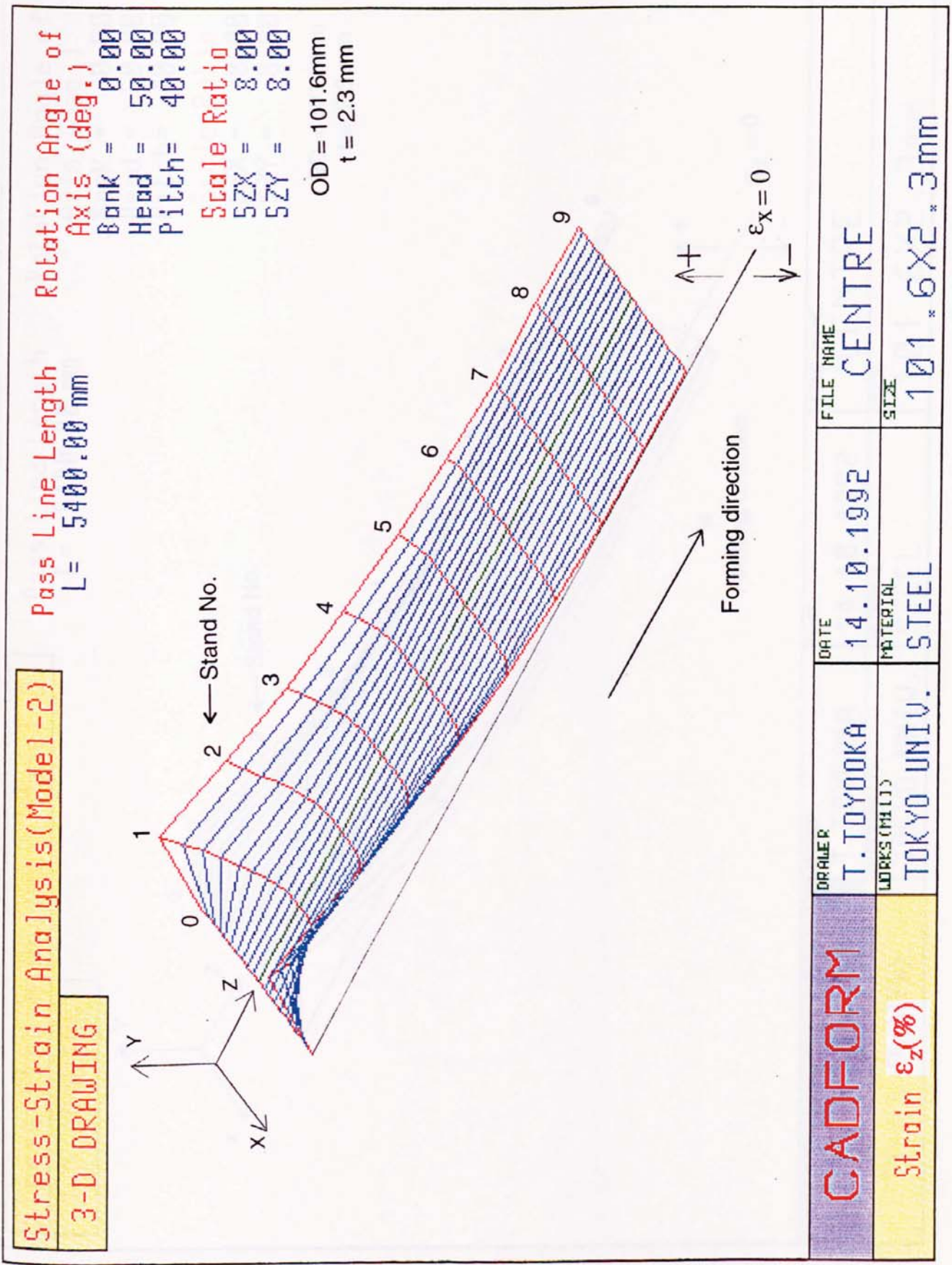


Fig.100 3-D graphic drawings of calculated longitudinal membrane strain ϵ_z for centre bending flower pattern

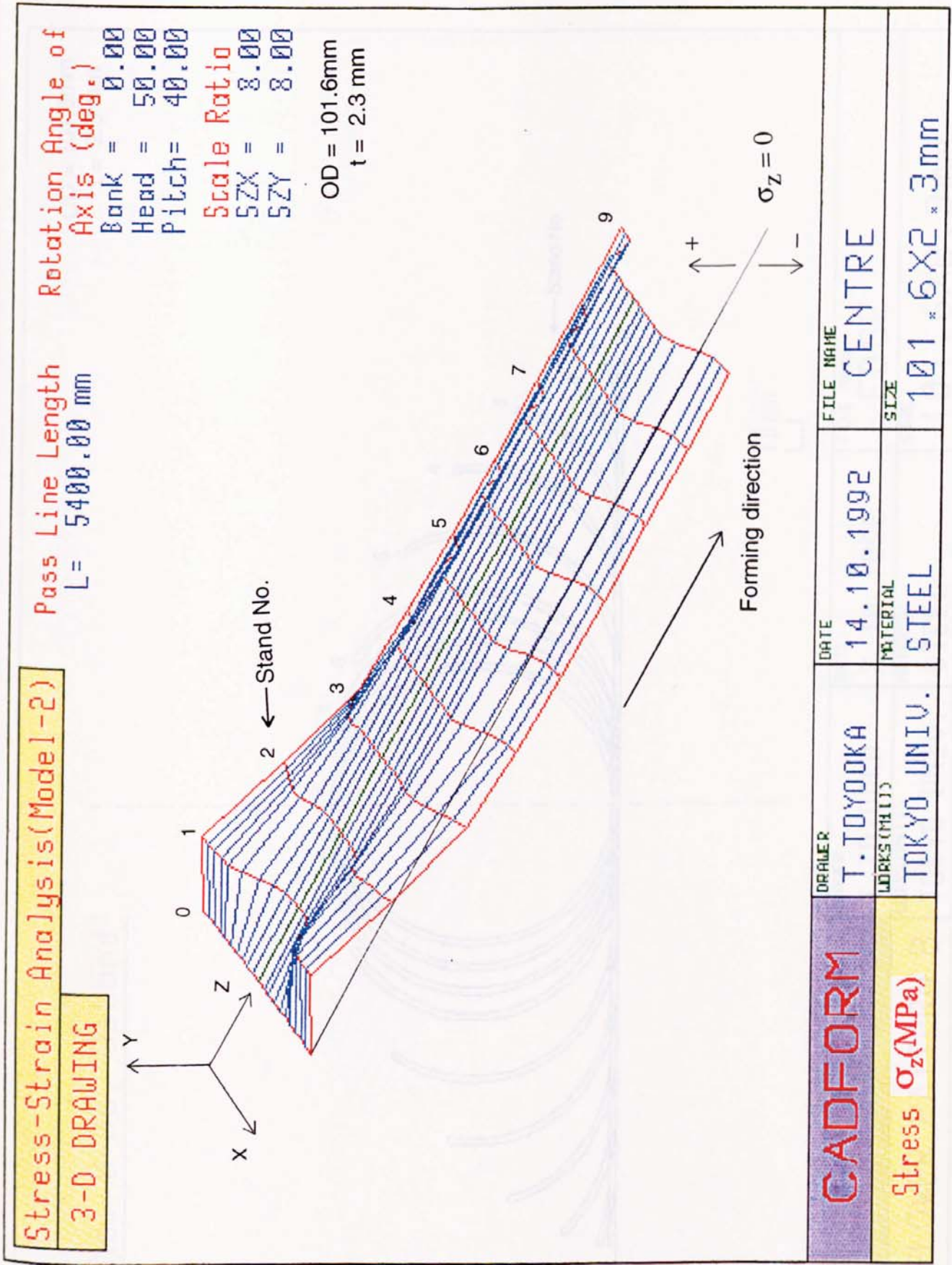
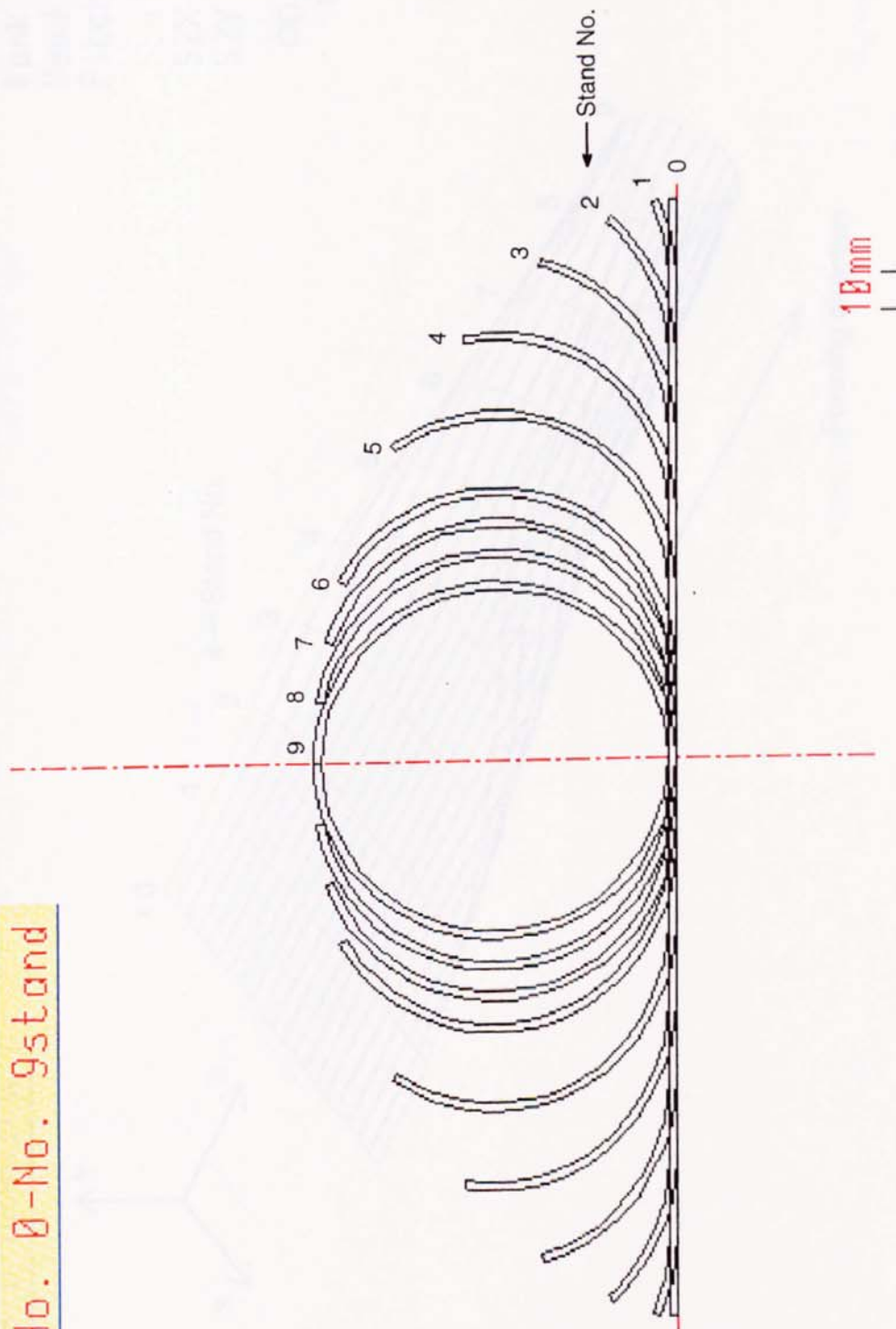


Fig.101 3-D graphic drawings of calculated longitudinal membrane stress σ_z for centre bending flower pattern

OD = 101.6mm
t = 2.3 mm

No. 0-No. 9stand



CADFORM	DRAWER T. TDYOOKA	DATE 8.10.1992	FILE NAME EDGE
FLOWER PATTERN B	WORKS (MILL) TOKYO UNIV.	MATERIAL STEEL	SIZE 101 * 6X2 * 3mm

Fig.102 Edge bending flower pattern by computer graphic drawing

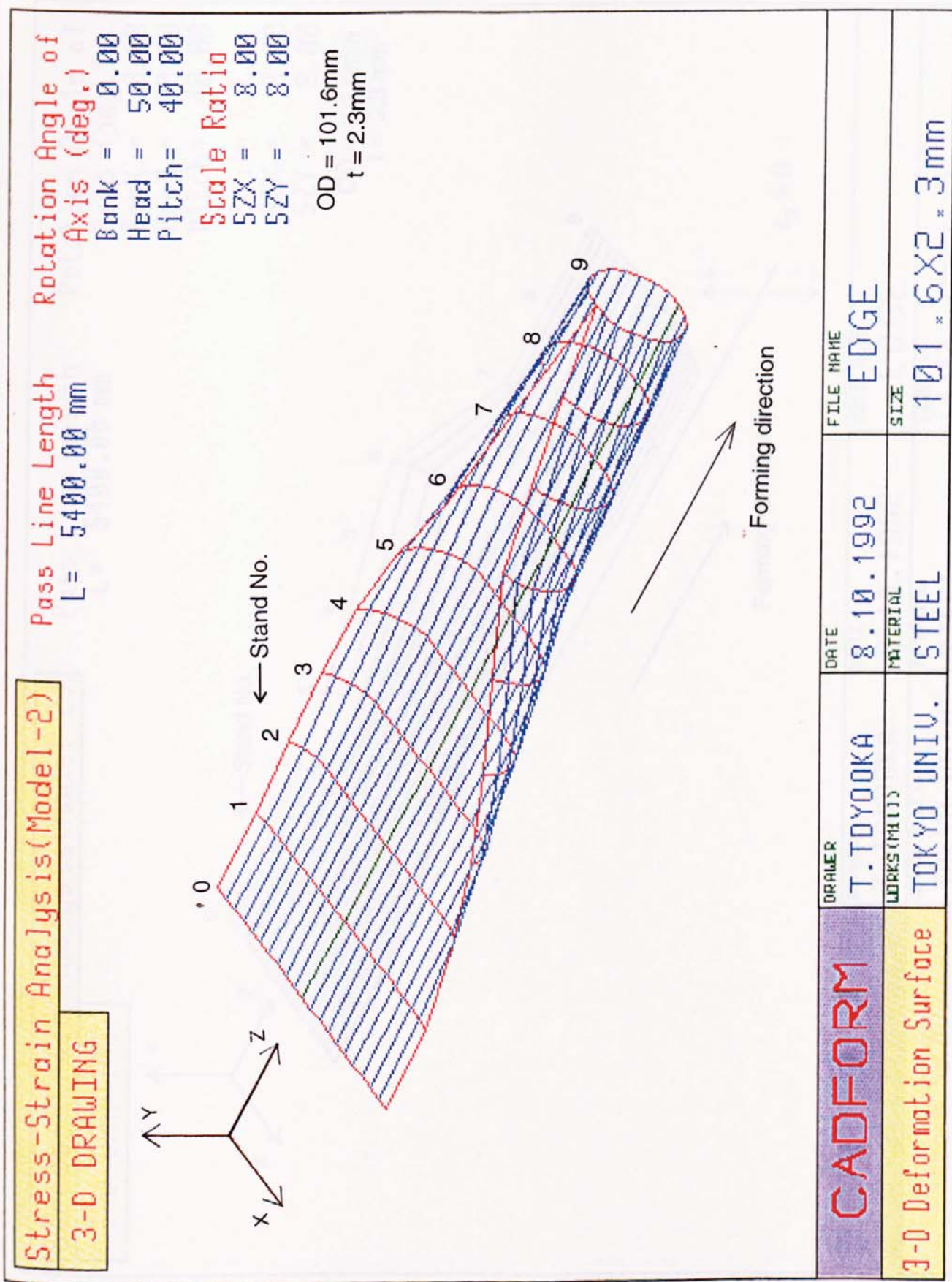


Fig.103 Computer graphic drawing of 3-D deformed surface of the strip for edge bending flower pattern

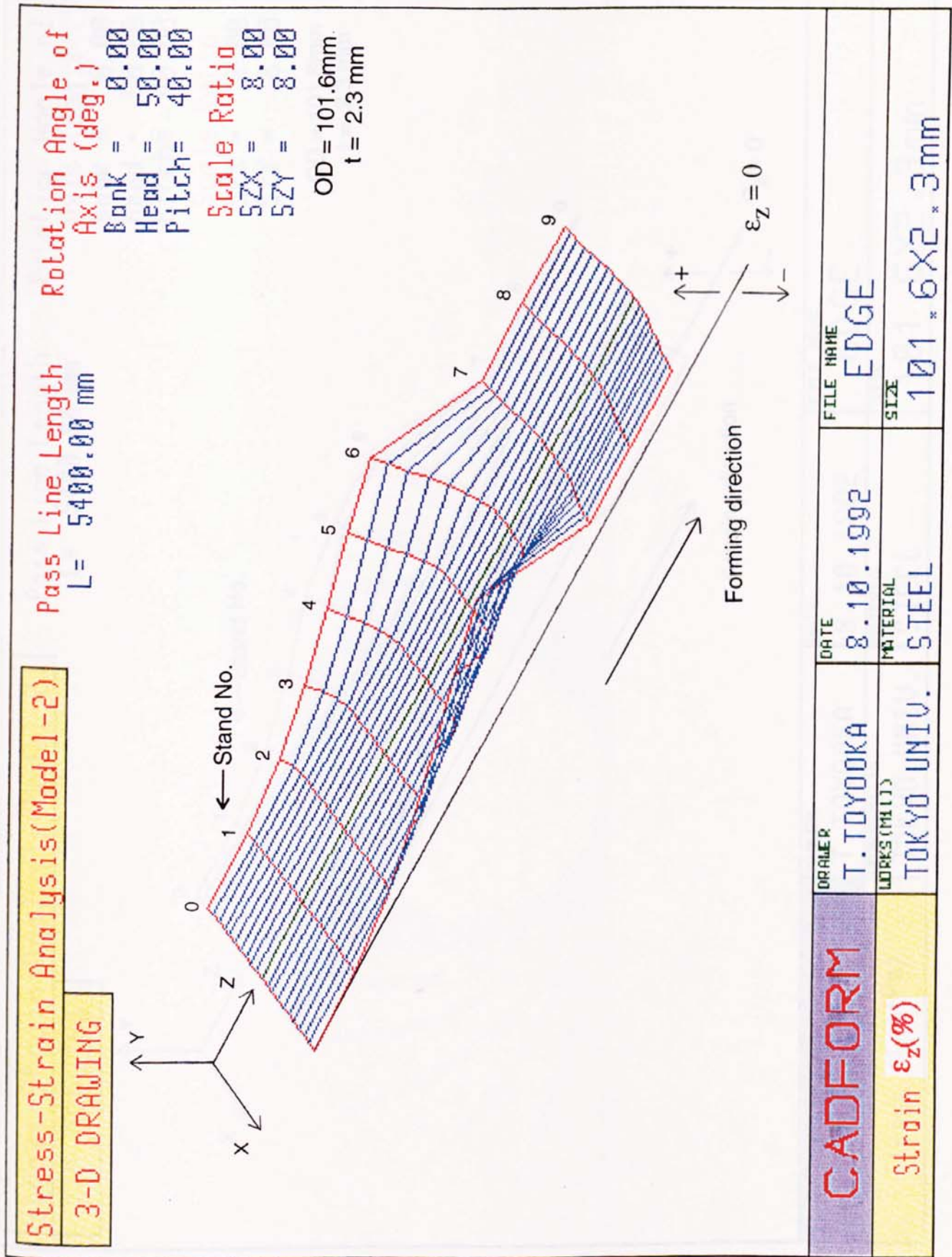


Fig.104 3-D graphic drawings of calculated longitudinal membrane strain ϵ_z for edge bending flower pattern

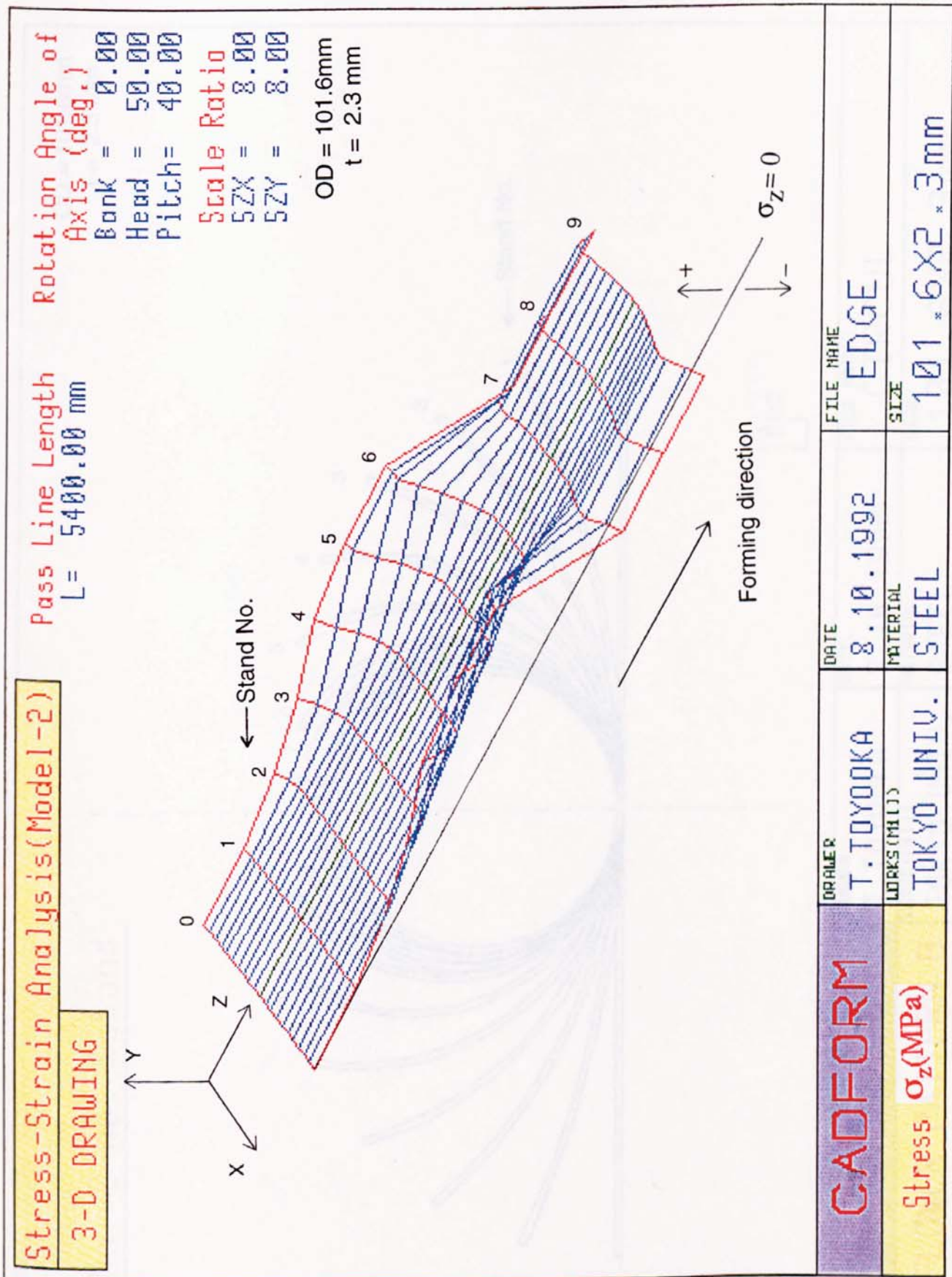
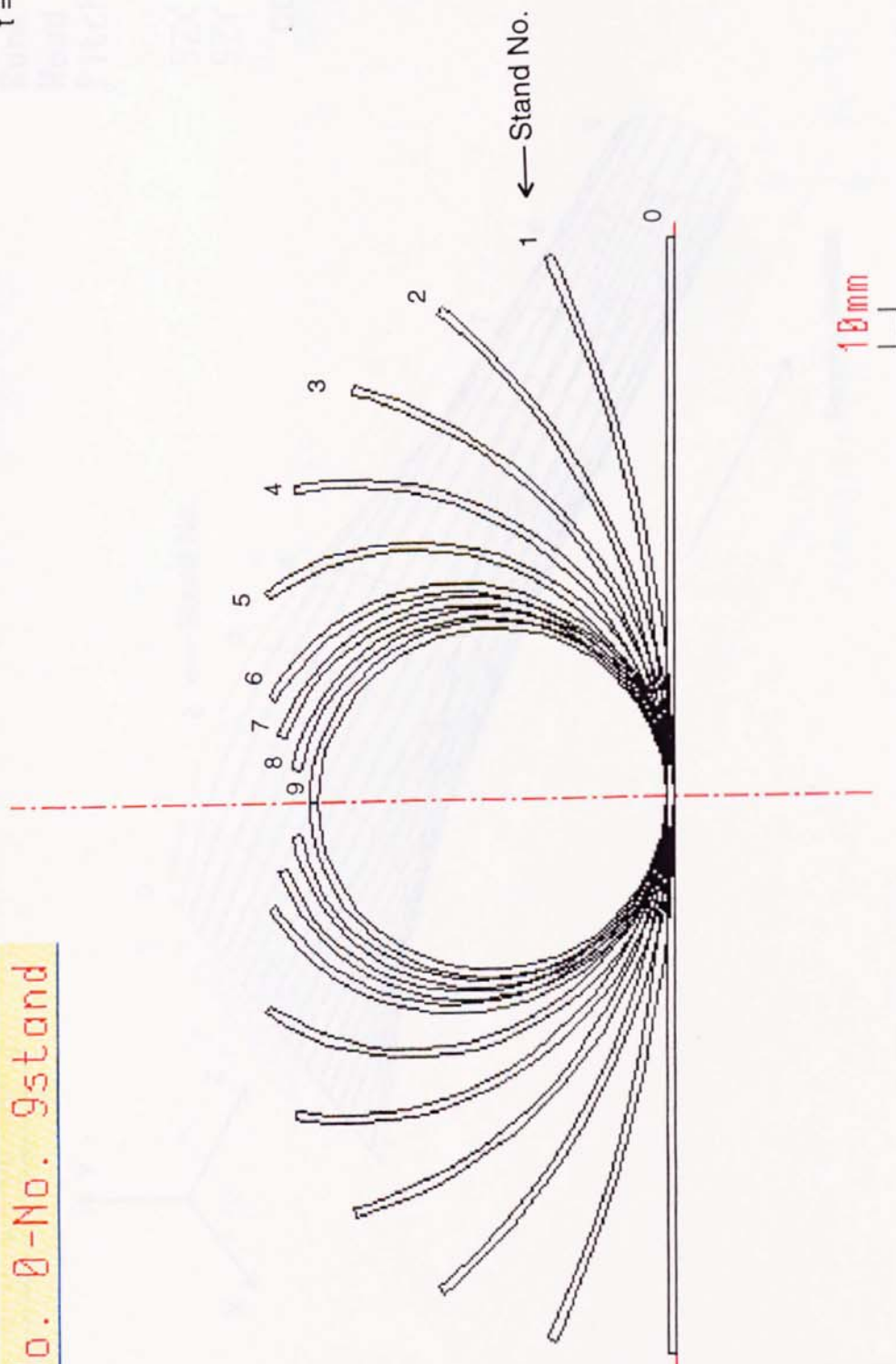


Fig.105 3-D graphic drawings of calculated longitudinal membrane stress σ_z for edge bending flower pattern

OD = 101.6mm
t = 2.3 mm

No. 0-No. 9stand



CADFORM	DRAWER T. TDYOOKA	DATE 8.10.1992	FILE NAME CIRCUL
FLOWER PATTERN B	WORKS (MILL) TOKYO UNIV.	MATERIAL STEEL	SIZE 101.6X2.3mm

Fig.106 Circular bending flower pattern by computer graphic drawing

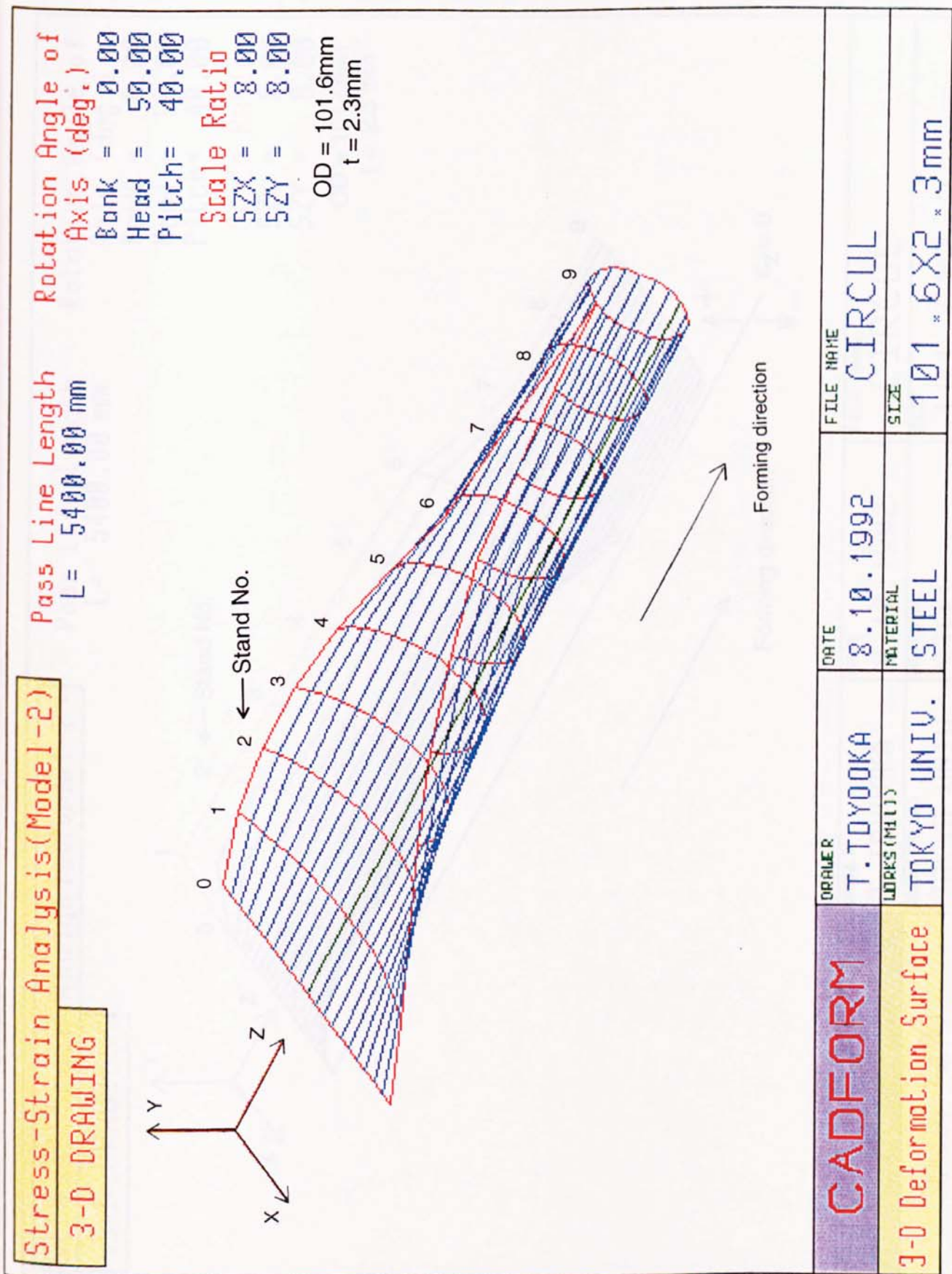


Fig.107

Computer graphic drawing of 3-D deformed surface of the strip for circular bending flower pattern

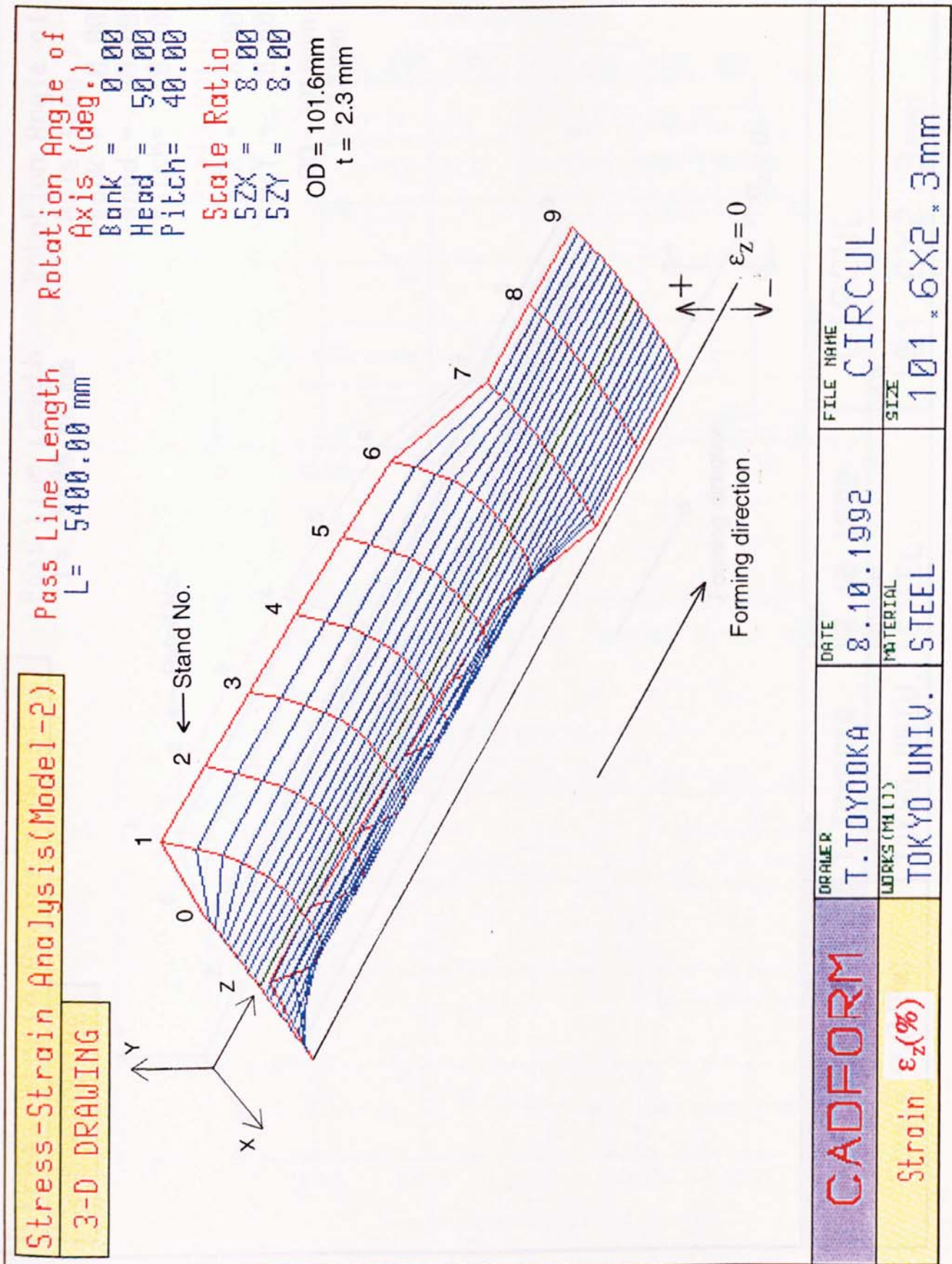


Fig.108 3-D graphic drawings of calculated longitudinal membrane strain ϵ_z for circular bending flower pattern

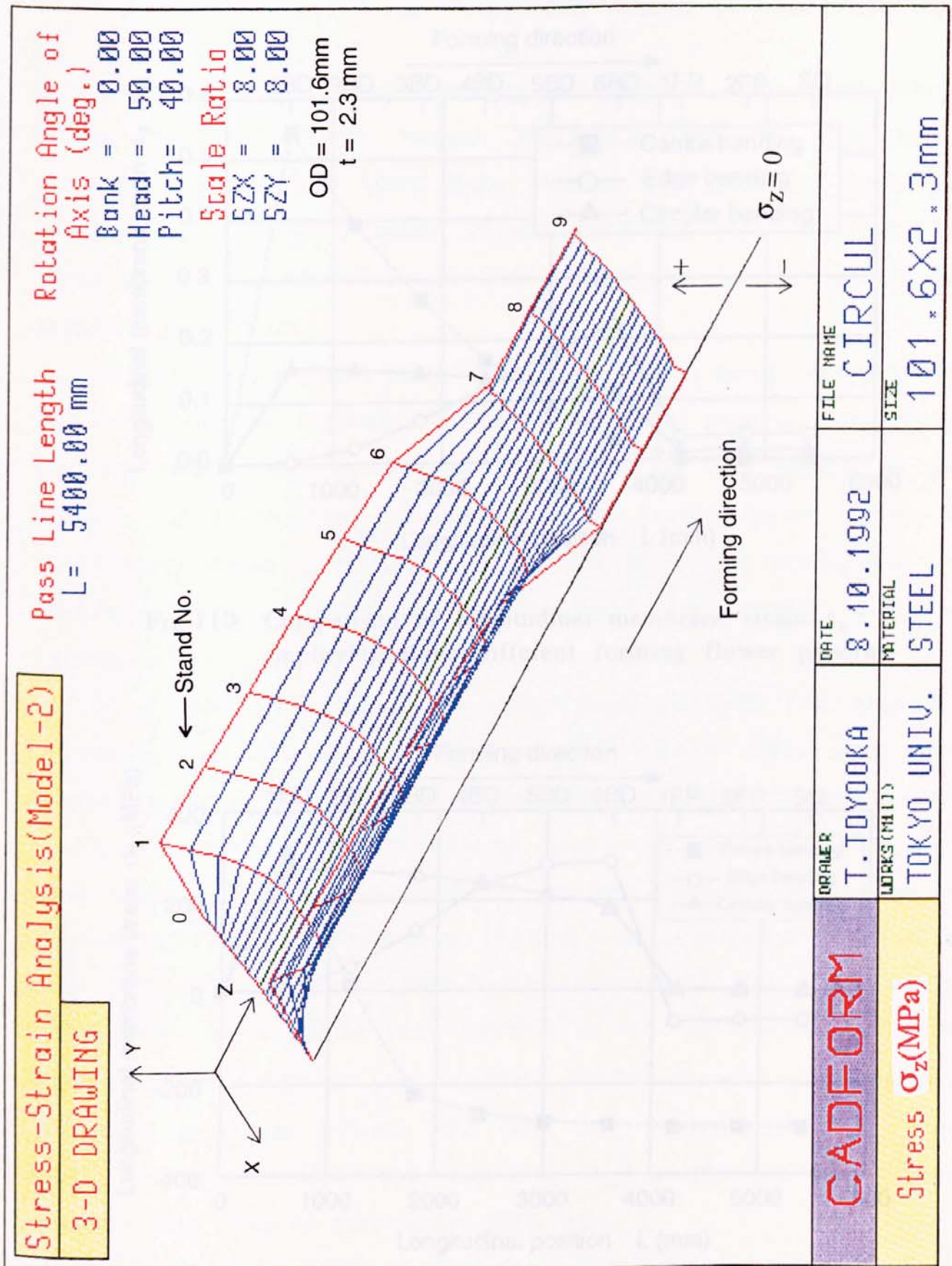


Fig.109 3-D graphic drawings of calculated longitudinal membrane stress σ_z for circular bending flower pattern

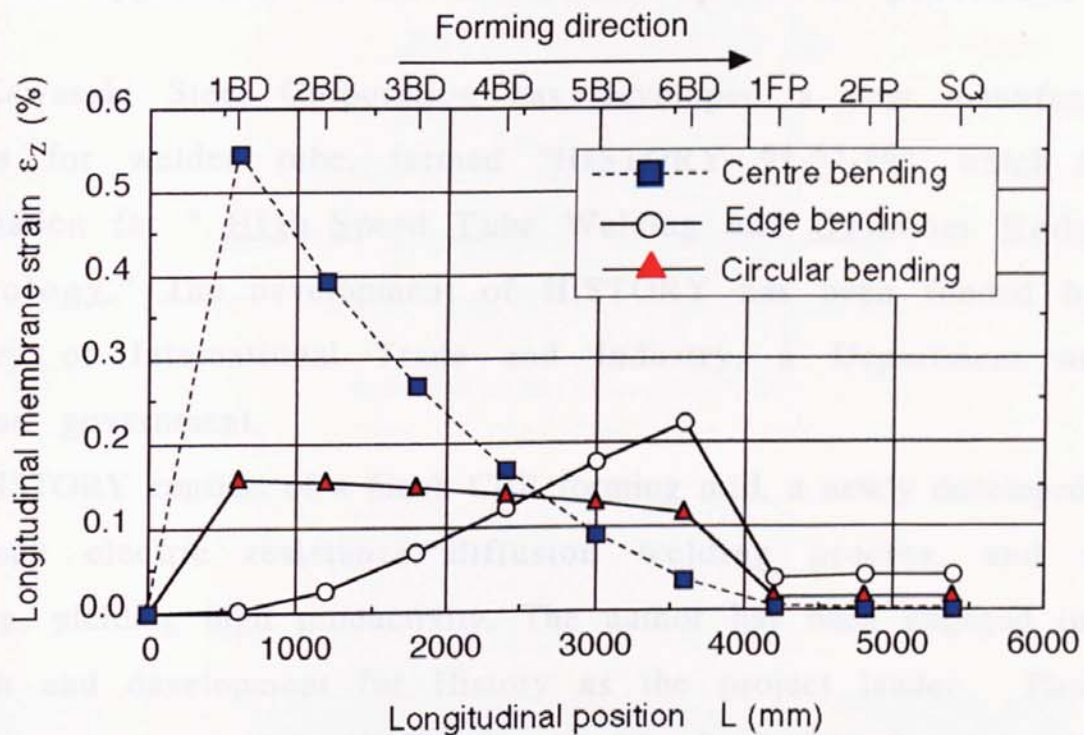


Fig.110 Comparison of longitudinal membrane strain ϵ_z employing three different forming flower patterns

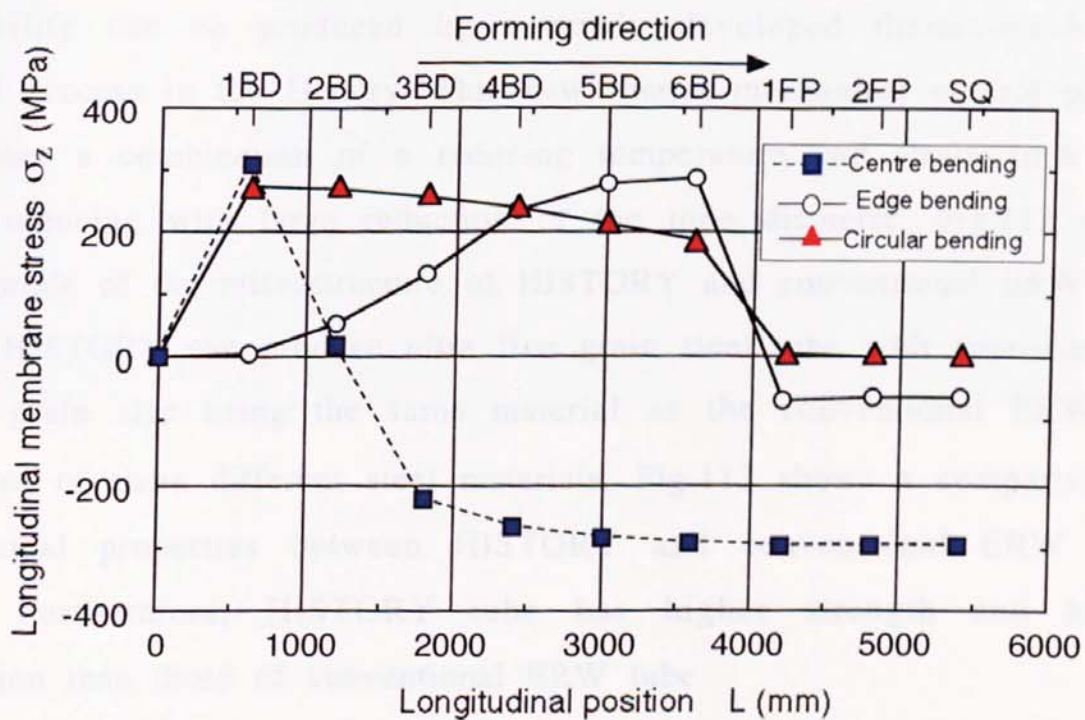


Fig.111 Comparison of longitudinal membrane stress σ_z employing three different forming flower patterns

8.5 Application of the CADFORM system to production mills

Kawasaki Steel Corporation has developed a new manufacturing process for welded tube, termed "HISTORY^{64,65,66}", which is the abbreviation for "High Speed Tube Welding and Optimum Reducing Technology." The development of HISTORY has been funded by the Ministry of International Trade and Industry, a Department of the Japanese government.

HISTORY consists of a 6inch CBR forming mill, a newly developed high frequency electric resistance diffusion welding process, and warm reducing, yielding high productivity. The author has been engaged in this research and development for History as the project leader. Photo.12 shows an appearance of the HISTORY mill. The 6inch CBR forming mill was introduced to manufacture thin walled tubes for machine structural purposes.

Ultra fine grain steel tube with high strength and excellent formability can be produced by a newly developed thermo-mechanical control process in the History. This new thermo-mechanical control process comprises a combination of a reducing temperature and strain such as a warm reducing with large reduction of the tube diameter. Fig.112 shows an example of the microstructure of HISTORY and conventional ERW steel tubes. HISTORY can produce ultra fine grain steel tube with approximately 1.2 μ m grain size using the same material as the conventional ERW. As examples of three different steel materials, Fig.113 shows a comparison of mechanical properties between HISTORY and conventional ERW steel tubes. Furthermore, HISTORY tube has higher strength and higher elongation than those of conventional ERW tube.

The CADFORM system was used to design the appropriate forming flower patterns. The tube size is $D = 146.0\text{mm}$ and $t = 2.0\text{mm}$. Details of the input data are shown in Appendix-8. Figures 114 and 115 show examples of the calculated results. It can be seen that the strip edges are

subjected to a large compressive stress condition in the longitudinal direction, before and after the No.1 fin-pass roll, as shown in Figures 114 (c) and 115. On the basis of the analysed results, the appropriate forming flower pattern was investigated in an attempt to decrease the longitudinal compressive stress. The CADFORM system is practically useful in designing the appropriate forming flower pattern for the production of the thin walled tubes.

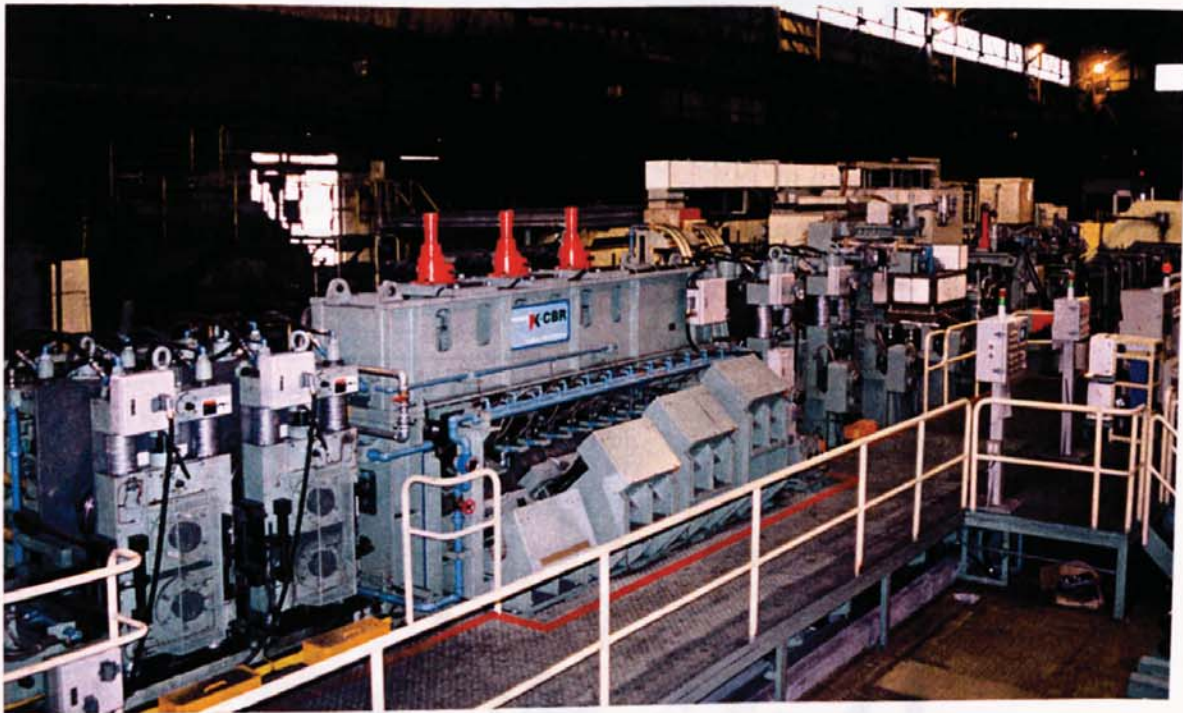
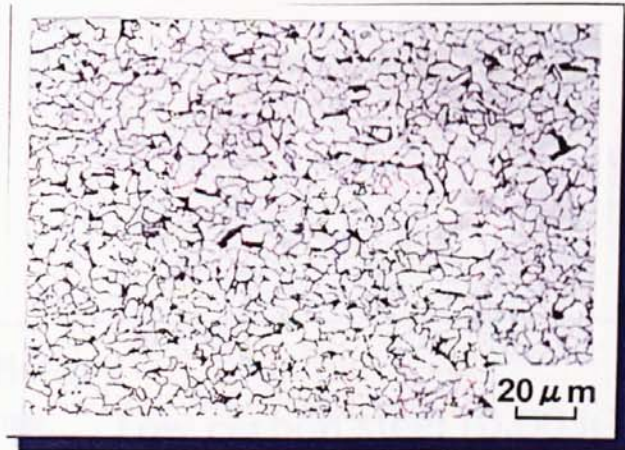
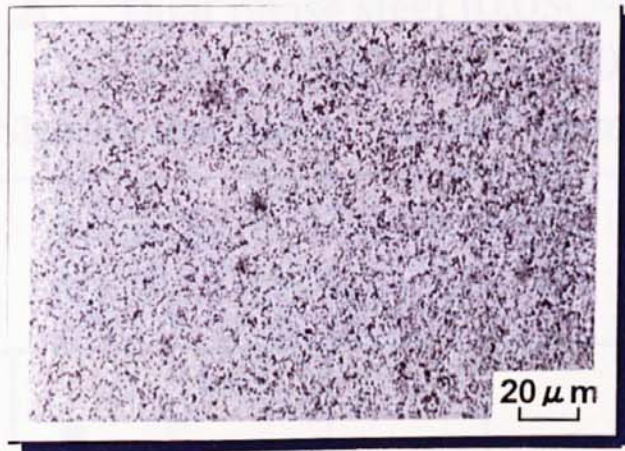


Photo. 12 Appearance of the HISTORY mill



Grain size= $6.8\ \mu\text{m}$

(a) Optical microstructure of conventional ERW steel tube



Grain size= $1.2\ \mu\text{m}$

(b) Optical microstructure of HISTORY steel tube



Grain size= $1.2\ \mu\text{m}$

(c) Scanning electron microstructure of HISTORY steel tube

Fig.112 Comparison of microstructure between HISTORY and conventional ERW steel tubes

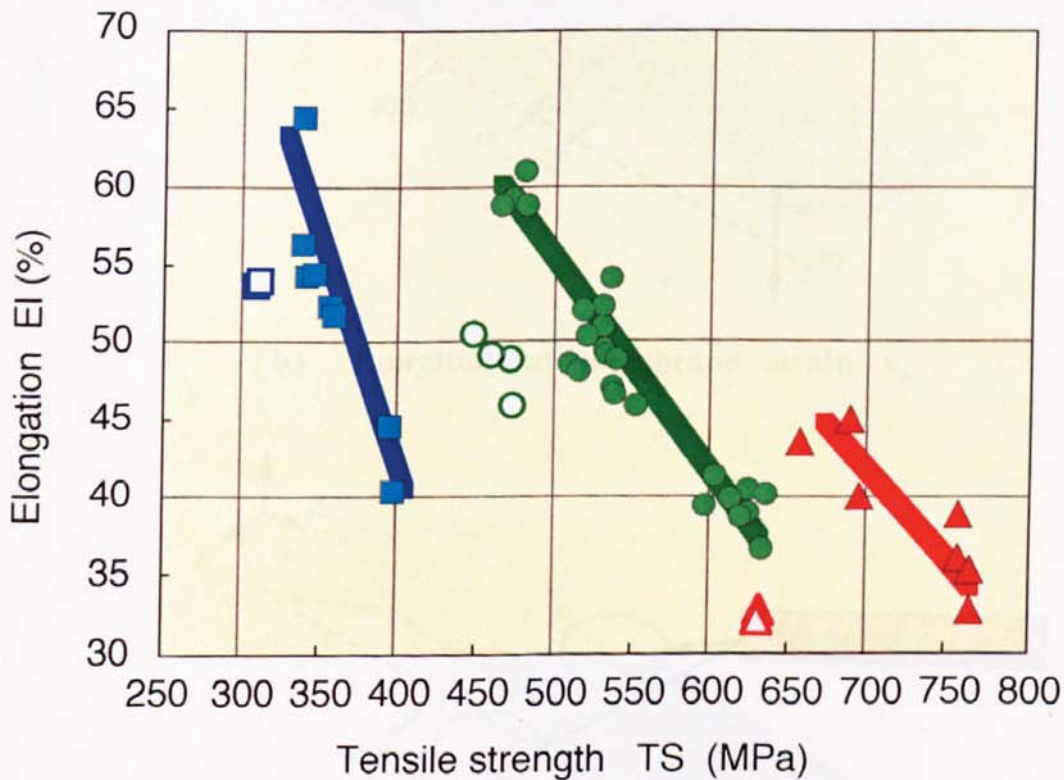
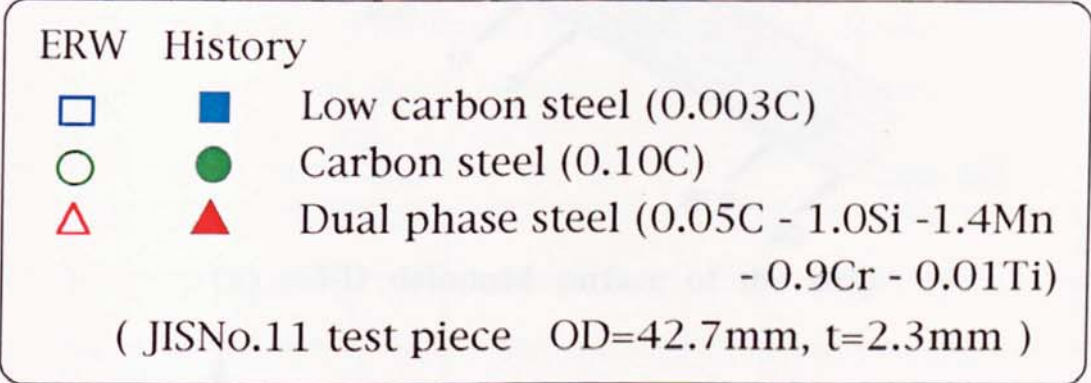
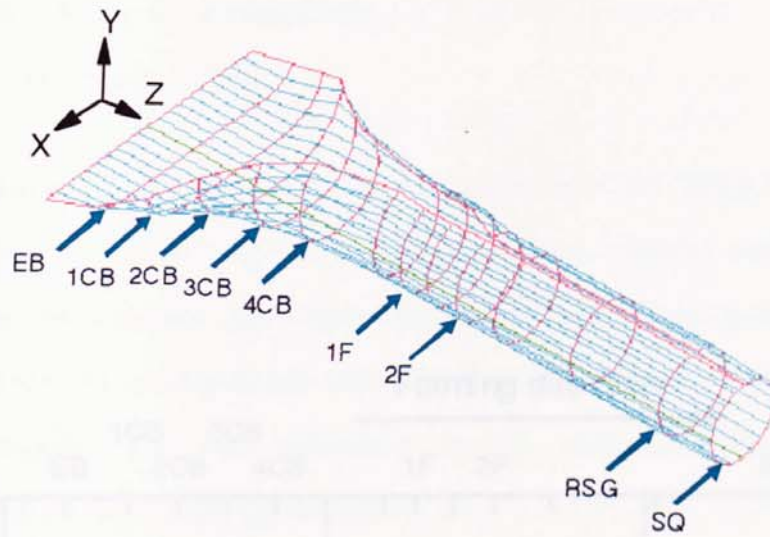
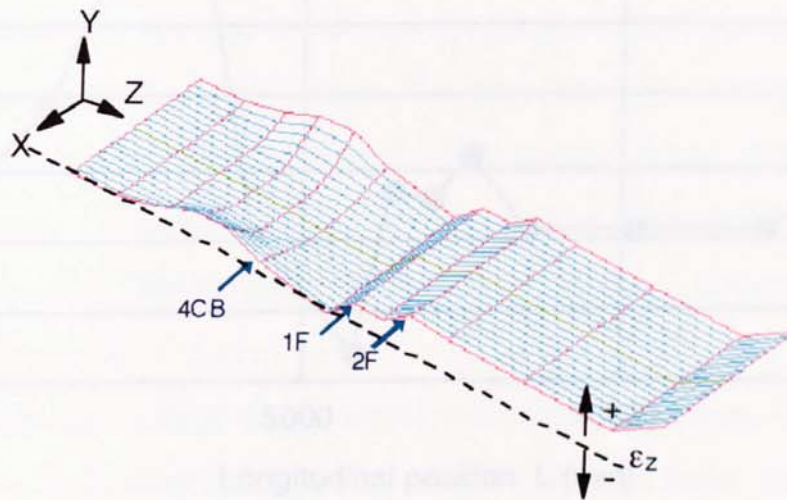


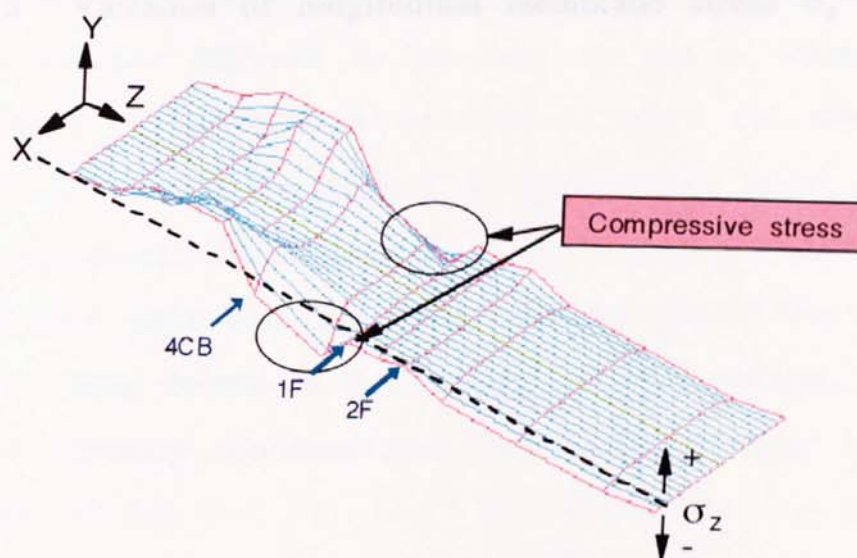
Fig.113 Comparison of mechanical properties between HISTORY and conventional ERW steel tubes



(a) 3-D deformed surface of the strip



(b) Longitudinal membrane strain ϵ_z



(c) Longitudinal membrane stress σ_z

Fig.114 Examples of calculated results in the 6 inch CBR forming mill of The HISTORY mill

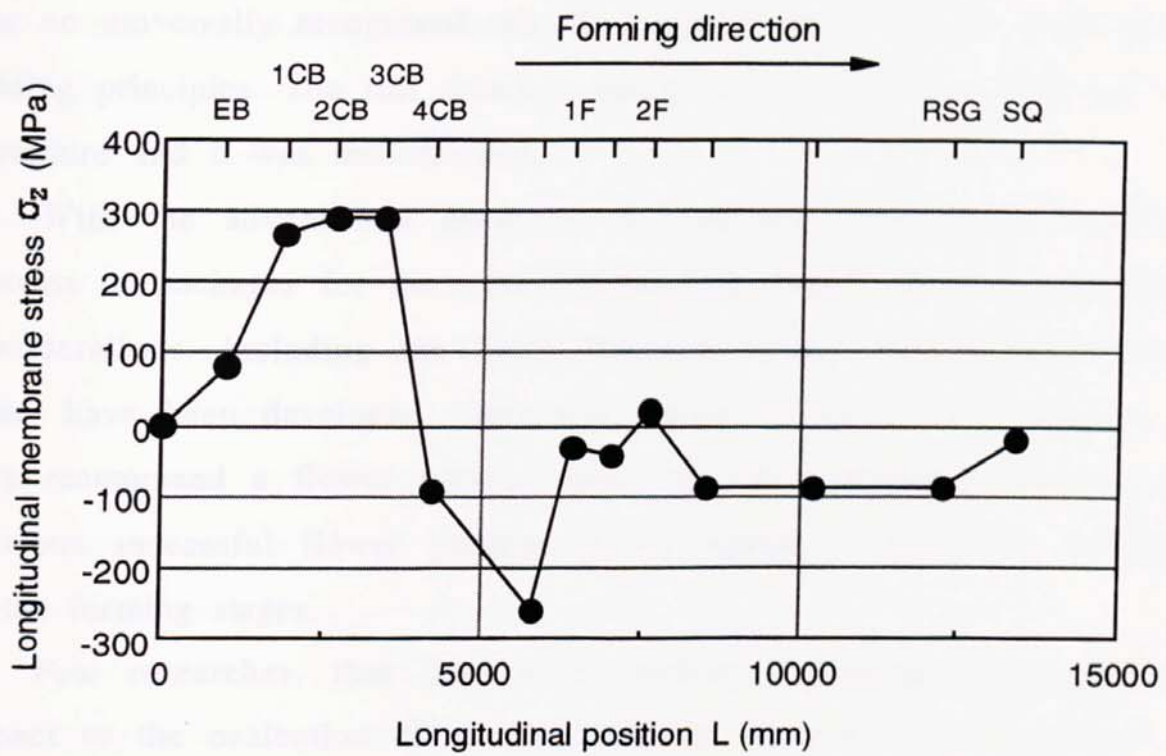


Fig.115 Variation of longitudinal membrane stress σ_z

Chapter 9 Conclusions

9.1 Introduction

The conventional design and manufacture of forming rolls depended on the individual skill of the roll designers. Such skills were normally based on the experience and knowledge gained from previous work. There was no universally recognized scientific design theory which could provide guiding principles. The roll schedule design was normally a trial and error procedure and it was not efficient.

With the advent and progress of computer technology, CAD/CAM systems or packages for the cold roll-forming, based on some geometrical considerations, including the basic bending theory and primitive design rules, have been developed. Generally, however, these CAD systems can only recommend a flower pattern based on the knowledge obtained from previous successful flower pattern, which lacked a theoretical evaluation of the forming stages.

Few researches, that deal with consistent forming simulation with respect to the evaluation of forming defects, have been conducted in the cold roll-forming process. This is because of the extremely complex three-dimensional deformation, with small strains and many uncertain boundary conditions, which are difficult to estimate or define. However, it is considered that it would become possible to carry out the consistent forming simulation by a modelling simplification based on radical assumptions. Theoretical simulation has been required, especially in the production of ERW tube and pipe, not only to predict the risk of the occurrence of forming defects in the forming of new products, but also to obtain optimum forming condition and procedures, in order to minimise forming defects.

9.2 Development of the CADFORM system

The development of the new interactive software package named "CADFORM", which requires knowledge of the integrated computer and graphics operation has provided the user with a consistent forming simulation for tube-making. This is a unique approach, which demonstrates a consistent forming simulation for tube-making by the cold roll-forming process.

Firstly, the application of the existing CAD/CAM system "ROLFOM" at Aston University to design the flower pattern of tube and pipe was tried, however there was a limitation in extending its application. Therefore, the new software package "CADFORM", that includes the elastic-plastic stress-strain analysis and the evaluation of edge buckling by a simplified model of the forming process, has been devised.

This system consists of four main programmes:

- (1) Flower pattern design programme with the data input and two-dimensional(2-D) drawing
- (2) Elastic-plastic stress-strain analysis programme
- (3) Evaluation of the edge buckling programme
- (4) Three-dimensional(3-D) graphics display and drawing programme

The interactive data input system has been created in order to provide easy use and access. Amendments of data, creating data files and calling the data from the file, by the interactive method, are also considered in order to give satisfactory operation for the designer. Furthermore, all main results are displayed on the Tektronix colour screen by a newly devised 2-D and 3-D graphics programmes associated with the GINO-F graphics package. These results are visualised in order to enable the designer to gain a rapid understanding and checking of the results.

The originality of this research is the realisation of predicting a forming

defect and to enable the designer to redesign the appropriate flower pattern based on the result of edge buckling evaluation. The consistent forming simulation, which consists of the construction of forming flower patterns, the analysis of stress-strain using the designed flower pattern and the evaluation of the edge buckling occurrence is the first realised proposal for more effective tube-making.

9.2.1 Flower pattern design

The flower pattern design programme is developed, which consists of the data input, the amendment of data, creating the files, calling the existing data file, and co-ordinating the 2-D graphics display and construction of the two kinds of flower patterns, with the interactive operation system. Thus, the two kinds of flower patterns developed, such as the individual drawing ("Flower pattern A") and the flower sequence drawing ("Flower pattern B") can also be visualized. Hence, the designer can easily design any flower pattern for tube and pipe, and can rapidly identify results. Furthermore, any size of tube and pipe can be drawn with this CADFORM system using the automatic scaling provision.

9.2.2 Elastic-plastic stress-strain analyses

This analysis utilises the membrane theory and adopts a geometrical deformation model, whereby deformation surface of strip between passes is divided into elements. The assumption is also made that the strip between passes is subjected to linear deformation in the longitudinal direction.

In the CADFORM system, two deformation models were devised: Model-1 and Model-2. Model-1 calculates the strain for the condition of no deformation of the lateral divided elements, whilst Model-2 calculates the strain by consideration of both the deformation of the laterally divided elements and the fin-pass roll reduction. The designer can also identify the outline of the stress-strain analysis results in the forming stages by the 3-D graphics display.

9.2.3 Verification of the CADFORM system

Verification of the calculated longitudinal strain was carried out for comparison with the measured forming strains by using the CBR forming pilot mill. The calculated longitudinal strain using Model-2 corresponds reasonably well with the measured longitudinal strain. However, the calculated longitudinal strain by Model-1 does not correspond with the measured longitudinal strain at the fin-pass roll forming stage. It is suggested that this discrepancy is due to no account being taken of the fin-pass reduction by Model-1.

Thus, the longitudinal forming strains of the strip can be approximately estimated by the CADFORM system. It is apparent that the longitudinal forming stress, which controls the occurrence of the edge buckling, can also be roughly estimated using these calculated strains by the CADFORM system.

9.2.4 Comparison of stress and strain by the two theoretical models

The calculated results by the two theoretical models are similar in the upper forming stages of the tube prior to the fin-pass roll forming stage. However, differences of stress and strain between Models-1 and -2 are noticeable at the fin-pass and squeeze roll forming stages. A number of effects of the fin-pass roll reduction on the strip deformation are apparent at the fin-pass roll and squeeze roll forming stages. Firstly, the longitudinal compressive stress is decreased by the addition of the fin-pass roll reductions. Secondly, as predicted by the calculated results from Model-2, the edge buckling can be suppressed by the fin-pass roll reduction.

9.2.5 Evaluation of edge buckling

The edge buckling model as thin walled columns was devised on the basis of the Euler⁶¹ theory. In this model, the Euler theory was applied to the elastic buckling in the elastic deformation and both of the tangent modulus theory and the reduced modulus theory were also applied to the plastic buckling in the plastic deformation.

Edge buckling rarely occurs in the upper forming stages since the analysed longitudinal stresses are all tensile stress. However, large increasing compressive stresses are added after the middle stage of the forming passes and becomes larger than the calculated elastic buckling stress. This compressive stress comes close to the plastic buckling stress over the critical elastic buckling stress between the middle forming stage

and the first fin-pass roll forming stage. It is therefore considered that the strip edges are subjected to a high critical condition of the elastic edge buckling.

In the fin-pass roll and squeeze roll forming stages, the longitudinal compressive stress calculated by the Model-1 becomes a little bit larger than the plastic buckling stress. It is apparent that the strip edges are subjected to a high critical condition of the plastic edge buckling.

On the other hand, the longitudinal compressive stress calculated by the Model-2 with the consideration of the fin-pass roll reduction is decreased less than the plastic buckling stress by the circumferential reduction of the strip. This suggests that the fin-pass roll reduction is more effective to suppress the occurrence of edge buckling.

Thus, it can be stated that the CADFORM stress-strain analysis can roughly predict the occurrence of edge buckling of the strip in tube-making by the cold roll-forming process.

9.2.6 Effects of the pass-line conditions

The longitudinal compressive stress is decreased at the forming stage, before the No.1 fin-pass roll, due to the effects of downhill pass-line forming. In the production mill, the downhill pass-line forming is generally applied to the forming of the thin walled tube. It is therefore considered that edge buckling can be suppressed by the downhill pass-line forming condition.

9.2.7 Effects of the number of laterally divided elements

In order to investigate the effect of the number of the laterally divided elements on the stress and strain in tube-making, the calculation for two cases of ten and twenty divided elements in a half width of strip were conducted. It is thus suggested that the effect of the number of lateral divided elements on the stress and strain is not significant for the condition of more than ten divided elements.

9.2.8 Effects of the forming flower patterns

Forming stresses and strains using the three fundamental forming flower patterns: edge bending, centre bending and circular bending, were calculated to study the effect of these forming patterns. It is noted that the strip utilising the centre bend forming pattern is subjected to the most critical condition of edge buckling occurrence.

However, the strip employing the circular bend forming pattern is subjected to the least critical condition of edge buckling occurrence.

Finally, the stress and strain features in the three fundamental flower patterns are clarified by the CADFORM system. Thus, the flower pattern design is very important in suppressing the occurrence of edge buckling.

9.4 Application of the CADFORM system

The CADFORM system was used to design the appropriate forming flower pattern for the 6inch CBR forming mill, the new manufacturing process for the welded tube, termed "HISTORY." By using the analysed results, the appropriate forming flower pattern was investigated to produce a decrease in the tube longitudinal compressive stress. The CADFORM system is practically useful in designing the appropriate forming flower pattern to suppress the occurrence of edge buckling, especially in the forming of thin walled tubes.

Chapter 10 Future Work

Compared with hot sheet rolling, hot bar rolling and cold sheet rolling, cold roll-forming is an extremely complex three-dimensional deformation process with small elastic-plastic deformation strains and many uncertain boundary conditions, which are difficult to estimate or define. However, it is considered that it would be possible to carry out consistent forming simulation by a modelling simplification based on several radical assumptions. Furthermore, the author considered that greater value would be attached to a consistent and complete forming simulation which can provide an approximate estimation, rather than a localised forming simulation with high accuracy in tube making by the cold roll-forming process.

Thus, the CADFORM system has been developed as the first attempt to give a consistent forming simulation with stress-strain analysis. The CADFORM stress-strain analysis can roughly predict the occurrence of edge buckling of the strip in tube-making by the cold roll-forming process. It has been confirmed that the CADFORM system is practically useful in designing the appropriate forming flower pattern to suppress the occurrence of edge buckling, especially in forming thin walled tubes. However, more work and improvements are necessary to get more accurate simulation results and to apply to a wider range of products by the cold roll-forming process.

The main subject areas for future work are as follows:

- (1) According to the results of some investigations, the ratio $d\epsilon_x(i, j)/d\epsilon_y(i, j)$ takes a value between 0.35 and 0.5. Thus, the value of 0.45 was applied in the calculation using the CADFORM system. However, the actual deformation of the semi-formed tube in the circumferential direction is not uniform at the fin-pass and squeeze roll forming stages.

Thus it is necessary to consider the variation of the ratio $d\epsilon_x(i, j)/d\epsilon_y(i, j)$ in the circumferential direction, based on the measured experimental data.

(2) In the evaluation of the edge buckling, a more accurate prediction might be obtained by using the known longitudinal stresses as boundary conditions in a FE model of a cylinder with an open slit in the longitudinal direction.

(3) The affected range of the edge buckling in the lateral direction of the strip has to be accurately investigated for different outside diameter pipes and different materials. Based on these results, the width of the laterally divided elements should be decided.

(4) The circumferential reduction of the strip is applied at the fin-pass roll reduction to suppress the edge buckling in the fin-pass roll forming stages. However, large fin-pass roll reduction causes the circumferential edge buckling in the edge portion of the strip. This circumferential edge buckling also becomes a serious problem. Therefore, an evaluation of the circumferential edge buckling should be simultaneously considered with the evaluation of the longitudinal edge buckling.

(5) In the CADFORM system, both of longitudinal bending and lateral bending are neglected to simplify the model. It is considered that the effects of lateral bending on the longitudinal edge buckling are not so large since the membrane stress has more influence on the longitudinal edge buckling than the bending stress and the lateral bending stress is not large.. However, the longitudinal bending of the semi-formed tube should be taken into consideration, especially in application of the downhill pass-line forming process, since the semi-formed tube behaves like a continuous beam.

(6) In this work, verification of the calculated longitudinal strain was carried out for comparison with one measured forming strain by using the CBR forming pilot mill. The calculated longitudinal strain using Model-2 corresponds reasonably well with the measured longitudinal strain. However, further measurements of forming strains in different sizes of pipes and different forming mills are necessary to verify the validity of the CADFORM system. In order to achieve this verification, the strain measurement procedure while the strip sheet is passing through the forming rolls has to be improved.

(7) A consistent forming simulation of tube-making by FEA will be able to provide more accurate results than the CADFORM system. However, it will take longer time to complete the calculation and it will be expensive.

REFERENCES

- 1) Sugayoshi T "Present Situation and Topics in the Production of ERW Tube and Pipe"
The 136th Symposium for Technology of Plasticity
'Recent Technology of Welded Tube and Pipe'
Tokyo (Japan) July 1991 pp1 [in Japanese]
- 2) Honjo W, Nakamura M Ishikawajima-Harima(IHI) Engineering Review
19, 1, 1, 1979 [in Japanese]
- 3) Yokoyama E, Toyooka T "Steel Sheet Deformation Behaviour and Forming Load Determination in 26 in Cage Forming ERW Pipe Mill"
Kawasaki Steel Technical Report No.4, pp72
Dec. 1981
- 4) Toyooka T "Recent Techniques of Roll Forming in the Medium Diameter ERW Mill"
Proceedings of the 3rd International Conference on Steel Rolling Tokyo (Japan) Sept. 1985
- 5) Toyooka T, Yokoyama E "Investigation on Steel Sheet Deformation in the Cage Roll Forming ERW Pipe Mill"
Proceedings of the 2nd International Conference on Rotary Metalworking Processes
Stratford-upon-Avon (U.K.) Oct. 1982
- 6) Onoda Y, Toyooka T "Effect of Down-hill Height and Fin Pass-Reduction Schedule on Shapes of Semi-pipe in Full Cage-type ERW Pipe Mill"
Journal of the Japan Society for Technology of Plasticity
30, 347, 1653, Dec. 1989 [in Japanese]
- 7) Toyooka T, Shiga A "Development of Chance-Free Bulge Roll Forming Process for Manufacturing ERW Tube and Pipe (1)"
Proceedings of the 1988 Japan Spring Conference for Technology of Plasticity
May (1988) 213 [in Japanese]
- 8) Toyooka T, Hashimoto Y "Development of Chance-Free Bulge Roll Forming Process for Manufacturing ERW Tube and Pipe (2)"
Proceedings of the 1988 Japan Spring Conference for Technology of Plasticity
May (1988) 221 [in Japanese]

- 9) Toyooka T, Shiga A "Development of Chance-Free Bulge Roll Forming Process for Manufacturing ERW Tube and Pipe (3)"
 Proceedings of the 40th Japan Joint Conference for Technology of Plasticity
 Oct. 1989, 357 [in Japanese]
- 10) Toyooka T, Hashimoto Y "Development of Chance-Free Bulge Roll Forming Process for Manufacturing ERW Tube and Pipe (4)"
 Proceedings of the 1990 Japan Spring Conference for Technology of Plasticity
 May 1990, 155 [in Japanese]
- 11) Toyooka T, Hashimoto Y "Development of Chance-Free Bulge Roll (CBR) Forming Process for Manufacturing ERW Pipe"
 Kawasaki Steel Technical Report No.25, pp59
 Sept. 1991 [in Japanese]
- 12) "Gino-F User Guide (Version 3.0)"
 Bradly Associates Ltd., Berkshire, 1990
- 13) "Gino-F Reference Manual (Version 3.0)"
 Bradly Associates Ltd., Berkshire, 1990
- 14) Jotaki M "Fortran 77"
 Omu(Publisher), 1990 [in Japanese]
- 15) "Programming in VAX FORTRAN"
 Digital Equipment Corporation Sept. 1984
- 16) Yoder U.S. Patent No.3472053 1969
- 17) Torrance U.S. Patent No.3417591 1968
- 18) Nicolai F "New Solution for Forming and Sizing in ERW Tube and Pipe Mills"
 Proceedings of I.T.A. International Conference and Exposition International Tube Association
 Philadelphia (USA) Sept. 1987
- 19) Duming H "CTA-a new Concept in Pipe and Tube Forming"
 Proceedings of I.T.A. International Conference and Exposition International Tube Association
 Philadelphia (USA) Sept. 1987
- 20) Nakata T "F.F.Mill, a new Generation of ERW Mill"
 Proceedings of I.T.A. International Conference and Exposition International Tube Association
 Philadelphia (USA) Sept. 1987

- 21) Nakago T Proceedings of the 39th Japan Joint Conference for
Technology of Plasticity
459, 1988 [in Japanese]
- 22) Adaka M Seitetsu Kenkyu 1988
(Nippon Steel Technical Report) [in Japanese]
- 23) Rhodes A "Computer Aided Design and Manufacture of Rolls
for Cold Roll-Forming"
Sheet Metal Industries 59, 643-651, 1982
- 24) Industrie Secco, Italy "Computer Aiding Design developed to
Assist in the Design of the Forming Sequence of
Cold Roll-Forming Profiles"
Proceedings of the 3rd International Conference on
Rotary Metalworking Processes
Kyoto (Japan) 1984 pp513-522
- 25) Riedlinger T "Roll Forming Die Design Time slashed from Days to
Hours"
Modern Metals 36, 38-40, 1980
- 26) Halmos G T "Computer Program Aids Roll Forming Designers"
Modern Metals 41, 22-26, 1985
- 27) Yuen W Y "New Development in CAD for Roll Forming"
The 1st International Conference on Technology of
Plasticity (Tokyo) Advanced Technology of
Plasticity 1, 514-519, 1984
- 28) Wong T N "Computer Aided Design and Manufacture of Form-
Rolls"
PhD thesis, University of Aston 1983
- 29) Matsune Journal of the Japan society for Technology of
Plasticity
23, 259, 786, 1983 [in Japanese]
- 30) Ona H,
Jimma T "A Computer Aided Design System for Cold Roll
Forming"
The 1st International Conference on Technology of
Plasticity (Tokyo) Advanced Technology of
Plasticity 1, 508-511, 1984

- 31) Sedlmaier A "Computer-Aided Production of Cold Rolled Profiles"
Tube International Nov. 1991 pp291
- 32) Baranowski R "Roll Design and Production System"
Tube International Jan. 1992 pp39
- 33) Masuda M, "Fundamental Research on the Cold Roll-Forming of Metals"
Murota T
Bulletin of the Japan Society of Mechanical Engineers 7, 28, 827-833 1964
See also: Journal of the Japan Society for Technology of Plasticity 6, 54, 379 1965 [in Japanese]
- 34) Sarantidis T M, "A Study of Cold Roll-Forming"
Noble C F
Proceedings of the 1st International Conference on Rotary Metalworking Processes
London 1979 pp411-422
- 35) Suzuki H, "Experimental Investigation on Cold Roll-Forming Process"
Kiuchi M
Report of the Institute of Industrial Science The University of Tokyo .22, 2, Sept. 1972
See also: Journal of the Japan Society for Technology of Plasticity
(1st Report 10, 97, 102 1969)
(2nd Report 10, 98, 157 1969)
(3rd Report 10, 102, 494 1969)
(4th Report 10, 102, 502 1969)
(5th Report 11, 110, 202 1970)
(6th Report 11, 112, 315 1970)
(7th Report 11, 119, 913 1970)
(8th Report 12, 130, 830 1971)
(9th Report 13, 133, 83 1972)
[all in Japanese]
- 36) Kiuchi M, "Characteristics of Cross-Sectional Profiles Formed by Fin-Rolls"
Shintani K
Journal of the Japan Society for Technology of Plasticity
27, 301, 280-286 1986 [in Japanese]
- 37) Jimma T, "Optimum Roll Pass Schedules of the Cold Roll Forming Process of Symmetrical Channels"
Ona H
Proceedings of the 21st International M.T.D.R. Conference Swansea (U.K.) 1980 pp63-68

- 38) Nakajima K, Seitetsu Kenkyu 299, 108 1979
Mizutani W Nippon Steel Technical Report
[in Japanese]
- 39) Kato K, "Effect of Metal Properties on Shape of Roll formed
Saito Y Products - Circular Arc Section"
Technology Reports of the Osaka University
30, 1561, 405-410 Oct. 1980
- 40) Kuriyama Y, Proceedings of the 34th Japan Joint Conference
Adaka M for Technology of Plasticity 465, 1983
- 41) Kasuga Y, "Experiments on Production of TIG Arc-Welded
Jimma T 304 Stainless Steel Pipes with Thin Walls"
Proceedings of the 3rd International Conference on
Steel Rolling Tokyo (Japan) Sept. 1985 pp327-334
- 42) Jimma T, "An Analysis of Cold Roll-Forming Process of
Morimoto H Channels using the Expanded Folded Paper Model"
Journal of the Japan Society for Technology of
Plasticity 27, 311, 1356-1362 1986
[in Japanese]
- 43) Kokado J, "On Edge Waves Occurring in Forming a Circular
Onoda Y Arc Groove with Wide Flanges through a Single
Stand Roll Mill"
Journal of the Japan Society for Technology of
Plasticity 17, 181, 92-100 1976
[in Japanese]
- 44) Kiuchi M, "Automated Design System of Optimum Roll
Koudabashi T Profiles for Cold Roll-Forming"
Proceedings of the 3rd International Conference
on Rotary Metalworking Processes
Kyoto (Japan) 1984 pp423-436
- 45) Kiuchi M, "Development of Simulation Model of Roll-Forming
Koudabashi T Processes"
Eto F Journal of the Japan Society for Technology of
Plasticity 27, 306,874-881 1986
[in Japanese]
- 46) Yamada Y "Plastic Stress-Strain Matrix and its Application for
Yoshimura N the Solution of Elastic-Plastic Problems by the
Sakurai T Finite Element Method"
Int. J. Mech. Sci. 10, 343-354 1968

- 47) Kiuchi M, Sato T "Study of Computational Simulation of Cold Roll Forming Process"
Report of Institute of Industrial Science
University of Tokyo 36, 7, 10-13 1984
- 48) Panton S M "Computer Aided Form Roll Design"
Ph D thesis, University Aston 1987
- 49) Bhattacharyya D, Smith P D "The Prediction of Deformation Length in Cold Roll Forming"
Journal of Mechanical Working Technology
9, 181-191 March 1984
- 50) Bhattacharyya D, Smith P D "The Prediction of Roll Load in Cold Roll Forming"
Journal of Mechanical Working Technology
14, 363-379 June 1987
- 51) Onoda Y "Finite Element Simulation of Deformation Features of Sheet Metal Formed by Fin Roll in ERW Pipe Mill"
Journal of the Japan Society for Technology of Plasticity 30, 346, 1554-1559 1989 [in Japanese]
- 52) Onoda Y, Nagamachi T, Toyooka T "Finite Element Simulation of Deformation Features of Sheet Metal Formed by Break-down Rolls in ERW Pipe Mill"
Proceedings of the 47th Japanese Joint Conference for the Technology of Plasticity
37-38, Nov. (1996) [in Japanese]
- 53) Onoda Y, Nagamachi T, Toyooka T "Finite Element Simulation of Deformation Features of Sheet Metal Formed by Fin Rolls in ERW Pipe Mill"
Proceedings of the 47th Japanese Joint Conference for the Technology of Plasticity
39-40, Nov. (1996) [in Japanese]
- 54) Onoda Y, Nagamachi T, Nakagome A, Kono M "Finite Element Simulation of Deformation Features of Steel Sheet Formed by Forming Rolls for Hat-Section"
Proceedings of the 46th Japanese Joint Conference for the Technology of Plasticity
367-368, Sept. (1995) [in Japanese]
- 55) Downes R J "Computer Simulation of Form-Roll Design"
PhD thesis, University Aston 1991
- 56) Itami Y, Ataka M, Shibata J "Effect of Sizing Process on Residual Stress of ERW Pipes"
Journal of the Japan Society for Technology of Plasticity
36, 419, 1373-1378(1995) [in Japanese]

- 57) Itami Y, Ataka M "Deformation Analysis of ERW Pipes Subjected to 2-Roll Sizer"
Journal of the Japan Society for Technology of Plasticity
37, 431, 1303-1308(1996) [in Japanese]
- 58) Kiuchi M, Wang F "Numerical Analysis of Deformation of Metal Sheet at Breakdown Forming Stage(1)"
Proceedings of the 1995 Japanese Spring Conference for the Technology of Plasticity
413-414, May (1995) [in Japanese]
- 59) Kiuchi M, Wang F "Numerical Analysis of Deformation of Metal Sheet at Breakdown Forming Stage(4)"
Proceedings of the 47th Japanese Joint Conference for the Technology of Plasticity
33-34, Nov. (1996) [in Japanese]
- 60) Kaltprofile Verlag Stahleisem MBH, Dusseldorf, 1969
- 61) Gere & Timoshenko Mechanics of Materials
Third SI edition Chapman&Hall, 1991
- 62) Roark R J, Young W C Formulas for Stress and Strain
Fifth edition McGraw-Hill 1975
- 63) Kiuchi M, Motogi K " Roll Forming "
Journal of the Japan Society for Technology of Plasticity 31, 350, 317-324 1990
[in Japanese]
- 64) Furukawa T, " Kawasaki's new History tube "
NEW STEEL
66, March (1999)
- 65) Toyooka T, " Development of ultra fine grain steel tube with high strength and excellent formability "
Current Advances in Materials and Processes
312, 2, 302(1999) [in Japanese]
- 66) Toyooka T, " Development of ultra fine grain steel tube with high strength and excellent formability "
Seoul 2000 FISITA World Automotive Congress
A420, June (2000)

Appendix -1 Programme of the CADFORM

```

C*****
*****
C**** This programme is Version-2 of CADFORM that consist of CADFORM.FOR;102,
FLOWERT.FOR;13 and SSA3DDSB.FOR;55. ****
C**** This programme analyse stress-stain with a consideration of Fin-pass and SQ reduction.
****
C*****
*****
C**** This programme is amended on 14th October,1992. *****
C*****
C
C
C*****
C*
C*      *****      *      *****      *****      *****      **      **      **
C*      *      *      *      *      *      *      *      *      *      *      *      *      *
C*      *      *      *      *      *****      *      *      *      *      *      *      *
C*      *      *****      *      *      *      *      *      *****      *      *      *
C*      *      *      *      *      *      *      *      *      *      *      *      *
C*      *****      *      *      *****      *      *      *      *      *      *
C*
C*
C*
C*      COMPUTER AIDED DESIGN AND ANALYSIS SYSTEM
C*
C*      BY TAKAAKI TOYOOKA      AT ASTON UNIVERSITY
C*
C*      ( 19TH. NOV.. 1991      VERSION 1.0 )
C*
C*****
C
C      ----*** NAIN      PROGRAM      ***-----
C***** This programme was amended on 8th October 1992 *****
C
C      PROGRAM MAIN
C
C      IMPLICIT      REAL*8(A-H,L,O-Z), INTEGER*4(I-K,M-N)
C      CHARACTER      FILE1*12, FILE2*12, AA*12, MA*8, M1*8, M2*8, SIZE*14,
%      DATE*10, DRAWER*12, WORKS*12, MATERIAL*12
C
C      DIMENSION      JC(0:25,5), JK(0:25,5)
C
C      COMMON/DAT1/ LS(0:26), TLS(0:26), DH(0:25), NR(0:25), R(0:25,5),
%      AN(0:25,5)
C      COMMON/DAT2/ D, WS, TS, KK, NN
C      COMMON/DAT3/ EE, SEQ0, HH, ANYU, BL, VV
C      COMMON/DAT4/ PE, ITD, IDH, IIDH, JF
C      COMMON/DAT5/ TLO(0:25), TLN1(0:25), AH(0:25), AW(0:25), WE(0:25),
%      AWY(0:25)
C      COMMON/DAT6/ RN(0:25,6), DLN(0:25,6), TLN(0:25,6), DLE(0:25)
C      COMMON/DAT7/ N1F, RSF
C      COMMON/POINT1/ PX0(0:25,0:5), PY0(0:25,0:5), CX(0:25,0:5),
%      CY(0:25,0:5), PXI(0:25,0:5), PYI(0:25,0:5),
%      RR(0:25,0:5)
C      COMMON/AAN/ AAN(0:25,0:5)
C      COMMON/POINT2/ PXE(0:25,-22:22), PYE(0:25,-22:22), PZ(0:25),
%      DB(0:25,0:21), TLE(0:25,0:21), ANE(0:25,0:22)
C      COMMON/STA1/ EZ(0:25,0:20), EX(0:25,0:20), DEZ(0:25,0:20),
%      DEX(0:25,0:20), DLZ(0:25,0:20), DZ(0:25,0:20), BB
C      COMMON/STA2/ HDEZ, HEZ, SDEX, HEX, SEX
C      COMMON/STA3/ PDEZ(0:25,-20:20), PEZ(0:25,-20:20),
%      PDEX(0:25,-20:20), PEX(0:25,-20:20)
C      COMMON/STA3A/ PEZE(0:25,0:20), PEXE(0:25,0:20), PEZP(0:25,0:20),
%      PEXP(0:25,0:20), PDEPSO(0:25,0:20)
C      COMMON/STA4/ FRD(0:10), DEXF(0:10,0:20), DEZF(0:10,0:20),
%      DBO(0:10,0:20), TLEO(0:10,0:20)
C      COMMON/STS1/ DSZ(0:25,-20:20), DSX(0:25,-20:20), SZ(0:25,-20:20),

```

```

%          SX(0:25,-20:20), SEQ(0:25,-20:20),
%          SOTOS(0:25,-20:20), EZE(0:25,0:20), EXE(0:25,0:20),
%          NHANT(0:25,0:20), EZP(0:25,0:20), EXP(0:25,0:20)
COMMON/STS2/ DEPSOT(0:25,0:20),
%          DWP(0:25,0:20), DWE(0:25,0:20), DW(0:25,0:20),
%          DWT(0:25,0:20), WT(0:25), WTR(0:25),
%          SWT(0:25),SWTR
COMMON/STS3/ HDSZ,SDSZ,HSZ, SSZ, HSX, SSX, HSOTOS, SSOTOS, HDW,
%          HWT, HWTR
COMMON/STS4/ PDSZ(0:25,-20:20), PDSX(0:25,-20:20),
%          PSZ(0:25,-20:20), PSX(0:25,-20:20),
%          PSEQ(0:25,-20:20), PSOTOS(0:25,-20:20),
%          /STS4A/ PDWE(0:25,0:20), PDWP(0:25,0:20),PDW(0:25,0:20),
%          PDWT(0:25,0:20), PWT(0:25), PWTR(0:25),
%          PSWT(0:25),PSWTR
COMMON/STS5/ DEZE(0:25,0:20),DEXE(0:25,0:20),
%          PDEZE(0:25,0:20),PDEXE(0:25,0:20)
DIMENSION DLO1(0:25,5),DLN1(0:25,5),
%          PDEXF(0:10,0:20),PDEZF(0:10,0:20)

```

```

C
DATA M1/'MODEL 1'/, M2/'MODEL 2'/

```

```

C
C
C
C
***** DEFINITION OF FUNCTION *****

```

```

PE=3.1415926535898/180

```

```

C
C
C
C
*****

```

```

820 WRITE(*,100)
100 FORMAT(//10X,'*****',
%10X,'*****',
%10X,'**',
%10X,'**  COMPUTER AIDED DESIGN AND ANALYSIS SYSTEM **',
%10X,'**      OF TUBE AND PIPE FORMING      **',
%10X,'**',
%10X,'**      BY T.TOYOOKA  ASTON UNIVERSITY      **',
%10X,'**      (19th. Nov. . 1991)      **',
%10X,'**',
%10X,'*****',
%10X,'*****')
PRINT*,

```

```

C
WRITE(*,101)
101 FORMAT(10X,'*****',
%10X,'**',
%10X,'**  CHOOSE THE WAY OF INPUTTING DATA  **',
%10X,'**',
%10X,'**  1. INPUT THE NEW DATA      ---> 1  **',
%10X,'**  2. CALL THE DATA FROM THE FILE ---> 2 **',
%10X,'**',
%10X,'*****')

```

```

C
13 WRITE(*,*)' ***** INPUT ONE NUMBER BETWEEN 1 AND 2 *****'
READ *, ITD

```

```

C
IF(ITD.NE.1.AND.ITD.NE.2) THEN
WRITE(*,102)
102 FORMAT(//4X,'* INPUT ERROR - INPUT THE CORRECT NUMBER AGAIN **/')
GO TO 13
ELSE
WRITE(*,*)'** INPUT THE FILE NAME IN ANY CASE **'
PRINT*,
WRITE(*,*)' FILE NAME=? '
READ(*,200) FILE1
200 FORMAT (A)

```



```

ENDIF
C
C***** FILE OPEN *****
C
OPEN( 1 ,FILE='D'//FILE1, STATUS='UNKNOWN')
C *OPEN( 2 ,FILE='P'//FILE1, STATUS='UNKNOWN')
OPEN( 3 ,FILE='R'//FILE1, STATUS='UNKNOWN')
C
C
IF(ITD.EQ.1) GO TO 11
IF(ITD.EQ.2) GO TO 12
C
C
11 WRITE(*,104)
104 FORMAT(//4X,'*****',
%/4X,'** INPUT THE NEW DATA. **',
%/4X,'*****'//)
C*****
C*** NEW DATA INPUT ***
C*****
C
JD=0
JV=0
C
WRITE(*,106)
106 FORMAT(//4X,'**USE THE UNIT OF LENGTH (mm) AND ANGLE',
%'(degree)**'//)
501 WRITE(*,108)
108 FORMAT(//4X,'OUTSIDE DIAMETER AT SQUEEZE ROLL:D(mm)=')
READ*, D
IF(JV.EQ.1) GO TO 506
502 WRITE(*,109)
109 FORMAT(//4X,'WIDTH OF SHEET:WS(mm)=')
READ*, WS

IF(JV.EQ.2) GO TO 506
503 WRITE(*,110)
110 FORMAT(//4X,'THICKNESS OF SHEET:TS(mm)=')
READ*, TS
IF(JV.EQ.3) GO TO 506
504 WRITE(*,111)
111 FORMAT(//4X,'NUMBER OF ROLL STANDS (Max.25):KK=')
READ*, KK
490 WRITE(*,492)
492 FORMAT(//4X,'STAND NUMBER OF 1st FIN-PASS ROLL:N1F=')
READ*,N1F

C
C***** CHECK AND AMEND THE DATA *****
C
506 WRITE(*,500)
500 FORMAT(//4X,'*****',
%/4X,'** DO YOU WANT TO CHANGE THE DATA THAT YOU **',
%/4X,'** INPUTTED JUST BEFORE? **',
%/4X,'**',
%/4X,'** 0. NO CHANGE ---> 0 **',
%/4X,'** 1. OUTSIDE DIAMETER ---> 1 **',
%/4X,'** 2. WIDTH OF SHEET ---> 2 **',
%/4X,'** 3. THICKNESS OF SHEET ---> 3 **',
%/4X,'** 4. NUMBER OF ROLL STANDS ---> 4 **',
%/4X,'** 5. STAND No. OF 1st FINPASS -> 5 **',
%/4X,'**',
%/4X,'*****'//)

```

```

PRINT*, '**--- INPUT THE PERMISSIBLE NUMBER FROM 0 TO 4. ---**'
READ*, JV
  IF(JV.EQ.0) GO TO 505
  IF(JV.EQ.1) GO TO 501
  IF(JV.EQ.2) GO TO 502
  IF(JV.EQ.3) GO TO 503
  IF(JV.EQ.4) GO TO 504
  IF(JV.EQ.5) GO TO 490
WRITE(*,508)
508 FORMAT(/4X,' ***** INPUT ERROR. *****',
  %4X,' INPUT THE PERMISSIBLE NUMBER AGAIN.'//)
  GO TO 506
505 IF(JD.EQ.1) GO TO 534
537 WRITE(*,112)
112 FORMAT(/4X,'DISTANCE OF EACH STAND:LS(mm)=')
  TLS(0)=0.0
  DO 10 I=1, KK
  II=I-1
  WRITE(*,113)II,I
113 FORMAT(/4X,'DISTANCE FROM ',I2,'st. TO ',I2,'st. =')
  READ*, LS(I)
  TLS(I)=TLS(I-1)+LS(I)
  10 CONTINUE
  IF(JV.EQ.1) GO TO 513
C
C***** INPUT THE DOWNHILL CONDITION *****
C
512 WRITE(*,114)
114 FORMAT(/4X,'**DOWNHILL AMOUNT OF EACH STAND:DH(mm)**')
C
14 WRITE(*,115)
115 FORMAT(/4X,'*****',
  %4X,' * IF YOU WANT THE BOTTOM CONSTANT, i.e. *',
  %4X,' * NO DOWNHILL FORMING, *',
  %4X,' * INPUT THE NUMBER 0(ZERO) *',
  %4X,' * AND THE OTHER CASE(DOWNHILL FORMING) *',
  %4X,' * INPUT THE NUMBER 1. *',
  %4X,'*****'//)
PRINT*, '*** INPUT THE NO. 0 OR 1. *****'
READ*, IDH
  IF(IDH.EQ.0) THEN
    DO 20 I=0, KK
    DH(I)=0.0
  20 CONTINUE
  ELSE IF(IDH.EQ.1) THEN
C***** INPUT THE CONDITION OF DOWNHILL OR UPHILL FORMING *****
WRITE(*,560)
560 FORMAT(/4X,'*****',
  %4X,' * IN CASE OF A DOWNHILL FORMING *',
  %4X,' * INPUT THE NUMBER 0(ZERO) ---> 0 *',
  %4X,' * IN CASE OF AN UPHILL FORMING *',
  %4X,' * INPUT THE NUMBER 1 ---> 1 *',
  %4X,'*****'//)
PRINT*, '***** INPUT THE NO. 0 OR 1. *****'
READ*, IIDH
PRINT*, '*****'
IF(IIDH.EQ.0) GO TO 210
IF(IIDH.EQ.1) GO TO 212
C
210 PRINT*, '** INPUT THE PLUS(+) VALUE IN A DOWNHILL FORMING.**'
  GO TO 214
212 PRINT*, '** INPUT THE MINUS(-) VALUE IN A UPHILL FORMING. **'
214 PRINT*, '*****'
C
  DO 30 I=0, KK
  WRITE(*,116) I,I

```

```

116 FORMAT(/4X,'DOWNHILL AMOUNT AT No.',I2,'st:DH(',I2,')=')
    READ*,DH(I)
30    CONTINUE
    ELSE
    WRITE(*,117)
117 FORMAT(/4X,'** INPUT ERROR --- INPUT 0 OR 1,AGAIN. **'//)
    GO TO 14
    ENDIF

```

```

C
C***** CHECKE AND AMEND THE DATA *****
C

```

```

513 WRITE(*,509)
509 FORMAT(/4X,'*****',
%4X,          '*** DO YOU WANT TO CHANGE THE DATA   **',
%4X,          '*** THAT YOU INPUTTED JUST BEFORE?   **',
%4X,          '***',
%4X,          '*** 0. NO CHANGE                ---> 0   **',
%4X,          '*** 1. DISTANCE OF EACH STAND    ---> 1   **',
%4X,          '*** 2. DOWNHILL AMOUNT            ---> 2   **',
%4X,          '***',
%4X,          '*****'//)
PRINT*, '-----INPUT THE NUMBER FROM 0 TO 2. -----'
READ*, JV
IF(JV.EQ.0) GO TO 511
IF(JV.EQ.1) GO TO 537
IF(JV.EQ.2) GO TO 512
WRITE(*,510)
510 FORMAT(/4X,'** INPUT ERROR.INPUT THE PERMISSIBLE No. AGAIN.**'//)
GO TO 513
511 IF(JD.EQ.2) GO TO 534

```

```

C
C***** INPUT THE DATA OF OUTSIDE RADII AND ANGLE OF HALF OF THE FLOWER AT EACH STAND.
*****
C

```

```

538 WRITE(*,118)
118 FORMAT(/4X,'*** INPUT THE DATA OF OUTSIDE RADII AND ANGLES OF ',
%4X,'HALF OF FLOWER ***',
%4X,' AT EACH STAND.',
%4X,' Max.NUMBER OF RADII IS 5(Max.5) INCLUDING ',
%4X,'THE LINEAR PARTS.'//)
WRITE(*,119)
119 FORMAT(/4X,'-----',
%4X,' IF FLOWER HAS LINEAR PARTS,',
%4X,' INPUT 0(ZERO) AS THE RADIUS AND',
%4X,' INPUT THE LENGTH OF LINEAR PART.',
%4X,'-----'//)
IF(JD.EQ.3) GO TO 90
GO TO 91
90 WRITE(*,92)
92 FORMAT(/4X,'*****',
%4X,' WHAT STAND DO YOU WANT TO CHANGE THE DATA OF? ',
%4X,' INPUT THE STAND NUMBER; I=.',
%4X,'*****'//)
READ*,I
GO TO 121

```

```

C
91 DO 40 I=1, KK
121 WRITE(*,120)I,I
120 FORMAT(/4X,'*****',
%4X,' INPUT THE NUMBER OF RADII',
%4X,' AT No.',I2,'st.:NR(',I2,')=')
READ*, NR(I)
IF(NR(I).GT.5.OR.NR(I).LT.1) THEN
WRITE(*,514)
514 FORMAT(/4X,'** INPUT ERROR. INPUT THE PERMISSIBLE NUMBER, ',
%4X,'AGAIN. **'//)

```

```

GO TO 121
ELSE
ENDIF
C
    JV=0
    WRITE(*,122) I
122 FORMAT(/4X,'***** No.',I2,' STAND *****',
    %/2X,'No.***',3X,'RADIUS(mm)',3X,'**ANGLE(degree) **'/)
    PRINT*,'-- For Example --'
    PRINT*,' 1 <----- This value is given automatically.'
    PRINT*,'@@@ YOU MUST INPUT THE REAL NUMBER LIKE 40.0 @@@'
    PRINT*,'45.6, 23.56 --You can put a space or , between values'
    PRINT*,' 0, 41.81 <---IN CASE OF LINEAR PART, ----- '
    PRINT*,'YOU MUST INPUT THE 0 AS A RADIUS AND A LINEAR LENGTH'
        DO 50 J=1, NR(I)
            JCC(I,J)=J
            JK(I,J)=I
517 WRITE(*,123) J
123 FORMAT(/2X,I3)
    READ(*,80) R(I,J), AN(I,J)
    80 FORMAT(F10.3, F15.10)
C
    IF(R(I,J).EQ.0.0) THEN
        R(I,J)=99999.999
        AN(I,J)=AN(I,J)/(R(I,J)*PE)
    ELSE
    ENDIF
    DL01(I,J)=R(I,J)*AN(I,J)*PE
    DLN1(I,J)=(R(I,J)-TS/2.0)*AN(I,J)*PE
C
    IF(JV.EQ.2) GO TO 518
    IF(JV.EQ.3) GO TO 518
50 CONTINUE
C
C***** CHECK AND AMEND THE DATA OF RADIUS AND ANGLE. *****
C
518 WRITE(*,515) I,I
515 FORMAT(/4X,'*****',
    %/4X,'** DO YOU WANT TO CHANGE THE DATA OF RADII **',
    %/4X,'**',
    %/4X,'** 0. NO CHANGE ---> 0 **',
    %/4X,'** 1. CHANGE ALL DATA AT SOME STAND ---> 1 **',
    %/4X,'** 2. CHANGE THE NUMBER OF RADII, RADII **',
    %/4X,'** AND ANGLE AT No.',I2,' STAND. ---> 2 **',
    %/4X,'** 3. CHANGE THE DATA OF ONE RADIUS ---> 3 **',
    %/4X,'** AND ANGLE AT No.',I2,' STAND. **',
    %/4X,'*****'//)
    PRINT*,'----- INPUT ONE NUMBER FROM 0 TO 2 ----'
    READ*, JV
    IF(JV.EQ.0) GO TO 519
    IF(JV.EQ.1) GO TO 90
    IF(JV.EQ.2) GO TO 121
521 WRITE(*,516) NR(I), NR(I)
516 FORMAT(/4X,'*****',
    %/4X,'* WHAT NUMBER OF RADIUS DO YOU WANT TO CHANGE *',
    %/4X,'* Max.RADIUS No.=',I1,' *',
    %/4X,'* INPUT ONE NUMBER FROM 1 TO ',I1,' *',
    %/4X,'*****'//)
    READ*, J
    IF(J.LE.NR(I).AND.J.GE.1) THEN
        WRITE(*,122) I
        GO TO 517
    ELSE
        WRITE(*,520)
520 FORMAT(/4X,'** INPUT EROOR. PLEASE INPUT THE PERMISSILE ',
    %'NUMBER, AGAIN.'//)

```

```

GO TO 521
ENDIF
519 IF(JD.EQ.3) GO TO 534
WRITE(*,*)'-----'
40 CONTINUE
C
C***** INPUT THE NUMBER OF DIVISION IN LATERAL DIRECTION *****
C***** (i.e. THE NUMBER OF ELEMENT IN LATERAL DIRECTION) *****
C
JV=0
522 WRITE(*,124)
124 FORMAT(/4X,'THE NUMBER OF DIVISION IN LATERAL DIRECTION OF SHEET
%',/10X,'Max.20 IN HALF OF WIDTH : NN=')
READ*,NN
IF (NN.GT.20.OR.NN.LT.1) THEN
WRITE(*,125)
125 FORMAT(/4X,'*** INPUT ERROR. INPUT THE PERMISSIBLE No. ',
%',AGAIN. *****/)
GO TO 522
ELSE
ENDIF
IF(JV.EQ.1) GO TO 524
C
C***** INPUT THE DATA OF MECHANICAL PROPERTY OF SHEET. *****
C
WRITE(*,126)
126 FORMAT(/4X,'*** INPUT THE MECHANICAL PROPERTY OF SHEET. ****/')
526 WRITE(*,127)
127 FORMAT(/4X,'YOUNG'S MODULUS:E(kgf/mm2)=')
READ*,EE
IF(JV.EQ.2) GO TO 524
527 WRITE(*,128)
128 FORMAT(/4X,'YIELD STRESS:Y(kgf/mm2)=')
READ*,SEQ0
IF(JV.EQ.3) GO TO 524
528 WRITE(*,129)
129 FORMAT(/4X,'WORK-HARDENING COEFFICIENT:H=(kgf/mm2)=')
READ*,HH
IF(JV.EQ.4) GO TO 524
529 WRITE(*,130)
130 FORMAT(/4X,'POISSON'S RATIO:PR=')
READ*,ANYU
IF(JV.EQ.5) GO TO 524
530 WRITE(*,131)
131 FORMAT(/4X,'RATIO OF LATERAL STRAIN TO LONGITUDINAL STRAIN',
%/4X,'IN THE FORMING WITHOUT REDUCTION :BL',
%/6X,'BL=E(y)/E(x)=0.0 - 1.0 BL=')
READ*,BL
494 WRITE(*,496)
496 FORMAT(/4X,'RATIO OF LONGITUDINAL STRAIN TO LATERAL STRAIN:RSF',
%/6X,'RSF=E(x)/E(y)=0.0 -1.0 RSF=')
READ*,RSF
599 WRITE(*,598)
598 FORMAT(/4X,'FORMING VELOCITY(m/min.):VV=')
READ*,VV
C
C***** CHECK AND AMEND THE DATA. *****
C
524 WRITE(*,523)
523 FORMAT(/4X,'*****',
%/4X,'** DO YOU WANT TO CHANGE THE DATA **',
%/4X,'** THAT YOU INPUTTED JUST BEFORE? **',
%/4X,'** **',
%/4X,'** 0. NO CHANGE ---> 0 **',
%/4X,'** 1. NUMBER OF DIVISION **',
%/4X,'** IN LATERAL DIRECTION ---> 1 **',
)

```

```

%/4X,      *** 2. YOUNG'S MODULUS          ---> 2  **',
%/4X,      *** 3. YIELD STRESS           ---> 3  **',
%/4X,      *** 4. WORK-HARDENING COEFFICIENT---> 4  **',
%/4X,      *** 5. POISSON'S RATIO        ---> 5  **',
%/4X,      *** 6. RATIO OF E(y)/E(x)     ---> 6  **',
%/4X,      *** 7. RATIO OF E(x)/E(y)     ---> 7  **',
%/4X,      ***   FOR FIN-PASS REDUCTION  ---> 8  **',
%/4X,      *** 8. FORMING VELOCITY       ---> 8  **',
%/4X,      ***
%/4X,      '*****'//)

```

```
PRINT*, '----- INPUT ONE NUMBER FROM 0 TO 7. -----'
```

```
READ*,JV
```

```
IF(JV.EQ.0) GO TO 525
```

```
IF(JV.EQ.1) GO TO 522
```

```
IF(JV.EQ.2) GO TO 526
```

```
IF(JV.EQ.3) GO TO 527
```

```
IF(JV.EQ.4) GO TO 528
```

```
IF(JV.EQ.5) GO TO 529
```

```
IF(JV.EQ.6) GO TO 530
```

```
IF(JV.EQ.7) GO TO 494
```

```
IF(JV.EQ.8) GO TO 599
```

```
WRITE(*,531)
```

```
531 FORMAT(/4X, '*** INPUT ERROR. INPUT THE PERMISSIBLE No. ',
%'AGAIN. ***'//)
```

```
GO TO 524
```

```
525 IF(JD.EQ.4) GO TO 534
```

C

```
C***** INPUT THE NEW TITLE BLOCK CONTENTS. *****
```

C

```
298 WRITE(*,299)
```

```
299 FORMAT(/10X, '*****',
```

```
%/10X,      **',
```

```
%/10X,      ** INPUT THE DATA FOR TITLE BLOCK CONTENTS **',
```

```
%/10X,      ** AND DIMENSIONS OF FLOWER. **',
```

```
%/10X,      **',
```

```
%/10X,      '*****'//)
```

C

```
PRINT*, '*** YOU CAN USE A FULL STOP(.). ***'
```

```
PRINT*, '*****'
```

C

```
300 WRITE(*,*) '*** INPUT THE DESCRIPTION OF "SIZE" WITHIN 14 CHARACTER
%S. **'
```

```
WRITE(*,*) '--- e.g. 38.1X1.75mm or 999.99X99.99mm -----'
```

```
WRITE(*,*) ' SIZE='
```

```
READ(*,301) SIZE
```

```
301 FORMAT(A)
```

```
IF(TJ.EQ.1)GO TO 310
```

```
302 WRITE(*,*) '*** INPUT THE DESCRIPTION OF "DATE" WITHIN 10 CHARACTER
%S. **'
```

```
WRITE(*,*) '--- e.g. 21.10.1992 -----'
```

```
WRITE(*,*) ' DATE='
```

```
READ(*,303) DATE
```

```
303 FORMAT(A)
```

```
IF(TJ.EQ.2)GO TO 310
```

```
304 WRITE(*,*) '*** INPUT THE DESCRIPTION OF "DRAWER" WITHIN 12 CHARACTE
%RS. **'
```

```
WRITE(*,*) '--- e.g. T.TOYOOKA -----'
```

```
WRITE(*,*) ' DRAWER='
```

```
READ(*,305) DRAWER
```

```
305 FORMAT(A)
```

```
IF(TJ.EQ.3)GO TO 310
```

```
306 WRITE(*,*) '*** INPUT THE DESCRIPTION OF "WORKS(MILL)" WITHIN 12 CHA
%RACTERS. **'
```

```
WRITE(*,*) '--- e.g. 2" MILL -----'
```

```
WRITE(*,*) ' WORKS='
```

```
READ(*,307) WORKS
```

```

307 FORMAT(A)
   IF(TJ.EQ.4)GO TO 310
308 WRITE(*,*)'*** INPUT THE DESCRIPTION OF "MATERIAL" WITHIN 12 CHARAC
   %TERS. **'
   WRITE(*,*)'--- e.g. STAINLESS -----'
   WRITE(*,*)' MATERIAL='
   READ(*,309) MATERIAL
309 FORMAT(A)
C
C***** CHECK AND AMEND THE DESCRIPTION INPUTED JUST BEFORE. *****
C
310 WRITE(*,312)
312 FORMAT(//4X,'*****',
   %/4X,'** DO YOU WANT TO CHANGE THE DESCRIPTION **',
   %/4X,'** THAT YOU INPUTTED BEFORE? **',
   %/4X,'** **',
   %/4X,'** 0. NO CHANGE ---> 0 **',
   %/4X,'** 1. SIZE ---> 1 **',
   %/4X,'** 2. DATE ---> 2 **',
   %/4X,'** 3. DRAWER ---> 3 **',
   %/4X,'** 4. WORKS(MILL) ---> 4 **',
   %/4X,'** 5. MATERIAL ---> 5 **',
   %/4X,'** **',
   %/4X,'*****'//)
   PRINT*, '**--- INPUT THE PERMISSIBLE NUMBER FROM 0 TO 5. ---**'
   READ*, TJ
   IF(TJ.EQ.0) GO TO 320
   IF(TJ.EQ.1) GO TO 300
   IF(TJ.EQ.2) GO TO 302
   IF(TJ.EQ.3) GO TO 304
   IF(TJ.EQ.4) GO TO 306
   IF(TJ.EQ.5) GO TO 308
   WRITE(*,314)
314 FORMAT(//4X,' ***** INPUT ERROR. *****',
   %/4X,' INPUT THE PERMISSIBLE NUMBER AGAIN.'//)
   GO TO 310
C
320 WRITE(*,556)SIZE,DATE,DRAWER,WORKS,MATERIAL
C
   IF(JD.EQ.5) GO TO 534
C
   WRITE(*,132)
132 FORMAT(//4X,'** YOU HAVE FINISHED TO INPUT THE ALL NEW DATA. **',
   %/4X,'* IT WILL BE COMMENCED TO WRITE THE INPUTTED NEW DATA'//)
   PRINT*, ' TO THE FILE NAMED D'//FILE1'//**'
C*****
   DO 82 I=1, KK
   TLN(I,0)=0.0
   DO 84 J=1, NR(I)
   RN(I,J)=R(I,J)-TS/2.0
   DLN(I,J)=RN(I,J)*AN(I,J)*PE
   TLN(I,J)=TLN(I,J-1)+DLN(I,J)
84 CONTINUE
82 CONTINUE
C*****
   WRITE(1,1) D,WS,TS, KK, N1F
1 FORMAT(5X,3(F10.2,5X),I5,10X,I5//)
C
   WRITE(1,2) (I,LS(I),TLS(I),I=1, KK)
2 FORMAT(1H ,5X,I5,5X,F10.2,5X,F10.2)
C
   WRITE(1,3) (I,DH(I),I=0, KK)
3 FORMAT(1H ,15X,I5,5X,F10.2)
C
   WRITE(1,4) (I,NR(I),I=1, KK)
4 FORMAT(1H ,5X,I5,5X,I3)

```

```

C
  WRITE(1,5) ((JK(I,J),JC(I,J),R(I,J),AN(I,J),DLO1(I,J),
%DLN1(I,J),TLN(I,J),J=1,NR(I)),I=1,KK)
5 FORMAT(1H ,5X,I3,4X,I2,3X,F10.3,5X,F15.10,5X,F10.4,5X,F10.4,5X,
%F10.4)
C
  WRITE(1,6) NN,EE,SEQ0,HH,ANYU,BL,RSF,VV
6 FORMAT(1H0,3X,I5,3X,2(F10.2,5X),F10.2,3(3X,F5.2),3X,F6.2)
  WRITE(1,7) IDH,IIDH
7 FORMAT(1H0,3X,I2,3X,I2)
  WRITE(1,8)SIZE,DATE,DRAWER,WORKS,MATERIAL
8 FORMAT(//4X,A16//4X,A10//4X,A12//4X,A12//4X,A12//)
GO TO 543
C
C***** CALL THE DATA FROM THE EXISTING FILE. *****
C
12 REWIND 1
  READ(1,1)D,WS,TS,KK,N1F
  READ(1,2)(I,LS(I),TLS(I),I=1,KK)
  READ(1,3)(I,DH(I),I=0,KK)
  READ(1,4)(I,NR(I),I=1,KK)
  READ(1,5)((JK(I,J),JC(I,J),R(I,J),AN(I,J),DLO1(I,J),
%DLN1(I,J),TLN(I,J),J=1,NR(I)),I=1,KK)
  READ(1,6)NN,EE,SEQ0,HH,ANYU,BL,RSF,VV
  READ(1,7) IDH,IIDH
  READ(1,8)SIZE,DATE,DRAWER,WORKS,MATERIAL
  WRITE(*,133)
133 FORMAT(//4X,'** ALL DATA HAVE BEEN CALLED FROM THE EXISTING',
%' FILE. **'//)
C
C***** CHANGE THE DATA CALLED FROM THE EXISTING FILE. *****
C
      JD=0
534 WRITE(*,532)
532 FORMAT(//4X,'*****',
%/4X,'** DO YOU WANT TO CHANGE THE DATA **',
%/4X,'** THAT YOU CALLED FROM THE EXISTING FILE **',
%/4X,'**',
%/4X,'** 0. NO CHANGE ---> 0 **',
%/4X,'** 1. D,WS,TS,KK,N1F ---> 1 **',
%/4X,'** 2. LS or DH ---> 2 **',
%/4X,'** 3. NR,R,AN ---> 3 **',
%/4X,'** 4. NN,EE,SEQ0,HH,ANYU,BL,RSF,VV --> 4 **',
%/4X,'** 5. DESCRIPTION OF ---> 5 **',
%/4X,'** TITLE BLOCK CONTENTS **',
%/4X,'**',
%/4X,'*****',//)
PRINT*,'----- INPUT ONE NUMBER FROM 0 TO 4. -----'
READ*,JD
IF(JD.EQ.0) GO TO 535
IF(JD.EQ.1) GO TO 506
IF(JD.EQ.2) GO TO 513
IF(JD.EQ.3) GO TO 538
IF(JD.EQ.4) GO TO 524
IF(JD.EQ.5) GO TO 310
C
142 WRITE(*,533)
533 FORMAT(//4X,'*** INPUT ERROR. INPUT THE PERMISSIBLE No.',
%' AGAIN. **'//)
GO TO 534
C
C***** MAKE A NEW FILE. *****
C
535      JF=0
542 WRITE(*,536)
536 FORMAT(//4X,'*****',

```



```

%/4X,      '**   IF YOU CHANGED THE DATA,      **',
%/4X,      '**   DO YOU WANT TO MAKE A NEW FILE?  **',
%/4X,      '**                                     **',
%/4X,      '**   0. NO (NOT TO MAKE)      ----> 0  **',
%/4X,      '**   1. YES (MAKE A NEW FILE)  ----> 1  **',
%/4X,      '**                                     **',
%/4X,      '*****'//)
PRINT*, '----- INPUT THE ONE No. BETWEEN 0 AND 1. -----'
READ*, JF
IF(JF.EQ.0) GO TO 539
IF(JF.EQ.1) GO TO 540
WRITE(*,541)
541 FORMAT(/4X, '** INPUT ERROR. INPUT THE PERMISSIBLE NUMBER',
%, AGAIN. **'//)
GO TO 542

C
C***** MAKE A NEW DATA FILE *****
C
540 WRITE(*,*) '** INPUT THE NEW FILE NAME. **'
WRITE(*,*) 'FILE NAME='
READ(*,201) FILE2
201 FORMAT(A)
C***** FILE OPEN *****
OPEN(4,FILE='D'//FILE2,STATUS='UNKNOWN')
C *OPEN(5,FILE='P'//FILE2,STATUS='UNKNOWN')
OPEN(6,FILE='R'//FILE2,STATUS='UNKNOWN')
C
C***** WRITING THE NEW DATA TO THE NEW FILE *****
C
WRITE(*,544)
544 FORMAT(/4X, '-----'//)
PRINT*, 'WRITING THE NEW DATA TO THE NEW FILE NAMED D'//FILE2
PRINT*, ' '
PRINT*, ' '
PRINT*, ' '
WRITE(4,1) D,WS,TS,KK,N1F
WRITE(4,2) (I,LS(I),TLS(I),I=1,KK)
WRITE(4,3) (I,DH(I),I=0,KK)
WRITE(4,4) (I,NR(I),I=1,KK)
WRITE(4,5) ((JK(I,J),JC(I,J),R(I,J),AN(I,J),DL01(I,J),
%DLN1(I,J),TLN(I,J),J=1,NR(I)),I=1,KK)
WRITE(4,6) NN,EE,SEQ0,HH,ANYU,BL,RSF,VV
WRITE(4,7) IDH,IIDH
WRITE(4,8)SIZE,DATE,DRAWER,WORKS,MATERIAL

C
C***** WRITING THE INPUT DATA TO THE RESULT FILE *****
C
WRITE(*,545)
545 FORMAT(/4X, '---- WRITING THE NEW INPUT DATA TO THE RESULT FILE ',
%'----')
PRINT*, ' NAMED R'//FILE2
WRITE(6,546)FILE2
546 FORMAT(1H1,/4X, '*****',
%/4X '** INITIAL INPUT DATA IN FILE R',A12,'**',
%/4X, '*****',/)
C
WRITE(6,547)
547 FORMAT(1H0,5X,'OUTER DIA.',5X,' WIDTH ',5X,' THICKNESS',
%5X,'NUMBER OF st.',5X,'Stand No. of 1st Finpass',/)
WRITE(6,1) D,WS,TS,KK,N1F
WRITE(6,548)
548 FORMAT(1H0,5X,'STAND',5X,' LS(I) ',5X,' TLS(I) '/')
WRITE(6,2)(I,LS(I),TLS(I),I=1,KK)
WRITE(6,549)
549 FORMAT(1H0,15X,'STAND',7X,'DOWNHILL AMOUNT'//)
WRITE(6,3)(I,DH(I),I=0,KK)

```

```

WRITE(6,550)
550 FORMAT(1H0,5X,'STAND',3X,'NUMBER OF RADIUS'/)
WRITE(6,4)(I,NR(I),I=1, KK)
WRITE(6,551)
551 FORMAT(1H0,3X,'STAND',4X,'No.R',3X,' RADIUS ',11X,' ANGLE . ',
%10X;'DLO',12X,'DLN',7X,'TLN(I,J)')/,
WRITE(6,5)(J,K(I,J),J,C(I,J),R(I,J), AN(I,J),DLO1(I,J),
%DLN1(I,J),TLN(I,J),J=1,NR(I)),I=1, KK)
WRITE(6,552) NN,EE,SEQ0,HH,ANYU,BL,RSF,VV
552 FORMAT(1H0,5X,'NUMBER OF DIVISION IN WIDTH=',I5/1H0,5X,'YOUNG''S',
%' MODULUS=',F10.2/1H0,5X,'YIELD STRESS=',F10.2/1H0,5X,'WORK-',
%'HARDENING COEFFICIENT=',F10.2/1H0,5X,'POISSON''S RATIO=',
%F5.2/1H0,5X,'RATIO OF E(y)/E(x)='F5.2,/1H0,5X,
%'RATIO OF E(x)/E(y)='F5.2,/1H0,5X,'FORMING VELOCITY='F6.2///)
WRITE(6,554) IDH,IIDH
554 FORMAT(1H0,5X,'IDH='I2,3X,'IIDH='I2//)
WRITE(6,556)SIZE,DATE,DRAWER,WORKS,MATERIAL
556 FORMAT(//4X,'SIZE='A16/4X,'DATE='A10/4X,'DRAWER='A12/4X,
%'WORKS='A12/4X,'MATERIAL='A12//)
GO TO 539
C
C***** IN CASE OF FIRST INPUT DATA *****
C
543 WRITE(3,553)FILE1
553 FORMAT(1H1,/,4X,'*****',
%/4X,'** INITIAL INPUT DATA IN FILE R',A12,'**',
%/4X,'@*****',/)
C
WRITE(3,547)
WRITE(3,1) D,WS,TS, KK,N1F
WRITE(3,548)
WRITE(3,2)(I,LS(I),TLS(I),I=1, KK)
WRITE(3,549)
WRITE(3,3)(I,DH(I),I=0, KK)
WRITE(3,550)
WRITE(3,4)(I,NR(I),I=1, KK)
WRITE(3,551)
WRITE(3,5)((J,K(I,J),J,C(I,J),R(I,J), AN(I,J),DLO1(I,J),
%DLN1(I,J),TLN(I,J),J=1,NR(I)),I=1, KK)
WRITE(3,552)NN,EE,SEQ0,HH,ANYU,BL,RSF,VV
WRITE(3,554) IDH,IIDH
WRITE(3,556) SIZE,DATE,DRAWER,WORKS,MATERIAL
C
539 WRITE(*,*)'** DATA INPUT HAS COMPLETED. NEXT IS DRAWING OF ',
%'FLOWER. **'
C
C***** 2-DIMENSIONAL DRAWING OF FORMING FLOWER *****
C
C***** SUBROUTINE FLOWER IS CALLED. *****
C
CALL FLOWER(FILE1,FILE2,SIZE,DATE,DRAWER,WORKS,MATERIAL)
C
C
C*****
C***** STRESS-STRAIN ANALYSIS AND 3D DRAWING *****
C*****
C
WRITE(*,856)
856 FORMAT(1H1,///,4X,
%'*****',
%/4X,'**',
%/4X,'** STRESS-STRAIN ANALYSIS AND 3-D DRAWING **',

```

```

%/4X, '**
%/4X, '**
%/4X, '*****', //)

```

July 1992

```

**
**
**

```

C
C

```

824 WRITE(*,822)
822 FORMAT(/,4X,
% '*****',
%/4X, '**
%/4X, '** What results do you want to get?
%/4X, '** 1.Stress-Strain Analysis Model-1 and Model-2 --> 1
%/4X, '** 2.Stress-Strain Analysis Model-1 --> 2
%/4X, '** 3.Stress-Strain Analysis Model-2 --> 3
%/4X, '** 4.Unnecessary --> 4
%/4X, '**
%/4X, '*****', //)

```

C

```

WRITE(*,*)'**** INPUT ONE NUMBER BETWEEN 1 AND 4. *****'
READ*,IR
IF(IR.NE.1.AND.IR.NE.2.AND.IR.NE.3.AND.IR.NE.4) THEN
WRITE(*,*)'@@@ INPUT ERROR - INPUT CORRECT NUMBER,AGAIN. @@@@'
GO TO 824
ELSE
WRITE(*,826)IR
826 FORMAT(/,4X,'IR=',I3,/)
ENDIF

```

C

```

IF(IR.EQ.1) GO TO 850
IF(IR.EQ.2) GO TO 850
IF(IR.EQ.3) GO TO 852
IF(IR.EQ.4) GO TO 860
GO TO 824

```

C

C

C***** Stress-Strain Analysis Model-1 *****

C

```

850 MA=M1
WRITE(*,600)MA
600 FORMAT(/,4X,
% '*****',
%/4X, '**
%/4X, '** STRESS-STRAIN ANALYSIS AND 3-D DRAWING ',A8, '
%/4X, '**
%/4X, '*****', //)

```

C

```

JW=0
DO 270 JJ=1,1000
JW=JW+1
270 CONTINUE

```

C

C***** CALL SUBROUTINE CAPOIN TO CALCULATE THE POINTS OF X, Y AND Z- AXIS OF THE DIVIDED MESHES *****

C

```
CALL CALPOIN(FILE1,FILE2,MA)
```

C

C***** CALL SUBROUTINE SNANA1 TO ANALYZE THE STRAIN WITHOUT CONSIDERING THE DEFORMATION OF MESHES IN THE LATERAL DIRECTION. *****

C

```
CALL SNANA1
```

C

C***** CALL SUBROUTINE SSANA TO ANALYZE THE STRESS IN DEFORMATION PROCESS. *****

C

```
CALL SSANA
```

C

C***** WRITING THE RESULTS OF STRESS, STRAIN, DEFORMATION WORK AND DEFORMATION WORK-RATE(POWER) *****

```

C
MM=1
700 OPEN(3,FILE='R'//FILE1,STATUS='UNKNOWN',ACCESS='APPEND')
    OPEN(6,FILE='R'//FILE2,STATUS='UNKNOWN',ACCESS='APPEND')
C
    IF(ITD.EQ.1) THEN
        NF=3
        AA=FILE1
    ELSE IF (ITD.EQ.2.AND.JF.EQ.1) THEN
        NF=6
        AA=FILE2
    ELSE
        GO TO 710
    ENDIF
    WRITE(NF,602)MA,AA
602 FORMAT(1H1,///,4X,
% '*****',
%/4X,'** OUTPUT DATA(RESULT) OF STRESS-STRAIN ANALISIS **',
%/4X,'** ',A8 ' IN THE FILE R',A12, '**',
%/4X,'*****',/)
C
C***** RESULTS OF STRAIN *****
C
    WRITE(NF,603)
603 FORMAT(/4X,'***** RESULTS OF STRAIN *****'/)
    WRITE(NF,604)D,TS,KK,N1F,NN,BL,RSF
604 FORMAT(4X,'OD=',F10.2,2X,'TS=',F10.2,5X,'NUMBER OF STAND=',I2,3X,
%'Stand No. of 1st Finpass=',I2,3X,
%/4X,'NUMBER OF DIVISION=',I2,3X,'Ex/Ez=',F5.2,3X,'Ez/Ex ',
%'in Finpass & SQ=',F5.2//4X,
%'*****',
%'*****'//)
C
    WRITE(NF,606)
606 FORMAT(2X,'ST.',2X,'Mesh',6X,'DEz(%)',7X,'Ez(%)',8X,'DEx(%)',7X,
%'Ex(%)',8X,'DEZE(%)',6X,'DEXE(%)',6X,'EzE(%)',7X,'ExE(%)',5X,
%'DEPSOT(%)'//)
C
    DO 610 I=0,KK
C
    DO 620 J=0,NN
C
        PDEZ(I,J)=DEZ(I,J)*100
        PEZ(I,J)=EZ(I,J)*100
        PDEX(I,J)=DEX(I,J)*100
        PEX(I,J)=EX(I,J)*100
        PEZE(I,J)=EZE(I,J)*100
        PEZE(I,J)=EZE(I,J)*100
        PDEXE(I,J)=DEXE(I,J)*100
        PDEXE(I,J)=DEXE(I,J)*100
        PDEPSO(I,J)=DEPSOT(I,J)*100
C
        WRITE(NF,608)I,J,PDEZ(I,J),PEZ(I,J),PDEX(I,J),PEX(I,J),PDEZE(I,J),
% PDEXE(I,J),PEZE(I,J),PEXE(I,J),PDEPSO(I,J)
608 FORMAT(1H ,2X,I3,2X,I3,3X,9(F11.6,2X))
620 CONTINUE
        WRITE(NF,621)
621 FORMAT(/4X,'-----'//)
610 CONTINUE
C
C***** RESULTS OF STRESS *****
C
    WRITE(NF,605)
605 FORMAT(1H1,///4X,'***** RESULTS OF STRESS *****'/)
    WRITE(NF,622)
622 FORMAT(/3X,'ST.',X,'Mesh',X,'NHAN',X,'DSz(kg/mm2)',7X,'DSx',8X,

```

```

%'Sz',9X,'Sx',9X,'SEQ',5X,'DSz(MPa)',7X,'DSx',9X,'Sz',9X,'Sx',9X,
%'SEQ'/)
C
DO 630 I=0, KK
C
DO 640 J=0, NN
C
PA=9.80665
PDSZ(I,J)=DSZ(I,J)*PA
PDSX(I,J)=DSX(I,J)*PA
PSZ(I,J)=SZ(I,J)*PA
PSX(I,J)=SX(I,J)*PA
PSEQ(I,J)=SEQ(I,J)*PA
C
WRITE(NF,624)I,J,NHANT(I,J),DSZ(I,J),DSX(I,J),SZ(I,J),SX(I,J),
%'SEQ(I,J),PDSZ(I,J),PDSX(I,J),PSZ(I,J),PSX(I,J),PSEQ(I,J)
624 FORMAT(1H ,3(2X,I3),2X,5(F10.4,X),5(F10.4,2X))
C
640 CONTINUE
C
WRITE(NF,626)
626 FORMAT(/4X,'-----'/)
630 CONTINUE
C
WRITE(NF,632)
632 FORMAT(1H1, //3X, 'ST. ',X, 'Mesh',X, 'NHAN',X, 'SOT/kg/mm2',2X,
%'DWe/kg*m/cm3',7X, 'DWp',9X, 'DW',7X, 'DWT/kg*m',4X, 'STO/MPa',4X,
%'DWe/J/cm3',5X, 'DWp',7X, 'DW',8X, 'DWT/J'/)
C
DO 650 I=0, KK
C
DO 660 J=0, NN
C
PSOTOS(I,J)=SOTOS(I,J)*PA
PDWE(I,J)=DWE(I,J)*PA
PDWP(I,J)=DWP(I,J)*PA
PDW(I,J)=DW(I,J)*PA
PDWT(I,J)=DWT(I,J)*PA
C
WRITE(NF,634)I,J,NHANT(I,J),SOTOS(I,J),DWE(I,J),DWP(I,J),DW(I,J),
%'DWT(I,J),PSOTOS(I,J),PDWE(I,J),PDWP(I,J),PDW(I,J),PDWT(I,J)
634 FORMAT(1H ,3(2X,I3),2X,5(F10.3,2X),5(F10.3,X))
660 CONTINUE
WRITE(NF,626)
650 CONTINUE
WRITE(NF,662)
662 FORMAT(1H1, //,13X, 'Deformation Work Increment',10X,
%'Total Deformation Work',8X, 'Deformation Work-Rate(Power)')
WRITE(NF,664)
664 FORMAT(1H ,2X, 'ST.No.',7X, 'WT/kg*m',10X, 'WT/J',13X,
%'WT/ kg*m',9X, 'WT/J',10X, 'WTR/kg*m/s',5X, 'WTR/J/s',/)
C
DO 670 I=0, KK
C
PWT(I)=WT(I)*PA
PWTR(I)=WTR(I)*PA
PSWT(I)=SWT(I)*PA
PSWTR= SWTR*PA
C
WRITE(NF,666)I,WT(I),PWT(I),SWT(I),PSWT(I),WTR(I),PWTR(I)
666 FORMAT(1H ,3X,I3,6X,F10.3,4X,F10.3,10X,F10.3,4X,F10.3,
%'9X,F10.3,2X,F10.3)
670 CONTINUE
WRITE(NF,626)
WRITE(NF,665)SWT(KK),PSWT(KK)
665 FORMAT(1H ,5X, 'Total Deformation Work of all stands =',F10.3,

```

```

        %'(kg*m) or ',F10.3,'(MPa)',/)
        WRITE(NF,667)SWTR,PSWTR
667 FORMAT(1H ,5X,'Total Deformation Work-Rate of all stands=',F10.3,
        %'(kg*m/s) or ',F10.3,'(J/s)',/)
C
        HDEZ=100*HDEZ
        HEZ=100*HEZ
        SDEX=100*SDEX
        HEX=100*HEX
        SEX=100*SEX
C
        WRITE(NF,668)HEZ,HEX,HDEZ,SEX,SDEX
668 FORMAT(1H1,////,4X,'Max.Ez(%)=' ,F11.6,6X,'Max.Ex(%)=' ,F11.6,
        %//4X,'Max.DEz(%)=' ,F11.6,5X,'Min.Ex(%)=' ,F11.6,5X,
        %'Min.DEx(%)=' ,F11.6,/)
C
C***** CHANGE THE UNIT TO (MPa) and (J) *****
C
        PHDSZ=HDSZ*PA
        PSDSZ=SDSZ*PA
        PHSZ=HSZ*PA
        PSSZ=SSZ*PA
        PHSX=HSX*PA
        PSSX=SSX*PA
        PHSOTO=HSOTOS*PA
        PSSOTO=SSOTOS*PA
        PHDW=HDW*PA
        PHWT=HWT*PA
        PHWTR=HWTR*PA
        WRITE(NF,672)HDSZ,PHDSZ,SDSZ,PSDSZ,HSZ,PHSZ,HSX,PHSX,SSZ,PSSZ,
        %
        % SSX,PSSX,HDW,HWT,HWTR,PHDW,PHWT,PHWTR
672 FORMAT(///,4X,'Max.DSz=' ,F10.4,'(kgf/mm2)',X,'or',X,F10.4,
        %'(MPa)',
        %//,4X,'Min.DSz=' ,F10.4,'(kgf/mm2)',X,'or',X,F10.4,'(MPa)',
        %//,4X,'Max.Sz=' ,F10.4,'(kgf/mm2)',X,'or',X,F10.4,
        %'(MPa)',10X,'Max.Sx=' ,F10.4,'(kgf/mm2)',X,'or',X,F10.4,'(MPa)',
        %//,4X,'Min.Sz=' ,F10.4,'(kgf/mm2)',X,'or',X,F10.4,'(MPa)',10X,
        %'Min.Sx=' ,F10.4,'(kgf/mm2)',X,'or',X,F10.4,'(MPa)',
        %//,4X,'Max.DW=' ,F10.3,'(kgf*m/cm3)',10X,'Max.WT=' ,F10.3,
        %'(kgf*m)',10X,'Max.WTR=' ,F10.3,'(kgf*m/s)',
        %//,4X,'Max.DW=' ,F10.3,'(J/cm3)',14X,'Max.WT=' ,F10.3,'(J)',14X,
        %'Max.WTR=' ,F10.3,'(J/s)'/////
        GO TO 712
710 PA=9.80665
        DO 720 I=0,KK
C
        DO 722 J=0,NN
C
        PDEZ(I,J)=DEZ(I,J)*100
        PEZ(I,J)=EZ(I,J)*100
        PDEX(I,J)=DEX(I,J)*100
        PEX(I,J)=EX(I,J)*100
        PEZE(I,J)=EZE(I,J)*100
        PEZE(I,J)=EXE(I,J)*100
        PDEZE(I,J)=DEZE(I,J)*100
        PDEXE(I,J)=DEXE(I,J)*100
        PDEPSO(I,J)=DEPSOT(I,J)*100
C
        PDSZ(I,J)=DSZ(I,J)*PA
        PDSX(I,J)=DSX(I,J)*PA
        PSZ(I,J)=SZ(I,J)*PA
        PSX(I,J)=SX(I,J)*PA
        PSEQ(I,J)=SEQ(I,J)*PA
C
722 CONTINUE
720 CONTINUE

```

```

C
  DO 750 I=0, KK
C
  DO 760 J=0, NN
C
  PSOTOS(I, J)=SOTOS(I, J)*PA
  PDWE(I, J)=DWE(I, J)*PA
  PDWP(I, J)=DWP(I, J)*PA
  PDW(I, J)=DW(I, J)*PA
  PDWT(I, J)=DWT(I, J)*PA
760 CONTINUE
750 CONTINUE
C
  DO 770 I=0, KK
C
  PWT(I)=WT(I)*PA
  PWTR(I)=WTR(I)*PA
770 CONTINUE
C
  HDEZ=100*HDEZ
  HEZ=100*HEZ
  SDEX=100*SDEX
  HEX=100*HEX
  SEX=100*SEX
C
C***** CHANGE THE UNIT TO (MPa) and (J) *****
C
  PHDSZ=HDSZ*PA
  PSDSZ=SDSZ*PA
  PHSZ=HSZ*PA
  PSSZ=SSZ*PA
  PHSX=HSX*PA
  PSSX=SSX*PA
  PHSOTO=HSOTOS*PA
  PSSOTO=SSOTOS*PA
  PHDW=HDW*PA
  PHWT=HWT*PA
  PHWTR=HWTR*PA
C
712 CLOSE(3, STATUS='KEEP')
  CLOSE(6, STATUS='KEEP')
C
C***** DRAWING 3-DIMENSIONAL VIEW(GRAPHS) OF DEFORMED SHEET, STRAIN AND STRESS *****
C
  IF(MM.EQ.2) GO TO 800
C
C***** CALL SUBROUTINE DRAW3D TO DRAW 3-D GRAPHICS OF RESULTS BY STRESS-STRAIN
ANALYSIS MODEL-2. *****
C
  CALL DRAW3D1(HDEZ, HEZ, SDEX, HEX, SEX, HDSZ, SDSZ, HSZ, SSZ, HSX, SSX,
% HSOTOS, PHDSZ, PSDSZ, PHSZ, PSSZ, PHSX, PSSX, PHSOTO, FILE1, FILE2, MM,
% SIZE, DATE, DRAWER, WORKS, MATERIAL)
C
  IF(IR.EQ.2) GO TO 860
C
  WRITE(*, 858)
858 FORMAT(///, 5X, 'Please input 0(zero) to advance to Model-2', //)
  READ*, MZ
  WRITE(*, 859) MZ
859 FORMAT(5X, 'MZ=', I3, //)
C
C
  WRITE(*, *) '**** Stress-strain Analysis Model-1 has completed. ***'
C
C
C***** Stress-strain Analysis Model-2 *****

```

```

C
C
852 MA=M2
WRITE(*,600)MA
C
C
IF(IR.EQ.3) THEN
DO 910 I=1, KK
TLN(I,0)=0.0
DO 920 J=1, NR(I)
C
RN(I,J)=R(I,J)-TS/2.0
DLN(I,J)=RN(I,J)*AN(I,J)*PE
TLN(I,J)=TLN(I,J-1)+DLN(I,J)
C
920 CONTINUE
910 CONTINUE
C
DO 930 I=0, KK
LAV=INT(TLS(KK)/2)
PZ(I)=TLS(I)-LAV
930 CONTINUE
C
ELSE
ENDIF
C
C***** CALL SUBROUTINE SNANAZ TO CALCULATE THE POINTS AND TO ANALYZE THE STRAIN WITH
CONSIDERING THE DEFORMATION OF MESHES IN THE LATERAL DIRECTION. *****
C
CALL SNANAZ
C
C***** WRITING THE POINT DATA OF DIVIDED ELEMENT INTO THE "R" FILE *****
C
IF(ITD.EQ.1) THEN
NF=3
AA=FILE1
GO TO 880
ELSE IF(ITD.EQ.2.AND.JF.EQ.1) THEN
NF=6
AA=FILE2
GO TO 880
ELSE
GO TO 882
ENDIF
C
880 OPEN(3, FILE='R'//FILE1, STATUS='UNKNOWN', ACCESS='APPEND')
OPEN(6, FILE='R'//FILE2, STATUS='UNKNOWN', ACCESS='APPEND')
C
WRITE(NF, 884)MA, AA
884 FORMAT(1H1, ///, 4X,
% '*****',
%/4X, '** OUTPUT DATA(RESULT) OF X-, Y- AND Z-AXES POINTS TO **',
%/4X, '** ANALYSE STRESS-STRAIN BY ', A8, ' **',
%/4X, '** IN THE FILE R', A12, ' **',
%/4X, '*****', /)
C
WRITE(NF, 886)
886 FORMAT(/6X, 'ST. ', 2X, 'Mesh', 5X, 'PXE(I,J)', 7X, 'PYE(I,J)', 8X,
%'PZ(I)', 9X, 'TLS(I)', 7X, 'ANE(I,J)', 8X, 'DB(I,J)', 7X, 'TLE(I,J)',
%5X, 'TLN1(I)/2', /)
C
DO 890 I=0, KK
DO 892 J=0, NN
WRITE(NF, 888)I, J, PXE(I, J), PYE(I, J), PZ(I), TLS(I), ANE(I, J),
%DB(I, J), TLE(I, J), TLN1(I)/2
888 FORMAT(1H , 4X, I3, 3X, I3, 3X, F10.3, 5X, F10.3, 5X, F10.3, 5X, F10.3,

```



```

%5X,F10.3,5X,F10.5,5X,F10.4,5X,F10.4)
892 CONTINUE
WRITE(NF,889)
889 FORMAT(/4X,'-----',
% '-----',/)
890 CONTINUE
WRITE(NF,870)
870 FORMAT(///4X,'ST.',2X,'Mesh',5X,'FRD(I)',9X,'DEZF(%)',8X,
%'DEXF(%)',7X,'DBO(I,J)',8X,'DB(I,J)',7X,'TLEO(I,J)',7X,
%'TLE(I,J)',6X,'TLN1(I)/2',/)
C
DO 872 I=N1F, KK
DO 874 J=0, NN
PDEZF(I,J)=100*DEZF(I,J)
PDEXF(I,J)=100*DEXF(I,J)
WRITE(NF,876)I,J,FRD(I),PDEZF(I,J),PDEXF(I,J),DBO(I,J),DB(I,J),
% TLEO(I,J),TLE(I,J),TLN1(I)/2
876 FORMAT(1H ,4X,I3,3X,I3,3X,6(F10.4,5X),F10.4,3X,F10.4)
C
874 CONTINUE
WRITE(NF,877)
877 FORMAT(/4X,'-----',
% '-----',/)
872 CONTINUE
C
CLOSE(3,STATUS='KEEP')
CLOSE(6,STATUS='KEEP')
C*****
*****
C
C***** CALL SUBROUTINE SSANA TO ANALIZE THE STRESS IN DEFORMATION PROCESS. *****
C
882 CALL SSANA
C
C***** WRITING THE RESULTS OF STRESS, STRAIN, DEFORMATION WORK AND DEFORMATION WORK-
RATE(POWER) *****
C
MM=2
GO TO 700
C
C***** THE SAME ROUTINE AS THE CASE OF MODEL1 IS ALSO USED IN THE MODEL2. *****
C
C***** CALL SUBROUTINE DRAW2 TO DRAW THE RESULTS BY STRESS-STRAIN ANALYSIS MODEL-2
*****
C
800 CALL DRAW3D2(HDEZ,HEZ,SDEX,HEX,SEX,HDSZ,SDSZ,HSZ,SSZ,HSX,SSX,
% HSOTOS,PHDSZ,PSDSZ,PHSZ,PSSZ,PHSX,PSSX,PHSOTO,FILE1,FILE2,MM,
% SIZE,DATE,DRAWER,WORKS,MATERIAL)
C*****
*****
C
WRITE(*,*)'*** Stress-strain Analysis Model-2 has completed. ****'
C
C
C
860 WRITE(*,*)'***** ALL JOB OF CADFORM HAVE COMPLETED. *****'
WRITE(*,810)
810 FORMAT(///10X,'*****',
%/10X,
% '*** **',
%/10X,
% '*** Do you want to analyse another data? **',
%/10X,
% '*** **',
%/10X,
% '*** 1. Yes/ Start from initial stage --> 1 **',
%/10X,
% '*** 2. No / Finish --> 2 **',
%/10X,
% '*** **',
%/10X,
% '*****'/)

```

```

C
812 WRITE(*,*)' ***** INPUT ONE NUMBER BETWEEN 1 AND 2. *****'
    READ*,IZ
C
    IF(IZ.NE.1.AND.IZ.NE.2) THEN
    WRITE(*,*)'@@@@ INPUT ERROR - INPUT CORRECT NUMBER AGAIN. @@@@'
    GO TO 812
    ELSE IF(IZ.EQ.1) THEN
    GO TO 820
    ELSE
    ENDIF
C
    STOP
    END

C*****
*****
C*****
C
C*****
C** THIS IS THE SUBROUTINE PROGRAM FOR 2-DIMENSIONAL FLOWER DRAWING IN CADFORM.
**
C*****
C%% Amendment on 18th September 1992 %%%
C***** SUBROUTINE FLOWER *****
C
    SUBROUTINE FLOWER(FILE1,FILE2,SIZE,DATE,DRAWER,WORKS,MATERIAL)
    IMPLICIT REAL*8(A-H,L,O-Z), INTEGER*4(I-K,M-N)
    CHARACTER FILE1*12,FILE2*12,SIZE*14,DATE*10,DRAWER*12,WORKS*12,
    % MATERIAL*12
C
    COMMON/DAT1/ LS(0:26),TLS(0:26),DH(0:25),NR(0:25),R(0:25,5),
    % AN(0:25,5)
    COMMON/DAT2/ D, WS, TS, KK, NN
    COMMON/DAT4/ PE, ITD, IDH, IIDH, JF
    COMMON/DAT5/ TLO(0:25),TLN1(0:25), AH(0:25), AW(0:25), WE(0:25),
    % AWY(0:25)
    COMMON/POINT1/ PXO(0:25,0:5), PYO(0:25,0:5), CX(0:25,0:5),
    % CY(0:25,0:5), PXI(0:25,0:5), PYI(0:25,0:5),
    % RR(0:25,0:5)
    COMMON/AAN/ AAN(0:25,0:5)
C
C
C
C
    WRITE(*,500)
500 FORMAT(/4X,'*****',
    %/4X, '** 2-DIMENSIONAL DRAWING OF FORMING FLOWER **',
    %/4X, '** USING GINO-F(Version3.0)GRAPHIC SOFTWARE **',
    %/4X, '*****'//)
C
C***** SUBROUTINE ZAHYOU IS CALLED TO CALUCULATE THE POINTS OF X AND Y AXIS ON FLOWER.
*****
    CALL ZAHYOU(FILE1,FILE2)
C
C***** SUBROUTINE DIMFLO IS CALLED TO CALUCULATE THE WIDTH AND HEIGHT OF FLOWERS.
*****
C
    CALL DIMFLO(FILE1,FILE2)
C
C
C
C
C * CLOSE(1,STATUS='KEEP')
C * CLOSE(2,STATUS='KEEP')
C * CLOSE(3,STATUS='KEEP')
C * CLOSE(4,STATUS='KEEP')
C * CLOSE(5,STATUS='KEEP')
C * CLOSE(6,STATUS='KEEP')

```

```

C
C*****--- CHOICE OF DRAWING FLOWER PATTERN BETWEEN PATTERN-A AND PATTERN-B -----*****
C
WRITE(*,510)
510 FORMAT(1H1,
  %//4X, '*****',
  %/4X, '**          CHOOSE THE FLOWER PATTERN.          **',
  %/4X, '**',
  %/4X, '**      1. FLOWER PATTERN-A AND -B    ---> 1    **',
  %/4X, '**      2. FLOWER PATTERN-A          ---> 2    **',
  %/4X, '**      3. FLOWER PATTERN-B            ---> 3    **',
  %/4X, '**      4. UNNECESSARY                  ---> 4    **',
  %/4X, '**',
  %/4X, '*****',//)
C
PRINT*, '----- INPUT ONE NUMBER FROM 1 TO 4. -----'
READ*,JP
WRITE(*,800)JP
800 FORMAT(//5X,'JP=',I2,/)
IF(JP.EQ.3) GO TO 310
IF(JP.EQ.4) GO TO 400
WRITE(*,*)'***** 2-DIMENSIONAL FLOWER PATTERN-A *****'
C
WRITE(*,562)
562 FORMAT(//4X, '*****',
  %/4X, '**      FROM WHAT STAND DO YOU WANT TO DRAW    **',
  %/4X, '**                                THE FLOWER    **',
  %/4X, '**      0. No.0 stand =(SHEET)          ---> 0    **',
  %/4X, '**      1. STAND No. WHICH YOU          ---> 1    **',
  %/4X, '**                                WANT TO DRAW    **',
  %/4X, '*****',//)
PRINT*, '----- INPUT ONE NUMBER IN ABOVE SHOWN NUMBER. -----'
READ*,JM
WRITE(*,810)JM
810 FORMAT(//5X,'JM=',I2,/)
C
C***** GINO-F IS CALLED TO DRAW THE FLOWER PATTERN. *****
C
310 CALL GINO
CALL T4510
CALL T4107
CALL UNITS(1.0)
IF(JP.EQ.3) GO TO 311
C
C***** IC IS THE INDICATER TO SKIP THE MENUE SCREEN OF DRAWING OF DIMENSION;HEIGHT,WIDTH AND
EDGE-WIDHT. *****
C
IC=0
C
C----- TO INITALIZE AND SWITCH TRANSFORMATION ON -----
C
100 CALL TRANSF(2)
CALL PICCLE
C***** SUBROUTINE FRAME1 IS CALLED TO DRAW THE FRAME OF GRAPH. *****
C
CALL FRAME1
C
C***** SUBROUTINE DRAW1 IS CALLED TO DRAW THE FLOWER PATTEN-A. *****
C
CALL DRAW1(JM,RA,XX,YY)
C
C***** WRITING THE SCALE VALUE:RA INTO THE RESULT FILE "R-FILE1" OR "R-FILE2" *****
C
IF(IC.EQ.0) THEN
OPEN(3,FILE='R'//FILE1,STATUS='UNKNOWN',ACCESS='APPEND')

```

```

OPEN(6,FILE='R'//FILE2,STATUS='UNKNOWN',ACCESS='APPEND')
GO TO 231
ELSE
GO TO 235
ENDIF
C
C
231 IF(ITD.EQ.1) THEN
NF=3
ELSE IF(ITD.EQ.2.AND.JF.EQ.1) THEN
NF=6
GO TO 230
ELSE
GO TO 232
ENDIF
WRITE(NF,234)FILE1
234 FORMAT(1H1,/,4X,
% '*****',
%/4X,'** OUT PUT OF SCALE VALUE IN FILE R',A12,' **',
%/4X,'*****'/)
GO TO 236
C
230 WRITE(NF,238)FILE2
238 FORMAT(1H1,/,4X,
% '*****',
%/4X,'** OUT PUT OF SCALE VALUE IN FILE R',A12,' **',
%/4X,'*****'/)
C
236 WRITE(NF,240) RA
240 FORMAT(4X,'*****',
%'*****',
%/6X,'THE VALUE OF DRAWING SCALE :RA=',F10.5,
%/4X,'*****',
%'*****'/)
C
C
232 CLOSE(3,STATUS='KEEP')
CLOSE(6,STATUS='KEEP')
C
C***** SUBROUTINE JISSUN IS CALLED TO DRAW THE ACTUAL LENGTH OF 10mm. *****
C
235 CALL JISSUN(RA,XX,YY)
C
C***** SUBROUTINE SUNPOU IS CALLED TO DRAW THE DIMENSION LINE. *****
C
CALL SUNPOU(JM,RA,XX,YY,IC,ND)
C
C***** SUBRIUTINE TITLE1 IS CALLED TO WRITE THE STATEMENT AND DIMENSION OF FLOWER. *****
C
CALL TITLE1(JM,RA,XX,YY,FILE1,FILE2,SIZE,DATE,DRAWER,WORKS,
% MATERIAL,ITD,JF)
C
C***** INPUT A DUMMY VALUE AFTER YOU GET A HARD-COPY OF THE FLOWER. *****
C***** INPUT ANY NUMBER i.e. FROM 1 TO 9. *****
C
READ*,JZ
C
CALL PICCLE
CALL CHAMOD
C
IF(JM.EQ.KK) GO TO 300
WRITE(*,200)
200 FORMAT(/10X,'*****',
%/10X,'** CHOOSE THE NEXT JOB TO DRAW THE FLOWER. **',
%/10X,'** 0. DRAW THE NEXT STAND ---> 0 **',
%/10X,'** 1. INPUT THE STAND No. **',

```

```

%10X,      '**          THAT YOU WANT TO DRAW.  ---> 1~25  **',
%10X,      '**    2. FINISH                      ---> 100  **',
%10X,      '*****'//)
C
220 WRITE(*,*)'***** INPUT THE NUMBER IN ABOVE SHOWN NUMBER. *****'
    READ *, JN
    WRITE(*,221)JN
221 FORMAT(/5X,'JN=',I3,/)
C
    IF(JN.EQ.100) GO TO 300
    IF(JN.EQ.0) GO TO 120
    GO TO 122
120   JM=JM+1
    IF(JM.GT.KK) GO TO 300
    GO TO 100
122  IF(JN.GE.1.AND.JN.LE.25) THEN
    JM=JN
    GO TO 100
    ELSE
    WRITE(*,*)'*** INPUT ERROR. INPUT THE PERMISSIBLE No.,AGAIN.',
    %' *****'
    GO TO 220
    ENDIF
C
300 WRITE(*,*)'***** 2-DIMENSIONAL FLOWER PATTERN-A FINISH. *****'
C
    IF(JP.EQ.2) GO TO 400
C
C*****-----< FLOWER PATTERN-B >-----*****
C
311 WRITE(*,*)'*****-----< 2-DIMENSIONAL FLOWER PATTERN-B >-----*****'
    WRITE(*,202)
202 FORMAT(/4X,'*****',
%4X,      '**    CHOOSE ONE NUMBER WHICH REPRESENT    **',
%4X,      '**          THE FLOWER PATTERN-B REQUIRED.      **',
%4X,      '**',
%4X,      '**    1. TO DRAW ALL STANDS          ---> 1    **',
%4X,      '**    2. SOME SEQUENCE OF STANDS        ---> 2    **',
%4X,      '**',
%4X,      '*****'//)
C
208 WRITE(*,*)'***** INPUT THE NUMBER FROM 1 OR 2 *****'
    READ *, JB
    WRITE(*,820)JB
820 FORMAT(/5X,'JB=',I2,/)
C
    IF(JB.EQ.1) GO TO 207
    IF(JB.EQ.2) THEN
    WRITE(*,204)
204 FORMAT(/10X,'*****',
%/10X,'INPUT THE STARTING STAND No. AND FINISHING STAND No.',
%'TO DRAW.'//)
    PRINT*,'          *** STARTING STAND No.='
    READ*,KS
    WRITE(*,206)
206 FORMAT(/10X,'*** FINISHING STAND No.=')
    READ*,KF
    ELSE
    ENDIF
C
207 CALL PICCLE
C
C***** SUBROUTINE FRAME1 IS CALLED TO DRAW THE FRAME OF GRAPH. *****
C
CALL TRANSF(2)

```

```

CALL FRAME1
C
  IF(JB.EQ.1) THEN
    JM=0
  ELSE IF(JB.EQ.2) THEN
    JM=KS
  ELSE
    WRITE(*,*)'*** INPUT ERROR. INPUT THE PERMISSIBLE No.,AGAIN. ***'
    GO TO 208
  ENDIF
C
C***** SUBROUTINE DRAW1 IS CALLED TO DRAW THE FLOWER PATTERN-B. *****
C
  CALL DRAW1(JM,RA,XX,YY)
C
C***** SUBROUTINE JISSUN IS CALLED TO DRAW THE ACTUAL LENGTH OF 10mm. *****
C
  CALL JISSUN(RA,XX,YY)
C
  WRITE(*,110)RA
  110 FORMAT(1H,5X,'** IN FLOWER PATTERN-B, THE DRAWING SCALE ',
    %'VALUE:RA=',F10.5,' ****',/)
C
C***** SUBROUTINE TITLE2 IS CALLED TO WRITE THE STATEMENT AND DIMENSION OF FLOWER. *****
C
  CALL TITLE2(JM,RA,XX,YY,FILE1,FILE2,SIZE,DATE,DRAWER,WORKS,
    % MATERIAL,JB,KF,ITD,JF)
C
  IF(JB.EQ.1) THEN
    DO 10 I=1,KK
C
C***** SUBROUTINE PLOT IS CALLED TO PLOT THE FLOWER AT EACH STAND. *****
C
  CALL LINCOL(1)
C
  CALL PLOT(I,RA)
C
  CALL SCALE2(-1.0,1.0)
C
  CALL PLOT(I,RA)
C
  CALL SCALE2(-1.0,1.0)
C
  10 CONTINUE
  GO TO 390
  ELSEIF(JB.EQ.2) THEN
    DO 20 I=KS+1,KF
C
C***** SUBROUTINE PLOT IS CALLED TO PLOT THE FLOWER AT EACH STAND. *****
C
  CALL LINCOL(1)
  CALL PLOT(I,RA)
  CALL SCALE2(-1.0,1.0)
  CALL PLOT(I,RA)
  CALL SCALE2(-1.0,1.0)
C
  20 CONTINUE
  ELSE
  ENDIF
C
C
  390 READ*,JZ
  CALL PICCLE
  PRINT*,'*****--< 2-DIMENSIONAL FLOWER PATTERN-B FINISH.--*****'
C
  CALL GINEND

```



```

    ENDIF
20  CONTINUE
    IF(AAN(I,NR(I)).GT.180) THEN
    WRITE(*,*)'!!!!!! AAN(I,NR(I)) EXCEED 180 DEGREE. !!!!!'
    WRITE(*,*)'**** CADFORM CAN'T WORK IN THIS CASE. ****'
    ELSE
    ENDIF
    GO TO 10
C
C***** CALCULATION OF THE POINT AT NO. 0 stand *****
C
30  J=0
    PXO(I,J)=0.0
    PYO(I,J)=-DH(I)
    CX(I,J)=0.0
    CY(I,J)=0.0
    J=1
    PXO(I,J)=WS/2.0
    PYO(I,J)=-DH(I)
    CX(I,J)=0.0
    CY(I,J)=0.0
10  CONTINUE
C
C***** CALUCULATION OF THE INSIDE POINTS OF FLOWER *****
C
    DO 40 I=1, KK
    DO 45 J=1, NR(I)
C
    RR(I,J)=R(I,J)-TS
45  CONTINUE
40  CONTINUE
C
    DO 50 I=0, KK
    IF(I.EQ.0) GO TO 70
C
    DO 55 J=0, NR(I)
    IF(J.EQ.0) THEN
    PXI(I,J)=0.0
    PYI(I,J)=-DH(I)+TS
    ELSE IF(J.EQ.1) THEN
    PXI(I,J)=FNS1(RR(I,J), AN(I,J))
    PYI(I,J)=RR(I,J)-FNS2(RR(I,J), AN(I,J))-DH(I)+TS
    ELSE
    PXI(I,J)=CX(I,J)+FNS1(RR(I,J), AAN(I,J))
    PYI(I,J)=CY(I,J)-FNS2(RR(I,J), AAN(I,J))
    ENDIF
55  CONTINUE
    GO TO 50
C
70  J=0
    PXI(I,J)=0.0
    PYI(I,J)=-DH(I)+TS
    J=1
    PXI(I,J)=WS/2.0
    PYI(I,J)=-DH(I)+TS
C
50  CONTINUE
C
    WRITE (*,*)'----- CALUCULATION OF ALL POINTS HAS BEEN COMPLETED. -
%-----'
    WRITE(*,100)
100 FORMAT(/,4X,'***** CALCULATED RESULTS OF THE POINTS OF FLOWER.',
%' *****'//,10X,'----- OUTSIDE POINTS -----')
    WRITE(*,102)
102 FORMAT(1H0,3X,1HI,3X,1HJ,4X,8HPXO(I,J),4X,8HPYO(I,J),6X,7HCX(I,J),
%6X,7HCY(I,J),4X,8HAAN(I,J),/)

```



```

        WRITE(*,104)((I,J,PX0(I,J),PY0(I,J),CX(I,J),CY(I,J),AAN(I,J),
        %J=0,NR(I)),I=0, KK)
104 FORMAT(1H ,2X,I2,2X,I2,2X,F10.3,2X,F10.3,3X,F10.3,3X,F10.3,2X,
        %F10.3)
C*****
C
C          PRINT*,'**** INPUT THE NUMBER 0 AFTER CHECKING THE DATA. ****'
C          READ*,NUM
C          WRITE(*,90)NUM
C          90 FORMAT(4X,I3,/)
C
        WRITE(*,106)
106 FORMAT(1H1,/,10X,'----- INSIDE POINTS -----')
        WRITE(*,108)
108 FORMAT(1H0,3X,1HI,3X,1HJ,4X,8HPXI(I,J),4X,8HPYI(I,J),6X,7HCX(I,J),
        %6X,7HCY(I,J),4X,8HAAN(I,J),/)
        WRITE(*,104)((I,J,PXI(I,J),PYI(I,J),CX(I,J),CY(I,J),AAN(I,J),
        %J=0,NR(I)),I=0, KK)
        PRINT*,' '
C*****
C
C          PRINT*,'**** INPUT THE NUMBER 0 AFTER CHECKING THE DATA. ****'
C          READ*,NUM
C          WRITE(*,92) NUM
C          92 FORMAT(4X,I3,/)
C
C***** WRITING THE ABOVE DATA TO THE RESULT FILE "R-FILE1" OR "R-FILE2" *****
C
        IF(ITD.EQ.1) THEN
            NF=3
        ELSE IF(ITD.EQ.2.AND.JF.EQ.1) THEN
            NF=6
            GO TO 210
        ELSE
            GO TO 204
        ENDIF
        WRITE(NF,208)FILE1
208 FORMAT(1H1,/,4X,
        % '*****',
        %/4X,'** OUT PUT DATA IN FILE R',A12,' **',
        %/4X,'*****'/)
        GO TO 214
C
210 WRITE(NF,212)FILE2
212 FORMAT(1H1,/,4X,
        % '*****',
        %/4X,'** OUT PUT DATA IN FILE R',A12,' **',
        %/4X,'*****'/)
C
214 WRITE(NF,216)
216 FORMAT(4X,'*****',
        %'*****',
        %/6X,'CALCULATED RESULTS OF AII POINTS OF X AND Y AXIS ON THE',
        %' FLOWER',
        %/4X,'*****',
        %'*****'/)
C
        WRITE(NF,100)
        WRITE(NF,102)
        WRITE(NF,104)((I,J,PX0(I,J),PY0(I,J),CX(I,J),CY(I,J),AAN(I,J),
        %J=0,NR(I)),I=0, KK)
        WRITE(NF,106)
        WRITE(NF,108)
        WRITE(NF,104)((I,J,PXI(I,J),PYI(I,J),CX(I,J),CY(I,J),AAN(I,J),
        %J=0,NR(I)),I=0, KK)
204 RETURN

```



```

ELSE IF(AAN(I,J).GE.90) THEN
  PXW(I,J)=CX(I,2)+R(I,2)
  AWY(I)=CY(I,J)
  ITH=1
ELSE
  PXW(I,J)=PX0(I,J)
ENDIF
PYH(I,J)=PY0(I,J)+DH(I)
GO TO 100

```

```

C
93 IF(ITH.EQ.1) THEN
  PXW(I,J)=PXW(I,J-1)
ELSE IF(AAN(I,J).GE.90) THEN
  PXW(I,J)=CX(I,3)+R(I,3)
  AWY(I)=CY(I,J)
  ITH=1
ELSE
  PXW(I,J)=PX0(I,J)
ENDIF
PYH(I,J)=PY0(I,J)+DH(I)
GO TO 100

```

```

C
94 IF(ITH.EQ.1) THEN
  PXW(I,J)=PXW(I,J-1)
ELSE IF(AAN(I,J).GE.90) THEN
  PXW(I,J)=CX(I,4)+R(I,4)
  AWY(I)=CY(I,J)
  ITH=1
ELSE
  PXW(I,J)=PX0(I,J)
ENDIF
PYH(I,J)=PY0(I,J)+DH(I)
GO TO 100

```

```

C
95 IF(ITH.EQ.1) THEN
  PXW(I,J)=PXW(I,J-1)
ELSE IF(AAN(I,J).GE.90) THEN
  PXW(I,J)=CX(I,5)+R(I,5)
  AWY(I)=CY(I,J)
  ITH=1
ELSE
  PXW(I,J)=PX0(I,J)
ENDIF
PYH(I,J)=PY0(I,J)+DH(I)

```

```

C
100 IF(2*PXW(I,J).GT.AW(I)) GO TO 10
15 IF(PYH(I,J).GT.AH(I)) GO TO 20
GO TO 25

```

```

C
10 AW(I)=2*PXW(I,J)
GO TO 15
20 AH(I)=PYH(I,J)
25 DLO(I,J)=R(I,J)*AN(I,J)*PE
TDLO(I,J)=TDLO(I,J-1)+DLO(I,J)
DLN1(I,J)=(R(I,J)-TS/2.0)*AN(I,J)*PE
TDLN1(I,J)=TDLN1(I,J-1)+DLN1(I,J)

```

```

85 CONTINUE

```

```

C
TLO(I)=2*TDLO(I,NR(I))
TLN1(I)=2*TDLN1(I,NR(I))
WE(I)=2*PX0(I,NR(I))
J=NR(I)
WRITE(*,30)
30 FORMAT(//6X,1HI,4X,1HJ,3X,5HNR(I),4X,9HTDLO(I,J),3X,
%13HTDLO(I,NR(I)),4X,6HTLO(I),5X,7HTLN1(I))
WRITE(*,31) I,J,NR(I),TDLO(I,J),TDLO(I,NR(I)),TLO(I),TLN1(I)

```

```

31 FORMAT(/4X,I3,2X,I3,2X,I3,4X,F10.2,4X,F10.2,4X,F10.2,2X,F10.3,/)
C
C PRINT*, '**** INPUT THE NUMBER 0 TO GO FURTHER. ****'
C PRINT*, 'NUM='
C READ*, NUM
C GO TO 80
C
32 AW(I)=WS
AH(I)=0.0
TLO(I)=WS
TLN1(I)=WS
WE(I)=WS
C
80 CONTINUE
C
WRITE(*,200)
200 FORMAT(1H1,/, '***< RESULTS OF CALUCULATION OF WIDTH AND',
%'HEIGHT OF FLOWER AT OUTSIDE SURFACE >***'/)
WRITE(*,201)
201 FORMAT(1H0, 'stand No.', 3X, 'C-LENGTH', 3X, 'N-LENGTH',
%' 5X, 'HEIGHT', 6X, 'WIDTH', 4X, 'E-WIDTH', 2X, 'PY/Max.WIDTH'//)
C
WRITE(*,202)(I, TLO(I), TLN1(I), AH(I), AW(I), WE(I), AWY(I), I=0, KK)
202 FORMAT(1H ,4X, I2, 4X, F10.3, X, F10.3, X, F10.3, X, F10.3, X, F10.3,
%' X, F10.3)
C
C PRINT*, ' **** INPUT THE NUMBER 0 TO GO FURTHER. ****'
C PRINT*, 'NUM='
C READ*, NUM
C
C***** WRITING THE ABOVE DATA TO THE RESULT FILE "R-FILE1" OR "R-FILE2" *****
C
IF(ITD.EQ.1) THEN
NF=3
ELSE IF(ITD.EQ.2.AND.JF.EQ.1) THEN
NF=6
GO TO 210
ELSE
GO TO 204
ENDIF
WRITE(NF,208)FILE1
208 FORMAT(1H1,/,4X,
%' *****',
%/4X, '** OUT PUT DATA IN FILE R', A12, ' **',
%/4X, '*****'/)
GO TO 214
C
210 WRITE(NF,212)FILE2
212 FORMAT(1H1,/,4X,
%' *****',
%/4X, '** OUT PUT DATA IN FILE R', A12, ' **',
%/4X, '*****'/)
C
214 WRITE(NF,216)
216 FORMAT(4X, '*****',
%'*****',
%/6X, 'CALCULATED RESULTS OF DIMENSIONS OF FLOWERS ABOUT ',
%/6X, 'THE CIRCUMFERENTIAL LENGTH, HEIGHT, WIDTH, EDGE WIDTH AND',
%/6X, 'PY OF Max.WIDTH AT OUTSIDE SURFACE AND THE CIRCUMFERENTIAL ',
%/6X, 'LENGTH OF NEUTRAL AXIS',
%/4X, '*****',
%'*****'/)
C
WRITE(NF,198)
198 FORMAT(/4X, '***< RESULTS OF CALUCULATION OF WIDTH AND',

```



```

C
C
C*****
*****
C THIS IS THE SUBROUTINE PROGRAM FOR DRAWING THE FLOWER PATTERN-A WHICH IS THE INDIVIDUAL
FLOWER AT EACH STAND.
C*****
*****
C
C***** SUBROUTINE DRAW1 *****
C
SUBROUTINE DRAW1(JM,RA,XX,YY)
C
IMPLICIT REAL*8(A-H,L,O-Z), INTEGER*4(I-K,M-N)
CHARACTER FILE1*12,FILE2*12
C
COMMON/DAT1/ LS(0:26),TLS(0:26),DH(0:25),NR(0:25),R(0:25,5),
% AN(0:25,5)
COMMON/DAT2/ D, WS, TS, KK, NN
COMMON/DAT4/ PE, ITD, IDH, IIDH, JF
COMMON/POINT1/ PXO(0:25,0:5), PYO(0:25,0:5), CX(0:25,0:5),
% CY(0:25,0:5), PXI(0:25,0:5), PYI(0:25,0:5),
% RR(0:25,0:5)
COMMON/AAN/ AAN(0:25,0:5)
C
C
C*****
*****
C-----"ITD":INDICATES THE CASE OF A NEW DATA INPUT OR THE CASE OF A EXISTING DATA CALL.
C-----"IDH":INDICATES THE CASE OF A BOTTOM CONSTANT OR THE CASE OF A DOWNHILL FORMING.
C-----"IIDH":INDICATES THE CASE OF A DOWNHILL FORMING OR UPHILL FORMING.
C-----"JF":INDICATES THE CASE OF CREATING A NEW FILE OR NOT DUE TO CHANGE OF EXISTING FILE.
C*****
*****
C
C
C***** THIS WRITE STATEMENT IS JUST ONLY FOR CHECK OF "IDH". *****
WRITE (*,100) IDH
100 FORMAT(/4X,'DOWNHILL INDEX:IDH=',I2//)
C
IF(IDH.EQ.0.OR.IIDH.EQ.1) THEN
XX=92.0
YY=64.0
CALL SHIFT2(XX,YY)
ELSE IF(IDH.EQ.1.AND.IIDH.EQ.0) THEN
XX=92.0
YY=94.0
CALL SHIFT2(XX,YY)
ELSE
WRITE(*,102)
102 FORMAT(/4X,'**** IDH IS'NT THE PERMISSIBLE VALUE THAT IS',
%' 0 OR 1. ****'//)
ENDIF
C
C***** DRAWING OF X-AXIS AND Y-AXIS *****
C
CALL LINCOL(2)
CALL PENTYP(1)
CALL MOVTO2(-XX+5.0,0.0)
CALL LINBY2(2*(XX-5.0),0.0)
CALL BROKEN(3)
CALL MOVTO2(0.0,-YY+34.0)
CALL LINTO2(0.0,165.0-YY)
C
C***** DECISION OF THE SCALE OF THE FLOWER TO DRAW DEPENDING ON THE WIDTH OF STEEL SHEET.

```



```

C
  WRITE(*,100)RA
100 FORMAT(1H ,4X,'***IN SUB SUNPOU, THE DRAWING SCALE:RA=',
  %F10.5//)
  CALL LINCOL(5)
  CALL BROKEN(0)
  CALL SCALE(RA)
  I=JM
  DO 10 J=1,NR(I)
  CALL MOVTO2(PXO(I,J),PYO(I,J))
  CALL LINTO2(CX(I,J),CY(I,J))
C
  IF(J.EQ.NR(I)) GO TO 20
C
  IF(J.EQ.5) GO TO 20
  CALL LINTO2(CX(I,J+1),CY(I,J+1))
C
10  CONTINUE
C
C***** THE DRAWING OF THE DIMENSIONS OF FLOWER:HEIGHT,WIDTH AND EDGE-WIDTH. *****
C
20  IF(IC.EQ.1) GO TO 80
  IF(IC.EQ.0) GO TO 22
  PRINT*,'##### ERROR HAPPENEND IN SUB SUNPOU.#####'
  STOP
C
22  WRITE(*,90)
90  FORMAT(///4X,'*****',
  %/4X,'** DO YOU WANT TO DRAW THE DIMENSIONS OF **',
  %/4X,'** FLOWER;HEIGHT,WIDTH AND EDGE-WIDTH? **',
  %/4X,'**',
  %/4X,'** 1. YES (DRAWING) -----> 1 **',
  %/4X,'** 2. NO (NO DRAWING) -----> 2 **',
  %/4X,'**',
  %/4X,'*****'/)
  PRINT*,'-----INPUT THE NUMBER FROM 1 TO 2. -----'
  READ*, ND
  IC=1
  IF(ND.EQ.1) GO TO 92
  IF(ND.EQ.2) GO TO 126
  WRITE(*,94)
94  FORMAT(/4X,'** INPUT ERROR. INPUT THE PERMISSIBLE No. AGAIN. **',
  %//)
  GO TO 22
C
80  IF(ND.EQ.2) GO TO 126
  IF(ND.EQ.1) GO TO 92
  PRINT*,'@@@ ERROR HAPPENED IN SUB SUNPOU. @@@@'
C
C***** DRAWING OF DIMENSION OF WIDTH *****
C
92  IF(I.EQ.0) GO TO 120
C
  IF(AAN(I,NR(I)).LT.90.0) THEN
  PX=AW(I)/2.0
  PY=AH(I)-DH(I)
  ELSE
  PX=AW(I)/2.0
  PY=AWY(I)
  ENDIF
C
122 CALL LINCOL(6)
  CALL MOVTO2(PX,PY)
  CALL LINTO2(PX,AH(I)-DH(I)+25.0/RA)
  CALL MOVBY2(-2*PX,0.0)
  CALL LINTO2(-PX,PY)
  CALL MOVTO2(-PX,AH(I)-DH(I)+23.0/RA)

```



```

$$$$$$$$$$$$$$$$$$$$$$$$$$$$$$$$$$$$$$$$$$$$$$$$$$$$$$$$$$$$
C
C
C
C*****
C THIS IS THE SUBROUTINE PROGRAM FOR DEAWING THE ACTUAL LENGTH OF 10mm.
C*****
C
C***** SUBROUTINE JISSUN *****
C
C SUBROUTINE JISSUN(RA,XX,YY)
C
C IMPLICIT REAL*8(A-H,L,O-Z), INTEGER*4(I-K,M-N)
C
C
C CALL LINCOL(1)
C CALL BROKEN(0)
C CALL SCALE(RA)
C
C CALL MOVT02((160.0-XX)/RA,(30.0-YY)/RA)
C CALL LINBY2(10.0,0.0)
C CALL LINBY2(0.0,3.0/RA)
C CALL MOVT02((160.0-XX)/RA,(30.0-YY)/RA)
C CALL LINBY2(0.0,3.0/RA)
C
C CALL LINCOL(2)
C CALL MOVBY2(-1.0,2.0/RA)
C CALL CHASIZ(3.0,4.0)
C CALL CHAINT(10,2)
C CALL CHASTR('mm')
C
C S=1.0/RA
C CALL SCALE(S)
C CALL CHAMOD
C RETURN
C END
C
C
$$$$$$$$$$$$$$$$$$$$$$$$$$$$$$$$$$$$$$$$$$$$$$$$$$$$$$$$$$$$
$$$$$$$$$$$$$$$$$$$$
C
C
C*****
C THIS IS THE SUBROUTINE PROGRAM FOR PLOTTING THE FLOWER AT EACH STAND.
C*****
C
C***** SUBROUTINE PLOT *****
C
C SUBROUTINE PLOT(I,RA)
C
C IMPLICIT REAL*8(A-H,L,O-Z), INTEGER*4(I-K,M-N)
C
C COMMON/DAT1/ LS(0:26),TLS(0:26),DH(0:25),NR(0:25),R(0:25,5),
% AN(0:25,5)
C COMMON/DAT2/ D, WS, TS, KK, NN
C COMMON/POINT1/ PXO(0:25,0:5), PYO(0:25,0:5), CX(0:25,0:5),
% CY(0:25,0:5), PXI(0:25,0:5), PYI(0:25,0:5),
% RR(0:25,0:5)
C DIMENSION PX(0:25,0:5),PY(0:25,0:5)
C
C
C
C WRITE(*,110)RA
C 110 FORMAT(1H ,5X,'** IN SUB PLOT, THE DRAWING SCALE VALUE:RA=',
C %F10.5//)
C CALL SCALE(RA)

```

```

CALL MOVTO2(0.0,0.0)
IF(I.EQ.0) THEN
CALL MOVTO2(PX0(I,0),PY0(I,0))
CALL LINTO2(PX0(I,1),PY0(I,1))
CALL LINTO2(PXI(I,1),PYI(I,1))
CALL LINTO2(PXI(I,0),PYI(I,0))
GO TO 100
ELSE
ENDIF

```

```

C
C***** IC IS THE INDICATER THAT REPRESENT THE POINT OF OUTSIDE SURFACE OR INSIDE SURFACE.
*****

```

```

IC=0

```

```

C
75 DO 80 J=1, NR(I)
IF(IC.EQ.0) THEN
PX(I,J-1)=PX0(I,J-1)
PY(I,J-1)=PY0(I,J-1)
PX(I,J)=PX0(I,J)
PY(I,J)=PY0(I,J)
ELSE
PX(I,J-1)=PXI(I,J-1)
PY(I,J-1)=PYI(I,J-1)
PX(I,J)=PXI(I,J)
PY(I,J)=PYI(I,J)
ENDIF

```

```

C
IF(R(I,J).EQ.9999.99) THEN
CALL MOVTO2(PX(I,J-1),PY(I,J-1))
CALL LINTO2(PX(I,J),PY(I,J))
ELSE
CALL MOVTO2(PX(I,J-1),PY(I,J-1))
CALL ARCTO2(CX(I,J),CY(I,J),PX(I,J),PY(I,J),1)
ENDIF

```

```

80 CONTINUE

```

```

IF(IC.EQ.1) GO TO 90

```

```

C***** DRAWING OF INSIDE LINE OF FLOWER *****

```

```

IC=1
GO TO 75

```

```

C
90 J=NR(I)
CALL MOVTO2(PXI(I,J),PYI(I,J))
CALL LINTO2(PX0(I,J),PY0(I,J))
100 CALL CHAMOD
S=1.0/RA
CALL SCALE(S)
RETURN
END

```

```

C
C*****
C** THIS IS THE SUBROUTINE PROGRAM FOR DRAWING TITLE BLOCK CONTENTS AND DIMENSIONS. **
C*****

```

```

C***** SUBROUTINE TITLE1 *****

```

```

SUBROUTINE TITLE1(JM,RA,XX,YY,FILE1,FILE2,SIZE,DATE,DRAWER,WORKS,
% MATERIAL,ITD,JF)

```

```

IMPLICIT REAL*8(A-H,L,O-Z), INTEGER*4(I-K,M-N)
CHARACTER FILE1*12,FILE2*12,SIZE*14,DATE*10,DRAWER*12,WORKS*12,
% MATERIAL*12

```

```

COMMON/DAT1/ LS(0:26),TLS(0:26),DH(0:25),NR(0:25),R(0:25,5),

```

```

%          AN(0:25,5)
COMMON/DAT2/ D, WS, TS, KK, NN
COMMON/DAT5/ TLO(0:25),TLN1(0:25), AH(0:25), AW(0:25), WE(0:25),
%          AWY(0:25)
COMMON/POINT1/ PXO(0:25,0:5), PYO(0:25,0:5), CX(0:25,0:5),
%          CY(0:25,0:5), PXI(0:25,0:5), PYI(0:25,0:5),
%          RR(0:25,0:5)
COMMON/AAN/ AAN(0:25,0:5)

```

C

C

C***** WRITING THE DESCRIPTION OF TITLE BLOCK CONTENTS USING GINO/LIB. *****

C

```

CALL SHIFT2(-XX,-YY)
CALL LINCOL(2)
CALL LINWID(0.5)

```

C

```

CALL MOVT02(12.0,15.0)
CALL CHASIZ(7.0,6.0)
CALL CHASTR('CADFORM')

```

C

```

CALL MOVT02(3.0,3.0)
CALL CHASIZ(4.0,5.0)
CALL CHASTR('FLOWER PATTERN A')
CALL LINWID(0.2)

```

C

```

CALL LINCOL(5)
CALL CHASIZ(2.0,2.0)
CALL MOVT02(71.0,9.0)
CALL CHASTR('WORKS(Mill)')
CALL MOVT02(71.0,21.0)
CALL CHASTR('DRAWER')
CALL MOVT02(116.0,21.0)
CALL CHASTR('DATE')
CALL MOVT02(116.0,9.0)
CALL CHASTR('MATERIAL')
CALL MOVT02(162.0,9.0)
CALL CHASTR('SIZE')
CALL MOVT02(162.0,21.0)
CALL CHASTR('FILE NAME')

```

C

```

CALL LINCOL(6)
CALL CHASIZ(5.0,5.0)
CALL MOVT02(165.0,2.0)
CALL CHASTR(SIZE)

```

C

```

CALL MOVT02(170.0,14.0)
IF(ITD.EQ.2.AND.JF.EQ.1) THEN
CALL CHASTR(FILE2)
ELSE
CALL CHASTR(FILE1)
ENDIF

```

C

```

CALL CHASIZ(3.5,4.0)
CALL MOVT02(118.0,2.0)
CALL CHASTR(MATERIAL)

```

C

```

CALL MOVT02(118.0,14.0)
CALL CHASTR(DATE)

```

C

```

CALL MOVT02(73.0,14.0)
CALL CHASTR(DRAWER)

```

C

```

CALL MOVT02(73.0,2.0)
CALL CHASTR(WORKS)

```

C

C***** THE DESCRIPTION OF VALUES OF DIMENSIONS *****

```

C
CALL RGBDEF(13,1.0,1.0,0.7)
CALL LINCOL(13)
CALL RFILL(0,0,3.0,158.0,57.0,168.0)
C
CALL LINCOL(2)
CALL CHASIZ(5.0,6.0)
CALL MOVTO2(5.0,160.0)
CALL CHASTR('No. ')
CALL CHAINT(JM,2)
CALL CHASTR('stand')
CALL LINCOL(6)
CALL MOVTO2(3.0,158.0)
CALL LINTO2(57.0,158.0)
CALL LINTO2(57.0,168.0)
CALL LINTO2(3.0,168.0)
CALL LINTO2(3.0,158.0)
C
CALL MOVTO2(187.0,164.0)
CALL CHASIZ(3.5,4.5)
CALL LINCOL(2)
CALL CHASTR('Unit:mm & deg. ')
C
DY1=10.0
DY2=8.0
I=JM
CALL MOVTO2(193.0,154.0)
CALL LINCOL(6)
CALL CHASTR('TLO=')
CALL CHAFIX(TLO(I),7,2)
C
CALL MOVTO2(193.0,144.0)
CALL CHASTR('TLN=')
CALL CHAFIX(TLN1(I),7,2)
BX=193.0
BY=134.0
IF(JM.EQ.0) GO TO 52
C
DO 50 J=1,NR(I)
CALL MOVTO2(BX,BY)
CALL CHASTR('R')
CALL CHAINT(J,1)
CALL CHASTR('=')
CALL CHAFIX(R(I,J),8,2)
CALL MOVTO2(BX,BY-DY2)
CALL CHASTR('A')
CALL CHAINT(J,1)
CALL CHASTR('=')
CALL CHAFIX(AN(I,J),8,2)
BY=BY-DY2-DY1
50 CONTINUE
C
52 CALL MOVTO2(BX,BY)
CALL CHASTR('DH=')
CALL CHAFIX(DH(I),8,2)
C
CALL MOVTO2(BX,BY-DY1)
CALL CHASIZ(3.0,4.0)
CALL CHASTR('SCALE=')
CALL CHAFIX(RA,6,4)
C
CALL MOVTO2(BX-1.0,BY-DY1-DY2)
CALL CHASIZ(3.0,4.0)
CALL CHASTR('R:Outer Radius')
CALL CHAMOD
C

```

```

C
    RETURN
    END
C
C*****
C** THIS IS THE SUBROUTINE PROGRAM FOR DRAWING TITLE BLOCK CONTENTS
**
C*****
C
C***** SUBROUTINE TITLE2 *****
C
    SUBROUTINE TITLE2(JM,RA,XX,YY,FILE1,FILE2,SIZE,DATE,DRAWER,WORKS,
%           MATERIAL,JB,KF,ITD,JF)
C
    IMPLICIT REAL*8(A-H,L,O-Z), INTEGER*4(I-K,M-N)
    CHARACTER FILE1*12,FILE2*12,SIZE*14,DATE*10,DRAWER*12,WORKS*12,
%           MATERIAL*12
C
    COMMON/DAT1/ LS(0:26),TLS(0:26),DH(0:25),NR(0:25),R(0:25,5),
%           AN(0:25,5)
    COMMON/DAT2/ D, WS, TS, KK, NN
C
C***** WRITING THE DESCRIPTION OF TITLE BLOCK CONTENTS USING GINO/LIB. *****
C
    CALL SHIFT2(-XX,-YY)
    CALL LINCOL(2)
    CALL LINWID(0.5)
C
    CALL MOVTO2(12.0,15.0)
    CALL CHASIZ(7.0,6.0)
    CALL CHASTR('CADFORM')
C
    CALL MOVTO2(3.0,3.0)
    CALL CHASIZ(4.0,5.0)
    CALL CHASTR('FLOWER PATTERN B')
    CALL LINWID(0.2)
C
    CALL LINCOL(5)
    CALL CHASIZ(2.0,2.0)
    CALL MOVTO2(71.0,9.0)
    CALL CHASTR('WORKS(Mill)')
    CALL MOVTO2(71.0,21.0)
    CALL CHASTR('DRAWER')
    CALL MOVTO2(116.0,21.0)
    CALL CHASTR('DATE')
    CALL MOVTO2(116.0,9.0)
    CALL CHASTR('MATERIAL')
    CALL MOVTO2(162.0,9.0)
    CALL CHASTR('SIZE')
    CALL MOVTO2(162.0,21.0)
    CALL CHASTR('FILE NAME')
C
    CALL LINCOL(6)
    CALL CHASIZ(5.0,5.0)
    CALL MOVTO2(165.0,2.0)
    CALL CHASTR(SIZE)
C
    CALL MOVTO2(170.0,14.0)
    IF(ITD.EQ.2.AND.JF.EQ.1) THEN
    CALL CHASTR(FILE2)
    ELSE
    CALL CHASTR(FILE1)
    ENDIF
C

```

```

CALL CHASIZ(3.5,4.0)
CALL MOVTO2(118.0,2.0)
CALL CHASTR(MATERIAL)
C
CALL MOVTO2(118.0,14.0)
CALL CHASTR(=DATE)
C
CALL MOVTO2(73.0,14.0)
CALL CHASTR(DRAWER)
C
CALL MOVTO2(73.0,2.0)
CALL CHASTR(WORKS)
C
C***** THE DESCRIPTION OF STAND No. THAT ARE DRAWN *****
C
CALL RGBDEF(13,1.0,1.0,0.7)
CALL LINCOL(13)
CALL RFILL(0,0,3.0,158.0,71.0,167.0)
C
CALL LINCOL(2)
CALL CHASIZ(4.0,5.0)
CALL MOVTO2(5.0,160.0)
CALL CHASTR('No. ')
CALL CHAINT(JM,2)
CALL CHASTR('- ')
CALL CHASTR('No. ')
IF(JB.EQ.1) THEN
CALL CHAINT(KK,2)
ELSE IF(JB.EQ.2) THEN
CALL CHAINT(KF,2)
ELSE
ENDIF
CALL CHASTR('stand')
CALL LINCOL(6)
CALL MOVTO2(3.0,158.0)
CALL LINTO2(71.0,158.0)
CALL CHAMOD
CALL SHIFT2(XX,YY)
C
C
RETURN
END
C*****
C***** THIS FILE INCLUDES ALL SUBROUTINES FOR STRESS-STRAIN ANALYSIS.
*****
C*****C
C Amendment of SSA3DDSB on 14th October 1992
C*****
*****
C***** THIS SUBROUTINE COMPUTE THE POINTS OF X-AXIS,Y-AXIS AND Z-AXIS AT THE DIVIDED POINTS
IN THE CIRCUMFERENTIAL LENGTH OF FLOWER. *****
C
C***** SUBROUTINE CALPOIN *****
C
SUBROUTINE CALPOIN(FILE1,FILE2,MA)
C
IMPLICIT REAL*8(A-H,L,O-Z), INTEGER*4(I-K,M-N)
CHARACTER FILE1*12,FILE2*12,AA*12,MA*8
C
COMMON/DAT1/ LS(0:26),TLS(0:26),DH(0:25),NR(0:25),R(0:25,5),
% AN(0:25,5)
COMMON/DAT2/ D, WS, TS, KK, NN
COMMON/DAT4/ PE, ITD, IDH, IIDH, JF
COMMON/DAT6/ RN(0:25,6), DLN(0:25,6), TLN(0:25,6),DLE(0:25)
COMMON/AAN/ AAN(0:25,0:5)

```

```

COMMON/POINTZ/ PXE(0:25,-22:22), PYE(0:25,-22:22), PZ(0:25),
%          DB(0:25,0:21), TLE(0:25,0:21), ANE(0:25,0:22)
C
C
C***** DEFINITION OF FUNCTION *****
C
FNS1(A,B)=A*DSIN(B*PE)
FNC1(A,B)=A*(1-DCOS(B*PE))
FNS2(A,B,C)=(A-B)*DSIN(C*PE)
FNC2(A,B,C)=A*(DCOS(B*PE)-DCOS(C*PE))
C
DO 10 I=1, KK
TLN(I,0)=0.0
DO 20 J=1, NR(I)
C
RN(I,J)=R(I,J)-TS/2.0
DLN(I,J)=RN(I,J)*AN(I,J)*PE
TLN(I,J)=TLN(I,J-1)+DLN(I,J)
C
20 CONTINUE
10 CONTINUE
C
C*****DEFINITION OF RN(I,NR(I)+1) TO AVOID THE CALCULATION OF DIVISION BY ZERO.
*****
C
DO 15 I=0, KK
C
RN(I,NR(I)+1)=RN(I,NR(I))
DLN(I,NR(I)+1)=RN(I,NR(I)+1)*AN(I,NR(I))*PE
TLN(I,NR(I)+1)=TLN(I,NR(I))+DLN(I,NR(I)+1)
C
15 CONTINUE
C***** CALCULATION OF DIVIDED POINTS *****
C
DO 30 I=0, KK
C
DO 50 N=0, NN
C
IF(I.EQ.0) THEN
C***** No.0 stand *****
C
PXE(I,N)=WS*N/(2*NN)
PYE(I,N)=-DH(I)
ANE(I,N)=0.0
TLE(I,N)=PXE(I,N)
GO TO 50
C
ELSE IF(N.EQ.0) THEN
C***** CENTER POINT *****
C
PXE(I,N)=0.0
PYE(I,N)=-DH(I)
ANE(I,N)=0.0
TLE(I,N)=0.0
GO TO 50
C
ELSE
DLE1=TLN(I,NR(I))/NN
DLE2=DLE1*100000.0
NDLE=DINT(DLE2)
DLE(I)=NDLE/100000.0
TLE(I,N)=DLE(I)*N
ENDIF
C

```



```

      IF(TLE(I,N).LE.TLN(I,1)) THEN
C
C***** IN THE AREA OF R(1) *****
C
      ANE(I,N)=TLE(I,N)/(RN(I,1)*PE)
      PXE(I,N)=FNS1(RN(I,1),ANE(I,N))
      PYE(I,N)=FNC1(RN(I,1),ANE(I,N))-DH(I)
      GO TO 50
C
      ELSE IF(TLE(I,N).LE.TLN(I,2)) THEN
C
C***** IN THE AREA OF R(2) *****
C
      ANE(I,N)=(TLE(I,N)-TLN(I,1))/(RN(I,2)*PE)+AAN(I,1)
      PXE(I,N)=FNS2(RN(I,1),RN(I,2),AN(I,1))+FNS1(RN(I,2),ANE(I,N))
      PYE(I,N)=FNC1(RN(I,1),AN(I,1))+FNC2(RN(I,2),AN(I,1),ANE(I,N))
      %-DH(I)
      GO TO 50
C
      ELSE IF(TLE(I,N).LE.TLN(I,3)) THEN
C
C***** IN THE AREA OF R(3) *****
C
      ANE(I,N)=(TLE(I,N)-TLN(I,2))/(RN(I,3)*PE)+AAN(I,2)
      PXE(I,N)=FNS2(RN(I,1),RN(I,2),AN(I,1))+
      %FNS2(RN(I,2),RN(I,3),AAN(I,2))+FNS1(RN(I,3),ANE(I,N))
      PYE(I,N)=FNC1(RN(I,1),AN(I,1))+FNC2(RN(I,2),AN(I,1),AAN(I,2))+
      %FNC2(RN(I,3),AAN(I,2),ANE(I,N))-DH(I)
      GO TO 50
C
      ELSE IF(TLE(I,N).LE.TLN(I,4)) THEN
C
C***** IN THE AREA OF R(4) *****
C
      ANE(I,N)=(TLE(I,N)-TLN(I,3))/(RN(I,4)*PE)+AAN(I,3)
      PXE(I,N)=FNS2(RN(I,1),RN(I,2),AN(I,1))+
      %FNS2(RN(I,2),RN(I,3),AAN(I,2))+FNS2(RN(I,3),RN(I,4),AAN(I,3))+
      %FNS1(RN(I,4),ANE(I,N))
      PYE(I,N)=FNC1(RN(I,1),AN(I,1))+FNC2(RN(I,2),AN(I,1),AAN(I,2))+
      %FNC2(RN(I,3),AAN(I,2),AAN(I,3))+FNC2(RN(I,4),AAN(I,3),ANE(I,N))-
      %DH(I)
      GO TO 50
C
      ELSE IF(TLE(I,N).GT.TLN(I,4)) THEN
C
C***** IN THE AREA OF R(5) *****
C
      ANE(I,N)=(TLE(I,N)-TLN(I,4))/(RN(I,5)*PE)+AAN(I,4)
      PXE(I,N)=FNS2(RN(I,1),RN(I,2),AN(I,1))+
      %FNS2(RN(I,2),RN(I,3),AAN(I,2))+FNS2(RN(I,3),RN(I,4),AAN(I,3))+
      %FNS2(RN(I,4),RN(I,5),AAN(I,4))+FNS1(RN(I,5),ANE(I,N))
      PYE(I,N)=FNC1(RN(I,1),AN(I,1))+FNC2(RN(I,2),AN(I,1),AAN(I,2))+
      %FNC2(RN(I,3),AAN(I,2),AAN(I,3))+FNC2(RN(I,4),AAN(I,3),AAN(I,4))+
      %FNC2(RN(I,5),AAN(I,4),ANE(I,N))-DH(I)
      GO TO 50
C
      ELSE
      WRITE(*,*)'**** ERROR HAPPENS IN THE CALCULATION OF DIVIDED POINTS
      % IN "SUB CALPOIN".****'
      STOP
      ENDIF
C
C
50 CONTINUE
30 CONTINUE
C

```

```

C***** POINTS OF Z-AXIS *****
C
  DO 60 I=0, KK
C
    LAV=INT(TLS(KK)/2)
    PZ(I)=TLS(I)-LAV
  60 CONTINUE
C
C***** WRITING THE POINT DATA OF DIVIDED ELEMENTE INTO THE "R" FILE *****
C
  IF(ITD.EQ.1) THEN
    NF=3
    AA=FILE1
    GO TO 100
  ELSE IF (ITD.EQ.2.AND.JF.EQ.1) THEN
    NF=6
    AA=FILE2
    GO TO 100
  ELSE
    GO TO 150
  ENDIF
C
  100 OPEN(3, FILE='R'//FILE1, STATUS='UNKNOWN', ACCESS='APPEND')
  OPEN(6, FILE='R'//FILE2, STATUS='UNKNOWN', ACCESS='APPEND')
C
  WRITE(NF, 102)MA, AA
  102 FORMAT(1H1, ///, 4X,
  % '*****',
  %/4X, '** OUTPUT DATA(RESULT) OF X-, Y- AND Z-AXIS POINTS TO **',
  %/4X, '** ANALIZE STRESS-STRAIN BY ', A8, ' **',
  %/4X, '** IN THE FILE R', A12, ' **',
  %/4X, '*****', /)
C
  WRITE(NF, 104)
  104 FORMAT(//6X, 'ST. ', 2X, 'Mesh', 5X, 'PXE(I, J)', 7X, 'PYE(I, J)', 8X,
  %'PZ(I)', 9X, 'TLS(I)', 7X, 'ANE(I, J)', 9X, 'DLE(I)', 7X, 'TLE(I, J)', /)
C
  DO 70 I=0, KK
  DO 80 N=0, NN
C
    WRITE(NF, 106)I, N, PXE(I, N), PYE(I, N), PZ(I), TLS(I), ANE(I, N), DLE(I),
  %TLE(I, N)
  106 FORMAT(1H , 4X, I3, 3X, I3, 3X, F10.3, 5X, F10.3, 5X, F10.3, 5X, F10.3,
  %5X, F10.3, 5X, F10.3, 5X, F10.3)
  80 CONTINUE
  WRITE(NF, 108)
  108 FORMAT(/4X, '-----'/)
  70 CONTINUE
C
  CLOSE(3, STATUS='KEEP')
  CLOSE(6, STATUS='KEEP')
C
  WRITE(*, 102)MA, AA
  DO 75 I=0, KK
C
  WRITE(*, 124)
  124 FORMAT(//X, 'ST. ', X, 'Mesh', 3X, 'PXE(I, J)', 5X, 'PYE(I, J)', 9X,
  %'PZ(I)', 7X, 'TLS(I)', 5X, 'ANE(I, N)', /)
C
  DO 85 N=0, NN
  WRITE(*, 126)I, N, PXE(I, N), PYE(I, N), PZ(I), TLS(I), ANE(I, N)
  126 FORMAT(1H , IZ, 2X, I3, 2X, F10.3, 3X, F10.3, 4X, F10.3, 3X, F10.3,
  %3X, F10.3)
  85 CONTINUE
  PRINT*, '-----'
C
C*****

```

```

C          WRITE(*,*)'**** INPUT ZERO(0) TO ADVANCE ****'
C          READ*,JJ
C
C          WRITE(*,108)
C          75 CONTINUE
C
C          150 WRITE(*,148)
C          148 FORMAT(/4X,'**** CALCULATION OF POINTS HAS COMPLETED.****',
C                %/2X,'*****',
C                %'*****'//)
C
C          RETURN
C          END
C
C*****
C
C***** THIS SUBROUTINE COMPUTE THE STRAIN WITHOUT CONSIDERING THE DEFORMATION OF MESH IN
C THR LATERAL DIRECTION. *****
C
C***** SUBROUTINE SNANA1 *****
C
C          SUBROUTINE SNANA1
C
C          IMPLICIT REAL*8(A-H,L,O-Z), INTEGER*4(I-K,M-N)
C
C          COMMON/DAT1/ LS(0:26),TLS(0:26),DH(0:25),NR(0:25),R(0:25,5),
C          %          AN(0:25,5)
C          COMMON/DAT2/ D, WS, TS, KK, NN
C          COMMON/DAT3/ EE,SEQ0, HH, ANYU, BL, VV
C          COMMON/POINT2/ PXE(0:25,-22:22), PYE(0:25,-22:22), PZ(0:25),
C          %          DB(0:25,0:21), TLE(0:25,0:21), ANE(0:25,0:22)
C          COMMON/STA1/ EZ(0:25,0:20), EX(0:25,0:20), DEZ(0:25,0:20),
C          %          DEX(0:25,0:20), DLZ(0:25,0:20), DZ(0:25,0:20), BB
C          COMMON/STA2/ HDEZ, HEZ, SDEX, HEX, SEX
C
C
C          WRITE(*,120)
C          120 FORMAT(/4X,'*****',
C                %/4X,'** THE STRAIN ANALYSIS "MODEL-1" START NOW. **',
C                %/4X,'*****'//)
C
C          WRITE(*,110)
C          110 FORMAT(/4X,'*** AT STRAIN ANALYSIS, INPUT ZERO(0)'
C                %' TO ADVANCE. *****'//)
C          READ*,JT
C
C***** HDEZ=Max.dEz/Increment Longitudinal Strain *****
C***** HEZ =Max. Ez/Longitudinal Strain *****
C***** SDEX=Min.dEx/Increment Lateral Strain *****
C***** HEX =Max. Ex/Lateral Strain *****
C***** SEX =Min. Ex/Lateral Strain *****
C
C          HDEZ=0.0
C          HEZ =0.0
C          SDEX=0.0
C          HEX =0.0
C          SEX =0.0
C          BB=WS/(2*NN)
C
C          DO 10 I=0, KK
C
C          DO 20 J=0, NN
C
C          IF(I.EQ.0) THEN
C
C***** INITIALIZING THE DATA AT No.0 stand *****

```

```

C
EZ(I,J)=0.0
EX(I,J)=0.0
DEZ(I,J)=0.0
DEX(I,J)=0.0
DLZ(I,J)=200.0
DZ(I,J)=200.0
GO TO 20

C
ELSE
DZ(I,J)=LS(I)
DLZ(I,J)=DSQRT(DZ(I,J)**2+(PXE(I,J)-PXE(I-1,J))**2+
% (PYE(I,J)-PYE(I-1,J))**2)
RX=DZ(I,J)/DZ(I-1,J)
DEZ(I,J)=DLOG(DLZ(I,J)/(DLZ(I-1,J)*RX))
ENDIF

C
IF(DEZ(I,J).GT.HDEZ) THEN
HDEZ=DEZ(I,J)
ELSE
ENDIF

C
DEX(I,J)=-BL*DEZ(I,J)

C
IF(DEX(I,J).LT.SDEX) THEN
SDEX=DEX(I,J)
ELSE
ENDIF

C
EZ(I,J)=EZ(I-1,J)+DEZ(I,J)

C
IF(EZ(I,J).GT.HEZ) THEN
HEZ=EZ(I,J)
ELSE
ENDIF

C
EX(I,J)=EX(I-1,J)+DEX(I,J)

C
IF(EX(I,J).GT.HEX) THEN
HEX=EX(I,J)
ELSE IF(EX(I,J).LT.SEX) THEN
SEX=EX(I,J)
ELSE
ENDIF

C
20 CONTINUE
10 CONTINUE

C
DO 30 I=0, KK
WRITE(*, 80)
80 FORMAT(/2X, 'ST.', 2X, 'MESH', 6X, 'DEZ ', 6X, 'DEX ', 7X,
%'EZ ', 7X, 'EX ', /)
DO 40 J=0, NN
WRITE(*, 82) I, J, DEZ(I, J), DEX(I, J), EZ(I, J), EX(I, J)
82 FORMAT(1H , 2X, I3, 2X, I3, 3X, 4(F10.6, 2X))

C
40 CONTINUE
C
***** INPUT ZERO(0) TO ADVANCE *****
READ*, JT

C
WRITE(*, 84)
84 FORMAT(/4X, '-----'/)
30 CONTINUE
C

```

```

WRITE(*,100)
100 FORMAT(/4X,'*** THE STRAIN ANALYSIS HAS BEEN COMPLETED. ****'//)
C
RETURN
END
C*****
*****
C
C*****
*****
C
C***** THIS SUBROUTINE DO THE STRESS ANALYSIS WITHOUT CONSIDERING THE DEFORMATION OF MESH
IN THR LATERAL DIRECTION. *****
C
C***** SUBROUTINE SSANA *****
C
SUBROUTINE SSANA
C
IMPLICIT REAL*8(A-H,L,O-Z), INTEGER*4(I-K,M-N)
C
COMMON/DAT1/ LS(0:26),TLS(0:26),DH(0:25),NR(0:25),R(0:25,5),
% AN(0:25,5)
COMMON/DAT2/ D, WS, TS, KK, NN
COMMON/DAT3/ EE,SEQ0,HH,ANYU,BL,VV
COMMON/STA1/ EZ(0:25,0:20), EX(0:25,0:20), DEZ(0:25,0:20),
% DEX(0:25,0:20), DLZ(0:25,0:20), DZ(0:25,0:20), BB
COMMON/STS1/ DSZ(0:25,-20:20), DSX(0:25,-20:20),SZ(0:25,-20:20),
% SX(0:25,-20:20), SEQ(0:25,-20:20),
% SOTOS(0:25,-20:20), EZE(0:25,0:20), EXE(0:25,0:20),
% NHANT(0:25,0:20), EZP(0:25,0:20), EXP(0:25,0:20)
COMMON/STS2/ DEPSOT(0:25,0:20),
% DWP(0:25,0:20), DWE(0:25,0:20), DW(0:25,0:20),
% DWT(0:25,0:20), WT(0:25), WTR(0:25),
% SWT(0:25),SWTR
COMMON/STS3/ HDSZ,SDSZ,HSZ, SSZ, HSX, SSX, HSOTOS, SSOTOS, HDW,
% HWT, HWTR
C
COMMON/STS5/ DEZE(0:25,0:20),DEXE(0:25,0:20),
% PDEZE(0:25,0:20),PDEXE(0:25,0:20)
C
C
C
C
WRITE(*,160)
160 FORMAT(/4X,'*****',
%/4X,'** THE STRESS ANALYSIS "MODEL-1" START NOW. **',
%/4X,'*****'//)
C
JW=0
DO 162 JJ=1,1000
JW=JW+1
162 CONTINUE
C
C***** HDSZ=Max.DSz/Longitudinal Stress Increment *****
C***** SDSZ=Min.DSz/Longitudinal Stress Increment *****
C***** HSZ=Max.Sz/Longitudinal Stress *****
C***** SSZ=Min.Sz/Longitudinal Stress *****
C***** HSX=Max.Sx/Lateral Stress *****
C***** SSX=Min.Sx/Lateral Stress *****
C***** HSOTOS=Max.SOTOS/Equivalent Stress *****
C***** SSOTOS=Min.SOTOS/Equivalent Stress *****
C***** HDW=Max.(DWe+DWp)/Elastic and Plastic Deformation Work per volume of a Mesh
*****
C***** HWT=Max.WT/Total Deformation Work along the width direction *****
C***** HWTR=Max.WTR/Deformation Work-Rate *****
C
HDSZ=0.0

```

```

SDSZ=0.0
HSZ=0.0
SSZ=0.0
HSX=0.0
SSX=0.0
HSOTOS=0.0
SSOTOS=0.0
HDW=0.0
HWT=0.0
HWTR=0.0

```

```

C
C***** INITIALIZING THE DATA AT No.0 stand *****
C

```

```

I=0
DO 10 J=0,NN
SZ(I,J)=0.0
SX(I,J)=0.0
SEQ(I,J)=SEQ0
SOTOS(I,J)=0.0
EZE(I,J)=0.0
EXE(I,J)=0.0
EZP(I,J)=0.0
EXP(I,J)=0.0
DEZE(I,J)=0.0
DEXE(I,J)=0.0
DEPSOT(I,J)=0.0

```

```

C
10 CONTINUE

```

```

C
C
C DO 20 I=1, KK

```

```

C WRITE(*,200)
C 200 FORMAT(/, 'ST. ', X, 'MESH', X, 'NHAN', 2X, 'DSZ(kg/mm2)', 3X, 'DSX',
C %8X, 'SZ', 9X, 'SX', 7X, 'SOTOS', 6X, 'SEQ' /)
C

```

```

C DO 30 J=0, NN

```

```

C***** CALCULATION OF STRESS IN THE ELASTIC DEFORMATION *****
C

```

```

ANA=EE/(1.0-ANYU**2)
DSZ(I,J)=ANA*(DEZ(I,J)+ANYU*DEX(I,J))
DSX(I,J)=ANA*(ANYU*DEZ(I,J)+DEX(I,J))
SZMAE=SZ(I-1,J)
SXMAE=SX(I-1,J)
SZ(I,J)=SZMAE+DSZ(I,J)
SX(I,J)=SXMAE+DSX(I,J)
SOTOS2=SZ(I,J)**2-SZ(I,J)*SX(I,J)+SX(I,J)**2
SOTOS(I,J)=DSQRT(SOTOS2)
SEQMAE=SEQ(I-1,J)

```

```

C IF(SOTOS(I,J).LE.SEQMAE) GO TO 50

```

```

C***** CALCULATION OF STRESS IN THE ELASTIC DEFORMATION AND THE ELASTIC-PLASTIC
DEFORMATION *****

```

```

C DEZIJ=DEZ(I,J)
C DEXIJ=DEX(I,J)
C SOTO=SOTOS(I-1,J)

```

```

C***** CALL SUBROUTINE EPDA/EPDA:(E)lastic-(P)lastic (D)eformation (A)nalysic *****
C

```

```

CALL EPDA(EE,HH,ANYU,SZMAE,SXMAE,SEQMAE,DEZIJ,DEXIJ,SOTO,DESOTO,

```

```

%DEZ1, DEX1, DSZ1, DSX1, DEZ2, DEX2, DSZ2, DSX2, DEPSO, NHAN)
C
IF(NHAN.GE.90) GO TO 100
C
NHANT(I,J)=NHAN
C
DSZ(I,J)=DSZ1+DSZ2
DSX(I,J)=DSX1+DSX2
C
C***** Elastic increment strain *****
C
DEZE(I,J)=DEZ1+(DSZ2-ANYU*DSX2)/EE
DEXE(I,J)=DEX1+(DSX2-ANYU*DSZ2)/EE
C
DEPSOT(I,J)=DEPSO
C***** DEPSOT: Increment of Equivalent Plastic Strain *****
C
SZ(I,J)=SZMAE+DSZ(I,J)
SX(I,J)=SXMAE+DSX(I,J)
C
SOTOS2=SZ(I,J)**2-SZ(I,J)*SX(I,J)+SX(I,J)**2
SOTOS(I,J)=DSQRT(SOTOS2)
SEQ(I,J)=SOTOS(I,J)
DWP(I,J)=(SEQ(I,J)+SEQMAE)*DEPSO/2.0
DWE(I,J)=(SZ(I,J)+SZ(I-1,J))*DEZE(I,J)/2.0+
% (SX(I,J)+SX(I-1,J))*DEXE(I,J)/2.0
DW(I,J)=DWP(I,J)+DWE(I,J)
GO TO 55
C
C***** STRESS ANALYSIS IN PURE ELASTIC DEFORMATION *****
C
50 NHANT(I,J)=1
SEQ(I,J)=SEQ(I-1,J)
DEZE(I,J)=DEZ(I,J)
DEXE(I,J)=DEX(I,J)
C
DWP(I,J)=0.0
DWE(I,J)=(SZ(I,J)+SZ(I-1,J))*DEZE(I,J)/2.0+
% (SX(I,J)+SX(I-1,J))*DEXE(I,J)/2.0
DW(I,J)=DWP(I,J)+DWE(I,J)
C
55 EZEMAE=EZE(I-1,J)
EXEMAE=EXE(I-1,J)
EZMAE=EZP(I-1,J)
EXMAE=EXP(I-1,J)
C
EZE(I,J)=EZEMAE+DEZE(I,J)
EXE(I,J)=EXEMAE+DEXE(I,J)
EZP(I,J)=EZMAE+DEZ(I,J)
EXP(I,J)=EXMAE+DEX(I,J)
C
IF(DSZ(I,J).GT.HDSZ) HDSZ=DSZ(I,J)
IF(DSZ(I,J).LT.SDSZ) SDSZ=DSZ(I,J)
IF(SZ(I,J).GT.HSZ) HSZ=SZ(I,J)
IF(SX(I,J).GT.HSX) HSX=SX(I,J)
IF(SZ(I,J).LT.SSZ) SSZ=SZ(I,J)
IF(SX(I,J).LT.SSX) SSX=SX(I,J)
IF(SOTOS(I,J).GT.HSOTOS) HSOTOS=SOTOS(I,J)
IF(SOTOS(I,J).LT.SSOTOS) SSOTOS=SOTOS(I,J)
IF(DW(I,J).GT.HDW) HDW=DW(I,J)
C
WRITE(*,202)I,J,NHANT(I,J),DSZ(I,J),DSX(I,J),SZ(I,J),SX(I,J),
C %SOTOS(I,J),SEQ(I,J)
C 202 FORMAT(1H ,I3,2X,I3,2X,I3,2X,6(F9.4,X))
C
30 CONTINUE

```

```

C
C*****
C*****
CC      WRITE(*,204)
CC 204  FORMAT(/4X,'***** INPUT ZERO(0) TO ADVANCE. *****',/)
CC      READ*,JG
C
C      WRITE(*,*)'-----'
C
C 20  CONTINUE
C
C***** CALCULATION OF TOTAL WORK AND WORK-RATE FOR DEFORMATION *****
C
C      SWT(0)=0.0
C      DO 60 I=1, KK
C      WT1=0.0
C
C      DO 70 J=0, NN
C
C      DWT(I,J)=TS*LS(I)*BB*DW(I,J)/1000
C      WT1=WT1+DWT(I,J)*2
C
C 70  CONTINUE
C
C***** WT:Total Deformation Work of all elements in width direction (kgf.m) or (J) *****
C
C      WT(I)=WT1
C      SWT(I)=SWT(I-1)+WT(I)
C
C***** SWT(I):Summation of WT(I) from 0 stand to i stand *****
C
C      IF(WT(I).GT.HWT) HWT=WT(I)
C      TT=(LS(I)/VV)*0.06
C      WTR(I)=WT(I)/TT
C
C***** WTR:Total Deformation Work-Rate at each stand (kgf.m/s) or (J/s) *****
C
C      IF(WTR(I).GT.HWTR) HWTR=WTR(I)
C 60  CONTINUE
C      TTT=(TLS(KK)/VV)*0.06
C      SWTR=SWT(KK)/TTT
C
C      GO TO 110
C
C 100 WRITE(*,101)I,J,NHAN
C 101  FORMAT(1H,'***** ERROR HAPPENED IN JUDGEMENT OF YIELD',
C        %' CONDITION OF STRESS-STRAIN *****',
C        %/4X,'STAND No.=',I3,3X,'MESH No.=',I3,3X,'NHAN=',I3,/)
C      STOP
C
C 110 WRITE(*,102)
C 102  FORMAT(/4X,'***** THE STRESS ANALYSIS HAS BEEN COMPLETED. ****'/)
C
C      RETURN
C      END
C*****
C*****
C*****
C*****
C***** THIS SUBROUTINE DO THE ELASTIC-PLASTIC DEFORMATION ANALYSIS. *****
C*****
C***** SUBROUTINE EPDA / EPDA:(E)lastic-(P)lastic (D)eformation (A)nalysis *****
C
C      SUBROUTINE EPDA(EE,HH,ANYU,SZ,SX,SEQ,DEZ,DEX,SOTO,DESOTO,

```



```

%DEZ1,DEX1,DSZ1,DSX1,DEZ2,DEX2,DSZ2,DSX2,DEPSO,NHAN)
C
  IMPLICIT  REAL*8(A-H,L,O-Z), INTEGER*4(I-K,M-N)
C
  WRITE(*,140)
140 FORMAT(/, '*****')
  WRITE(*,*) '** THE STRESS ANALYSIS "SUB. EPDA" START NOW. **'
  WRITE(*,*) '*****'
C
  ANA=EE/(1.0-ANYU**2)
  DNA=SEQ**2-SOTO**2
C
  SZD=(2.0*SZ-SX)/3.0
  SXD=(2.0*SX-SZ)/3.0
C
  IF(DABS(DEZ).LE.1.0D-15) GO TO 1
C
  BNA=1.0+ANYU*DEX/DEZ
  CNA=ANYU+DEX/DEZ
  SA=ANA**2*(BNA**2-BNA*CNA+CNA**2)
  SB=3.0*ANA*(SZD*BNA+SXD*CNA)
  SC=-DNA
  ABC=SB**2-4.0*SA*SC
  RTABC=DSQRT(ABC)
C
  IF(DEZ.LT.0.0) GO TO 2
C***** IN CASE OF dEz>=0 *****
  IF(SOTO.NE.SEQ) GO TO 3
  IF(SB.GT.0.0) GO TO 4
  IF(SB.LT.0.0) GO TO 5
  IF(SB.EQ.0.0) GO TO 6
C
  NHAN=99
  GO TO 50
C
  3 NHAN=21
  DEZ1=(-SB+RTABC)/2.0/SA
  GO TO 7
  4 NHAN=22
  DEZ1=0.0
  GO TO 7
  5 NHAN=23
  DEZ1=(-SB+RTABC)/2.0/SA
  GO TO 7
  6 NHAN=24
  DEZ1=0.0
  GO TO 7
C
C***** IN CASE OF dEz<0 *****
  2 IF(SOTO.NE.SEQ) GO TO 8
  IF(SB.GT.0.0) GO TO 9
  IF(SB.LT.0.0) GO TO 10
  IF(SB.EQ.0.0) GO TO 11
C
  NHAN=98
  GO TO 50
C
  8 NHAN=31
  DEZ1=(-SB-RTABC)/2.0/SA
  GO TO 7
  9 NHAN=33
  DEZ1=(-SB-RTABC)/2.0/SA
  GO TO 7
  10 NHAN=32
  DEZ1=0.0
  GO TO 7

```

```

11 NHAN=34
   DEZ1=0.0
C
7 DEX1=DEX*DEZ1/DEZ
  DSZ1=(DEZ1+ANYU*DEX1)*ANA
  DSX1=(ANYU*DEZ1+DEX1)*ANA
C
C***** THE STRAIN OF PLASTIC DEFORMATION WITH INCREMENT OF ELASTIC STRAIN IN THE PLSTIC
DEFORMATION. *****
C
   DEZ2=DEZ-DEZ1
   DEX2=DEX-DEX1
C
C***** STRESS IN THE Z-AXIS AND X-AXIS DIRECTION AT YIELDING. *****
C
   SZB=SZ+DSZ1
   SXB=SX+DSX1
C
C***** RE-DIVIDING A INCREMENT STRAIN IN PLASTIC DEFORMATION TO GET A FINE(PRECISE)
ANALYSIS. *****
C
   M=10
   DDEZ2=DEZ2/FLOAT(M)
   DDEX2=DEX2/FLOAT(M)
   DSZ2=0.0
   DSX2=0.0
   DESOTO=0.0
C
C   WRITE(*,700)
C 700 FORMAT(/,2X,'M',6X,'SZB',6X,'SXB',5X,'SZDB',5X,'SXDB',
C      %4X,'SOTOB',7X,'PB',7X,'RB',7X,'QB',/)
C
   DO 100 I=1,M
   SZDB=(2.0*SZB-SXB)/3.0
   SXDB=(2.0*SXB-SZB)/3.0
   SOTOB2=SZB**2.0-SZB*SXB+SXB**2.0
   SOTOB=DSQRT(SOTOB2)
   IF(I.EQ.1) SOTOB1=SOTOB
   PB=2.0*HH*SOTOB**2.0/(9.0*EE)
   RB=SZDB**2.0+2.0*ANYU*SZDB*SXDB+SXDB**2.0
   QB=RB+2.0*(1.0-ANYU**2.0)*PB
C
C   WRITE(*,702)M,SZB,SXB,SZDB,SXDB,SOTOB,PB,RB,QB
C 702 FORMAT(1H ,I2,X,8(F8.4,X))
C
   SL=SXDB**2.0+2.0*PB
   SM=-SZDB*SXDB+2.0*ANYU*PB
   SQ=SZDB**2.0+2.0*PB
C
   DDSZ2=EE*(SL*DDEZ2+SM*DDEX2)/QB
   DDSX2=EE*(SM*DDEZ2+SQ*DDEX2)/QB
C
   SZB=SZB+DDSZ2
   SXB=SXB+DDSX2
C***** INCREMENT OF THE PLASTIC STRESS *****
   DSZ2=DSZ2+DDSZ2
   DSX2=DSX2+DDSX2
100 CONTINUE
C
C***** INCREMENT OF THE EQUIVALENT PLASTIC STRAIN *****
C

```

```

SOTOBZ=SZB**2.0-SZB*SXB+SXB**2.0
SOTOBF=DSQRT(SOTOBZ)
DSOTO=SOTOBF-SOTOB1
DEPSO=DSOTO*(1.0/HH-1.0/EE)
GO TO 50

```

C

```

1 WRITE(*,*)'**** THIS IS THE CASE OF dEz<= 1.0D-15: the same as 1.0
%E-15. *****'
DEZ1=0.0
DEX1=0.0
DEZ2=0.0
DEX2=0.0
DSZ1=0.0
DSX1=0.0
DSZ2=0.0
DSX2=0.0
DESOTO=0.0
NHAN=50

```

C

```

50 WRITE(*,120)
120 FORMAT(/4X,'**** SUB. EPDA HAS DONE. THIS IS FOR CHECKING. ***'/)

```

C

```

RETURN
END

```

```

C*****
*****
C*****
*****

```

C

```

C***** THIS SUBROUTINE DEALS WITH THE 3-DIMENSIONAL DRAWING OF THE RESULTS IN THIS STRESS-
STRAIN ANALYSIS. *****

```

C

```

C***** SUBROUTINE DRAW3D1 *****

```

C

```

SUBROUTINE DRAW3D1(HDEZ,HEZ,SDEX,HEX,SEX,HDSZ,SDSZ,HSZ,SSZ,HSX,
% SSX,HSOTOS,PHDSZ,PSDSZ,PHSZ,PSSZ,PHSX,PSSX,PHSOTO,FILE1,FILE2,
% MM,SIZE,DATE,DRAWER,WORKS,MATERIAL)

```

C

```

IMPLICIT REAL*8(A-H,L,O-Z), INTEGER*4(I-K,M-N)
CHARACTER FILE1*12,FILE2*12,SIZE*14,DATE*10,DRAWER*12,WORKS*12,
% MATERIAL*12

```

C

C

```

COMMON/DAT1/ LS(0:26),TLS(0:26),DH(0:25),NR(0:25),R(0:25,5),
% AN(0:25,5)
COMMON/DAT2/ D, WS, TS, KK, NN
COMMON/DAT4/ PE, ITD, IDH, IIDH, JF
COMMON/DAT5/ TLO(0:25),TLN1(0:25), AH(0:25), AW(0:25), WE(0:25),
% AWY(0:25)
COMMON/POINTZ/ PXE(0:25,-22:22), PYE(0:25,-22:22), PZ(0:25),
% DB(0:25,0:21), TLE(0:25,0:21), ANE(0:25,0:22)
COMMON/STA3/ PDEZ(0:25,-20:20), PEZ(0:25,-20:20),
% PDEX(0:25,-20:20), PEX(0:25,-20:20)
% /STA3A/ PEZE(0:25,0:20), PEXE(0:25,0:20),PEZP(0:25,0:20),
% PEXP(0:25,0:20), PDEPSO(0:25,0:20)
COMMON/STS1/ DSZ(0:25,-20:20), DSX(0:25,-20:20),SZ(0:25,-20:20),
% SX(0:25,-20:20), SEQ(0:25,-20:20),
% SOTOS(0:25,-20:20), EZE(0:25,0:20), EXE(0:25,0:20),
% NHANT(0:25,0:20), EZP(0:25,0:20), EXP(0:25,0:20)
COMMON/STS4/ PDSZ(0:25,-20:20), PDSX(0:25,-20:20),
% PSZ(0:25,-20:20), PSX(0:25,-20:20),
% PSEQ(0:25,-20:20), PSOTOS(0:25,-20:20),
% /STS4A/ PDWE(0:25,0:20), PDWP(0:25,0:20),PDW(0:25,0:20),
% PDWT(0:25,0:20), PWT(0:25), PWTR(0:25),
% PSWT(0:25),PSWTR
DIMENSION XX(-20:20)

```

```

C
  WRITE(*,260)
260 FORMAT(/4X,'*****',
  %/4X,      '**',
  %/4X,      '** 3-DIMENSIONAL DRAWING OF THE RESULTS OF **',
  %/4X,      '**          STRESS-STRAIN ANALYSIS          **',
  %/4X,      '**',
  %/4X,      '*****'//)

C
C*****THIS COMAND MAKE THE TIME TO DISPLAY THE ABOVE DESCRIPTION. *****
  WRITE(*,266)
266 FORMAT(/4X,'**** INPUT ZERO(0) TO ADVANCE FURTHER STEP. ****'/)
  READ*,JA

C
C***** CALL GINO GRAPHIC PACAGE *****
C
  CALL GINO
  CALL T4510
  CALL T4107
  CALL UNITS(1.0)
  CALL TRANSF(2)
  CALL PICCLE
  GO TO 998

C
99 CALL SCALE(1.0/SA)
  CALL TRANSF(2)

C
998 WRITE(*,100)
100 FORMAT(/4X,'*****',
  %/4X,      '** CHOOSE A ITEM THAT YOU WANT TO DRAW. **',
  %/4X,      '**',
  %/4X,      '** 1. 3-DIMENSIONAL DEFORMED SURFACE --> 1 **',
  %/4X,      '** 2. STRAIN(Ez and Ex) --> 2 **',
  %/4X,      '** 3. INCREMENT STRAIN(dEz and DEx) --> 3 **',
  %/4X,      '** 4. STRESS (Sz and Sx)Unit=[MPa] --> 4 **',
  %/4X,      '** 5. STRESS (Sz and Sx)Unit=[kgf/mm2]--> 5 **',
  %/4X,      '** 6. STRESS INCREMENT(DSz and DSx)',
  %/4X,      '      Unit=[MPa] --> 6 **',
  %/4X,      '** 7. STRESS INCREMENT(DSz and DSx)',
  %/4X,      '      Unit=[kgf/mm2]--> 7 **',
  %/4X,      '** 8. EQUIVALENT STRESS Unit=[MPa] --> 8 **',
  %/4X,      '** 9. EQUIVALENT STRESS Unit=[kgf/mm2]--> 9 **',
  %/4X,      '** 0. FINISH --> 0 **',
  %/4X,      '**',
  %/4X,      '*****'//)
  PRINT*, '----- INPUT ONE NUMBER FROM 0 TO 9. -----'
  READ*,JN
  IF(JN.EQ.0) GO TO 400

C
C
  IF(JN.EQ.1.) THEN
    NF=11
  ELSE IF(JN.EQ.2.OR.JN.EQ.3) THEN
    NF=12
  ELSE IF(JN.EQ.4.OR.JN.EQ.5) THEN
    NF=13
  ELSE IF(JN.EQ.6.OR.JN.EQ.7) THEN
    NF=14
  ELSE IF(JN.EQ.8.OR.JN.EQ.9) THEN
    NF=15
  ELSE
    ENDIF
  GO TO 98

C
96 CALL SCALE(1.0/SA)
  CALL TRANSF(2)

```

```

IF(JS.EQ.1) THEN
GO TO 98
ELSE IF(JS.EQ.2) THEN
GO TO 97
ELSE
ENDIF

```

C

```

98 WRITE(*,102)
102 FORMAT(/4X,'*****',
%/4X, '** INPUT THE ANGLE OF PITCH, HEADING AND **',
%/4X, '** BANK OF THE AXIS OF X, Y AND Z. **',
%/4X, '** BANK:Rotation of Z-axis(longitudinal) **',
%/4X, '** HEADING:Rotation of Y-axis(height) **',
%/4X, '** PITCH:Rotation of X-axis(width) **',
%/4X, '**<Newly first Input> **',
%/4X, '** 1. Input or change when you newly --->1 **',
%/4X, '** input the data(ITD=1) **',
%/4X, '**<Call existing data> **',
%/4X, '** 2. Call the data from existing file -->2 **',
%/4X, '** 3. Change data in existing file --->3 **',
%/4X, '** Before change, you must choose No.2 **',
%/4X, '**<Call existing data and create new file> **',
%/4X, '** 4. Call the data from existing file -->4 **',
%/4X, '** and transfer them to the new file **',
%/4X, '** 5. Input or change when the data --->5 **',
%/4X, '** were called from existing file **',
%/4X, '** and create new file (ITD=2 AND JF=1) **',
%/4X, '**<Call the data from newly created file> **',
%/4X, '** 6. Call the data from new file --->6 **',
%/4X, '** that was created in No.4 and No.5 **',
%/4X, '*****'/)
PRINT*, '**--- INPUT THE PERMISSIBLE NUMBER FROM 1 TO 6. ---**'
READ*, JM

```

C

```
IF (JM.EQ.6) GO TO 888
```

C

```

OPEN(11,FILE='G1'//FILE1,STATUS='UNKNOWN')
OPEN(12,FILE='G2'//FILE1,STATUS='UNKNOWN')
OPEN(13,FILE='G3'//FILE1,STATUS='UNKNOWN')
OPEN(14,FILE='G4'//FILE1,STATUS='UNKNOWN')
OPEN(15,FILE='G5'//FILE1,STATUS='UNKNOWN')

```

C

```

IF(JM.EQ.1.OR.JM.EQ.3.OR.JM.EQ.5) THEN
WRITE(*,104)
104 FORMAT(/4X,'*****',
%/10X,'Bank of Z-axis(deg.)=',)
READ*,ABZ1
ABZ=ABZ1*PE
WRITE(*,106)
106 FORMAT(/10X,'Heading of Y-axis(deg.)=',)
READ*,AHY1
AHY=AHY1*PE
WRITE(*,108)
108 FORMAT(/10X,'Pitch of X-axis(deg.)=',)
READ*,APX1
APX=APX1*PE

```

C

```
ELSE IF((JM.EQ.2.OR.JM.EQ.4).AND.ITD.EQ.2) THEN
```

C

```
C***** CALL THE DATA FROM THE EXISTING FILE *****
```

C

```

REWIND NF
READ(NF,601)ABZ1,AHY1,APX1
ABZ=ABZ1*PE
AHY=AHY1*PE
APX=APX1*PE

```

```

C
601 FORMAT(1H1,///5X,3(F10.6,5X)/)
    ELSE IF (JM.EQ.2.AND.ITD.EQ.1) THEN
        PRINT 220
220 FORMAT(4X, '*** INPUT THE No. 1 BECAUSE OF ITD=1. ***'/)
    GO TO 98
    ELSE
        PRINT 222
222 FORMAT(4X, '*** INPUT THE PERMISSIBLE No. FROM 1 TO 2, AGAIN. ***'/)
    GO TO 98
    ENDIF
C***** CALL THE DATA FROM THE EXISTING FILE *****
    IF(JS.EQ.1) GO TO 300
    IF((JM.EQ.2.OR.JM.EQ.4).AND.ITD.EQ.2) THEN
C
        READ(NF,602)SZX,SZY
602 FORMAT(/5X,F10.4,5X,F10.4/)
        JP=0
C
        CLOSE(11,STATUS='KEEP')
        CLOSE(12,STATUS='KEEP')
        CLOSE(13,STATUS='KEEP')
        CLOSE(14,STATUS='KEEP')
        CLOSE(15,STATUS='KEEP')
C
        GO TO 300
    ELSE
C
97 WRITE(*,110)
110 FORMAT(/4X, '*****',
    /4X, '** Input the scale ratio of Z-axis vs X-axis and **',
    /4X, '** of Z-axis vs Y-axis. **',
    /4X, '**',
    /4X, '** 1. Input or change when you newly ---> 1 **',
    /4X, '** input the data(ITD=1) **',
    /4X, '** 2. Change the data in existing file ---> 2 **',
    /4X, '** 3. Input or change when the data ---> 3 **',
    /4X, '** were called from existing file **',
    /4X, '** and create new file(ITD=2 AND JF=1) **',
    /4X, '*****'/)
    PRINT*, '**--- INPUT THE PERMISSIBLE NUMBER FROM 1 TO 3. ---**'
    READ*, JP
    WRITE(*,111)
111 FORMAT(/4X, '*****',
    /10X, 'The Scale ratio of Z-axis vs X-axis:(Zscale/Xscale)=')
    READ*,SZX
    WRITE(*,112)
112 FORMAT(/10X, 'The Scale ratio of Z-axis vs Y-axis:',
    /10X, '(Zscale/Yscale)=')
    READ*,SZY
    ENDIF
    GO TO 300
C***** Call the data from newly created file. *****
C
888 OPEN(21,FILE='G1'//FILE2,STATUS='UNKNOWN')
    OPEN(22,FILE='G2'//FILE2,STATUS='UNKNOWN')
    OPEN(23,FILE='G3'//FILE2,STATUS='UNKNOWN')
    OPEN(24,FILE='G4'//FILE2,STATUS='UNKNOWN')
    OPEN(25,FILE='G5'//FILE2,STATUS='UNKNOWN')
C
    IF(NF.EQ.11) THEN
        NH=21
C
    ELSE IF(NF.EQ.12) THEN
        NH=22
C

```

```

ELSE IF(NF.EQ.13) THEN
NH=23
C
ELSE IF(NF.EQ.14) THEN
NH=24
C
ELSE IF(NF.EQ.15) THEN
NH=25
ELSE
ENDIF
C
REWIND NH
READ(NH,601)ABZ1,AHY1,APX1
READ(NH,602)SZX,SZY
C
CLOSE(21,STATUS='KEEP')
CLOSE(22,STATUS='KEEP')
CLOSE(23,STATUS='KEEP')
CLOSE(24,STATUS='KEEP')
CLOSE(25,STATUS='KEEP')
C
C***** Max.Height of the flower in all stands *****
300 HM=0.0
DO 15 I=0, KK
IF(AH(I).GT.HM) HM=AH(I)
15 CONTINUE
C
C***** DISTANCE OF PLOTTING AT X-AXIS WHEN STRESS OR STRAIN IS PLOTTED. *****
C
DO 17 J=-20,20
XX(J)=(D/NN)*J
17 CONTINUE
C
C***** MAKING THE DATA OF POINTS IN THE MINUS REAGION *****
C
DO 10 I=0, KK
C
DO 20 J=1, NN
C
PXE(I, -J)=-PXE(I, J)
PYE(I, -J)=PYE(I, J)
C
PEZ(I, -J)=PEZ(I, J)
PEX(I, -J)=PEX(I, J)
C
PDEZ(I, -J)=PDEZ(I, J)
PDEX(I, -J)=PDEX(I, J)
C
DSZ(I, -J)=DSZ(I, J)
DSX(I, -J)=DSX(I, J)
PDSZ(I, -J)=PDSZ(I, J)
PDSX(I, -J)=PDSX(I, J)
SZ(I, -J)=SZ(I, J)
SX(I, -J)=SX(I, J)
PSZ(I, -J)=PSZ(I, J)
PSX(I, -J)=PSX(I, J)
SOTOS(I, -J)=SOTOS(I, J)
PSOTOS(I, -J)=PSOTOS(I, J)
SEQ(I, -J)=SEQ(I, J)
PSEQ(I, -J)=PSEQ(I, J)
20 CONTINUE
10 CONTINUE
C
C***** DEFINITION OF 0 POINT AND A SCALE *****
C
XV=119.0

```

```

C      YV=95.0
C      CALL SHIFT2(XV,YV)
C
C***** SCALE TO DRAWING *****
C
C      AAR=239.0/(1.4*TLS(KK))
C      AAR=AAR*10000
C      AAR=IDINT(AAR)
C      SA=AAR/10000
C      ZL=TLS(KK)
C
C      CALL SCALE(SA)
C
C
C
C      JT=0
C      JD=0
C
C***** DRAWING FRAME OF 3-D GRAPHICS *****
C*****CALL SUBROUTINE FRAMEZ *****
C
C      64 CALL FRAMEZ(SA,XV,YV)
C
C      CALL LINCOL(2)
C      JL=1
C      JU=0
C
C      DO 30 I=0, KK
C
C      DO 40 J=-NN, NN, 1
C
C      80 IF(JT.EQ.0) THEN
C          GO TO(1,2,3,4,5,6,7,8,9), JN
C      ELSE IF(JT.NE.0) THEN
C          GO TO (52,53,54,55,56,57), JT
C      ELSE
C          ENDIF
C
C      WRITE(*,*)'*** INPUT ERROR. INPUT THE CORRECT NUMBER, AGAIN. ****'
C      GO TO 99
C
C***** 3D.DEFORMED SURFACE *****
C
C      1 X=PXE(I,J)*ZL/(SZX*D)
C        Y=(PYE(I,J)-HM/2.0)*ZL/(SZY*D)
C        Z=PZ(I)
C        GO TO 50
C
C***** STRAIN *****
C
C      2 Y=PEZ(I,J)*ZL/(SZY*DABS(HEZ))
C        GO TO 48
C
C      52 Y=PEX(I,J)*ZL/(SZY*DABS(HEZ))
C        GO TO 48
C
C***** INCREMENT STRAIN *****
C
C      3 Y=PDEZ(I,J)*ZL/(SZY*DABS(HDEZ))
C        GO TO 48
C
C      53 Y=PDEX(I,J)*ZL/(SZY*DABS(HDEZ))
C        GO TO 48
C
C***** STRESS Unit=(MPa) *****

```



```

C
  4 Y=PSZ(I,J)*ZL/(SZY*DABS(PHSZ-PSSZ))
    GO TO 48
C
  54 Y=PSX(I,J)*ZL/(SZY*DABS(PHSZ-PSSZ))
    GO TO 48
C
C***** STRESS Unit(kgf/mm2) *****
C
  5 Y=SZ(I,J)*ZL/(SZY*DABS(HSZ-SSZ))
    GO TO 48
C
  55 Y=SX(I,J)*ZL/(SZY*DABS(HSZ-SSZ))
    GO TO 48
C
C***** STRESS INCREMENT Unit=(MPa) *****
C
  6 Y=PDSZ(I,J)*ZL/(SZY*DABS(PHDSZ-PSDSZ))
    GO TO 48
C
  56 Y=PDSX(I,J)*ZL/(SZY*DABS(PHDSZ-PSDSZ))
    GO TO 48
C
C***** STRESS INCREMENT Unit=(kgf/mm2) *****
C
  7 Y=DSZ(I,J)*ZL/(SZY*DABS(HDSZ-SDSZ))
    GO TO 48
C
  57 Y=DSX(I,J)*ZL/(SZY*DABS(HDSZ-SDSZ))
    GO TO 48
C
C***** EQUIVALENT STRESS Unit=(MPa) *****
C
  8 Y=PSOTOS(I,J)*ZL/(SZY*DABS(PHSOTO))
    GO TO 48
C
C***** EQUIVALENT STRESS Unit=(kgf/mm2) *****
C
  9 Y=SOTOS(I,J)*ZL/(SZY*DABS(HSOTOS))
    GO TO 48
C
  48 X=XX(J)*ZL/(SZX*D)
    Z=PZ(I)
C
C***** ROTATION OF Z-AXIS/ BANK *****
  50 XA=X*COS(ABZ)-Y*SIN(ABZ)
    YA=X*SIN(ABZ)+Y*COS(ABZ)
    X=XA
    Y=YA
C
C***** ROTATION OF Y-AXIS/ HEADING *****
  ZA=Z*COS(AHY)-X*SIN(AHY)
  XA=Z*SIN(AHY)+X*COS(AHY)
  Z=ZA
  X=XA
C
C***** ROTATION OF X-AXIS/ PITCH *****
  ZA= Z*COS(APX)+Y*SIN(APX)
  YA=-Z*SIN(APX)+Y*COS(APX)
  Z=ZA
  Y=YA
C
  GO TO (74,76,78,79),JU
  IF(JL.EQ.2) GO TO 62
C
C***** DRAWING THE LINE IN THE CIRCUMFERENTIAL DIRECTION *****

```

```

C
  IF(J.EQ.-NN) THEN
  CALL MOVT02(X,Y)
  ELSE
  CALL LINT02(X,Y)
  ENDIF
40 CONTINUE
30 CONTINUE
C
C***** DRAWING THE LINE IN THE LONGITUDINAL DIRECTION *****
C
  JL=2
C
  DO 60 J=-NN,NN,1
C
  DO 70 I=0, KK
  GO TO 80
C
62 IF(I.EQ.0) THEN
  CALL MOVT02(X,Y)
  GO TO 70
  ELSE IF(J.EQ.-NN.OR.J.EQ.NN) THEN
  CALL LINC02(2)
  ELSE IF(J.EQ.0) THEN
  CALL LINC02(5)
  ELSE
  CALL LINC02(6)
  ENDIF
  CALL LINT02(X,Y)
C
70 CONTINUE
60 CONTINUE
C
  IF(JN.NE.1) GO TO 72
  IF(D.LE.100.0) THEN
    ZU=400.0
    XU=50.0
    YU=50.0
  ELSE IF(D.LE.400) THEN
    ZU=700.0
    XU=100.0
    YU=100.0
  ELSE
    ZU=1000.0
    XU=500.0
    YU=500.0
  ENDIF
C
  JU=1
C
  X1=-XU*ZL/(SZX*D)
  Y1=(YU-HM/2.0)*ZL/(SZY*D)
  Z1=-1.5*ZU+PZ(0)
C
  X=0.0
  Y=(0.0-HM/2.0)*ZL/(SZY*D)
  Z=Z1
  CALL LINC02(3)
  GO TO 50
C
74 XB=X
  YB=Y
  CALL MOVT02(XB,YB)
  JU=2
  X=X1
  Y=(0.0-HM/2.0)*ZL/(SZY*D)

```

```

      Z=Z1
      GO TO 50
C
76 CALL LINTO2(X,Y)
   JU=3
   CALL MOVT02(XB,YB)
   X=0.0
   Y=Y1
   Z=Z1
   GO TO 50
C
78 CALL LINTO2(X,Y)
   JU=4
   CALL MOVT02(XB,YB)
   X=0.0
   Y=(0.0-HM/2.0)*ZL/(SZY*D)
   Z=-0.5*ZU+PZ(0)
   GO TO 50
79 CALL LINTO2(X,Y)
   JD=1
72 CALL CHAMOD
C
C***** CALL SUBROUTINE TITLE3 TO DRAW THE TITLE BOCKS *****
C
      CALL TITLE3(JN,SA,XV,YV,FILE1,FILE2,SIZE,DATE,DRAWER,WORKS,
%          MATERIAL,MM,JT,ABZ1,AHY1,APX1, SZX,SZY,ITD,JF)
C
C***** CALL SUBROUTINE LINE TO DRAW THE SCALE LINE *****
C
      CALL LINE
C
      PRINTZ00
200 FORMAT(/4X, '*** INPUT 0(ZERO) TO GO TO FURTHER SETP. **'/)
      READ*,JZ
      WRITE(*,202) JZ
202 FORMAT(5X, 'JZ=',I3/)
      CALL PICCLE
C
      IF(JD.EQ.1) GO TO 232
      IF(JN.EQ.2) THEN
         JT=1
         JD=1
         GO TO 64
      ELSE IF(JN.EQ.3) THEN
         JT=2
         JD=1
         GO TO 64
      ELSE IF(JN.EQ.4) THEN
         JT=3
         JD=1
         GO TO 64
      ELSE IF(JN.EQ.5) THEN
         JT=4
         JD=1
         GO TO 64
      ELSE IF(JN.EQ.6) THEN
         JT=5
         JD=1
         GO TO 64
      ELSE IF(JN.EQ.7) THEN
         JT=6
         JD=1
         GO TO 64
      ELSE
         ENDIF
C

```

```

232 WRITE(*,230)
230 FORMAT(/4X, '*****',
%4X, '**',
%4X, '** DO YOU WANT TO CHANGE THE DATA **',
%4X, '** AS SHOWN BELOW. **',
%4X, '** INPUT THE NUMBER **',
%4X, '**',
%4X, '** 1.ANGLE OF PITCH,HEADING AND BANK ---> 1 **',
%4X, '** 2.SCALE RATIO OF Z VS X AND Z VS Y ---> 2 **',
%4X, '** 3.NO CHANGE (TO STORE ---> 3 **',
%4X, '** THE UP-TO-DATE DATA TO THE FILE) **',
%4X, '** 4.NO CHANGE (NOT TO STORE ---> 4 **',
%4X, '** THE UP-TO-DATE DATA TO THE FILE) **',
%4X, '** 5.FINISH ---> 5 **',
%4X, '*****'//)
PRINT*, '**--- INPUT THE PERMISSIBLE NUMBER FROM 1 TO 5. ---**'
READ*, JS
IF(JS.EQ.1) GO TO 96
IF(JS.EQ.2) GO TO 96
IF(JS.EQ.3) GO TO 302
IF(JS.EQ.4) GO TO 99
IF(JS.EQ.5) GO TO 400
C
PRINT*, '** INPUT YHE PERMISSIBLE No.,AGAIN. *****'
GO TO 232
C
302 WRITE(*,304)
304 FORMAT(/4X, '** YOU HAVE COMPLETED THE DRAWING OF THE DATA. **',
%4X, '** THE DATA IS WRITTEN TO G FILE. *****'//)
C
IF(JM.EQ.2) THEN
PRINT*, '@@@@ You must choose No.4. @@@@'
GO TO 232
ELSE
ENDIF
C
IF(JM.EQ.6) THEN
PRINT*, '@@ You cannot store it and choose No.4. @@'
GO TO 232
ELSE
ENDIF
C
IF(JM.EQ.4.OR.JM.EQ.5.OR.JP.EQ.3) GO TO 350
C
OPEN(11,FILE='G1'//FILE1,STATUS='UNKNOWN')
OPEN(12,FILE='G2'//FILE1,STATUS='UNKNOWN')
OPEN(13,FILE='G3'//FILE1,STATUS='UNKNOWN')
OPEN(14,FILE='G4'//FILE1,STATUS='UNKNOWN')
OPEN(15,FILE='G5'//FILE1,STATUS='UNKNOWN')
C
IF(NF.EQ.11) THEN
NH=11
C
ELSE IF(NF.EQ.12) THEN
NH=12
C
ELSE IF(NF.EQ.13) THEN
NH=13
C
ELSE IF(NF.EQ.14) THEN
NH=14
C
ELSE IF(NF.EQ.15) THEN
NH=15
ELSE
ENDIF

```

```

C
WRITE(NH,601)ABZ1,AHY1,APX1
WRITE(NH,602)SZX,SZY
C
CLOSE(11,STATUS='KEEP')
CLOSE(12,STATUS='KEEP')
CLOSE(13,STATUS='KEEP')
CLOSE(14,STATUS='KEEP')
CLOSE(15,STATUS='KEEP')
GO TO 348
C
350 IF(JM.EQ.4.OR.JM.EQ.5.OR.JP.EQ.3) GO TO 356
PRINT*,'**** ERROR HAPPENED IN DRWA3DSB ****'
STOP
C
356 OPEN(21,FILE='G1'//FILE2,STATUS='UNKNOWN')
OPEN(22,FILE='G2'//FILE2,STATUS='UNKNOWN')
OPEN(23,FILE='G3'//FILE2,STATUS='UNKNOWN')
OPEN(24,FILE='G4'//FILE2,STATUS='UNKNOWN')
OPEN(25,FILE='G5'//FILE2,STATUS='UNKNOWN')
C
IF(NF.EQ.11) THEN
NH=21
C
ELSE IF(NF.EQ.12) THEN
NH=22
C
ELSE IF(NF.EQ.13) THEN
NH=23
C
ELSE IF(NF.EQ.14) THEN
NH=24
C
ELSE IF(NF.EQ.15) THEN
NH=25
ELSE
ENDIF
C
WRITE(NH,601)ABZ1,AHY1,APX1
WRITE(NH,602)SZX,SZY
C
CLOSE(21,STATUS='KEEP')
CLOSE(22,STATUS='KEEP')
CLOSE(23,STATUS='KEEP')
CLOSE(24,STATUS='KEEP')
CLOSE(25,STATUS='KEEP')
GO TO 352
C
C***** WRITING THE DATA FOR DRAWING TO THE RESULT FILE *****
C
348 WRITE(*,310) FILE1
310 FORMAT(/4X,'*** WRITING THE DATA FOR DRAWING TO THE RESULT ',
%/10X,'FILE R',A12,' **',/)
C
OPEN(3,FILE='R'//FILE1,STATUS='UNKNOWN',ACCESS='APPEND')
C
IF(JM.EQ.3.OR.JP.EQ.2) THEN
WRITE(3,311)
311 FORMAT(/4X,'@ Change the data of the existing file. @')
ELSE
ENDIF
C
WRITE(3,312)
312 FORMAT(/4X,'*****THE DATA TO DRAW THE 3-D GRAPH *****')
C
WRITE(3,314)JN,ABZ1,AHY1,APX1

```

```

314 FORMAT(/4X,'JN=',I3,
    %/4X,'Bank of Z-axis(deg.)= ',F10.6,
    %/4X,'Heading of Y-axis(deg.)=',F10.6,
    %/4X,'Pitch of X-axis(deg.)= ',F10.6,/)

    WRITE(3,316)SZX,SZY
316 FORMAT(/4X,'SCALE RATIO OF Z-AXIS VS X-AXIS=',F10.4,
    %4X,'SCALE RATIO OF Z-AXIS VS Y-AXIS=',F10.4,/)
C
    CLOSE(3,STATUS='KEEP')
    GO TO 99
C
352 WRITE(*,320) FILEZ
320 FORMAT(/4X,'*** WRITING THE DATA FOR DRAWING TO THE RESULT ',
    %/10X,'FILE R',A12,' **',/)
C
    OPEN(6,FILE='R'//FILEZ,STATUS='UNKNOWN',ACCESS='APPEND')
C
    WRITE(6,322)
322 FORMAT(/4X,'****THE DATA TO DRAW THE 3-D GRAPH *****/)
C
    WRITE(6,324)JN,ABZ1,AHY1,APX1
324 FORMAT(/4X,'JN=',I3,
    %/4X,'Bank of Z-axis(deg.)= ',F10.6,
    %/4X,'Heading of Y-axis(deg.)=',F10.6,
    %/4X,'Pitch of X-axis(deg.)= ',F10.6,/)

    WRITE(6,326)SZX,SZY
326 FORMAT(/4X,'SCALE RATIO OF Z-AXIS VS X-AXIS=',F10.4,
    %4X,'SCALE RATIO OF Z-AXIS VS Y-AXIS=',F10.4,/)
C
    CLOSE(6,STATUS='KEEP')
    GO TO 99
C
C***** FINISH OF THE 3-D DRAWING *****
C
400 CALL GINEND
    WRITE(*,*)'**** YOU HAVE COMPLETED THE 3-D DRAWUNG. ****'
    RETURN
    END
C-----
-----
C*****
C*****
C***** THIS IS THE SUBROUTINE PROGRAMME FOR DRAWING THE FRAME OF 3-D GRAPHICS. *****
C*****
*****
C
C***** SUBROUTINE FRAME2 *****
C
    SUBROUTINE FRAME2(SA,XV,YV)
C
    CALL SCALE(1.0/SA)
    CALL SHIFT2(-XV,-YV)
C
    CALL RGBDEF(12,0.7,0.8,1.0)
    CALL LINCOL(12)
    CALL RFILL(0,0,0.0,12.0,70.0,24.0)
C
    CALL RGBDEF(13,1.0,1.0,0.7)
    CALL LINCOL(13)
    CALL RFILL(0,0,0.0,0.0,70.0,12.0)
C
    CALL LINCOL(1)

```

```

CALL BROKEN(0)
CALL MOVT02(0.0,0.0)
CALL LINWID(0.4)
CALL LINT02(239.0,0.0)
CALL LINT02(239.0,179.0)
CALL LINT02(0.0,179.0)
CALL LINT02(0.0,0.0)
C
CALL LINWID(0.3)
CALL MOVT02(0.0,24.0)
CALL LINT02(239.0,24.0)
C
C* CALL MOVT02(0.0,36.0)
C* CALL LINT02(70.0,36.0)
C* CALL LINT02(70.0,24.0)
C
CALL LINWID(0.2)
CALL MOVT02(239.0,12.0)
CALL LINT02(0.5,12.0)
CALL MOVT02(70.0,0.0)
CALL LINT02(70.0,24.0)
CALL MOVT02(115.0,0.0)
CALL LINT02(115.0,24.0)
CALL MOVT02(160.0,0.0)
CALL LINT02(160.0,24.0)
C
CALL CHAMOD
C
CALL SHIFT2(XV,YV)
CALL SCALE(SA)
C
RETURN
END
C-----
-----
C*****
*****
C** THIS IS THE SUBROUTINE PROGRAMME FOR DRAWING TITLE BLOCK CONTENTS AND DIMENSIONS.
**
C*****
*****
C
C***** SUBROUTINE TITLE3 FOR MODEL-1 OF STRESS-STRAIN ANALYSIS *****
C
SUBROUTINE TITLE3(JN,SA,XV,YV,FILE1,FILE2,SIZE,DATE,DRAWER,WORKS,
% MATERIAL,MM,JT,ABZ1,AHY1,APX1, SZX,SZY,ITD,JF)
C
IMPLICIT REAL*8(A-H,L,O-Z), INTEGER*4(I-K,M-N)
CHARACTER FILE1*12,FILE2*12,SIZE*14,DATE*10,DRAWER*12,WORKS*12,
% MATERIAL*12
C
COMMON/DAT1/ LS(0:26),TLS(0:26),DH(0:25),NR(0:25),R(0:25,5),
% AN(0:25,5)
COMMON/DAT2/ D, WS, TS, KK, NN
C
DIMENSION XARR(4),YARR(4)
C
C
C***** WRITING THE DESCRIPTION OF TITLE BLOCK CONTENTS USING GINO/LIB. *****
C
CALL SCALE(1.0/SA)
CALL SHIFT2(-XV,-YV)
C
CALL RGBDEF(16,0.5,1.0,1.0)
CALL LINC0L(16)
C
XARR(1)=0.0

```

```

C      XARR(2)=70.0
C      XARR(3)=70.0
C      XARR(4)=0.0
C      YARR(1)=12.0
C      YARR(2)=12.0
C      YARR(3)=24.0
C      YARR(4)=24.0
C      CALL MOVTO2(XARR(1),YARR(1))
C      CALL POLTO2(XARR,YARR,4)
C      CALL POFTO2(0,0,0,XARR,YARR,4)
C
C      CALL LINCOL(2)
C      CALL LINWID(0.5)
C
C      CALL MOVTO2(12.0,15.0)
C      CALL CHASIZ(7.0,6.0)
C      CALL CHASTR('CADFORM')
C
C*     CALL MOVTO2(12.0,15.0)
C*     CALL CHASIZ(4.0,5.0)
C*     CALL CHASTR('3-D DRAWING')
C
C      CALL LINWID(0.2)
C      CALL MOVTO2(2.0,3.0)
C      CALL CHASIZ(2.8,4.5)
C
C      IF(JN.EQ.1) THEN
C        CALL CHASTR('3-D Deformation Surface')
C      ELSE IF(JN.EQ.2.AND.JT.EQ.0) THEN
C        CALL CHASTR('  Strain Ez(%)')
C      ELSE IF(JN.EQ.2.AND.JT.EQ.1) THEN
C        CALL CHASTR('  Strain Ex(%)')
C      ELSE IF(JN.EQ.3.AND.JT.EQ.0) THEN
C        CALL CHASTR('Strain Increment dEz(%)')
C      ELSE IF(JN.EQ.3.AND.JT.EQ.2) THEN
C        CALL CHASTR('Strain Increment dEx(%)')
C      ELSE IF(JN.EQ.4.AND.JT.EQ.0) THEN
C        CALL CHASTR('  Stress Sz(MPa)')
C      ELSE IF(JN.EQ.4.AND.JT.EQ.3) THEN
C        CALL CHASTR('  Stress Sx(MPa)')
C      ELSE IF(JN.EQ.5.AND.JT.EQ.0) THEN
C        CALL CHASTR('  Stress Sz(kgf/mm2)')
C      ELSE IF(JN.EQ.5.AND.JT.EQ.4) THEN
C        CALL CHASTR('  Stress Sx(kgf/mm2)')
C      ELSE IF(JN.EQ.6.AND.JT.EQ.0) THEN
C        CALL CHASTR('Stress Ince. dSz(MPa)')
C      ELSE IF(JN.EQ.6.AND.JT.EQ.5) THEN
C        CALL CHASTR('Stress Incr. dSx(MPa)')
C      ELSE IF(JN.EQ.7.AND.JT.EQ.0) THEN
C        CALL CHASTR('Stress Incr.dSz(kgf/mm2)')
C      ELSE IF(JN.EQ.7.AND.JT.EQ.6) THEN
C        CALL CHASTR('Stress Incr.dSx(kgf/mm2)')
C      ELSE IF(JN.EQ.8) THEN
C        CALL CHASTR('Equivalent Stress (MPa)')
C      ELSE IF(JN.EQ.9) THEN
C        CALL CHASTR('Equiv. Stress (kgf/mm2)')
C      ELSE
C      ENDIF
C
C      CALL LINCOL(5)
C      CALL CHASIZ(2.0,2.0)
C      CALL MOVTO2(71.0,9.0)
C      CALL CHASTR('WORKS(Mill)')
C      CALL MOVTO2(71.0,21.0)

```



```

CALL CHASTR('DRAWER')
CALL MOVTO2(116.0,21.0)
CALL CHASTR('DATE')
CALL MOVTO2(116.0,9.0)
CALL CHASTR('MATERIAL')
CALL MOVTO2(162.0,9.0)
CALL CHASTR('SIZE')
CALL MOVTO2(162.0,21.0)
CALL CHASTR('FILE NAME')
C
CALL LINCOL(6)
CALL CHASIZ(5.0,5.0)
CALL MOVTO2(165.0,2.0)
CALL CHASTR(SIZE)
C
CALL MOVTO2(170.0,14.0)
IF(ITD.EQ.2.AND.JF.EQ.1) THEN
CALL CHASTR(FILE2)
ELSE
CALL CHASTR(FILE1)
ENDIF
C
CALL CHASIZ(3.5,4.0)
CALL MOVTO2(118.0,2.0)
CALL CHASTR(MATERIAL)
C
CALL MOVTO2(118.0,14.0)
CALL CHASTR(DATE)
C
CALL MOVTO2(73.0,14.0)
CALL CHASTR(DRAWER)
C
CALL MOVTO2(73.0,2.0)
CALL CHASTR(WORKS)
C
C***** THE DESCRIPTION OF STAND No. THAT ARE DRAWN *****
C
CALL RGBDEF(13,1.0,1.0,0.7)
CALL LINCOL(13)
CALL RFILL(0,0,3.0,159.0,51.0,168.0)
CALL RFILL(0,0,3.0,168.0,114.0,177.0)
C
CALL LINCOL(2)
CALL CHASIZ(3.5,4.5)
CALL MOVTO2(5.0,170.0)
CALL CHASTR('Stress-Strain Analysis')
IF(MM.EQ.1) THEN
CALL CHASTR('(Model-1)')
ELSE IF(MM.EQ.2) THEN
CALL CHASTR('(Model-2)')
ELSE
ENDIF
CALL MOVTO2(5.0,161.0)
CALL CHASTR(' 3-D DRAWING ')
CALL LINCOL(1)
CALL MOVTO2(3.0,168.0)
CALL LINTO2(114.0,168.0)
CALL LINTO2(114.0,177.0)
CALL LINTO2(3.0,177.0)
CALL LINTO2(3.0,159.0)
CALL LINTO2(51.0,159.0)
CALL LINTO2(51.0,168.0)
C
CALL MOVTO2(185.0,170.0)
CALL CHASIZ(3.0,4.0)
CALL LINCOL(2)

```

```

CALL CHASTR('Rotation Angle of')
CALL MOVT02(185.0,164.0)
CALL CHASTR(' Axis (deg.)')
CALL LINC0L(6)
CALL MOVT02(197.0,158.0)
CALL CHASTR('Bank =')
CALL CHAFIX(ABZ1,7,2)
CALL MOVT02(197.0,152.0)
CALL CHASTR('Head =')
CALL CHAFIX(AHY1,7,2)
CALL MOVT02(197.0,146.0)
CALL CHASTR('Pitch=')
CALL CHAFIX(APX1,7,2)
C
CALL MOVT02(200.0,138.0)
CALL LINC0L(2)
CALL CHASTR('Scale Ratio')
CALL LINC0L(6)
CALL MOVT02(200.0,132.0)
CALL CHASTR('SZX =')
CALL CHAFIX(SZX,7,2)
CALL MOVT02(200.0,126.0)
CALL CHASTR('SZY =')
CALL CHAFIX(SZY,7,2)
C
CALL MOVT02(125.0,170.0)
CALL LINC0L(2)
CALL CHASTR('Pass Line Length')
CALL LINC0L(6)
CALL MOVT02(130.0,164.0)
CALL CHASTR('L=')
CALL CHAFIX(TLS(KK),9,2)
CALL MOVT02(165.0,164.0)
CALL CHASTR('mm')
C
CALL CHAMOD
CALL SHIFT2(XV,YV)
CALL SCALE(SA)
C
C
RETURN
END
-----
C*****
*****
C** THIS IS THE SUBROUTINE PROGRAMME FOR STRESS-STRAIN ANALYSIS MODEL-2.
**
C*****
*****
C THIS SUBROUTINE COMPUTE POINTS OF DEVIDED MESH OF FLOWER AND STRAIN WITH CONSIDERATION OF
LATERAL CONTRACTION OF MESH.
C*****
*****
C
SUBROUTINE SNANAZ
C
IMPLICIT REAL*8(A-H,L,O-Z), INTEGER*4(I-K,M-N)
C
COMMON/DAT1/ LS(0:26),TLS(0:26),DH(0:25),NR(0:25),R(0:25,5),
% AN(0:25,5)
COMMON/DAT2/ D, WS, TS, KK, NN
COMMON/DAT3/ EE,SEQ0, HH, ANYU, BL, VV
COMMON/DAT4/ PE, ITD, IDH, IIDH, JF
COMMON/DAT5/ TLO(0:25),TLN1(0:25), AH(0:25), AW(0:25), WE(0:25),
% AWY(0:25)

```

```

COMMON/DAT6/ RN(0:25,6), DLN(0:25,6), TLN(0:25,6),DLE(0:25)
COMMON/DAT7/ N1F,RSF
COMMON/AAN/ AAN(0:25,0:5)
COMMON/POINT2/ PXE(0:25,-22:22), PYE(0:25,-22:22), PZ(0:25),
%          DB(0:25,0:21), TLE(0:25,0:21), ANE(0:25,0:22)
COMMON/STA1/ EZ(0:25,0:20), EX(0:25,0:20), DEZ(0:25,0:20),
%          DEX(0:25,0:20), DLZ(0:25,0:20), DZ(0:25,0:20), BB
COMMON/STA2/ HDEZ, HEZ, SDEX, HEX, SEX
COMMON/STA4/ FRD(0:10),DEXF(0:10,0:20),DEZF(0:10,0:20),
%          DBO(0:10,0:20),TLEO(0:10,0:20)

C
C ***** DEFINITION OF FUNCTION *****
C          PE=3.1415926535898/180
C *****
C
C          FNS1(A,B)=A*DSIN(B*PE)
C          FNC1(A,B)=A*(1-DCOS(B*PE))
C          FNS2(A,B,C)=(A-B)*DSIN(C*PE)
C          FNCZ(A,B,C)=A*(DCOS(B*PE)-DCOS(C*PE))

C          PRINT*,'***** Strain Analysis Model-2 start. *****'
C
C *****
C          WRITE(*,520)
C          520 FORMAT(1H1,6X,'I',6X,'J',6X,'RN(I,J)',6X,'AN(I,J)',
C          %6X,'TLN(I,J)',//)
C          DO 530 I=1, KK
C          DO 540 J=1, NR(I)
C          WRITE(*,542)I,J,RN(I,J),AN(I,J),TLN(I,J)
C          542 FORMAT(/,4X,I3,4X,I3,4X,F10.4,4X,F10.4,4X,F10.4)
C          540 CONTINUE
C          WRITE(*,*)'*****'
C          530 CONTINUE
C *****
C          HDEZ=0.0
C          HEZ=0.0
C          SDEX=0.0
C          HEX=0.0
C          SEX=0.0

C
C          BB1=WS/(2*NN)
C          BB2=BB1*100000.0
C          NB3=IDNINT(BB2)
C          BB4=NB3/100000.0
C          BB=BB4

C          WRITE(*,200)BB1, BB2, NB3, BB4, BB
C          200 FORMAT(///4X,'BB1= ',F10.5,/,4X,'BB2=',F12.2,/,4X,'BB3= ',I9,
C          %/,4X,'BB4= ',F10.5,/,4X,'BB= ',F10.5,///)

C          WRITE(*,*)'**** INPUT ZERO TO ADVANCE *****'
C          READ*,NC

C
C ***** Definition of RN(I,NR(I)+1) to avoid the calculation of division by zero. *****
C
C          DO 50 I=0, KK
C
C          RN(I,NR(I)+1)=RN(I,NR(I))
C          DLN(I,NR(I)+1)=RN(I,NR(I)+1)*AN(I,NR(I))*PE
C          TLN(I,NR(I)+1)=TLN(I,NR(I))+10*DLN(I,NR(I)+1)

C          50 CONTINUE
C *****
C          WRITE(*,22)
C          22 FORMAT(1H1,X,'I',3X,'J',3X,'RN(I,4)',4X,'RN(I,5)',2X,
C          %'DB(I,J)',2X,'TLE(IJ)',2X,'TLN(I2)',2X,'TLN(I3)',2X,

```

```

      %'TLN(I4)',2X,'TLN(I5)',/)
C*****
      DO 10 I=0, KK
C
      DO 20 J=0, NN
C
      IF(I.EQ.0) THEN
C***** Initialising data at No.0 stand *****
C
      PXE(I,J)=BB*J
      PYE(I,J)=-DH(I)
      TLE(I,J)=BB*(J+1)
      ANE(I,J)=0.0
      EZ(I,J)=0.0
      EX(I,J)=0.0
      DEZ(I,J)=0.0
      DEX(I,J)=0.0
      DB(I,J)=BB
      DLZ(I,J)=200.0
      DZ(I,J)=200.0
      GO TO 20
C
      ELSE IF(J.EQ.0) THEN
      PXE(I,J)=0.0
      PYE(I,J)=-DH(I)
      ANE(I,J)=0.0
      ELSE
      ENDIF
C
      DZ(I,J)=LS(I)
      DLZ(I,J)=DSQRT(DZ(I,J)**2+(PXE(I,J)-PXE(I-1,J))**2+
% (PYE(I,J)-PYE(I-1,J))**2)
      RX=DZ(I,J)/DZ(I-1,J)
      DEZ(I,J)=DLOG(DLZ(I,J)/(DLZ(I-1,J)*RX))
      DEX(I,J)=-BL*DEZ(I,J)
      EZ(I,J)=EZ(I-1,J)+DEZ(I,J)
      EX(I,J)=EX(I-1,J)+DEX(I,J)
C
      DB(I,J)=DB(I-1,J)*DEXP(DEX(I,J))
C
      IF(DEZ(I,J).GT.HDEZ) HDEZ=DEZ(I,J)
      IF(EZ(I,J).GT.HEZ) HEZ=EZ(I,J)
      IF(DEX(I,J).LT.SDEX) SDEX=DEX(I,J)
      IF(EX(I,J).GT.HEX) HEX=EX(I,J)
      IF(EX(I,J).LT.SEX) SEX=EX(I,J)
C
      IF(J.EQ.0) THEN
      TLE(I,J)=DB(I,J)
      ELSE
      TLE(I,J)=TLE(I,J-1)+DB(I,J)
      ENDIF
C*****
C
      WRITE(*,25)I,J,RN(I,4),RN(I,5),DB(I,J),TLE(I,J),TLN(I,2),
      %TLN(I,3),TLN(I,4),TLN(I,5)
      25 FORMAT(/,I2,2X,I2,2X,F10.3,2X,F7.2,2X,F7.3,2X,F7.2,2X,F7.2,
      %2X,F7.2,2X,F7.2,2X,F7.2)
C*****
      IF(TLE(I,J).LE.TLN(I,1)) THEN
C*****
C      WRITE(*,502)TLE(I,J),TLN(I,1)
C      502 FORMAT(/,5X,'PART(1)',4X,'TLE(I,J)=' ,F10.4,4X,
C      %'TLN(I,1)=' ,F10.4,/)
C*****
C
      ANEZ=TLE(I,J)/(RN(I,1)*PE)

```

```

C
C*****
C   WRITE(*,504)ANE2,RN(I,1),PE
C 504 FORMAT(/,2X,'ANE2=',F10.4,4X,'RN(I,1)=' ,F10.4,4X,
C   %'PE=' ,F15.10,/)
C   WRITE(*,*)'-----INPUT ZERO TO ADVANCE. -----'
C   READ*,NNK
C*****
C   PX2=FNS1(RN(I,1),ANE2)
C   PY2=FNC1(RN(I,1),ANE2)-DH(I)
C
C   GO TO 30
C
C   ELSE IF(TLE(I,J).LE.TLN(I,2)) THEN
C*****
C   WRITE(*,506)TLE(I,J),TLN(I,1),TLN(I,2)
C 506 FORMAT(/,5X,'PART(2)',4X,'TLE(I,J)=' ,F10.4,4X,
C   %'TLN(I,1)' ,F10.4,4X,'TLN(I,2)=' ,F10.4,/)
C*****
C
C   ANE2=(TLE(I,J)-TLN(I,1))/(RN(I,2)*PE)+AAN(I,1)
C
C*****
C   WRITE(*,507)ANE2,RN(I,2),PE
C 507 FORMAT(/,2X,'ANE2=' ,F10.4,4X,'RN(I,2)=' ,F10.4,4X,
C   %'PE=' ,F15.10,/)
C   WRITE(*,*)'-----INPUT ZERO TO ADVANCE. -----'
C   READ*,NNK
C
C   PX2=FNS2(RN(I,1),RN(I,2),AN(I,1))+FNS1(RN(I,2),ANE2)
C   PY2=FNC1(RN(I,1),AN(I,1))+FNC2(RN(I,2),AN(I,1),ANE2)-DH(I)
C   GO TO 30
C*****
C   ELSE IF(TLE(I,J).LE.TLN(I,3)) THEN
C*****
C   WRITE(*,508)TLE(I,J),TLN(I,3)
C 508 FORMAT(/,5X,'PART(3)',4X,'TLE(I,J)=' ,F10.4,4X,
C   %'TLN(I,3)=' ,F10.4,/)
C*****
C
C   ANE2=(TLE(I,J)-TLN(I,2))/(RN(I,3)*PE)+AAN(I,2)
C
C*****
C   WRITE(*,510)ANE2,RN(I,3),PE
C 510 FORMAT(/,2X,'ANE2=' ,F10.4,4X,'RN(I,3)=' ,F10.4,4X,
C   %'PE=' ,F15.10,/)
C   WRITE(*,*)'-----INPUT ZERO TO ADVANCE. -----'
C   READ*,NNK
C*****
C   PX2=FNS2(RN(I,1),RN(I,2),AN(I,1))+FNS2(RN(I,2),RN(I,3),AAN(I,2))+
C   %FNS1(RN(I,3),ANE2)
C   PY2=FNC1(RN(I,1),AN(I,1))+FNC2(RN(I,2),AN(I,1),AAN(I,2))+
C   %FNC2(RN(I,3),AAN(I,2),ANE2)-DH(I)
C   GO TO 30
C
C   ELSE IF(TLE(I,J).LE.TLN(I,4)) THEN
C
C   ANE2=(TLE(I,J)-TLN(I,3))/(RN(I,4)*PE)+AAN(I,3)
C   PX2=FNS2(RN(I,1),RN(I,2),AN(I,1))+FNS2(RN(I,2),RN(I,3),AAN(I,2))+
C   %FNS2(RN(I,3),RN(I,4),AAN(I,3))+FNS1(RN(I,4),ANE2)
C   PY2=FNC1(RN(I,1),AN(I,1))+FNC2(RN(I,2),AN(I,1),AAN(I,2))+
C   %FNC2(RN(I,3),AAN(I,2),AAN(I,3))+FNC2(RN(I,4),AAN(I,3),ANE2)-DH(I)
C   GO TO 30
C
C   ELSE IF(TLE(I,J).GT.TLN(I,4)) THEN

```

```

ANEZ=(TLE(I,J)-TLN(I,4))/(RN(I,5)*PE)+AAN(I,4)
PX2=FNS2(RN(I,1),RN(I,2),AN(I,1))+FNS2(RN(I,2),RN(I,3),AAN(I,2))+
%FNS2(RN(I,3),RN(I,4),AAN(I,3))+FNS2(RN(I,4),RN(I,5),AAN(I,4))+
%FNS1(RN(I,5),ANEZ)
PY2=FNC1(RN(I,1),AN(I,1))+FNC2(RN(I,2),AN(I,1),AAN(I,2))+
%FNC2(RN(I,3),AAN(I,2),AAN(I,3))+FNC2(RN(I,4),AAN(I,3),AAN(I,4))+
%FNC2(RN(I,5),AAN(I,4),ANEZ)-DH(I)
GO TO 30

```

```

C
ELSE

```

```

-----
WRITE(*,100)
100 FORMAT(/,'$$$$$ Error happened in the calculation of divided',
%' points',/, ' in subroutine SNANAZ. $$$$$$',/)
STOP
-----

```

```

C
ENDIF

```

```

C
C*****

```

```

C 30 IF(I.GE.N1F)THEN
C WRITE(*,500) TLE(I,J),RN(I,1),ANEZ
C 500 FORMAT(/,4X,'TLE(I,J)=',F10.4,4X,'RN(I,1)=',F10.4,4X,
C %'ANEZ=',F10.4,/)
C WRITE(*,*)'*** INPUT ZERO(0) TO ADVANCE. ****'
C READ*,NKK
C ELSE
C ENDF

```

```

C*****

```

```

30 ANE(I,J+1)=ANEZ
PXE(I,J+1)=PX2
PYE(I,J+1)=PY2

```

```

C
20 CONTINUE

```

```

C
IF(I.EQ.0) GO TO 10

```

```

C
WRITE(*,*)'*****'

```

```

C
C*****
C** Consideration of Fin-pass Reduction (17th Sept. 1992) **
C*****

```

```

C
IF(I.LT.N1F) GO TO 12

```

```

C
TLE2=2*TLE(I,NN-1)
IF(TLE2.LE.TLN1(I)) GO TO 12

```

```

C
C**** Calculation of Fin-pass Reduction ****

```

```

C
FRD(I)=DLOG(TLE2/TLN1(I))

```

```

C
WRITE(*,62)
62 FORMAT(1H1,X,'I',3X,'J',2X,'FRD(I)',3X,'DBO(I,J)',3X,'DB(I,J)',
%2X,'TLE0(I,J)',2X,'TLE(I,J)',3X,'TLN1(I)/2',/)

```

```

C
DO 60 J=0,NN

```

```

C
DEXF(I,J)=-FRD(I)
DEZF(I,J)=-RSF*DEXF(I,J)

```

```

C
DEZ(I,J)=DEZ(I,J)+DEZF(I,J)
DEX(I,J)=DEX(I,J)+DEXF(I,J)

```

```

C
EZ(I,J)=EZ(I,J)+DEZF(I,J)
EX(I,J)=EX(I,J)+DEXF(I,J)

```

```

C

```

```

DBO(I,J)=DB(I,J)
DB(I,J)=DB(I,J)/DEXP(FRD(I))
TLEO(I,J)=TLE(I,J)
TLE(I,J)=TLE(I,J)/DEXP(FRD(I))
C
IF(DEZ(I,J).GT.HDEZ) HDEZ=DEZ(I,J)
IF(EZ(I,J).GT.HEZ) HEZ=EZ(I,J)
IF(DEX(I,J).LT.SDEX) SDEX=DEX(I,J)
IF(EX(I,J).GT.HEX) HEX=EX(I,J)
IF(EX(I,J).LT.SEX) SEX=EX(I,J)
C
IF(TLE(I,J).LE.TLN(I,1)) THEN
C
ANEZ=TLE(I,J)/(RN(I,1)*PE)
PX2=FNS1(RN(I,1),ANEZ)
PY2=FNC1(RN(I,1),ANEZ)-DH(I)
GO TO 65
C
ELSE IF(TLE(I,J).LE.TLN(I,2)) THEN
C
ANEZ=(TLE(I,J)-TLN(I,1))/(RN(I,2)*PE)+AAN(I,1)
PX2=FNS2(RN(I,1),RN(I,2),AN(I,1))+FNS1(RN(I,2),ANEZ)
PY2=FNC1(RN(I,1),AN(I,1))+FNC2(RN(I,2),AN(I,1),ANEZ)-DH(I)
GO TO 65
C
ELSE IF(TLE(I,J).LE.TLN(I,3)) THEN
C
ANEZ=(TLE(I,J)-TLN(I,2))/(RN(I,3)*PE)+AAN(I,2)
PX2=FNS2(RN(I,1),RN(I,2),AN(I,1))+FNS2(RN(I,2),RN(I,3),AAN(I,2))+
%FNS1(RN(I,3),ANEZ)
PY2=FNC1(RN(I,1),AN(I,1))+FNC2(RN(I,2),AN(I,1),AAN(I,2))+
%FNC2(RN(I,3),AAN(I,2),ANEZ)-DH(I)
GO TO 65
C
ELSE IF(TLE(I,J).LE.TLN(I,4)) THEN
C
ANEZ=(TLE(I,J)-TLN(I,3))/(RN(I,4)*PE)+AAN(I,3)
PX2=FNS2(RN(I,1),RN(I,2),AN(I,1))+FNS2(RN(I,2),RN(I,3),AAN(I,2))+
%FNS2(RN(I,3),RN(I,4),AAN(I,3))+FNS1(RN(I,4),ANEZ)
PY2=FNC1(RN(I,1),AN(I,1))+FNC2(RN(I,2),AN(I,1),AAN(I,2))+
%FNC2(RN(I,3),AAN(I,2),AAN(I,3))+FNC2(RN(I,4),AAN(I,3),ANEZ)-DH(I)
GO TO 65
C
ELSE IF(TLE(I,J).GT.TLN(I,4)) THEN
C
ANEZ=(TLE(I,J)-TLN(I,4))/(RN(I,5)*PE)+AAN(I,4)
PX2=FNS2(RN(I,1),RN(I,2),AN(I,1))+FNS2(RN(I,2),RN(I,3),AAN(I,2))+
%FNS2(RN(I,3),RN(I,4),AAN(I,3))+FNS2(RN(I,4),RN(I,5),AAN(I,4))+
%FNS1(RN(I,5),ANEZ)
PY2=FNC1(RN(I,1),AN(I,1))+FNC2(RN(I,2),AN(I,1),AAN(I,2))+
%FNC2(RN(I,3),AAN(I,2),AAN(I,3))+FNC2(RN(I,4),AAN(I,3),AAN(I,4))+
%FNC2(RN(I,5),AAN(I,4),ANEZ)-DH(I)
GO TO 65
C
ELSE
C-----
WRITE(*,102)
102 FORMAT(/,'$$$$$ Error happened in the calculation of divided',
%' points',/, ' in subroutine SNANA2. $$$$$$',/)
STOP
C-----
ENDIF
C
65 ANE(I,J+1)=ANEZ
PXE(I,J+1)=PX2
PYE(I,J+1)=PYZ

```

```

C      WRITE(*,64)I,J,FRD(I),DBO(I,J),DB(I,J),TLEO(I,J),TLE(I,J),
%      TLN1(I)/2
64 FORMAT(/,I2,2X,I2,2X,5(2X,F10.3),4X,F10.3)
C
60 CONTINUE
C
12 WRITE(*,*)'@@@@@@@@@@@@@@@@@@@@@@@@@@@@@@@@@@@@@@@@@@@@@@@@@@@@@@@@@@@@'.
C
10 CONTINUE
C
      RETURN
      END
C-----
-----
C*****
*****
C*****
*****
C
C*****
*****
C** THIS SUBROUTINE IS FOR 3-D DRAWING OF RESULTS BY STRESS-STRAIN ANALYSIS MODEL-2. *****
C*****
*****
C
C***** SUBROUTINE DRAW3D2 *****
C
      SUBROUTINE DRAW3D2(HDEZ,HEZ,SDEX,HEX,SEX,HDSZ,SDSZ,HSZ,SSZ,HSX,
%SSX,HSOTOS,PHDSZ,PSDSZ,PHSZ,PSSZ,PHSX,PSSX,PHSOTO,FILE1,FILE2,
%MM,SIZE,DATE,DRAWER,WORKS,MATERIAL)
C
      IMPLICIT REAL*8(A-H,L,O-Z), INTEGER*4(I-K,M-N)
      CHARACTER FILE1*12,FILE2*12,SIZE*14,DATE*10,DRAWER*12,WORKS*12,
%      MATERIAL*12
C
C
      COMMON/DAT1/ LS(0:26),TLS(0:26),DH(0:25),NR(0:25),R(0:25,5),
%      AN(0:25,5)
      COMMON/DAT2/ D, WS, TS, KK, NN
      COMMON/DAT4/ PE, ITD, IDH, IIDH, JF
      COMMON/DAT5/ TLO(0:25),TLN1(0:25), AH(0:25), AW(0:25), WE(0:25),
%      AWY(0:25)
      COMMON/POINT2/ PXE(0:25,-22:22),PYE(0:25,-22:22),PZ(0:25),
%      DB(0:25,0:21),TLE(0:25,0:21),ANE(0:25,0:22)
      COMMON/STA3/ PDEZ(0:25,-20:20),PEZ(0:25,-20:20),
%      PDEX(0:25,-20:20),PEX(0:25,-20:20)
%      /STA3A/ PEZE(0:25,0:20),PEXE(0:25,0:20),PEZP(0:25,0:20),
%      PEXP(0:25,0:20),PDEPSO(0:25,0:20)
      COMMON/STS1/ DSZ(0:25,-20:20),DSX(0:25,-20:20),SZ(0:25,-20:20),
%      SX(0:25,-20:20),SEQ(0:25,-20:20),
%      SOTOS(0:25,-20:20),EZE(0:25,0:20),EXE(0:25,0:20),
%      NHANT(0:25,0:20),EZP(0:25,0:20),EXP(0:25,0:20)
      COMMON/STS4/ PDSZ(0:25,-20:20),PDSX(0:25,-20:20),
%      PSZ(0:25,-20:20),PSX(0:25,-20:20),
%      PSEQ(0:25,-20:20),PSOTOS(0:25,-20:20),
%      /STS4A/ PDWE(0:25,0:20),PDWP(0:25,0:20),PDW(0:25,0:20),
%      PDWT(0:25,0:20),PWT(0:25),PWTR(0:25),
%      PSWT(0:25),PSWTR
      DIMENSION XX(-20:20)
C
      WRITE(*,450)FILE1,FILE2
450 FORMAT(///,5X,'FILE1=',A12,/,5X,'FILE2=',A12,///)
C
      WRITE(*,260)
260 FORMAT(/4X,'*****',

```



```

%4X,      ***
%4X,      *** 3-DIMENSIONAL DRAWING OF THE RESULTS OF ***
%4X,      *** STRESS-STRAIN ANALYSIS MODEL-2 ***
%4X,      ***
%4X,      *****'///)
C
C*****THIS COMAND MAKE THE TIME TO DISPLAY THE ABOVE DESCRIPTION. *****
WRITE(*,266)
266 FORMAT(/4X,'**** INPUT ZERO(0) TO ADVANCE FURTHER STEP. ****'/)
READ*,JA
C
C***** CALL GINO GRAPHIC PACAGE *****
C
CALL GINO
CALL T4510
CALL T4107
CALL UNITS(1.0)
CALL TRANSF(2)
CALL PICCLE
GO TO 998
C
99 CALL SCALE(1.0/SA)
CALL TRANSF(2)
C
998 WRITE(*,100)
100 FORMAT(/4X,'*****',
%4X,      '** CHOOSE A ITEM THAT YOU WANT TO DRAW. **',
%4X,      '**
%4X,      '** 1. 3-DIMENSIONAL DEFORMED SURFACE --> 1 **',
%4X,      '** 2. STRAIN(Ez and Ex) --> 2 **',
%4X,      '** 3. INCREMENT STRAIN(dEz and DEx) --> 3 **',
%4X,      '** 4. STRESS (Sz and Sx)Unit=[MPa] --> 4 **',
%4X,      '** 5. STRESS (Sz and Sx)Unit=[kgf/mm2]--> 5 **',
%4X,      '** 6. STRESS INCREMENT(DSz and DSx)
%4X,      '** Unit=[MPa] --> 6 **',
%4X,      '** 7. STRESS INCREMENT(DSz and DSx)
%4X,      '** Unit=[kgf/mm2]--> 7 **',
%4X,      '** 8. EQUIVALENT STRESS Unit=[MPa] --> 8 **',
%4X,      '** 9. EQUIVALENT STRESS Unit=[kgf/mm2]--> 9 **',
%4X,      '** 0. FINISH --> 0 **',
%4X,      '**
%4X,      *****'///)
PRINT*,'----- INPUT ONE NUMBER FROM 0 TO 9. -----'
READ*,JN
IF(JN.EQ.0) GO TO 400
C
C
IF(JN.EQ.1.) THEN
NF=31
ELSE IF(JN.EQ.2.OR.JN.EQ.3) THEN
NF=32
ELSE IF(JN.EQ.4.OR.JN.EQ.5) THEN
NF=33
ELSE IF(JN.EQ.6.OR.JN.EQ.7) THEN
NF=34
ELSE IF(JN.EQ.8.OR.JN.EQ.9) THEN
NF=35
ELSE
ENDIF
GO TO 98
C
96 CALL SCALE(1.0/SA)
CALL TRANSF(2)
IF(JS.EQ.1) THEN
GO TO 98
ELSE IF(JS.EQ.2) THEN

```

```

GO TO 97
ELSE
ENDIF

```

C

```

98 WRITE(*,102)
102 FORMAT(/4X,'*****',
%/4X,      '** INPUT THE ANGLE OF PITCH, HEADING AND **',
%/4X,      '**   BANK OF THE AXIS OF X, Y AND Z.   **',
%/4X,      '** BANK:Rotation of Z-axis(longitudinal) **',
%/4X,      '** HEADING:Rotation of Y-axis(height)  **',
%/4X,      '** PITCH:Rotation of X-axis(width)     **',
%/4X,      '**<Newly first Input>                       **',
%/4X,      '** 1. Input or change when you newly   --->1 **',
%/4X,      '**       input the data(ITD=1)                 **',
%/4X,      '**<Call existing data>                       **',
%/4X,      '** 2. Call the data from existing file -->2 **',
%/4X,      '** 3. Change data in existing file   --->3 **',
%/4X,      '**       Before change, you must choose No.2 **',
%/4X,      '**<Call existing data and create new file> **',
%/4X,      '** 4. Call the data from existing file -->4 **',
%/4X,      '**       and transfer them to the new file   **',
%/4X,      '** 5. Input or change when the data   --->5 **',
%/4X,      '**       were called from existing file       **',
%/4X,      '**       and create new file (ITD=2 AND JF=1) **',
%/4X,      '**<Call the data from newly created file> **',
%/4X,      '** 6. Call the data from new file     --->6 **',
%/4X,      '**       that was created in No.4 and No.5   **',
%/4X,      '*******'/)
PRINT*, '**--- INPUT THE PERMISSIBLE NUMBER FROM 1 TO 6. ---**'
READ*, JM

```

C

```
IF (JM.EQ.6) GO TO 888
```

C

```
WRITE(*,*)'$$$$ OPEN FILE $$$$$$'
```

C

```
WRITE(*,*)'***** INPUT ZERO TO ADVANCE *****'
```

C

```
READ*,NS
```

C

C

```

OPEN(31,FILE='H1'//FILE1,STATUS='UNKNOWN')
OPEN(32,FILE='H2'//FILE1,STATUS='UNKNOWN')
OPEN(33,FILE='H3'//FILE1,STATUS='UNKNOWN')
OPEN(34,FILE='H4'//FILE1,STATUS='UNKNOWN')
OPEN(35,FILE='H5'//FILE1,STATUS='UNKNOWN')

```

C

```
IF(JM.EQ.1.OR.JM.EQ.3.OR.JM.EQ.5) THEN
```

```
WRITE(*,104)
```

```
104 FORMAT(/4X,'*****',
```

```
%/10X,'Bank of Z-axis(deg.)=')
```

```
READ*,ABZ1
```

```
ABZ=ABZ1*PE
```

```
WRITE(*,106)
```

```
106 FORMAT(/10X,'Heading of Y-axis(deg.)=')
```

```
READ*,AHY1
```

```
AHY=AHY1*PE
```

```
WRITE(*,108)
```

```
108 FORMAT(/10X,'Pitch of X-axis(deg.)=')
```

```
READ*,APX1
```

```
APX=APX1*PE
```

C

```
ELSE IF((JM.EQ.2.OR.JM.EQ.4).AND.ITD.EQ.2) THEN
```

C

```
C***** CALL THE DATA FROM THE EXISTING FILE *****
```

C

```
REWIND NF
```

```
READ(NF,601)ABZ1,AHY1,APX1
```

```
ABZ=ABZ1*PE
```

```

    AHY=AHY1*PE
    APX=APX1*PE
C
601 FORMAT(1H1,///5X,3(F10.6,5X)//)
    ELSE IF (JM.EQ.2.AND.ITD.EQ.1) THEN
    PRINT 220
220 FORMAT(4X,'*** INPUT THE No. 1 BECAUSE OF ITD=1. ***'//)
    GO TO 98
    ELSE
    PRINT 222
222 FORMAT(4X,'*** INPUT THE PERMISSIBLE No. FROM 1 TO 2,AGAIN. ***'//)
    GO TO 98
    ENDIF
C***** CALL THE DATA FROM THE EXISTING FILE *****
IF(J5.EQ.1) GO TO 300
IF((JM.EQ.2.OR.JM.EQ.4).AND.ITD.EQ.2) THEN
C
    READ(NF,602)SZX,SZY
602 FORMAT(/5X,F10.4,5X,F10.4//)
    JP=0
C
    CLOSE(31,STATUS='KEEP')
    CLOSE(32,STATUS='KEEP')
    CLOSE(33,STATUS='KEEP')
    CLOSE(34,STATUS='KEEP')
    CLOSE(35,STATUS='KEEP')
C
    GO TO 300
    ELSE
C
97 WRITE(*,110)
110 FORMAT(/4X,'*****',
%/4X, '*** Input the scale ratio of Z-axis vs X-axis and ***',
%/4X, '*** of Z-axis vs Y-axis. ***',
%/4X, '*** ***',
%/4X, '*** 1. Input or change when you newly ---> 1 ***',
%/4X, '*** input the data(ITD=1) ***',
%/4X, '*** 2. Change the data in existing file ---> 2 ***',
%/4X, '*** 3. Input or change when the data ---> 3 ***',
%/4X, '*** were called from existing file ***',
%/4X, '*** and create new file(ITD=2 AND JF=1) ***',
%/4X, '*****'//)
    PRINT*, '***--- INPUT THE PERMISSIBLE NUMBER FROM 1 TO 3. ---***'
    READ*, JP
    WRITE(*,111)
111 FORMAT(/4X,'*****',
%/10X,'The Scale ratio of Z-axis vs X-axis:(Zscale/Xscale)=')
    READ*,SZX
    WRITE(*,112)
112 FORMAT(/10X,'The Scale ratio of Z-axis vs Y-axis:',
%/10X,'(Zscale/Yscale)=')
    READ*,SZY
    ENDIF
    GO TO 300
C***** Call the data from newly created file. *****
C
888 OPEN(41,FILE='H1'//FILE2,STATUS='UNKNOWN')
    OPEN(42,FILE='H2'//FILE2,STATUS='UNKNOWN')
    OPEN(43,FILE='H3'//FILE2,STATUS='UNKNOWN')
    OPEN(44,FILE='H4'//FILE2,STATUS='UNKNOWN')
    OPEN(45,FILE='H5'//FILE2,STATUS='UNKNOWN')
C
    IF(NF.EQ.11) THEN
    NH=41
C
    ELSE IF(NF.EQ.12) THEN

```

```

      NH=42
C
      ELSE IF(NF.EQ.13) THEN
      NH=43
C
      ELSE: IF(NF.EQ.14) THEN
      NH=44
C
      ELSE IF(NF.EQ.15) THEN
      NH=45
      ELSE
      ENDIF
C
      REWIND NH
      READ(NH,601)ABZ1,AHY1,APX1
      READ(NH,602)SZX,SZY
C
      CLOSE(41,STATUS='KEEP')
      CLOSE(42,STATUS='KEEP')
      CLOSE(43,STATUS='KEEP')
      CLOSE(44,STATUS='KEEP')
      CLOSE(45,STATUS='KEEP')
C
C***** Max.Height of the flower in all stands *****
      300 HM=0.0
      DO 15 I=0,KK
      IF(AH(I).GT.HM) HM=AH(I)
      15 CONTINUE
C
C***** DISTANCE OF PLOTTING AT X-AXIS WHEN STRESS OR STRAIN IS PLOTTED. *****
C
      DO 17 J=-20,20
      XX(J)=(D/NN)*J
      17 CONTINUE
C
C***** MAKING THE DATA OF POINTS IN THE MINUS REAGION *****
C
      DO 10 I=0,KK
C
      DO 20 J=1,NN
C
      PXE(I,-J)=-PXE(I,J)
      PYE(I,-J)=-PYE(I,J)
C
      PEZ(I,-J)=PEZ(I,J)
      PEX(I,-J)=PEX(I,J)
C
      PDEZ(I,-J)=PDEZ(I,J)
      PDEX(I,-J)=PDEX(I,J)
C
      DSZ(I,-J)=DSZ(I,J)
      DSX(I,-J)=DSX(I,J)
      PDSZ(I,-J)=PDSZ(I,J)
      PDSX(I,-J)=PDSX(I,J)
      SZ(I,-J)=SZ(I,J)
      SX(I,-J)=SX(I,J)
      PSZ(I,-J)=PSZ(I,J)
      PSX(I,-J)=PSX(I,J)
      SOTOS(I,-J)=SOTOS(I,J)
      PSOTOS(I,-J)=PSOTOS(I,J)
      SEQ(I,-J)=SEQ(I,J)
      PSEQ(I,-J)=PSEQ(I,J)
      20 CONTINUE
      10 CONTINUE
C
C***** DEFINITION OF 0 POINT AND A SCALE *****

```

```

C
  XV=119.0
  YV=95.0
C
  CALL SHIFT2(XV,YV)
C
C***** SCALE TO DRAWING *****
C
  AAR=239.0/(1.4*TLS(KK))
  AAR=AAR*10000
  AAR=IDINT(AAR)
  SA=AAR/10000
  ZL=TLS(KK)
C
  CALL SCALE(SA)
C
C
C
  JT=0
  JD=0
C
C***** DRAWING FRAME OF 3-D GRAPHICS *****
C*****CALL SUBROUTINE FRAME2 *****
C
  64 CALL FRAME2(SA,XV,YV)
C
  CALL LINCOL(2)
  JL=1
  JU=0
C
  DO 30 I=0, KK
C
  DO 40 J=-NN, NN, 1
C
  80 IF(JT.EQ.0) THEN
    GO TO(1,2,3,4,5,6,7,8,9), JN
  ELSE IF(JT.NE.0) THEN
    GO TO (52,53,54,55,56,57), JT
  ELSE
    ENDIF
C
  WRITE(*,*)'*** INPUT ERROR. INPUT THE CORRECT NUMBER, AGAIN. ****'
  GO TO 99
C
C***** 3D.DEFORMED SURFACE *****
C
  1 X=PXE(I,J)*ZL/(SZX*D)
  Y=(PYE(I,J)-HM/2.0)*ZL/(SZY*D)
  Z=PZ(I)
  GO TO 50
C
C***** STRAIN *****
C
  2 Y=PEZ(I,J)*ZL/(SZY*DABS(HEZ))
  GO TO 48
C
  52 Y=PEX(I,J)*ZL/(SZY*DABS(HEZ))
  GO TO 48
C
C***** INCREMENT STRAIN *****
C
  3 Y=PDEZ(I,J)*ZL/(SZY*DABS(HDEZ))
  GO TO 48
C
  53 Y=PDEX(I,J)*ZL/(SZY*DABS(HDEZ))
  GO TO 48

```

```

C
C***** STRESS Unit=(MPa) *****
C
  4 Y=PSZ(I,J)*ZL/(SZY*DABS(PHSZ-PSSZ))
    GO TO 48
C
  54 Y=PSX(I,J)*ZL/(SZY*DABS(PHSZ-PSSZ))
    GO TO 48
C
C***** STRESS Unit(kgf/mm2) *****
C
  5 Y=SZ(I,J)*ZL/(SZY*DABS(HSZ-SSZ))
    GO TO 48
C
  55 Y=SX(I,J)*ZL/(SZY*DABS(HSZ-SSZ))
    GO TO 48
C
C***** STRESS INCREMENT Unit=(MPa) *****
C
  6 Y=PDSZ(I,J)*ZL/(SZY*DABS(PHDSZ-PSDSZ))
    GO TO 48
C
  56 Y=PDSX(I,J)*ZL/(SZY*DABS(PHDSZ-PSDSZ))
    GO TO 48
C
C***** STRESS INCREMENT Unit=(kgf/mm2) *****
C
  7 Y=DSZ(I,J)*ZL/(SZY*DABS(HDSZ-SDSZ))
    GO TO 48
C
  57 Y=DSX(I,J)*ZL/(SZY*DABS(HDSZ-SDSZ))
    GO TO 48
C
C***** EQUIVALENT STRESS Unit=(MPa) *****
C
  8 Y=PSOTOS(I,J)*ZL/(SZY*DABS(PHSOTO))
    GO TO 48
C
C***** EQUIVALENT STRESS Unit=(kgf/mm2) *****
C
  9 Y=SOTOS(I,J)*ZL/(SZY*DABS(HSOTOS))
    GO TO 48
C
  48 X=XX(J)*ZL/(SZX*D)
    Z=PZ(I)
C
C***** ROTATION OF Z-AXIS/ BANK *****
  50 XA=X*COS(ABZ)-Y*SIN(ABZ)
    YA=X*SIN(ABZ)+Y*COS(ABZ)
    X=XA
    Y=YA
C
C***** ROTATION OF Y-AXIS/ HEADING *****
  ZA=Z*COS(AHY)-X*SIN(AHY)
  XA=Z*SIN(AHY)+X*COS(AHY)
  Z=ZA
  X=XA
C
C***** ROTATION OF X-AXIS/ PITCH *****
  ZA= Z*COS(APX)+Y*SIN(APX)
  YA=-Z*SIN(APX)+Y*COS(APX)
  Z=ZA
  Y=YA
C
  GO TO (74,76,78,79),JU
  IF(JL.EQ.2) GO TO 62

```

```

C
C***** DRAWING THE LINE IN THE CIRCUMFERENTIAL DIRECTION *****
C
    IF(J.EQ.-NN) THEN
    CALL MOVTO2(X,Y)
    ELSE
    CALL LINTO2(X,Y)
    ENDIF
40 CONTINUE
30 CONTINUE
C
C***** DRAWING THE LINE IN THE LONGITUDINAL DIRECTION *****
C
    JL=2
C
    DO 60 J=-NN,NN,1
C
    DO 70 I=0, KK
    GO TO 80
C
62 IF(I.EQ.0) THEN
    CALL MOVTO2(X,Y)
    GO TO 70
    ELSE IF(J.EQ.-NN.OR.J.EQ.NN) THEN
    CALL LINCOL(2)
    ELSE IF(J.EQ.0) THEN
    CALL LINCOL(5)
    ELSE
    CALL LINCOL(6)
    ENDIF
    CALL LINTO2(X,Y)
C
70 CONTINUE
60 CONTINUE
C
    IF(JN.NE.1) GO TO 72
    IF(D.LE.100.0) THEN
        ZU=400.0
        XU=50.0
        YU=50.0
    ELSE IF(D.LE.400) THEN
        ZU=700.0
        XU=100.0
        YU=100.0
    ELSE
        ZU=1000.0
        XU=500.0
        YU=500.0
    ENDIF
C
    JU=1
C
    X1=-XU*ZL/(SZX*D)
    Y1=(YU-HM/2.0)*ZL/(SZY*D)
    Z1=-1.5*ZU+PZ(0)
C
    X=0.0
    Y=(0.0-HM/2.0)*ZL/(SZY*D)
    Z=Z1
    CALL LINCOL(3)
    GO TO 50
C
74 XB=X
    YB=Y
    CALL MOVTO2(XB,YB)
    JU=2

```

```

X=X1
Y=(0.0-HM/2.0)*ZL/(SZY*D)
Z=Z1
GO TO 50
C
76 CALL LINT02(X,Y)
JU=3
CALL MOVT02(XB,YB)
X=0.0
Y=Y1
Z=Z1
GO TO 50
C
78 CALL LINT02(X,Y)
JU=4
CALL MOVT02(XB,YB)
X=0.0
Y=(0.0-HM/2.0)*ZL/(SZY*D)
Z=-0.5*ZU+PZ(0)
GO TO 50
79 CALL LINT02(X,Y)
JD=1
72 CALL CHAMOD
C
C***** CALL SUBROUTINE TITLE3 TO DRAW THE TITLE BOCKS *****
C
CALL TITLE3(JN,SA,XV,YV,FILE1,FILE2,SIZE,DATE,DRAWER,WORKS,
% MATERIAL,MM,JT,ABZ1,AHY1,APX1,SZX,SZY,ITD,JF)
C
C***** CALL SUBROUTINE LINE TO DRAW THE SCALE LINE *****
C
CALL LINE
C
PRINT200
200 FORMAT(4X,'** INPUT 0(ZERO) TO GO TO FURTHER SETP. **/')
READ*,JZ
WRITE(*,202) JZ
202 FORMAT(5X,'JZ=',I3/)
CALL PICCLE
C
IF(JD.EQ.1) GO TO 232
IF(JN.EQ.2) THEN
JT=1
JD=1
GO TO 64
ELSE IF(JN.EQ.3) THEN
JT=2
JD=1
GO TO 64
ELSE IF(JN.EQ.4) THEN
JT=3
JD=1
GO TO 64
ELSE IF(JN.EQ.5) THEN
JT=4
JD=1
GO TO 64
ELSE IF(JN.EQ.6) THEN
JT=5
JD=1
GO TO 64
ELSE IF(JN.EQ.7) THEN
JT=6
JD=1
GO TO 64
ELSE

```


ENDIF

C

```
232 WRITE(*,230)
230 FORMAT(/4X, '*****',
%4X, '**',
%4X, '** DO YOU WANT TO CHANGE THE DATA **',
%4X, '** AS SHOWN BELOW. **',
%4X, '** INPUT THE NUMBER **',
%4X, '**',
%4X, '** 1.ANGLE OF PITCH,HEADING AND BANK ---> 1 **',
%4X, '** 2.SCALE RATIO OF Z VS X AND Z VS Y ---> 2 **',
%4X, '** 3.NO CHANGE (TO STORE ---> 3 **',
%4X, '** THE UP-TO-DATE DATA TO THE FILE) **',
%4X, '** 4.NO CHANGE (NOT TO STORE ---> 4 **',
%4X, '** THE UP-TO-DATE DATA TO THE FILE) **',
%4X, '** 5.FINISH ---> 5 **',
%4X, '*****//)
PRINT*, '**--- INPUT THE PERMISSIBLE NUMBER FROM 1 TO 5. ---**'
READ*, JS
IF(JS.EQ.1) GO TO 96
IF(JS.EQ.2) GO TO 96
IF(JS.EQ.3) GO TO 302
IF(JS.EQ.4) GO TO 99
IF(JS.EQ.5) GO TO 400
```

C

```
PRINT*, '** INPUT YHE PERMISSIBLE No.,AGAIN. *****'
GO TO 232
```

C

```
302 WRITE(*,304)
304 FORMAT(/4X, '** YOU HAVE COMPLETED THE DRAWING OF THE DATA. **',
%4X, '** THE DATA IS WRITTEN TO G FILE. *****'//)
```

C

```
IF(JM.EQ.2) THEN
PRINT*, '**** You must choose No.4. ****'
GO TO 232
ELSE
ENDIF
```

C

```
IF(JM.EQ.6) THEN
PRINT*, '@@ You cannot store it and choose No.4. @@'
GO TO 232
ELSE
ENDIF
```

C

```
IF(JM.EQ.4.OR.JM.EQ.5.OR.JP.EQ.3) GO TO 350
```

C

```
OPEN(31,FILE='H1'//FILE1,STATUS='UNKNOWN')
OPEN(32,FILE='H2'//FILE1,STATUS='UNKNOWN')
OPEN(33,FILE='H3'//FILE1,STATUS='UNKNOWN')
OPEN(34,FILE='H4'//FILE1,STATUS='UNKNOWN')
OPEN(35,FILE='H5'//FILE1,STATUS='UNKNOWN')
```

C

```
IF(NF.EQ.31) THEN
NH=31
```

C

```
ELSE IF(NF.EQ.32) THEN
NH=32
```

C

```
ELSE IF(NF.EQ.33) THEN
NH=33
```

C

```
ELSE IF(NF.EQ.34) THEN
NH=34
```

C

```
ELSE IF(NF.EQ.35) THEN
NH=35
```

```

ELSE
ENDIF
C
WRITE(NH,601)ABZ1,AHY1,APX1
WRITE(NH,602)SZX,SZY
C
CLOSE(31,STATUS='KEEP')
CLOSE(32,STATUS='KEEP')
CLOSE(33,STATUS='KEEP')
CLOSE(34,STATUS='KEEP')
CLOSE(35,STATUS='KEEP')
GO TO 348
C
350 IF(JM.EQ.4.OR.JM.EQ.5.OR.JP.EQ.3) GO TO 356
PRINT*,'***** ERROR HAPPENED IN DRWA3DSB *****'
STOP
C
356 OPEN(41,FILE='H1'//FILE2,STATUS='UNKNOWN')
OPEN(42,FILE='H2'//FILE2,STATUS='UNKNOWN')
OPEN(43,FILE='H3'//FILE2,STATUS='UNKNOWN')
OPEN(44,FILE='H4'//FILE2,STATUS='UNKNOWN')
OPEN(45,FILE='H5'//FILE2,STATUS='UNKNOWN')
C
IF(NF.EQ.31) THEN
NH=41
C
ELSE IF(NF.EQ.32) THEN
NH=42
C
ELSE IF(NF.EQ.33) THEN
NH=43
C
ELSE IF(NF.EQ.34) THEN
NH=44
C
ELSE IF(NF.EQ.35) THEN
NH=45
ELSE
ENDIF
C
WRITE(NH,601)ABZ1,AHY1,APX1
WRITE(NH,602)SZX,SZY
C
CLOSE(41,STATUS='KEEP')
CLOSE(42,STATUS='KEEP')
CLOSE(43,STATUS='KEEP')
CLOSE(44,STATUS='KEEP')
CLOSE(45,STATUS='KEEP')
GO TO 352
C
***** WRITING THE DATA FOR DRAWING TO THE RESULT FILE *****
C
348 WRITE(*,310) FILE1
310 FORMAT(/4X,'*** WRITING THE DATA FOR DRAWING TO THE RESULT ',
%/10X,'FILE R',A12,' **',/)
C
OPEN(3,FILE='R'//FILE1,STATUS='UNKNOWN',ACCESS='APPEND')
C
IF(JM.EQ.3.OR.JP.EQ.2) THEN
WRITE(3,311)
311 FORMAT(/4X,'@@@@@ Change the data of the existing file. @@@@@')
ELSE
ENDIF
C
WRITE(3,312)
312 FORMAT(/4X,'*****THE DATA TO DRAW THE 3-D GRAPH *****')

```

```

C
  WRITE(3,314)JN,ABZ1,AHY1,APX1
314 FORMAT(/4X,'JN=',I3,
  %/4X,'Bank of Z-axis(deg.)= ',F10.6,
  %/4X,'Heading of Y-axis(deg.)=',F10.6,
  %/4X,'Pitch of X-axis(deg.)= ',F10.6,/)

  WRITE(3,316)SZX,SZY
316 FORMAT(/4X,'SCALE RATIO OF Z-AXIS VS X-AXIS=',F10.4,
  %4X,'SCALE RATIO OF Z-AXIS VS Y-AXIS=',F10.4,/)
C
  CLOSE(3,STATUS='KEEP')
  GO TO 99
C
352 WRITE(*,320) FILE2
320 FORMAT(/4X,'*** WRITING THE DATA FOR DRAWING TO THE RESULT ',
  %/10X,'FILE R',A12,' **',/)
C
  OPEN(6,FILE='R'//FILE2,STATUS='UNKNOWN',ACCESS='APPEND')
C
  WRITE(6,322)
322 FORMAT(/4X,'****THE DATA TO DRAW THE 3-D GRAPH *****/)
C
  WRITE(6,324)JN,ABZ1,AHY1,APX1
324 FORMAT(/4X,'JN=',I3,
  %/4X,'Bank of Z-axis(deg.)= ',F10.6,
  %/4X,'Heading of Y-axis(deg.)=',F10.6,
  %/4X,'Pitch of X-axis(deg.)= ',F10.6,/)

  WRITE(6,326)SZX,SZY
326 FORMAT(/4X,'SCALE RATIO OF Z-AXIS VS X-AXIS=',F10.4,
  %4X,'SCALE RATIO OF Z-AXIS VS Y-AXIS=',F10.4,/)
C
  CLOSE(6,STATUS='KEEP')
  GO TO 99
C
C***** FINISH OF THE 3-D DRAWING *****
C
400 CALL GINEND
  WRITE(*,*)'*** YOU HAVE COMPLETED THE 3-D DRAWUNG. *****'
  RETURN
  END
C*****

```

Appendix -2 Input data of D=60.5mm x t=1.75mm

 ** INITIAL INPUT DATA IN FILE RCBR60-5BC **

OUTER DIA.	WIDTH	THICKNESS	NUMBER OF st.	Stand No. of 1st Finpass
60.50	187.08	1.75	8	6

STAND	LS(I)	TLS(I)
1	600.00	600.00
2	600.00	1200.00
3	450.00	1650.00
4	450.00	2100.00
5	450.00	2550.00
6	1050.00	3600.00
7	320.00	3920.00
8	900.00	4820.00

STAND	DOWNHILL AMOUNT
0	0.00
1	0.00
2	0.00
3	0.00
4	0.00
5	0.00
6	0.00
7	0.00
8	0.00

STAND	NUMBER OF RADIUS
1	2
2	3
3	4
4	4
5	4
6	5
7	5
8	1

STAND	No. R	RADIUS	ANGLE	DLO	DLN	TLN(I,J)
1	1	99999.999	0.0385887082	67.3500	67.3494	67.3494
1	2	26.910	57.6400000000	27.0717	26.1914	93.5408
2	1	99999.999	0.0195836978	34.1800	34.1797	34.1797
2	2	63.230	30.4800000000	33.6369	33.1714	67.3511
2	3	28.900	53.5500000000	27.0106	26.1928	93.5439
3	1	148.260	8.0000000000	20.7010	20.5788	20.5788
3	2	52.520	22.8300000000	20.9270	20.5784	41.1572
3	3	76.010	19.9700000000	26.4927	26.1877	67.3449
3	4	28.900	53.5500000000	27.0106	26.1928	93.5378
4	1	109.250	10.8800000000	20.7457	20.5795	20.5795
4	2	26.820	45.4500000000	21.2750	20.5809	41.1605
4	3	76.010	19.9700000000	26.4927	26.1877	67.3482
4	4	28.900	53.5500000000	27.0106	26.1928	93.5410
5	1	43.690	27.5400000000	21.0002	20.5796	20.5796
5	2	26.820	45.4500000000	21.2750	20.5809	41.1605
5	3	76.010	19.9700000000	26.4927	26.1877	67.3483
5	4	28.900	53.5500000000	27.0106	26.1928	93.5411
6	1	32.080	38.1100000000	21.3379	20.7558	20.7558

6	2	28.790	38.5800000000	19.3857	18.7965	39.5524
6	3	51.370	26.6300000000	23.8758	23.4691	63.0215
6	4	28.790	38.5800000000	19.3857	18.7965	81.8180
6	5	30.140	22.5800000000	11.8780	11.5332	93.3512
7	1	34.620	41.3500000000	24.9850	24.3536	24.3536
7	2	30.420	32.2800000000	17.1384	16.6454	40.9990
7	3	34.620	32.7400000000	19.7826	19.2826	60.2816
7	4	30.420	32.2800000000	17.1384	16.6454	76.9270
7	5	30.160	31.9600000000	16.8235	16.3354	93.2624
8	1	30.400	180.0000000000	95.5044	92.7555	0.0000

NUMBER OF DIVISION IN WIDTH= 10

YOUNG'S MODULUS= 21000.00

YIELD STRESS= 30.00

WORK-HARDENING COEFFICIENT= 200.00

POISSON'S RATIO= 0.30

RATIO OF E(y)/E(x)= 0.50

RATIO OF E(x)/E(y)= 0.45

FORMING VELOCITY= 60.00

IDH= 0 IIDH= 0

SIZE= 60.5X1.75mm

DATE=30. 9.1992

DRAWER=T.TOYOOKA

WORKS=2"MILL

MATERIAL=STEEL

Appendix -3 Input data of D=42.7mm x t=1.5mm

 ** INITIAL INPUT DATA IN FILE RCBR42-7M **
 @*****

0	OUTER DIA.	WIDTH	THICKNESS	NUMBER OF st.	Stand No. of 1st Finpass
	42.7	136.00	1.50	9	6

0	STAND	LS(I)	TLS(I)
	1	400.00	400.00
	2	400.00	800.00
	3	400.00	1200.00
	4	400.00	1600.00
	5	400.00	2000.00
	6	850.00	2850.00
	7	400.00	3250.00
	8	400.00	3650.00
	9	600.00	4250.00

0	STAND	DOWNHILL AMOUNT
	0	0.00
	1	0.00
	2	0.00
	3	0.00
	4	0.00
	5	0.00
	6	0.00
	7	0.00
	8	0.00
	9	0.00

0	STAND	NUMBER OF RADIUS
	1	2
	2	3
	3	4
	4	4
	5	4
	6	5
	7	5
	8	5
	9	1

0	STAND	No.R	RADIUS	ANGLE	DLO	DLN	TLN(I,J)
	1	1	28052.500	0.1000000000	48.9608	48.9595	48.9595
	1	2	22.480	49.6300000000	19.4723	18.8227	67.7822
	2	1	13860.300	0.1000000000	24.1908	24.1895	24.1895
	2	2	54.530	26.2700000000	25.0019	24.6580	48.8475
	2	3	23.830	46.7600000000	19.4480	18.8360	67.6835
	3	1	108.650	8.0000000000	15.1704	15.0657	15.0657
	3	2	42.960	20.0000000000	14.9959	14.7341	29.7998
	3	3	54.530	20.1900000000	19.2154	18.9511	48.7509
	3	4	25.060	44.4200000000	19.4284	18.8469	67.5978
	4	1	80.020	10.8800000000	15.1951	15.0527	15.0527
	4	2	20.000	43.5400000000	15.1983	14.6284	29.6811
	4	3	54.530	20.1900000000	19.2154	18.9511	48.6322
	4	4	25.060	44.4200000000	19.4284	18.8469	67.4792
	5	1	32.190	27.3000000000	15.3377	14.9804	14.9804
	5	2	20.000	43.5400000000	15.1983	14.6284	29.6088
	5	3	54.530	20.1900000000	19.2154	18.9511	48.5599

5	4	25.060	44.4200000000	19.4284	18.8469	67.4068
6	1	23.200	38.1100000000	15.4314	14.9325	14.9325
6	2	20.850	38.5800000000	14.0393	13.5343	28.4668
6	3	37.000	26.6300000000	17.1969	16.8483	45.3151
6	4	20.850	38.5800000000	14.0393	13.5343	58.8494
6	5	21.810	22.5800000000	8.5952	8.2996	67.1491
7	1	25.000	41.3500000000	18.0423	17.5011	17.5011
7	2	22.000	32.2800000000	12.3946	11.9721	29.4732
7	3	25.000	32.7400000000	14.2855	13.8570	43.3301
7	4	22.000	32.2800000000	12.3946	11.9721	55.3022
7	5	21.810	31.9600000000	12.1658	11.7474	67.0496
8	1	27.610	40.0000000000	19.2754	18.7518	18.7518
8	2	26.600	10.0000000000	4.6426	4.5117	23.2635
8	3	20.580	80.0000000000	28.7351	27.6879	50.9514
8	4	26.600	10.0000000000	4.6426	4.5117	55.4631
8	5	22.890	30.0000000000	11.9852	11.5925	67.0555
9	1	21.810	180.0000000000	68.5181	66.1619	66.1619

0 NUMBER OF DIVISION IN WIDTH= 10
 0 YOUNG'S MODULUS= 21000.00
 0 YIELD STRESS= 30.00
 0 WORK-HARDENING COEFFICIENT= 200.00
 0 POISSON'S RATIO= 0.30
 0 RATIO OF E(y)/E(x)= 0.50
 0 RATIO OF E(x)/E(y)= 0.45
 0 FORMING VELOCITY= 5.00

0 IDH= 0 IIDH= 0

SIZE= 42.7x1.5mm
 DATE=19. 5.1994
 DRAWER=T.TOYOOKA
 WORKS=CBR Model mi
 MATERIAL=STAINLESS

Appendix -4 Input and output data of D=100mm x t=1.0mm

 ** INITIAL INPUT DATA IN FILE RY100BC **

OUTER DIA.	WIDTH	THICKNESS	NUMBER OF st.	Stand No. of 1st Finpass
100.00	315.00	1.00	9	6

STAND	LS(I)	TLS(I)
1	444.65	444.65
2	323.35	768.00
3	625.00	1393.00
4	460.00	1853.00
5	574.01	2427.01
6	260.99	2688.00
7	440.00	3128.00
8	440.00	3568.00
9	500.00	4068.00

STAND	DOWNHILL AMOUNT
0	0.00
1	0.00
2	0.00
3	0.00
4	0.00
5	0.00
6	0.00
7	0.00
8	0.00
9	0.00

STAND	NUMBER OF RADIUS
1	3
2	3
3	3
4	3
5	3
6	5
7	5
8	5
9	1

STAND	No.R	RADIUS	ANGLE	DLO	DLN	TLN(I,J)
1	1	99999.999	0.0173262440	30.2400	30.2398	30.2398
1	2	244.930	8.0800000000	34.5407	34.4702	64.7100
1	3	99999.999	0.0531647548	92.7900	92.7895	157.4995
2	1	99999.999	0.0173262440	30.2400	30.2398	30.2398
2	2	89.220	22.2500000000	34.6473	34.4531	64.6930
2	3	99999.999	0.0531647548	92.7900	92.7895	157.4825
3	1	99999.999	0.0173262440	30.2400	30.2398	30.2398
3	2	40.000	50.0000000000	34.9066	34.4703	64.7101
3	3	99999.999	0.0531647548	92.7900	92.7895	157.4996
4	1	69.470	25.1200000000	30.4575	30.2383	30.2383
4	2	40.000	50.0000000000	34.9066	34.4703	64.7085
4	3	99999.999	0.0531647548	92.7900	92.7895	157.4981
5	1	43.810	40.0000000000	30.5851	30.2361	30.2361
5	2	36.410	55.0000000000	34.9511	34.4711	64.7072
5	3	2261.830	2.3500000000	92.7695	92.7490	157.4562
6	1	50.000	35.0000000000	30.5433	30.2378	30.2378
6	2	40.000	50.0000000000	34.9066	34.4703	64.7081
6	3	250.000	11.7000000000	51.0509	50.9488	115.6569
6	4	37.390	43.3000000000	28.2567	27.8788	143.5356
6	5	50.000	15.0000000000	13.0900	12.9591	156.4947
7	1	50.000	40.0000000000	34.9066	34.5575	34.5575
7	2	44.000	45.0000000000	34.5575	34.1648	68.7223
7	3	152.120	14.4600000000	38.3912	38.2650	106.9874
7	4	42.000	50.0000000000	36.6519	36.2156	143.2030
7	5	50.000	15.0000000000	13.0900	12.9591	156.1620
8	1	50.000	50.0000000000	43.6332	43.1969	43.1969
8	2	49.000	30.0000000000	25.6563	25.3945	68.5914
8	3	79.880	16.9000000000	23.5615	23.4140	92.0054
8	4	49.000	50.0000000000	42.7606	42.3242	134.3296
8	5	50.000	25.0000000000	21.8166	21.5984	155.9281

9 1 50.000 180.0000000000 157.0796 155.5088 155.5088
NUMBER OF DIVISION IN WIDTH= 10
YOUNG'S MODULUS= 21000.00
YIELD STRESS= 34.40
WORK-HARDENING COEFFICIENT= 200.00
POISSON'S RATIO= 0.30
RATIO OF E(y)/E(x)= 0.50
RATIO OF E(x)/E(y)= 0.45
FORMING VELOCITY= 7.50

IDH= 0 IIDH= 0

SIZE= 100.0X1.0mm
DATE=30. 9.1992
DRAWER=T.TOYOOKA
WORKS=YAMANASHI
MATERIAL=STEEL(KTH45)

 ** OUT PUT DATA IN FILE RY1008C **

 CALCULATED RESULTS OF AII POINTS OF X AND Y AXIS ON THE FLOWER

***** CALCULATED RESULTS OF THE POINTS OF FLOWER. *****

----- OUTSIDE POINTS -----

I	J	PXO(I,J)	PYO(I,J)	CX(I,J)	CY(I,J)	AAN(I,J)
0	0	0.000	0.000	0.000	0.000	0.000
1	0	0.000	0.000	0.000	0.000	0.000
1	1	30.240	0.005	0.000	99999.999	0.017
1	2	64.666	2.446	30.166	244.935	8.097
1	3	156.524	15.559	-14020.837	99005.469	8.150
2	0	0.000	0.000	0.000	0.000	0.000
2	1	30.240	0.005	0.000	99999.999	0.017
2	2	64.021	6.658	30.213	89.225	22.267
2	3	149.875	41.859	-37828.827	92549.253	22.320
3	0	0.000	0.000	0.000	0.000	0.000
3	1	30.240	0.005	0.000	99999.999	0.017
3	2	60.877	14.302	30.228	40.005	50.017
3	3	120.467	85.429	-76563.000	64269.895	50.070
4	0	0.000	0.000	0.000	0.000	0.000
4	1	29.491	6.570	0.000	69.470	25.120
4	2	51.169	32.515	12.510	42.787	75.120
4	3	74.956	122.205	-96595.407	25712.061	75.173
5	0	0.000	0.000	0.000	0.000	0.000
5	1	28.161	10.250	0.000	43.810	40.000
5	2	41.028	41.315	4.757	38.141	95.000
5	3	31.050	133.539	-2212.195	-155.817	97.350
6	0	0.000	0.000	0.000	0.000	0.000
6	1	28.679	9.042	0.000	50.000	35.000
6	2	45.584	38.322	5.736	41.808	85.000
6	3	44.828	89.279	-203.465	60.111	96.700
6	4	31.727	113.559	7.693	84.917	140.000
6	5	20.718	120.572	-0.413	75.257	155.000
7	0	0.000	0.000	0.000	0.000	0.000
7	1	32.139	11.698	0.000	50.000	40.000
7	2	47.689	41.569	3.857	45.404	85.000
7	3	46.199	79.829	-103.852	54.827	99.460
7	4	26.112	109.100	4.771	72.926	149.460
7	5	14.101	114.208	0.705	66.036	164.460
8	0	0.000	0.000	0.000	0.000	0.000
8	1	38.302	17.861	0.000	50.000	50.000
8	2	49.022	40.848	0.766	49.357	80.000
8	3	49.657	64.316	-29.645	54.719	96.900
8	4	27.771	99.478	1.012	58.429	146.900
8	5	7.510	107.093	0.465	57.592	171.900
9	0	0.000	0.000	0.000	0.000	0.000
9	1	0.000	100.000	0.000	50.000	180.000

----- INSIDE POINTS -----

I	J	PXI(I,J)	PYI(I,J)	CX(I,J)	CY(I,J)	AAN(I,J)
0	0	0.000	1.000	0.000	0.000	0.000
1	0	0.000	1.000	0.000	0.000	0.000
1	1	30.240	1.005	0.000	99999.999	0.017
1	2	64.525	3.436	30.166	244.935	8.097
1	3	156.383	16.549	-14020.837	99005.469	8.150
2	0	0.000	1.000	0.000	0.000	0.000
2	1	30.240	1.005	0.000	99999.999	0.017
2	2	63.642	7.583	30.213	89.225	22.267
2	3	149.495	42.784	-37828.827	92549.253	22.320
3	0	0.000	1.000	0.000	0.000	0.000
3	1	30.240	1.005	0.000	99999.999	0.017
3	2	60.111	14.945	30.228	40.005	50.017
3	3	119.700	86.071	-76563.000	64269.895	50.070
4	0	0.000	1.000	0.000	0.000	0.000
4	1	29.067	7.476	0.000	69.470	25.120
4	2	50.203	32.772	12.510	42.787	75.120
4	3	73.989	122.461	-96595.407	25712.061	75.173
5	0	0.000	1.000	0.000	0.000	0.000
5	1	27.518	11.016	0.000	43.810	40.000
5	2	40.032	41.227	4.757	38.141	95.000
5	3	30.058	133.411	-2212.195	-155.817	97.350
6	0	0.000	1.000	0.000	0.000	0.000
6	1	28.105	9.862	0.000	50.000	35.000
6	2	44.587	38.409	5.736	41.808	85.000
6	3	43.834	89.162	-203.465	60.111	96.700
6	4	31.084	112.793	7.693	84.917	140.000
6	5	20.296	119.666	-0.413	75.257	155.000
7	0	0.000	1.000	0.000	0.000	0.000
7	1	31.497	12.464	0.000	50.000	40.000
7	2	46.693	41.656	3.857	45.404	85.000
7	3	45.213	79.665	-103.852	54.827	99.460
7	4	25.604	108.238	4.771	72.926	149.460
7	5	13.833	113.245	0.705	66.036	164.460
8	0	0.000	1.000	0.000	0.000	0.000
8	1	37.536	18.503	0.000	50.000	50.000
8	2	48.037	41.022	0.766	49.357	80.000
8	3	48.664	64.196	-29.645	54.719	96.900
8	4	27.224	98.640	1.012	58.429	146.900
8	5	7.370	106.103	0.465	57.592	171.900
9	0	0.000	1.000	0.000	0.000	0.000
9	1	0.000	99.000	0.000	50.000	180.000

 ** OUT PUT DATA IN FILE RY100BC **

 CALCULATED RESULTS OF DIMENSIONS OF FLOWERS ABOUT
 THE CIRCUMFERENTIAL LENGTH, HEIGHT, WIDTH, EDGE WIDTH AND
 PY OF Max.WIDTH AT OUTSIDE SURFACE AND THE CIRCUMFERENTIAL
 LENGTH OF NEUTRAL AXIS

< RESULTS OF CALUCULATION OF WIDTH ANDHEIGHT OF FLOWER >

band No.	C-LENGTH	N-LENGTH	HEIGHT	WIDTH	E-WIDTH	PY/Max.WIDTH
0	315.000	315.000	0.000	315.000	315.000	0.000
1	315.141	314.999	15.559	313.049	313.049	0.000
2	315.355	314.965	41.859	299.750	299.750	0.000
3	315.873	314.999	85.429	240.934	240.934	0.000
4	316.308	314.996	122.205	149.911	149.911	0.000
5	316.611	314.912	133.539	82.333	62.100	38.141
6	315.695	312.989	120.572	93.070	41.437	60.111
7	315.194	312.324	114.208	96.536	28.202	54.827
8	314.856	311.856	107.093	100.470	15.021	54.719
9	314.159	311.018	100.000	100.000	0.000	50.000

** OUT PUT OF SCALE VALUE IN FILE RY100BC **

THE VALUE-OF DRAWING SCALE :RA= 0.53960

 ** OUTPUT DATA(RERESULT) OF X-,Y- AND Z-AXIS POINTS TO **
 ** ANALYZE STRESS-STRAIN BY MODEL 1 **
 ** IN THE FILE RY100BC **

ST.	Mesh	PXE(I,J)	PYE(I,J)	PZ(I)	TLS(I)	ANE(I,J)	DLE(I)	TLE(I,J)
0	0	0.000	0.000	-2034.000	0.000	0.000	0.000	0.000
0	1	15.750	0.000	-2034.000	0.000	0.000	0.000	15.750
0	2	31.500	0.000	-2034.000	0.000	0.000	0.000	31.500
0	3	47.250	0.000	-2034.000	0.000	0.000	0.000	47.250
0	4	63.000	0.000	-2034.000	0.000	0.000	0.000	63.000
0	5	78.750	0.000	-2034.000	0.000	0.000	0.000	78.750
0	6	94.500	0.000	-2034.000	0.000	0.000	0.000	94.500
0	7	110.250	0.000	-2034.000	0.000	0.000	0.000	110.250
0	8	126.000	0.000	-2034.000	0.000	0.000	0.000	126.000
0	9	141.750	0.000	-2034.000	0.000	0.000	0.000	141.750
0	10	157.500	0.000	-2034.000	0.000	0.000	0.000	157.500

1	0	0.000	0.000	-1589.350	444.650	0.000	15.750	0.000
1	1	15.750	0.001	-1589.350	444.650	0.009	15.750	15.750
1	2	31.500	0.008	-1589.350	444.650	0.031	15.750	31.500
1	3	47.236	0.001	-1589.350	444.650	4.005	15.750	47.250
1	4	62.901	2.207	-1589.350	444.650	7.696	15.750	63.000
1	5	78.495	4.420	-1589.350	444.650	8.105	15.750	78.750
1	6	94.087	6.642	-1589.350	444.650	8.114	15.750	94.500
1	7	109.679	8.866	-1589.350	444.650	8.123	15.750	110.250
1	8	125.271	11.093	-1589.350	444.650	8.132	15.750	126.000
1	9	140.862	13.322	-1589.350	444.650	8.141	15.750	141.750
1	10	156.453	15.554	-1589.350	444.650	8.150	15.750	157.500

2	0	0.000	0.000	-1266.000	768.000	0.000	15.748	0.000
2	1	15.748	0.001	-1266.000	768.000	0.009	15.748	15.748
2	2	31.496	0.014	-1266.000	768.000	0.829	15.748	31.497
2	3	47.140	1.634	-1266.000	768.000	10.999	15.748	47.245
2	4	62.252	5.992	-1266.000	768.000	21.169	15.748	62.993
2	5	76.832	11.945	-1266.000	768.000	22.275	15.748	78.741
2	6	91.404	17.916	-1266.000	768.000	22.284	15.748	94.490
2	7	105.976	23.889	-1266.000	768.000	22.293	15.748	110.238
2	8	120.547	29.864	-1266.000	768.000	22.302	15.748	125.986
2	9	135.116	35.841	-1266.000	768.000	22.311	15.748	141.734
2	10	149.685	41.821	-1266.000	768.000	22.320	15.748	157.483

3	0	0.000	0.000	-641.000	1393.000	0.000	15.750	0.000
3	1	15.750	0.001	-641.000	1393.000	0.009	15.750	15.750
3	2	31.500	0.025	-641.000	1393.000	1.845	15.750	31.500
3	3	46.728	3.616	-641.000	1393.000	24.691	15.750	47.250
3	4	59.367	12.837	-641.000	1393.000	47.537	15.750	63.000
3	5	69.515	24.882	-641.000	1393.000	50.025	15.750	78.750
3	6	79.632	36.952	-641.000	1393.000	50.034	15.750	94.500
3	7	89.748	49.024	-641.000	1393.000	50.043	15.750	110.250
3	8	99.862	61.098	-641.000	1393.000	50.052	15.750	126.000
3	9	109.974	73.173	-641.000	1393.000	50.061	15.750	141.750
3	10	120.084	85.250	-641.000	1393.000	50.070	15.750	157.500

4	0	0.000	0.000	-181.000	1853.000	0.000	15.750	0.000
4	1	15.613	1.790	-181.000	1853.000	13.084	15.750	15.750
4	2	30.412	7.077	-181.000	1853.000	26.950	15.750	31.500
4	3	42.678	16.789	-181.000	1853.000	49.795	15.750	47.249
4	4	50.211	30.502	-181.000	1853.000	72.641	15.750	62.999
4	5	54.290	45.714	-181.000	1853.000	75.128	15.750	78.749
4	6	58.332	60.936	-181.000	1853.000	75.137	15.750	94.499
4	7	62.370	76.159	-181.000	1853.000	75.146	15.750	110.249
4	8	66.407	91.383	-181.000	1853.000	75.155	15.750	125.998
4	9	70.441	106.608	-181.000	1853.000	75.164	15.750	141.748
4	10	74.472	121.833	-181.000	1853.000	75.173	15.750	157.498

5	0	0.000	0.000	393.010	2427.010	0.000	15.746	0.000
5	1	15.401	2.831	393.010	2427.010	20.830	15.746	15.746
5	2	28.786	10.956	393.010	2427.010	42.003	15.746	31.491
5	3	37.843	23.682	393.010	2427.010	67.125	15.746	47.237
5	4	40.639	39.050	393.010	2427.010	92.248	15.746	62.982
5	5	39.265	54.735	393.010	2427.010	95.355	15.746	78.728
5	6	37.741	70.406	393.010	2427.010	95.754	15.746	94.474

5	7	36.107	86.067	393.010	2427.010	96.153	15.746	110.219
5	8	34.365	101.716	393.010	2427.010	96.552	15.746	125.965
5	9	32.514	117.352	393.010	2427.010	96.951	15.746	141.710
5	10	30.554	132.975	393.010	2427.010	97.350	15.746	157.456

6	0	0.000	0.000	654.000	2688.000	0.000	15.649	0.000
6	1	15.390	2.453	654.000	2688.000	18.114	15.649	15.649
6	2	29.253	9.572	654.000	2688.000	36.539	15.649	31.299
6	3	39.678	21.106	654.000	2688.000	59.239	15.649	46.948
6	4	44.845	35.770	654.000	2688.000	81.939	15.649	62.598
6	5	45.899	51.379	654.000	2688.000	88.109	15.649	78.247
6	6	45.925	67.026	654.000	2688.000	91.703	15.649	93.897
6	7	44.969	82.644	654.000	2688.000	95.297	15.649	109.546
6	8	42.012	97.946	654.000	2688.000	111.515	15.649	125.196
6	9	33.401	110.873	654.000	2688.000	135.821	15.649	140.845
6	10	20.507	119.619	654.000	2688.000	155.000	15.649	156.495

7	0	0.000	0.000	1094.000	3128.000	0.000	15.616	0.000
7	1	15.358	2.443	1094.000	3128.000	18.076	15.616	15.616
7	2	29.201	9.531	1094.000	3128.000	36.151	15.616	31.232
7	3	40.000	20.698	1094.000	3128.000	56.189	15.616	46.849
7	4	46.200	34.939	1094.000	3128.000	76.758	15.616	62.465
7	5	47.719	50.455	1094.000	3128.000	88.537	15.616	78.081
7	6	47.314	66.059	1094.000	3128.000	94.438	15.616	93.697
7	7	45.260	81.530	1094.000	3128.000	102.671	15.616	109.313
7	8	39.082	95.772	1094.000	3128.000	124.231	15.616	124.930
7	9	28.102	106.747	1094.000	3128.000	145.791	15.616	140.546
7	10	13.967	113.226	1094.000	3128.000	164.460	15.616	156.162

8	0	0.000	0.000	1534.000	3568.000	0.000	15.593	0.000
8	1	15.336	2.436	1534.000	3568.000	18.049	15.593	15.593
8	2	29.163	9.503	1534.000	3568.000	36.097	15.593	31.186
8	3	40.118	20.508	1534.000	3568.000	54.231	15.593	46.778
8	4	47.060	34.395	1534.000	3568.000	72.652	15.593	62.371
8	5	49.609	49.740	1534.000	3568.000	86.765	15.593	77.964
8	6	48.949	65.293	1534.000	3568.000	98.733	15.593	93.557
8	7	44.166	80.063	1534.000	3568.000	117.153	15.593	109.150
8	8	34.961	92.566	1534.000	3568.000	135.574	15.593	124.742
8	9	22.280	101.525	1534.000	3568.000	153.851	15.593	140.335
8	10	7.440	106.098	1534.000	3568.000	171.900	15.593	155.928

9	0	0.000	0.000	2034.000	4068.000	0.000	15.551	0.000
9	1	15.296	2.423	2034.000	4068.000	18.000	15.551	15.551
9	2	29.095	9.454	2034.000	4068.000	36.000	15.551	31.102
9	3	40.046	20.405	2034.000	4068.000	54.000	15.551	46.653
9	4	47.077	34.204	2034.000	4068.000	72.000	15.551	62.204
9	5	49.500	49.500	2034.000	4068.000	90.000	15.551	77.754
9	6	47.077	64.796	2034.000	4068.000	108.000	15.551	93.305
9	7	40.046	78.595	2034.000	4068.000	126.000	15.551	108.856
9	8	29.095	89.546	2034.000	4068.000	144.000	15.551	124.407
9	9	15.296	96.577	2034.000	4068.000	162.000	15.551	139.958
9	10	0.000	99.000	2034.000	4068.000	180.000	15.551	155.509

 ** OUTPUT DATA(RESULT) OF STRESS-STRAIN ANALYSIS **
 ** MODEL 1 IN THE FILE RY1008C **

***** RESULTS OF STRAIN *****

OD= 100.00 TS= 1.00 NUMBER OF STAND= 9 Stand No. of 1st Finpass= 6
 NUMBER OF DIVISION=10 Ex/Ez= 0.50 Ez/Ex in Finpass & SQ= 0.45

ST.	Mesh	DEz(%)	Ez(%)	DEx(%)	Ex(%)	DEZE(%)	DEXE(%)	EzE(%)	ExE(%)	DEPSOT(%)
0	0	0.000000	0.000000	0.000000	0.000000	0.000000	0.000000	0.000000	0.000000	0.000000
0	1	0.000000	0.000000	0.000000	0.000000	0.000000	0.000000	0.000000	0.000000	0.000000
0	2	0.000000	0.000000	0.000000	0.000000	0.000000	0.000000	0.000000	0.000000	0.000000
0	3	0.000000	0.000000	0.000000	0.000000	0.000000	0.000000	0.000000	0.000000	0.000000
0	4	0.000000	0.000000	0.000000	0.000000	0.000000	0.000000	0.000000	0.000000	0.000000
0	5	0.000000	0.000000	0.000000	0.000000	0.000000	0.000000	0.000000	0.000000	0.000000
0	6	0.000000	0.000000	0.000000	0.000000	0.000000	0.000000	0.000000	0.000000	0.000000
0	7	0.000000	0.000000	0.000000	0.000000	0.000000	0.000000	0.000000	0.000000	0.000000
0	8	0.000000	0.000000	0.000000	0.000000	0.000000	0.000000	0.000000	0.000000	0.000000
0	9	0.000000	0.000000	0.000000	0.000000	0.000000	0.000000	0.000000	0.000000	0.000000
0	10	0.000000	0.000000	0.000000	0.000000	0.000000	0.000000	0.000000	0.000000	0.000000

1	0	0.000000	0.000000	0.000000	0.000000	0.000000	0.000000	0.000000	0.000000	0.000000
1	1	0.000000	0.000000	0.000000	0.000000	0.000000	0.000000	0.000000	0.000000	0.000000
1	2	0.000000	0.000000	0.000000	0.000000	0.000000	0.000000	0.000000	0.000000	0.000000
1	3	0.000091	0.000091	-0.000046	-0.000046	0.000091	-0.000046	0.000091	-0.000046	0.000000
1	4	0.001234	0.001234	-0.000617	-0.000617	0.001234	-0.000617	0.001234	-0.000617	0.000000
1	5	0.004957	0.004957	-0.002478	-0.002478	0.004957	-0.002478	0.004957	-0.002478	0.000000
1	6	0.011198	0.011198	-0.005599	-0.005599	0.011198	-0.005599	0.011198	-0.005599	0.000000
1	7	0.019958	0.019958	-0.009979	-0.009979	0.019958	-0.009979	0.019958	-0.009979	0.000000
1	8	0.031244	0.031244	-0.015622	-0.015622	0.031244	-0.015622	0.031244	-0.015622	0.000000
1	9	0.045063	0.045063	-0.022531	-0.022531	0.045063	-0.022531	0.045063	-0.022531	0.000000
1	10	0.061420	0.061420	-0.030710	-0.030710	0.061420	-0.030710	0.061420	-0.030710	0.017152

2	0	0.000000	0.000000	0.000000	0.000000	0.000000	0.000000	0.000000	0.000000	0.000000
2	1	0.000000	0.000000	0.000000	0.000000	0.000000	0.000000	0.000000	0.000000	0.000000
2	2	0.000000	0.000000	0.000000	0.000000	0.000000	0.000000	0.000000	0.000000	0.000000
2	3	0.000423	0.000515	-0.000212	-0.000257	0.000423	-0.000212	0.000515	-0.000257	0.000000
2	4	0.005819	0.007053	-0.002909	-0.003526	0.005819	-0.002909	0.007053	-0.003526	0.000000
2	5	0.023437	0.028393	-0.011718	-0.014197	0.023437	-0.011718	0.028393	-0.014197	0.000000
2	6	0.052983	0.064181	-0.026491	-0.032090	0.052983	-0.026491	0.064181	-0.032090	0.000000
2	7	0.094389	0.114347	-0.047195	-0.057174	0.094389	-0.047195	0.114347	-0.057174	0.000000
2	8	0.147606	0.178850	-0.073803	-0.089425	0.147606	-0.073803	0.178850	-0.089425	0.023463
2	9	0.212571	0.257633	-0.106285	-0.128817	0.212571	-0.106285	0.257633	-0.128817	0.102335
2	10	0.289209	0.350629	-0.144605	-0.175315	0.289209	-0.144605	0.350629	-0.175315	0.198656

3	0	0.000000	0.000000	0.000000	0.000000	0.000000	0.000000	0.000000	0.000000	0.000000
3	1	0.000000	0.000000	0.000000	0.000000	0.000000	0.000000	0.000000	0.000000	0.000000
3	2	0.000000	0.000000	0.000000	0.000000	0.000000	0.000000	0.000000	0.000000	0.000000
3	3	0.000010	0.000524	-0.000005	-0.000262	0.000010	-0.000005	0.000524	-0.000262	0.000000
3	4	0.000011	0.007063	-0.000005	-0.003532	0.000011	-0.000005	0.007063	-0.003532	0.000000
3	5	-0.000126	0.028268	0.000063	-0.014134	-0.000126	0.000063	0.028268	-0.014134	0.000000
3	6	-0.000097	0.064084	0.000048	-0.032042	-0.000097	0.000048	0.064084	-0.032042	0.000000
3	7	0.000101	0.114449	-0.000051	-0.057224	0.000101	-0.000051	0.114449	-0.057224	0.000000
3	8	0.000468	0.179318	-0.000234	-0.089659	0.000468	-0.000234	0.179318	-0.089659	0.000444
3	9	0.001002	0.258635	-0.000501	-0.129318	0.001002	-0.000501	0.258635	-0.129318	0.000961
3	10	0.001702	0.352331	-0.000851	-0.176166	0.001702	-0.000851	0.352331	-0.176166	0.001648

4	0	0.000000	0.000000	0.000000	0.000000	0.000000	0.000000	0.000000	0.000000	0.000000
4	1	0.000761	0.000761	-0.000380	-0.000380	0.000761	-0.000380	0.000761	-0.000380	0.000000
4	2	0.012028	0.012028	-0.006014	-0.006014	0.012028	-0.006014	0.012028	-0.006014	0.000000
4	3	0.044336	0.044860	-0.022168	-0.022430	0.044336	-0.022168	0.044860	-0.022430	0.000000
4	4	0.086391	0.093454	-0.043195	-0.046727	0.086391	-0.043195	0.093454	-0.046727	0.000000
4	5	0.128797	0.157065	-0.064398	-0.078532	0.128797	-0.064398	0.154535	-0.076870	0.002550
4	6	0.178462	0.242546	-0.089231	-0.121273	0.094816	-0.036369	0.158900	-0.068411	0.086950
4	7	0.235423	0.349871	-0.117711	-0.174936	0.048103	-0.003990	0.162552	-0.061215	0.197865
4	8	0.299582	0.478899	-0.149791	-0.239450	0.009543	0.018142	0.165382	-0.056257	0.303911
4	9	0.370827	0.629462	-0.185414	-0.314731	0.008053	0.013546	0.167604	-0.053570	0.369485
4	10	0.449034	0.801365	-0.224517	-0.400683	0.007028	0.008641	0.169644	-0.052454	0.442816

5	0	0.000000	0.000000	0.000000	0.000000	0.000000	0.000000	0.000000	0.000000	0.000000

5	1	-0.000590	0.000171	0.000295	-0.000086	-0.000590	0.000295	0.000171	-0.000086	0.000000
5	2	-0.009343	0.002685	0.004672	-0.001342	-0.009343	0.004672	0.002685	-0.001342	0.000000
5	3	-0.034102	0.010758	0.017051	-0.005379	-0.034102	0.017051	0.010758	-0.005379	0.000000
5	4	-0.068467	0.024987	0.034234	-0.012493	-0.068467	0.034234	0.024987	-0.012493	0.000000
5	5	-0.110476	0.046589	0.055238	-0.023294	-0.110476	0.055238	0.044059	-0.021632	0.000000
5	6	-0.164657	0.077889	0.082328	-0.038945	-0.164657	0.082328	-0.005757	0.013918	0.000000
5	7	-0.230449	0.119422	0.115225	-0.059711	-0.230449	0.115225	-0.067897	0.054010	0.000000
5	8	-0.307197	0.171702	0.153598	-0.085851	-0.307197	0.153598	-0.141815	0.097342	0.000000
5	9	-0.394215	0.235247	0.197108	-0.117623	-0.322537	0.142496	-0.154933	0.088926	0.083228
5	10	-0.490794	0.310571	0.245397	-0.155286	-0.332780	0.130736	-0.163136	0.078282	0.195009

6	0	0.000000	0.000000	0.000000	0.000000	0.000000	0.000000	0.000000	0.000000	0.000000
6	1	-0.000066	0.000105	0.000033	-0.000052	-0.000066	0.000033	0.000105	-0.000052	0.000000
6	2	-0.001119	0.001566	0.000560	-0.000783	-0.001119	0.000560	0.001566	-0.000783	0.000000
6	3	-0.003412	0.007346	0.001706	-0.003673	-0.003412	0.001706	0.007346	-0.003673	0.000000
6	4	-0.004104	0.020883	0.002052	-0.010441	-0.004104	0.002052	0.020883	-0.010441	0.000000
6	5	-0.006031	0.040558	0.003015	-0.020279	-0.006031	0.003015	0.038028	-0.018617	0.000000
6	6	-0.020368	0.057521	0.010184	-0.028761	-0.020368	0.010184	-0.026125	0.024102	0.000000
6	7	-0.053214	0.066208	0.026607	-0.033104	-0.053214	0.026607	-0.121111	0.080617	0.000000
6	8	-0.118372	0.053330	0.059186	-0.026665	-0.115586	-0.015880	-0.157401	0.081461	0.119900
6	9	-0.203863	0.031384	0.101932	-0.015692	-0.011717	-0.021763	-0.166650	0.067163	0.213066
6	10	-0.105944	0.204627	0.052972	-0.102313	-0.004761	-0.009376	-0.167897	0.068906	0.104524

7	0	0.000000	0.000000	0.000000	0.000000	0.000000	0.000000	0.000000	0.000000	0.000000
7	1	-0.000104	0.000000	0.000052	0.000000	-0.000104	0.000052	0.000000	0.000000	0.000000
7	2	-0.001564	0.000001	0.000782	-0.000001	-0.001564	0.000782	0.000001	-0.000001	0.000000
7	3	-0.007277	0.000070	0.003638	-0.000035	-0.007277	0.003638	0.000070	-0.000035	0.000000
7	4	-0.020231	0.000652	0.010116	-0.000326	-0.020231	0.010116	0.000652	-0.000326	0.000000
7	5	-0.039482	0.001076	0.019741	-0.000538	-0.039482	0.019741	-0.001454	0.001124	0.000000
7	6	-0.056781	0.000740	0.028391	-0.000370	-0.056781	0.028391	-0.082907	0.052492	0.000000
7	7	-0.065866	0.000342	0.032933	-0.000171	-0.030804	0.007063	-0.151915	0.087680	0.037802
7	8	-0.049891	0.003439	0.024945	-0.001720	-0.003056	-0.005726	-0.160456	0.075735	0.043444
7	9	-0.019735	0.011649	0.009867	-0.005824	-0.000615	-0.001219	-0.167265	0.065944	0.019074
7	10	-0.183032	0.021595	0.091516	-0.010797	-0.004717	-0.008861	-0.172614	0.060044	0.180228

8	0	0.000000	0.000000	0.000000	0.000000	0.000000	0.000000	0.000000	0.000000	0.000000
8	1	0.000000	0.000000	0.000000	0.000000	0.000000	0.000000	0.000000	0.000000	0.000000
8	2	-0.000001	0.000001	0.000000	0.000000	-0.000001	0.000000	0.000001	0.000000	0.000000
8	3	-0.000057	0.000013	0.000028	-0.000006	-0.000057	0.000028	0.000013	-0.000006	0.000000
8	4	-0.000385	0.000267	0.000192	-0.000134	-0.000385	0.000192	0.000267	-0.000134	0.000000
8	5	-0.000021	0.001054	0.000011	-0.000527	-0.000021	0.000011	-0.001475	0.001135	0.000000
8	6	0.000103	0.000842	-0.000051	-0.000421	0.000103	-0.000051	-0.082804	0.052441	0.000000
8	7	0.000522	0.000864	-0.000261	-0.000432	0.000522	-0.000261	-0.151393	0.087419	0.000000
8	8	0.003600	0.007039	-0.001800	-0.003519	0.003600	-0.001800	-0.156857	0.073935	0.000000
8	9	0.004143	0.015792	-0.002072	-0.007896	0.004143	-0.002072	-0.163122	0.063872	0.000000
8	10	0.002526	0.024121	-0.001263	-0.012061	0.002526	-0.001263	-0.170088	0.058781	0.000000

9	0	0.000000	0.000000	0.000000	0.000000	0.000000	0.000000	0.000000	0.000000	0.000000
9	1	0.000000	0.000000	0.000000	0.000000	0.000000	0.000000	0.000000	0.000000	0.000000
9	2	0.000001	0.000001	0.000000	-0.000001	0.000001	0.000000	0.000001	-0.000001	0.000000
9	3	-0.000010	0.000003	0.000005	-0.000002	-0.000010	0.000005	0.000003	-0.000002	0.000000
9	4	-0.000260	0.000007	0.000130	-0.000004	-0.000260	0.000130	0.000007	-0.000004	0.000000
9	5	-0.001041	0.000014	0.000520	-0.000007	-0.001041	0.000520	-0.002516	0.001655	0.000000
9	6	-0.000092	0.000750	0.000046	-0.000375	-0.000092	0.000046	-0.082896	0.052487	0.000000
9	7	0.002962	0.003826	-0.001481	-0.001913	0.002962	-0.001481	-0.148432	0.085938	0.000000
9	8	0.001665	0.008704	-0.000832	-0.004352	0.001665	-0.000832	-0.155192	0.073103	0.000000
9	9	-0.001143	0.014649	0.000571	-0.007325	-0.001143	0.000571	-0.164265	0.064444	0.000000
9	10	-0.002979	0.021142	0.001490	-0.010571	-0.002535	0.001250	-0.172622	0.060031	0.000441

***** RESULTS OF STRESS *****

ST.	Mesh	NHAN	DSz(kg/mm2)	DSx	Sz	Sx	SEQ	DSz(MPa)	DSx	Sz	Sx	SEQ
0	0	0	0.0000	0.0000	0.0000	0.0000	34.4000	0.0000	0.0000	0.0000	0.0000	337.3488
0	1	0	0.0000	0.0000	0.0000	0.0000	34.4000	0.0000	0.0000	0.0000	0.0000	337.3488
0	2	0	0.0000	0.0000	0.0000	0.0000	34.4000	0.0000	0.0000	0.0000	0.0000	337.3488
0	3	0	0.0000	0.0000	0.0000	0.0000	34.4000	0.0000	0.0000	0.0000	0.0000	337.3488
0	4	0	0.0000	0.0000	0.0000	0.0000	34.4000	0.0000	0.0000	0.0000	0.0000	337.3488
0	5	0	0.0000	0.0000	0.0000	0.0000	34.4000	0.0000	0.0000	0.0000	0.0000	337.3488
0	6	0	0.0000	0.0000	0.0000	0.0000	34.4000	0.0000	0.0000	0.0000	0.0000	337.3488
0	7	0	0.0000	0.0000	0.0000	0.0000	34.4000	0.0000	0.0000	0.0000	0.0000	337.3488
0	8	0	0.0000	0.0000	0.0000	0.0000	34.4000	0.0000	0.0000	0.0000	0.0000	337.3488
0	9	0	0.0000	0.0000	0.0000	0.0000	34.4000	0.0000	0.0000	0.0000	0.0000	337.3488
0	10	0	0.0000	0.0000	0.0000	0.0000	34.4000	0.0000	0.0000	0.0000	0.0000	337.3488

1	0	1	0.0000	0.0000	0.0000	0.0000	34.4000	0.0000	0.0000	0.0000	0.0000	337.3488
1	1	1	0.0000	0.0000	0.0000	0.0000	34.4000	0.0000	0.0000	0.0000	0.0000	337.3488
1	2	1	0.0000	0.0000	0.0000	0.0000	34.4000	0.0000	0.0000	0.0000	0.0000	337.3488
1	3	1	0.0179	-0.0042	0.0179	-0.0042	34.4000	0.1760	-0.0414	0.1760	-0.0414	337.3488
1	4	1	0.2420	-0.0569	0.2420	-0.0569	34.4000	2.3732	-0.5584	2.3732	-0.5584	337.3488
1	5	1	0.9723	-0.2288	0.9723	-0.2288	34.4000	9.5350	-2.2435	9.5350	-2.2435	337.3488
1	6	1	2.1965	-0.5168	2.1965	-0.5168	34.4000	21.5407	-5.0684	21.5407	-5.0684	337.3488
1	7	1	3.9149	-0.9211	3.9149	-0.9211	34.4000	38.3917	-9.0333	38.3917	-9.0333	337.3488
1	8	1	6.1287	-1.4420	6.1287	-1.4420	34.4000	60.1016	-14.1415	60.1016	-14.1415	337.3488
1	9	1	8.8392	-2.0798	8.8392	-2.0798	34.4000	86.6831	-20.3960	86.6831	-20.3960	337.3488
1	10	1	12.0478	-2.8348	12.0478	-2.8348	34.4000	118.1484	-27.7996	118.1484	-27.7996	337.3488

2	0	1	0.0000	0.0000	0.0000	0.0000	34.4000	0.0000	0.0000	0.0000	0.0000	337.3488
2	1	1	0.0000	0.0000	0.0000	0.0000	34.4000	0.0000	0.0000	0.0000	0.0000	337.3488
2	2	1	0.0000	0.0000	0.0000	0.0000	34.4000	0.0000	0.0000	0.0000	0.0000	337.3488
2	3	1	0.0830	-0.0195	0.1010	-0.0238	34.4000	0.8141	-0.1915	0.9901	-0.2330	337.3488
2	4	1	1.1414	-0.2686	1.3834	-0.3255	34.4000	11.1934	-2.6337	13.5665	-3.1921	337.3488
2	5	1	4.5972	-1.0817	5.5695	-1.3105	34.4000	45.0828	-10.6077	54.6179	-12.8513	337.3488
2	6	1	10.3928	-2.4454	12.5893	-2.9622	34.4000	101.9182	-23.9808	123.4590	-29.0492	337.3488
2	7	1	18.5148	-4.3564	22.4297	-5.2776	34.4000	181.5684	-42.7220	219.9601	-51.7553	337.3488
2	8	21	24.6742	-4.9512	30.8029	-6.3933	34.4474	241.9715	-48.5549	302.0730	-62.6965	337.8134
2	9	21	23.3198	-2.3825	32.1590	-4.4623	34.6066	228.6894	-23.3642	315.3725	-43.7603	339.3752
2	10	21	21.2338	-0.0275	33.2816	-2.8623	34.8011	208.2325	-0.2700	326.3809	-28.0696	341.2825

3	0	1	0.0000	0.0000	0.0000	0.0000	34.4000	0.0000	0.0000	0.0000	0.0000	337.3488
3	1	1	0.0000	0.0000	0.0000	0.0000	34.4000	0.0000	0.0000	0.0000	0.0000	337.3488
3	2	1	0.0000	0.0000	0.0000	0.0000	34.4000	0.0000	0.0000	0.0000	0.0000	337.3488
3	3	1	0.0019	-0.0004	0.1029	-0.0242	34.4000	0.0186	-0.0044	1.0086	-0.2373	337.3488
3	4	1	0.0021	-0.0005	1.3855	-0.3260	34.4000	0.0203	-0.0048	13.5869	-3.1969	337.3488
3	5	1	-0.0246	0.0058	5.5448	-1.3047	34.4000	-0.2417	0.0569	54.3762	-12.7944	337.3488
3	6	1	-0.0190	0.0045	12.5703	-2.9577	34.4000	-0.1861	0.0438	123.2729	-29.0054	337.3488
3	7	1	0.0199	-0.0047	22.4496	-5.2823	34.4000	0.1949	-0.0459	220.1550	-51.8012	337.3488
3	8	22	0.0094	0.0132	30.8122	-6.3801	34.4483	0.0918	0.1293	302.1648	-62.5671	337.8222
3	9	22	0.0138	0.0199	32.1729	-4.4424	34.6086	0.1356	0.1950	315.5081	-43.5652	339.3942
3	10	22	0.0155	0.0216	33.2971	-2.8407	34.8045	0.1518	0.2120	326.5327	-27.8575	341.3152

4	0	1	0.0000	0.0000	0.0000	0.0000	34.4000	0.0000	0.0000	0.0000	0.0000	337.3488
4	1	1	0.1493	-0.0351	0.1493	-0.0351	34.4000	1.4636	-0.3444	1.4637	-0.3444	337.3488
4	2	1	2.3594	-0.5551	2.3594	-0.5551	34.4000	23.1373	-5.4441	23.1374	-5.4441	337.3488
4	3	1	8.6967	-2.0463	8.7995	-2.0705	34.4000	85.2850	-20.0671	86.2937	-20.3044	337.3488
4	4	1	16.9459	-3.9873	18.3314	-4.3133	34.4000	166.1825	-39.1018	179.7693	-42.2987	337.3488
4	5	21	24.7953	-5.7361	30.3402	-7.0407	34.4051	243.1592	-56.2516	297.5353	-69.0460	337.3993
4	6	21	19.3627	-1.8286	31.9330	-4.7864	34.5756	189.8831	-17.9329	313.1559	-46.9382	339.0705
4	7	21	10.8245	2.4093	33.2740	-2.8729	34.7995	106.1517	23.6276	326.3068	-28.1735	341.2669
4	8	22	3.4581	4.8472	34.2704	-1.5328	35.0619	33.9128	47.5351	336.0776	-15.0320	343.8402
4	9	22	2.7962	3.6834	34.9691	-0.7590	35.3547	27.4212	36.1222	342.9293	-7.4431	346.7107
4	10	22	2.2201	2.4806	35.5172	-0.3601	35.6986	21.7720	24.3261	348.3047	-3.5314	350.0837

5	0	1	0.0000	0.0000	0.0000	0.0000	34.4000	0.0000	0.0000	0.0000	0.0000	337.3488
5	1	1	-0.1157	0.0272	0.0336	-0.0079	34.4000	-1.1346	0.2670	0.3291	-0.0774	337.3488
5	2	1	-1.8327	0.4312	0.5266	-0.1239	34.4000	-17.9730	4.2289	5.1644	-1.2152	337.3488
5	3	1	-6.6892	1.5739	2.1103	-0.4965	34.4000	-65.5988	15.4350	20.6948	-4.8694	337.3488
5	4	1	-13.4301	3.1600	4.9013	-1.1532	34.4000	-131.7042	30.9892	48.0651	-11.3094	337.3488
5	5	1	-21.6703	5.0989	8.6699	-1.9418	34.4051	-212.5131	50.0031	85.0222	-19.0429	337.3993
5	6	1	-32.2981	7.5995	-0.3650	-2.8132	34.5756	-316.7357	74.5261	-3.5798	27.5878	339.0705
5	7	1	-45.2035	10.6361	-11.9295	7.7632	34.7995	-443.2950	104.3047	-116.9882	76.1312	341.2669
5	8	1	-60.2579	14.1783	-25.9875	12.6455	35.0619	-590.9279	139.0419	-254.8502	124.0098	343.8402
5	9	33	-64.5665	10.5541	-29.5974	9.7952	35.5227	-633.1807	103.5007	-290.2514	96.0577	348.3588
5	10	33	-67.7445	7.1311	-32.2273	6.7710	36.0924	-664.3467	69.9326	-316.0421	66.4012	353.9453

6	0	1	0.0000	0.0000	0.0000	0.0000	34.4000	0.0000	0.0000	0.0000	0.0000	337.3488
6	1	1	-0.0130	0.0031	0.0205	-0.0048	34.4000	-0.1276	0.0300	0.2015	-0.0474	337.3488
6	2	1	-0.2195	0.0517	0.3071	-0.0723	34.4000	-2.1530	0.5066	3.0114	-0.7086	337.3488
6	3	1	-0.6693	0.1575	1.4410	-0.3391	34.4000	-6.5631	1.5443	14.1317	-3.3251	337.3488
6	4	1	-0.8050	0.1894	4.0963	-0.9638	34.4000	-7.8945	1.8575	40.1706	-9.4519	337.3488
6	5	1	-1.1830	0.2783	7.4869	-1.6635	34.4051	-11.6009	2.7296	73.4214	-16.3133	337.3993
6	6	1	-3.9953	0.9401	-4.3604	3.7533	34.5756	-39.1808	9.2190	-42.7606	36.8068	339.0705
6	7	1	-10.4380	2.4560	-22.3675	10.2192	34.7995	-102.3623	24.0852	-219.3505	100.2164	341.2669
6	8	31	-4.6961	-4.7437	-30.6836	7.9018	35.3040	-46.0529	-46.5197	-300.9031	77.4901	346.2144
6	9	32	-4.2105	-5.8333	-33.8079	3.9619	35.9529	-41.2910	-57.2050	+331.5424	38.8526	352.5779
6	10	32	-1.7478	-2.4934	-33.9751	4.2777	36.3034	-17.1397	-24.4515	-333.1817	41.9497	356.0151

7	0	1	0.0000	0.0000	0.0000	0.0000	34.4000	0.0000	0.0000	0.0000	0.0000	337.3488
7	1	1	-0.0205	0.0048	0.0001	0.0000	34.4000	-0.2009	0.0473	0.0005	-0.0001	337.3488
7	2	1	-0.3069	0.0722	0.0002	-0.0001	34.4000	-3.0092	0.7081	0.0022	-0.0005	337.3488
7	3	1	-1.4274	0.3359	0.0137	-0.0032	34.4000	-13.9977	3.2936	0.1340	-0.0315	337.3488
7	4	1	-3.9684	0.9337	0.1279	-0.0301	34.4000	-38.9166	9.1568	1.2540	-0.2951	337.3488
7	5	1	-7.7446	1.8223	-0.2577	0.1588	34.4051	-75.9483	17.8702	-2.5269	1.5569	337.3993
7	6	1	-11.1379	2.6207	-15.4982	6.3739	34.5756	-109.2252	25.7000	-151.9858	62.5069	339.0705
7	7	31	-6.6197	-0.5027	-28.9872	9.7166	34.8759	-64.9169	-4.9294	-284.2673	95.2870	342.0154
7	8	32	-1.1016	-1.5330	-31.7851	6.3688	35.4019	-10.8026	-15.0332	-311.7058	62.4569	347.1736
7	9	32	-0.2264	-0.3239	-34.0343	3.6379	35.9915	-2.2204	-3.1768	-333.7628	35.6758	352.9556
7	10	32	-1.7020	-2.3715	-35.6771	1.9062	36.6674	-16.6907	-23.2560	-349.8725	18.6937	359.5839

8	0	1	0.0000	0.0000	0.0000	0.0000	34.4000	0.0000	0.0000	0.0000	0.0000	337.3488
8	1	1	0.0000	0.0000	0.0000	0.0000	34.4000	-0.0003	0.0001	0.0003	-0.0001	337.3488
8	2	1	-0.0001	0.0000	0.0001	0.0000	34.4000	-0.0011	0.0003	0.0011	-0.0003	337.3488
8	3	1	-0.0111	0.0026	0.0025	-0.0006	34.4000	-0.1092	0.0257	0.0248	-0.0058	337.3488
8	4	1	-0.0755	0.0178	0.0524	-0.0123	34.4000	-0.7399	0.1741	0.5141	-0.1210	337.3488
8	5	1	-0.0042	0.0010	-0.2618	0.1597	34.4051	-0.0409	0.0096	-2.5678	1.5665	337.3993
8	6	1	0.0202	-0.0047	-15.4781	6.3692	34.5756	0.1977	-0.0465	-151.7881	62.4604	339.0705
8	7	1	0.1023	-0.0241	-28.8849	9.6925	34.8759	1.0037	-0.2362	-283.2636	95.0509	342.0154
8	8	1	0.7061	-0.1661	-31.0791	6.2027	35.4019	6.9243	-1.6292	-304.7815	60.8277	347.1736
8	9	1	0.8127	-0.1912	-33.2216	3.4467	35.9915	7.9699	-1.8753	-325.7929	33.8006	352.9556
8	10	1	0.4956	-0.1166	-35.1815	1.7896	36.6674	4.8598	-1.1435	-345.0127	17.5502	359.5839

9	0	1	0.0000	0.0000	0.0000	0.0000	34.4000	0.0000	0.0000	0.0000	0.0000	337.3488
9	1	1	0.0000	0.0000	0.0001	0.0000	34.4000	0.0004	-0.0001	0.0007	-0.0002	337.3488
9	2	1	0.0002	0.0000	0.0003	-0.0001	34.4000	0.0016	-0.0004	0.0027	-0.0006	337.3488
9	3	1	-0.0019	0.0004	0.0006	-0.0001	34.4000	-0.0188	0.0044	0.0061	-0.0014	337.3488
9	4	1	-0.0510	0.0120	0.0015	-0.0003	34.4000	-0.4998	0.1176	0.0143	-0.0034	337.3488
9	5	1	-0.2041	0.0480	-0.4660	0.2078	34.4051	-2.0017	0.4710	-4.5695	2.0375	337.3993
9	6	1	-0.0181	0.0043	-15.4962	6.3734	34.5756	-0.1776	0.0418	-151.9657	62.5022	339.0705
9	7	1	0.5809	-0.1367	-28.3039	9.5558	34.8759	5.6969	-1.3405	-277.5667	93.7104	342.0154
9	8	1	0.3265	-0.0768	-30.7525	6.1259	35.4019	3.2021	-0.7534	-301.5794	60.0743	347.1736
9	9	1	-0.2242	0.0527	-33.4458	3.4994	35.9915	-2.1982	0.5172	-327.9910	34.3178	352.9556
9	10	31	-0.4984	0.1130	-35.6799	1.9026	36.6682	-4.8876	1.1080	-349.9003	18.6582	359.5926

 ** OUTPUT DATA(RESULT) OF X-,Y- AND Z-AXES POINTS TO **
 ** ANALYSE STRESS-STRAIN BY MODEL 2 **
 ** IN THE FILE RY100BC **

ST.	Mesh	PXE(I,J)	PYE(I,J)	PZ(I)	TLS(I)	ANE(I,J)	DB(I,J)	TLE(I,J)	TLN1(I)/2
0	0	0.000	0.000	-2034.000	0.000	0.000	15.75000	15.7500	157.5000
0	1	15.750	0.000	-2034.000	0.000	0.000	15.75000	31.5000	157.5000
0	2	31.500	0.000	-2034.000	0.000	0.000	15.75000	47.2500	157.5000
0	3	47.250	0.000	-2034.000	0.000	0.000	15.75000	63.0000	157.5000
0	4	63.000	0.000	-2034.000	0.000	0.000	15.75000	78.7500	157.5000
0	5	78.750	0.000	-2034.000	0.000	0.000	15.75000	94.5000	157.5000
0	6	94.500	0.000	-2034.000	0.000	0.000	15.75000	110.2500	157.5000
0	7	110.250	0.000	-2034.000	0.000	0.000	15.75000	126.0000	157.5000
0	8	126.000	0.000	-2034.000	0.000	0.000	15.75000	141.7500	157.5000
0	9	141.750	0.000	-2034.000	0.000	0.000	15.75000	157.5000	157.5000
0	10	157.500	0.000	-2034.000	0.000	0.000	15.75000	173.2500	157.5000

1	0	0.000	0.000	-1589.350	444.650	0.000	15.75000	15.7500	157.4995
1	1	15.750	0.001	-1589.350	444.650	0.009	15.75000	31.5000	157.4995
1	2	31.500	0.008	-1589.350	444.650	0.313	15.75000	47.2500	157.4995
1	3	47.236	0.601	-1589.350	444.650	4.005	15.74999	63.0000	157.4995
1	4	62.901	2.207	-1589.350	444.650	7.696	15.74990	78.7499	157.4995
1	5	78.495	4.420	-1589.350	444.650	8.105	15.74961	94.4995	157.4995
1	6	94.087	6.642	-1589.350	444.650	8.114	15.74912	110.2486	157.4995
1	7	109.678	8.866	-1589.350	444.650	8.123	15.74843	125.9971	157.4995
1	8	125.269	11.093	-1589.350	444.650	8.132	15.74754	141.7446	157.4995
1	9	140.858	13.322	-1589.350	444.650	8.141	15.74645	157.4910	157.4995
1	10	156.445	15.553	-1589.350	444.650	8.150	15.74516	173.2362	157.4995

2	0	0.000	0.000	-1266.000	768.000	0.000	15.75000	15.7500	157.4825
2	1	15.750	0.001	-1266.000	768.000	0.009	15.75000	31.5000	157.4825
2	2	31.500	0.014	-1266.000	768.000	0.831	15.75000	47.2500	157.4825
2	3	47.145	1.635	-1266.000	768.000	11.003	15.74996	63.0000	157.4825
2	4	62.259	5.994	-1266.000	768.000	21.174	15.74944	78.7494	157.4825
2	5	76.839	11.948	-1266.000	768.000	22.275	15.74776	94.4972	157.4825
2	6	91.411	17.919	-1266.000	768.000	22.284	15.74495	110.2421	157.4825
2	7	105.980	23.890	-1266.000	768.000	22.293	15.74100	125.9831	157.4825
2	8	120.544	29.863	-1266.000	768.000	22.302	15.73592	141.7190	157.4825
2	9	135.102	35.836	-1266.000	768.000	22.311	15.72973	157.4488	157.4825
2	10	149.654	41.808	-1266.000	768.000	22.320	15.72242	173.1712	157.4825

3	0	0.000	0.000	-641.000	1393.000	0.000	15.75000	15.7500	157.4996
3	1	15.750	0.001	-641.000	1393.000	0.009	15.75000	31.5000	157.4996
3	2	31.500	0.025	-641.000	1393.000	1.845	15.75000	47.2500	157.4996
3	3	46.728	3.616	-641.000	1393.000	24.691	15.74996	63.0000	157.4996
3	4	59.367	12.837	-641.000	1393.000	47.537	15.74944	78.7494	157.4996
3	5	69.515	24.882	-641.000	1393.000	50.025	15.74777	94.4972	157.4996
3	6	79.631	36.950	-641.000	1393.000	50.034	15.74495	110.2421	157.4996
3	7	89.743	49.019	-641.000	1393.000	50.043	15.74099	125.9831	157.4996
3	8	99.851	61.085	-641.000	1393.000	50.052	15.73589	141.7190	157.4996
3	9	109.954	73.150	-641.000	1393.000	50.061	15.72966	157.4487	157.4996
3	10	120.051	85.211	-641.000	1393.000	50.070	15.72230	173.1710	157.4996

4	0	0.000	0.000	-181.000	1853.000	0.000	15.75000	15.7500	157.4981
4	1	15.613	1.791	-181.000	1853.000	13.084	15.74994	31.4999	157.4981
4	2	30.412	7.077	-181.000	1853.000	26.950	15.74905	47.2490	157.4981
4	3	42.678	16.789	-181.000	1853.000	49.794	15.74647	62.9955	157.4981
4	4	50.210	30.498	-181.000	1853.000	72.635	15.74264	78.7381	157.4981
4	5	54.288	45.703	-181.000	1853.000	75.128	15.73764	94.4757	157.4981
4	6	58.326	60.914	-181.000	1853.000	75.137	15.73093	110.2067	157.4981
4	7	62.360	76.119	-181.000	1853.000	75.146	15.72250	125.9292	157.4981
4	8	66.389	91.316	-181.000	1853.000	75.155	15.71238	141.6416	157.4981
4	9	70.413	106.505	-181.000	1853.000	75.164	15.70059	157.3422	157.4981
4	10	74.432	121.682	-181.000	1853.000	75.173	15.68716	173.0293	157.4981

5	0	0.000	0.000	393.010	2427.010	0.000	15.75000	15.7500	157.4562
5	1	15.405	2.832	393.010	2427.010	20.836	15.74999	31.5000	157.4562
5	2	28.793	10.962	393.010	2427.010	42.017	15.74979	47.2498	157.4562
5	3	37.848	23.694	393.010	2427.010	67.146	15.74915	62.9989	157.4562
5	4	40.638	39.066	393.010	2427.010	92.274	15.74803	78.7470	157.4562
5	5	39.263	54.753	393.010	2427.010	95.356	15.74633	94.4933	157.4562
5	6	37.739	70.426	393.010	2427.010	95.755	15.74386	110.2371	157.4562

5	7	36.105	86.085	393.010	2427.010	96.154	15.74059	125.9777	157.4562
5	8	34.364	101.729	393.010	2427.010	96.552	15.73648	141.7142	157.4562
5	9	32.514	117.356	393.010	2427.010	96.951	15.73148	157.4457	157.4562
5	10	30.555	132.965	393.010	2427.010	97.350	15.72557	173.1713	157.4562

6	0	0.000	0.000	654.000	2688.000	0.000	15.65147	15.6515	156.4947
6	1	15.392	2.454	654.000	2688.000	18.116	15.65146	31.3029	156.4947
6	2	29.256	9.575	654.000	2688.000	36.545	15.65136	46.9543	156.4947
6	3	39.681	21.111	654.000	2688.000	59.248	15.65093	62.6052	156.4947
6	4	44.847	35.777	654.000	2688.000	81.950	15.64994	78.2552	156.4947
6	5	45.899	51.387	654.000	2688.000	88.111	15.64845	93.9036	156.4947
6	6	45.924	67.033	654.000	2688.000	91.705	15.64719	109.5508	156.4947
6	7	44.969	82.648	654.000	2688.000	95.298	15.64659	125.1974	156.4947
6	8	42.012	97.948	654.000	2688.000	111.518	15.64783	140.8452	156.4947
6	9	33.401	110.873	654.000	2688.000	135.821	15.64949	156.4947	156.4947
6	10	20.507	119.619	654.000	2688.000	155.000	15.63501	172.1297	156.4947

7	0	0.000	0.000	1094.000	3128.000	0.000	15.61634	15.6163	156.1620
7	1	15.359	2.443	1094.000	3128.000	18.076	15.61634	31.2327	156.1620
7	2	29.201	9.531	1094.000	3128.000	36.152	15.61634	46.8490	156.1620
7	3	40.000	20.698	1094.000	3128.000	56.190	15.61634	62.4654	156.1620
7	4	46.200	34.940	1094.000	3128.000	76.759	15.61629	78.0817	156.1620
7	5	47.719	50.455	1094.000	3128.000	88.537	15.61626	93.6979	156.1620
7	6	47.314	66.060	1094.000	3128.000	94.438	15.61629	109.3142	156.1620
7	7	45.260	81.530	1094.000	3128.000	102.672	15.61633	124.9305	156.1620
7	8	39.081	95.772	1094.000	3128.000	124.233	15.61607	140.5466	156.1620
7	9	28.101	106.747	1094.000	3128.000	145.793	15.61541	156.1620	156.1620
7	10	13.967	113.226	1094.000	3128.000	164.460	15.61459	171.7766	156.1620

8	0	0.000	0.000	1534.000	3568.000	0.000	15.59301	15.5930	155.9281
8	1	15.336	2.436	1534.000	3568.000	18.049	15.59301	31.1860	155.9281
8	2	29.163	9.503	1534.000	3568.000	36.098	15.59301	46.7790	155.9281
8	3	40.118	20.509	1534.000	3568.000	54.232	15.59301	62.3721	155.9281
8	4	47.060	34.396	1534.000	3568.000	72.653	15.59299	77.9650	155.9281
8	5	49.609	49.741	1534.000	3568.000	86.766	15.59293	93.5580	155.9281
8	6	48.949	65.294	1534.000	3568.000	98.734	15.59295	109.1509	155.9281
8	7	44.166	80.065	1534.000	3568.000	117.155	15.59295	124.7439	155.9281
8	8	34.960	92.567	1534.000	3568.000	135.576	15.59246	140.3363	155.9281
8	9	22.279	101.526	1534.000	3568.000	153.853	15.59176	155.9281	155.9281
8	10	7.440	106.098	1534.000	3568.000	171.900	15.59108	171.5192	155.9281

9	0	0.000	0.000	2034.000	4068.000	0.000	15.55111	15.5511	155.5088
9	1	15.297	2.423	2034.000	4068.000	18.000	15.55111	31.1022	155.5088
9	2	29.096	9.454	2034.000	4068.000	36.001	15.55111	46.6533	155.5088
9	3	40.047	20.405	2034.000	4068.000	54.001	15.55111	62.2044	155.5088
9	4	47.078	34.205	2034.000	4068.000	72.001	15.55111	77.7556	155.5088
9	5	49.500	49.501	2034.000	4068.000	90.001	15.55111	93.3067	155.5088
9	6	47.077	64.798	2034.000	4068.000	108.002	15.55105	108.8577	155.5088
9	7	40.045	78.597	2034.000	4068.000	126.002	15.55080	124.4085	155.5088
9	8	29.094	89.547	2034.000	4068.000	144.002	15.55040	139.9589	155.5088
9	9	15.295	96.578	2034.000	4068.000	162.001	15.54991	155.5088	155.5088
9	10	0.000	99.000	2034.000	4068.000	180.000	15.54937	171.0582	155.5088

ST.	Mesh	FRD(I)	DEZF(%)	DEXF(%)	DBO(I,J)	DB(I,J)	TLEO(I,J)	TLE(I,J)	TLN1(I)/2
6	0	0.0063	0.2824	-0.6276	15.7500	15.6515	15.7500	15.6515	156.4947
6	1	0.0063	0.2824	-0.6276	15.7500	15.6515	31.5000	31.3029	156.4947
6	2	0.0063	0.2824	-0.6276	15.7499	15.6514	47.2499	46.9543	156.4947
6	3	0.0063	0.2824	-0.6276	15.7495	15.6509	62.9993	62.6052	156.4947
6	4	0.0063	0.2824	-0.6276	15.7485	15.6499	78.7478	78.2552	156.4947
6	5	0.0063	0.2824	-0.6276	15.7470	15.6485	94.4948	93.9036	156.4947
6	6	0.0063	0.2824	-0.6276	15.7457	15.6472	110.2405	109.5508	156.4947
6	7	0.0063	0.2824	-0.6276	15.7451	15.6466	125.9856	125.1974	156.4947
6	8	0.0063	0.2824	-0.6276	15.7463	15.6478	141.7319	140.8452	156.4947
6	9	0.0063	0.2824	-0.6276	15.7480	15.6495	157.4799	156.4947	156.4947
6	10	0.0063	0.2824	-0.6276	15.7334	15.6350	173.2133	172.1297	156.4947

7	0	0.0022	0.1011	-0.2247	15.6515	15.6163	15.6515	15.6163	156.1620
7	1	0.0022	0.1011	-0.2247	15.6515	15.6163	31.3029	31.2327	156.1620
7	2	0.0022	0.1011	-0.2247	15.6515	15.6163	46.9544	46.8490	156.1620
7	3	0.0022	0.1011	-0.2247	15.6515	15.6163	62.6059	62.4654	156.1620
7	4	0.0022	0.1011	-0.2247	15.6514	15.6163	78.2573	78.0817	156.1620
7	5	0.0022	0.1011	-0.2247	15.6514	15.6163	93.9087	93.6979	156.1620
7	6	0.0022	0.1011	-0.2247	15.6514	15.6163	109.5601	109.3142	156.1620
7	7	0.0022	0.1011	-0.2247	15.6515	15.6163	125.2116	124.9305	156.1620

7	8	0.0022	0.1011	-0.2247	15.6512	15.6161	140.8628	140.5466	156.1620
7	9	0.0022	0.1011	-0.2247	15.6505	15.6154	156.5133	156.1620	156.1620
7	10	0.0022	0.1011	-0.2247	15.6497	15.6146	172.1630	171.7766	156.1620

8	0	0.0015	0.0673	-0.1495	15.6163	15.5930	15.6163	15.5930	155.9281
8	1	0.0015	0.0673	-0.1495	15.6163	15.5930	31.2327	31.1860	155.9281
8	2	0.0015	0.0673	-0.1495	15.6163	15.5930	46.8490	46.7790	155.9281
8	3	0.0015	0.0673	-0.1495	15.6163	15.5930	62.4654	62.3721	155.9281
8	4	0.0015	0.0673	-0.1495	15.6163	15.5930	78.0817	77.9650	155.9281
8	5	0.0015	0.0673	-0.1495	15.6163	15.5929	93.6980	93.5580	155.9281
8	6	0.0015	0.0673	-0.1495	15.6163	15.5930	109.3142	109.1509	155.9281
8	7	0.0015	0.0673	-0.1495	15.6163	15.5930	124.9305	124.7439	155.9281
8	8	0.0015	0.0673	-0.1495	15.6158	15.5925	140.5463	140.3363	155.9281
8	9	0.0015	0.0673	-0.1495	15.6151	15.5918	156.1614	155.9281	155.9281
8	10	0.0015	0.0673	-0.1495	15.6144	15.5911	171.7758	171.5192	155.9281

9	0	0.0027	0.1211	-0.2691	15.5930	15.5511	15.5930	15.5511	155.5088
9	1	0.0027	0.1211	-0.2691	15.5930	15.5511	31.1860	31.1022	155.5088
9	2	0.0027	0.1211	-0.2691	15.5930	15.5511	46.7790	46.6533	155.5088
9	3	0.0027	0.1211	-0.2691	15.5930	15.5511	62.3721	62.2044	155.5088
9	4	0.0027	0.1211	-0.2691	15.5930	15.5511	77.9651	77.7556	155.5088
9	5	0.0027	0.1211	-0.2691	15.5930	15.5511	93.5581	93.3067	155.5088
9	6	0.0027	0.1211	-0.2691	15.5930	15.5511	109.1510	108.8577	155.5088
9	7	0.0027	0.1211	-0.2691	15.5927	15.5508	124.7437	124.4085	155.5088
9	8	0.0027	0.1211	-0.2691	15.5923	15.5504	140.3360	139.9589	155.5088
9	9	0.0027	0.1211	-0.2691	15.5918	15.5499	155.9278	155.5088	155.5088
9	10	0.0027	0.1211	-0.2691	15.5913	15.5494	171.5191	171.0582	155.5088

 ** OUTPUT DATA(RESULT) OF STRESS-STRAIN ANALYSIS **
 ** MODEL 2 IN THE FILE RY100BC **

***** RESULTS OF STRAIN *****

OD= 100.00 TS= 1.00 NUMBER OF STAND= 9 Stand No. of 1st Finpass= 6
 NUMBER OF DIVISION=10 Ex/Ez= 0.50 Ez/Ex in Finpass & SQ= 0.45

ST.	Mesh	DEz(%)	Ez(%)	DEx(%)	Ex(%)	DEZE(%)	DEXE(%)	EzE(%)	ExE(%)	DEPSOT(%)
0	0	0.000000	0.000000	0.000000	0.000000	0.000000	0.000000	0.000000	0.000000	0.000000
0	1	0.000000	0.000000	0.000000	0.000000	0.000000	0.000000	0.000000	0.000000	0.000000
0	2	0.000000	0.000000	0.000000	0.000000	0.000000	0.000000	0.000000	0.000000	0.000000
0	3	0.000000	0.000000	0.000000	0.000000	0.000000	0.000000	0.000000	0.000000	0.000000
0	4	0.000000	0.000000	0.000000	0.000000	0.000000	0.000000	0.000000	0.000000	0.000000
0	5	0.000000	0.000000	0.000000	0.000000	0.000000	0.000000	0.000000	0.000000	0.000000
0	6	0.000000	0.000000	0.000000	0.000000	0.000000	0.000000	0.000000	0.000000	0.000000
0	7	0.000000	0.000000	0.000000	0.000000	0.000000	0.000000	0.000000	0.000000	0.000000
0	8	0.000000	0.000000	0.000000	0.000000	0.000000	0.000000	0.000000	0.000000	0.000000
0	9	0.000000	0.000000	0.000000	0.000000	0.000000	0.000000	0.000000	0.000000	0.000000
0	10	0.000000	0.000000	0.000000	0.000000	0.000000	0.000000	0.000000	0.000000	0.000000

1	0	0.000000	0.000000	0.000000	0.000000	0.000000	0.000000	0.000000	0.000000	0.000000
1	1	0.000000	0.000000	0.000000	0.000000	0.000000	0.000000	0.000000	0.000000	0.000000
1	2	0.000000	0.000000	0.000000	0.000000	0.000000	0.000000	0.000000	0.000000	0.000000
1	3	0.000091	0.000091	-0.000046	-0.000046	0.000091	-0.000046	0.000091	-0.000046	0.000000
1	4	0.001234	0.001234	-0.000617	-0.000617	0.001234	-0.000617	0.001234	-0.000617	0.000000
1	5	0.004957	0.004957	-0.002478	-0.002478	0.004957	-0.002478	0.004957	-0.002478	0.000000
1	6	0.011198	0.011198	-0.005599	-0.005599	0.011198	-0.005599	0.011198	-0.005599	0.000000
1	7	0.019958	0.019958	-0.009979	-0.009979	0.019958	-0.009979	0.019958	-0.009979	0.000000
1	8	0.031243	0.031243	-0.015622	-0.015622	0.031243	-0.015622	0.031243	-0.015622	0.000000
1	9	0.045060	0.045060	-0.022530	-0.022530	0.045060	-0.022530	0.045060	-0.022530	0.000000
1	10	0.061415	0.061415	-0.030708	-0.030708	0.061415	-0.030708	0.061415	-0.030708	0.017152

2	0	0.000000	0.000000	0.000000	0.000000	0.000000	0.000000	0.000000	0.000000	0.000000
2	1	0.000000	0.000000	0.000000	0.000000	0.000000	0.000000	0.000000	0.000000	0.000000
2	2	0.000000	0.000000	0.000000	0.000000	0.000000	0.000000	0.000000	0.000000	0.000000
2	3	0.000424	0.000515	-0.000212	-0.000258	0.000424	-0.000212	0.000515	-0.000258	0.000000
2	4	0.005824	0.007058	-0.002912	-0.003529	0.005824	-0.002912	0.007058	-0.003529	0.000000
2	5	0.023447	0.028404	-0.011723	-0.014202	0.023447	-0.011723	0.028404	-0.014202	0.000000
2	6	0.052996	0.064194	-0.026498	-0.032097	0.052996	-0.026498	0.064194	-0.032097	0.000000
2	7	0.094398	0.114355	-0.047199	-0.057178	0.094398	-0.047199	0.114355	-0.057178	0.000000
2	8	0.147595	0.178838	-0.073797	-0.089419	0.147595	-0.073797	0.178838	-0.089419	0.023451
2	9	0.212514	0.257575	-0.106257	-0.128787	0.212514	-0.106257	0.257575	-0.128787	0.102276
2	10	0.289072	0.350487	-0.144536	-0.175243	0.289072	-0.144536	0.350487	-0.175243	0.198507

3	0	0.000000	0.000000	0.000000	0.000000	0.000000	0.000000	0.000000	0.000000	0.000000
3	1	0.000000	0.000000	0.000000	0.000000	0.000000	0.000000	0.000000	0.000000	0.000000
3	2	0.000000	0.000000	0.000000	0.000000	0.000000	0.000000	0.000000	0.000000	0.000000
3	3	0.000009	0.000524	-0.000005	-0.000262	0.000009	-0.000005	0.000524	-0.000262	0.000000
3	4	0.000006	0.007064	-0.000003	-0.003532	0.000006	-0.000003	0.007064	-0.003532	0.000000
3	5	-0.000133	0.028271	0.000066	-0.014136	-0.000133	0.000066	0.028271	-0.014136	0.000000
3	6	-0.000107	0.064087	0.000054	-0.032043	-0.000107	0.000054	0.064087	-0.032043	0.000000
3	7	0.000082	0.114438	-0.000041	-0.057219	0.000082	-0.000041	0.114438	-0.057219	0.000000
3	8	0.000430	0.179268	-0.000215	-0.089634	0.000430	-0.000215	0.179268	-0.089634	0.000408
3	9	0.000928	0.258503	-0.000464	-0.129251	0.000928	-0.000464	0.258503	-0.129251	0.000890
3	10	0.001566	0.352053	-0.000783	-0.176026	0.000939	-0.000783	0.352053	-0.176026	0.001516

4	0	0.000000	0.000000	0.000000	0.000000	0.000000	0.000000	0.000000	0.000000	0.000000
4	1	0.000761	0.000761	-0.000380	-0.000380	0.000761	-0.000380	0.000761	-0.000380	0.000000
4	2	0.012028	0.012028	-0.006014	-0.006014	0.012028	-0.006014	0.012028	-0.006014	0.000000
4	3	0.044334	0.044859	-0.022167	-0.022429	0.044334	-0.022167	0.044859	-0.022429	0.000000
4	4	0.086365	0.093429	-0.043183	-0.046714	0.086365	-0.043183	0.093429	-0.046714	0.000000
4	5	0.128711	0.156983	-0.064356	-0.078491	0.128711	-0.064356	0.156983	-0.078491	0.002473
4	6	0.178273	0.242360	-0.089137	-0.121180	0.094805	-0.036383	0.158892	-0.068426	0.086761
4	7	0.235067	0.349505	-0.117534	-0.174753	0.048104	-0.004015	0.162542	-0.061234	0.197482
4	8	0.298975	0.478243	-0.149488	-0.239121	0.009533	0.018129	0.165370	-0.056275	0.303288
4	9	0.369860	0.628363	-0.184930	-0.314181	0.008043	0.013543	0.167589	-0.053583	0.368520
4	10	0.447569	0.799622	-0.223784	-0.399811	0.007016	0.008649	0.169625	-0.052459	0.441372

5	0	0.000000	0.000000	0.000000	0.000000	0.000000	0.000000	0.000000	0.000000	0.000000

5	1	-0.000590	0.000171	0.000295	-0.000086	-0.000590	0.000295	0.000171	-0.000086	0.000000
5	2	-0.009340	0.002688	0.004670	-0.001344	-0.009340	0.004670	0.002688	-0.001344	0.000000
5	3	-0.034083	0.010776	0.017041	-0.005388	-0.034083	0.017041	0.010776	-0.005388	0.000000
5	4	-0.068391	0.025038	0.034196	-0.012519	-0.068391	0.034196	0.025038	-0.012519	0.000000
5	5	-0.110318	0.046664	0.055159	-0.023332	-0.110318	0.055159	0.044212	-0.021721	0.000000
5	6	-0.164375	0.077985	0.082187	-0.038992	-0.164375	0.082187	-0.035483	0.013761	0.000000
5	7	-0.229978	0.119527	0.114989	-0.059764	-0.229978	0.114989	-0.067436	0.053755	0.000000
5	8	-0.306448	0.171795	0.153224	-0.085897	-0.306448	0.153224	-0.141078	0.096949	0.000000
5	9	-0.393075	0.235288	0.196538	-0.117644	-0.322413	0.142665	-0.154824	0.089082	0.081965
5	10	-0.489122	0.310500	0.244561	-0.155250	-0.332646	0.130915	-0.163022	0.078455	0.192986

6	0	0.282399	0.282399	-0.627553	-0.627553	0.043959	-0.169961	0.043959	-0.169961	0.492912
6	1	0.282321	0.282492	-0.627514	-0.627600	0.043780	-0.169881	0.043951	-0.169966	0.493271
6	2	0.281177	0.283865	-0.626942	-0.628286	0.041147	-0.168700	0.043835	-0.170044	0.498710
6	3	0.278493	0.289269	-0.625600	-0.630988	0.032907	-0.164887	0.043683	-0.170275	0.518589
6	4	0.276857	0.301894	-0.624782	-0.637301	0.019062	-0.158122	0.044100	-0.170641	0.562381
6	5	0.274266	0.320930	-0.623487	-0.646819	0.000347	-0.149621	0.044559	-0.171342	0.637481
6	6	0.259116	0.337101	-0.615912	-0.654904	0.044504	-0.185216	0.039021	-0.171455	0.467593
6	7	0.225215	0.344743	-0.598961	-0.658725	0.093383	-0.226985	0.025947	-0.173230	0.376791
6	8	0.157083	0.328878	-0.564895	-0.650792	0.138620	-0.273087	-0.002457	-0.176138	0.547731
6	9	0.072465	0.307753	-0.522586	-0.640230	0.124440	-0.266493	-0.030384	-0.177411	0.904432
6	10	0.182280	0.492781	-0.577494	-0.732744	0.166341	-0.262477	0.003320	-0.184022	0.801807

7	0	0.101107	0.383506	-0.224682	-0.852235	-0.001246	-0.002473	0.042713	-0.172434	0.220430
7	1	0.101013	0.383506	-0.224635	-0.852235	-0.001283	-0.002479	0.042669	-0.172446	0.220384
7	2	0.099640	0.383506	-0.223949	-0.852235	-0.001822	-0.002568	0.042013	-0.172611	0.219718
7	3	0.094301	0.383570	-0.221279	-0.852267	-0.004152	-0.002933	0.039531	-0.173208	0.217358
7	4	0.082234	0.384128	-0.215245	-0.852546	-0.010068	-0.003764	0.034032	-0.174406	0.213772
7	5	0.063582	0.384512	-0.205919	-0.852738	-0.019471	-0.004730	0.025088	-0.176072	0.213291
7	6	0.047042	0.384143	-0.197649	-0.852553	-0.024731	-0.004236	0.014290	-0.175692	0.214038
7	7	0.038977	0.383719	-0.193617	-0.852342	-0.020955	-0.002461	0.004991	-0.175691	0.207985
7	8	0.058069	0.386946	-0.203163	-0.853955	0.008556	-0.002570	0.006099	-0.178707	0.209326
7	9	0.087769	0.395522	-0.218013	-0.858243	0.044688	-0.007893	0.014305	-0.185305	0.283720
7	10	-0.086811	0.405970	-0.130723	-0.863467	-0.084263	0.020237	-0.080943	-0.163785	0.391899

8	0	0.067278	0.450784	-0.149507	-1.001741	-0.000097	-0.001507	0.042617	-0.173941	0.146792
8	1	0.067278	0.450784	-0.149507	-1.001741	-0.000074	-0.001503	0.042595	-0.173948	0.146797
8	2	0.067278	0.450784	-0.149507	-1.001741	0.000270	-0.001442	0.042283	-0.174053	0.146875
8	3	0.067225	0.450795	-0.149480	-1.001747	0.001545	-0.001234	0.041077	-0.174442	0.147199
8	4	0.066912	0.451040	-0.149324	-1.001870	0.004294	-0.000892	0.038325	-0.175297	0.148119
8	5	0.067293	0.451805	-0.149514	-1.002252	0.009341	-0.000575	0.034428	-0.176647	0.151293
8	6	0.067415	0.451558	-0.149575	-1.002129	0.015236	-0.000713	0.029526	-0.176405	0.156630
8	7	0.067868	0.451587	-0.149801	-1.002143	0.020708	-0.001255	0.025700	-0.176945	0.163391
8	8	0.070954	0.457901	-0.151345	-1.005300	0.022078	-0.001071	0.028177	-0.179778	0.166403
8	9	0.071385	0.466907	-0.151560	-1.009803	0.018230	-0.000561	0.032535	-0.185866	0.161238
8	10	0.069609	0.475579	-0.150672	-1.014139	0.070542	-0.025852	-0.010402	-0.189637	0.301193

9	0	0.121087	0.571871	-0.269082	-1.270824	0.000316	-0.002625	0.042933	-0.176566	0.264308
9	1	0.121087	0.571871	-0.269082	-1.270824	0.000332	-0.002622	0.042928	-0.176570	0.264311
9	2	0.121087	0.571871	-0.269082	-1.270824	0.000570	-0.002580	0.042853	-0.176633	0.264366
9	3	0.121076	0.571871	-0.269077	-1.270824	0.001484	-0.002426	0.042560	-0.176868	0.264605
9	4	0.120831	0.571872	-0.268955	-1.270824	0.003477	-0.002123	0.041803	-0.177420	0.265218
9	5	0.120068	0.571873	-0.268573	-1.270825	0.006161	-0.001795	0.040590	-0.178442	0.266257
9	6	0.121087	0.572645	-0.269082	-1.271211	0.010142	-0.001414	0.039669	-0.177818	0.269602
9	7	0.124273	0.575860	-0.270676	-1.272818	0.014454	-0.001062	0.040153	-0.178008	0.275277
9	8	0.123097	0.580998	-0.270088	-1.275387	0.012522	-0.001195	0.040699	-0.180974	0.272592
9	9	0.120417	0.587324	-0.268747	-1.278550	0.009071	-0.001508	0.041605	-0.187374	0.268273
9	10	0.118720	0.594299	-0.267899	-1.282038	0.040727	-0.003892	0.030325	-0.193529	0.319970

***** RESULTS OF STRESS *****

ST.	Mesh	NHAN	DSz(kg/mm2)	DSx	Sz	Sx	SEQ	DSz(MPa)	DSx	Sz	Sx	SEQ
0	0	0	0.0000	0.0000	0.0000	0.0000	34.4000	0.0000	0.0000	0.0000	0.0000	337.3488
0	1	0	0.0000	0.0000	0.0000	0.0000	34.4000	0.0000	0.0000	0.0000	0.0000	337.3488
0	2	0	0.0000	0.0000	0.0000	0.0000	34.4000	0.0000	0.0000	0.0000	0.0000	337.3488
0	3	0	0.0000	0.0000	0.0000	0.0000	34.4000	0.0000	0.0000	0.0000	0.0000	337.3488
0	4	0	0.0000	0.0000	0.0000	0.0000	34.4000	0.0000	0.0000	0.0000	0.0000	337.3488
0	5	0	0.0000	0.0000	0.0000	0.0000	34.4000	0.0000	0.0000	0.0000	0.0000	337.3488
0	6	0	0.0000	0.0000	0.0000	0.0000	34.4000	0.0000	0.0000	0.0000	0.0000	337.3488
0	7	0	0.0000	0.0000	0.0000	0.0000	34.4000	0.0000	0.0000	0.0000	0.0000	337.3488
0	8	0	0.0000	0.0000	0.0000	0.0000	34.4000	0.0000	0.0000	0.0000	0.0000	337.3488
0	9	0	0.0000	0.0000	0.0000	0.0000	34.4000	0.0000	0.0000	0.0000	0.0000	337.3488
0	10	0	0.0000	0.0000	0.0000	0.0000	34.4000	0.0000	0.0000	0.0000	0.0000	337.3488

1	0	1	0.0000	0.0000	0.0000	0.0000	34.4000	0.0000	0.0000	0.0000	0.0000	337.3488
1	1	1	0.0000	0.0000	0.0000	0.0000	34.4000	0.0000	0.0000	0.0000	0.0000	337.3488
1	2	1	0.0000	0.0000	0.0000	0.0000	34.4000	0.0000	0.0000	0.0000	0.0000	337.3488
1	3	1	0.0179	-0.0042	0.0179	-0.0042	34.4000	0.1760	-0.0414	0.1760	-0.0414	337.3488
1	4	1	0.2420	-0.0569	0.2420	-0.0569	34.4000	2.3732	-0.5584	2.3732	-0.5584	337.3488
1	5	1	0.9723	-0.2288	0.9723	-0.2288	34.4000	9.5351	-2.2436	9.5351	-2.2436	337.3488
1	6	1	2.1965	-0.5168	2.1965	-0.5168	34.4000	21.5406	-5.0684	21.5406	-5.0684	337.3488
1	7	1	3.9148	-0.9211	3.9148	-0.9211	34.4000	38.3910	-9.0332	38.3910	-9.0332	337.3488
1	8	1	6.1284	-1.4420	6.1284	-1.4420	34.4000	60.0995	-14.1410	60.0995	-14.1410	337.3488
1	9	1	8.8387	-2.0797	8.8387	-2.0797	34.4000	86.6782	-20.3949	86.6782	-20.3949	337.3488
1	10	1	12.0468	-2.8345	12.0468	-2.8345	34.4000	118.1388	-27.7974	118.1388	-27.7974	337.3488

2	0	1	0.0000	0.0000	0.0000	0.0000	34.4000	0.0000	0.0000	0.0000	0.0000	337.3488
2	1	1	0.0000	0.0000	0.0000	0.0000	34.4000	0.0000	0.0000	0.0000	0.0000	337.3488
2	2	1	0.0000	0.0000	0.0000	0.0000	34.4000	0.0000	0.0000	0.0000	0.0000	337.3488
2	3	1	0.0831	-0.0196	0.1011	-0.0238	34.4000	0.8151	-0.1918	0.9911	-0.2332	337.3488
2	4	1	1.1424	-0.2688	1.3844	-0.3257	34.4000	11.2032	-2.6360	13.5764	-3.1944	337.3488
2	5	1	4.5992	-1.0822	5.5715	-1.3109	34.4000	45.1027	-10.6124	54.6378	-12.8560	337.3488
2	6	1	10.3953	-2.4460	12.5919	-2.9628	34.4000	101.9433	-23.9867	123.4839	-29.0550	337.3488
2	7	1	18.5165	-4.3568	22.4313	-5.2779	34.4000	181.5844	-42.7257	219.9754	-51.7589	337.3488
2	8	21	24.6742	-4.9516	30.8026	-6.3936	34.4474	241.9711	-48.5589	302.0705	-62.7000	337.8131
2	9	21	23.3195	-2.3838	32.1582	-4.4635	34.6065	228.6859	-23.3773	315.3641	-43.7722	339.3740
2	10	21	21.2334	-0.0298	33.2802	-2.8643	34.8008	208.2282	-0.2918	326.3670	-28.0891	341.2796

3	0	1	0.0000	0.0000	0.0000	0.0000	34.4000	0.0000	0.0000	0.0000	0.0000	337.3488
3	1	1	0.0000	0.0000	0.0000	0.0000	34.4000	0.0000	0.0000	0.0000	0.0000	337.3488
3	2	1	0.0000	0.0000	0.0000	0.0000	34.4000	0.0000	0.0000	0.0000	0.0000	337.3488
3	3	1	0.0018	-0.0004	0.1029	-0.0242	34.4000	0.0176	-0.0042	1.0087	-0.2373	337.3488
3	4	1	0.0012	-0.0003	1.3856	-0.3260	34.4000	0.0114	-0.0027	13.5878	-3.1971	337.3488
3	5	1	-0.0260	0.0061	5.5455	-1.3048	34.4000	-0.2551	0.0600	54.3827	-12.7959	337.3488
3	6	1	-0.0210	0.0049	12.5708	-2.9578	34.4000	-0.2061	0.0485	123.2778	-29.0065	337.3488
3	7	1	0.0162	-0.0038	22.4474	-5.2817	34.4000	0.1584	-0.0373	220.1338	-51.7962	337.3488
3	8	22	0.0086	0.0121	30.8112	-6.3815	34.4482	0.0844	0.1189	302.1549	-62.5811	337.8212
3	9	22	0.0128	0.0184	32.1710	-4.4451	34.6083	0.1256	0.1807	315.4898	-43.5915	339.3916
3	10	22	0.0143	0.0199	33.2944	-2.8444	34.8039	0.1398	0.1953	326.5068	-27.8938	341.3096

4	0	1	0.0000	0.0000	0.0000	0.0000	34.4000	0.0000	0.0000	0.0000	0.0000	337.3488
4	1	1	0.1493	-0.0351	0.1493	-0.0351	34.4000	1.4637	-0.3444	1.4637	-0.3444	337.3488
4	2	1	2.3594	-0.5552	2.3594	-0.5552	34.4000	23.1381	-5.4443	23.1381	-5.4443	337.3488
4	3	1	8.6863	-2.0462	8.7992	-2.0704	34.4000	85.2820	-20.0664	86.2907	-20.3037	337.3488
4	4	1	16.9408	-3.9861	18.3264	-4.3121	34.4000	166.1329	-39.0901	179.7207	-42.2872	337.3488
4	5	21	24.7928	-5.7385	30.3383	-7.0433	34.4050	243.1348	-56.2750	297.5174	-69.0709	337.3977
4	6	21	19.3593	-1.8327	31.9301	-4.7905	34.5752	189.8499	-17.9722	313.1277	-46.9787	339.0668
4	7	21	10.8230	2.4037	33.2704	-2.8780	34.7988	106.1370	23.5723	326.2709	-28.2239	341.2593
4	8	22	3.4551	4.8436	34.2663	-1.5379	35.0606	33.8831	47.4997	336.0381	-15.0813	343.8269
4	9	22	2.7938	3.6821	34.9648	-0.7630	35.3524	27.3974	36.1089	342.8871	-7.4826	346.6890
4	10	22	2.2179	2.4816	35.5124	-0.3628	35.6951	21.7505	24.3363	348.2573	-3.5575	350.0496

5	0	1	0.0000	0.0000	0.0000	0.0000	34.4000	0.0000	0.0000	0.0000	0.0000	337.3488
5	1	1	-0.1157	0.0272	0.0336	-0.0079	34.4000	-1.1342	0.2669	0.3295	-0.0775	337.3488
5	2	1	-1.8321	0.4311	0.5273	-0.1241	34.4000	-17.9666	4.2274	5.1715	-1.2168	337.3488
5	3	1	-6.6854	1.5730	2.1138	-0.4974	34.4000	-65.5615	15.4262	20.7292	-4.8775	337.3488
5	4	1	-13.4152	3.1565	4.9112	-1.1556	34.4000	-131.5581	30.9548	48.1626	-11.3324	337.3488
5	5	1	-21.6394	5.0916	8.6990	-1.9517	34.4050	-212.2096	49.9317	85.3079	-19.1393	337.3977
5	6	1	-32.2428	7.5865	-0.3126	2.7960	34.5752	-316.1935	74.3985	-3.0658	27.4198	339.0668
5	7	1	-45.1110	10.6144	-11.8407	7.7363	34.7988	-442.3883	104.0914	-116.1174	75.8675	341.2593
5	8	1	-60.1109	14.1438	-25.8446	12.6059	35.0606	-589.4870	138.7028	-253.4490	123.6215	343.8269
5	9	33	-64.5262	10.6017	-29.5614	9.8387	35.5179	-632.7859	103.9672	-289.8988	96.4845	348.3121
5	10	33	-67.7012	7.1817	-32.1889	6.8189	36.0848	-663.9221	70.4283	-315.6649	66.8707	353.8711

6	0	21	-1.6221	-36.1785	-1.6221	-36.1785	35.3953	-15.9071	-354.7894	-15.9071	-354.7894	347.1093
6	1	21	-1.6578	-36.1723	-1.6242	-36.1802	35.3960	-16.2579	-354.7289	-15.9284	-354.8065	347.1165
6	2	21	-2.1838	-36.0821	-1.6564	-36.2062	35.4070	-21.4157	-353.8444	-16.2442	-355.0612	347.2242
6	3	21	-3.8213	-35.7727	-1.7076	-36.2701	35.4472	-37.4746	-350.8104	-16.7454	-355.6879	347.6178
6	4	21	-6.5480	-35.1701	-1.6367	-36.3257	35.5356	-64.2135	-344.9007	-16.0509	-356.2331	348.4850
6	5	21	-10.2783	-34.5040	-1.5793	-36.4556	35.6922	-100.7953	-338.3684	-15.4874	-357.5077	350.0211
6	6	21	-2.5524	-39.6612	-2.8651	-36.8651	35.5194	-25.0309	-388.9432	-28.0968	-361.5235	348.3260
6	7	21	5.8356	-45.9161	-6.0051	-38.1798	35.5596	57.2277	-450.2833	-58.8897	-374.4158	348.7204
6	8	21	13.0833	-53.4232	-12.7613	-40.8173	36.1666	128.3038	-523.9025	-125.1452	-400.2810	354.6730
6	9	23	10.2675	-52.8832	-19.2939	-43.0445	37.3442	100.6901	-518.6073	-189.2087	-422.1227	366.2216
6	10	23	20.2150	-49.0557	-11.9739	-42.2368	37.7038	198.2414	-481.0718	-117.4235	-414.2011	369.7484

7	0	22	-0.4587	-0.6570	-2.0808	-36.8355	35.8404	-4.4988	-6.4432	-20.4059	-361.2327	351.4743
7	1	22	-0.4676	-0.6610	-2.0919	-36.8412	35.8410	-4.5860	-6.4819	-20.5144	-361.2884	351.4805
7	2	22	-0.5983	-0.7187	-2.2548	-36.9248	35.8507	-5.8674	-7.0477	-22.1116	-362.1089	351.5750
7	3	22	-1.1612	-0.9642	-2.8687	-37.2343	35.8860	-11.3871	-9.4559	-28.1325	-365.1438	351.9219
7	4	22	-2.5840	-1.5657	-4.2208	-37.8914	35.9672	-25.3406	-15.3545	-41.3915	-371.5876	352.7181
7	5	22	-4.8209	-2.4396	-6.4001	-38.8952	36.1229	-47.2765	-23.9239	-62.7639	-381.4316	354.2446
7	6	22	-6.0005	-2.6898	-8.8656	-39.5549	35.9516	-58.8447	-26.3780	-86.9415	-387.9015	352.5644
7	7	22	-5.0063	-2.0187	-11.0113	-40.1985	35.9796	-49.0947	-19.7967	-107.9844	-394.2125	352.8389
7	8	22	1.7967	-0.0006	-10.9646	-40.8179	36.5893	17.6193	-0.0062	-107.5260	-400.8872	358.8180
7	9	22	9.7663	1.2723	-9.5277	-41.7723	37.9171	95.7743	12.4767	-93.4344	-409.6460	371.8397
7	10	32	-18.0443	-1.1635	-30.0182	-43.4003	38.4952	-176.9543	-11.4104	-294.3778	-425.6114	377.5087

8	0	22	-0.1267	-0.3545	-2.2075	-37.1900	36.1368	-1.2425	-3.4763	-21.6483	-364.7089	354.3810
8	1	22	-0.1210	-0.3519	-2.2129	-37.1931	36.1375	-1.1869	-3.4509	-21.7012	-364.7393	354.3873
8	2	22	-0.0375	-0.3140	-2.2923	-37.2388	36.1472	-0.3682	-3.0794	-22.4797	-365.1883	354.4834
8	3	22	0.2712	-0.1777	-2.5975	-37.4121	36.1833	2.6593	-1.7431	-25.4732	-366.8869	354.8367
8	4	22	0.9291	0.0915	-3.2916	-37.7999	36.2663	9.1116	0.8969	-32.2799	-370.6907	355.6511
8	5	22	2.1157	0.5141	-4.2844	-38.3811	36.4284	20.7482	5.0412	-42.0157	-376.3905	357.2405
8	6	22	3.4667	0.8903	-5.3989	-38.6646	36.2678	33.9968	8.7311	-52.9447	-379.1704	355.6659
8	7	22	4.6920	1.1441	-6.3194	-39.0544	36.3095	46.0123	11.2200	-61.9721	-382.9925	356.0744
8	8	22	5.0208	1.2813	-5.9438	-39.5366	36.9253	49.2368	12.5652	-58.2892	-387.7219	362.1131
8	9	22	4.1680	1.1325	-5.3596	-40.6398	38.2427	40.8744	11.1060	-52.5600	-398.5400	375.0326
8	10	22	14.4891	-1.0822	-15.5291	-44.4825	39.1034	142.0895	-10.6128	-152.2883	-436.2242	383.4729

9	0	22	-0.1088	-0.5838	-2.3163	-37.7737	36.6705	-1.0665	-5.7249	-22.7149	-370.4338	359.6148
9	1	22	-0.1048	-0.5820	-2.3177	-37.7751	36.6712	-1.0280	-5.7074	-22.7292	-370.4467	359.6212
9	2	22	-0.0470	-0.5559	-2.3393	-37.7947	36.6811	-0.4607	-5.4512	-22.9404	-370.6395	359.7183
9	3	22	0.1745	-0.4570	-2.4231	-37.8691	36.7176	1.7109	-4.4821	-23.7623	-371.3690	360.0764
9	4	22	0.6555	-0.2491	-2.6361	-38.0490	36.8019	6.4283	-2.4429	-25.8515	-373.1336	360.9029
9	5	22	1.2976	0.0123	-2.9868	-38.3688	36.9660	12.7252	0.1209	-29.2905	-376.2696	362.5129
9	6	22	2.2427	0.3759	-3.1562	-38.2887	36.8122	21.9932	3.6866	-30.9515	-375.4838	361.0046
9	7	22	3.2620	0.7555	-3.0574	-38.2988	36.8653	31.9888	7.4092	-29.9833	-375.5833	361.5254
9	8	22	2.8071	0.5911	-3.1368	-38.9455	37.4757	27.5278	5.7971	-30.7613	-381.9248	367.5110
9	9	22	1.9888	0.2800	-3.3708	-40.3598	38.7844	19.5039	2.7460	-33.0560	-395.7940	380.3449
9	10	22	9.1290	1.9213	-6.4001	-42.5612	39.7494	89.5247	18.8418	-62.7636	-417.3825	389.8089

Appendix -5 Input data of centre bend flower pattern

 ** INITIAL INPUT DATA IN FILE RCENTRE **
 @*****

OUTER DIA.	WIDTH	THICKNESS	NUMBER OF st.	Stand No. of 1st Finpass
101.60	311.96	2.30	9	7

STAND	LS(I)	TLS(I)
1	600.00	600.00
2	600.00	1200.00
3	600.00	1800.00
4	600.00	2400.00
5	600.00	3000.00
6	600.00	3600.00
7	600.00	4200.00
8	600.00	4800.00
9	600.00	5400.00

STAND	DOWNHILL AMOUNT
0	0.00
1	0.00
2	0.00
3	0.00
4	0.00
5	0.00
6	0.00
7	0.00
8	0.00
9	0.00

STAND	NUMBER OF RADIUS
1	2
2	2
3	2
4	2
5	2
6	2
7	2
8	2
9	1

STAND	No.R	RADIUS	ANGLE	DLO	DLN	TLN(I,J)
1	1	50.800	25.0000000000	22.1657	21.6639	21.6639
1	2	99999.999	0.0769575037	134.3162	134.3146	155.9785
2	1	50.800	50.0000000000	44.3314	43.3278	43.3278
2	2	99999.999	0.0645450031	112.6523	112.6510	155.9788
3	1	50.800	75.0000000000	66.4970	64.9917	64.9917
3	2	99999.999	0.0521325008	90.9884	90.9873	155.9790
4	1	50.800	100.0000000000	88.6627	86.6556	86.6556
4	2	99999.999	0.0397200008	69.3245	69.3237	155.9793
5	1	50.800	125.0000000000	110.8284	108.3195	108.3195
5	2	99999.999	0.0273075002	47.6606	47.6600	155.9795
6	1	50.800	150.0000000000	132.9941	129.9834	129.9834
6	2	99999.999	0.0148950001	25.9967	25.9964	155.9798
7	1	50.800	160.0000000000	141.8604	138.6490	138.6490
7	2	99999.999	0.0099299999	17.3311	17.3309	155.9799
8	1	50.800	170.0000000000	150.7266	147.3145	147.3145
8	2	99999.999	0.0049650001	8.6656	8.6655	155.9800

9 1 50.800 180.0000000000 159.5929 155.9801 155.9801

NUMBER OF DIVISION IN WIDTH= 10

YOUNG'S MODULUS= 21000.00

YIELD STRESS= 31.50

WORK-HARDENING COEFFICIENT= 80.00

POISSON'S RATIO= 0.30

RATIO OF $E(y)/E(x)$ = 0.50

RATIO OF $E(x)/E(y)$ = 0.45

FORMING VELOCITY= 40.00

IDH= 0 IIDH= 0

SIZE= 101.6X2.3mm
DATE=14.10.1992
DRAWER=T.TOYOOKA
WORKS=TOKYO UNIV.
MATERIAL=STEEL

Appendix -6 Input data of edge bend flower pattern

 ** INITIAL INPUT DATA IN FILE REDGEB **

OUTER DIA.	WIDTH	THICKNESS	NUMBER OF st.	Stand No. of 1st Finpass
101.60	311.96	2.30	9	7

STAND	LS(I)	TLS(I)
1	600.00	600.00
2	600.00	1200.00
3	600.00	1800.00
4	600.00	2400.00
5	600.00	3000.00
6	600.00	3600.00
7	600.00	4200.00
8	600.00	4800.00
9	600.00	5400.00

STAND	DOWNHILL AMOUNT
0	0.00
1	0.00
2	0.00
3	0.00
4	0.00
5	0.00
6	0.00
7	0.00
8	0.00
9	0.00

STAND	NUMBER OF RADIUS
1	2
2	2
3	2
4	2
5	2
6	2
7	2
8	2
9	1

STAND	No.R	RADIUS	ANGLE	DLO	DLN	TLN(I,J)
1	1	99999.999	0.0769575037	134.3162	134.3146	134.3146
1	2	50.800	25.0000000000	22.1657	21.6639	155.9785
2	1	99999.999	0.0645450031	112.6523	112.6510	112.6510
2	2	50.800	50.0000000000	44.3314	43.3278	155.9788
3	1	99999.999	0.0521325008	90.9884	90.9873	90.9873
3	2	50.800	75.0000000000	66.4970	64.9917	155.9790
4	1	99999.999	0.0397200008	69.3245	69.3237	69.3237
4	2	50.800	100.0000000000	88.6627	86.6556	155.9793
5	1	99999.999	0.0273075002	47.6606	47.6600	47.6600
5	2	50.800	125.0000000000	110.8284	108.3195	155.9795
6	1	99999.999	0.0148950001	25.9967	25.9964	25.9964
6	2	50.800	150.0000000000	132.9941	129.9834	155.9798
7	1	99999.999	0.0099299999	17.3311	17.3309	17.3309
7	2	50.800	160.0000000000	141.8604	138.6490	155.9799
8	1	99999.999	0.0049650001	8.6656	8.6655	8.6655
8	2	50.800	170.0000000000	150.7266	147.3145	155.9800
9	1	50.800	180.0000000000	159.5929	155.9801	155.9801

NUMBER OF DIVISION IN WIDTH= 10
YOUNG'S MODULUS= 21000.00
YIELD STRESS= 31.50
WORK-HARDENING COEFFICIENT= 80.00
POISSON'S RATIO= 0.30
RATIO OF E(y)/E(x)= 0.50
RATIO OF E(x)/E(y)= 0.45
FORMING VELOCITY= 40.00

IDH= 0 IIDH= 0

SIZE= 101.6X2.3mm
DATE=8.10.1992
DRAWER=T. TOYOOKA
WORKS=TOKYO UNIV.
MATERIAL=STEEL

Appendix -7 Input data of circular bend flower pattern

 ** INITIAL INPUT DATA IN FILE RCIRCULB **

OUTER DIA.	WIDTH	THICKNESS	NUMBER OF st.	Stand No. of 1st Finpass
101.60	311.96	2.30	9	7

STAND	LS(I)	TLS(I)
1	600.00	600.00
2	600.00	1200.00
3	600.00	1800.00
4	600.00	2400.00
5	600.00	3000.00
6	600.00	3600.00
7	600.00	4200.00
8	600.00	4800.00
9	600.00	5400.00

STAND	DOWNHILL AMOUNT
0	0.00
1	0.00
2	0.00
3	0.00
4	0.00
5	0.00
6	0.00
7	0.00
8	0.00
9	0.00

STAND	NUMBER OF RADIUS
1	1
2	1
3	1
4	1
5	1
6	1
7	1
8	1
9	1

STAND	No.R	RADIUS	ANGLE	DLO	DLN	TLN(I,J)
1	1	358.630	25.0000000000	156.4819	155.9801	155.9801
2	1	179.890	50.0000000000	156.9836	155.9801	155.9801
3	1	120.310	75.0000000000	157.4854	155.9801	155.9801
4	1	90.520	100.0000000000	157.9872	155.9801	155.9801
5	1	72.646	125.0000000000	158.4890	155.9801	155.9801
6	1	60.730	150.0000000000	158.9908	155.9801	155.9801
7	1	57.006	160.0000000000	159.1908	155.9794	155.9801
8	1	53.721	170.0000000000	159.3934	155.9813	155.9801
9	1	50.800	180.0000000000	159.5929	155.9801	155.9801

NUMBER OF DIVISION IN WIDTH= 10

YOUNG'S MODULUS= 21000.00

YIELD STRESS= 31.50

WORK-HARDENING COEFFICIENT= 80.00

POISSON'S RATIO= 0.30

RATIO OF $E(y)/E(x)$ = 0.50

RATIO OF $E(x)/E(y)$ = 0.45

FORMING VELOCITY= 40.00

IDH= 0 IIDH= 0

SIZE= 101.6X2.3mm
DATE=8.10.1992
DRAWER=T.TOYOOKA
WORKS=TOKYO UNIV.
MATERIAL=STEEL

Appendix -8 Input data of D=146.0mm x t=2.0mm

 ** INITIAL INPUT DATA IN FILE RH146-1 **

0	OUTER DIA.	WIDTH	THICKNESS	NUMBER OF st.	Stand No. of 1st Finpass
	146.00	461.26	2.00	13	7

0	STAND	LS(I)	TLS(I)
	1	1000.00	1000.00
	2	900.00	1900.00
	3	780.00	2680.00
	4	780.00	3460.00
	5	780.00	4240.00
	6	1540.00	5780.00
	7	625.00	6405.00
	8	625.00	7030.00
	9	625.00	7655.00
	10	870.00	8525.00
	11	1730.00	10255.00
	12	1995.00	12250.00
	13	1150.00	13400.00

0	STAND	DOWNHILL AMOUNT
	0	0.00
	1	0.00
	2	0.00
	3	0.00
	4	0.00
	5	0.00
	6	0.00
	7	0.00
	8	0.00
	9	0.00
	10	0.00
	11	0.00
	12	0.00
	13	0.00

0	STAND	NUMBER OF RADIUS
	1	2
	2	3
	3	4
	4	4
	5	4
	6	4
	7	5
	8	5
	9	5
	10	5
	11	5
	12	5
	13	1

0	STAND	No.R	RADIUS	ANGLE	DLO	DLN	TLN(I,J)
	1	1	99999.999	0.0942458294	164.4900	164.4884	164.4884
	1	2	75.000	50.2100000000	65.7247	64.8484	229.3368
	2	1	99999.999	0.0575937186	100.5200	100.5190	100.5190
	2	2	111.210	33.5600000000	65.1393	64.5536	165.0726
	2	3	83.500	44.9700000000	65.5370	64.7522	229.8247
	3	1	361.980	8.0000000000	50.5419	50.4023	50.4023
	3	2	147.610	19.7800000000	50.9588	50.6136	101.0159
	3	3	131.400	28.3200000000	64.9480	64.4538	165.4697
	3	4	83.500	44.9700000000	65.5370	64.7522	230.2218
	4	1	266.710	10.8800000000	50.6460	50.4562	50.4562

4	2	66.460	44.6700000000	51.8148	51.0351	101.4913
4	3	131.400	28.3200000000	64.9480	64.4538	165.9450
4	4	83.500	44.9700000000	65.5370	64.7522	230.6972
5	1	107.260	27.3600000000	51.2190	50.7415	50.7415
5	2	66.460	44.6700000000	51.8148	51.0351	101.7766
5	3	131.400	28.3200000000	64.9480	64.4538	166.2304
5	4	83.500	44.9700000000	65.5370	64.7522	230.9825
6	1	78.560	37.6200000000	51.5819	50.9253	50.9253
6	2	66.460	44.6700000000	51.8148	51.0351	101.9605
6	3	131.400	28.3200000000	64.9480	64.4538	166.4142
6	4	83.500	44.9700000000	65.5370	64.7522	231.1664
7	1	77.650	38.1100000000	51.6485	50.9834	50.9834
7	2	69.830	38.5800000000	47.0199	46.3465	97.3299
7	3	123.610	26.6300000000	57.4516	56.9868	154.3167
7	4	69.830	38.5800000000	47.0199	46.3465	200.6633
7	5	73.040	22.5800000000	28.7847	28.3906	229.0539
8	1	77.650	38.1100000000	51.6485	50.9834	50.9834
8	2	69.830	38.5800000000	47.0199	46.3465	97.3299
8	3	123.610	26.6300000000	57.4516	56.9868	154.3167
8	4	69.830	38.5800000000	47.0199	46.3465	200.6633
8	5	73.040	22.5800000000	28.7847	28.3906	229.0539
9	1	74.730	52.5000000000	68.4749	67.5586	67.5586
9	2	71.930	30.0000000000	37.6625	37.1389	104.6975
9	3	96.620	15.0000000000	25.2951	25.0333	129.7308
9	4	71.930	30.0000000000	37.6625	37.1389	166.8696
9	5	72.630	49.0000000000	62.1140	61.2588	228.1284
10	1	74.730	52.5000000000	68.4749	67.5586	67.5586
10	2	71.930	30.0000000000	37.6625	37.1389	104.6975
10	3	96.620	15.0000000000	25.2951	25.0333	129.7308
10	4	71.930	30.0000000000	37.6625	37.1389	166.8696
10	5	72.630	49.0000000000	62.1140	61.2588	228.1284
11	1	74.730	52.5000000000	68.4749	67.5586	67.5586
11	2	71.930	30.0000000000	37.6625	37.1389	104.6975
11	3	96.620	15.0000000000	25.2951	25.0333	129.7308
11	4	71.930	30.0000000000	37.6625	37.1389	166.8696
11	5	72.630	49.0000000000	62.1140	61.2588	228.1284
12	1	74.730	52.5000000000	68.4749	67.5586	67.5586
12	2	71.930	30.0000000000	37.6625	37.1389	104.6975
12	3	96.620	15.0000000000	25.2951	25.0333	129.7308
12	4	71.930	30.0000000000	37.6625	37.1389	166.8696
12	5	72.630	49.0000000000	62.1140	61.2588	228.1284
13	1	73.000	180.0000000000	229.3363	226.1947	226.1947

0 NUMBER OF DIVISION IN WIDTH= 10
 0 YOUNG'S MODULUS= 21000.00
 0 YIELD STRESS= 30.00
 0 WORK-HARDENING COEFFICIENT= 200.00
 0 POISSON'S RATIO= 0.30
 0 RATIO OF E(y)/E(x)= 0.50
 0 RATIO OF E(x)/E(y)= 0.45
 0 FORMING VELOCITY= 40.00

0 IDH= 0 IIDH= 0

SIZE= 146x2.0mm
 DATE=20.10.1998
 DRAWER=M.ARATANI
 WORKS=HISTORY
 MATERIAL=SAPH440